Rainwater Harvesting in Rural Jordan

A GIS and remote sensing-based analysis of ancient and modern adaptations to water scarcity in a changing environment

————

Barbara Sophia
Brilmayer Bakti

0   50   100 m

Dissertation

Submitted to the

Combined Faculty of Natural Sciences and Mathematics

Heidelberg University, Germany

for the degree of

Doctor of Natural Sciences (Dr. rer. nat.)

Presented by

Barbara Sophia Brilmayer Bakti

Oral examination: December 17, 2019

Rainwater Harvesting in Rural Jordan

A GIS and remote sensing-based analysis of ancient and modern adaptations to water scarcity in a changing environment

Dedicated to those who made this work possible

and contributed to its successful realization,

and those who will read and value it.

Supervisor / 1st referee: Prof. Dr. Olaf Bubenzer

2nd referee: Prof. Dr. Hans Gebhardt

Contents

Figures

Tables

Abbreviations and acronyms

ACSAD	Arab Center for the Studies of Arid Zone and Dry Lands
AFE	Automatic Feature Extraction (model)
ALOS	Advanced Land Observing Satellite, "Daichi"; for ALOS PRISM see PRISM
ALOS DEM	Custom-made digital elevation model for the study area, produced by Geoserve B.V., based on ALOS PRISM triplet imagery
ANUDEM	Australian National University DEM
ArcGIS (Desktop)	ArcGIS Desktop, Advanced, versions 10.0-10.6, ESRI 2010-2018, including all applications (e.g. ArcMap), tools, and extensions available with the named licensing level and versions; also see references
Arc Hydro	Arc Hydro for ArcGIS, Arc Hydro Tools, versions 2.0.1.156-10.5.0.50 for ArcGIS versions 10.0-10.5, ESRI 2014-2017; also see references
ArcMap	Application, part of ArcGIS Desktop software package (see above)
ASTER	Advanced Spaceborne Thermal Emission and Reflection Radiometer (satellite sensor), on board Terra, NASA's first Earth Observing System satellite
ASTER GDEM (V2)	Global Digital Elevation Model (Version 2) produced based on ASTER data, ASTGTMv002, NASA ET AL. 2009; also see references
ATCOR	Atmospheric and Topographic Corrections, ATCOR for ERDAS IMAGINE, version(s) 2010 and 2011, RICHTER ET AL. 2010-2011; also see references
ATCOR3	Module ATCOR3 – for Rugged Terrain, part of ATCOR (see above)
CI	Confidence interval
COT	Commercial off-the-shelf product, usually referring to software solutions
DEM	Digital elevation model, generic term that can refer to a DSM or DTM or anything in-between
DoA	Department of Antiquities, here referring to Jordan
DoPS	Department of Population Statistics, here referring to Jordan
DoS	Department of Statistics, here referring to Jordan
DSM	Digital surface model, representing the surface of the landscape including all objects in it (buildings, trees, etc.)
DSS	Decision support system
DTM	Digital Terrain Model, in contrast to the DSM, here objects of the earth's surface (e.g. buildings, trees, etc.) have been removed
ENVI FX	ENVI Feature Extraction Module, L3Harris Geospatial
EORC	Earth Observation Research Center, affiliated with JAXA
EPE	Estimated position error (in GPS based measurements)
ERDAS IMAGINE	ERDAS IMAGINE Professional, versions 2010 and 2011, ERDAS 2009-2011; also see references
ESRI	Environmental Systems Research Institute, Inc.
FA	Feature Analyst for ArcGIS, professional, versions 5.0.0.119-5.2.0.4, OVERWATCH / TEXTRON SYSTEMS 2012-2017; also see references
FAO	Food and Agriculture Organization of the United Nations
(The) GCI	(The) Getty Conservation Institute
GCP	Ground control point
GEOBIA	Geospatial/geographical object-based image analysis
GIS	Geographic information system
GPS	Global Positioning System

IPCC	Intergovernmental Panel on Climate Change
IRCSA	International Rainwater Catchment Systems Association
JADIS	Jordan Antiquities Database and Information System, precursor of the MEGA-Jordan database
JAXA	Japan Aerospace Exploration Agency
JICA	Japan International Cooperation Agency
JOSCIS	Jordan Soil and Climate Information System
JPL	Jet Propulsion Laboratory, California Institute of Technology (Caltech)
JUST	Jordan University of Science and Technology
LiDAR	Light detection and ranging, active remote sensing method
LU/LC	Land Use/Land Cover
MCM	Million cubic meter
Ma	Mega anni, million years (before present)
MEGA-Jordan	Middle Eastern Geodatabase for Antiquities, database for Jordan; online database, also see references
MENA	Middle East and North Africa region
METI	Ministry of Economy, Trade, and Industry of Japan
MoA	Ministry of Agriculture, here referring to Jordan
MoE	Ministry of Environment, here referring to Jordan
MoP	Ministry of Planning, here referring to Jordan
MS (bands)	Multi spectral bands (satellite imagery)
MWI	Ministry of Water and Irrigation, here referring to Jordan
NASA	U.S. National Aeronautics and Space Administration
NGO	Non-governmental organization
NIR	Near infrared, here concerning the corresponding band in satellite images
NPO	Non-profit organization
NSM&LUP	National Soil Map and Land Use Project, here referring to Jordan
OBIA	Object-based image analysis
OSL	Optically stimulated luminescence, chronometric (absolute) dating method
(ALOS) PRISM	Panchromatic Remote Sensing Instrument for Stereo Mapping, on board ALOS
RC	Runoff coefficient
RMS / RMSE	Root Mean Square Error
RRWH	Rooftop rainwater harvesting
RWH	Rainwater harvesting
SBAS	Satellite Based Augmentation System
SCS / SCS-CN	Soil Conservation Service / Soil Conservation Service Curve Number (method), a method of runoff estimation developed by the SCS
SD	Standard deviation
SDSS	Spatial decision support system, DSS based on geodata and a GIS
SWAT	Soil and Water Assessment Tool, Arc SWAT, add-on for ArcGIS Desktop
UNDP	United Nations Development Programme
UNESCO	United Nations Educational, Scientific and Cultural Organization
USDA / US Soil Taxonomy	U.S. Department of Agriculture/U.S. Soil Taxonomy (soil classification system of the United States of America)
UV (light)	Ultraviolet light
VHR	Very high resolution
WAJ	Water Authority of Jordan
WH	Water harvesting
WRB	World Reference Base for Soil Resources

Abstract

This study investigates the topic of rainwater harvesting on the Karak Plateau located in rural Jordan. The term rainwater harvesting describes various methods and structures employed for the collection, storage and use of rainwater and resulting (on-site) surface runoff. Within the scope of traditional water management, over millennia, many of these techniques were developed, refined and applied in Jordan, as well as in other, especially semiarid, regions of the world. This tradition is rooted in the natural water shortage of the plateau and frequent absence of other reliable sources of freshwater. Today, population growth, climate change and local effects of globalization and global change are leading to growing water shortages in the MENA region (Middle East and North Africa) and many other parts of the world. In the search for sustainable solutions for this problem, traditional as well as new strategies of rainwater harvesting have recently been receiving increasing interest.

The present study contributes to an enhanced understanding of the applicability and the potential of some of the most widely-used, traditional rainwater harvesting methods, especially the use of cisterns. The mapped structures were examined taking into account the settlement history and the respective circumstances of the natural and human environment. Possible determining factors concerning site preferences and resulting patterns in the spatial distribution of rainwater harvesting sites have been detected. The diachronic comparative analysis revealed changes in human-environment-interactions, particularly with regard to the significance and management of local water resources under natural shortage. The collected data enabled the detailed estimation of the rainwater harvesting potential and the suggestion of possible ways to improve and expand current rainwater harvesting schemes and efforts. The integration and possible role of rainwater harvesting strategies were discussed with regard to modern, sustainable water management and supply. Additionally, the applicability of modern geoinformation techniques was evaluated. Remote sensing techniques and methods of image analysis, particularly with regard to the interpretation of satellite images of very high resolution, were examined especially. The combination of ground truth and other information from field work and remote sensing-based data and techniques has proven most suitable and efficient. The mostly remote sensing-based mapping of rainwater harvesting structures and the establishment of a comprehensive database formed the basis for all subsequent analysis and possible further, sustainable planning steps. The semiautomatic analysis of the satellite imagery provided detailed information on land use/land cover and building rooftops and thus decisively contributed to the improvement of the (input) data basis.

All in all, the collected data enabled a significantly enhanced, quantitative estimation of the rainwater harvesting potential of the study area. Many of the gained findings and insights can be transferred onto other dry areas and regions with similar environmental or socio-economic conditions.

Kurzzusammenfassung

Anhand des Karak-Plateaus, einer ländlichen Region in Jordanien, wird der Ansatz des *Rainwater Harvesting* näher untersucht. Dabei handelt es sich um Methoden zur Sammlung und Nutzung von Regenwasser und unmittelbar daraus entstehendem Oberflächenabfluss, die häufig im Rahmen des traditionellen Wassermanagements über Jahrtausende entwickelt und genutzt wurden, sowohl in Jordanien als auch in anderen, v.a. semiariden, Regionen. Ihre Tradition ist auf die natürliche Wasserknappheit und den häufigen Mangel an alternativen, verlässlichen Wasserquellen zurückzuführen. Durch Bevölkerungszunahme, Klimawandel und lokale Auswirkungen globaler Veränderungen zeichnet sich vor allem in der MENA-Region (*Middle East and North Africa*) eine Verschärfung der Wasserknappheit ab. Auf der Suche nach Lösungsstrategien hierfür erfahren traditionelle sowie moderne *Rainwater Harvesting*-Strategien zunehmende Beachtung.

Die vorliegende Studie leistet einen Beitrag zum besseren Verständnis des Einsatzes und des Potentials einiger weitverbreiteter, traditioneller *Rainwater Harvesting*-Methoden, insbesondere der Nutzung von Zisternen. Die kartierten Anlagen werden in Zusammenhang mit der Siedlungsgeschichte und den physio- sowie anthropogeographischen Rahmenbedingungen der Region untersucht und räumliche Verteilungsmuster sowie mögliche determinierende Faktoren herausgearbeitet. In der diachronen Betrachtung werden Veränderungen in der Mensch-Umwelt-Beziehung deutlich, v.a. hinsichtlich der Bedeutung und des Managements von lokalen Wasserressourcen bei natürlicher Knappheit. Die erhobenen Daten ermöglichen eine detaillierte Abschätzung des *Rainwater Harvesting*-Potentials und zeigen Wege zur Verbesserung und Erweiterung der bestehenden Strategien und Systeme auf. Zudem werden die Integration und die mögliche Rolle von *Rainwater Harvesting*-Methoden im Rahmen einer modernen Wasserversorgung und eines nachhaltigen Wassermanagements diskutiert. Weiterhin wird der Einsatz von modernen Methoden der Geoinformatik evaluiert. Techniken der Fernerkundung und der Bildanalyse bzw. der Interpretation von hochauflösenden Satellitenbildern finden dabei besondere Beachtung. Insgesamt erweist sich die Kombination von Bodendaten sowie Erkenntnissen aus Geländearbeit und Fernerkundungsmethoden und -daten als besonders zielführend und effizient. Die größtenteils fernerkundungsgestützte, flächendeckende Kartierung von *Rainwater Harvesting*-Systemen und der Aufbau einer umfassenden Datenbank schaffen die Basis für weiterführende Analysen und zukünftige nachhaltigere Planungsschritte. Die semi-automatische Auswertung hochauflösender Satellitenbilder liefert detaillierte Informationen zu Landnutzung und Gebäudedachflächen und trägt so entscheidend bei zur Verbesserung der Datengrundlage.

Insgesamt erlauben die gewonnen Daten eine deutlich genauere, quantifizierende Einschätzung des *Rainwater Harvesting*-Potentials im Untersuchungsgebiet. Viele der erarbeiteten Ergebnisse und Erkenntnisse lassen sich auch auf andere Trockengebiete und Regionen mit ähnlichen Rahmenbedingungen übertragen.

1 Introduction

In most arid and semiarid areas of the world, the first human settlers had to develop strategies for securing their water needs in order to survive. In the absence of springs, perennial streams or other reliable sources of surface water, the collection, storage and use of rainwater and resulting runoff became an essential strategy for survival. Over the centuries, different approaches were developed independently all over the world. These included channels, dikes, ridges and shallow walls for the (re-) direction, diversion, and collection of runoff as well as dams, reservoirs and cisterns for water storage. In areas with the necessary preconditions, even shallow groundwater aquifers were exploited through wells and qanat systems (also named karez, foggara or khettara). The choice, development and design of specific structures and techniques most likely depended on the prevailing natural conditions at the respective location and the socio-cultural settings during that time. Changes in either the human or the environmental set of factors, or in both, probably led to different preferences, modifications or even to the abandonment of strategies. However, over time, some approaches proved to be particularly advantageous, reliable and sustainable, allowing societies to survive and flourish even in less favorable or hostile dry environments. Over the centuries and millennia, these water management and supply strategies were refined to fit local environmental conditions in as optimally a way as possible, forming long traditions. These in turn were then passed down for generations, often from ancient to modern times.

In recent years, the increasing water shortage in many dry areas of the world, such as the Middle East and North Africa (MENA region), has led to a renewed interest in traditional ways of water management and supply, including rainwater harvesting (RWH) strategies. Many countries with very limited natural freshwater resources are faced with a growing water demand due to high population growth rates (natural and resulting from migration dynamics), changes in lifestyle that are associated with an increase in water consumption, geopolitical situations and globalization which induces (geographical) shifts in production strategies and value chains. The resulting water shortage is aggravated by climate change that entails modified precipitation patterns, reduced precipitation amounts and higher evaporation rates in many regions. In search of long-term (i.e. sustainable) solutions to this problem, ancient and traditional strategies of water management and supply are being re-examined regarding their potential for alleviating current and future water shortage.

The optimal application of RWH techniques typically requires comprehensive, in-depth knowledge of the history, tradition and potential of RWH as well as a thorough understanding of possible interdependencies between RWH schemes and the natural environmental conditions and cultural, socio-economic and political circumstances. In consideration of the multifaceted nature of the subject, the present study

attempts to integrate aspects from a variety of disciplines besides (physical) geography, such as anthropology, archaeology, natural and cultural heritage conservation, climate change investigation, agricultural sciences, computing and (geo-) informatics, land use planning, engineering and development aid, as well as water resources research. The methodological approach is similarly broad and combines different techniques such as GIS analyses, application of remote sensing products and image interpretation, as well as field work including GPS based mapping, measurements and photographic documentation. The different aspects and partial research questions addressed in the study at hand are presented in Table 1. In principle, the objectives of the present study can be divided into two scopes. On the one hand, the gathered information and outcomes are intended to contribute to an enhanced understanding of RWH practices and ancient water management and supply strategies. On the other hand, data and findings of the present study can provide a basis for suggestions on the implementation and improvement of modern RWH strategies. Moreover, the study aims to estimate the RWH potential and discusses the possible role of RWH in both a modern society and a semiarid area. Finally, it evaluates, from a methodological point of view, the applicability and suitability of GIS and remote sensing techniques with regard to the objectives of the present study and similar purposes.

The research questions concerning ancient and modern RWH, especially in semiarid areas, are addressed here using the example of a rural area in Jordan. The country is part of the MENA region and commonly ranked among the ten driest countries in the world with respect to their (per capita) water resources. In recent years, water shortage and associated problems have been aggravated by climate change and high population growth rates. The latter is partially a result of migration dynamics that are associated with political instabilities in the wider region. Jordan possesses a long and rich cultural history in which water management and supply strategies have always played a prominent role due to the natural water scarcity of the country. The geographical situation, between the Mediterranean Sea and the vast desert areas of the Arabian Peninsula in the east, entails a transitional character that can be observed in many features of Jordan, most evidently in its climate. Natural environments like that of Jordan, and transitional, semiarid areas or desert fringes in general, are believed to be particularly sensitive to climate change and other natural shifts and anthropogenic influences, especially with respect to water related changes. The described circumstances along with the political stability and the general openness and friendliness of the Jordanian people make the country an ideal study area, from which insights can be gained that may (partially) apply to other areas of the world, particularly other semiarid and arid regions.

Table 1: Subtopics and partial research questions with increasing levels of complexity from descriptive (level 1) to analytical, deductive and interpretive (levels 2 and 3) and finally reflective (evaluation and transfer, levels 4 and 5).

Level of Complexity	Subtopics and Questions
1	**Existing rainwater harvesting infrastructure** • What strategies of traditional water management and rainwater harvesting have been or are currently employed? • What rainwater harvesting infrastructure now exists and how can it be mapped? • What rainwater harvesting structures have been given up and what are still in use? • Of what age are the rainwater harvesting structures and in which condition are they?
2	**Site characteristics and spatial patterns** • What factors of the natural or human environment play a crucial role during site selection for rainwater harvesting structures? • Do site preferences differ depending on the employed rainwater harvesting method? • Are there any spatial patterns observable in the distribution of rainwater harvesting sites? • From a diachronic point of view, are there any changes in these patterns and rainwater harvesting strategies in general?
3	**Rainwater harvesting potential and strategies** • What is the rainwater harvesting potential of the area and how does it relate to the water demand? • For what purposes can rainwater harvesting be applied? • How can the area benefit from rainwater harvesting? • Which types of rainwater harvesting strategies seem most suitable? • How can the existing rainwater harvesting infrastructure be improved and complemented?
4	**Methodological evaluation** • How can modern geoinformatics support rainwater harvesting research and planning? • Which tools and approaches are suitable for addressing which questions? • What data need to be collected for improved rainwater harvesting planning and research?
5	**Synopsis and transferability** • What new insights on rainwater harvesting were gained? • What role can rainwater harvesting play in a rural, semiarid environment and how has this changed? • Which areas might be suitable for similar rainwater harvesting strategies? • Regarding its benefits and drawbacks, what can be the future role of rainwater harvesting, particularly concerning water stress alleviation?

The vertical axis spanning the levels reads: Description – Analysis / Synthesis / Interpretation – Evaluation – Transfer

2 Rainwater harvesting: state of knowledge and previous research

The term water harvesting (WH) has been defined in many ways and by several authors since its first use which is ascribed to H.J. Geddes of the University of Sydney in 1963 (MYERS 1975). One often cited definition is that of CRITCHLEY & SIEGERT (1991, p. 9) who describe WH as the "collection of runoff for its productive use". Similar explanations can also be found in MYERS (1975) and FRASIER (1998). While CRITCHLEY & SIEGERT (1991) and PRINZ (1996) center on WH for agricultural purposes, which indeed is one of the most common application areas, other scholars attempt to give a broader understanding of the term. Here, a more general definition of WH comprising "methods to induce, collect, and store runoff from various sources and for various purposes" (BOERS & BEN-ASHER 1982, p. 146) is preferred. Useful descriptions of WH explaining the term in a comprehensive manner can also be found in OWEIS ET AL. (2012). Although both expressions, WH and rainwater harvesting (RWH), are often used synonymously (cf. BOERS & BEN-ASHER 1982), it should correctly be distinguished between the more general term WH and the subordinated, more specialized term RWH. While WH encompasses the collection and use of all forms of precipitation (e.g. snow, fog, rain) and runoff (also that of ephemeral streams), typically for agricultural purposes (MALIVA & MISSIMER 2012), RWH refers only to precipitation in the form of rain and directly resulting runoff (cf. PACEY & CULLIS 1986). Therefore, RWH "can be succinctly defined as the collection, storage, and reuse of rainwater" (MALIVA & MISSIMER 2012, p. 529). CRITCHLEY & SIEGERT (1991) see RWH as opposed to floodwater harvesting while both are subsumed under the term WH. Other scholars do not differentiate between WH and RWH but rather only use the expression WH which is subdivided into other categories such as micro- or macrocatchment WH according to the dimensions of systems or their application area (cf. OWEIS ET AL. 2001). The same techniques are elsewhere subsumed under the generic term RWH (cf. PACEY & CULLIS 1986, MALIVA & MISSIMER 2012).

Closely related to the terms RWH and WH is the label traditional water use (or management) that is often applied to the same or similar techniques and approaches, typically when a historical perspective is taken and times before the establishment of the (modern) terms WH and RWH are discussed. As the expression traditional water use does not represent a fixed technical term with a clear, restrictive definition, it can be observed being applied to a variety of contexts involving water allocation, water management, water rights, and archaeological or historical investigations on water supply and consumption (cf. e.g. MILLER 1980, LEIN 2004, INTWATER n.d.). From a linguistic point of view, the expression primarily denotes ways of water utilization that were established over a long period of time. It is therefore often associated with historic irrigation schemes (LEIN 2004, RAPPOLD 2005, INTWATER n.d.). However, there have always been more ways of water use and as "water use necessitates water storage" (LANCASTER & LANCASTER 1999, p. 131) – at least in the absence of a permanent source of freshwater which

often is the case in arid lands – the field consequently opens up to a wider range of topics such as water supply and resources development, water (demand) management, and agricultural applications. What all studies have in common is their historical aspect, since they investigate strategies and concepts which have been developed and used over long periods of time. Similar expressions found in literature are traditional (water) technologies, traditional water supply systems, traditional techniques of water management, and traditional water systems (e.g. UNESCO & ACSAD 1986, LAUREANO 2004, HUSSAIN ET AL. 2008, ALI ET AL. 2009). Sometimes the word traditional is also replaced by indigenous, referring to long-established, old techniques of water management as indigenous knowledge (cf. VAN DIJK & REIJ 1994, OWEIS ET AL. 2004).

For millennia, RWH has played a fundamental role in water management. It often was the primary or an important additional source of water, at least in dry areas where other reliable sources of freshwater, such as springs or perennial rivers, were absent or insufficient. Thus, RWH approaches form an integral part of traditional water use and supply strategies. Many, if not most, of the RWH methods known today have been in use over millennia and therefore can be traced back to long traditions in many parts of the world. This overlapping field of traditional water management and RWH represents the main focus of this study.

2.1 Origins and tradition of rainwater harvesting

The exact beginning of RWH activities is difficult to identify and depends on how narrow the term is defined, i.e. which actions are seen as RWH strategies. Understanding RWH in the broadest sense, which may include even the digging of holes by desert animals to trap water, LAUREANO (2004) states that RWH with dikes and built surfaces had already been practiced by the first hominids and by *Homo sapiens* during the Paleolithic period. In contrast, most scholars see the first evidence for RWH dating from Neolithic times or even earlier periods (BIENERT 2000, GEBEL 2004, FUJII 2007, MAYS 2010, MITHEN 2010). Not surprisingly, considering the effort and labor required for most RWH schemes, the advancement of RWH is tied to the beginning of sedentism. Early populations probably deliberately chose the locations worth investing in RWH, while sites of permanent settlement surely had a higher priority in securing access to sufficient water resources as a matter of survival and convenience. In analogy to other developments during that time, e.g. agriculture and animal husbandry, early water management strategies are sometimes characterized as the "domestication of water" (GEBEL 2004, MITHEN 2010). Independent of the exact definition of RWH, in the last 6,000 years, techniques for the collection, storage, and use of precipitation and subsequent runoff have been developed at similar times all around the world. Hence, the traces and remains of ancient RWH schemes can be found in many parts of the world, e.g.

in the MENA region (EVENARI ET AL. 1982, LAVEE ET AL. 1997, BIENERT & HÄSER 2004, OWEIS ET AL. 2004, ABDELKHALEQ & ALHAJ AHMED 2007), the Mediterranean (MAYS ET AL. 2007, SHOWLEH 2007, ANTONIOU ET AL. 2014, SCHÄFER ET AL. 2014), as well as in Asia (LI ET AL. 2002, PANDEY ET AL. 2003) and South America (MAYS & GOROKHOVICH 2010, MALIVA & MISSIMER 2012). Further details on the evolution, tradition, and history of RWH, with reference to findings from different regions, can also be found in GOULD & NISSEN-PETERSEN (1999), PANDEY ET AL. (2003), MAYS (2010) and AKPINAR FERRAND & CECUNJANIN (2014).

2.2 Rainwater harvesting strategies: types and classification

RWH strategies can be subdivided into several categories according to different criteria, such as the size of structures (e.g. macro- vs. micro-catchment water harvesting), the main purposes of use of the harvested water (e.g. domestic vs. agricultural purposes), or the origin of the harvested water, i.e. the form of precipitation that is collected (e.g. flood water, fog, surface or subsurface runoff, etc.). All these criteria are used in an attempt to structure and classify the huge variety of RWH techniques known today. Besides the specialized literature on individual techniques, PACEY & CULLIS (1986), MALIVA & MISSIMER (2012) and OWEIS ET AL. (2012) provide a good overview of the common practices. The latter comprise various micro- and macro-catchment techniques as well as particular forms of RWH, such as rooftop rainwater harvesting (RRWH) and modern artificial groundwater recharge (also called managed aquifer recharge). While flood or stormwater harvesting schemes operate on a large scale, micro-catchment systems are employed on a smaller scale. Micro-catchment water harvesting methods are quite diverse and encompass miscellaneous earthworks and small stone structures such as shallow walls, dikes, channels, check dams, terraces, bunds, and ridges which are intended to slow down, divert, spread, redirect, or hold back surface runoff (overland and rill flow). They are typically constructed to support rainfed agriculture in semiarid to arid areas and are often also called runoff farming systems (BRUINS ET AL. 1986, CRITCHLEY & SIEGERT 1991, FRASIER 1994). The harvested water is usually stored in the soil profile or partially directly used by the plants, although it can also be collected and stored in open reservoirs or excavated underground chambers (cisterns) for later use (OWEIS 2005). Due to the huge variety and wide geographical distribution of micro- and macro-catchment WH methods, plenty of local names exist for individual techniques which are often used under different labels in several regions, while identical or similar names can also denote slightly different practices (CRITCHLEY & SIEGERT 1991, see FULLER RENNER & FRASIER 1995 and OWEIS ET AL. 2012 for examples of different RWH techniques and local names). However, not all methods are employed everywhere, i.e. in all areas where RWH is practiced, due to historical, socio-economical, or cultural reasons and differences in land suitability. An overview of the geographical distribution of RWH methods in the Arab world can be

found in UNESCO & ACSAD (1986) while examples from various regions were compiled by MALIVA & MISSIMER 2012.

The plurality of RWH practices known today encompasses some very old techniques like qanat systems, (also named foggara or karez) which tap on shallow groundwater aquifers on mountain hillsides and convey the water to the point of use with an elaborate tunnel and shaft system (LIGHTFOOT 2000, HUSSAIN ET AL. 2008, REMINI ET AL. 2014). These systems have been given up in most parts of the world. At the same time, new, modern RWH techniques were developed, such as e.g. the intentional enrichment of groundwater resources with collected precipitation and surface runoff. The harvested water is fed directly into aquifers for storage and protection from evaporation and pollution. This method is termed artificial groundwater recharge or managed aquifer recharge. It can represent an integral part of RWH systems or an independent practice when other sources of water are employed (PRINZ 2002, WOLF ET AL. 2008, MALIVA & MISSIMER 2012). The majority of RWH strategies possess a long record of diachronic use. Most of the different micro- and macro-catchment WH techniques that are applied in agriculture as well as small reservoirs and cisterns for water storage, belong to the traditional practices which were established in prehistoric or ancient times and are still in use today in vast areas of the world (PRINZ 1996, OWEIS ET AL. 2004, ALI ET AL. 2009). Several studies have built on this traditional knowledge and illustrate its reuse potential within a modern setting (e.g. UNESCO & ACSAD 1986, LA BIANCA 1995, REGNER 2002, OWEIS ET AL. 2004, ALI ET AL. 2009).

2.3 General advantages and disadvantages of rainwater harvesting

The benefits of RWH have been pointed out in numerous studies (e.g. BRUINS ET AL. 1986, FEWKES 2006, BARRON 2009, WISSER ET AL. 2010). The significance of the different strategies has probably changed since ancient times during which they were indispensable to cover essential water needs for survival. Nevertheless, the traditional, old techniques of RWH still represent valuable, additional sources of water which can complement other modern approaches of water resources development and management (GUTTMANN-BOND 2010, AKPINAR FERRAND & CECUNJANIN 2014). The main advantages of RWH are commonly seen in the decentralized way of water supply and acquisition, the normally relatively low technological requirements and the small financial input required (depending on methods and conditions). Moreover, the potential of increasing resilience to climate change effects and natural hazards (e.g. droughts or floods), the enhancement of agricultural production and plant growth and the sustainable character of RWH approaches are perceived as typical benefits (e.g. PANDEY ET AL. 2003, STURM ET AL. 2009, DILE ET AL. 2013). However, depending on the respective setting, there may also be several drawbacks and limitations (VOHLAND & BARRY 2009), such as economic

constraints, e.g. a negative or neutral cost-benefit analysis (FLESKENS ET AL. 2005, ROEBUCK ET AL. 2011), and disadvantageous hydrological impacts, like a decrease in the replenishment of groundwater resources (STAHN & TOMINI 2009) or minimized runoff and discharge or flow of streams at downstream locations (NGIGI 2003). Possible drawbacks and benefits can vary, largely depending on the specific area or region of the world, individual local environmental preconditions, the socio-economic setting and the intended field of application of RWH schemes (e.g. residential, commercial, or agricultural).

2.4 Geographical dissemination of rainwater harvesting: source and target areas

The origins, traditions and history of RWH in different parts of the world have already been briefly described earlier in this chapter (see 2.1). Semiarid and arid areas have been the focus of RWH strategies ever since their beginning. This arises from the widespread lack of alternative sources of freshwater, e.g. springs or perennial streams in those regions, and the resulting necessity to develop water resources through planning and engineering efforts. Hence, dry areas, as well as densely populated and intensively agriculturally used areas, have been the source and target areas of RWH schemes throughout every time period. However, to some extent, various techniques of RWH have been practiced in almost every part and country of the world up to now. This illustrates the general applicability of RWH in nearly all environmental and socio-economic settings. Nevertheless, not all strategies are suitable for all conditions and the selection of appropriate techniques also depends on the intended function of the RWH schemes. The main contradictions exist between dry and humid climates, from an environmental point of view, and developing and developed countries, from a socio-economic perspective. In all areas with a pronounced temporal concentration of precipitation and a complementary dry season, the central idea of RWH is to balance temporal differences in water availability, i.e. to store the water surplus of the wet season to cover water demands during the dry season. This is especially crucial for the dry areas of the world where the occurrence of precipitation is erratic and annual precipitation amounts are low. Through RWH, additional water, which otherwise would mostly be lost to evaporation, can be made available for use. Thus, for example, agricultural production can be enhanced and the risks of crop failure due to droughts or flashfloods can be minimized. Therefore, the significance and value of RWH strategies are highest in vulnerable, semiarid to arid, rural and agriculturally used areas. This applies especially to developing countries in which livelihood security largely depends on agricultural production (cf. e.g. BRUINS ET AL. 1986, OWEIS 2005, BARRON 2009, HELMREICH & HORN 2009, DILE ET AL. 2013). However, developed countries can also benefit from RWH (e.g. STEFFEN ET AL. 2013). Commonly, all types of micro- and macro-catchment RWH techniques, including RRWH, can be employed, depending on the intended uses of the harvested water. Regions that meet the aforementioned climatic criteria and are

particularly suitable for RWH are large parts of the subtropics or areas with Mediterranean climates, parts of the American continent, Australia, and especially the MENA region.

RWH is also frequently applied to areas with sufficient to high amounts of total annual precipitation but strong seasonal discrepancies, i.e. concentrated precipitation patterns. These conditions are typically found in large parts of the tropics or regions with monsoon climates, such as south and south-east Asia (e.g. India, Bangladesh, Myanmar). Here, aside from an increased water availability in times with little or no precipitation, another advantage of RWH is the reduction of concentrated runoff (floods). RWH structures are able to retard, spread, and reduce runoff and thus can diminish negative impacts from large amounts of concentrated runoff. For this purpose, especially macro-catchment RWH or flood/storm water harvesting techniques may be suitable, although many other RWH strategies and particularly RRWH can prove beneficial as well (cf. e.g. AGARWAL & NARAIN 1997, GUNNELL & KRISHNAMURTHY 2003, SHARMA 2009, ISLAM ET AL. 2010, DOMÈNECH ET AL. 2012).

Depending on the grade of development of a country, different aspects play a major role in the adoption of RWH and the selection of suitable techniques. For developing countries, the main reasons for the application of RWH are commonly livelihood improvement, including health benefits through improved access to clean water (e.g. FRY ET AL. 2010, DOMÈNECH ET AL. 2012), poverty reduction, and the enhancement of agriculture, i.e. food production. Hence, all kinds of RWH strategies can be rewarding, depending on local conditions. In developing countries, sustainability aspects can play a certain role, whereas these are usually a key concern in developed countries (cf. DOMÈNECH & SAURÍ 2011). In addition to ecological considerations, economic benefits such as the saving of potable water and a reduction of water treatment expenses may represent principal reasons for the implementation of RWH in developed countries (LI ET AL. 2010, FARRENY ET AL. 2011a, RAHMAN ET AL. 2012, MATOS SILVA ET AL. 2015). Typically, RRWH is practiced on different scales (residential, commercial, neighborhood scale) (e.g. THOMAS ET AL. 2014) while RWH strategies supporting agricultural production (e.g. runoff farming) are less significant. However, under certain conditions, e.g. in areas with semiarid or Mediterranean climates and intensive agriculture or livestock grazing, these RWH practices can prove beneficial especially in terms of sustainability and ecosystem conservation (VAN WESEMAEL ET AL. 1998, JIMÉNEZ ET AL. 2004, FROT ET AL. 2008). In urban areas, the increasing extent of sealed surfaces can lead to high amounts of runoff in short periods of time after the onset of precipitation. The retention of runoff by RRWH/ RWH systems, e.g. in associated storage tanks, can improve problems related to concentrated runoff such as e.g. sewer overflow (e.g. FARAHBAKHSH ET AL. 2009, STEFFEN ET AL. 2013). Finally, another advantage of RWH lies in its decentralized character which makes it suitable for remote areas where no connection to the public water supply system exists, in developing as well as developed countries (e.g. FEWKES 2006, DOMÈNECH ET AL. 2012, VAN DER STERREN ET AL. 2012).

2.5 Fields of previous and current research

Since the late 1960s to the 1970s, a steadily increasing number of papers on modern RWH have been published. Here, only a short overview of some main topics can be given, which is by no means exhaustive. During the 1980s and 90s, handbooks were issued with detailed instructions for the planning, construction, and successful operation of RWH systems, mainly micro-catchment schemes (e.g. FRASIER & MYERS 1983, CRITCHLEY & SIEGERT 1991). These publications provided the basic knowledge for the skillful inducement, collection and storage of runoff, and mainly focused on agricultural purposes (i.e. primarily runoff farming). Besides physical and technical considerations, socio-economic aspects were also discussed (FRASIER 1987, FULLER RENNER & FRASIER 1995). The work of PACEY & CULLIES (1986), a highly cited benchmark paper, is probably one of the most comprehensive in the field of RWH/WH and runoff farming with micro-catchments. In 1994, the FAO also issued a wide-ranging collection of research papers entitled "Water harvesting for improved agricultural production". More recent publications on WH and supplemental irrigation are the ones by OWEIS ET AL. (1999), OWEIS (2005) and OWEIS & HACHUM (2006). OWEIS ET AL. (2012) also compiled the recent encyclopedic benchmark paper "Water harvesting for agriculture in the dry areas". Besides research papers in established scientific media, numerous reports and other publications focusing on the application of WH in the context of (agricultural) engineering and development aid projects and studies have been issued by various organizations (e.g. NGOs, NPOs) (ANSCHÜTZ ET AL. 2003, BALKE 2009, BARRON 2009).

An extensive review and compilation of existing information and literature on RRWH has recently been prepared by DEBUSK & HUNT (2014). For this type of RWH, there are also several guidelines and manual-like publications which range from essential, short technical instructions for the private end-user and layman to broader and more comprehensive papers concerning the design and operation of more complex residential and commercial RRWH systems (TEXAS WATER DEVELOPMENT BOARD 2005, PORTER ET AL. 2008, CHIBI & VAN DUUREN 2010). A good overview that includes various technological, quality and economic aspects can be found in FEWKES (2006).

Furthermore, there is also plenty of specialized literature on particular RWH techniques like fog water harvesting (e.g. KLEMM ET AL. 2012), artificial groundwater recharge (e.g. WOLF ET AL. 2008, TAHERI TIZRO ET AL. 2009), or the combination of RRWH and artificial groundwater recharge (SHARMA 2009). Papers on RWH including (underground) cisterns are particularly relevant for the present study. Detailed information in this regard can be found e.g. in ALI ET AL. (2009) and AL-SALAYMEH ET AL. (2011) as well as in the proceedings of the international conference on rainwater catchment systems (IRCSA n.d.a, n.d.b).

More recently, i.e. since the late 1990s/early 2000s, the use of geoinformatics, i.e. the application of geographic information systems (GIS), remote sensing and related techniques, has been established in

various fields, including RWH planning and performance assessment. PRINZ ET AL. (1994) probably were the first to suggest the systematic use of GIS and remote sensing to identify suitable sites for RWH. This approach has later been adopted in several studies on small, local scales, as well as larger, regional scales (e.g. DE WINNAAR ET AL. 2007, MBILINYI ET AL. 2007, MWENGE KAHINDA ET AL. 2008, MWENGE KAHINDA ET AL. 2009, MAHMOUD ET AL. 2015). The (spatial) decision support systems (SDSS/DSS) employed in these studies were GIS based and integrated all data, of which a part was acquired through remote sensing, for best possible results (e.g. section of RWH sites, suitability maps). Moreover, geographic information systems are often applied to assess the water harvesting potential of an area (SEKAR & RANDHIR 2007, NAPOLI ET AL. 2014, YOUSIF & BUBENZER 2015). The use of GIS allows the spatially explicit estimation of runoff amounts and RWH potentials that reflect spatial heterogeneities in local environmental conditions and input data (e.g. slope, soil characteristics, land use, etc.). In addition, the SWAT model, available as an extension for several GIS solutions, and various other more or less complex models, are used for the spatially explicit assessment of runoff and RWH potentials, i.e. the amount of water that can be collected or becomes available for plant growth in a given area (ANDERSSON ET AL. 2009, OUESSAR ET AL. 2009, SHADEED & LANGE 2010). Runoff and RWH potentials are also estimated using empiric approaches that are based on field data collected from test sites (runoff plots) or lumped models like the water balance model (FROT ET AL. 2008, ALI ET AL. 2010). Furthermore, the benefits and impacts of RWH practices have been studied with respect to different aspects such as changes in runoff and erosion (OUESSAR ET AL. 2004, AL-SEEKH & MOHAMMAD 2009), groundwater replenishment (STAHN & TOMINI 2009), regional development and environmental conservation (LI ET AL. 2002), and water yield and socio-economic effects (BALDERAMA 2014).

Finally, there are many studies which investigated specific details of RWH, for example the necessary environmental preconditions for the successful application of RWH for agricultural purposes (BULCOCK & JEWITT 2013). In the aforementioned study, recommendations from literature and observed practices were compared to distinguish between sufficient, suitable, and optimal conditions for RWH. LI ET AL. (2004) examined the possibilities of increasing runoff through different types of surface treatment of catchment areas. FLESKENS ET AL. (2005) and SCHIETTECATTE ET AL. (2005) evaluated the performance of a specific RWH technique, the jess(ou)r in Tunisia, in terms of the availability of additional amounts of water, changes in infiltration properties, and effects on olive tree growth and yields. For RRWH systems, the variability of rainfall and resulting consequences for the planning of storage capacities were studied by SU ET AL. (2009) and YOUN ET AL. (2012). The latter study also took into consideration the effects of climate change. MATOS ET AL. (2013) compared storage tank sizes to different demand scenarios. The economic aspects of shared RRWH systems (community systems) were analyzed by GURUNG & SHARMA (2014), whereas DOMÈNECH & SAURÍ (2011) investigated socio-economic aspects of smaller, individually owned RRWH systems. WARD ET AL. (2010, 2012) assessed the performance of RRWH systems with continuous modeling for an improved, more accurate estimation of suitable dimensions of storage tanks. They also included economic and demand concerns in their studies. The

optimal design of RRWH systems for residential houses was investigated by BOCANEGRA-MARTÍNEZ ET AL. (2014), while FARRENY ET AL. (2011b) examined the suitability of different roof types for RRWH, with regard to water quantity and quality aspects. Many studies address the question of the quality of water from RWH systems as a side issue, while it represents the central topic of the papers of e.g. GOULD (1999), MEERA & MANSOOR AHAMMED (2006), SAZAKLI ET AL. (2007), and DE KWAADSTENIET ET AL. (2013). The aforementioned studies exemplify the broad variety of research in the field of RWH.

2.6 Research on rainwater harvesting in Jordan

RWH in Jordan is discussed as a major topic or side issue in many research papers in several disciplines. The interest in RWH is largely rooted in Jordan's natural water scarcity which mainly is a result of the country's location within a region of a semiarid to arid climate. Additionally, Jordan is a country of the upper middle income class for which agricultural production plays an important role (HAYEK 2009, MOE & UNDP 2009, THE WORLD BANK GROUP 2015). Since sufficient rainfall occurs in only 5% of the land, agriculture often requires (supplemental) irrigation which accounts for around 60% of the kingdom's annual water demand (MWI 2016a). Aspects concerning the application of modern RWH schemes, for agricultural and other purposes and in the context of sustainable development, therefore constitute important fields of ongoing research. Moreover, due to the long settlement history that probably goes back to the Paleolithic period, Jordan has a long tradition of water management and RWH and a rich heritage of associated structures and facilities. This setting provides ideal conditions for investigations from historical or archaeological perspectives.

Numerous places in Jordan exhibit remains and traces of old water management infrastructure elements like dikes, channels, reservoirs, cisterns, small dams and stone walls. Many of these structures that were used for the collection, (re-) direction and storage of runoff have been documented in archaeological studies. Since perennial rivers and springs were absent in vast areas of Jordan during all its historical periods, most of the major and minor ancient settlements had to rely on some kind of RWH to cover their water demand. Therefore, prominent archaeological sites like the ones of Petra and Gadara (Umm Qais), as well as smaller sites in more remote areas, made use of a multitude of basic to sophisticated water management structures and RWH facilities (e.g. HELMS 1981, BETTS & HELMS 1989, LANCASTER & LANCASTER 1995b, OLESON 1995, ORTLOFF 2005, FUJII 2007, KEILHOLZ 2007). Although questions concerning water management and supply are often included only as side issues in archaeological surveys, there are also a considerable number of studies that concentrate on the subject and the associated infrastructure (e.g. BIENERT & HÄSER 2004, also see Table 2, part 1). A summary of the topic and the

main findings can be found in BIENERT (2000), OLESON (2001), ABDELKHALEQ & ALHAJ AHMED (2007), and AL-AZEEZ SHQIARAT (2008). Additionally, FARDOUS ET AL. (2004) and ABU SHMAIS (2007) compiled an overview of known ancient RWH structures in Jordan, including their location, type, estimated storage capacity and period of construction or use. The age of individual structures is typically inferred from other archaeological traces that are found at the same site or in their immediate surroundings. Water facilities with a rather permanent character, such as dams, reservoirs and cisterns, often exhibit specific construction details that enable their assignment to particular periods of history. In contrast, bunds, dikes, ridges, check dams and similar elements are rather ephemeral structures which usually lack specific characteristics that could be linked to certain eras. The absolute determination of the age of water infrastructure elements is possible by means of 14C dating of some of the construction materials such as mortar or plaster (e.g. AL-BASHAIREH & HODGINS 2011, LICHTENBERGER ET AL. 2015). However, later phases of repair, e.g. renovation of the plaster lining used for waterproofing, can complicate the identification of likely construction ages. In some cases, locally accumulated sediments and OSL dating could offer additional clues regarding the last time of use or the possible (minimum) age of abandoned water facilities (runoff farming systems, cisterns) (BECKERS ET AL. 2013, KRAUSHAAR ET AL. 2015). When considering the time of their construction, for most water management facilities, the attribution to a specific period of history is either impossible or remains rather tentative. The Jordanian database of archaeological sites (MEGA-Jordan) (THE GCI ET AL. 2010) includes water infrastructure elements, especially when they are associated with other archaeological traces found at the same site. However, nearly all of the water related structures are listed as being of unknown age.

The RWH structures at Jawa are believed to date from the Chalcolithic period (4th millennium B.C.) and to be the oldest in Jordan (MILLER 1980, HELMS 1981, BIENERT 2000). Preliminary findings of some recent studies suggest that there might be even older RWH structures, e.g. in the vicinity of the Jafr basin (FUJII 2007) or near Petra (GEBEL 2004). Remains of ancient water management facilities that were associated with more recent periods of history, especially the Nabataean, the Roman and the Byzantine eras, were identified in many places throughout Jordan. These structures have been documented and described in a number of studies (see Table 2, part 1 for examples). Besides site-specific investigations, there are also overarching studies on water management strategies during particular eras of history (e.g. MILLER 1980, OLESON 1995, OLESON 2007, AL-AZEEZ SHQIARAT 2008) as well as studies on specific RWH techniques, schemes and structures like cisterns (PACE 1996, WÅHLIN 1997), qanats (LIGHTFOOT 1997) and mahafir (AGNEW ET AL. 1995). In some papers, the modern reuse potential of the ancient water infrastructures and possible associated benefits were discussed (e.g. LABIANCA 1995, FARDOUS ET AL. 2004, SALAMEH 2004).

A short synopsis of traditional RWH practices that have been or are still used in Jordan can be found in UNESCO & ACSAD (1986). In the named study, based on findings from neighboring countries, also further RWH techniques that could be adopted in Jordan are pointed out. Overviews of modern RWH

strategies which are currently being employed or have been tested in Jordan are provided by AL-LABADI (1994), SHATANAWI (1994), ALKHADDAR ET AL. (2003), and FARDOUS ET AL. (2004). Studies on modern RWH that refer to specific areas or (test) sites and examine particular techniques or aspects are presented in Table 2 (part 2) and Figure 1. Additionally, there are several other studies which examine modern RWH on a broader, region- or nationwide scale. Moreover, empirical research on RWH is frequently carried out within the scope of Master's theses and remains unpublished (e.g. YOUSSEF 1998, ALKHATEEB 2007). Apart from research purposes, RWH schemes are often implemented in the framework of development projects that are commonly conducted and/or funded by development aid agencies and other international organizations in cooperation with Jordanian government agencies (e.g. MOP & JICA 1990, THE HASHEMITE KINGDOM OF JORDAN 2001). Experiences and outcomes of these projects are mostly only documented in unpublished reports for the internal use of involved stakeholders and donors. While the aforementioned academic studies and gray literature are not included in Table 2, they are considered in the present study where appropriate.

Research on modern RWH in Jordan generally covers a similar range of topics and aspects like that described earlier, either referring to other parts of the world or to no specific region (see section 2.5). Individual RWH techniques that have been investigated in Jordan encompass the collection of runoff with earth ponds (ALKHADDAR 2003) and sand ditches (ABU-ZREIG ET AL. 2000, ABU-ZREIG & TAMIMI 2011) as well as fog harvesting (TARAWNEH 2004). The recent, nationwide study of ASSAYED ET AL. (2013) concentrated on the optimal use of cisterns and associated benefits. Further topics that have been investigated in RWH studies (also see Table 2) comprise the estimation of runoff and the evaluation of negarims, a specific form of micro-catchment RWH schemes (AL ALI 2012), the improvement of micro-catchment RWH techniques with regard to agricultural purposes (OWEIS & TAIMEH 1996, GAMMOH 2013), surface crust formation in soils and its influence on (harvestable) runoff (ABU-AWWAD & SHATANAWI 1997) as well as water quality aspects (RADAIDEH ET AL. 2009). Modern geoinformatics have been applied e.g. to identify suitable sites for RWH and to assess the RWH potential of a given area in a spatially explicit manner (AL-ADAMAT ET AL. 2010, HADADIN ET AL. 2012, ZIADAT ET AL. 2012). There is also a sustained interest in RRWH which seems to be a promising option for Jordan. The approach and its potential have been studied by PREUL (1994), ABDULLA & AL-SHAREEF (2009), and ABU-ZREIG & HAZAYMEH (2012). Finally, the role of RWH in the safe, sustainable long-term management of Jordan's water resources and the safeguarding of an adequate water supply in the future has been evaluated by JABER & MOHSEN (2001).

Table 2: Previous studies on ancient water management and rainwater harvesting in Jordan. Corresponding sites and areas of previous research are displayed in Figure 1.

No.	Study	Subject	Study area (in Jordan)
— Part 1 – sites where ancient water management was studied			
1	KEILHOLZ 2007, 2014	Ancient water management, cisterns, Hellenistic period	Gadara/ Umm Qais
1-2	DÖRING 2008	Qanat Firaun	Gadara - Abila/ Quweilbeh
3-4	AL-ANSARI ET AL. 2013	Ancient RWH schemes	Umm El-Jimal, Jawa
4	HELMS 1981	Ancient water management in a desert environment	Jawa
5	GHRAYYIB & RONZA 2007	Water distribution and storage system (Umayyad period)	Qasr al-Hallabat
6	ARCE 2004	Ummayad hydraulic system	Amman
7	BASTERT & LAMPRICHS 2004	Ancient techniques of water usage and storage	Wadi Qattar
8	BETTS & HELMS 1989	Water harvesting and storage system	Ibn El-Ghazzi
9-10	AGNEW ET AL. 1995	Mahafir: function of old RWH system	Maharouta, Anka (Badia)
11	PRAG 2007	Water strategies and old water installations	Iktanu Region (southern ghawrs)
12	LABIANCA 1995	On-site RWH, ancient RWH strategies and potential of modern reuse/ adaptation	Tall Hisban
13	BIKAI 2004	Water system	Madaba
14	DAVIAU & FOLEY 2007	Nabataean water management systems	Wadi ath-Thamad catchment
15-31	PACE 1996	Cisterns, diachronic description	Karak Plateau (17 sites)
27	MATTINGLY ET AL. 1998	Ancient water catchment system	Nakhl (Karak Plateau)
32	DE VRIES 1987	Water system	el-Lejjun (Karak Plateau)
33	CROOK 2009	Old irrigation system	Wadi Faynan
34-35	FUJII 2007, 2010	Neolithic runoff collection and barrage systems	Wadi Abu Tulayha and Wadi Ruweishid ash-Sharqi (Jafr area)
36	GEBEL 2004	Neolithic water control	Ba'ja (Shara mountains, Petra area)
37-38	BECKERS ET AL. 2013	OSL and 14C dating of runoff terraces	Seil Wadi Mousa/ Umm Ratam and Wadi el-Ghurab (Petra area)
39	ORTLOFF 2005	Water supply and distribution system, 300 B.C.-300 A.D.	Petra
	JOUKOWSKY & CLOKE 2007	Water infrastructure of the Great Temple	
	BELLWALD 2008	Hydraulic infrastructure	
	AL-BASHAIREH & HODGINS 2011	14C dating of ancient water infrastructure	
	BECKERS 2012	Geoarchaeological perspective on RWH	
40	LAVENTO ET AL. 2004	Ancient water management system	Jabal Haroun (Petra area)
41	SCHMID 2008	Ancient water supply	Wadi Farasa (Petra area)
42	AKASHEH 2004	Nabataean and modern watershed management	Siq, Wadi Musa (Petra area)

Table 2 continued

No.	Study	Subject	Study area (in Jordan)
Part 1 – sites where ancient water management was studied		
43	AL-AZEEZ SHQIARAT ET AL. 2010	Water management, cisterns	Udhruh/ Udhruh region
	ABUDANH 2007	Old water supply systems (Nabataean to modern), e.g. reservoirs, cisterns, qanats	
44	LINDNER 2005	Ancient water supply and management	Sabra (Petra area)
45	EADIE & OLESON 1986	Nabataean and Roman water supply system	Humayma
	OLESON 1991	Nabataean and Roman water supply, aqueducts, cisterns	Auara (Humayma)
	OLESON 2007	Nabataean water supply systems	Hawra (Humayma)
46	HEEMEIER ET AL. 2008	Water infrastructure of a prehistoric settlement	Tall Hujayrat al-Ghuzlan
Part 2 – sites (a-u) and areas (I-VIII) where modern RWH was studied		
a-d; I-IV	RADAIDEH ET AL. 2009	Quality of cistern water	Governorates Irbid, Ajloun, Jarash, Zarqa (multiple sites each)
e	ABU-ZREIG ET AL. 2000, ABU-ZREIG & TAMIMI 2011	RWH with sand ditches	Ramtha (JUST Campus)
f	AL-ALI 2012	Micro-catchment WH, Negarim, soil water conservation, runoff estimation	Al-Khanasri research station (NE Jordan)
f, t	YOUSSEF 1998	Evaluation of different micro-catchment WH techniques, runoff calculation and measurements	Al-Khanasri Research Station (NE Jordan), Mhai (Karak)
g-l	ALAYYASH ET AL. 2012	Runoff estimation for suggested RWH sites	Watersheds Ghadeer al-Naqa, al-Manareh (al-Ghuliasi), Alaasra, Wadi Ali (Al-Abed), and al-Subhi (Badia)
m	TAQIEDDIN ET AL. 1995	Estimation of runoff and RWH potential	Safawi (Badia)
n	ABU-AWWAD & SHATANAWI 1997	Influence of surface crust formation in soils on WH	Muwaqqar watershed (Univ. of Jordan research station)
	GAMMOH 2013	Improved micro-catchment WH, enhanced technique, evaluation; agricultural applications	
	OWEIS & TAIMEH 1996	Evaluation of a small basin WH system, negarim, micro-catchment WH	
o	ZIADAT ET AL. 2006, ZIADAT ET AL. 2012	WH suitability assessment of land using GIS, participatory approach	Muhareb/ Mharib watershed (Amman governorate)
p-u	TARAWNEH 2004	Fog water harvesting, evaluation of potential	Taibih, Dhabab, Moab, Mahy, Abiad (Mazar-Karak area)
V	AL-ADAMAT ET AL. 2012	RHW siting with GIS	Badia
VI	HADADIN ET AL. 2012	WH potential, spatial hydrological analysis using GIS	North-eastern desert (Badia)
VII	ALKHADDAR 2003	WH with earth ponds	Northern Badia
VIII	AL-ADAMAT 2008, AL-ADAMAT ET AL. 2010	WH pond siting, decision support system using GIS	Azraq basin (NE Jordan, Badia)
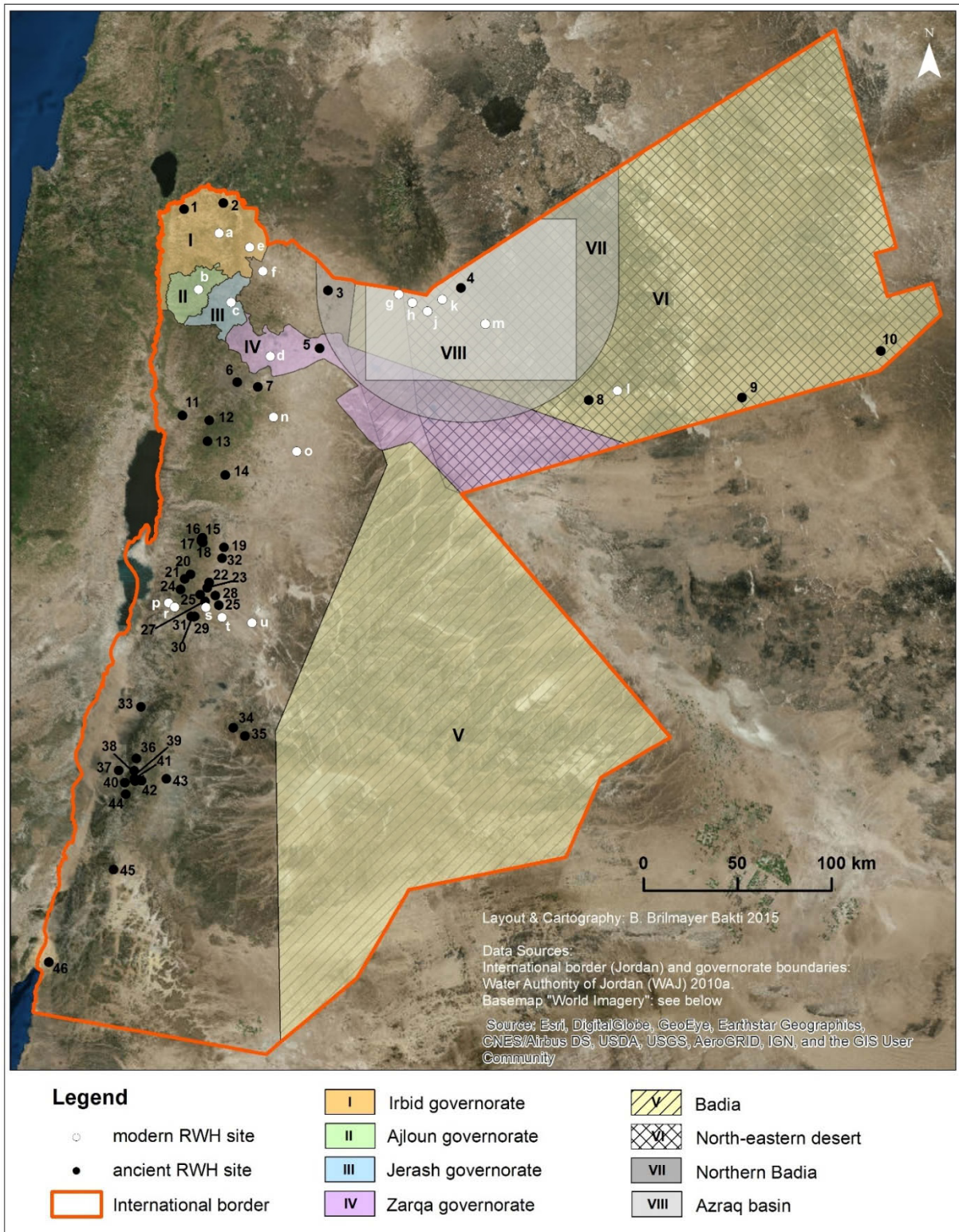
Fig. 1: Sites and areas of previous studies on ancient water management or (modern) rainwater harvesting (RWH) in Jordan. For explanation of the numbers and associated studies see Table 2.

2.7 Research gaps, open questions, and objectives of the present study

The research summary given in the previous chapters has already shown that the link between ancient water management and modern RWH strategies is poorly established and barely explored. Typically, studies either focus on ancient water management, usually from an archaeological point of view, or they concentrate on modern RWH approaches. The connection between both fields is mostly limited to remarks on the reuse potential of some of the ancient water management techniques and the long traditions of currently applied RWH strategies. Occasionally, the systematic rehabilitation and expansion old RWH facilities, including cisterns, have been suggested (e.g. AGNEW ET AL. 1995, LABIANCA 1995). However, no major research has been conducted in this regard. At the same time, new RWH schemes are implemented within the scope of regional development programs that typically are not connected in any way to recent or ongoing research.

On the other hand, progress in (geo-) information technology and the increasing availability of novel remote sensing products and methods offer new possibilities for RWH research as well as applied projects. Remote sensing techniques and a growing automation of analytical processes considerably facilitate the access to quantitative aspects. Larger datasets can be analyzed efficiently, e.g. to discover (spatial) patterns and trace changes through data comparison. Up to now, geoinformatics have been employed in RWH studies primarily for the estimation of runoff and in the form of spatial decision support systems. Yet, the available data and methods may offer great potential for a variety of other purposes and research questions too.

As a first step, a survey of the existing RWH infrastructure needs to be conducted. For this purpose, a remote sensing-based approach is recommended, since the interpretation of satellite images with a very high spatial resolution facilitates the collection of high amounts of detailed information within a short time. Thus, a comprehensive database can be established that includes ancient as well as modern RWH structures. The database can then be used for further analyses and to address various research questions, such as e.g. comparisons of ancient and modern RWH practices. It can also be employed to identify deficits in current RWH strategies and thus, improve the (central) planning of new RWH projects. Consequently, the still weak connection between research, on the one hand, and development projects on the other, can be substantiated.

With regard to the promising method of RRWH and the estimation of collectable runoff from rooftops, in addition to precipitation information, accurate and reliable building data are needed. Since the latter typically are not readily available, proxies, such as other census data, have often been used in previous studies to estimate rooftop areas (ABDULLA & AL-SHAREEF 2009, ABU-ZREIG & HAZAYMEH 2012). However, this can lead to inaccurate estimations of the RRWH potential, especially on a local scale (e.g. individual villages or towns). LANGE ET AL. 2012 manually identified rooftops in images. Yet, due to

the time-consuming nature of this approach it can usually only be applied to small areas. In order to improve the assessment of RRWH potentials on every scale, straightforward, efficient and yet accurate procedures need to be developed that allow the extraction of building data from readily available remote sensing products like aerial or satellite images. Possibilities of automation of image analysis processes should be examined in this regard.

3 Study area: the Karak Plateau, Jordan

The study area is located in central West Jordan, ca. 65 km south of the capital Amman and 20 km east of the Dead Sea. It extends from 31°15' to 31°26' north and 35°44' to 35°50' east, thus comprising around 150 km^2 of land in the northern part of the Karak Governorate. The governorate, which corresponds to ancient and biblical Moab, is named after the regional capital Karak that is situated approximately in the center of the plateau and about 15 km south of the studied territory (see Fig. 2). The King's Highway, which leads from the south to the north of Jordan, crosses the Karak Plateau longitudinally and runs parallel to the Dead Sea Highway in the west and the Desert Highway in the east. It divides the highland area into a western and an eastern part of which the latter forms the main focus of the present study.

3.1 Relief, geomorphology, and hydrology

The territory of the Karak Governorate largely consists of a plateau with altitudes of 700 to over 1,200 m above sea level (see Fig. 2). As the tableland slightly dips northeastwards, the highest elevations are found in its southwestern part. Steep slopes lead down to the Dead Sea (over 400 m below sea level) in the west and the wadis al Mujib and al Hasa, which form the northern and the southern border of the plateau respectively (see Fig. 2). The eastern fringes of the highland are characterized by a smooth transition into the lower areas of the eastern desert of Jordan (Badia). Since there is no natural boundary, the Desert Highway is usually perceived as the eastern most limit of the plateau. The study area itself takes up the northeastern quarter of the highland, roughly extending between the King's Highway and a southward trending branch of the Wadi al Mujib (Wadi Nukhayla). The highest parts, with slightly over 1,000 m above sea level, belong to the outskirts of Mount Shihan (see Fig. 2). Otherwise, softly undulating terrain with elevations between 665 to 1,000 m above sea level constitutes the relief. Only in its south-eastern corner does the land become more rugged in the context of the incision of the Wadi Nukhayla and its numerous small tributaries.

All surface runoff in the study area is ultimately directed westwards towards the Dead Sea, although runoff on the plateau mainly flows northwards and northeastwards towards the Wadi al Mujib and its tributaries. Only a small part in the southwestern corner of the study area, west of ar-Rabba, belongs to the catchment of the Wadi Ibn Hammad which drains westwards and forms part of the Dead Sea surface water basin. The major part of the study area, around 97%, belong to the drainage basin of the Wadi al

Mujib which is the fifth largest surface water basin of Jordan (WAJ 2010c). In addition to the rivers Jordan, Yarmouk, and Zarqa, the Mujib is also one of the major perennial streams of Jordan. North of the study area, it has formed a deep canyon, across which a dam has recently been built at the confluence of its eastward and southward trending branches, the Wadi Su'eida and the Wadi Nukhayla (for location of wadis see section 5.4, Fig. 38) (EL-NAQA 1993, WAITZBAUER & PETUTSCHNIG 2004c). While the valley of the Wadi Nukhayla represents the eastern boundary of the study area, its tributary, the Wadi Balua, cuts into the plateau area from northeast to southwest. Almost half of the territory under study belong to the catchment of the Wadi Balua (see 5.4, Fig. 38 and Table 14). A detailed description of the hydrological situation in the study area is given in chapter 5.4.
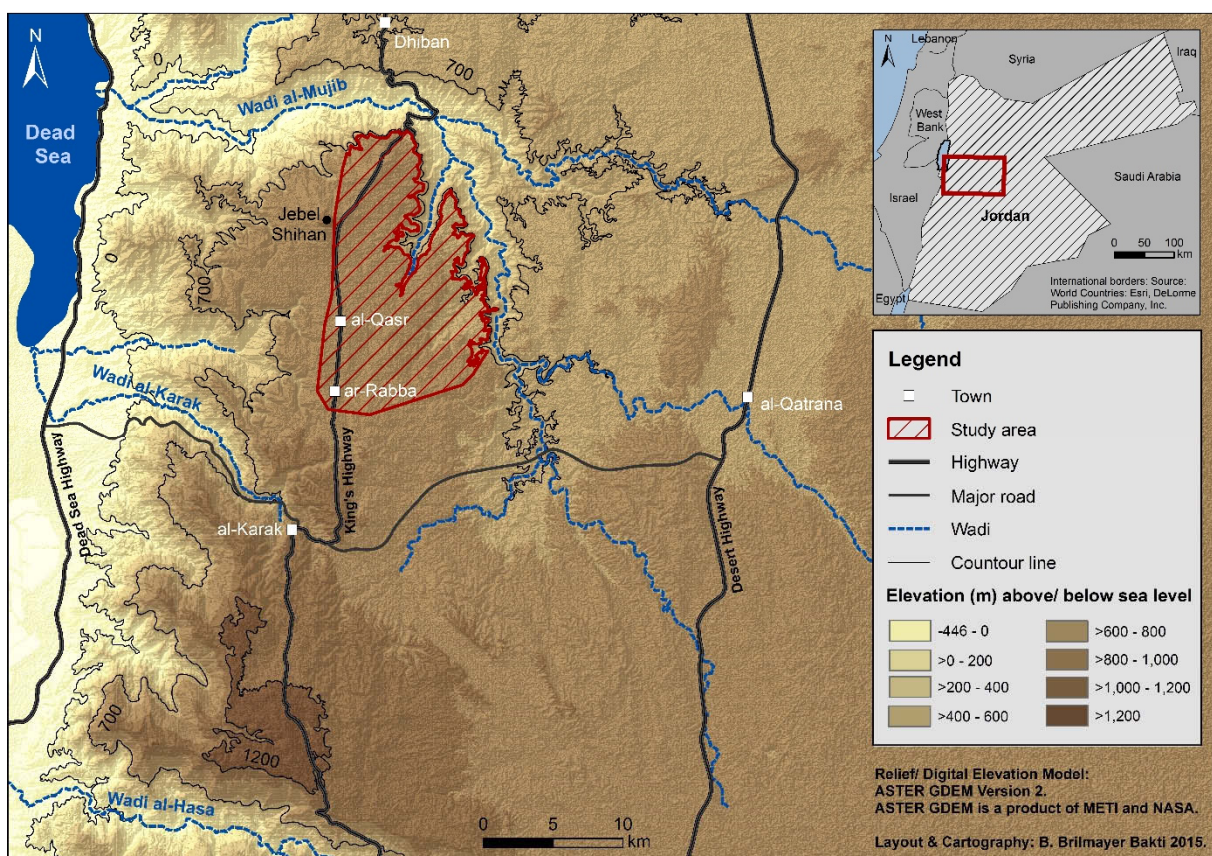
Figure 2: Location and extent of the study area. The main map shows the Karak Plateau while the regional setting of the area is displayed in the inset map (the red rectangle indicates the extent of the main map).

Drainage lines, i.e. perennial streams and intermittent wadis, commonly follow zones of structural weakness such as faults in the underground (DE JAEGER & DE DAPPER 2002). Hence, their course is mostly controlled tectonically. The deep incision of the wadis results mainly from the high relief energy, i.e. the large differences in elevation between the plateau area and the base level of the Dead Sea basin over short distances. This steep regional topographical gradient, together with climatic characteristics such as concentrated precipitation events (see chapter 3.3), provide a high erosion potential which leads locally to gully formation in the study area (cf. DE JAEGER & DE DAPPER 2002). The mean annual flow of the Mujib and its tributaries is composed of a base flow constituting 50-90% of the total annual discharge

and additional large floods (SALAMEH 1997, GREENBAUM ET AL. 2006). High discharge rates in winter show a strong connection to the temporal precipitation pattern (winter rains) in the area, while the annual base flow is sustained primarily by springs which occur at the fringes of the table land and at the slopes of valleys. Within the flat terrain of the plateau itself, springs and other perennial sources of freshwater are absent.

3.2 Geology

Detailed knowledge of the geological situation is essential for the present study as subterranean conditions immediately influence the applicability and functioning of some RWH structures, primarily cisterns, which are excavated in the underground. The presence of different rock types also affects the availability of building materials and thus, the construction of other, above-ground RWH structures (check dams, bunds, shallow walls, etc.). Hydrogeological characteristics determine the accessibility and availability of groundwater as an alternative source of water and the applicability of some RWH schemes that involve the intentional recharge of groundwater stored in aquifers, for example.

In this chapter, the Cenozoic environmental history of the study area is initially outlined. Changing environmental conditions and tectonic movements shaped the relief and thus explain the evolution of the landscape described in the previous section. At the same time, the aforementioned changes led to the deposition and erosion of different sediments and hence, formed the present composition of lithostratigraphic units in the underground. The resulting geological formations and their spatial occurrence in the study area are described in section 3.2.2. Subsequently, the stratigraphy, lithology, and hydrological characteristics of the different layers are presented in section 3.2.3 and 3.2.4.

3.2.1 Paleogeography and evolution of the present environment

The Karak Plateau forms the eastern elevated shoulder of the Jordan Valley/Dead Sea graben which is associated with the African rift valley system. Subsidence within the forming rift valley, i.e. in the area of the south-north trending Dead Sea transform, and uplift of the land masses on its western and eastern side, i.e. the Palestine block and the Transjordan block respectively, probably started in the late Oligocene to early Miocene (BENDER 1975, GARFUNKEL & BEN-AVRAHAM 1996, BANDEL & SHINAQ 2003). However, taphrogenetic movements took place mainly during the Pliocene-Pleistocene transition and in Pleistocene times (BENDER 1968). This phase of intense faulting and tectonic movements probably ended during the Middle Pleistocene and was associated with a period of basalt volcanism (BENDER

1968, WAITZBAUER & PETUTSCHNIG 2004b). While some of the basaltic rocks indeed seem to be of Pleistocene age (see BENDER 1975 for details), some other, e.g. most of the basalts of Mount Shihan in the study area, are older, originating from late Miocene to Pliocene time (DE JAEGER & DE DAPPER 2002, IBRAHIM ET AL. 2014).

Parallel to the uplift of the eastern graben shoulder, the Transjordan block, incision of antecedent wadis such as the Wadi al Mujib and its tributaries took place (DE JAEGER & DE DAPPER 2002, GREENBAUM ET AL. 2006). Although the structure of the drainage system, i.e. the course of the wadis such as the Wadi Balua for example, is principally controlled tectonically, climatic alterations during the Pleistocene, including several glacials and interglacials, substantially expedited rock weathering and fluvial incision. The lowering of the Dead Sea level during the Holocene further added to the aforementioned factors (SALAMEH 1997). In summary, the development of the regional drainage system can be explained as follows: "While the inherited tectonic structures in the area are the base for the drainage pattern in plan-view, it is the combined effect of tectonic activity and changing climatic conditions that adjusted the slope- and river profiles in elevation-view" (DE JAEGER & DE DAPPER 2002, p. 92).

3.2.2 Geological formations and their spatial distribution

Vast areas of the softly undulating relief of the tableland are covered by deep soils (see chapter 3.4) which overlay basalt formations in the northern part, around the volcano Mount Shihan (DE JAEGER & DE DAPPER 2002, IBRAHIM ET AL. 2014), and the marly limestone, coquina, and phosphate layers of the Al Hisa formation in the rest of the area (cf. Fig. 3-5 and Table 3). The volcanic rocks of the Shihan Basaltic Group outcrop only at a few and comparably small sites on the tableland, e.g. at the volcanic center of Mount Shihan and east of al-Qasr, as well as at the fringes of the plateau, particularly around the Wadi Balua. While the basalts of the northern half are of late Tertiary (Miocene to Pliocene) age, those of the Judaiyida formation in the southern part of the study area are younger, dating from the Pleistocene epoch (DE JAEGER & DE DAPPER 2002, IBRAHIM ET AL. 2014, also see Table 3).

Around Mount Shihan (see Fig. 2 for location), especially northwest to northeast of it, and around the villages of al-'Aliya in the north and ar-Rabba in the south, as well as at a few other sites, calcrete formations (caliche) have formed on older sediments and volcanic rocks (see Fig. 3, for details on calcrete formations see BENDER 1968 and 1975). In the southeastern section of the study area, where the relief gradually becomes more rugged towards the east, the different coquina, marly limestone, and phosphate layers of the Al Hisa formation surface. Younger geological formations such as the Muwaqqar Chalk Marl of the Late Cretaceous to Paleocene epochs, the Sanina and Judaiyida Basalts of the Miocene to Pliocene and Pleistocene epochs, and Pleistocene fluviatile and lacustrine gravels can only be found east of the areas of the Al Hisa Phosphorite formation. There, the Wadi Ghuwayta (see section

5.4, Fig. 38) has incised into the plateau in a northeast to southwest trending direction that is prescribed by a large fault system. The Wadi Ghuwayta and its tributaries, together with other minor wadis draining into the Wadi Nukhayla (cf. 5.4, Fig. 38), and the intricate system of faults, have led to the formation of a rugged and vividly dissected terrain in this part of the study area. This in turn induces the absence of deep soils and the exposure of the underlying geological formations. Older strata than those of the Al Hisa Phosphorite and its members are only encountered at a few sites of limited extent between the aforementioned Wadi Ghuwayta and Wadi Balua. At these sites, the limestone, chert, and phosphate layers of the Amman Silicified Limestone formation surface.
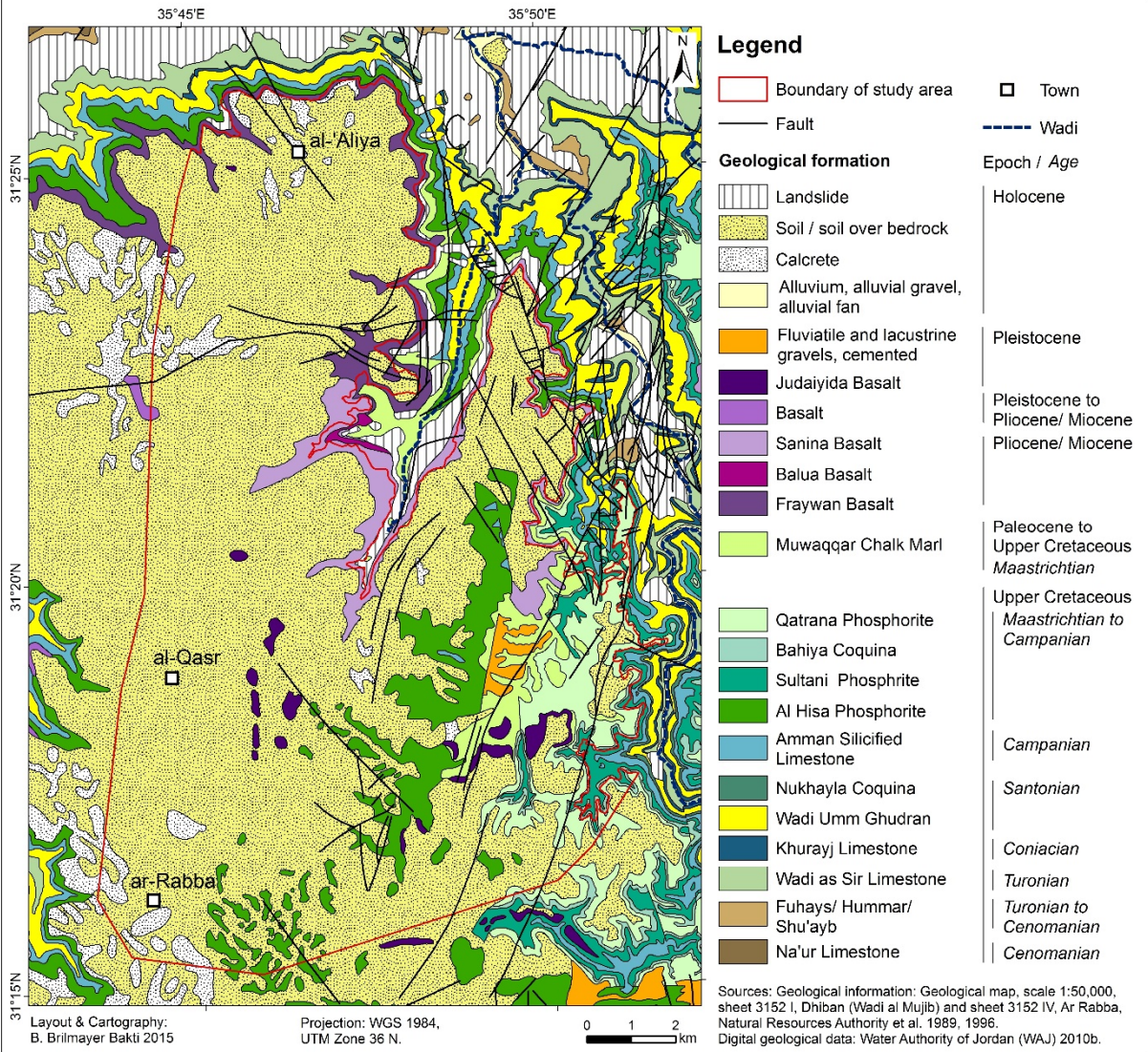
Fig. 3: Geological map of the study area and its surroundings. For stratigraphic and lithological information see Table 3.

3.2.3 Stratigraphy and lithology

North and east of the study area itself, the Wadi al Mujib and its tributaries such as the Wadi Nukhayla and the Wadi Balua, have cut deep into the different rock formations that constitute the plateau. Thus, the thickness and sequence of the geological strata are revealed (see Fig. 4). However, large parts of the wadi slopes are affected by mass movements and landslide masses covering vast areas of the middle and lower parts of wadi slopes, disguising in-situ geological formations. Where this is not the case, youngest to oldest rocks are exposed from upper slopes towards the wadi beds, i.e. ages of strata increase with decreasing elevation. A cross section, from north to south across the canyon of the Wadi al Mujib, illustrates the stratigraphy (see Fig. 4). The Kurnub Sandstone of the Lower to Upper Cretaceous epoch represents the base of the approximately 700 m thick sediments which were deposited later. It is overlain by the limestone and marl layers of the Ajloun group which consists of, from bottom to top, the Na'ur Limestone, the Fuhays, the Hummar, and the Shu'ayb formation, the Wadi as Sir Limestone, and the Khurayj Limestone (see Table 3). During later phases of the Upper Cretaceous, the layers of the Belqa group were deposited. Besides limestone and marl, these strata also comprise chalk, coquinas, and phosphate beds. The oldest formations of this group are the Wadi Umm Ghudran, which encompasses the Mujib Chalk, the Tafila member, the Nukhayla Coquina, and the Dhiban Chalk, as well as the Amman Silicified Limestone formation that includes the Mutarammil Coquina (see Table 3). The following Al Hisa Phosphorite unit and its members, namely the Sultani Phosphorite, the Siwaqa Coquina, the Bahiya Coquina, and the Qatrana Phosphorite, constitute the youngest and therefore topmost strata of sediments in vast areas of the Karak Plateau. The younger Muwaqqar Chalk Marl formation occurs only in the
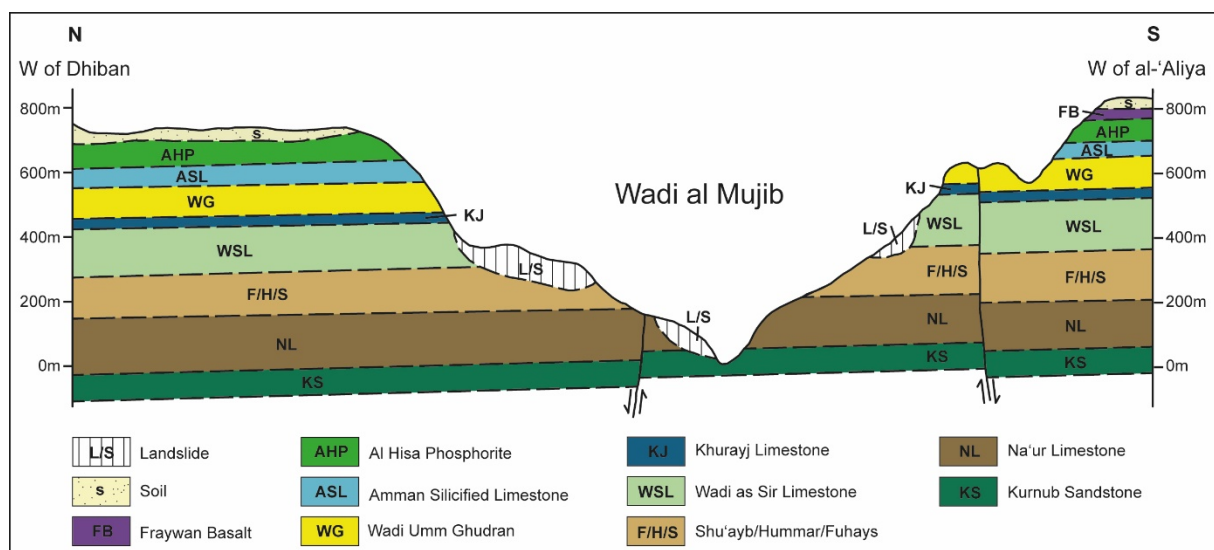
Fig. 4: Geological cross section of Wadi al Mujib, from west of Dhiban (31°29'56''N, 35°45'08''E) in the north to west of al-'Aliya (31°25'21''N, 35°45'21''E) on the Karak Plateau in the south. For locations of villages see Fig. 2 (Dhiban) and Fig. 3 (al-'Aliya). For stratigraphic and lithological information see Table 3. Modified from NATURAL RESOURCES AUTHORITY ET AL. 1996.

eastern section of the tableland, in the catchment of the Wadi Ghuwayta. There, it was probably protected from erosion due to the slightly lower altitude and it was also not covered by later formations. Hence, in the described areas, the Muwaqqar Chalk Marl overlies the Al Hisa Phosphorite and forms the uppermost part of the Belqa group. Finally, where occurring, the local basalt flows of the Miocene to Pliocene and Pleistocene epochs buried the sediments of the Upper Cretaceous. Fluviatile gravels that were often cemented later were deposited in the southeastern part of the study area during the Pleistocene (see Fig. 3). The typically thick soil layers that cover vast areas of the highland formed during the Holocene. The sediments were deposited conformably and exhibit a horizontal stratification. In combination with the homogenous uplift of the tableland, this led to the relatively flat, softly undulating relief of the plateau. Substantial differences in elevation between individual blocks and corresponding strata are absent (see Fig. 4).

For each geological unit, the essential lithological information is presented in Table 3. The lithology and stratigraphy have been described in detail, e.g. by QUENNEL (1951), BURDON (1959), BENDER (1968 and 1975), POWELL (1989), and POWELL & MOH'D (2011). Differences between studies mainly concern the designation and delineation of individual geological units. The terminology that is currently used to describe the situation in Jordan is employed in this chapter and has been introduced in parts by QUENNEL (1951) and several later scholars (e.g. POWELL 1989). The different units were named after type localities. Across the region, various designations are applied to strata of the same age (cf. e.g. BANDEL & SHINAQ 2003, BANDEL & SALAMEH 2013). In contrast to the information given in Table 3, BENDER (1968 and 1975) groups the strata into different units and relates them to QUENNEL'S (1951) series.

Lithological compositions of the sediments reflect varying conditions and different depositional environments during the respective times of their formation. These changes were induced by several marine ingressions and regressions of the Tethys Ocean during the Paleozoic, Mesozoic, and early Cenozoic eras. From the north, the west, and the northwest, the Tethys Ocean expanded into the Jordanian hinterland up to different limits. While the sea during the Triassic and the Jurassic only reached as far as the present-day Jordan Valley/Wadi Arava, it extended further to the east, beyond the location of the modern town of Karak, during the Albian age of the Lower Cretaceous (BENDER 1968). In the Upper Cretaceous, most of Jordan was covered by the ocean. Apart from smaller oscillations, the transgression lasted until the Oligocene epoch and the beginning of the tectonic movements associated with the formation of the Dead Sea rift valley (BENDER 1975).

The long period of time, during which the region was covered by the sea, allowed thick layers of marine sediments to accumulate. The coarse- to medium- and fine-grained, varicolored sandstones of the Kurnub formation were mainly deposited by braided and meandering paleocurrents in a continental, alluvial environment (POWELL & MOH'D 2011). With the marine ingression beginning in the Cenomanian, several thick and thin layers of carbonate rocks, primarily marls and different kinds of limestone, started to form. These comprise nodular, dolomitic, massive, (algal-) laminated, and marly limestones

(POWELL 1989). Based on the abundant fossils contained therein, the strata can be assigned to Cenomanian, Turonian, and Coniacian to Santonian ages. BENDER (1968, 1975) describes these sediments as the Nodular, the Echinoid, and the Massive Limestone Members. These units correspond to the Ajlun Group of QUENNEL (1951) that comprises the Na'ur Limestone, the Fuhays, Hummar, and Shu'ayb formation, the Wadi as Sir Limestone, and the Khurayj Limestone (POWELL 1989). Gypsum beds (Na'ur, Fuhays/Hummar/ Shu'ayb, and lower Wadi as Sir formation), silt- or mudstone layers (lower Na'ur and upper Fuhays/ Hummar/Shu'ayb), dolomite, and sandstone (upper part of the Wadi as Sir formation) are intercalated with the different limestone strata (see Table 3). The deposited sequence is a result of changes in the depositional environment that are primarily associated with sea-level fluctuations. Shallow marine to fully marine, subtidal, low-energy conditions on a carbonate shelf (Ajlun Group) and later a pelagic ramp (Belqa Group) prevailed most of the time. Intermittent periods were characterized by emergence and supratidal, possibly lagoonal, and intertidal conditions (e.g. POWELL & MOH'D 2011). The members of the Wadi Umm Ghudran formation (lower Belqa Group) testify to these different conditions which must have alternated over a comparatively short period of time, mainly during the Santonian in the middle of the Upper Cretaceous epoch. Relatively stable, moderately deep to deep marine conditions that also occurred during that time, allowed the accumulation of thick layers of chalk (Mujib Chalk, Dhiban Chalk) (POWELL & MOH'D 2011).

Later, during the Maastrichtian and the Paleocene, similar conditions led to the deposition of the thick, soft, chalky and marly beds of the Muwaqqar Chalk Marl Formation that constitutes the upper part of the Belqa Group (POWELL 1989). In the time between the development of the Mujib Chalk and the Muwaqqar Chalk Marl, comparably thin layers with heterogeneous lithology formed in shallow marine, subtidal to intertidal, tidal, or estuarine environments (cf. SHINAQ ET AL. 2006, POWELL & MOH'D 2011). In addition to the hitherto described sediments, some of these strata also consist of dolomite, chert, and phosphorite, as well as coquinas in some locations. This heterogeneous composition characterizes the Tafila Member that lacks phosphorite, but includes rocks of the tripoli type, the Amman Silicified Limestone, and the overlaying Al Hisa Phosphorite Formation (see Table 3) (POWELL 1989). In contrast to the underlying Amman Silicified Limestone unit, which primarily encompasses beds of hard chert and (silicified) limestone, the Al Hisa Formation mainly consists of phosphorite, chalky marl, and limestone and contains less chert (cf. SHINAQ ET AL. 2006). Similar to the oolitic limestone of the Wadi as Sir unit, coquinas or (oyster) shell marble rocks formed in an intertidal or other shallow marine, high energy environment, e.g. on submarine swells, barriers, and banks. The coquinas are composed of reworked, abraded, and moderately cemented shell fragments and occur locally as members of the Wadi Umm Ghudran, the Amman Silicified Limestone, and the Al Hisa Phosphorite formations (Nukhayla, Mutarammil, and Siwaqa and Bahiya Coquinas, respectively) (see Table 3).

Table 3: Lithology and stratigraphy of geological formations in the study area (see Fig. 3). For ages in Ma before present see COHEN ET AL. (2013, updated). For legend to the depicted lithology see Figure 5. Sources: NATURAL RESOURCES AUTHORITY ET AL. 1989, 1996 (geological information, schematic sketch of composite lithology), CO-HEN ET AL. 2013, updated (age and epoch names).

Composite Lithology* *for legend see Fig. 5*	Symbol Thickness	Member	Formation	Group	Lithology description (from top to base respectively)	Age (Age, *Epoch*)
	JB		Judaiyida Basalt		basalt	*Pleistocene*
	SB		Sanina Basalt	Shihan Basaltic Group	basalt, jointed	*Miocene/ Pliocene*
	BB SBG		Balua Basalt		upper part: volcanic tuff, lower part: basalt with columnar jointing	*Miocene/ Pliocene*
	FB		Fraywan Basalt		scoria and tuff, basalt with vertical and horizontal jointing	*Miocene/ Pliocene*
	MCM 100m		Muwaqqar Chalk Marl		upper part: alternating layers of mainly limestone and chert; lower part: thick, soft beds of chalk marl interbedded with thin layers of chert and marl; bituminous in parts; limestone concretions in several horizons	Maastrichtian, *Upper Cretaceous* to *Paleocene*
	QP	Qatrana Phosphorite			phosphorite, phosphatic chert, limestone	
	BC	Bahiya Coquina			coquinal limestone, mega cross-bedded	Campanian to
	SC AHP	Siwaqa Coquina	Al Hisa Phosphorite	Belqa	coquinal limestone, mega cross-bedded	Maastrichtian, *Upper Cretaceous*
	SP 70m	Sultani Phosphorite			phosphorite, phosphatic chert, interbedded with marly limestone	
	MC	Mutarammil Coquina			coquinal limestone	Campanian,
	ASL 60-90m		Amman Silicified Limestone		concretions and thin beds of (phosphatic) chert, (silicified) limestone, partly brecciated; dolomitic chalky marl	*Upper Cretaceous*
	DNC	Dhiban Chalk			chalk	
	NC WG	Nukhayla Coquina			coquina, mega cross-bedded	Santonian,
	TF 90-93m	Tafila	Wadi Umm Ghudran		tripoli, (phosphatic) chert; dolomite, (phosphatic) limestone	*Upper Cretaceous*
	MBC	Mujib Chalk			chalk	
	KJ 25m	Khurayj Limestone			limestones and marls	Coniacian, *Upper Cretaceous*
	WSL 120-125m		Wadi as Sir Limestone		limestone, thin and thickly bedded, occasionally beds with chert nodules; dolomitic and oolitic limestone; dolomite; upper part: thin to medium beds of limestone, massive beds of dolomitic limestone, thin bed of trough cross-bedding sandstone; near base: gypsum	Turonian, *Upper Cretaceous*
	F/H/S 140-150m		Shu'ayb Hummar Fuhays (Undifferentiated)	Ajlun	uppermost part: red mudstone unit with thin beds of gypsum and marls; upper and middle part: marls, limestone, dolomitic, nodular and marly limestones; lower part (Wala and Karak Limestone Members): alternating thin beds of limestone, marly limestone, and marls; partly bituminous at base	Cenomanian to Turonian, *Upper Cretaceous*
	NL 130-170m		Na'ur Limestone		upper part: dolomitic and nodular limestone, marls and marly limestone intercalated with massive limestone beds; lower part (Juhayra member): (limonitic/quartzose) sandstone, thin beds of glauconitic siltstone, mudstone	Cenomanian, *Upper Cretaceous*
	KS 40-250m			Kurnub	coarse-, medium-, and fine grained white and varicolored sandstones with planar and trough cross bedding; plant fragments in parts	Albian to early Cenomanian, *Lower to Upper Cretaceous*

Fig. 5: Legend to the composite lithology presented in Table 3. Modified from NATURAL RESOURCES AUTHORITY ET AL. *1989 and 1996.*

The volcanic rocks of the Shihan Basaltic Group can be divided into four to five members dating from the Miocene to Pliocene and the Pleistocene (see Table 3) (NATURAL RESOURCES AUTHORITY AL. 1996, IBRAHIM ET AL. 2014). They were formed by "successive basaltic flows and partly of fragments of ejecta, indicating intermittent volcanic activity" (IBRAHIM ET AL. 2014, p. 544). Therefore, the Shihan Basaltic Group consists of basalts (from basaltic flows) of various thickness which are occasionally separated by intermediate layers of scoria (see Table 3). The rocks are mostly alkali basalts and typically exhibit columnar jointing (IBRAHIM ET AL. 2014). The different members and basalts can be distinguished primarily based on their geochemistry and secondarily on grounds of additional characteristics such as their texture. Occasionally, basalts can cover fluviatile gravels, calcrete crusts, or paleosols and include fragments of underlying sediments (BENDER 1968 and 1975, IBRAHIM ET AL. 2014). In contrast to the other members of the Shihan Basaltic Group, the Jad'a member described by IBRAHIM ET AL. (2014) is made up of lapilli tuff that stems from volcanic eruption. With respect to the lithological information, the Jad'a member most likely corresponds to (a portion of) the upper part of the Balua Basalt (see Table 3). While the older three to four units, namely the Fraywan, the Balua, (the Jad'a,) and the Sanina members are associated with the first stage of volcanic activity of Mount Shihan during the Messinian (approx. 5.3-7.2 Ma ago), the Judaiyida Formation is of a younger, probably Middle Pleistocene age (IBRAHIM ET AL. 2014). Only the Judaiyida unit, which occurs about 25 km south to southeast of Mount Shihan, is considered a wadi-fill flow. The basalt flows of the other, older units are supposed to have preceded the fluvial incision of the major wadis (DE JAEGER & DE DAPPER 2002, IBRAHIM ET AL. 2014). Distribution and local extents of the basalt cover may even have influenced the incision and thus, the present-day course of Wadi al Mujib (DE JAEGER & DE DAPPER 2002).

3.2.4 Hydrogeology

The hydrological characteristics of the different geological units and the overall hydrogeological situation are outlined below. Regarding the latter, a different stratigraphical nomenclature is usually applied, which groups the strata of the Belqa Group into units B1 - B3 and those of the Ajlun Group into units A1 - A7 (cf. e.g. POWELL 1989, EL-NAQA 1993 and 1994, MARGANE ET AL. 2002). In the following, the designations of the approximately corresponding hydrogeological units are given in parentheses.

The Al Hisa Phosphorite (B2b), the Amman Silicified Limestone (B2a), and the middle part of the Wadi as Sir Limestone (A7b) formation together constitute the Amman-Wadi Sir or B2/A7 aquifer system (EL-NAQA 1993 and 1994). Units B2 and A7 are considered to be interconnected hydraulically although they are separated by the Wadi Umm Ghudran (B1) formation which comprises strata acting as aquicludes (Dhiban Chalk or B1c, Mujib Chalk or B1a) and aquitards (Tafila Member or B1b) (EL-NAQA 1993). The older sediments of the Ajlun Group (A1-A6, from base to top) underlie the B2/A7 aquifer system and exhibit an overall low permeability. Therefore, they are regarded as aquitards, although parts of the Na'ur Limestone (A1/ A2) may act as aquifers. Recharge to the B2/A7 aquifer system mainly occurs in elevated areas to the north and the south of the study area and in the western parts of the Karak Plateau where water enters fractured outcrops of the corresponding units (EL-NAQA 1993). Further east, the Muwaqqar Chalk Marl (B3) overlies the aquifer system and impedes recharge as the strata of the formation are largely impermeable and thus, form an aquiclude (MARGANE ET AL. 2002). The vertical and horizontal permeability, as well as the transmissivity of the B2/A7 aquifer system, vary spatially, depending on the presence of joints and fractures and possible degrees of karstification (EL-NAQA 1994). Although karstification can potentially affect several of the strata consisting of carbonate rocks, primarily limestone, it is largely limited to the Wadi as Sir Limestone formation and corresponding areas in Jordan (WERZ 2006, cf. also KEMPE ET AL. 2006). In most parts of the country, necessary preconditions for karstification, such as tectonic deformation leading to fractures and joints in rocks, are not, or only insufficiently fulfilled (cf. also section 3.2.3 and Fig. 4).

3.3 Climate

Jordan represents a transitionary zone between the Mediterranean in the west and the desert environment in the east (cf. KIRK 1998). Therefore, its climate exhibits a strong longitudinal gradient which is additionally modified by orographic influences. When including the weaker latitudinal gradient, the country can broadly be divided into three larger climatic regions. These are the hot and dry climate of the Dead Sea/Wadi Arava valley and southeast Jordan, the cooler desert climate of northeast and eastern Jordan,

and the more humid, Mediterranean climate that prevails in the highlands to the east of the Jordan Valley/ Wadi Arava (cf. AL-EISAWI 1985, TARAWNEH & KADIOGLU 2003, AL-BAKRI ET AL. 2011). Cool and warm steppe climates can be found in the transitional areas, for example around the eastern fringes of the highlands (see Fig. 6).

One trait that all climate subtypes have in common is the Mediterranean pattern in the distribution of temperature and precipitation over the year (ZOHARY 1973, WAITZBAUER & PETUTSCHNIG 2004a). Warm to hot and dry summers are followed by moderately cold to cold and humid winters, while the transitional periods of spring and autumn are very short and less defined. Differences between climatic regions (see Fig. 6) are mainly of a quantitative nature and concern temperatures as well as precipitation (WAITZBAUER & PETUTSCHNIG 2004a).

During the winter half-year, i.e. from November to March, the weather is influenced by cyclones and low pressure systems over the eastern Mediterranean, which are associated with a lower position of the westerlies and the polar front (SHEHADEH 1985, KIRK 1998). Cold artic and polar air masses then invade the region. A combination of the above factors and eastward moving frontal depressions results in precipitation (SHEHADEH 1985, FREIWAN & KADIOGLU 2008). Towards the east, and particularly the southeast of Jordan, the climate becomes more continental due to increasing distances from the Mediterranean Sea (SHEHADEH 1985, WAITZBAUER & PETUTSCHNIG 2004a). Accordingly, precipitation decreases in the same directions. Moist air masses coming from the Mediterranean Sea, and moving to the east, bring precipitation to the highlands on both sides of the rift valley. Further east, lee effects lead to a rain shadow and lower amounts of annual precipitation (see Fig. 7).

In the winter months, the weather is dictated by frontal depressions. In terms of intensity and frequency, their influence dimishes towards the south, thus leading to reduced amounts of annual precipitation (see Fig. 7) (SHEHADEH 1985). The north is more directly exposed to frontal depressions, whereas air masses reaching southern Jordan have lost most of their humidity along their track over the Sinai desert (TARAWNEH & KADIOGLU 2003). The Cyprus Low, a depression center in the southeastern Mediterranean, represents the main source area of cyclones entering Jordan during the winter. Wind directions are usually west and northwest for most parts of the country (KIRK 1998, TARAWNEH & KADIOGLU 2003, CORDOVA 2007). Changes in the number and intensity of frontal depressions reaching the country in the winter half-year are responsible for interannual variances in precipitation. In terms of percentage, interannual variances increase with decreasing amounts of annual precipitation. Extreme weather events, especially extreme precipitation events, are also more likely to occur in the drier eastern and southern parts of Jordan (FREIWAN & KADIOGLU 2008).

During the summer, Jordan is influenced by the subtropical high-pressure belt, when the activity and formation of cyclones is blocked. This leads to stable conditions associated with hot and dry, continental air masses over the country (SHEHADEH 1985). Practically, no precipitation occurs during the summer

except for some rare cases of extreme events. Occasionally, a seasonal wind called the Shamal affects the region and brings dust from the desert areas in the north and northeast to the Western Highlands (CORDOVA 2007).
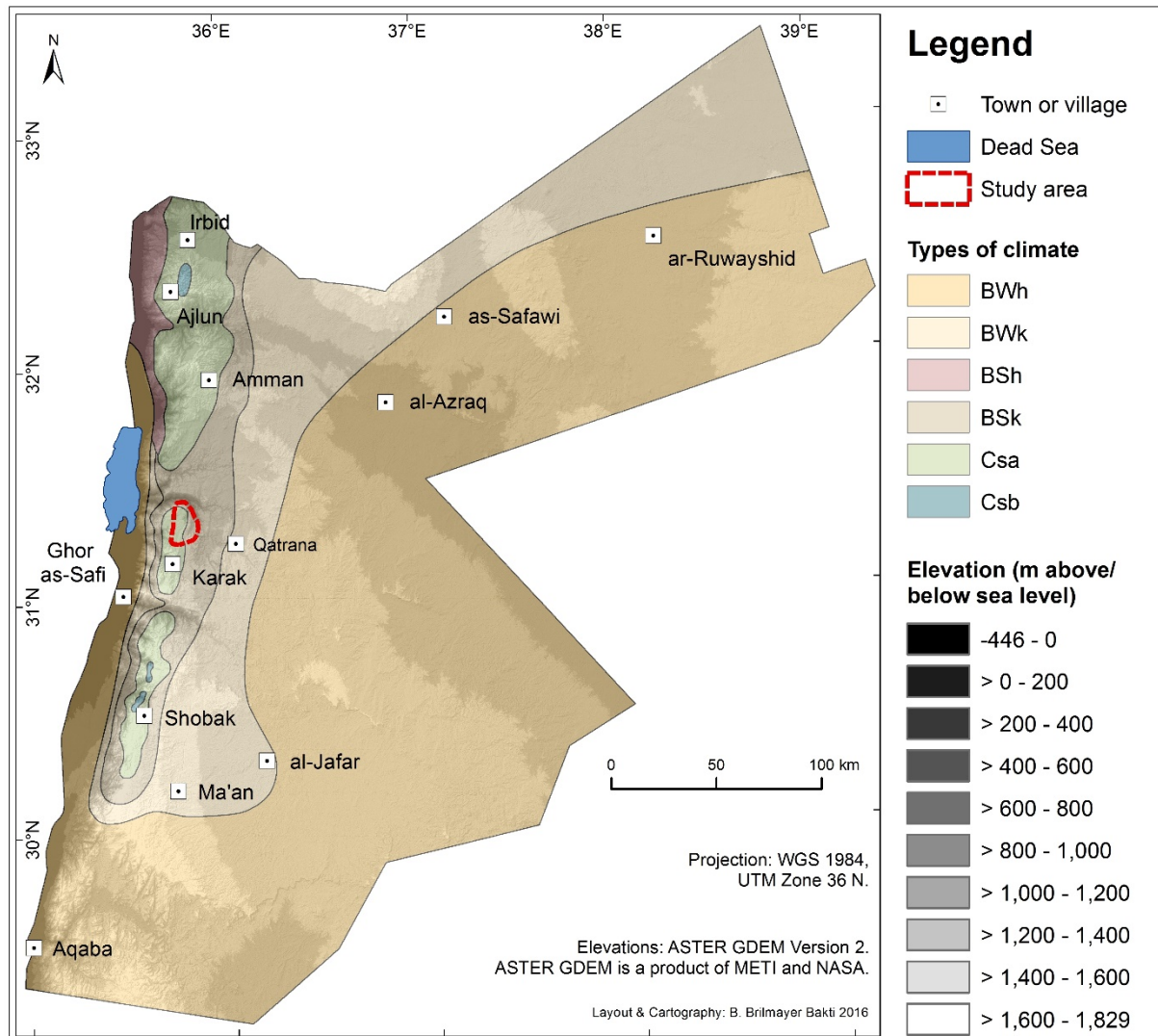
Fig. 6: Climatic regions of Jordan according to the classification of Koeppen & Geiger. Delineation of climatic regions according to CORDOVA 2007.

The transitional seasons, spring and autumn, are characterized by unstable weather conditions due to alternating influences of frontal cyclonic systems in the north and northwest and thermal troughs in the south and southeast (FREIWAN & KADIOGLU 2008). During spring, Khamsin (also called Saharan) depressions can occur. They are associated with a regional, hot and dry, dusty wind of the same name that blows from the desert areas in the south and southeast, and particularly, affects southern Jordan (SHEHADEH 1985, WAITZBAUER & PETUTSCHNIG 2004a, CORDOVA 2007). Although most of the precipitation falls during the winter rainy season from October to April, with a maximum in January, seasonal rainfall of lesser and highly variable amounts can occur in autumn and especially in spring (TARAWNEH & KADIOGLU 2003). Rainfall in the transitional seasons contributes particularly to the total

annual precipitation amounts of the dry areas in the east and southeast of Jordan. These regions are especially affected by unstable weather conditions and convective rainfall events that are connected to the extension of the thermal Red Sea trough (TARAWNEH & KADIOGLU 2003, FREIWAN & KADIOGLU 2008).
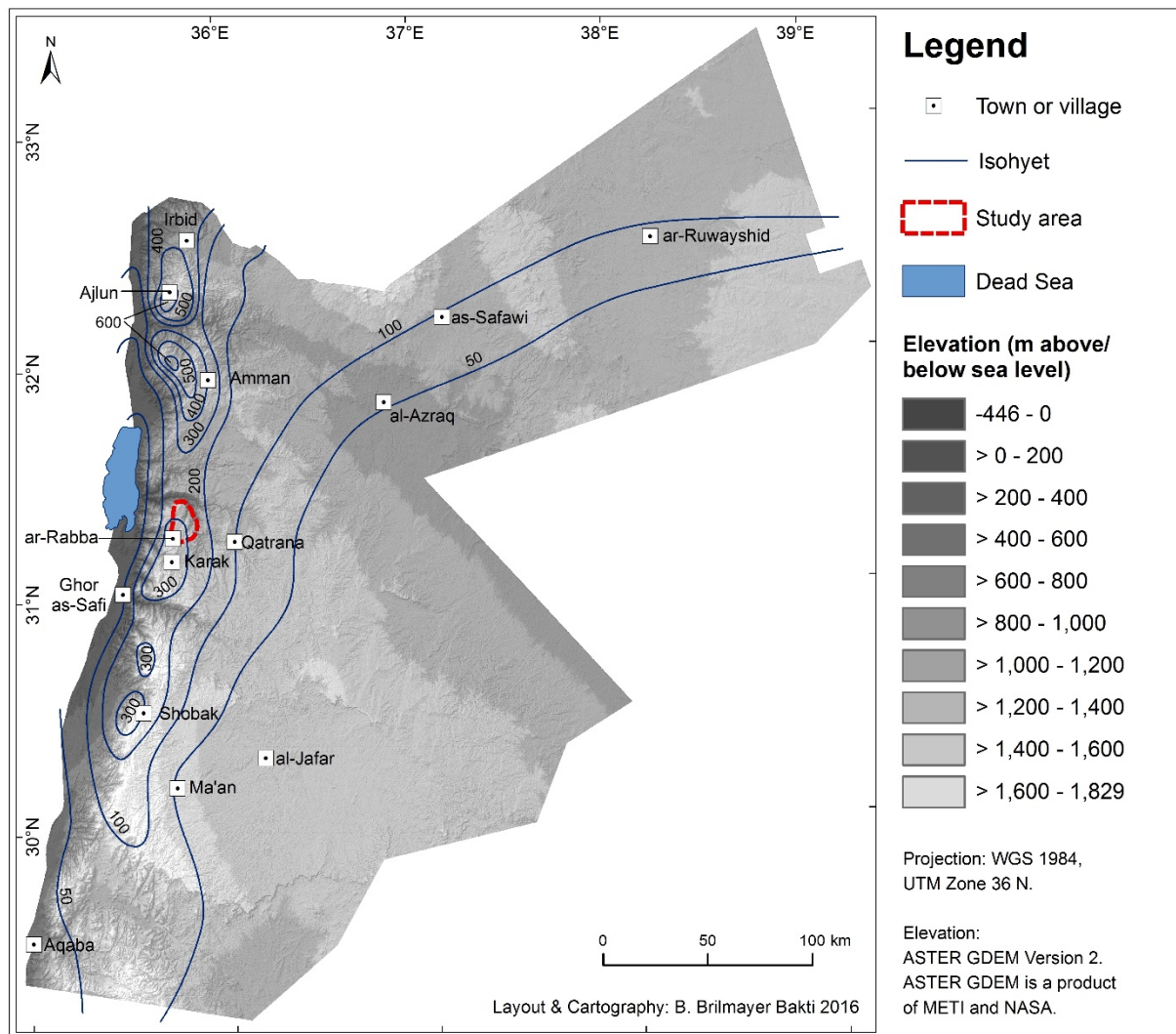
Fig. 7: Average annual precipitation amounts in Jordan. Delineation of isohyets based on AL FARAJAT (2001) and AL-HOMOUD ET AL. (1995). Sources of isohyets/precipitation information: Higher Council for Science and Technology (HCST) in Jordan, as cited in AL-HOMOUD ET AL. 1995, AL FARAJAT 2001.

Climatically, the study area itself is located between the hot desert climate of the Dead Sea valley in the west and the cooler steppe and desert climates in the east (see Fig. 6). Climate stations included in Figure 8 roughly correspond to a transect from west to east (see Fig. 7 for locations). Thus, the associated diagrams illustrate longitudinal changes in climate in the region. According to the classification scheme of Koeppen and Geiger, the climate of Ghor as-Safi in the Dead Sea valley is that of a hot desert (BWh type). The climate of this area is dictated by the low elevations and Foehn wind effects, i.e. dry and warm, descending winds from the Judean Mountains in the west (TARAWNEH & KADIOGLU 2003). In the highlands east of the Dead Sea, at altitudes over 700 m above sea level, a Mediterranean climate of

the Csa type dominates, which is exemplified by the diagram of ar-Rabba (see Fig. 8). At al-Qatrana, further to the east, a cooler desert climate of the BWk type prevails. This is a result of the altitude, which is similar to that of the highlands, and the increasing continentality towards the east. The transitional area, between the central part of the Karak Plateau (ar-Rabba) and the Badia (al-Qatrana), is characterized by a relatively cool steppe climate of the BSk type (see Fig. 6).
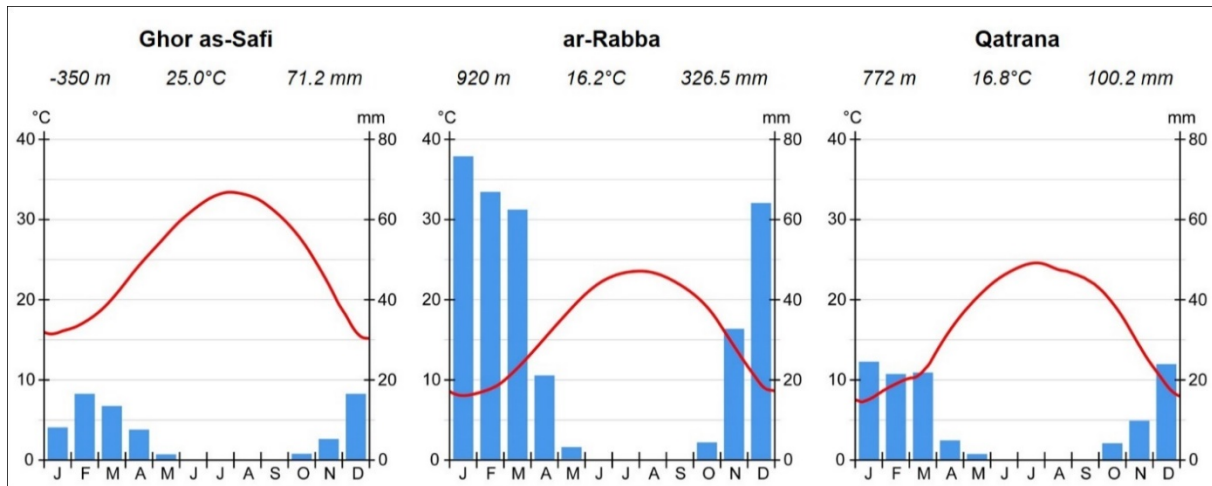
Fig. 8: Climate diagrams of three selected stations within and around the study area (cross-section from southwest to northeast). Locations of climate stations are shown in Figure 7. Below the name of each station, its elevation below or above sea level, the mean annual temperature, and the mean annual precipitation amount is given. Red curves represent mean monthly temperatures, blue columns show mean monthly precipitation amounts. Figures refer to the observation periods 1974-1987 for Ghor as-Safi, 1952-1987 (precipitation) and 1961-1987 (temperature) for ar-Rabba, and 1976-1987 for Qatrana. Sources of climate data: Jordanian Ministry of Agriculture & Meteorological Department, as cited in OTT 1998. Modified from OTT 1998.

All described climates show the same pattern regarding the temporal distribution of temperature and precipitation over the year. Yet, significant differences can be observed in terms of quantity. Compared to the Dead Sea area, climates of the highland and the eastward adjacent region are characterized by overall lower temperatures due to comparatively high elevations above sea level. Hence, ar-Rabba in the center of the Karak Plateau and al-Qatrana on the outskirts of the Eastern Desert exhibit almost identical curves of mean monthly temperatures (see Fig. 8). However, diurnal temperature curves become steeper, indicating pronounced differences between hot day and cold night temperatures towards the desert in the east. This contrast between day and night temperatures is typical for desert areas. Throughout the discussed region, mean monthly temperatures are very similar in areas of comparable altitude. In contrast, annual precipitation amounts show larger differences and a decreasing trend towards the east. Thus, a distinct longitudinal gradient can be identified. Therefore, on average, only one third of the annual precipitation occurring in ar-Rabba is recorded at al-Qatrana (see Fig. 8). Towards the east, the likelihood of extreme events, in addition to the interannual variability in precipitation increases, along with the growing aridity. As annual precipitation amounts decrease markedly, over short

distances from west to east, a gradual transition from a Mediterranean to a steppe climate can be observed within the study area. Thus, the area reflects the transitional character of Jordan in general, but on a smaller scale.

3.4 Soils

The soils of Jordan have been studied on different levels of detail within the scope of the NATIONAL SOIL MAP AND LAND USE PROJECT (NSM&LUP) (NSM&LUP ET AL. 1993a,b, 1994a,b). Besides reports on the characteristics and distribution of different soils, soil maps were produced for large parts of Jordan. Collected information on soils and land use have also been integrated into a nationwide database; the Jordan Soil and Climate Information System (JOSCIS). The area under study is covered by the reconnaissance soil survey (level 1) as well as a semi-detailed study (level 2). Available information, especially from the latter, are compiled in Fig. 9 and Table 4. An overview of the soils in Jordan can also be found in AL QUDAH (2001) and LUCKE ET AL. (2013). Older publications containing information on the soils of the country are those of BENDER (1968) and MOORMAN (1959). Specific aspects such as the characteristics and occurrence of certain soil types or the link between soils and geoarchaeological questions were studied e.g. by TAIMEH & KHRESAT (1988), KHRESAT & TAIMEH (1998), KHRESAT (2001), CORDOVA ET AL. (2005), SCHMIDT ET AL. (2006), LUCKE (2007), KHRESAT ET AL. (2008), and LUCKE ET AL. (2014).

The mosaic of soils occurring in the study area (see Fig. 9) arises from an intricate interplay of a number of different factors. These include the relief, geomorphological processes, geological formations and substrates, as well as climatic conditions. The latter largely determine moisture availability, which in turn represents a limiting factor for soil development in the study area. Time and the geological and paleogeographical history of the area also affected the formation of different soils. The resulting spatial pattern of different soils is illustrated in Figure 9. In the map, areas with similar combinations and percentages of individual soil types are assigned to the same unit. Key characteristics and major soil types of each unit are presented in Table 4. The information given in Figure 9 and Table 4 are based on the findings of the soil surveys conducted by the NSM&LUP ET AL. (1993a,b, 1994a,b). Although inadequately published and therefore of limited availability, the data of these surveys currently represent the most comprehensive information on the soils of Jordan (cf. LUCKE ET AL. 2013). In the surveys, soils were classified and described according to the USDA taxonomy from 1990 (SOIL SURVEY STAFF 1990). Therefore, the following explanations comprise several references to this classification scheme. The taxonomy and terminology of the WRB (World Reference Base for Soil Resources) (IUSS WORKING GROUP WRB 2007) is now more and more established as the international standard for soil description

and classification. An overview of approximate equivalences between relevant soil types of different classification schemes is presented in Table 5. Soil types described in older publication (e.g. MOORMAN 1959, BENDER 1968) are included. Due to fundamental differences in classification schemes, approaches, and methods, correlations established in Table 5 must be seen as approximations.

Deep fertile soils cover vast areas of the Karak Plateau, especially in its central and northern parts, where the relief is mostly flat to softly undulating, and a Mediterranean semi-arid climate prevails with annual precipitation amounts of around 300 mm. Towards the east and southeast, where the terrain becomes more rugged and annual precipitation amounts decrease to around 200 mm, soils are typically shallower and rather poorly developed. Precipitation plays a key role in soil development and determines the degree to which pedogenic processes can take place. In the study area, the dominant pedogenic processes are clay eluviation and illuviation, as well as carbonate leaching and secondary accumulation of carbonate in the subsoil. The latter processes commonly result in the formation of a calcic horizon in soil profiles (cf. KHRESAT 2001).

In the US Soil Taxonomy, different climatic conditions are reflected in corresponding soil moisture regimes. All soils in the study area are characterized by either a xeric, or a transitional, xeric to aridic moisture regime (NSM&LUP ET AL. 1994a). Xerochrepts and shallow (lithic) Xerorthents are associated with a xeric moisture regime (see Table 4). Soils of these two Great Groups account for over 84% of the soil cover in the area and hence represent the majority of soils (see Table 5). They are particularly common in the central and northern part of the plateau where annual precipitation amounts range between 250 and over 300 mm. There, mostly deep Xerochrepts occur on flat land and gentle slopes, while shallow, stony Xerorthents are typically found on steep and eroded slopes (AL QUDAH 2001). Chromoxererts which correspond to the Red Mediterranean Soils described by MOORMAN (1959) and others (BENDER 1968, SCHMIDT ET AL. 2006, CORDOVA 2007), are not mentioned explicitly in the description of soil units (see Table 4) (cf. NSM&LUP ET AL. 1994a,b). Nevertheless, it seems likely that conditions allowed the development of Chromoxererts in certain areas (cf. BENDER 1968, CORDOVA ET AL. 2005). A transitional, xeric to aridic moisture regime characterizes the soils in the eastern and southeastern parts of the study area. There, the terrain is covered by associations of Camborthids, Calciorthids, and Torriorthents (see Fig. 9 and Table 4). While Torriorthents only occur in a lithic form, i.e. with a maximum depth of 50 cm above the C horizon or the bedrock, Camborthids and Calciorthids can be deeper. Since this transitional zone constitutes a minor part of the study area, the aforementioned Great Groups of soils each account for only 2-3% of the total soil cover of the area.

In terms of taxonomic classes, the soils of the study area can be grouped into Inceptisols, Entisols, and Aridisols. On a subordinated level, in the study area, each class is represented by one suborder and one or two Great Groups (within this suborder). Most of the soils (71%) belong to the class of Inceptisols. These are characterized by a relatively young age and a limited profile development (EITEL 2001, BLUME ET AL. 2010). The class of Inceptisols encompasses the Great Group of Xerochrepts of which

the subgroup of Calcixerollic Xerochrepts is the dominant soil type in the area (see Table 5). With a share of 17% in the soil cover, Entisols are the second most common soil types. These are very young soils with (almost) no horizon development (AL QUDAH 2001, CHESWORTH 2008). They comprise the suborder of Orthents and the two Great Groups of Torriorthents and Xerorthents (SOIL SURVEY STAFF 1990). Torriorthents, and especially Xerorthents, account for most of the shallow (lithic) soils in the study area. In the classification scheme of the WRB, these soils correspond to Leptosols (see Table 5). Entisols typically occur in the desert areas of Jordan and are often associated with Aridisols that are characteristic for the steppe region of the country (AL QUDAH 2001). Although Aridisols cover vast areas (around 60%) of Jordan, they only account for a minor share (ca. 6%) in the soil cover of the study
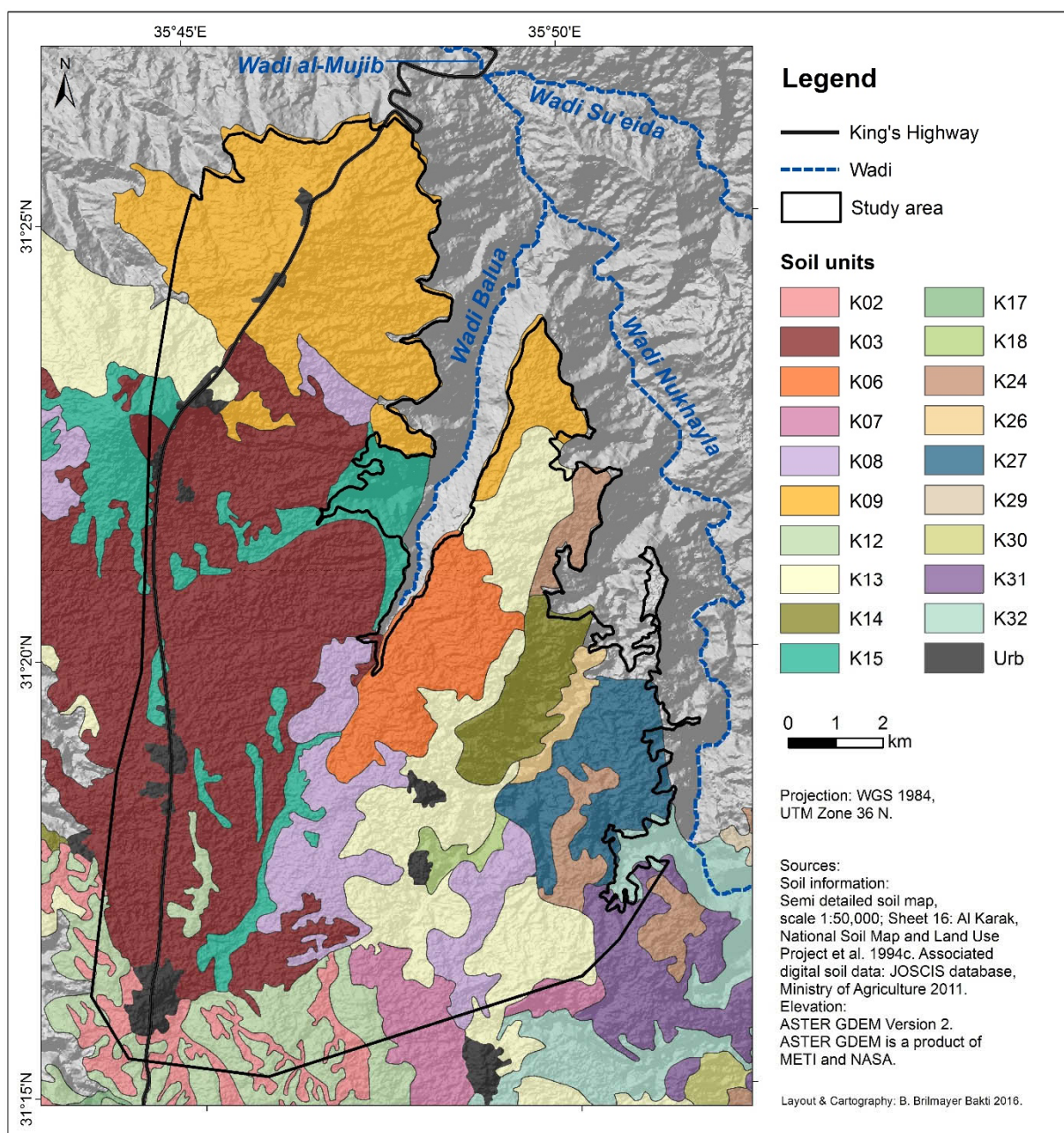
Fig. 9: Soil map of the study area. Areas assigned to the category "Urb" correspond to settlement or built-up areas. Further information concerning individual soil map units and their composition can be found in Table 4.

Table 4: Description of the different units in the soil map (Fig. 9). The composition, main soil types, and essential characteristics of each unit are displayed below. Soil types are defined according to the US Soil Taxonomy of 1990 (SOIL SURVEY STAFF 1990). Modified from NATIONAL SOIL MAP AND LAND USE PROJECT (NSM&LUP) ET AL. 1994a.

Map unit	Soil type (US Soil Taxonomy 1990, subgroups)	Share in unit	Average soil depth	Percentage of shallow soils	Stones and rock outcrops	Geomorphology and parent material	Altitude (m above sea level)	Slope range (%)	Moisture regime	Mean annual precipitation (mm)
K02	Calcixerollic Xerochrepts	40 %	81 cm	25 %	few stones and rock outcrops	undulating plains: more concave sites; deep colluvial mantle	800–1050	0–8	Xeric	325–375
	Vertic Xerochrepts	35 %								
	Lithic Xerorthents	20 %								
K03	Calcixerollic Xerochrepts	55 %	78 cm	20 %	localized stones and rock outcrops (20 %)	flat to very gently undulating plains: deep colluvial and aeolian mantle	800–810	0–4	Xeric	300–350
	Vertic Xerochrepts	25 %								
K06	Calcixerollic Xerochrepts	75 %	77 cm	15 %	few stones, little or no rock outcrops	undulating plains: moderately deep colluvial and aeolian mantle over limestone; dense drainage network	800–1080	0–4 (5–8)	Xeric (drier parts)	275–325
	Lithic Xerorthents	15 %								
K07	Calcixerollic Xerochrepts	55 %	76 cm	20 %	few stones, localized rock outcrops (<10 %)	undulating to rolling plains: deep aeolian and colluvial mantle	800–1080	0–8 (9–16)	Xeric	300–325
K08	Calcixerollic Xerochrepts	65 %	66 cm	35 %	numerous stones, localized rock outcrops (25 %)	gently undulating plain with frequent low and rounded limestone outcrops; moderately deep colluvium	730–780	0–4	Xeric	300–350
	Lithic Xerorthents	15 %								
K09	Calcixerollic Xerochrepts	70 %	80 cm	20 %	numerous stones, localized rock outcrops (10 %)	undulating to rolling plain in limestone with basalt capping; erosion problematic	520–770	0–8 (9–16)	Xeric (drier parts)	270–320
K12	Lithic Xerorthents	35 %	65 cm	45 %	numerous stones and rock outcrops (20 %)	rolling limestone plain incl. less sloping plateau sites with some moderately deep colluvium	1040–1190	0–25	Xeric	320–340
	Calcixerollic Xerochrepts	30 %								
	Lithic Xerochrepts	15 %								
	Vertic Xerochrepts	15 %								
K13	Calcixerollic Xerochrepts	45 %	45 cm	40 %	abundant boulders and stones, localized rock outcrops (20 %)	gently to moderately sloping margins of undulating plain	800–840	0–16 (16–25)	Xeric (drier parts)	260–300
	Lithic Xerorthents	30 %								
K14	Lithic Xerorthents	45 %	44 cm	60 %	abundant stones and rock outcrops (40 %)	complex of rolling upland with rocky and shallow soils and narrow valley bottom with deep soils	960–1180	0–25	Xeric	300–350
	Vertic Xerochrepts	20 %								
	Calcixerollic Xerochrepts	15 %								
	Typic Xerochrepts	10 %								
K15	Lithic Xerorthents	30 %	45 cm	75 %	abundant boulders and stones and rock outcrops (40 %)	rolling plain with frequent low outcrops of basalt rocks and boulders	770–780	——	Xeric	310–340
	Calcixerollic Xerochrepts	30 %								
	Vertic Xerochrepts	10 %								
K18	Typic Xerochrepts	50 %	56 cm	50 %	abundant boulders and stones and rock outcrops (50 %)	steep uppermost slopes of escarpment; abundant limestone rock outcrops	800–1240	16–60	Xeric	320–370
	Lithic Xerorthents	25 %								
K24	Xerochreptic Calciorthids	35 %	62 cm	35 %	few stones, little or no rock outcrops	gently sloping; moderately deep colluvium and aeolian material; fairly dense drainage network; erosion problematic	640–870	0–8	Transitional (drier parts)	150–200
	Xerochreptic Camborthids	25 %								
	Lithic Xeric Torriorthents	15 %								
K26	Xerochreptic Camborthids	30 %	57 cm	55 %	abundant boulders and stones and rock outcrops (50 %)	valley sides, concave footslopes and alluvial toeslopes; dissected basalt plateau	720–1040	0–16	Transitional (wetter parts)	220–290
	Lithic Xeric Torriorthents	25 %								
	Xerochreptic Calciorthids	20 %								
	Lithic Xerochreptic Camborthids	15 %								
K27	Lithic Xeric Torriorthents	40 %	50 cm	50 %	abundant small stones (30 %) and rock outcrops (10 %)	rolling plains on limestone, shallow colluvium	700–1080	0–16	Transitional	200–300
	Xerochreptic Camborthids	35 %								
	Xerochreptic Calciorthids	15 %								
K31	Lithic Xeric Torriorthents	45 %	31 cm	80 %	abundant stones in surface horizon (30–50 %)	highly dissected upper and midslopes of edges of limestone plateau; dense drainage network	710–820	0–16	Transitional (drier parts)	150–200
	Xerochreptic Camborthids	35 %								
	Lithic Xerochreptic Camborthids	10 %								
K32	Rock Outcrops	40 %		——	very bouldery, abundant rock outcrops (40 %)	steep scarp slopes descending to major Wadis	560–800	25–60	Transitional Dry	175–250

Table 5: Soil types in the study area according to Figure 9 and Table 4 and corresponding soil types of different classification schemes. "Other soil names" are those used in older publications, e.g. by MOORMAN (1959) and BENDER (1968). Where more than one of these names could apply to the specific soil type (first column), the most likely equivalent has been underlined. The area covered by each soil type was calculated from the share of this soil type in individual soil units (Table 4, third column) and the extent of these soil units in the study area. Where, in a given soil unit, shares of individual soil types and rock outcrops did not amount to 100%, the remaining parts were assigned to the category "other soils not specified". The category "not classified" contains the parts of the study area that were not covered by the semi-detailed soil survey of the NSM&LUP ET AL. (1994c) (see Fig. 9). Approximate equivalences between soil types of different classification systems were established based on NSM&LUP ET AL. (1994b), CORDOVA (2007), LUCKE (2007), CHESWORTH (2008), and LUCKE ET AL. (2013).

Soil type US Soil Taxonomy 1990 or category	Soil type FAO/WRB (IUSS WORKING GROUP WRB 2007)	Other soil names (e.g. MOORMAN 1959, BENDER 1968)	Extent (km²)	Share in study area
Calcixerollic Xerochrepts	Calcaric Cambisols	Yellow Mediterranean Soil, Red Mediterranean Soil	77.31	47.3 %
Lithic Xerorthents	Leptosols	Rendzina	17.74	10.9 %
Vertic Xerochrepts	Vertic Cambisols	Vertisol, Red Mediterranean Soil	14.95	9.2 %
Lithic Xeric Torriorthents	Leptosols	Rendzina, Yellow Soil	4.47	2.7 %
Xerochreptic Camborthids	Yermic Cambisols	Yellow Soil	4.43	2.7 %
Xerochreptic Calciorthids	Haplic Calcisols	Yellow Soil	2.77	1.7 %
Lithic Xerochrepts	Dystric Leptosols	Rendzina, Yellow Mediterranean Soil, Red Mediterranean Soil	1.1	0.7 %
Typic Xerochrepts	Chromic Cambisols	Red Mediterranean Soil	1.05	0.6 %
Lithic Xerochreptic Camborthids	Yermic Leptosols	Redzina, Yellow Soil	0.33	0.2 %
other soils not specified			8.72	5.3 %
rock outcrops			28.1	17.2 %
area not classified			2.31	1.4 %

area. In the surveys of the NSM&LUP ET AL. (1994a), Vertisols were not detected in the study area itself but in the surroundings where similar conditions prevail. Other scholars (TAIMEH & KHRESAT 1988, KHRESAT & TAIMEH 1998) who particularly focused on Vertisols also located typical soil profiles in the vicinity of ar-Rabba, within the study area. Due to strong similarities, it can often be difficult to distinguish Vertisols from Vertic Xerochrepts and Typic Xerochrepts (cf. NSM&LUP ET AL. 1994a). Therefore, some of the soils in the study area could be Vertisols.

Moderately deep to deep soils, i.e. soils with a profile depth of ca. 75cm to 1m and more, have formed in vast areas with gently undulating and flat terrain. In these areas, slope gradients commonly vary between 0 to 4 or 6%, although steeper slopes with gradients of no more than 16% are occasionally included (NSM&LUP ET AL. 1994a). In the flattest parts of the tableland and where a Mediterranean climate prevails, deep Vertic Xerochrepts could develop. Under identical climatic, but a wider range of topographic conditions, Calcixerollic and Typic Xerochrepts formed. In a similar terrain, but under drier climatic conditions, Xerochreptic Camborthids and Calciorthids developed (see Fig. 9 and Table 4). The parent material, however, is largely the same for all soil types. It mainly consists of colluvium derived from the weathering of local rocks, primarily limestone, and additionally chert and basalt (NSM&LUP ET AL. 1994a,b). Occasionally, alluvial material is included and shares of Aeolian admixture can vary from marginal to significant (NSM&LUP ET AL. 1994a, SCHMIDT ET AL. 2006). Soil colors range from dark and strong brown to (pale) yellowish brown, brownish or reddish yellow, yellow, and yellowish

red. According to Munsell's soil color charts, the colors can be classified as 7.5YR and 10YR, 5R which rarely occurs in the area, and 7.5YR 6/6 to 3/4 and 10YR 6/6 to 3/4 (NSM&LUP ET AL. 1994a,b, VÖGELE 2012). The latter numbers are the most frequently observed in soils of the Karak Plateau. Therefore, the soils and soil series found in the study area have mostly been described as brown (cf. NSM&LUP ET AL. 1994a). Vertic and Calcixerollic Xerochrepts were also often classified as red soils. Reddish hues are a result of rubification, i.e. the formation of hematite in soils. Due to conditions required for this process, reddish colors suggest the presence of a moister Mediterranean climate in the past (SCHMIDT ET AL. 2006, CORDOVA 2007). Paler color shades, particularly in surface horizons, are typically attributed to high calcium carbonate contents and the involvement of Aeolian material (cf. e.g. EITEL 2001, CORDOVA 2007). Soils with these colors correspond to the Yellow Mediterranean Soil and Yellow Soils described in older publications (e.g. MOORMAN 1959, BENDER 1968). They occur primarily in the eastern part of the study area where a transitional, xeric to aridic moisture regime prevails.

Regarding grain size distribution patterns, all soil types that form deep profiles are characterized by high amounts of very fine and fine particles, i.e. clay and silt contents of 40-50% and 30-40% respectively (cf. NSM&LUP ET AL. 1994b). Soils are usually not sandy with 10-15% of the soil mass belonging to the sand fraction (VÖGELE 2012). Vertic and Typic Xerochrepts exhibit the highest clay contents of around 50% and more (NSM&LUP ET AL. 1994b, VÖGELE 2012). Calcixerollic Xerochrepts are mostly characterized by a similar composition, with slightly higher percentages of silt and lower percentages of clay (NSM&LUP ET AL. 1994b, CORDOVA 2007). Xerochreptic Camborthids and Calciorthids, the deep soils of the transitional steppe area, typically show slightly higher contents (up to 20%) of sand, a significantly higher silt content of around 50%, to well over 60%, and a markedly lower percentage (20-30%) of clay (NSM&LUP ET AL. 1994b). Higher silt contents suggest limited chemical weathering due to drier climatic conditions and significant eolian admixtures of material from adjacent areas (cf. EITEL 2001) such as e.g. the deserts in the east. Soil types with higher percentages of clay are usually found in areas with higher amounts (around 300 mm) of annual precipitation (cf. also SCHMIDT ET AL. 2006). This correlation between clay content and precipitation is paralleled by changes in clay mineralogy. Only the soils with the highest clay content, i.e. Vertic Xerochrepts and Vertisols, have been classified as montmorillonitic, while all other soil types exhibit a mixed clay mineralogy (NSM&LUP ET AL. 1994a). Smectites, such as montmorillonite, also show some of the strongest swelling potentials with seasonal drying and wetting and hence, largely influence soil properties (EITEL 2001).

Observed soil textures reflect the patterns of grain size distribution that were described above. Therefore, the textures of most soils can be defined as clay loam to (silty) clay. Subsoils, Vertic and Typic Xerochrepts, and most Calcixerollic Xerochrepts usually exhibit a more clayey texture, whereas topsoils and Xerochreptic Camborthids and Calciorthids are normally characterized by a more silty and loamy texture. In most cases, soil structures are medium subangular blocky, but they can range from coarse to fine subangular blocky (NSM&LUP ET AL. 1994a). Prismatic, platy and crumb structures have also been

found, e.g. in Vertic Xerochrepts and Calcixerollic Xerochrepts (NSM&LUP ET AL. 1994a, VÖGELE 2012). With amounts of 1-2% or less, organic contents are typically low to very low in all soils (VÖGELE 2012) due to dominant types of land use and land cover, climatic conditions, and vegetation dynamics. All soils are calcareous to some degree (slightly, moderately, or highly). In most cases, calcium carbonate contents were found to be around 30% (NSM&LUP ET AL. 1994a). Lower percentages of less than 10-20% of $CaCO_3$ are observed in Vertic Xerochrepts, some Xerochreptic Camborthids, and Typic Xerochrepts (NSM&LUP ET AL. 1994a, VÖGELE 2012). Calcixerollic Xerochrepts exhibit the greatest variety of $CaCO_3$-Levels that can range from 15% to over 50% (NSM&LUP ET AL. 1994a,b).

Carbonate leaching and clay illuviation lead to the formation of distinctive horizons in subsoils. However, intensity and extent of these processes are limited due to the relatively young age of the soils and the restricted moisture availability that results from semiarid to arid climatic conditions. Hence, horizons of clay accumulation and secondary carbonate precipitation are found at various depths in soil profiles. Clay contents usually increase with depth but they can also reach their maximum in the upper middle of subsoils (NSM&LUP ET AL. 1994b, CORDOVA 2007). The accumulation of clay characteristically leads to the formation of a Bt horizon while calcic or Bk horizons are a result of secondary carbonate accumulation. Calcic horizons typically occur in steppe soils, i.e. Xerochreptic Camborthids and Calciorthids, as well as in many Calcixerollic Xerochrepts (cf. NSM&LUP ET AL. 1994b, CORDOVA 2007, VÖGELE 2012). The latter, Calcixerollic Xerochrepts, can also lack a calcic horizon. Where no calcic horizons were observed, they might exist in depths not investigated in surveys (NSM&LUP ET AL. 1994a). Soft and hard $CaCO_3$ concretions of various sizes occur in almost all soils, in specific horizons or throughout the subsoil. While their amount can vary considerably, they are particularly abundant in calcic horizons (NSM&LUP ET AL. 1994a,b, VÖGELE 2012). Besides simple concretions, $CaCO_3$ accumulations can also take the form of filaments or threads, nodules, or carbonate coatings on pebbles and gravel (cf. KHRESAT 2001).

Other horizons frequently observed in the soils of the area are ochric, i.e. pale surface horizons (see above on color) and cambic subsoil horizons (NSM&LUP ET AL. 1994a,b). A cambic subsoil horizon is found in most soils, except for some Calcixerollic Xerochrepts and all Vertic Xerochrepts which feature a vertic instead of a cambic subsoil horizon (NSM&LUP ET AL. 1994b, VÖGELE 2012). High clay contents, which are typical for Vertic and Typic Xerochrepts, often enable the formation of shiny ped faces. These are a result of clay coatings on peds or represent pressure faces which are related to the shrink-swell phenomena of clay minerals (cf. NSM&LUP ET AL. 1994a,b). Argilliturbation (or peloturbation) can lead to polished surfaces such as slickensides which can easily be confused with shiny ped faces. However, according to the US Soil Taxonomy, only horizons with real slickensides are classified as Bss horizons (NSM&LUP ET AL. 1994a, SOIL SURVEY STAFF 1990). They are often found in the deeper subsoils of Vertic Xerochrepts and some Calcixerollic Xerochrepts (NSM&LUP ET AL. 1994b, VÖGELE 2012). During summer, the drying out of clay minerals induces vertical cracks of various widths and

depths in topsoils and upper subsoils. Rewetting in winter and the resulting shrink-swell dynamic lead to churning movements (peloturbation) and self-mulching (cf. e.g. CHESWORTH 2008). The described phenomena can occur, to varying degrees, in all deep soils with high clay contents, i.e. deep Xerochrepts, especially Vertic Xerochrepts, and partially in Typic and Calcixerollic Xerochrepts (NSM&LUP ET AL. 1994a). Due to the high percentages of clay, deeper layers of these soil types can show compaction (NSM&LUP ET AL. 1994a,b).

Shallow soils or Leptosols cover most of the mid and upper slopes, hills and hill crests, as well as other areas with moderate gradients of 10-20% and some parts of steeper sloping terrain with gradients of up to 40-60% (NSM&LUP ET AL. 1994a). In the drier southeastern corner of the study area, (Lithic) Xerochreptic Camborthids and Lithic Xeric Torriorthents occur together with shallow and gravelly varieties of Xerochreptic Calciorthids (see Fig. 9 and Table 4) (NSM&LUP ET AL. 1994a). In the rest of the study area, where a xeric moisture regime prevails, Lithic Xerorthents constitute the most common type of shallow soils (see Fig. 9 and Table 4). In some areas, they are associated with or are replaced by Lithic Xerochrepts. Together, Lithic Xerochrepts and Lithic Xerochreptic Camborthids cover less than 1% of the study area (see Table 5). With depths of around 37 cm, they usually represent less shallow soils (NSM&LUP ET AL. 1994a). In contrast, Lithic Xeric Torriorthents and the prevalent Lithic Xerorthents are typically very shallow and exhibit soil depths of less than 19 cm (NSM&LUP ET AL. 1994a,b).

The parent material of the Leptosols on the Karak Plateau is nearly identical to that of the other, deeper soils in the area. Hence, the soils show large similarities in their properties, for example, regarding the range of soil colors. Often the parental material, primarily colluvium from weathered limestone and other types of rock, is gravelly or stony and so are many of the Lithic Xerochreptic Camborthids and other shallow soils that developed from it (NSM&LUP ET AL. 1994a,b). Grain size distributions exhibit broad variations, often including significant percentages of the coarser or gravel fraction. Within the fine earth fraction, the shallow soils generally tend to have a sand content of about 20% or more, a silt content of around 50% or more and a clay content of ca. 30% or less (NSM&LUP ET AL. 1994b). Consequently, textures range from silt to clay loam and loam to sandy and gravelly. While the latter is quite common, sandy textures are rather rare. Silty clay loams represent the dominant type of texture (NSM&LUP ET AL. 1994a). Structures are primarily fine subangular blocky to crumbly, although some soils exhibit little or no structure (NSM&LUP ET AL. 1994a,b). Almost all soils are strongly calcareous with $CaCO_3$ contents of 30% and more (NSM&LUP ET AL. 1994b). Calcium carbonate contents of around 50% are frequently found in Lithic Xerorthents (NSM&LUP ET AL. 1994b). Usually, a topsoil and a shallow subsoil horizon can be distinguished in deeper Leptosols, i.e. those with depths of over 19 cm (NSM&LUP ET AL. 1994a,b). However, no diagnostic (subsoil) horizons are described for Leptosols. Where a top- and a subsoil layer can be identified, clay contents are typically higher in the subsoil layer than in the topsoil layer (NSM&LUP ET AL. 1994b). Clay accumulation in the subsoil indicates

incipient soil development. Calcium carbonate is usually distributed uniformly throughout the soil profile but $CaCO_3$ contents can also be the highest in the topsoil (NSM&LUP ET AL. 1994b). Occasionally, few soft $CaCO_3$ concretions and carbonate coatings on gravel are observed (NSM&LUP ET AL. 1994a). Finally, the shallow soils are frequently associated with rock outcrops (see Table 4).

High clay and silt contents in the topsoils of all soils in the study area often lead to the formation of a hard, dry surface and surface sealing (NSM&LUP ET AL. 1994a, ABU-AWWAD & SHATANAWI 1997). While surface capping hinders wind erosion, it fosters runoff and all types of erosion by water, i.e. sheet, rill, and gully erosion (NSM&LUP ET AL. 1994a, SCHMIDT ET AL. 2006). Although in principle, all soils are affected by these processes, magnitudes vary largely with local conditions. Land use and agricultural practices strongly influence soil characteristics, runoff, and erosion. The shallow soils (Leptosols) are usually covered by a root mat which can be patchy or rudimentary but nonetheless stabilizes the soil and protects it against erosion (NSM&LUP ET AL. 1994a). Tillage destroys and removes this root mat and enhances stratification. The latter entails compaction in subsoils and accumulation of gravel at the surface, especially in shallow soils (NSM&LUP ET AL. 1994a, KHRESAT ET AL. 2008).

In many cases, plant growth and the productive use of soils (e.g. for agriculture) are limited by edaphic aridity, high contents of gravel and $CaCO_3$, salinity, and an inherently low to very low fertility due to the scarcity of organic matter. Moisture deficits occur primarily in shallow and gravelly soils that have a very low water retention potential (NSM&LUP ET AL. 1994a). In contrast, high percentages of clay ensure great water holding capacities in corresponding soils. However, they can also reduce the share of soil water that is available for plants. High clay contents in soils, typically found e.g. in Vertisols and Vertic or Typic Xerochrepts, are often associated with compaction which entails rootability problems and insufficient aeration (cf. KHRESAT & TAIMEH 1998, AL QUDAH 2001). Additionally, limited drainage can lead to a build-up of salts, especially in soils under agricultural use (cf. e.g. CHESWORTH 2008). Depending on their size and depth, surface cracks, which often form in clayey soils, may damage trees roots (AL QUDAH 2001). Low to moderate levels of salinity are usually observed in the subsoils of Xerochreptic Camborthids and Calciorthids, Lithic Xerochreptic Camborthids, Lithic Xeric Torriorthents, and Lithic Xerorthents (NSM&LUP ET AL. 1994a,b). Salinity it is a typical trait of the soils of the drier and transitional areas, whereas the Xerochrepts that cover most of the study area, are normally nonsaline. While gypsum percentages are usually very low, i.e. in the range of 2-4% or lower, calcium carbonate concentrations are typically (very) high. Elevated levels of $CaCO_3$ often lead to nutrient imbalances and thus can impede plant growth (NSM&LUP ET AL. 1994a). This applies to many Calcixerollic Xerochrepts and to almost all shallow soils.

The described limitations render all Leptosols inappropriate for most agricultural purposes, although these soils can be marginally suitable for the use as rangeland or even for forestry and agriculture with drip irrigation (NSM&LUP ET AL. 1994a). However, the individual suitability largely depends on local conditions, particularly the soil depth, relief, gravel content, and moisture availability at a given site.

The deeper soils of the transitional area, i.e. Xerochreptic Camborthids and Calciorthids, are likewise mostly unsuitable for rainfed agriculture, primarily due to their salinity, their gravel contents, and the generally low amounts of soil moisture. These soils usually possess a moderate or marginal potential for use as rangeland, for forestry, and irrigated agriculture (NSM&LUP ET AL. 1994a). In contrast, Vertic, Typic, and Calcixerollic Xerochrepts, which cover most of the study area, constitute the best soils for all purposes, including rainfed agriculture (AL QUDAH 2001). High $CaCO_3$ concentrations in many Calcixerollic Xerochrepts and deficits in soil moisture due to climatic factors reduce the suitability of the named soils to a moderate level (NSM&LUP ET AL. 1994a). Similarly, Vertic Xerochrepts are only moderately appropriate for tree plantations and forestry due to their vertic properties which may damage tree roots.

3.5 Vegetation and land use

The vegetation cover of Jordan largely depends on climatic characteristics; primarily annual precipitation amounts. Additionally, minimum and maximum temperatures during the winter and summer are decisive. The aforementioned aspects are included in the Emberger quotient based on which Jordan was divided into nine bioclimatological regions (AL-EISAWI 1985). Each region encompasses areas with similar climatological conditions for vegetation growth. With regard to the origin and composition of the actual present-day flora, four phytogeographical territories have been delineated, namely the Mediterranean, the Irano-Turanian, the Saharo-Arabian, and the Sudanian or Tropical region (ZOHARY 1962, AL-EISAWI 1985). The different territories are distinguished according to their dominant plant associations. This approach also places the country in the wider context of the MENA region in terms of common characteristic flora elements and plant associations. The four main phytogeographical territories can be further subdivided into vegetation units based on additional aspects such as topography, geomorphology, lithology (substrate), degree and nature of human influence, etc. (ZOHARY 1962, AL-EISAWI 1985, ALBERT ET AL. 2004). Thus, a more detailed vegetation map of the country can be drawn (see Fig. 10). However, in vast areas of Jordan, including the study area, the natural vegetation has been altered or overridden during the long history of human land use and agriculture. Therefore, in the following, characteristics of the potential natural and the actual (natural) vegetation are firstly outlined, before particularities of the land use and the corresponding parts of the actual vegetation are described.

Figure 10 shows the distribution and extents of the four flora regions and their subordinated vegetation units in Jordan. While the delineation of individual phytogeographical territories is mostly similar in all vegetation studies (FEINBRUN & ZOHARY 1955, ZOHARY 1962, AL-EISAWI 1985 and 1996, ALBERT ET
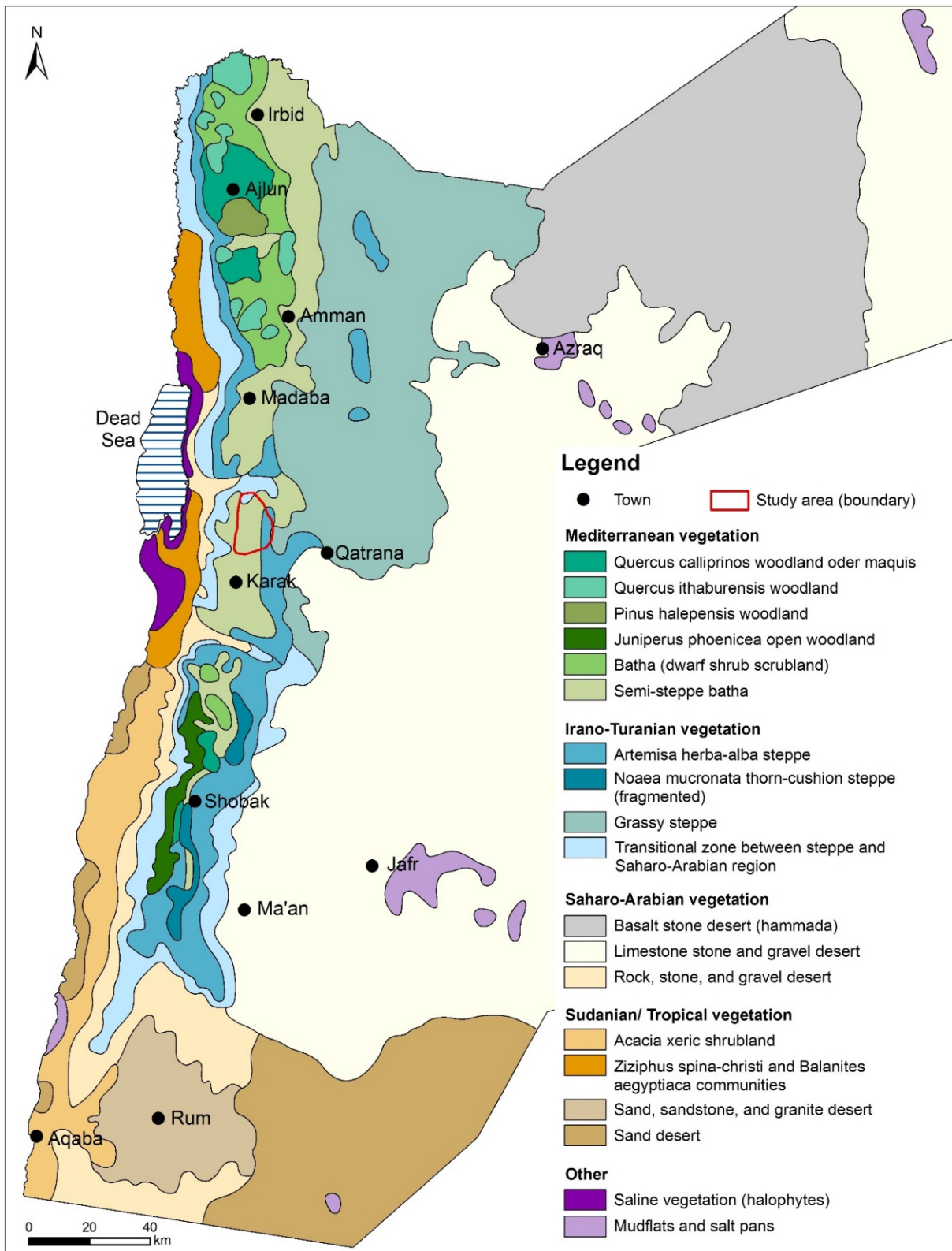
Fig. 10: Vegetation map of Jordan. Vegetation units are symbolized with different colors. In the legend, they are arranged according to the major flora regions. Vegetation units labeled as deserts (various types) commonly consist of open scrubland with different dwarf shrub communities, depending on substrates. Modified from Albert et al. 2004.

AL. 2004), more differences exist with regard to subordinated vegetation classes. Discrepancies mainly concern the number of classes, class names, and spatial extents of individual class, whereas the underlying broad concept is largely identical in all studies. The classification scheme is based on the distinction between areas with Mediterranean trees and shrubs (maquis, garrigue, batha, etc.), those with steppe vegetation consisting primarily of shrubs and grasses, and desert areas with sparse xerophytic vegetation. Different types of Mediterranean vegetation are found in the highlands of West Jordan. This flora region is surrounded by the Irano-Turanian steppe zone which shades off into the Saharo-Arabian desert vegetation that covers vast areas of eastern Jordan (see Fig. 10). The flora of the Sudanian or Tropical class is limited to the driest and hottest parts of the country, namely the Dead Sea and the Wadi Arava valley, and southern Jordan. The study area extends over two phytogeographical regions (see Fig. 10). Most of the area belongs to the Mediterranean region while the eastern quarter is typically assigned to the Irano-Turanian zone.

3.5.1 Flora of the Mediterranean and the Irano-Turanian territory

The Mediterranean flora appears as semi-steppe batha (ZOHARY 1962, ALBERT ET AL. 2004, DANIN 2003-2016b) or Mediterranean non-forest vegetation (AL-EISAWI 1985). It principally consists of dwarf-shrubs (chamaephytes) and bushes which are complemented by herbs, grasses, and some trees. In contrast to the batha, the semi-steppe batha is composed of more drought tolerant plants and many Irano-Turanian flora elements (ALBERT ET AL. 2004). Within the Mediterranean territory, it occupies the drier parts that are still characterized by annual precipitation amounts of 300 mm or more. The area of the semi-steppe batha corresponds to a transitional zone between the areas of the Mediterranean woodland or maquis and the steppe (DANIN 2003-2016b). Consequently, the vegetation contains primarily Irano-Turanian flora elements but also Mediterranean and bi- or pluriregional taxa (ALBERT ET AL. 2004). Plant communities in the study region are dominated by dwarf-shrub associations of *Ononis natrix* and *Ballota undulata* which are Mediterranean and pluriregional species respectively (FEINBRUN & ZOHARY 1955, ZOHARY 1962). They can often be complemented by *Noaea mucronata*, an Irano-Turanian dwarf-shrub, and *Sarcopoterium spinosum*, a Mediterranean chamaephyte which represents the plant indicator of the batha. However, the latter has not been found on the Karak Plateau (FEINBRUN & ZOHARY 1955, ALBERT ET AL. 2004, DANIN 2003-2016a,b). On rock outcrops and stony ground, Mediterranean shrubs such as *Capparis spinosa* and *Varthemia iphionoides* are found (ZOHARY 1962, ALBERT ET AL. 2004). These plants root in chasms. Other dwarf-shrubs that form part of the regional vegetation of the semi-steppe batha are *Rhamnus palaestinus*, *Calycotome villosa*, *Cistus spp.*, *Thymus capitatus*, *Tecrium polium*, and *Salvia dominica,* all belonging to the Mediterreanean flora, and the Irano-Turanian elements *Astragalus bethlehemiticus*, *Phlomis brachyodom*, *Verbascum eremobium*, and *Artemisia herba-alba* (AL-EISAWI 1985, ALBERT ET AL. 2004, DANIN 2003-2016a). The latter dominates the vegetation of the

adjacent steppe and hence, becomes a more prominent element of the flora composition towards the fringes of the semi-steppe batha area.

Besides dwarf-shrubs, the vegetation of the semi-steppe batha comprises numerous perennial herbaceous plants (hemicryptophytes), many of which are bi- or pluriregional species like *Dactylis glomerata*, *Hordeum bulbosum*, *Poa bulbosa*, and *Anchusa strigosa*, whereas others, such as *Psoralea bituminosa*, *Carlina libanotica*, *Scrophularia xanthoglossa*, *Sanguisorba minor*, *Eryngium glomeratum*, and *Convolvulus dorycnium* clearly belong to the Mediterranean flora (AL-EISAWI 1985 and 1996, DANIN 2003-2016a). *Echinops polyceras* is the only common hemicryptophyte of the Iranio-Turanian flora (ALBERT ET AL. 2004). Finally, the vegetation also contains several Mediterranean and Irano-Turanian annuals such as *Lathyrus cicera*, *Rhagadiolus stellatus*, *Crupina crupinastrum*, several *Bromus* species, *Minuartia picta*, *Chardinia orientalis*, and some steppe grass species of the family *Poaceae*, e.g. *Aegilops kotschyi*, *Boissiera squarrosa*, *Taeniatherum crinitum* (AL-EISAWI 1996, ALBERT ET AL. 2004). Often, Mediterranean geophytes like *Ophrys sphegodes*, *Asphodelus microcarpus*, and *Asparagus aphyllus* further contribute to the plant diversity of the area (AL-EISAWI 1985, 1996).

Trees, which rarely occur in the semi-steppe batha region, are usually pistachio (*Pistacia atlantica*), hawthorn (*Crataegus azarolus*), and almond (*Amygdalus communis*) trees (ZOHARY 1962, CORDOVA 2007). Isolated trees or groups of trees have sometimes been interpreted as relics of former woodlands and indicators of a potential climax or former natural vegetation which was degraded or altered by human influence, e.g. through forest clearance, agriculture, and animal husbandry with intensified grazing activity (AL-EISAWI 1996, CORDOVA 2007). Often, the Mediterranean maquis, garrigue, and batha are regarded as degraded woodlands or different states of vegetation within the desertification process (CORDOVA 2007, ALBERT ET AL. 2004). However, the former existence of woodlands on the Karak Plateau remains questionable. Certainly, the area and its vegetation have already been influenced by human activities for a long time (see 3.5.2 and 3.6). As a result, today, a transformed, seminatural to cultural vegetation is observed. Large similarities in environmental conditions on the Karak Plateau, on the one hand, and the wooded highlands further in the north and the south, on the other hand, further nourish the hypothesis of the former existence of forests that were destroyed by human activities (AL-EISAWI 1996). However, natural shifts in climate and slight topographic and bioclimatic differences between the Karak Plateau and the highlands in the north and the south could be responsible for some changes and differences in vegetation as well (ALBERT ET AL. 2004).

The eastern part of the Karak Plateau belongs to the Irano-Turanian phytogeographical region which is governed by different types of steppe vegetation (see Fig. 10) (ZOHARY 1962, AL-EISAWI 1985). The Irano-Turanian region represents a transitional zone between the Mediterranean territory and the desert region and is confined to areas with precipitation amounts of more than 100-150 mm and less than 250-350 mm annually (AL-EISAWI 1996, ALBERT ET AL. 2004). Due to the aridity that marks the dry timber line, the vegetation is generally characterized by a dominance of shrubs and the absence of trees (AL-

EISAWI 1985). Although herbaceous plants, grass species, annuals, and geophytes also occur, these play a minor role in comparison to the dwarf-shrubs (CORDOVA 2007). The dominance of dwarf-shrubs in today's steppe vegetation could be a result of anthropogenic influences, primarily the grazing of (farm) animals (ALBERT ET AL. 2004, CORDOVA 2007). Prolonged grazing pressure diminishes the natural occurrence of plant species that serve as fodder plants, such as many steppe grass species, and allows unpalatable and more resilient plants to thrive. Considering its composition, the present vegetation of the Irano-Turanian territory rather corresponds to a semidesert formation of low shrubs than to the term steppe, in the strict sense, which denotes open grassland. What distinguishes the steppe areas of Jordan from the actual semidesert and desert regions of the Saharo-Arabian and the Sudanian territory is a more or less closed vegetation cover and a different flora composition (see below) (DAVIES & FALL 2001, ALBERT ET AL. 2004). Grasses are supposed to have formed larger parts of the former natural vegetation of the Jordanian steppe before the onset of anthropogenic influences. The same is thought to apply to the potential climax vegetation. These assumptions are based on observations concerning plant successions at several sites after shrub clearance or protection from grazing (ALBERT ET AL. 2004, CORDOVA 2007). The natural vegetation of the steppe zone most likely included wild species of cereals before the advent of agriculture in the Neolithic. This could have been a favorable aspect that contributed to the early settlement of this area (ALBERT ET AL. 2004, CORDOVA 2007).

Plant associations vary broadly within the steppe region and reflect differences in local edaphic, topographic, and (micro) climatic conditions. Therefore, attempts have been made to define subregions within the steppe zone according to different flora compositions (ZOHARY 1962, ALBERT ET AL. 2004). However, the complex mosaic of local conditions and the generally transitional character of the vegetation form obstacles in this regard and led to mixed results (AL-EISAWI 1985). Nonetheless, in Figure 10, four subregions are shown for the Irano-Turanian territory. The delineated subregions or vegetation units may illustrate some general differences and tendencies in the corresponding flora. According to this concept, the eastern part of the study area falls into the vegetation unit of the *Artemsia herba-alba* steppe. Minor areas at the fringes of the highland belong to the grassy steppe and the transitional zone (ecotone) that shades off into the Saharo-Arabian flora region (see Fig. 10). *Artemisia herba-alba* is also the plant indicator for the Jordanian steppe regions in general. Together with *Noaea mucronata*, it occurs throughout the Irano-Turanian territory and beyond due to the broad ecological spectrum of both dwarf-shrub species (ALBERT ET AL. 2004).

Several plants, particularly dwarf-shrubs, spread in the process of secondary succession after human interference, e.g. through agriculture and grazing of livestock. This applies especially to dwarf-shrubs of the families *Chenopodiaceae* (e.g. *Salsola spp.*, *Anabasis spp.*, *Noaea mucronata*, *Hammada spp.*), *Asteraceae* (particularly *Artemisia herba-alba*), and *Fabaceae* (*Astragalus spp.*) (ALBERT ET AL. 2004, CORDOVA 2007). Thistle species such as *Cousinia spp.*, *Echinops spp.*, *Notobasis syriaca*, and *Gundelia tournefortii* also flourish under these circumstances (ALBERT ET AL. 2004). Although *Artemisia herba-*

alba occurs under grazing conditions in general, it is reduced and substituted by *Chenopodiaceae* under severe grazing, particularly in drier areas (ALBERT ET AL. 2004, CORDOVA 2007). Where *Artemisia herba-alba* is cut back and exploited for several purposes, herbs and grass species such as *Poa bulbosa* and *Carex pachystylis* succeed (ALBERT ET AL. 2004). On saline soils, *Artemisia herba-alba* is replaced by the dwarf-shrubs *Salsola vermiculata* and *Atriplex stylosa* (ALBERT ET AL. 2004, CORDOVA 2007). In agricultural fields at the desert fringe, *Artemisia herba-alba* is diminished in favor of *Hammada scoparia* and particularly *Anabasis syriaca,* which form deeper roots that remain in the soil during ploughing and removal of the vegetation cover (AL-EISAWI 1996, ALBERT ET AL. 2004). This allows these species to revive during fallow periods. Deep rooting also enables plants to access water from deeper layers of the subsurface and hence, represents one of the several adaption strategies to aridity and environmental conditions of steppes and semideserts. Synoptic descriptions of other, similar adaption strategies can be found in ZOHARY (1962) and ALBERT ET AL. (2004).

Apart from the aforementioned influences on plant associations, within the steppe zone, vegetation composition changes gradually from west to east. While *Noaea mucronata* is typically found in the slightly moister and cooler parts of the steppe region, *Artemisia herba-alba* is more thermophile and drought tolerant and covers rocky substrates (ALBERT ET AL. 2004, CORDOVA 2007). In the transitional area, towards the desert in the east (badia), the flora shows a gradual decrease in *Artemisia herba-alba* and an increasing appearance of dwarf-shrubs of the *Chenopodiaceae* family, such as *Anabasis syriaca* and *articulata*, *Atriplex stylosa*, *Halogeton alopecuroides*, *Hammada scoparia*, and *Salsola vermiculata,* (ALBERT ET AL. 2004). These represent typical plant species of the semideserts and deserts of the Middle East (DAVIES & FALL 2001). Intensive livestock grazing also fosters the invasion and spreading of Saharo-Arabian plant species such as *Anabasis articulata* and *Halogeton alopecuroides* in the steppe zone (ALBERT ET AL. 2004).

In conclusion, the vegetation of the Irano-Turanian territory, whether natural or synanthropic, can include dwarf-shrubs of Irano-Turanian (i.a. *Artemisia herba-alba, Astragalus spinosus*, *Anabasis syriaca*, *Noaea mucronata*) and Saharo-Arabian origin (*Anabasis articulate, Halogeton alopecuroides*) as well as bi-regional species from both territories (*Atriplex stylosa* and *leucoclada*, *Hammada scoparia*, *Salsola vermiculata*) (AL-EISAWI 1985 and 1996, ALBERT ET AL. 2004, DANIN 2003-2016a). Plant associations featuring *Artemisia herba-alba* dominate and characterize vast areas of the steppe region (AL-EISAWI 1996, DAVIES & FALL 2001, CORDOVA 2007). The perennial herbs that occur in the Irano-Turanian region encompass pluri-regional and Mediterranean species such as *Poa bulbosa* and *Asphodelus microcarpus/aestivus* (Al-Eisawi 1996, Danin 2003-2016a). Hemicrytophytes have been reported as part of the Irano-Turanian flora by AL-EISAWI (1996) and ALBERT ET AL. (2004), but may not be present in the area according to DANIN (2003-2016a). The geophytes that are discussed as possible members of the steppe flora of Jordan are *Ranunculus damascenus*, *Tulipa polychroma*, *Carex pachystylis*, *Ixiolirion*

tataricum, *Iris atrofusca* and *petrana*, which are all of Irano-Turanian origin, as well as *Urginea maritima* and *Sternbergia clusiana* which are Mediterranean and bi-regional species, respectively (AL-EISAWI 1996, ALBERT ET AL. 2004, DANIN 2003-2016a). The steppe vegetation also includes several annuals. According to ALBERT ET AL. (2004) and DANIN (2003-2016a) these comprise elements of the Irano-Turanian flora such as *Torularia torulosa* and *Loliolum subulatum*, bi-regional species like *Astragalus cruciatus* and *Lophochloa berythea*, and *Erucaria boveana* that is of Saharo-Arabian origin. The few taller shrubs and trees that may occasionally occur in the Irano-Turanian region usually belong to the species *Atriplex halimus, Retama raetam, Tamarix spp., Pistacia atlantica, Capparis decidua*, and *Ziziphus lotus* or *spina-christi* (AL-EISAWI 1985 and 1996, CORDOVA 2007). They are primarily found in some smaller subareas of the Irano-Turanian territory, including wadi or valley bottoms, and the western slopes of the Dead Sea valley (cf. DAVIES & FALL 2001). There, as well as on rock outcrops and in areas of higher altitudes, flora compositions often differ from the rest of the steppe region due to specific local conditions (ALBERT ET AL. 2004).

3.5.2 Land use

Vast parts of the study area are used for agriculture due to the favorable geomorphological and climatological conditions. The Karak Plateau forms the southern part of the Transjordanian Mediterranean Belt, a zone where agriculture has been practiced since the Neolithic (CORDOVA 2007). Today, probably about one third of the area of the Karak Governorate is under cultivation according to estimates by OTT (1998) (see Fig. 11). The semi-detailed survey of the NSM&LUP ET AL. (1994a) probably represents the most extensive and detailed study of the land use of the Karak Plateau. In the named survey, land use was mapped through the interpretation of satellite images in combination with ground truth. Results, i.e. the produced land use data, and their characteristics are closely linked to the details of the mapping procedure, e.g. the selected classes of land use and the recording date (season) and spatial resolution of the satellite images.

In the central part of the plateau and thus, the western, largest share of the study area, rainfed agriculture is the main type of land use (see Fig. 11). There, the flat to softly undulating relief, the deep soils, and annual precipitation amounts of around 300 mm provide favorable conditions for the cultivation of cereals, primarily wheat and barley (CORDOVA 2007). Agricultural practices can, but do not necessarily, include fallowing (OTT 1998). Areas of permanently uncultivated land typically correspond to convex upper slopes and hill crests with shallow soils or rock outcrops (NSM&LUP ET AL. 1994a). In the drier eastern part of the study area, where the relief is more rugged and soils are usually less well developed and shallower, the rainfed cultivation of field crops is confined to smaller areas with more favorable

conditions, such as footslopes and valley bottoms (see Fig. 11) (NSM&LUP ET AL. 1994a). In the transitional area toward the steppe, typically dry farming is practiced which encompasses specific crop rotations and one or more years of fallow at regular intervals in order to restore soil moisture reserves (LANCASTER & LANCASTER 1995a, OTT 1998). While in the western part of study area, precipitation is usually sufficient to sustain annual field crops even in dry years, in the eastern part, rainfed crop cultivation is limited to wetter years. Consequently, the limits of Mediterranean rainfed agriculture fluctuate with interannual variances in precipitation and shift to the east in wet years and to the west in dry years (OTT 1998, CORDOVA 2007). Despite precautionary measures like regular fallowing and sowing only after the first significant rainfall in the winter half-year, crop failures are reported to occur every four to five years (OTT 1998).
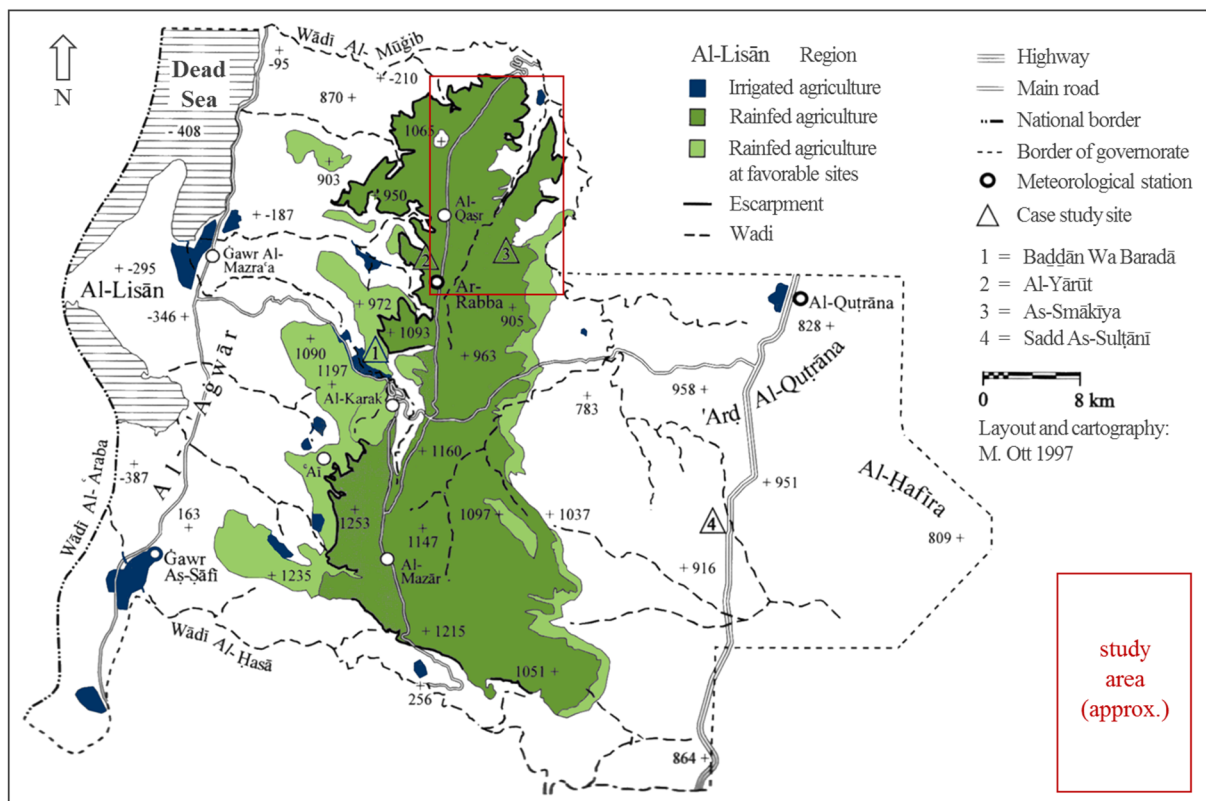
Fig. 11: Areas of different agricultural use within the Karak Governorate. Slightly modified from OTT 1998.

Among the agricultural plants grown on the tableland, annual crops, particularly cereals, predominate. Permanent crops, especially olive trees, are cultivated on a smaller scale. Barley and wheat are the most prevalent annual crops, although sorghum and legumes are also widely grown (LANCASTER & LANCASTER 1995a, CORDOVA 2007). On the Karak Plateau, annual crops are usually cultivated without irrigation and therefore can only be grown during the rainy season, i.e. in the winter half-year (see also Fig. 11). The prevalence of cultivated plant species varies across the table land due to differences in local conditions and requirements of individual plant species (LANCASTER & LANCASTER 1995a, OTT 1998). The amount and temporal distribution of necessary water supply are especially decisive in this regard

and can vary largely between species. For example, barley can usually be grown successfully in the drier steppe region while wheat is less well adapted to these levels of dryness (CORDOVA 2007). Permanent crops on the Karak Plateau are primarily olive trees, while other kinds of fruit trees are also cultivated. In the central part of the plateau, these can be grown without irrigation whereas in the drier, eastern areas permanent crops typically cannot survive without (supplemental) irrigation (OTT 1998). Therefore, most olive plantations are found in the central part of the plateau where precipitation is sufficient to sustain these trees. Towards the east, the number and extents of areas with permanent crop cultivation decrease (OTT 1998, CORDOVA 2007). On a smaller scale, vegetables, various fruits, and olives are grown within and in the immediate surroundings of settlements, i.e. around residential buildings (NSM&LUP ET AL. 1994a). This form of horticulture (usually home gardens) is practiced everywhere in the study area and normally requires irrigation. Frequently, supplemental irrigation, mostly in the form of drip irrigation, is applied to permanent crops all over the Karak Plateau, in order to increase crop yields (OTT 1998).

Livestock grazing is practiced everywhere on the tableland. In the drier eastern parts, it represents the main form of land use (LANCASTER & LANCASTER 1995a, AL-EISAWI 1996). In the summer half-year, nomads and local farmers graze their herds on agricultural fields on the Karak Plateau, thus exploiting the stubbles that remain from crop production in the winter half-year (LANCASTER & LANCASTER 1995a, OTT 1998). During the cooler, rainy winter season, from autumn to late spring, nomads and their herds typically retreat into the steppe and desert areas further to the east (OTT 1998, CORDOVA 2007). These seasonal movements (i.e. transhumance) represent an adaptation to local environmental conditions and spatial variances in these, which largely follow a longitudinal gradient. Grazing animals are mostly sheep and goats. Throughout the region, preferences for species of one or the other of the two genera vary, which partly may be explained by differences in grazing habits between sheep and goats (COR-DOVA 2007). Overall, the number of sheep is reported to be slightly higher than those of goats (LAN-CASTER & LANCASTER 1995a, OTT 1998). Reafforestation efforts are typically limited to areas with a minimum of 250 mm of mean annual precipitation. Thus, in most cases, for example northeast of as-Smakiya, reafforestation occurs in areas of natural range and grazing land (NSM&LUP ET AL. 1994a, OTT 1998). Natural woodlands were not found in the study area.

Some studies on land use and agricultural practices on the Karak Plateau (e.g. LANCASTER & LANCAS-TER 1995a, OTT 1998) also describe the use of cisterns and include sketch-maps of cistern sites. This indicates the role cisterns play in the lifestyle habits and economic activities (mainly farming and animal husbandry) of people in the region. Although cistern water can serve a variety of different purposes, it is mainly used to water livestock during the summer dry period (LANCASTER & LANCASTER 1995a). Today, flocks are increasingly supplied with water and additional fodder by trucks. This practice allows herds to stay longer in a given area (AL-EISAWI 1996). However, in combination with a higher number of grazing animals, this often leads to severe overgrazing which is associated with adverse effects on vegetation cover and biodiversity (see 3.5.1) (ALBERT ET AL. 2004, CORDOVA 2007). In this regard, the

natural range land of the transitional, steppe, and (semi-) desert areas is particularly at risk. Another major problem is the expansion of episodic agriculture towards the east, into the steppe region which is typically less resilient to (anthropogenic) disturbances. Tillage practices, including ploughing, do not only remove the vegetation cover but also effectively destroy the root mat of most plants and destabilize soil aggregates (NSM&LUP ET AL. 1994a, AL-EISAWI 1996). Resulting areas of bare soil are then more prone to erosion. Over time, secondary vegetation can develop. However, it usually consists of fewer plant species and thus represents a reduction in biodiversity (AL-EISAWI 1996, CORDOVA 2007). Despite these problems, for a variety of reasons, agricultural growth is still promoted by the government with grants and special conditions (OTT 1998, THE AGRICULTURAL COMMITTEE 2002, MINISTRY OF AGRICULTURE 2013/ 2014). However, more sustainable forms of agriculture are sought to reduce associated water consumption and soil erosion (cf. e.g. ABU-SHARAR 2006, AL-BAKRI ET AL. 2008, MINISTRY OF ENVIRONMENT 2006 and 2015).

3.6 Modern settlement structure and history of the area

Depending on the source, 12-13 individual settlements are identified in the study area (see Fig. 12 and Table 6). Resident numbers in the respective villages and towns ranged from less than 200, to well over 7,000, in 2015 (see Table 6) (DOPS 2015). In total, 23,614 people were assumed to be living in the study area. Over the last decades, the population has grown significantly, in the whole country, as well as in the Karak Governorate. While this growth mostly did not lead to the foundation of new settlements, existing settlements were considerably expanded (cf. DOS 1994, LANCASTER & LANCASTER 1995a, DOPS 2015). During this expansion, size proportions between individual settlements were either roughly preserved or amplified. Thus, the biggest settlements also experienced the highest increase in absolute numbers of residents. The largest towns, namely ar-Rabba, al-Qasr and Jad'a, are located along the King's Highway in the central part of the Karak Plateau, while the two smallest settlements, Hmud and Rashadiya, are situated in the rather remote southeastern part of the study area, at the desert fringe (see Table 6 and Fig. 12). In terms of administrative units, most of the study area belongs to the district of Qasr. Only the northern part of the terrain is assigned to the Mujib district. According to the latest census in 2015, slightly more than 3% of the country's population live in the Karak Governorate, while less than 10% of this share were citizens of the district of Qasr (DOPS 2015). In 2013, roughly two-thirds of the residents of the governorate were assigned to the rural population which is defined as living in settlements with less than 5,000 inhabitants (DOS 2013). The population density in the Karak Governorate in 2013 was estimated at ca. 73 persons per km^2, which is roughly equivalent to the mean figure for the whole country (DOS 2013). Based on the census data from 2015 (see Table 6), the population density in the study area itself is calculated at 145 inhabitants per km^2. More than half of the 23,614 residents

in the study area are living in ar-Rabba and al-Qasr. With respect to the size of these towns and the definition given above, the residents of ar-Rabba and al-Qasr, and thus, more than half of population in the area, can be classified as urban. Nonetheless, the study area in general represents a rural, averagely populated part of Jordan with a mainly agrarian character (see 3.5.2). Beyond the importance of agriculture in the area, the local economy has been characterized as a multi-resource system in which income is generated from various economic activities in different sectors (LANCASTER & LANCASTER 1995a).

Table 6: Settlements in the study area and corresponding population figures in 2015. The residential area of Mansura (see Fig. 12) is included in the village of Shihan below. Source: DEPARTMENT OF POPULATION STATISTICS (DoPS) 2015.

Settlement	Residents	Households	Settlement	Residents	Households
ar-Rabba	7,208	1,430	Ariha (Riha)	741	136
al-Qasr	6,127	1,261	Shihan	655	137
Jad'a	3,865	774	Mis'r	626	121
Mghayyer	1,522	317	Abu Traba	292	66
as-Smakiya	1,372	334	Hmud	284	72
al-'Aliya	749	126	Rashadiya	173	31

Villages and towns currently existing in the study area mostly formed during the last two hundred years, while each settlement is usually associated with one or more tribal group (JOHNS 1992, KANA'AN & MCQUITTY 1994, LANCASTER & LANCASTER 1995a). However, the area possesses a long history of human occupation that probably began in the Paleolithic. Most of the modern settlements have ancient roots and were built in the places or in the immediate vicinity of ancient ruins and other archaeological finds and remains (see Fig. 12). For example, the modern town of ar-Rabba roughly developed in and around the place of Roman Rabbathmoab or Areopolis (CALZINI GYSENS 2008) while the buildings of al-Qasr cluster around a Nabataean temple (GLUECK 1939, KANA'AN & MCQUITTY 1994). Traces and remains of the long history of human occupation in the area have been documented in several archaeological surveys, e.g. by GLUECK (1934), MILLER and PINKERTON (MILLER 1979, 1991) and in the *Limes Arabicus* Project (PARKER 1987, 2006). The most recent, broad survey of the area is that of the Karak Resources Project (e.g. MATTINGLY 1996a, MATTINGLY & PACE 2007). The project focused particularly on human-environment interactions during different periods of the past. Additionally, specific sites or subareas were examined in numerous other archaeological studies. The MEGA-Jordan online database (THE GCI ET AL. 2010, described in MYERS & DALGITY 2012) provides comprehensive information on all known archaeological sites of Jordan.

The history of human occupation is reconstructed from various sources, among which archaeological finds and remains are particularly important, since for some periods, such as e.g. prehistory, they represent the only source of information. While the abundance of finds and remains is associated with prosperity and expansion, the scarcity of traces from a certain era or culture is typically seen as evidence of deterioration and recession. Besides quantitative aspects, such as the number of sites and related objects,

qualitative properties like the type of relics (e.g. sherds, artifacts, ruins and other structures) can offer valuable information about a specific culture or period of history. Fig. 13 displays the number of sites that were associated with each period, based on archaeological finds and remains. The diagram roughly provides a visual summary of the settlement history outlined below.
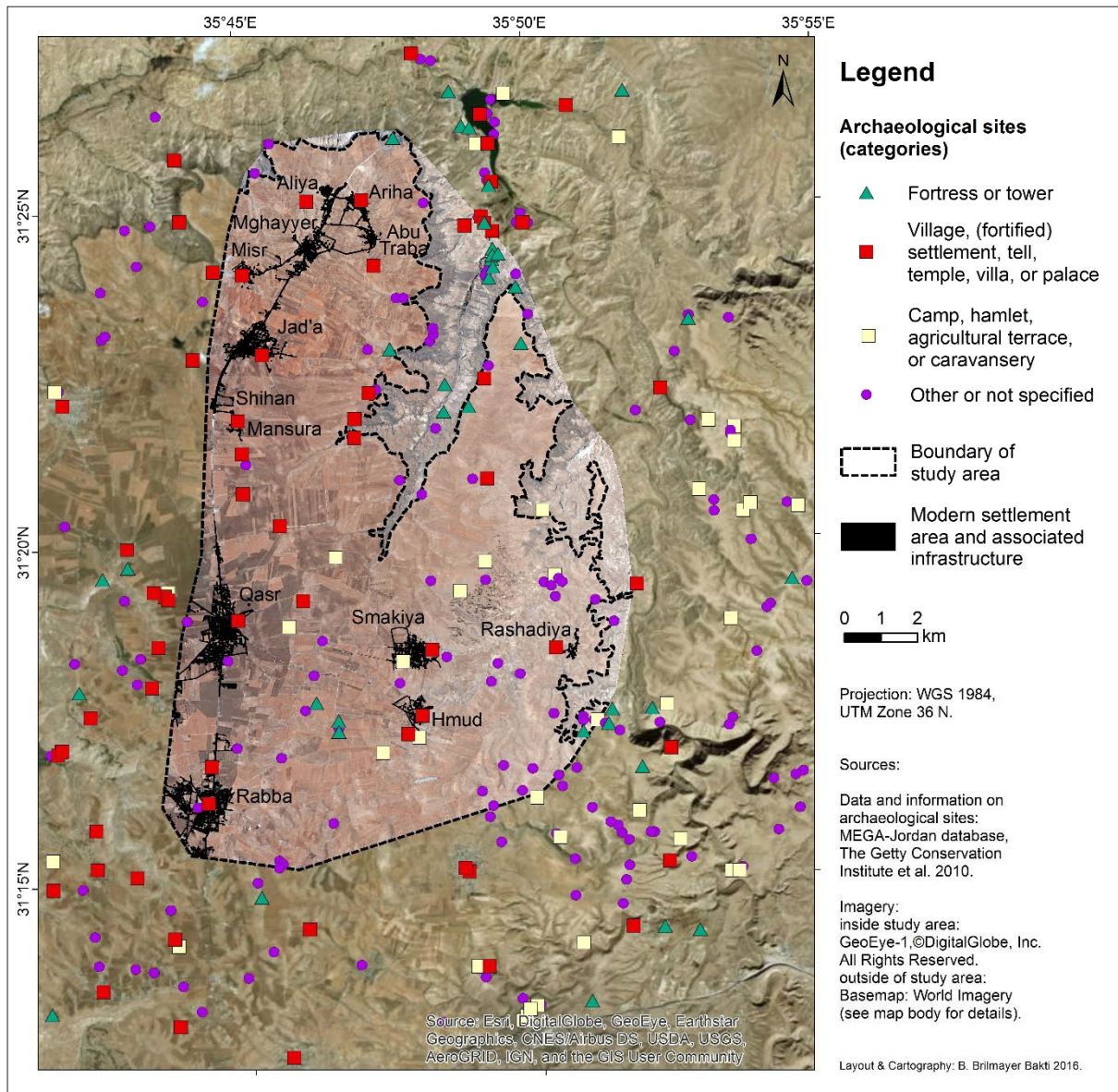
Fig. 12: Map of current settlements and archaeological sites within and in the vicinity of the study area. A total of 83 archaeological sites of different types (see categories) have been identified in the study area. Another 233 sites were found within a maximum distance of 6 km. Among the sites with structural remains, villages represent the most common site type. Many sites were used for different purposes during multiple periods of history (see Fig. 13). However, based on the broad definition of categories here, sites could usually clearly be assigned to one class. Where an overlap between different classes of site functions existed, sites were placed in the dominant category (according to the number of finds, remains and associated periods). The group of "other or not specified" sites primarily comprises places of surface finds (e.g. sherds and other artifacts).

Epoch	No. of sites in total	No. of new sites	
Paleolithic (1.5 Mio. - 17000 BC)	9	9	
Epipaleolithic (17000 - 8500 BC)	2	0	
Neolithic (8500 - 4500 BC)	2	1	
Chalcolithic (4500 - 3200 BC)	5	3	
Early Bronze Age (3200 - 2200 BC)	21	14	
Middle Bronze Age (2200 - 1550 BC)	13	3	
Late Bronze Age (1500 - 1200 BC)	13	2	
Iron Age (1200 - 331 BC)	39	20	
Hellenistic (331 - 63 BC)	11	2	
Nabataean (312 BC - 106 AD)	60	17	
Roman (63 BC/ 106 AD - 324 AD)	59	8	
Byzantine (324 - 636 AD)	53	2	
Islamic (636 - 1516 AD)	31	0	
Ottoman (1516 - 1918 AD)	46	2	

Fig. 13: Periods of history and number of sites that were associated with each period based on archaeological evidence. All known places of finds and remains were considered as archaeological sites, regardless of the type, the number and the significance of the discovered objects or structures. The category of new sites includes all places where traces from the respective period but not from any earlier one were found. Sources: chronology, periods and corresponding time spans: HOMÈS-FREDERICQ & FRANKEN 1986 and DEPARTMENT OF ANTIQUITIES n.d., information on archaeological sites: MEGA-Jordan database: THE GCI ET AL. 2010.

Knowledge about prehistoric periods, i.e. the Paleolithic, Epipaleolithic, Neolithic, and Chalcolithic, is still rather limited and associated with larger uncertainties. Archaeological evidence of these periods was found only at a few sites and mostly dated to the Paleolithic and the Chalcolithic periods (see Fig. 13) (MILLER 1979, KOUCKY 1987a, WORSCHECH 1992). The number of sites with traces from the corresponding eras started to increase from the Chalcolithic onward, including many locations in the steppe and desert regions, east of the study area (GREEN 2004a). This expansion might have been related to favorable, moister climatic conditions during these times (cf. e.g. MACDONALD 2001). Concerning the plateau area, a significant increase in the number of sites, well beyond that of previous times, is documented for the Early Bronze Age (see Fig. 13). However, only the first half of the period was characterized by prosperity, population growth and expansion, whereas the second half of the Early Bronze Age was associated with a decrease in local population and an abandonment of sites, probably due to an aridification of climate, among other reasons (HARLAN 1985, HARRISON 1997, GREEN 2004a). Aside from some outstanding places which exhibit signs of continued occupation, relatively few sites were recorded for the Middle and the Late Bronze Age, particularly in the steppe zone (WORSCHECH 1992, GREEN 2004a). Although drier climatic conditions probably continued during the Iron Age (e.g. MAC-DONALD 2001), an unprecedented prosperity with significant settlement activity occurred which also led to the occupation of many new sites that apparently had not been used before (see number of new sites in Fig. 13) (PARKER 1992, WORSCHECH 1992). However, given the suggested aridity, this expansion and prosperity may have been limited to the plateau area and a few suitable locations, e.g. adjacent to wadis, further to the east (GREEN 2004a, PORTER ET AL. 2014).

During the Iron Age, the study area was part of the tribal kingdom of Moab (DEARMAN 1989, LABIANCA & YOUNKER 1998, ROUTLEDGE 2004, ABUJABER 2007). An important relic, the Mesha stele or Moabite stone, was preserved from this time and found at Dhiban, in the vicinity of the study area. The inscription of the stone provides valuable information on the Moabite culture and living conditions during that time. To further fortify the eastern border of the Moabite kingdom, watchtowers, forts and similar structures were established around the fringe of the plateau (see also Fig. 12) (KOUCKY 1987a, WORSCHECH 1992). It is assumed that, again, a decline set in towards the end of the Iron Age and for this reason archaeological evidence of the Persian (ca. 539-331 B.C.) and the Hellenistic (ca. 331-63 B.C.) period is either absent or comparatively scarce (MILLER 1991, PARKER 1992, WORSCHECH 1992, GREEN 2004a). The limited number of sites and traces from the Hellenistic period is commonly seen as being linked to a smaller sedentary population in the study area during this time. However, numerous finds and remains at many places have been associated with the Nabataean culture (see Fig. 13). The era of the existence of the Nabataean kingdom, which comprised vast areas of Jordan, including the Karak Plateau, largely overlapped with the Hellenistic and the early Roman period. This coexistence, as well as possible similarities, resulting uncertainties and misattributions of finds and remains could have led to a blurred image of that time and may offer an additional explanation for the limited number of sites, structures and objects that have been dated to the Hellenistic period (PARKER 1992).

During the Nabataean and the partly contemporaneous Early Roman period, the region experienced its greatest prosperity and population density (PARKER 1992). This is reflected by the abundance of finds, remains and archaeological sites attributed to these two periods (see Fig. 13) (also cf. PARKER 1987 and 2006, MILLER 1991). The prosperity of societies and communities in the region were probably primarily a result of favorable socio-political circumstances, although moister climatic conditions might have contributed as well, at least during some phases of the Nabatean and the Roman periods (PARKER 1992, GREEN 2004a). The formation of larger states brought about several benefits, such as new opportunities for trade and exchange and enhanced protection against outside aggressors. The improvement and fortification of major traffic routes, such as the *Via Nova Traiana*, which in large parts corresponds to today's King's Highway, represented important achievements and cornerstones of development during Roman times (MATTINGLY 1996b, PARKER 2007). In terms of security and protection, monitoring and controlling access to the Karak Plateau especially from the eastern desert region, were of utmost importance. This can be inferred from the reoccupation and re-establishment of many Iron Age watchtowers and the construction of several additional towers, forts and similar structures in the Nabataean and the Roman era (also see Fig. 12) (KOUCKY 1987a). When the tableland was part of the Roman client kingdom of Nabataea (until 106 AD) and later the Roman province of Arabia, the desert frontier that formed its eastern border was fortified with the *Limes Arabicus* to protect the highland in the west against invaders from the east (GREEN 2004b, PARKER 2007). During Late Roman times (ca. 135-324 AD) again, apparently a period of decline and site abandonment occurred, which was most noticeable in the steppe zone (KOUCKY 1987a, MILLER 1991, PARKER 1992). Climate change probably cannot explain

this recession satisfactorily, especially since recent studies (GREEN 2004a, LEROY 2010) suggest rather favorable climatic conditions with increased moisture availability for this time, in contrast to the dry period mentioned in older studies (KOUCKY 1987b). In the 4th and 5th century, i.e. the Early Byzantine period, the region flourished and the local population probably increased again, as numerous finds and remains from this period indicate (PARKER 1992). Most likely, this prosperity was enabled by persistent, favorable socio-political circumstances and suitable, slightly cooler and moister climatic conditions (KOUCKY 1987a, PARKER 1992, LEROY 2010). The continued maintenance of the Roman Limes may have played an important role in this regard, as it probably significantly contributed to the security and protection of the highland area. By the 6th century, towards the end of the Byzantine period, a notable decline had set in which most likely involved a depopulation of the area and an abandonment of sites, especially in the eastern parts of the tableland (GREEN 2004a). In the course of socio-political changes, the *Limes Arabicus* and most frontier forts were also given up, which altogether must have caused a renewed vulnerability of the area, especially around the desert fringe (PARKER 1992, 2007). Climate change that led to an increased aridity probably further contributed to the observed deterioration of the area, which continued well into the Early Islamic period (GREEN 2004a, LEROY 2010).

The number of occupied sites and population figures remained at comparatively low levels throughout Islamic times, including the Ottoman era. During the Islamic period, the region was subsequently ruled by different Muslim dynasties, namely the Umayyad, the Abbasid, the Ayyubid and the Mamluk. Although a certain degree of general settlement continuity has been suggested, several major and minor fluctuations probably occurred over the centuries in terms of the number of occupied sites, the population size and the role and significance of the area within the larger empire (JOHNS 1992, MILWRIGHT 2008). These variations included short-term, as well as long-term, consequences of changes that happened within a specific era or between different periods of history. According to the available data and records, on the Karak Plateau, the sharpest decline in settlement and agricultural activities apparently occurred in the Early Islamic, i.e. the Umayyad period (JOHNS 1992, PARKER 1992, LEROY 2010). Up to now, very few archaeological finds and remains have been associated with the Abbasid period (cf. MILLER 1991). Around the 12th century and the era of the Crusaders, the area obviously experienced some prosperity again, although this positive general trend was most likely interrupted by shorter episodes of upheaval, insecurity and destruction (JOHNS 1992). The Ayyubid and the Mamluk periods are also considered times of rural prosperity which lasted until the 16th century (ABUJABER 2007; cf. also MILLER 1991, WORSCHECH 1992, LANCASTER & LANCASTER 1995a). In the following centuries, local Arab tribes gained influence and power. A general tendency towards nomadic pastoralism has been associated with this time (JOHNS 1992, MILWRIGHT 2008). Finally, towards the end of the 19th century, a gradual return to sedentary agriculture could be observed and most of the currently existing settlements were built (JOHNS 1992, LANCASTER & LANCASTER 1995a).

Throughout history, the role of the Karak Plateau and the study area was predominantly that of an agricultural back country whose importance otherwise resulted from its strategic position at the crossroads of important north-south and east-west connections (cf. e.g. MATTINGLY 1996b). Military, trade, caravan and pilgrim routes of all periods passed through the area, linking the Arabian hinterland with the Mediterranean coast and the major cities and centers in the north, e.g. in the Decapolis region and Syria, with the Red Sea and Egypt in the south (LANCASTER & LANCASTER 1995a, MATTINGLY 1996b, ZAYADINE 1985, 2007). Local produce from agriculture and livestock farming was primarily intended for covering the demands of the local population, while any surpluses were traded regionally or served as supplies for travelers crossing the tableland (LANCASTER & LANCASTER 1995a). Over the centuries and millennia, the number of settlements and the size of the associated population changed repeatedly, indicating several alternating periods of prosperity and decline of various intensities. These variances have been attributed to changes in socio-political circumstances and climate. While individual triggers or causes and their significance usually cannot be determined clearly, the coincidence and interplay of cultural and environmental factors represent the most likely explanation for the above outlined fluctuations (GREEN 2004a). Marginal areas such as the transitional steppe zone were often affected most severely and changes became most noticeable there, which shows the particular sensitivity and vulnerability of these areas.

4 Methods and raw input data

This chapter consists of two parts, the first of which (4.1) focuses on the methods applied in the processing of the raw input data and the preparation of the materials (box 1 and 2 in Fig. 14) used in the subsequent analyses. Details of the main analyses (box 4 in Fig. 14) are then presented in the second part (4.2). The prepared information layers (box 3 in Fig. 14) which are employed in the analyses are described in chapter 5. An overview of the study design, the overall workflow and the involved materials and methods are given below.

1. RAW INPUT DATA	2. DATA PROCESSING	3. INTERMEDIATE OUTPUT
from field work: • GPS points • photographs and measurements remote sensing products: • satellite images • DEMs (based on satellite imagery) other data: • geological information • archaeological information • precipitation records	• preprocessing of satellite images: orthorectification, atmospheric corrections, pan-sharpening, etc. • mapping and image interpretation: on-screen digitization • semi-automatic image analysis: feature extraction and image classification • hydrological analysis • examination, editing, and integration of data in GIS; generation of derivative and ancillary data • spatial interpolation	• (RWH inventory: see 5.) • hydrological information (drainage lines, catchments) • precipitation maps • Land Use/Land Cover data and map • data on buildings/rooftops • revised DEM and slope map • revised geological data • revised, selected, and compiled archaeological data

5. FINAL RESULTS	4. ANALYSES
• inventory of RWH structures (database) • storage capacities (of cisterns) • characteristics of RWH sites • distances and possible spatial relationships between features • comparison of findings for old and modern RWH facilities • general RWH potential, specific RRWH potential → data, figures, tables, and maps	• extraction of site information from intermediate output layers • database queries • determination of distances between features (near analysis) • computation of local runoff (RWH potential) under different precipitation scenarios • computation of runoff from rooftops (RRWH potential) under different precipitation scenarios

interpretation and discussion

Fig. 14: Overview of the different datasets and processes employed in the present study. Stages one, two, and four are described in this chapter while the intermediate and the final results are presented in chapters 5 and 6. All intermediate results (box 3), except for the RWH inventory, are included in chapter 5 as they have primarily been created as input layers for the actual analysis (box 4). The RWH inventory also represents one of the major outcomes of the present study and therefore is described in detail in the final results section (chapter 6).

4.1 Data acquisition and processing

In order to be able to address the research questions of the present study, the necessary data and information (materials), as well as suitable methods, analyses, and procedures had to be identified. Once the required materials were defined, potential sources, appropriate methods of data acquisition, and suitable processing steps needed to be determined. The selection of adequate materials and methods was based on a balanced consideration of different aspects such as availability, feasibility, and optimal suitability for the objectives of the study.

Two different approaches were adopted for the collection of necessary information: fieldwork and remote sensing. Both strategies mutually complement each other, as remote sensing can enable the up-scaling of findings from fieldwork while the latter provides ground truth for the assessment and calibration of remotely sensed data. Although the most accurate data on the characteristics of an area may be obtained through field surveys, this also represents a time and cost intensive method of data acquisition. Therefore, fieldwork has been applied primarily where it was indispensable. Large portions of the required information were collected through remote sensing, i.e. the recording of data from a distance, usually from air or space. Remote sensing techniques represent time and cost efficient strategies especially for the detection of larger datasets. However, they are not applicable to all kinds of information and research questions and their advantageous utilization largely depends on the availability of suitable raw products (e.g. images) and adequate analysis techniques.

Complementary to the information that had to be gathered through fieldwork and remote sensing, some readily available datasets could be obtained e.g. from local authorities and online resources (see section 4.1.5). As the quality of input information largely influences the results of the subsequent analyses, special attention was given to the stage of data preparation. Significant efforts were dedicated to ensure a high quality in the prepared datasets that were used as input for the following analyses (see Fig. 14).

4.1.1 Fieldwork: mapping and documentation of rainwater harvesting structures

A comprehensive inventory of the currently existing RWH facilities in the area was a prerequisite for all further analyses of RWH strategies. Therefore, in late summer 2010, a first field survey was conducted which concentrated on mapping cisterns. These underground water storage containers are discernable on the earth's surface only by small, often fortified manholes, which provide access to the interior of the cisterns. Representatives of local authorities and residents showed the location of cisterns and contributed further valuable information, e.g. on the ages, modifications, and current uses of these cisterns. Due to the abundance of cisterns and other RWH structures, the survey focused on a subset of

objects, namely old cisterns as indicated by the local guides. The alleged age was used as a working hypothesis which should be substantiated by further evidence, e.g. construction details suggesting a specific building period. Field records encompassed notes and photographs documenting the condition, current use, construction characteristics, depth, water content, and further details on each cistern. Documentation of all available information accompanied the actual mapping, i.e. the registration of the positions of individual objects (see Fig. 15).

The mapping was conducted with a professional hand-held GPS device, the Magellan® MobileMapper™ 6. Its GPS accuracy has been stated at 2-5 m (real time SBAS) or 1-2 m with appropriate post-processing (MAGELLAN NAVIGATION 2008). The actual remaining position error, however, essentially depends on environmental conditions during recording, particularly the number and characteristics of satellites available for positioning. Given the advances in this field in recent years, now real time GPS accuracies of less than 2 m (SBAS, horizontal RMS) are possible (TRIMBLE NAVIGATION LIMITED 2013). With 9-10 satellites commonly available, and open sky view during recording, the estimated position error (EPE) automatically determined by the device was ranged between 1 and 2.5 m, with a mean EPE of 1.4 m. Double registration of a few cistern locations on different days and subsequent comparison of resulting points yielded differences of 0.3-1.4 m and 0.75 m, on average. These comparatively low discrepancies, which include possible slight aberrations in recording positions, further point to a satisfactory GPS accuracy for the given task.

During the second field survey in late summer 2011, some of the previously mapped cisterns were studied in detail and ground truth data was collected to assess the reliability of remotely sensed information. Field inspections again focused on cisterns as their detection with remote sensing commonly comprises greater ambiguities due to the variable appearance and small size of their above-ground components that led to their identification. Nonetheless, for a sample set of 15 cisterns, the mapping approach with remote sensing could be confirmed since all features were found exactly at the location predicted from satellite image interpretation (see chapter 4.1.2.2). In addition to the objects recorded during the first field survey and those mapped with remote sensing, two more cisterns were discovered during the second field survey which previously had not been identified on the satellite image. Although this suggests a slight underestimation resulting from the remote sensing approach, the conducted survey is insufficient for a final appraisal of the method which would require further investigations comprising a systematic sampling strategy, a larger sample size, and more ground truth data. Based on the present study, false positives, i.e. structures misinterpreted as cisterns on the satellite image, cannot definitely be excluded. This applies mainly to the dataset of possible additional cisterns (see section 4.1.2.2). Yet, the collected ground truth data and small sample survey allow for a first positive preliminary estimation of the applicability of the remote sensing supported mapping approach.

A sample set of 7 allegedly old cisterns located in different parts of the study area was chosen for closer examination. Criteria for the selection were old age, as suggested by promising surface characteristics

and proximity to known archaeological sites, appropriate location, with regard to a widespread and balanced spatial distribution of sample features, and accessibility. The interior of the chosen cisterns was investigated to reveal further construction details as well as typical shapes and storage volumes (see Fig. 15). Digital laser distance measuring was applied at crucial spots within the cisterns to capture their dimensions. Individual water storage capacities were then calculated based on these measurements and three-dimensional geometric figures, which corresponded approximately to the actual shape of the cistern interior (cf. KOELBEL 2009 following a similar approach). Digital photography was employed to document details of the interior and the construction, e.g. the condition and type of plaster lining (see Fig. 15). Findings from inside inspections provided further valuable clues for age estimation of objects.

Fig. 15: Mapping and inspection of cisterns. Logging of cistern locations with a hand-held GPS device and exploration of depth and water level (a). Due to narrow manholes representing the only entrance, most cisterns can solely be accessed with a rope ladder despite their large subterranean dimensions (b, c). Photographs: B. Brilmayer Bakti (a) and A. Vögele (b, c).

In the framework of the second field survey, some exemplary soil profiles were also studied. In addition to field observations and descriptions, samples were taken for subsequent analysis of basic soil parameters such as grain size distribution. Findings are described by VÖGELE (2012). Information on soils is closely related to water harvesting strategies since soil characteristics play a key role for surface runoff generation, water storage potential in the soil profile, and (potential) land use, particularly agriculture.

4.1.2 Satellite imagery, image interpretation, and related data processing

Very high resolution (VHR) satellite imagery was applied for two purposes: the generation of a digital elevation model (DEM) of the relief of the area (see 4.1.3) and the derivation of data on land cover and

specific features such as buildings, drainage lines, and RWH structures (see chapters 4.1.2.2-4.1.2.5). Two different sets of satellite imagery were employed, both of which belong to the domain of optical remote sensing products. Details on the images and their processing are given in the following sections. Two main approaches can be distinguished regarding the interpretation of the imagery for the production of thematic maps and layers: the visual-manual method, including on-screen digitization by an expert (see 4.1.2.2) and the semi-automatic image analysis process with the software Feature Analyst (see 4.1.2.3-4.1.2.5). Some advantages and limitations of the application of remote sensing have already been pointed out above (section 4.1). Primarily, in the context of the present study, remote sensing allowed for the time and cost efficient acquisition of large datasets of new, nonexistent information, thus providing access to quantitative aspects. This is indispensable for comparative analyses, the tracing of (spatial) patterns, and representativeness and robustness of results.

4.1.2.1 Satellite imagery: characteristics and preprocessing

GeoEye-1 imagery from late summer 2010 was employed for all mapping purposes (see following chapters). This choice was based on image suitability, stock availability, and economic considerations. The raw data bundle obtained encompassed four multi-spectral and one pan-chromatic band with 2 m and 0.5 m spatial resolution respectively. At the time of acquisition, this was the highest spatial resolution commercially available due to governmental restrictions. Specifications of the GeoEye-1 sensor and the acquired imagery product are displayed in Table 7. In order to cover the study area, two datasets recorded with a time difference of about one week had to be combined (see Fig. 16). Prior to its interpretation, the imagery was subjected to a thorough preparatory processing (preprocessing) including orthorectification, atmospheric corrections, and pan-sharpening (resolution merge). This procedure was implemented to ensure the best possible image interpretation results. For further details on the relevance of thorough image preprocessing also see e.g. LUEBKER & SCHAAB (2008). In the present case, preprocessing especially enhanced inter-image matching of the two complementary datasets covering the study area. All processing steps were conducted using ERDAS IMAGINE, unless stated otherwise.

Raw source images were geometrically corrected to eliminate distortions resulting from relief and angle of view during image recording. In contrast to true orthorectification, the procedure applied here only accounts for the correction of terrain displacement (cf. LILLESAND ET AL. 2015). True orthorectification is applied mainly to urban areas and requires VHR digital surface models (DSM) which accurately represent the relief and heights of large surface objects such as buildings. Since necessary DSMs are still costly and not commonly available, true orthorectification is usually only applied where it is indispensable, due to characteristics of the study area and/or research questions. For the purposes of the present study, the generation of orthoimages in the sense of terrain corrected satellite images was sufficient, particularly since the study area has a rural character and lacks tall buildings or forests which would alter the surface relief significantly.

Table 7: Specifications of the GeoEye-1 sensor and the acquired Geo imagery product. Two image tiles were obtained as bundles comprising five files respectively, one for each of the four multispectral (MS) bands and one for the panchromatic (Pan) band. Source: GEOEYE 2009, 2010.

Selected parameters of satellite:		Selected parameters of imagery:	
geometrical resolution		number of source images	2
Pan (nominal at nadir)	0.41 m *	bit depth	11 bit
MS (nominal at nadir)	1.65 m *	dynamic range adjustment	off
spectral range and bands	450-800 nm (pan)	product type / processing level	Geo™ (bundle)
	450-510 nm (blue)		standard geometric correction
	510-580 nm (green)		radiometric correction
	655-690 nm (red)		rectification to a map projection
	780-920 nm (NIR)	coordinate system	WGS 1984, UTM Zone 36 N
radiometric resolution (dynamic range)	11 bit	acquisition date and time	2010-07-21, 08:35 GMT (image 1) 2010-07-29, 08:27 GMT (image 2)
swath width (at nadir)	15.2 km	file format	GeoTiff
revisit time	ca. 3 days	percent cloud cover	1% (image 1) / 0% (image 2)
orbital altitude	681 km	supplementary data (included with product)	sensor camera model in rational polynomial coefficient (RPC) format, metadata text file
launch date	September 6, 2008		

* resampled to 0.5 m (Pan) and 2.0 m (MS) resolution for product delivery due to governmental restrictions at the time of acquisition.

During orthorectification, the terrain was represented by the DEM derived from ALOS PRISM satellite images (see chapters 4.1.3 and 5.3). In order to match the resolution of multispectral and panchromatic images, the DEM was resampled to 2 m and 0.5 m resolution respectively. Orthorectification in ERDAS IMAGINE further employed a geometric model specifically designed for GeoEye-1 imagery. The model is configured to incorporate the RPC files accompanying each GeoEye-1 image.

To ensure an adequate location accuracy, GPS reference data from fieldwork was included in the orthorectification process. Due to the absence of other points with higher spatial accuracy, location data of previously mapped cisterns served as ground control points (GCP). For the first source image covering the northern part of the study area, GPS points of 16 cistern locations were used, while 12 GCPs were employed for the rectification of the second source image covering the southern part of the study area. The GPS data use as GCPs were selected based on two criteria. Firstly, the establishment of the relationship between recorded GPS points and visible features in satellite images had to be unambiguous, i.e. the respective cisterns needed to be clearly discernible in the images. Secondly, a balanced and widespread distribution of GCPs over the area was important for the best outcomes of the rectification and referencing procedure. Remaining root-mean-squared errors (RMSE), resulting from the orthorectification process, amounted to around 2 m on average and more specifically to 1.76 m for the northern and 2.36 m for the southern source images.

Before conducting further preprocessing steps, a layer stack was created in order to compile the images of all MS bands into one single file for each source image while preserving individual bands. Images then were clipped to the extent of the study area which was equivalent to the coverage of the ALOS-based DEM and hence the extent of orthorectification (see Fig. 16). Subsequently, data were subjected to atmospheric corrections with ATCOR, an add-on program for ERDAS IMAGINE (see NEUBERT &

MEINEL (2005), GEOSYSTEMS (2011), and RICHTER & SCHLAEPFER (2011) for a detailed description). The module ATCOR3 was applied allowing "for the radiometric correction of satellite imagery over rugged terrain to remove atmospheric and topographic effects" (GEOSYSTEMS 2011, p. 102). Typically, this is believed to improve results of subsequent image interpretation, particularly with (semi-)automatic classification procedures (LUEBKER & SCHAAB 2008, GEOSYSTEMS 2011). The elimination of atmospheric and topographic influences and hence, the computation of actual surface reflectance values, is especially important when images recorded at different points in time should be merged or compared (NEUBERT & MEINEL 2005). Within the present study, atmospheric corrections substantially improved inter-image matching of the two source images.

To correct topographic effects in ATCOR3, the terrain itself, as well as the associated information such as slope, aspect, shadow, and sky view, must be represented digitally. Once a DEM is provided, all other necessary layers can be derived from it, either in ATCOR3 or other suitable programs, e.g. ArcGIS. Here, the DEM based on ALOS PRISM data has been employed as it offered the highest spatial resolution of all DEMs available for the present study. It was resampled to half meter pixel size to fit the resolution of the panchromatic images and fulfill optimal conditions of one quarter of the image resolution (cf. GEOSYSTEMS 2011) for the MS layer stacks. The preparation of the terrain files, i.e. the DEM and the aforementioned derivative information layers, also encompassed several filtering, smoothing and correction procedures in order to avoid artifacts in the final ATCOR3 corrected output images (cf. NEUBERT & MEINEL 2005, RICHTER & SCHLAEPFER 2011). Details on the applied methods can be found in chapter 4.1.3.

The necessary input parameters for the atmospheric correction in ATCOR3, such as date and time of acquisition and recording details, were retrieved from the metadata file of the GeoEye-1 imagery. Metadata, more precisely radiometric information contained therein, also allowed to create and use a sensor calibration file that specifically matched the concerned imagery (cf. RICHTER & SCHLAEPFER 2011). Atmospheric conditions represented by the atmospheric model, atmosphere type, and scene visibility, were estimated, tested, and adjusted in order to identify optimal values and choices.

In the output, i.e. the atmospherically corrected images, reflectance values of dark objects such as dense vegetation, dark asphalt, and shadow areas, were often so small that they resulted in no data areas; appearing as "holes" in the final images. A stepwise procedure has been suggested to attain higher reflectance values to solve this problem (GEOSYSTEMS 2012). Initially, scene visibility values should be raised. Setting them to the maximum of 120 km yielded optimal results for the MS images of the present study. However, this procedure was insufficient for the panchromatic images. Here, the sensor calibration file had to be additionally modified by adding an adequate offset. A trial and error calibration approach needed to be taken to find the most suitable offset value in combination with an appropriate scene visibility. Too high offset and/or scene visibility values resulted in hazy output images, while too low numbers did not raise reflectance values sufficiently. Optimal offset values varied and had to be

identified for each source image separately. Alternatively, atmospheric corrections could have been skipped for the panchromatic images and limited to the MS layer stacks. Although the performance of atmospheric corrections on panchromatic images is reported to be less decisive, it still enhances the quality of output imagery. Therefore, ATCOR3 was also applied to panchromatic images to ensure best results, i.e. clearer and sharper ("crisp") preprocessed images.

Atmospheric corrections were the most computationally intensive part of the preprocessing chain, demanding extensive computing resources and entailing long computing times. This is caused by the complexity of the correction procedures, on the one hand, and high data volumes due to the fine spatial resolution of the satellite imagery, on the other. Symptomatically, the second (southern) source image had to be split into two parts for the processing in ATCOR3 due to limitations in computing resources and tolerable temporary file size. The empiric calibration approach that had to be adopted in large parts (see previous paragraph) further contributed to the complexity and costliness (in terms of time) of this part of the preprocessing.
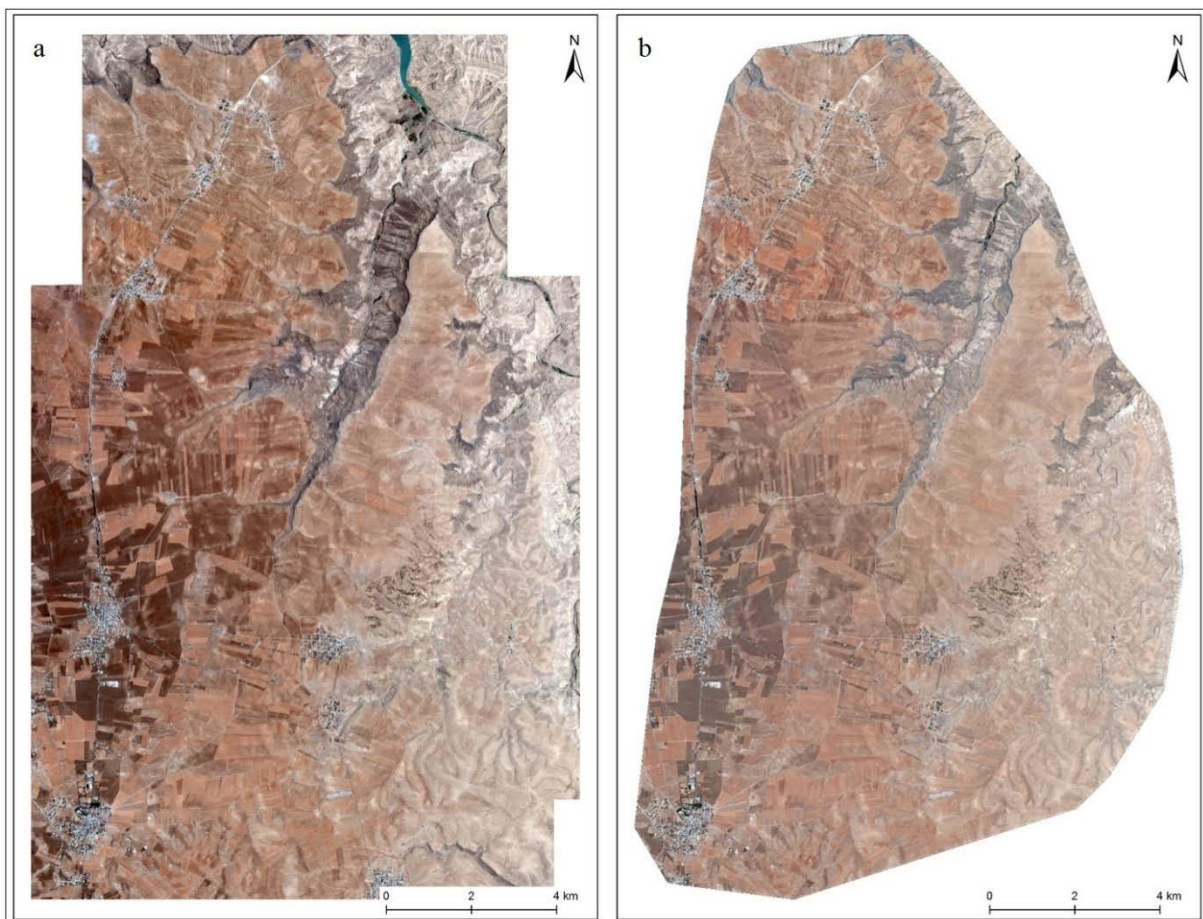
Fig. 16: GeoEye-1 satellite imagery before (a) and after preprocessing (b). Both are true color (RGB) images attained by the band combination 3-2-1 in a multispectral layer stack. On the left (a), the raw imagery as acquired from the vendor is displayed. On the right (b), the final preprocessed image (mosaic) after orthorectification, atmospheric corrections, and pan-sharpening is presented. Source: GeoEye-1 satellite imagery ©DigitalGlobe, Inc. All Rights Reserved.

A panchromatic sharpening (pan-sharpening) was subsequently performed on the atmospherically corrected images. Pan-sharpening is an image fusion technique used to increase the spatial resolution of multispectral imagery by merging panchromatic images with a higher resolution with multispectral images with a lower resolution. In ERDAS IMAGINE, several algorithms are available for this purpose. For VHR images with four MS bands and characteristics similar to that of GeoEye-1 (e.g. QuickBird), the subtractive resolution merge technique has been developed (ERDAS 2010). It has been employed for data fusion and assessed in several studies with varying results (e.g. ASHRAF ET AL. 2012, YANG ET AL. 2012, WITHARANA ET AL. 2013). The choice of the optimal data fusion algorithm depends on the scene and its content, the target features, and the intended use (cf. e.g. WITHARANA ET AL. 2013). For the present study, the subtractive resolution merge approach proved most suitable, based on the visual evaluation of the results of different pan-sharpening techniques available in ERDAS IMAGINE. Suitable values for crucial parameters used by this technique, such as e.g. sharpening filter center value and pan contribution weight, had to be determined empirically and adjusted as necessary. Finally, the two preprocessed image tiles were combined into one image using the MosaicPro module in ERDAS IMAGINE. The resulting output image (see Fig. 16) represented the basis for all subsequent interpretative steps.

4.1.2.2 Visual interpretation of satellite imagery and on-screen digitization

Visual image interpretation has been employed for the mapping of features, which can be identified on the satellite image by a trained user but not with automatic feature extraction approaches, at least not with adequate results. The superiority of image interpretation by an expert, compared to even the most sophisticated currently available automatic methods, originates from the complexity of human visual perception, information processing, and decision making which often involve additional background knowledge and "convergence of evidence" (LILLESAND ET AL. 2015, p. 66). However, the expert has to invest a substantial amount of time in the interpretation of the images and must have specific training. The expenditure of time increases with the complexity of the interpretative task and the quantity of target objects. Therefore, in the present survey, the visual image interpretation approach has been limited to what is absolutely necessary, i.e. the identification of objects which could not be detected (semi-) automatically. Besides this, visual image interpretation also complemented and formed part of the semi-automatic image analysis procedures described in chapters 4.1.2.3-4.1.2.6.

In general, (semi-) automatic feature extraction methods tend to fail and visual image interpretation through an expert becomes indispensable when target objects exhibit a great variance in their visual appearance and the image context varies largely. This is also true when their characteristics can easily be confused with those of other objects, and when a number of different or alternative criteria are used for their reliable identification. This was the case for visible drainage lines (wadis, channels, and similar) and all types of RWH structures, i.e. bunds, dikes, ridges, and check dams, made of earth or stones,

as well as cisterns. Upon recognition of the aforementioned targets, their location was captured with on-screen digitization in ArcMap. Features were digitally represented as points in case of cisterns, and lines in case of drainage channels (wadis and similar) and linear RWH structures like bunds, dikes, ridges, dams, and shallow walls.

Visual identification of linear RWH elements (bunds, walls, dikes, etc.) and most drainage lines was straightforward and unambiguous (see Fig. 17). Where wadis and natural channels were less incised due to flat terrain, hard underground, or recent onset of formation, their precise course occasionally was more difficult to trace on the satellite image. Here, the drainage line network, as calculated by a preliminary hydrological analysis based on the DEM (see 4.1.4 for details), could be used as auxiliary information to corroborate tentative visual interpretation and thus, enhance the reliability of the results. In contrast to the aforementioned cases, the remote sensing supported detection of underground cisterns proved more intricate as it had to be based on minor indicative surface features. These are commonly small in size and exhibit a great variety of appearances (see Fig. 17), whereas the largest part of the object, i.e. the cistern body, is hidden belowground and therefore invisible in the imagery.
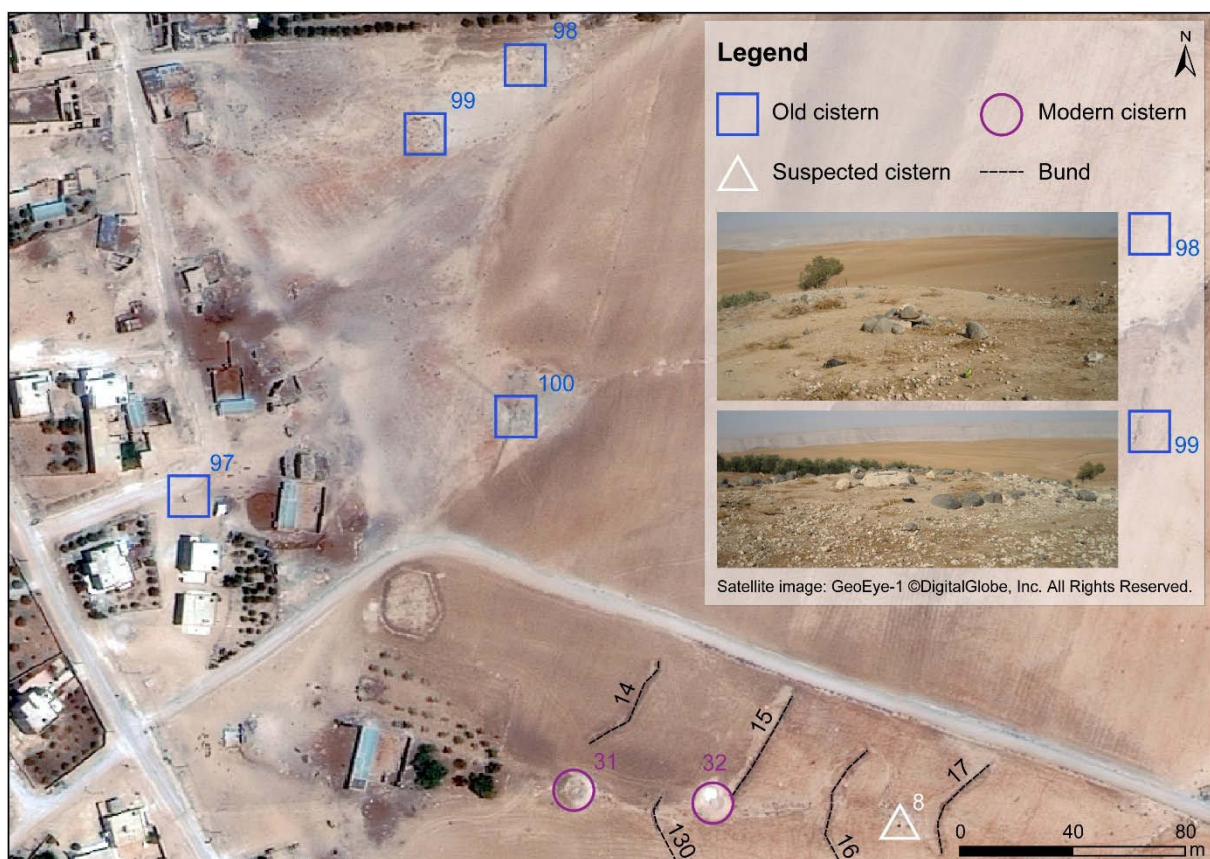
Fig. 17: Appearance of different RWH structures in the satellite image and in the field (cisterns no. 98 and 99). Features named "old cisterns" have been mapped with fieldwork (chapter 4.1.1) and used as examples in the visual image interpretation approach. Additional cisterns which could be identified with sufficient certitude on the satellite image have been labeled as "modern cisterns". Possible further cistern locations are included in the class "suspected cisterns". Photographs, design and layout: B. Brilmayer Bakti.

GPS points of cisterns previously mapped in a field survey (see 4.1.1) were used as training examples in order to identify characteristic, visible signs of cisterns on the earth's surface and on the satellite image. Thus, the following criteria could be derived: a usually round, bright spot of relatively small size, often with a contrasting tiny dark feature in the middle, that correspond to the cemented area around the cistern and the manhole indicated a cistern. Cement, especially when new, shows high reflection values in all bands and therefore appears as bright areas in the satellite image (see Fig. 17). In contrast, metal closing lids or (basalt) stones which are often used to cover manholes, usually exhibit low reflection values. For the identification as cisterns, the combination of arrangement, size, shape, and particularly contrast, is more important than absolute reflection values. Additional clues for the interpretation can be found in the image context. Cisterns are usually located on contrasting, homogeneous bare ground, often appearing in groups, and are frequently associated with feeding channels, bunds, deflection walls, or similar structures that are used to decelerate runoff and direct it towards the cistern (see Fig. 17). However, the described criteria are often not all fulfilled, thus complicating the interpretation decision. Reliable and unambiguous identification is more difficult or sometimes even impossible for cisterns within a different setting, e.g. especially in less contrasting settlement areas, or old cisterns missing a characteristic cemented area. Therefore, two categories of features were created. One class contained all cisterns which mostly fulfilled the mentioned characteristics and therefore could be identified with sufficient certainty. The other class included all points where cisterns are suspected, due to certain clues but ground check would be necessary for clarification.

Ground truth data, which was acquired through fieldwork (see section 4.1.1), was applied to evaluate mapping results derived from visual interpretation of the satellite image. This approach could be confirmed for the class of clearly identified cisterns. No false positives, i.e. nonexistent cisterns, have been detected in comparison to ground truth (see 4.1.1 for further details). Substantial homogeneity in this group of features, regarding their characteristics and associated certainty of identification, allowed for the generalization of findings from a sample set of objects (see 4.1.1). In contrast, strong heterogeneity in the group of potential further cisterns requires the confirmation of the nature of every single entity through fieldwork. Hence, no estimation of reliability and feasibility of the mapping approach can be given for this class since findings from single features cannot be upscaled. Remote sensing based mapping with visual image interpretation thus seemed suitable and reliable for a significant share of cisterns, whereas it was not applicable to the detection of all cisterns. Objects which can be well identified in the satellite image are usually modern, newly constructed cisterns in a contrasting bare ground environment outside settlement areas. Cisterns with largely different characteristics either cannot be recognized in the satellite imagery at all or not with sufficient certitude. Nonetheless, the data of possible additional cisterns as derived from visual image interpretation may serve as a valuable guide for the mapping of cisterns in field work.

4.1.2.3 Semi-automatic image analysis: the Feature Analyst approach

Automatic image analysis is the complementary approach to visual image interpretation and manual digitization of features as presented in the previous section (4.1.2.2). Both strategies can either be applied in isolation or in combination; mutually complementing each other. Due to their differing advantages and disadvantages, they are suited to different tasks. Automatic procedures are commonly employed for the extraction of larger datasets such as objects or land use/land cover (LU/LC) classes from satellite or aerial imagery covering substantial areas. For these purposes, automatic approaches are favored over visual-manual interpretation, as they enable the acquisition of highly consistent results within a short time. However, automatic image interpretation is not optimally suited to all tasks since the objects or LU/LC areas which should be detected usually need to meet some requirements in order to be identified reliably by the software. In regard to their appearance in the image, objects or areas of the same category typically need to share adequate homogeneities in their characteristics and sufficient differences to those of other classes or the rest of the image. In relation to the study at hand, the preparation of a simple LU/LC map and the detection of rooftops seemed to fulfill the necessary requirements for automatic procedures.

Automatic image interpretation approaches should be differentiated into completely automatic and de facto semi-automatic procedures. With fully automatic methods, the whole object extraction and image classification process is conducted by the software while the user only specifies parameters or sets up rules. All other approaches must be properly referred to as semi-automatic procedures. These methods typically involve the digitization of training examples by the user, which are then employed by the software to classify the image. The method adopted in this study belongs to the semi-automatic approaches as described below.

Besides the degree of automatization, image interpretation methods can be divided into two large categories: the pixel-based classification approach and the object-based image analysis (OBIA). In traditional pixel-based approaches, each pixel of an image is classified individually based on its spectral values ("color"), i.e. the combination of digital numbers in the different spectral bands. In contrast to that, OBIA methods try to mimic human visual interpretation by taking into account further attributes such as size, shape, texture, pattern, and environment, just like the human interpreter does. The integration of these additional aspects in the classification process can enhance reliability and accuracy of analysis results. In principal, the pixel-based approach has been developed for low resolution imagery where larger areas are represented by one pixel, whereas the OBIA approach better suits high resolution imagery. With increasing resolution, heterogeneity in spectral values within an area commonly grows. Just like an impressionistic painting or a mosaic with many small parts, the area of one LU/LC class or object then comprises a larger number of pixels with highly diverse spectral values. Hence, a traditional pixel-based classification can lead to problems like the "salt and pepper effect" when individual pixels of an area belonging to the same LU/LC category are assigned to different classes based on their spectral

characteristics. Therefore, as a first step in the classification process, OBIA methods usually encompass a segmentation procedure in which pixels are grouped into relatively homogenous areas (cf. e.g. APLIN & SMITH 2008, BLASCHKE 2010). This typically reduces computing time in the following analysis since segments are classified instead of individual pixels, whose number can be enormous in very high resolution imagery, especially when larger areas are covered. Due to the described considerations, an OBIA approach seemed most adequate for the automatic analysis of the VHR satellite imagery in the present study. The integration of further attributes, in addition to spectral values, was particularly important in order to be able to distinguish buildings, i.e. rooftops, from other cemented areas with mostly identical spectral characteristics such as backyards, parking lots, driveways, and the like.

Further details on the OBIA approach in the domain of remote sensing can be found in BLASCHKE ET AL. (2008) and BLASCHKE (2010). For reasons of simplicity, in the present study, the term OBIA is used in a generalized manner subsuming all alternative or more specific names and associated concepts such as geospatial/geographical object-based image analysis (GEOBIA), object-oriented image analysis, or (automated) feature/object extraction/recognition (BLASCHKE ET AL. 2008, BLASCHKE 2010). In the context of the OBIA approach, different software solutions have been developed and are currently available as COTS (commercial off-the-shelf products), e.g. IMAGINE Objective, an add-on for ERDAS IMAGINE (Hexagon Geospatial), ENVI FX, the feature extraction module for ENVI (L3Harris Geospatial), Feature Analyst (Overwatch Systems, Ltd., Textron Systems Corporation), an extension of ESRI's ArcGIS, and eCognition (Trimble Geospatial). The first successful and still most widely used OBIA software is Timble's eCognition (formerly Definiens) which has, until recently, been employed in around half of the published scientific studies (BLASCHKE 2010). However, depending on the specific classification or object extraction task, some of the newer software packages can represent reasonable alternative solutions and offer considerable advantages. The selection of the most suitable software for the present study was based on a combination of different criteria. Besides economic considerations, i.e. expenses for the acquisition of or the subscription to a software, its user-friendliness, and thus the required expert knowledge or necessary training with the software, were taken into account. Expectable classification and feature extraction results, and hence the suitability of the software for the intended purposes, were inferred from published findings of previous studies.

With regard to the aforementioned aspects, the software solution Feature Analyst (FA) was chosen for all semi-automatic image analysis tasks. Since FA is available as an extension to ESRI's ArcGIS Desktop software, it perfectly integrated with the databases, tools and other procedures applied in this study. The software is only offered in a subscription-based mode. Costs of a one-year academic license are moderate and similar to, or lower than, those of other OBIA software solutions. One major advantage of FA compared to most other commercial software packages is its user friendliness. A machine learning approach, relying largely on training examples digitized by the user, the availability of default parameters for a variety of object categories and LU/LC classes, as well as an optimized user interface make

the application of the software convenient, especially for users familiar with the ArcGIS environment (cf. e.g. BLUNDELL & OPITZ 2006). Consequently, users are usually able to obtain acceptable results with a minimum of training and within a short time. FA has been employed and evaluated in a number of studies and for a broad range of purposes (e.g. LAVIGNE ET AL. 2006, YUAN 2008, MADSEN ET AL. 2011, CZEREPOWICZ ET AL. 2012, GÜNERALP ET AL. 2014). Classification and object extraction tasks identical or similar to those of the present study were investigated by FREIRE ET AL. (2010), TSAI ET AL.(2011) and CAGGIANO ET AL. (2016) who detected buildings, as well as KUNAPO ET AL.(2005) and MILLER ET AL. (2009) who produced a basic LU/LC map that distinguished between impervious and pervious surfaces.

The functionality and underlying methodology of FA have been described by BLUNDELL & OPITZ (2006) and OPITZ & BLUNDELL (2008b). The software is rooted in a machine learning approach in which several inductive learning algorithms are used to identify objects that match individual user-defined templates (QUACKENBUSH 2004, OPITZ & BLUNDELL 2008b, GÜNERALP ET AL. 2014). FA differs from other software solutions and "true OBIA approaches" in that it does not involve an evident segmentation step, but rather classifies individual pixels, considering spectral, spatial and contextual characteristics (TSAI ET AL. 2011). The system, also called "learner" as it learns from examples provided by the user, thus imitates human visual image interpretation and develops a model that identifies objects similar to the provided templates (OPITZ & BLUNDELL 2008b). Since the methodology is inherently adaptive, it can be applied to a variety of object extraction and classification tasks. Details on the science behind FA and its algorithms remain proprietary and hidden from the user as the algorithms run in the background during learning and classification. However, the major strength of the software is seen in its use of ensemble learning in which genetic algorithms are employed to develop an optimal set of classifiers (BLUNDELL & OPITZ 2006, OPITZ & BLUNDELL 2008b). An ensemble consists of several basic classification algorithms that are selected individually and automatically by the software based on the input data. These classification algorithms encompass artificial neural networks and variants thereof, decision trees, Bayesian learning and K-nearest neighbor (OPITZ & BLUNDELL 2008b).

Like many other image analysis software solutions, FA offers two different classification approaches, an unsupervised and a supervised one. Here, as in most cases, the latter is employed since usually only a supervised classification allows to extract specific target objects. Hence, the described procedure of image classification and object extraction refers to the supervised approach. The workflow starts with manual digitization of templates that indicate target objects or areas of the intended LU/LC classes. This step represents a common characteristic of FA and traditional, pixel-based image classification approaches e.g. in ERDAS IMAGINE. Based on the training examples provided by the user, the software then performs a learning and classification process which detects further objects or areas potentially belonging to the target group. Suitable default learning parameters are available for the extraction of many common object and LU/LC categories. These settings can serve as a starting point and can be

modified as needed (see Fig. 18). Optimal adjustments are usually identified through a trial and error process. The selection of a suitable input representation is especially crucial. Similar to the view from a window, the surrounding part of the image provides the necessary contextual information for the classification of an individual pixel in the center. The input representation allows defining the size of the "window" and the way the environment of the center pixel is taken into account during classification (see Fig. 19). In order to minimize the amount of data and the number of pixels which need to be considered, lower resolutions or selected individual pixels or group of pixels are used with increasing distance from the center. The method borrows its idea from the visual perception of humans and many animal species, which exhibit a declining visual acuity from the center towards the boundaries of the
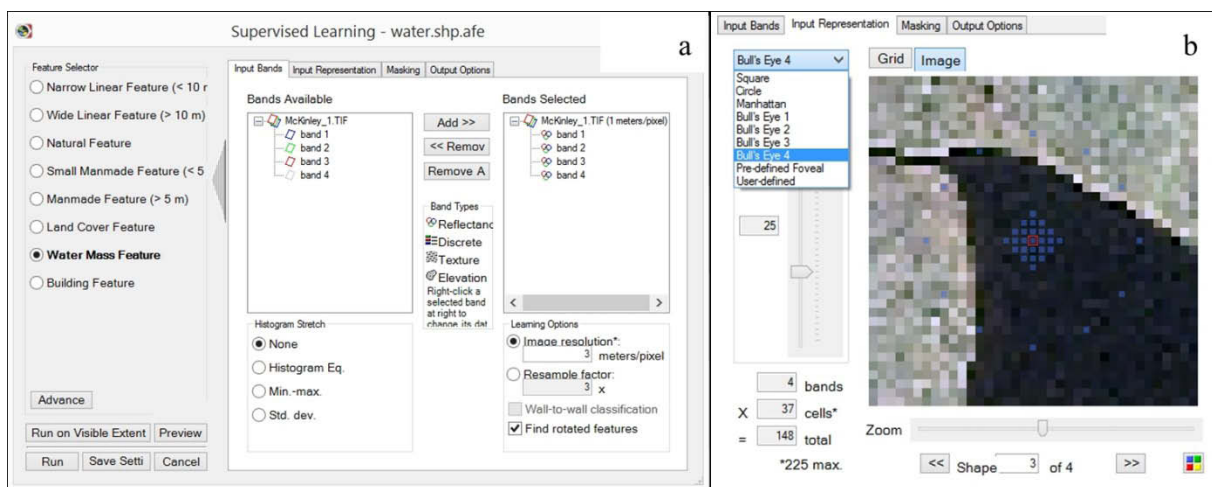
Fig. 18: Feature Analyst supervised learning window (a) and details of the input presentation (b). The number and arrangement of auxiliary pixels (blue squares) that are considered in the classification of the center pixel (red frame) depend on the selected pattern (here Bull's Eye 4) and the pattern width (here 25). The input representation resulting from the selected settings are shown on the satellite image.
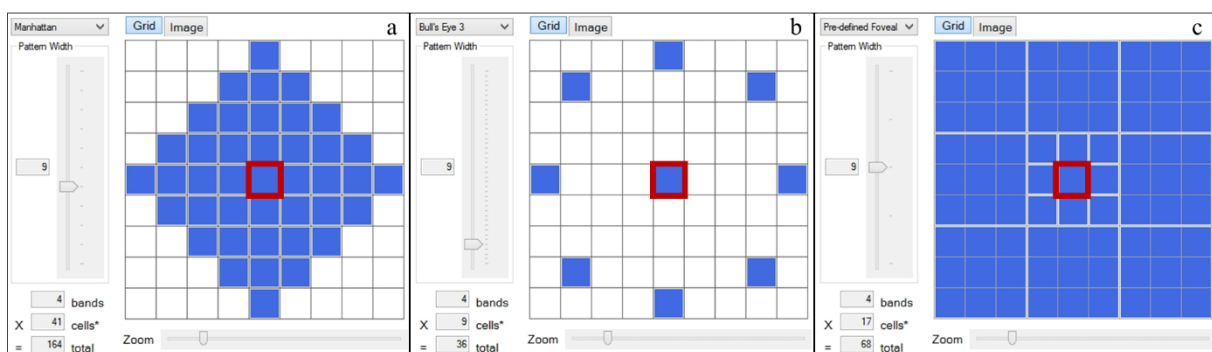
Fig. 19: Different input representation patterns available in Feature Analyst. All patterns are shown with a pattern width of 9, i.e. a potential window of 9×9 pixel. Patterns determine the number and arrangement of auxiliary pixels (blue) used during the classification of the center pixel (red box). Auxiliary pixels represent the spatial context. Higher numbers of pixels entail larger computing times and therefore should be reduced to the necessary minimum to capture spatial characteristics and the context of features. Hence, the selection of a suitable input representation pattern and pattern width is probably the most crucial parameter of the supervised learning setting. Exemplary patterns illustrated here are Manhattan (a), Bull's Eye 3 (b), and Pre-defined Foveal (c). The latter (c) groups the outer pixels into boxes of 3×3 pixel. Average (spectral) values are calculated from the individual pixels of each box and used during classification. This allows for the consideration of a higher number of pixels without significantly increasing computing time.

visual field. This type of perception is described as foveal and peripheral vision. Accordingly, during the classification of each pixel, FA uses a higher resolution, and thus a larger number of pixels in the center and a lower resolution with fewer pixels around the margins of the "window", i.e. the considered subset of the image. Different search kernels (patterns) and kernel sizes can be chosen or defined for this purpose (see Fig. 19) (cf. Tsai et al. 2011). Further details on this concept can also be found in Opitz & Blundell (2008b) and Güneralp et al. (2014).

Subsequently, the output of the learning and classification process can be assessed by the user, usually through visual examination. Based on findings, initial classification results can be refined through a process named "Hierarchical Learning", in which the user specifies correctly and wrongly classified areas or objects, or digitizes additional examples. The associated steps called "Clutter Removal" and "Add missed features" are applied to mitigate over- and underclassification respectively and are always followed by a subsequent learning pass. Thereby background classification algorithms and parameters can be refined and classification results improved. The procedure can be repeated as often as necessary to achieve the best possible outcomes. However, there is evidence that excessive application of hierarchical learning produces intricate classification models without significantly enhancing the results (Miller et al. 2009, Overwatch 2010, Wiginton et al. 2010). With the optional hierarchical learning procedure, classification becomes an iterative process, including intermediate results and feedback provided by the user. Once the most suitable classification model has been developed, it can easily be transferred to other images using the "Batch Processing" option. For this purpose, FA automatically creates a script or Automatic Feature Extraction (AFE) Model for each step of the classification workflow. These AFE models can be viewed, modified, and applied to analyze and classify any other image.

4.1.2.4 Preparation of the land use/land cover map

When classifying satellite images, an appropriate balance must be found between the desired information and the possible LU/LC classes or objects which can be distinguished by the software. Individual objects or areas must exhibit sufficient similarities with the other items of the same class and adequate differences to objects or areas of other classes in terms of the spectral and/or spatial characteristics (cf. e.g. Lillesand et al. 2015). For the study at hand, a minimum number of extractable LU/LC classes was defined based on broad differences between various land surfaces concerning their hydrological qualities, particularly water infiltration and runoff formation. The major divide occurs between sealed or impervious surfaces with high runoff values and pervious land with higher infiltration and low to very low runoff values. Impervious areas correspond mostly to built-up or settlement areas and surfaces of associated infrastructure elements. The category of pervious surfaces comprises a broad variety of different types of LU/LC such as e.g. agricultural fields, vegetated areas, range land, and bare soil. These differences are associated with large variations in runoff coefficients, i.e. the percentage of precipitation which is converted into surface runoff. Consequently, it would be desirable to further define LU/LC

subcategories within the broad class of pervious surfaces and thus distinguish between e.g. vegetated and non-vegetated areas or patches with shallow soils or bare rock and those with deep soils. However, there are a number of obstacles inherent to the method of remote sensing or the specific satellite image which impede a more detailed classification. For example, digital mapping of different soil types and soil characteristics is more intricate and requires a more comprehensive methodological approach than a regular classification of a four band multispectral satellite image (cf. e.g. MULDER ET AL. 2011 on digital soil mapping with remote sensing). In contrast, living or photosynthetic vegetation can easily, and highly reliably, be detected in optical remote sensing products, owing to typical high reflectance values in the fourth band (near infrared) (cf. e.g. LILLESAND ET AL. 2015 on spectral signatures of different types of LU/LC). Since the acquired GeoEye-1 satellite imagery was recorded in late summer, only information on the vegetation cover in summer can be derived from this dataset. The growing season of most plants, including annual (agricultural) crops which are grown in vast areas of the plateau, coincides with the rainy winter half-year (see chapters 3.3 and 3.5). The summer vegetation in the area largely corresponds to permanent plants like olive, fruit and other trees and horticulture. The latter types of vegetation often need (supplemental) irrigation and hence are of particular relevance with regard to water demand, water storage, and water harvesting schemes.

Based on the aforementioned considerations, the following three LU/LC classes were defined and derived from the preprocessed GeoEye-1 satellite image through semi-automatic image analysis: impervious surfaces, pervious surfaces, except (photosynthetic) vegetation, and vegetation. The first category of impervious areas contained all different types of sealed surfaces and man-made objects such as buildings, parking lots, (asphalt) streets, and the like. The class of pervious surfaces encompassed agricultural fields, fallow and range land with no or negligible (living) vegetation, areas of bare earth or bare rock, wadi beds, and similar kinds of unsealed surfaces and open land inside and outside of settlements. Plantations, trees, yards, areas of horticulture, and other land with a significant (mainly photosynthetic) vegetation cover were assigned to the class of vegetation. While this category is comparatively homogeneous in terms of the covered range of spectral signatures, the two other classes, the impervious and the pervious one, are more heterogeneous in their spectral and spatial characteristics due to the broader range of different types of land cover they contain.

The workflow leading to the LU/LC map, using the three classes described above, is visualized in Fig. 20. It largely builds on the basic LU/LC classification, with two classes, that was conducted by BAICU (2012) and discriminated between impervious and pervious surfaces. Upon visual examination, the outputs of the stepwise multi-class extraction accomplished by BAICU (2012) were refined with minor manual editing. Results were complemented by a single class object extraction for the class of vegetation.

The basic LU/LC map produced by BAICU (2012) consisted of two classes, impervious, sealed and pervious, unsealed surfaces, while the latter also included vegetated areas. A description of the exact semi-automatic classification procedure that was performed by Feature Analyst and based on the GeoEye-1

imagery of the present study, can be found in BAICU (2012). A basic accuracy assessment of the outcomes showed an overall accuracy of 90 % and a Kappa score of 0.8 (BAICU 2012). These results suggest substantial accuracy and reliability of classification results. Nonetheless, a visual examination revealed several larger spots of misclassification. Mainly pervious areas, such as gravelly or stony wadi beds, bare rock, particularly bare limestone areas, and bare ground with a very shallow soil cover, were occasionally interpreted wrongly as impervious surfaces by the software, due to similar extents, shapes, and spectral signatures. Since larger areas of misclassification primarily occurred in clusters within more or less circumscribed regions of otherwise pervious ground, initial results of the semi-automatic classification could be improved substantially with manual editing, requiring comparatively little time and effort.
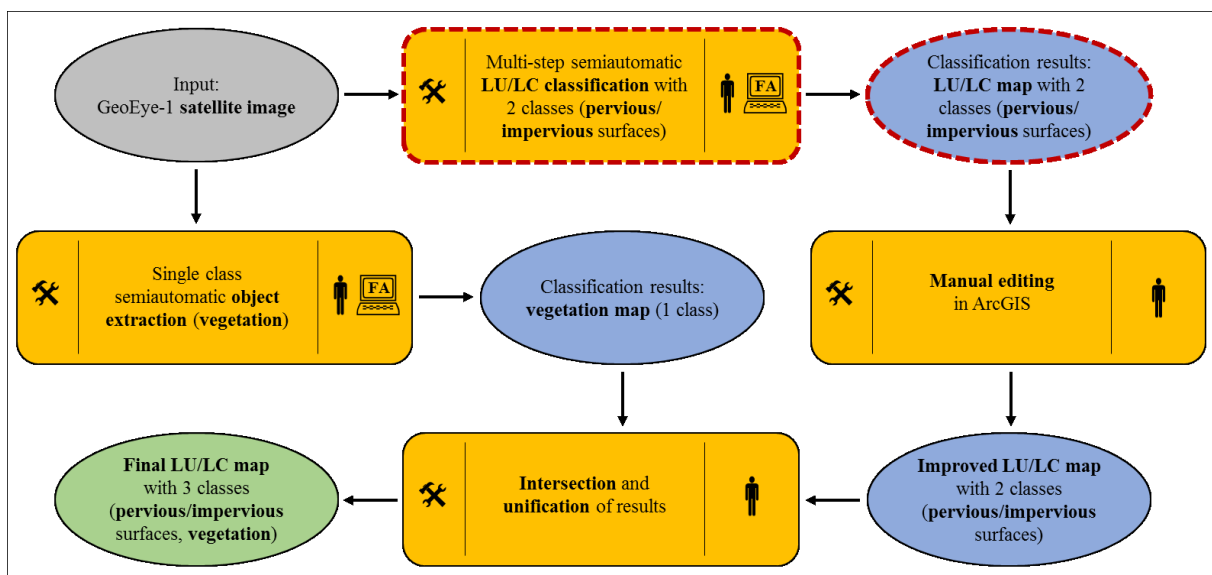
Fig. 20: Workflow of the production of the LU/LC map. Processes are shown as yellow boxes and marked with a hammer and wrench symbol. Input, intermediate and output datasets are represented by blue ovals, except for the initial input and the final results which are depicted as a grey and a green oval respectively. The parts of the work that were completed by BAICU (2012) are indicated with a red, broken outline. The man icon indicates largely manual operations, including the application of ArcGIS tools that are mainly controlled by the user. Semi-automatic classification steps performed with Feature Analyst are marked by a combination of the computer and the man icon.

BAICU's classification results were available as vector data stored in a shapefile. Manual editing of the data mainly consisted of reassigning wrongly classified features to the correct class, and to a minor degree, of reshaping features to eliminate larger misclassified parts. All editing operations were primarily aimed at reducing the overclassification tendency in the impervious class and the associated underclassification in the pervious class. In most cases, features wrongly identified as impervious surfaces could simply be assigned to or merged with neighboring or surrounding features of the pervious class. Occasionally, the boundary between impervious and pervious areas needed to be reshaped, usually to "cut off" parts of the impervious feature and add them to an existing pervious feature. Manual editing was limited to larger areas of obvious misclassification as identified through visual examination. With

manual editing, the number of features in the impervious class was reduced by two-thirds, while the extent of the class decreased only by one third (see Table 8). Simultaneously, the extent of the pervious class increased, although the relative change was marginal (1 %) due to the already large areal extent of the class. After editing, a smaller number of features and larger feature sizes on average were observed in both classes. The respective share of each category in the study area remained comparatively stable (see Table 8 and Fig. 21). The unedited classification results of BAICU (2012) included clouded areas which were assigned to the impervious category. Since the cloud covered areas were adequately captured and distinguished from the surrounding pervious areas, the corresponding features could simply be reassigned to the category of clouds during the manual editing process. Only a small part of the boundary of one feature had to be reshaped manually.

The existing vegetation discernible in the imagery was detected with Feature Analyst using a single class object extraction approach. The classification workflow is visualized in Figure 22. In order to facilitate the classification process and reduce computing time, the satellite image was cut into three parts which were analyzed successively. Initially, a task-specific classification model was developed which optimally captured the vegetation. The AFE model was established based on a relatively small subset of the satellite image that still covered all different types of vegetation. Once satisfying classification results and hence a suitable AFE model were attained for this image subset, the model could be applied onto other images through batch processing.

The starting point of vegetation detection was the manual digitization of training examples as input for the subsequent machine learning process (see Fig. 22). Manual delineation of templates closely followed the best practice recommendations given in OVERWATCH (2010). These suggest that training examples should capture the outlines of target objects or areas as accurately as possible and reflect the variety of shapes, sizes, spectral values and contexts that occur in the respective class. Moreover, templates should be distributed homogeneously over the input image, if possible. In the present case, 16 training examples (see Fig. 23 for one example) were sufficient to fulfill the aforementioned criteria.

Table 8: Properties of the two LU/LC classes before and after manual editing and quantitative changes. "Before editing" refers to the classification results produced by BAICU (2012). Due to the exclusion of cloud covered parts, the total area that is classified as impervious or pervious shrinks from 163.087 km² to 163.040 km² after manual editing.

Key parameter	LU/LC class	Before editing	After editing
Number of features	Impervious	5,266	1,771
	Pervious	1,367	890
Range of feature sizes	Impervious	< 1 m² - 3.769 km²	< 1 m² - 3.507 km²
	Pervious	< 1 m² - 84.225 km²	< 1 m² - 86.126 km²
Mean feature size	Impervious	1,202 m²	2,392 m²
	Pervious	114,667 m²	178,431 m²
Total extent of class	Impervious	6.328 km²	4.237 km²
	Pervious	156.750 km²	158.803 km²
Share in study area	Impervious	3.9 %	2.6 %
	Pervious	96.1 %	97.4 %
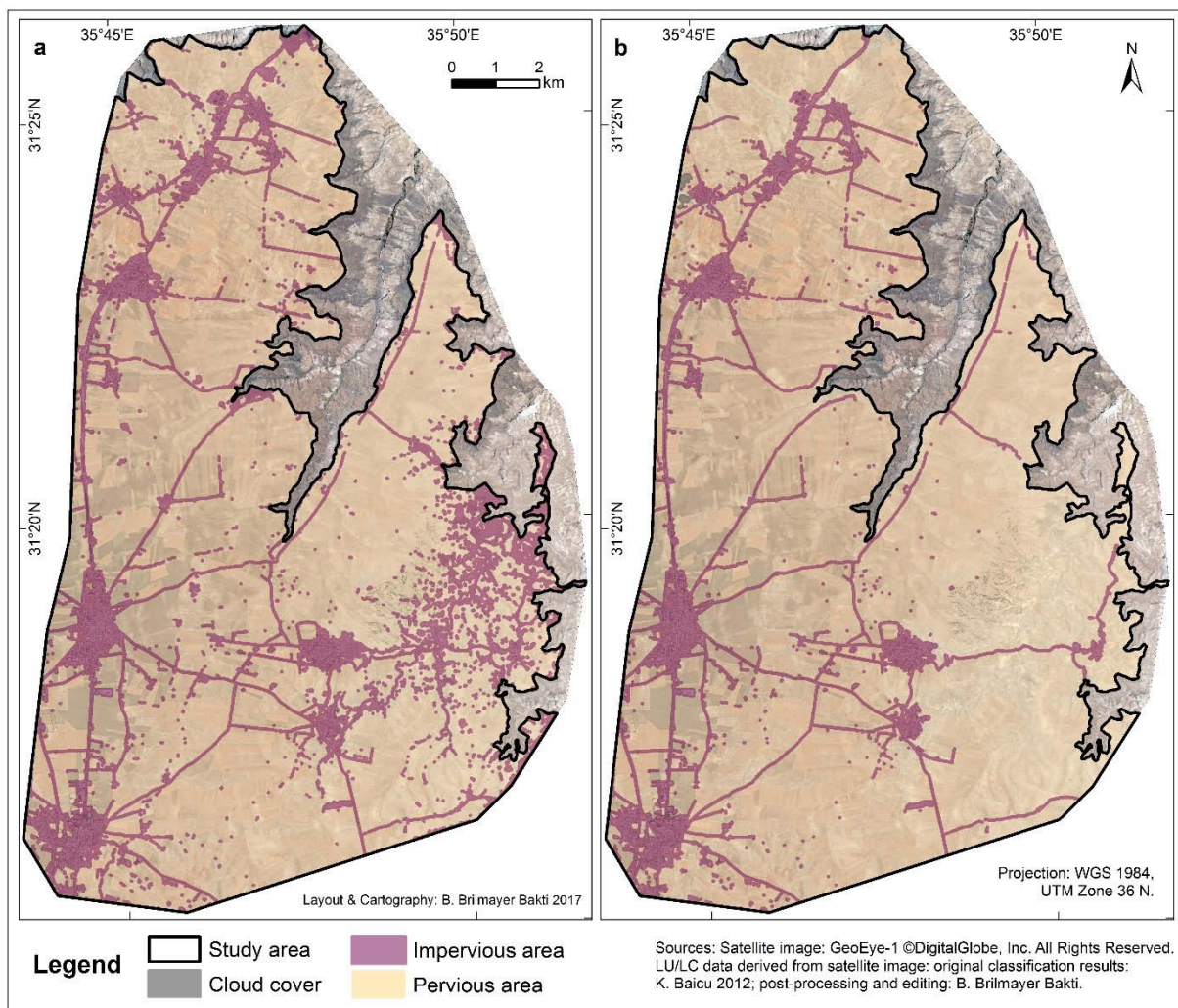
Fig. 21: LU/LC map showing impervious and pervious areas before and after manual editing. In the editing process, cloud covered areas were assigned to a separate category. Overestimation of the impervious category was reduced.

Subsequently, a supervised learning pass was conducted based on the digitized training examples. Selected supervised learning settings are presented in Figure 23. They remained mostly identical during all supervised learning passes (see Fig. 22) and represent an adaptation of the predefined settings for "natural features". Suitable learning settings were identified empirically through the experimental adjustment of individual parameters followed by the visual evaluation of corresponding classification results. During the first supervised learning pass of Model 1 (see Fig. 22), outputs were aggregated to a minimum area of 2 m^2 per feature. Specific masks that further constrain the area to be classified were not employed. However, masks formed an inherent part of all the hierarchical learning processes. In the clutter removal procedure, by default, previous classification results were masked as regions of interest. When adding missed features, previous classification results defined the mask of the region to exclude in the corresponding learning process. The masks further narrowed the area down that should be classified, in order to either focus on the re-evaluation of previous results (in the case of clutter removal) or on the search for additional areas belonging to the target class, outside of previously identified regions

95

(in the case of add missed features). During clutter removal, the option "remove clutter based on shape attributes, too" was selected in the output parameters sections of the learning settings. Besides the described exceptions, the supervised learning setting as shown in Fig. 23 was employed for the classification of the imagery.

Initial classification results (box "classification results 1" in Fig. 22) appeared generally suitable but still contained a substantial degree of overclassification. False positives primarily concerned areas that resembled vegetation with no or low photosynthetic activity. In order to address this issue, hierarchical learning was applied with two successive passes of clutter removal (see Fig. 22). The procedure involved the marking up of positive, i.e. correctly classified, and negative, i.e. false positive examples, by manually selecting features or delineating suitable parts of features. These edits were made to the clutter removal layer which was created automatically for this purpose and comprised the previous classification results. Afterwards, a supervised learning pass was conducted based on the specified examples to refine the classification model and algorithms. In order to avoid a significant underclassification in the outcomes of a clutter removal process, it is recommended to indicate considerably more positive than negative examples (OVERWATCH 2010). The applied clutter removal procedure successfully reduced overclassification and lead to a decrease of the identified vegetation area by 13 % (see Fig. 22). The existing vegetation was captured with satisfactory completeness and no severe underclassification was observed. The assessment of classification results and their suitability was based on comprehensive visual examination.

Using the batch processing function of FA, the AFE model that was developed on the subset of the imagery (Model 1 in Fig. 22) was then applied to the three image tiles which together covered the whole study area. Careful visual inspection of the outputs revealed that the application of the initially developed model (Model 1) did not lead to equally suitable classification results for all image tiles. This may be due to variances in land cover in different parts of the satellite image. Therefore, classification results from batch processing and the associated initial AFE model (Model 1) were refined with further hierarchical learning steps (see Fig. 22). The classification results of the southern image tile (S3) exhibited a considerable degree of underestimation of the vegetation cover. Consequently, the "add missed features" procedure was employed to detect further vegetation areas (see Fig. 22). Although only a single additional template was digitized for the subsequent supervised learning pass, the area identified as vegetation (classification results 5 in Fig. 22) increased substantially, resulting in a considerable overclassification. This shortcoming could be overcome with another pass of clutter removal and the classification model and its outcomes could be improved significantly. The detected vegetation area increased by 45 % through the "add missed features" procedure and decreased by 16 % through clutter removal. Thus, the vegetation area in the final output, after hierarchical learning, was still 22 % larger than that of the initial results from batch processing (see Fig. 22).
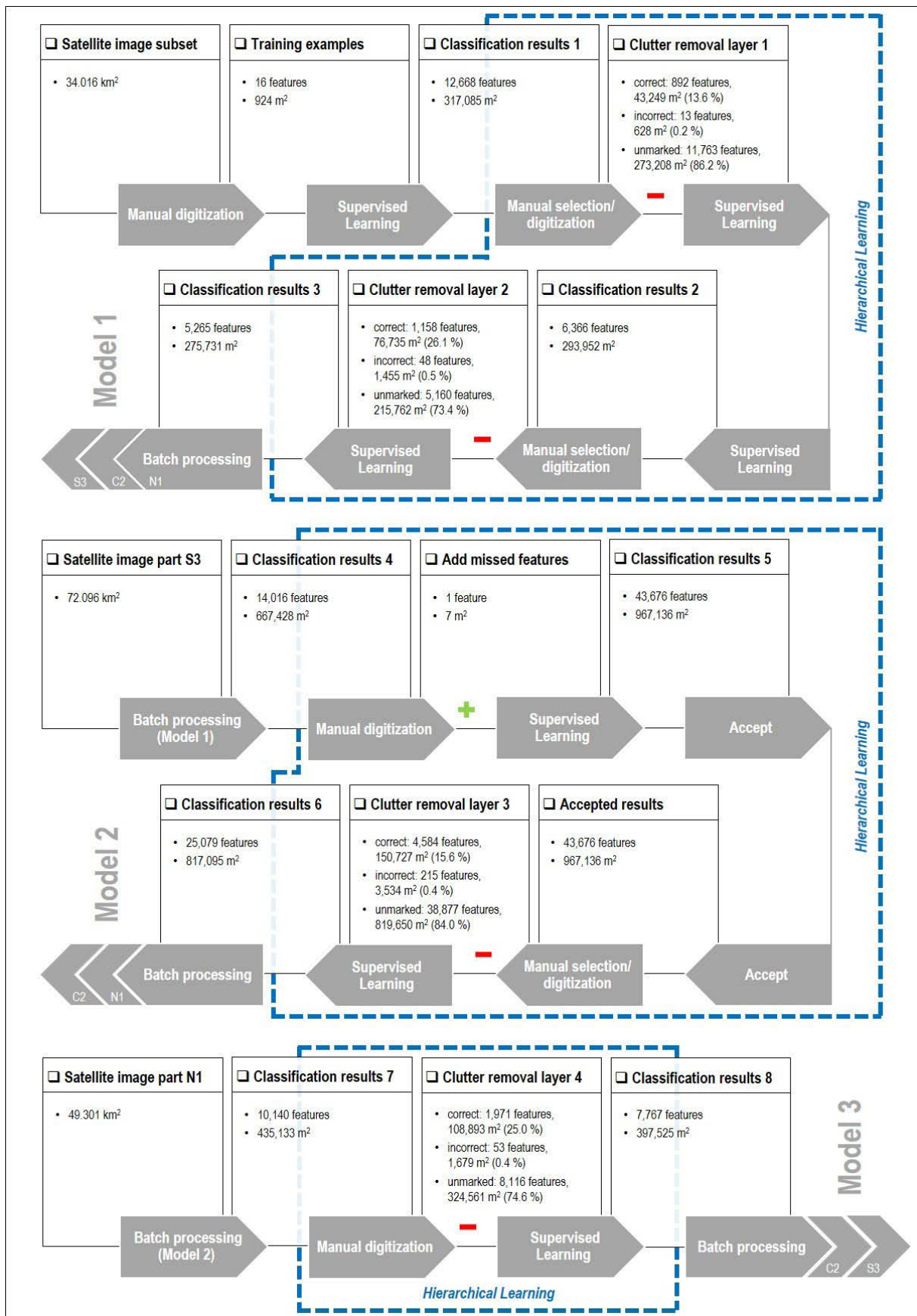
Fig. 22: Workflow of the vegetation extraction procedure with Feature Analyst. The characters N1, C2 and S3 refer to the three different image tiles, the northern (N1), the central (C2), and the southern part (S3), that were produced from the satellite image of the whole study area. Boxes represent individual input and output vector datasets while arrows symbolize processes. For details concerning the supervised learning settings see Fig. 23.
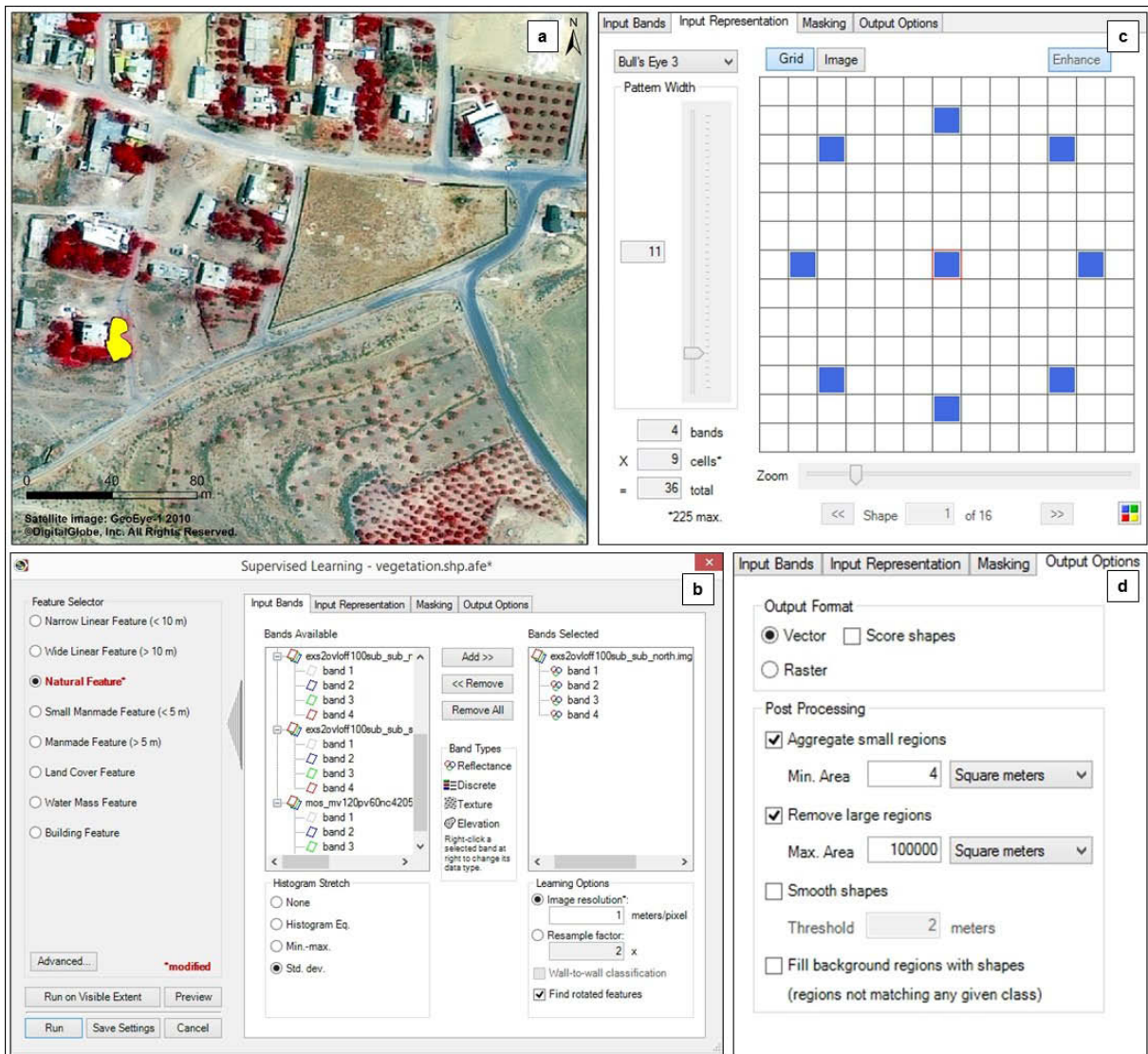
Fig. 23: Manually digitized training example (a) and supervised learning settings (c-d) used in the vegetation detection process (see Fig. 22).

The new, improved AFE model (Model 2 in Fig. 22) could then be applied to the other image tiles via batch processing. Upon close visual examination, outcomes showed a considerable amount of overclassification for the northern image tile (N1). Therefore, again, a careful clutter removal was performed to enhance the suitability of the classification results and the AFE model (Model 3 in Fig. 22). Clutter removal reduced the area identified as vegetation by 9%, in comparison to the initial batch processing results obtained with Model 2 (see Fig. 22, classification results 7 and 8).

Subsequently, all three AFE models (see Fig. 22) were applied to all the image parts, and classification outputs were compared and evaluated visually. The main differences in the classification results were observed in relation to parts with diffuse vegetation and vegetation with no or very low photosynthetic activity. Since they mostly lacked the high reflectance values in the fourth band (NIR) which characterize active, photosynthetic vegetation, these types of vegetation were comparatively hard to distinguish

from other land cover elements with similar appearances. Hence, where significant under- or overclassifications were noticed in classification outcomes, they mainly concerned these areas. The best possible classification results showed a good balance of accuracy and completeness and thus were largely free from severe biases of either over- or underclassification.

For each of the three parts of the imagery (tiles N1, C2 and S3), a different AFE model was found to be most suitable. For the central part (tile C2), the first model yielded optimal results, while for the southern part (tile S3), the second and for the northern part (tile N1) the third AFE model led to the best classification outcomes (see Fig. 22 for AFE models and their development).

Finally, all collected LU/LC data, i.e. the (edited) dataset of the pervious and the impervious class, the vegetation detection results and the data on identified cloud covered areas were integrated into one file. The resulting dataset was stored in the raster and the vector file format. For the latter, two versions were produced, an unsmoothed vector file directly corresponding to the raster data and a smoothed vector file in which feature outlines were slightly simplified, primarily to eliminate shape biases resulting from pixel boundaries. While the smoothed data is more appealing to the human eye, and often matches natural boundaries of objects or areas of different classes better, the unsmoothed version more accurately reflects actual classification results based on image pixels. Therefore, each version of the final, integrated LU/LC dataset may serve different purposes.

For the integration of the LU/LC data, two workflows were employed, one for the production of the final raster dataset and the corresponding unsmoothed vector data, and one for the creation of the smoothed vector dataset. The first step in the preparation of the raster dataset was the conversion of the manually edited vector data of the impervious, the pervious and the clouded areas into the raster data format. Subsequently, the resulting raster file could be unified with the raster data of the vegetation extraction process. In the unification process, the vegetation data was set as the dominant layer. Thus, the vegetated areas were subtracted from the regions of the other classes, in effect, the pervious and the impervious ones, as no overlap with clouded areas existed. In the output raster file, each cell was assigned to exactly one LU/LC class. To eliminate smaller residual patches resulting from the data integration process, the aggregation tool of FA was applied. Patches smaller than 4 m^2 were incorporated into surrounding or neighboring areas of other classes to form larger regions. The output represented the final, integrated LU/LC dataset in the raster file format. It was converted into the vector format using the standard tool available for this purpose in ArcGIS.

For the smoothed version of the LU/LC data in the vector format, a slightly different approach was adopted. The actual smoothing was done in FA, either by using the smoothing option in the last step of the classification process or with a separate smoothing process. All LU/LC vector data was smoothed with the same algorithm (Bezier) and parameters which were described in BAICU (2012). The smoothed datasets then were combined into one vector data file (shapefile) using the Integrate and the Identity tool

in ArcMap. As in the processing of the raster data, the vegetation dataset was set as the dominant layer and vegetated areas were subtracted from the regions of other LU/LC classes. The output neither contained overlapping nor unclassified areas. An aggregation procedure was applied to remove areas of less than 4 m^2 extent in the pervious and the impervious class. Aggregation was limited to the aforementioned two classes since smaller patches in these categories clearly resulted from the data integration procedure. In contrast, smaller areas (min. 1 m^2) in the vegetation class usually existed before data integration and mostly corresponded to small patches of vegetation such as e.g. single trees. Moreover, due to the comparatively small total area of the vegetation, any changes resulting from post-classification processing would have had a greater proportional impact on the estimated total extent of the class. In general, smoothing and simplification operations typically entail changes in the extents of individual LU/LC classes and amplify size differences between classes. Here, this would have led to a marked decrease in the total area of the vegetation and a corresponding increase in the extent of the pervious class. Therefore, a conservative smoothing procedure was applied to ensure the best possible congruence of unsmoothed and smoothed LU/LC data in terms of the total area of each class.

As a last step, a dataset representing the extent and location of modern settlements was derived from the final LU/LC data. For this purpose, the boundaries of modern settlements were delineated manually. The dataset was then used to clip the regions of the impervious class and thus extract the settlement areas.

4.1.2.5 Semi-automatic detection of rooftops

The semi-automatic detection of rooftops was done separately for each settlement within the study area. The object extraction strategy, in its core, involved the development of a suitable AFE model, based on a subset of the preprocessed GeoEye-1 imagery, and its subsequent application to the rest of the imagery via batch processing. This approach allowed the time-efficient, largely automated extraction of building data. The reapplication of the developed AFE model for the classification of several image parts was facilitated by the similarity of the settlements and the associated building inventory.

Firstly, 12 image subsets, each covering one of the settlements in the study area, were produced from the preprocessed GeoEye-1 satellite image. The extent of each image subset was adjusted to show the respective settlement entirely, while excluding surrounding areas as far as possible. In this way, processing times of individual images could be reduced and the classification process expedited.

For the development of an AFE model that optimally captures rooftop areas in the imagery, three image subsets were selected. The choice was based on the sizes of image tiles and corresponding settlements, according to the population figures displayed in Table 6 (see chapter 3.6). The three selected subsets were the largest ones and covered the three biggest settlements in the area, ar-Rabba, al-Qasr and Jad'a

(cf. Table 6). Due to the sizes, the highest number and greatest variety of rooftops were expected in those images. This was seen as providing optimal conditions for the development of a robust, suitable and broadly applicable AFE model.

The complete workflow, which led to three AFE models that seemed similarly suitable for the extraction of rooftops from the satellite imagery, is visualized in Figure 24. The initial classification model was developed based on the image tile with the greatest extent and the largest anticipated total area of rooftops, due to the described considerations. A relatively small set of training examples (see Fig. 24 and Fig. 25, a) formed the input and basis of the first learning pass which produced the initial classification results (see Fig. 25, b). Suitable training examples were chosen according to the recommendations on good training data and digitized as accurately as possible (see 4.1.2.3 and OVERWATCH 2010). Subsequently, the first classification results and the associated AFE model were improved with several steps of hierarchical learning (Fig. 24 and Fig. 25, c-h). Thus, an optimally suited AFE model and the best possible object extraction results could be attained. In the final output, no significant under- or overestimation of the total area of rooftops could be observed and the detected rooftops showed an adequate location accuracy.

Hierarchical learning was limited to three cycles (cf. Fig. 24), since more passes did not seem to be connected to a substantial, further improvement of classification results. This observation is in good accordance with the recommendations for hierarchical learning given in the reference manual of FA (OVERWATCH 2010). In regard to the learning parameters employed in each classification pass, no universally suitable settings could be identified. Instead, the use of varying values, especially in input representations, pattern widths and thresholds for the maximum area of output features, proved particularly beneficial for the improvement of classification results. Therefore, the settings were adjusted individually in each learning pass. The selected learning parameters are displayed in Figure 24 (light pink boxes).

After each learning pass, the suitability of the object extraction results (see Fig. 25) and hence, the employed AFE model, were evaluated in two ways. Visual examination allowed to quickly assess location accuracy, i.e. how well the automatically identified objects matched observable buildings in the satellite image. However, visually, the quantitative accuracy of outcomes could be assessed only roughly by identifying larger areas of over- or underclassification. Apparently well-matched results had to be compared to reference data (see 4.1.2.6) for a more precise assessment of their quantitative correctness. Here, classification outcomes were checked against reference data (manually digitized rooftops) only in terms of the total area. The combination of this basic quantitative evaluation and the visual examination allowed the quick estimation of the quality of outcomes from each learning pass. Based on the findings, the necessity for improvement and the next steps in the classification process could be determined.

Model 1

❑ Satellite image
- subset
- settlement: Qasr
- 6.873 km²

Manual digitization

❑ Training examples
- 73 features
- total: 12,961 m²
- min. 82 m² - max. 366 m²
- mean: 178 m²
- SD: 63 m²

Supervised Learning
- Building Feature template
- image resolution: 1 m²
- input representation: Bull's Eye 3
- pattern width: 17
- aggregate small regions: min. 49 m²

❑ Classification results 1
- 344 features
- total: 667,752 m²
- min. 49 m² - max. 232,037 m²
- mean: 1,941 m²
- SD: 16,939 m²

Manual selection/ digitization

❑ Clutter removal layer 1
- correct: 37 features, 421,719 m² (63 %)
- incorrect: 13 features, 29,506 m² (4 %)
- unmarked: 304 features, 216,528 m² (33 %)
(−)

❑ Classification results 3
- 535 additional features
- additional area 190,284 m²
- min. 40 m² - max. 13,620 m²
- mean: 356 m²
- SD: 956 m²

Supervised Learning
- Land Cover Feature template (modified)
- image resolution: 2 m²
- input representation: Manhattan
- pattern width: 11
- aggregate small regions: min. 39 m²
- remove large regions: max. 50,000 m²

❑ Add missed features 1
- 7 features
- total: 2,204 m²
- min. 145 m² - max. 681 m²
- mean: 315 m²
- SD: 186 m²
(+)

Manual digitization

❑ Classification results 2
- 745 features
- total: 305,513 m²
- min. 39 m² - max. 17,087 m²
- mean: 410 m²
- SD: 833 m²

Supervised Learning
- Manmade Feature template (modified)
- image resolution: 1 m²
- input representation: Manhattan
- pattern width: 11
- aggregate small regions: min. 39 m²
- remove large regions: max. 50,000 m²

Hierarchical Learning

Accept results

❑ Accepted results 1
- 1,280 features
- total: 495,797 m²
- min. 39 m² - max. 17,087 m²
- mean: 387 m²
- SD: 887 m²

Manual selection/ digitization

❑ Clutter removal layer 2
- correct: 152 features, 70,046 m² (14 %)
- incorrect: 37 features, 17,085 m² (4 %)
- unmarked: 1,122 features, 408,667 m² (82 %)
(−)

Supervised Learning
- Building Feature template (modified)
- image resolution: 1 m²
- input representation: Bull's Eye 3
- pattern width: 17
- aggregate small regions: min. 12 m²
- remove large regions: max. 50,000 m²

❑ Classification results 4
- 537 features
- total: 182,329 m²
- min. 13 m² - max. 5,344 m²
- mean: 340 m²
- SD: 381 m²

Model 1

Model 2

❑ Satellite image
- subset
- settlement: Rabba
- 4.440 km²

Batch Processing with Model 1

❑ Classification results 5
- 489 features
- total: 149,588 m²
- min. 16 m² - max. 3,575 m²
- mean: 306 m²
- SD: 344 m²

Manual digitization

❑ Add missed features 2
- 6 features
- total: 958 m²
- min. 82 m² - max. 320 m²
- mean: 160 m²
- SD: 76 m²
(+)

Supervised Learning
- Land Cover Feature template (modified)
- image resolution: 1 m²
- input representation: Manhattan
- pattern width: 11
- aggregate small regions: min. 39 m²
- remove large regions: max. 10,000 m²

❑ Classification results 6
- 679 additional features
- additional area: 202,215 m²
- min. 39 m² - max. 7,021 m²
- mean: 298 m²
- SD: 601 m²

Hierarchical Learning

Model 2

❑ Classification results 7
- 821 features
- total: 160,597 m²
- min. 14 m² - max. 4,129 m²
- mean: 196 m²
- SD: 318 m²

Supervised Learning
- Building Feature template (modified)
- image resolution: 0.5 m²
- input representation: Bull's Eye 3
- pattern width: 17
- aggregate small regions: min. 14 m²
- remove large regions: max. 8,000 m²

❑ Clutter removal layer 3
- correct: 106 features, 41,020 m² (12 %)
- incorrect: 21 features, 6,192 m² (2 %)
- unmarked: 1,043 features, 304,591 m² (86 %)
(−)

Manual selection/ digitization

❑ Accepted results 2
- 1,168 features
- total: 351,803 m²
- min. 16 m² - max. 7,021 m²
- mean: 301 m²
- SD: 510 m²

Accept results

Model 3

❑ Satellite image
- subset
- settlement: Jad'a
- 2.018 km²

Batch Processing with Model 1

❑ Classification results 8
- 308 features
- total: 74,798 m²
- min. 12 m² - max. 2,323 m²
- mean: 243 m²
- SD: 206 m²

Manual digitization

❑ Add missed features 3
- 5 features
- total: 732 m²
- min. 82 m² - max. 176 m²
- mean: 146 m²
- SD: 34 m²
(+)

Supervised Learning
- Building Feature template (modified)
- image resolution: 0.5 m²
- input representation: Pre-defined Foveal
- pattern width: 9
- aggregate small regions: min. 14 m²
- remove large regions: max. 500 m²

❑ Classification results 9
- 478 additional features
- additional area: 38,092 m²
- min. 14 m² - max. 482 m²
- mean: 80 m²
- SD: 92 m²

Hierarchical Learning

Model 3

❑ Classification results 10
- 449 features
- total: 85,743 m²
- min. 14 m² - max. 2,076 m²
- mean: 191 m²
- SD: 181 m²

Supervised Learning
- Building Feature template (modified)
- image resolution: 0.5 m²
- input representation: Manhattan
- pattern width: 11
- aggregate small regions: min. 14 m²
- remove large regions: max. 8,000 m²

❑ Clutter removal layer 4
- correct: 99 features, 24,667 m² (22 %)
- incorrect: 9 features, 1,517 m² (1 %)
- unmarked: 678 features, 86,706 m² (77 %)
(−)

Manual selection/ digitization

❑ Accepted results 3
- 786 features
- total: 112,890 m²
- min. 12 m² - max. 2,323 m²
- mean: 144 m²
- SD: 168 m²

Accept results

Fig. 24: Workflow of the development of three AFE models for the automatic detection of rooftops in the prepro- cessed GeoEye-1 satellite image. Hierarchical learning steps are circumscribed by black, dashed lines. The plus symbol marks processes intended to broaden object extraction results and counteract underclassification. The minus symbol marks processes used to narrow down outcomes and reduce overclassification.

Legend

Buildings/rooftops

User input

- Training examples
- Features/parts marked as correct
- Features/parts marked as incorrect
- Examples of missed features

Feature Analyst output

- Classification results
- Added features/areas

0   400   800
m

Fig. 25: Development of the initial AFE model for the detection of rooftops: user input (a, c, e, g) and classification results (b, d, f, h) of the different stages of model development. Part a shows the initial training examples used to obtain the first classification results (b). Outcomes were improved with subsequent steps of hierarchical learning. A first pass of clutter removal (c, d) was followed by a step of adding missed features (e, f) and another pass of clutter removal (g, h) which led to the final classification results (h).

With the above described procedure, satisfactory classification results and a suitable initial AFE model could be obtained for the image subset of Qasr (see Fig. 24 and 25). Next, the transferability and robustness of this first model were tested by applying it to the second largest image tile which covered the town of Rabba. The object extraction results then were evaluated as outlined above. In contrast to the results from the first image, outcomes from the batch processing of the second image (Rabba) seemed less well-matched. Consequently, an attempt was made to improve the classification results and the existing AFE model with additional steps of hierarchical learning (see Fig. 24). Since the initial outcomes from batch processing exhibited a pronounced tendency towards underclassification, the procedure for adding missed features was applied. This operation commonly leads to a significant overclassification, which could also be observed in the present case. Therefore, another pass of clutter removal was performed to counteract this tendency. The resulting second AFE model was able to produce slightly better object extraction results for the image of Rabba than the first model.

In two batch processing procedures, each of the aforementioned AFE models was then employed to detect rooftops in a third image. This image subset covered the village of Jad'a, the third largest settlement in the study area in terms of the number of residents. Outputs of the batch processing procedure were evaluated individually as described before. Upon comparison of the findings, the results from the application of the first AFE model seemed more appropriate than those of the second AFE model. Nonetheless, the outcomes apparently exhibited a slightly lower quality than the results of the first image tile (Qasr). Therefore, again an attempt was made to improve the initial AFE model. The employed stepwise procedure of hierarchical learning was similar to the one leading to the development of the second AFE model. Details of the workflow and the selected parameters are displayed in Figure 24. Thus, a third AFE model was attained which, like the second model, also built on the first AFE model. For the image subset of Jad'a, the third AFE model yielded the best-suited rooftop detection outcomes.

Since the ultimate goal was to create a robust AFE model with broad suitability, all hitherto developed models were tested in the classification of other images via batch processing. For this purpose, the three AFE models, one at a time, were applied to the three aforementioned image tiles (Qasr, Rabba and Jad'a, cf. Fig. 24) as well as to three further image subsets, which had not been utilized in the development of the models. The latter images covered the villages of Smakiya, Mghayyer and Shihan, respectively. These represented the largest of the remaining settlements in terms of household numbers (see chapter 3.6, Table 6) and hence, high total areas of rooftops were expected there. The batch processing outputs, i.e. rooftop detection results from all images were then evaluated with a detailed accuracy assessment procedure (see following chapter). Findings from the evaluation allowed to identify the AFE model with the best overall suitability and broadest applicability. Via batch processing, the selected model was then used to automatically detect rooftops in the image subsets of the remaining six settlements in the study area.

4.1.2.6 Accuracy assessment of semi-automatically extracted datasets

An accuracy assessment was conducted to estimate the quality of the outcomes from the semi-automatic image classification and object extraction procedures (see chapters 4.1.2.4 and 4.1.2.5 for methods and 5.1 and 5.2 for results). Different approaches were used in the evaluation of the LU/LC data and the rooftop data, respectively. The assessment of the LU/LC data was limited to the outcomes of the semi-automatic extraction of the vegetation information. The raw, unedited image classification results of the other LU/LC classes, i.e. the pervious and the impervious category, had previously been evaluated by BAICU (2012). In the present study, the aforementioned data of the pervious and the impervious class were edited manually (see 4.1.2.4). Due to this blending of different methods and the previous evaluation, the corresponding classes were exempt from the accuracy assessment here.

The procedure of the accuracy assessment of the vegetation data is described below. The original, unsmoothed vegetation detection outcomes which were integrated with the other LU/LC data (see 4.1.2.4) were evaluated here. The accuracy assessment procedure itself consisted of sampling, i.e. the collection of a subset of test data from the classification results and the acquisition of reference data for the same locations, and subsequent comparison of the two sample datasets.

The sampling strategy essentially corresponded to a stratified random approach in which the same number of samples was collected from the two strata, the vegetation and the background or non-vegetation class. As LI & GUO (2013) pointed out, to avoid major biases, the evaluation of a single LU/LC class must include the sampling and assessment of background data when common assessment techniques and traditional statistical measures of accuracy are employed. Since random sampling would have led to an underrepresentation of samples from the vegetation category, due to the comparatively small extent of this class (see 5.1), a stratified random sampling strategy was selected. Furthermore, a suitable sample size and an appropriate sampling unit had to be determined. With regard to the sample size, CONGALTON's (1991) rule of thumb, which suggests at least 50 samples per class, provided a first orientation. In view of the high number of individual detected patches of vegetation (features) and their relatively broad spectrum of properties, the number of samples per class was increased to 100. Thus, the best possible reliability and representativeness could be ensured in the collected sample data and the associated accuracy outcomes, while maintaining an acceptable level of feasibility. Due to the large extent and the high resolution of the satellite imagery, derived classification results also consisted of an enormous quantity of individual pixels. Therefore, the commonly used sampling unit of one pixel did not seem suitable. Instead, a cluster of pixels, here a rectangle of 3 × 3 pixels, was chosen as the sampling unit. Each pixel of the cluster is assessed separately by assigning a classification and a reference label to it (STEHMAN & WICKHAM 2011, in contrast to CONGALTON & GREEN2009). Hence, a sample unit in parts can be attributed to different LU/LC classes. Here, this was necessary where smaller patches of vegetation (minimum area 4 m^2 or four pixels, see 4.1.2.4) or the boundaries of features were included in the samples. If instead, a block of the same size (3 × 3 pixels) had been chosen as the sampling unit, each

sample would have had to be assigned in its entirety to one category, since a block is considered as a single entity. Mixed samples including parts of different classes therefore would have had to be excluded or relabeled, e.g. based on the majority of pixels in the respective block. However, this could have introduced further biases into the accuracy assessment procedure and corresponding outcomes.

In the absence of real ground truth, in this case GPS data of existing vegetation in the study area, reference data was acquired through visual interpretation of the preprocessed GeoEye-1 satellite image and manual delineation of vegetation areas. Although preferably real ground truth in the form of field data should be used, for feasibility reasons, the acquisition of reference data through interpretation of aerial or satellite imagery is common practice. CONGALTON & GREEN (2009) also considered this approach an acceptable solution for basic classification tasks with few, broad and clearly distinguishable LU/LC classes. Nonetheless, an accuracy assessment without field data does not allow to estimate the quality of classification results accurately with regard to real world conditions. It rather represents a methodological evaluation in which the outcomes from two different remote sensing-based techniques of image analysis are compared. However, visual-manual image interpretation is considered the best practice, with which the most accurate and reliable thematic data can be derived from remote sensing images. Therefore, the accuracy assessment is able to provide valuable information about the quality of classification results, particularly with regard to the suitability of the selected methodological approach as well.

All processing, including the acquisition of reference data, sampling and data evaluation, was done in ArcMap. For each of the 200 samples in total (100 per category, consisting of a window of 3×3 pixels, respectively), classification outputs and reference data were compared on a per pixel basis. The results were integrated into an error matrix which not only served presentation purposes but also formed the basis for the calculation of the common statistical measures of accuracy (see chapter 5.1, Table 10).

Results from the semi-automatic detection of rooftops were evaluated comprehensively and in detail with a spatially explicit approach in order to determine their accuracy and reliability. All outcomes from the application of the three different AFE models to the six image tiles that were used for the development and the evaluation of the models, were assessed in the same way. Accuracy findings of original classification results, i.e. outputs from a given AFE model for the image subset based on which the model had been developed, indicated the appropriateness of the specific outcomes and the AFE model in the particular case. In contrast, findings from the assessment of feature extraction results that were obtained through batch processing, additionally allowed to judge the transferability of the respective AFE model. To facilitate the comparison and evaluation of the three AFE models in terms of their performance, suitability and transferability, results from the accuracy assessment of batch processing outputs were also aggregated by AFE model (see chapter 5.2, Table 13).

In total, 18 datasets which resulted from the classification of six image tiles with three different AFE models, were evaluated. No sampling was employed and classification outputs were assessed in their

entirety. Automatically detected rooftops were compared to reference data for each image and settlement individually. Since no real ground truth, such as measurements of rooftop areas of buildings, were available, reference data was created through visual interpretation of the preprocessed GeoEye-1 satellite imagery and manual digitization of the discernible rooftops. In ArcMap, the classification and the reference data were then intersected to identify overlaps and discrepancies between rooftop areas in the two named datasets. The findings were entered into an error matrix which discriminated between two categories, rooftop and non-rooftop or background areas (see Table 11 and 12, chapter 5.2). Based on the error matrix of each of the 18 datasets of semi-automatically detected rooftops, the traditional statistical measures of accuracy (user's, producer's and overall accuracy) and Cohen's kappa were respectively calculated. Additionally, the number of overlapping features was determined from the intersection of classification results and reference data and a corresponding accuracy index termed "Feature Score" was developed. The object- or feature-based error matrixes and the associated measures of accuracy were configured and calculated in the same way as the other, area-related error matrixes and traditional statistical measures of accuracy. In combination with the latter, the object-related figures provided further, more holistic information about the appropriateness of classification results. Furthermore, they were able to deliver insight into the type, location and possible sources of classification errors. The design of the described customized accuracy assessment, including object-related measures, in many ways parallels other approaches for the evaluation of building detection results (e.g. FREIRE ET AL. 2010, TSAI ET AL. 2011, ZENG ET AL. 2013). Concerning the outcomes of OBIA processes, the development of better suited assessment procedures and more apt measures of accuracy were also postulated by PERSELLO & BRUZZONE (2010) who employed geometric indices, and PONTIUS JR & MILLONES (2011) who advocated the use of quantity and allocation disagreement.

Finally, as a part of the accuracy assessment, classification results and reference data were also compared in terms of the respective total area of rooftops identified. Thus, the amount of over- or underclassification could also be estimated (see 5.2, Table 11 and 12). Although valuable, this index of quantity appropriateness is not spatially explicit and hence does not reflect the spatial or location accuracy of the corresponding classification results. Consequently, this figure must always be interpreted in conjunction with other indices, such as e.g. the feature scores, which express the spatial accuracy of outcomes.

Based on the accuracy assessment results, the most appropriate AFE model was determined for the semi-automatic extraction of rooftops from the remaining image subsets that covered the six smaller settlements in the study area. In the selection process, special attention was given to the assessment results of batch processing outputs, since these were most indicative of the transferability of the respective AFE model. The aggregation of the corresponding outcomes (see 5.2, Table 13) allowed for the estimation of the characteristic performance of each AFE model. Thus, also the likely quality of classification results for the six remaining image subsets could be anticipated. Since the AFE models showed mixed results for the different statistical measures of accuracy, some indices had to be defined as the most

decisive ones for the selection of a single, best suited AFE model. Priority was given to the appropriateness of the total area of detected rooftops, i.e. the least amount of over- or underclassification, and the relative spatial accuracy of outcomes which is expressed in feature scores.

4.1.3 Processing of digital elevation models

With regard to digital elevation models (DEM), it is necessary to define the surface to which the model refers. In principal, a DEM can visualize the surface of a landscape including any man-made and natural objects (e.g. buildings, trees, etc.), or it can represent the surface of the terrain, i.e. the relief of the bare earth. In the case of the latter, the term digital terrain model (DTM) has been established whereas in the case of the former, the expression digital surface model (DSM) is used. Both terms are more specific than the inherently ambiguous expression DEM which can be seen as an umbrella term for both DTMs and DSMs. Sometimes DEM is also used as a synonym for DTM (HIRT 2014). It is crucial to distinguish between DTMs and DSMs in areas where differences between both are greatest, for example in forested or built-up areas. In open range land and similar rural areas, differences between DSMs and DTMs are typically marginal. Another decisive factor in this regard is the spatial resolution of a DEM, since with higher resolutions minor height differences and surface features become increasingly evident. The DEMs employed for the study at hand are technically DSMs since vegetation or buildings heights were not explicitly removed. Nonetheless, they largely correspond to DTMs due to the characteristics of the study area and the spatial resolution of the models. The study area has a rural character and mostly consists of open range land. Surface objects (trees, low-rise buildings, etc.) are rather small and few in numbers and thus do not significantly influence the relief depicted in the models. Due to the expected overlap between DSMs and DTMs in this case, here, the more generic term DEM is used, as it is common practice for remote sensing derived models (cf. HIRT 2014).

In the study at hand, two DEMs with different spatial resolution and coverage were used. The ASTER GDEM (Version 2) has an almost global coverage and a resolution of 1 arc second (approximately 30 m) and is based on stereoscopic imagery recorded by the ASTER satellite sensor (ASTER GDEM VALIDATION TEAM 2011, JPL ET AL. 2012). It is provided at no cost by NASA and METI and represents the relief of the earth with vertical accuracies (RSME) of better than 10 m (ASTER GDEM VALIDATION TEAM 2011, HIRT 2014). The ASTER GDEM V2 was used primarily in this study where elevation data outside the study area itself was needed, e.g. for the broader, regional hydrological analysis (chapter 4.1.4) and the spatial interpolation of precipitation data (see 4.1.6).

A DEM with a higher spatial resolution of 5 m pixel size was acquired for the study area itself (see inset map in Fig. 26). It was created through spatio-triangulation of two sets of ALOS PRISM triplet satellite images which had a resolution of 2.5 m and were recorded in January 2011 (for details on ALOSPRISM imagery see JAXA & EORC n.d.). The DEM was produced by Geoserve B.V. During the production

process, 14 GCPs based on the GeoEye-1 imagery (preliminary, largely unprocessed version) served as collateral data and 12 tie points were used. The resulting DEM exhibited relative accuracy values of better than 7.5 m in the horizontal (XY) and better than 10 m in the vertical (Z) dimension (CE90 and LE90 respectively). The model itself, as well as its derivative data layers, such as e.g. the slope map, were employed for a variety of purposes in the present study. This included the extraction of elevation information for specific points or areas (see 4.2.1), a detailed hydrological analysis for the study area (see 4.1.4), and the preprocessing of the GeoEye-1 satellite imagery (orthorectification and atmospheric corrections, see 4.1.2.1).

For several of the intended purposes of the DEM, a smoothing and filtering procedure had to be applied to the original ALOS-based DEM and the derivative datasets, in order to minimize or eliminate minor artefacts, errors and distortions (see Fig. 26). Apart from the quality of the DEM, the necessary degree of modification depended on the intended use. In the orthorectification process (see 4.1.2.1) and for the hydrological analysis (4.1.4) the original, unaltered DEM was used. For all other purposes, particularly the atmospheric corrections of the GeoEye-1 imagery with ATCOR3 (see 4.1.2.1), the DEM was modified as described below.

Initially, the original, custom-made ALOS DEM with 5 m resolution was resampled to a half meter resolution to artificially refine its level of detail. Then, all small closed depressions, so-called sinks, were leveled using the Fill tool available from the toolbox of the Spatial Analyst extension in ArcGIS (cf. Fig. 26 a, b). Subsequently, in ArcMap, for each meter of elevation difference, contour lines were created and generalized to reduce the number of vertices in each line and eliminate staircase effects from pixels. Afterwards, a DEM was interpolated from the contour lines with the Topo to Raster tool in ArcGIS. The named function produces a topologically and hydrologically correct DEM based on the ANUDEM approach developed by HUTCHINSON (1989, 1996) (ESRI 2016; for further information about ANUDEM see HUTCHINSON & GALLANT 2000, HUTCHINSON ET AL. 2009, 2011). As an integral part of the interpolation process, several optional parameters, such as e.g. the discretization error factor, the vertical standard error and the maximum number of iterations, allowed adjusting the smoothness of the resulting DEM. Here, suitable settings were chosen to limit smoothing to the necessary degree. This allowed the creation of a suitable DEM while preserving elevation values and details of the original DEM as far as possible. Although the procedure led to a generally satisfactory output, the resulting DEM still contained several minor erroneous spots along the fringes of the model. In order to remove these artifacts, contour lines with 1 m spacing were again derived from the modified DEM. Where necessary, the contours then were edited and adjusted manually. From the corrected contours, the final DEM was interpolated with the Topo to Raster procedure described above. Differences in elevation values between the original and the final modified DEM varied between -22 and +28 m with an average of +/- 3 m. More than 98% of all raster cells exhibited a difference of 3 m or less, indicating that elevation values

were not altered significantly in the editing process. Larger changes mainly concerned closed depressions in the original DEM and hence can be attributed to the sink filling procedure.
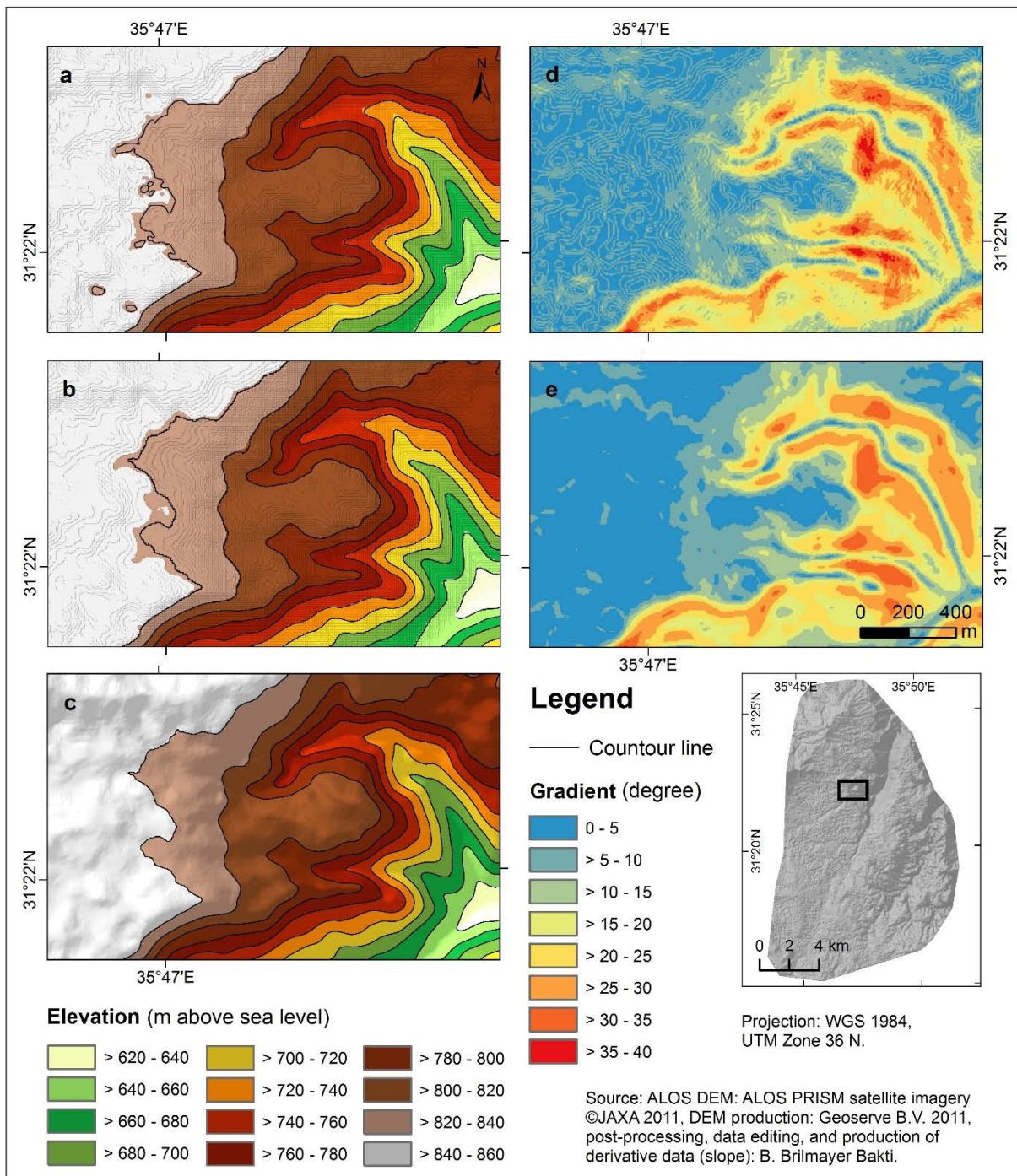
Fig. 26: Effects of modifications on the ALOS DEM and derivative data layers (slope map). In the original DEM (a) and the corresponding slope map (d) artifacts are visible. In contrast, the final modified DEM (b, c) and the slope map (e) derived from it, appear smoother and largely free from artifacts. Using the floating point raster type (c) whenever possible avoids the staircase effect occuring in a raster when elevations are represented by integer cell values (b). Location and extent of the subsets (a-e) are indicated by the black rectangle in the inset map showing the complete ALOS DEM.

The degree to which the relief displayed by the DEM appears natural and smooth, is also determined by the properties of the raster file, particularly the pixel type and pixel depth. Rasters of the floating point type, such as the output of the Topo to Raster function, are generally more suitable for the representation of continuous data and exhibit a smoother model surface than rasters of the integer type (see Fig. 26 b, c). However, for its use in ATCOR, the DEM inevitably had to be available as a raster file of the 16 bit unsigned integer type. This introduced systematic artifacts resembling the imprint of contour lines (see Fig. 26 a, b) which were especially evident in derivative data, i.e. terrain files calculated based on the DEM (see slope map in Fig. 26 d). In order to compensate for this effect, in ERDAS IMAGINE a low pass filter with a kernel size of 11×11 pixels was applied to all terrain files once or twice, depending on individual necessities. The slope map which reflects the steepness of the terrain, i.e. the change in elevation from one raster cell to its neighboring one, was created in ArcMap as this led to better, more suitable results than computing the corresponding file with ATCOR3. All terrain files were derived from the final, modified ALOS DEM (see above). The DEM and all derivative datasets initially were produced with a spatial resolution of 5 m. They were resampled to a resolution of 0.5 m in order to match the image of the panchromatic band of GeoEye-1 in terms of resolution (see section 4.1.2.1, Table 7). RICHTER & SCHLAEPFER (2011) suggested that resampling, where necessary, should be performed as the last step when preparing terrain files for atmospheric corrections with ATCOR. Thus, the appearance of further artifacts, and consequently, an increased need for filtering and smoothing can be avoided.

4.1.4 Hydrological analysis and preparation of surface drainage data

In order to gain detailed information about the (potential) surface drainage network of the study area and the surrounding wider region, hydrological analyses were conducted on different scales using Arc Hydro for ArcGIS. By applying a series of different Arc Hydro tools, several relevant data layers containing e.g. information on drainage lines and catchments, could be derived from the DEM (see Fig. 27). In total, the sequence of operations which formed the hydrological analysis was performed three times with different input data and parameters. The first hydrological analysis (workflow a in Fig. 27) was based on the ASTER GDEM V2 (see 4.1.3) and served to identify the major wadis (drainage lines) and their watersheds in the broader region (see 5.4, Fig. 37). Thus, the regional setting of surface water drainage could be revealed in which the study area and its drainage network are embedded. The second hydrological analysis (see Fig. 27, a) was limited to the study area itself and used the ALOS DEM as input (see 5.4, Fig. 38). The outcomes were evaluated by comparing the computed drainage lines to those discernible in the GeoEye-1 satellite image. In general, the network of drainage lines derived from the (original) ALOS DEM largely was in accordance with the wadis, channels, gullies and rills visible in the satellite image. Nonetheless, quite a number of minor, and a few major discrepancies, were ob-

served (cf. 5.4, Fig. 39 b and c). Differences between computed (synthetic) drainage lines and visually identified drainage lines were strongest and most common in areas with low relief energy, i.e. mostly flat terrain. Similar observations were mentioned in other studies (e.g. SEYLER ET AL. 2009). Parallel double or longer straight lines and similar atypical forms usually represent artifacts in the computed drainage network. These also primarily occurred in areas with very little variances in elevation (see Fig. 39). Due to the described perceived deficits in the drainage data derived from the DEM, a third hydrological analysis was carried out. This time, in addition to the ALOS DEM, a dataset of drainage lines, which were digitized manually, based on visual interpretation of the satellite image (see 4.1.2.2), was used as input (see Fig. 27, b). Thus, the assets of both input datasets could be combined to further enhance the reliability and accuracy of the outputs. In the hydrological analysis, the information contained in each dataset, the manually digitized drainage lines and the elevation data of the DEM, were integrated. The process in which the drainage lines were "burned" into the relief of the DEM, roughly corresponded to a hydrological correction of the DEM. A similar approach had also been adopted e.g. by SEYLER ET AL. (2009).

The exact steps and the detailed procedure of the conducted hydrological analyses are visualized in Figure 27. In all cases, the pit or sink filling process which eliminates closed depressions in the DEM, was an essential, indispensable part of the workflow. As no real closed depressions with ponding water or subterranean drainage were known to exist in the area, all sinks were filled without exception. This was necessary to enable the computation of a completely dendritic drainage network. In tests, the use of the modified ALOS DEM in the second hydrological analysis (see workflow a in Fig. 27) was not associated with more suitable outcomes, as the visual evaluation of the computed drainage lines (synthetic streams) indicated, in comparison with the satellite image. Therefore, in order to minimize the degree of modifications made to the elevation data, the original, unaltered ALOS DEM was employed in all hydrological analyses that focused on the study area itself.

Moreover, for all hydrological analyses relying solely on a DEM (workflow a in Fig. 27), the threshold for stream initiation is decisive. It defines the minimum catchment area required for headwaters, i.e. the beginning of a drainage line, and must be specified in the stream definition process. The selected threshold also determines the level of detail exhibited by the computed network of drainage lines and the corresponding catchment data. In the region-wide hydrological analysis, which was based on the ASTER GDEM and used for overview purposes, the threshold of stream initiation was set to 50 km^2, whereas for the detailed, study area-specific analysis, which relied on the ALOS DEM, an area of 0.025 km^2 was chosen. The smaller threshold selected in the study-area-specific analysis ensured that the automatically computed network of drainage lines showed a similar level of detail as the manually digitized one. This allowed the direct comparison of both datasets and corresponding analysis outcomes (see chapter 5.4, Fig. 39 and Table 14).
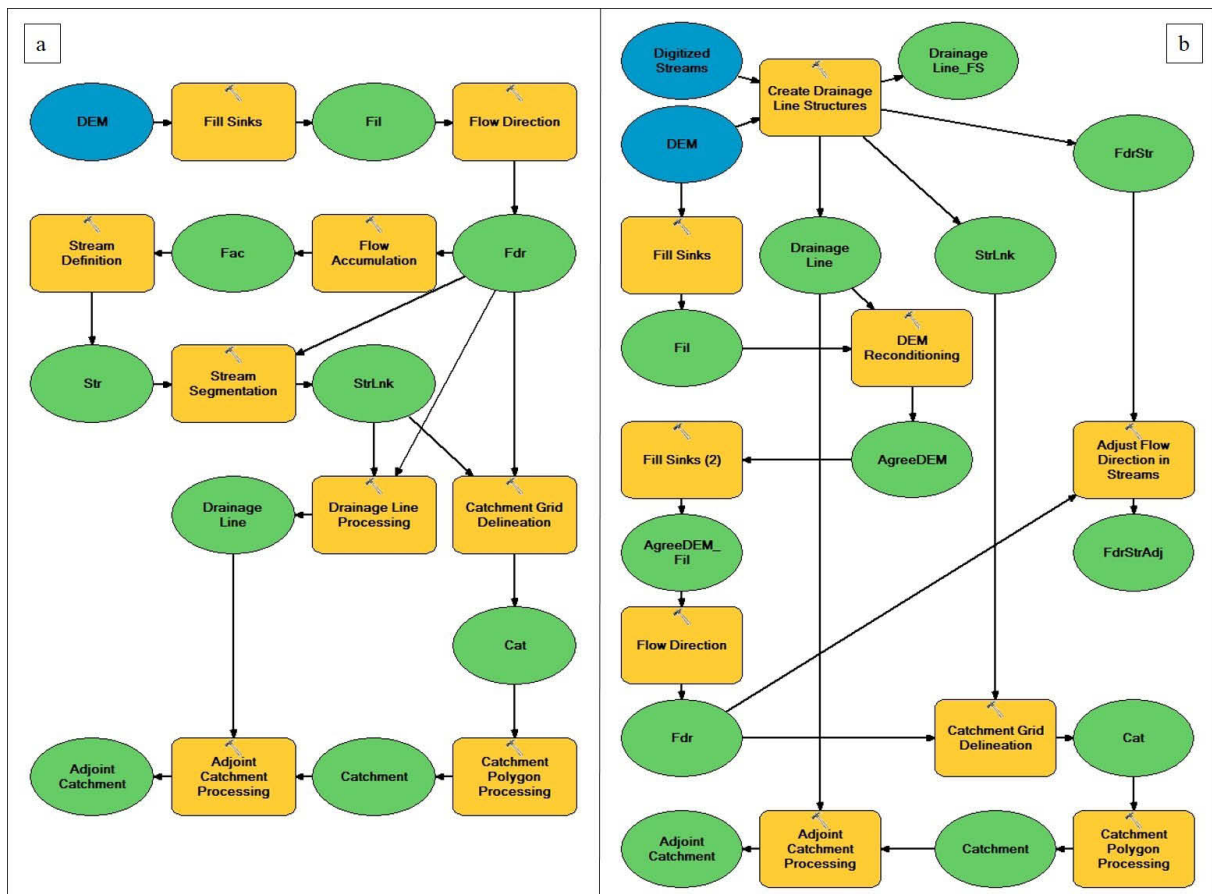
Fig. 27: Hydrological analyses: workflows/models. Each model shows the sequence of Arc Hydro operations executed in the respective analysis. Input and (intermediate) output datasets are depicted as blue and green ovals, respectively. Intermediate outputs serve as input for the next processing step. Tools are represented by yellow boxes with a hammer symbol. Arrows indicate the processing direction and relations (input/output) between individual elements. Models were set up and managed with the ModelBuilder application of ArcGIS Desktop. Diagram a illustrates the workflow of the hydrological analyses that relied solely on a DEM, i.e. the ASTER GDEM V2 for the region-wide analysis and the ALOS DEM for the preliminary, study area-specific analysis, as input data. Diagram b visualizes the workflow of the study area-specific hydrological analysis which used the ALOS DEM and the manually digitized drainage lines as input.

4.1.5 Acquisition of geological and archaeological data

Geological data and information about the sites of archaeological finds and remains were included in the present study, particularly with regard to the identification of common properties of RWH sites and their possible relations to other natural and man-made objects in the environment (see chapter 4.2.1). The geological and archaeological data were obtained from external sources and processed and edited as necessary in order to be able to integrate them into the study's database containing all other datasets and to use them in the subsequent analyses (see 4.2.1).

The geological data layer (see chapter 5.5) was derived from the digital, nationwide vector dataset (WAJ 2010b) which comprised the information of the available (printed) geological maps of the scale 1:50,000

for Jordan. A subset of the named dataset was created for the study area and the contained information was compared to those given in the two geological maps (sheets 3152 I, Dhiban/Wadi al Mujib and 3152 IV, Ar Rabba) of the same scale (1:50,000) (NATURAL RESOURCES AUTHORITY ET AL. 1989, 1996) that together covered the study area. Discrepancies were eliminated by editing the digital dataset to match the geological maps. Further modifications mainly concerned the attribute table of the geological dataset. The stored information was consolidated, complemented and modified as necessary to produce a suitable, conveniently manageable dataset with all relevant, available geological information. A concise description of the content of the prepared data layer can be found in chapter 5.5.

Data on archaeological sites was retrieved from the MEGA-Jordan online database which stores information about all archaeological finds and remains in conjunction with their respective location where they were found in Jordan (THE GCI ET AL. 2010). In a first step, the database was queried for archaeological sites within the study area or a distance of max. 6 km around it. Results were exported as a table which included one pair of coordinates (x, y) for each archaeological site. In ArcMap, this information was imported and converted into a vector dataset in which each archaeological site and its corresponding location were represented by one point feature. With subsequent queries of the MEGA-Jordan database, further information about the extracted subset of archaeological sites was gathered and added to the aforementioned vector dataset. There, the collected information about each site was stored as attributes of the corresponding feature (point). Thus, for each feature (archaeological site), the created data layer contained a number of relevant details, such as e.g. the type(s) of archaeological finds or remains (broad categories), the associated archaeological period(s) and whether the discoveries included water structures or not.

Subsequently, the archaeological sites (point features) in the created dataset were grouped into three different categories according to their location. The first class encompassed all sites that were situated on the Karak Plateau and within the study area itself (see 3.6, Fig. 12). The remaining archaeological sites in the zone of a maximum distance of 6 km around the study area were classified into two groups, depending on whether they were located on the tableland, i.e. at elevations of at least 700 m above sea level, or in the valleys of major wadis and thus, at lower elevations. This discrimination was necessary due to the differences between the Karak Plateau and the surrounding areas at lower elevations in terms of environmental conditions, especially with regard to the available freshwater resources. These differences in altitude and associated natural circumstances, including water availability, need to be considered in the distance analyses and the deduction of possible spatial relations (see chapters 4.2.1, 6.2.2 and 7.3). For example, an ancient cistern located at the fringes of the Karak Plateau more likely served as a crucial water resource for a nearby ancient settlement on the tableland than for one in the Mujib valley, at a similar distance but at substantially lower elevations. Therefore, two broad areas with similar environmental conditions were defined. The contour line indicating an altitude of 700 m above sea level was

used to separate the tableland from areas of lower elevations. For each archaeological site, the category to which it had been assigned, was recorded in the attribute table of the data layer.

4.1.6 Spatial interpolation of precipitation data

Of all climatic parameters, precipitation was the most decisive for the present study, particularly with respect to the estimation of runoff and RWH potentials (see chapter 4.2.2). Therefore, detailed, comprehensive precipitation data was acquired and processed as described below. Due to practical considerations including limited data availability, costs of data acquisition and methodological feasibility within the scope of the present study, the use of detailed climate data was limited to precipitation records. All other climatic parameters were taken into account more generally. Indirectly, they were expressed in e.g. suitable runoff coefficients and thus, also influenced the estimation of runoff (see 4.2.2).

Daily precipitation records of four weather stations (Jada', Qasr, Rabba, Hemud) within the study area, and 24 further ones situated in the surrounding area (see Fig. 28), gave an account of the amount of precipitation (in mm) measured at the respective location at a given date. Through spatial interpolation of this point data, continuous raster files were produced that covered the defined region and showed the daily amount of precipitation on a per cell basis. The distribution, locations, and names of the weather stations that provided the precipitation data are displayed in Figure 28.

The available precipitation records of the 28 weather stations covered different time spans and occasionally included shorter or longer periods (one day to several months, or even years) with no data or estimates instead of measured precipitation. For a reasonable representation of the climate of a given area, an observation period of 30 years is commonly recommended. A sufficiently long observation period was particularly important for the present study since the semi-arid climate of the region is characterized by large interannual variances, especially in precipitation (see 3.3 and 5.6, Fig. 41). Upon examination of the available precipitation data of the 28 weather stations in the region, the 30 year period of 1963 - 1992 was identified as the one with the best data coverage (see Fig. 29). The chosen time span largely overlaps with the currently recommended climate normal reference period of the years 1961-1990, which is used e.g. by the IPCC (cf. MCCARTHY ET AL. 2001). Thus, the employed data should be comparable to that of other regions of the world and suitable as reference to trace the impact of climate change on precipitation in the data of later periods. The slight deviance of the selected observation period from the recommended time span 1961-1990 was a result of data coverage. When determining a suitable 30 year period, the availability of as many precipitation records from different weather stations as possible was given priority. This should ensure the best possible validity, representativeness and reliability of interpolation outcomes, i.e. the maps of daily and long-term average precipitation.
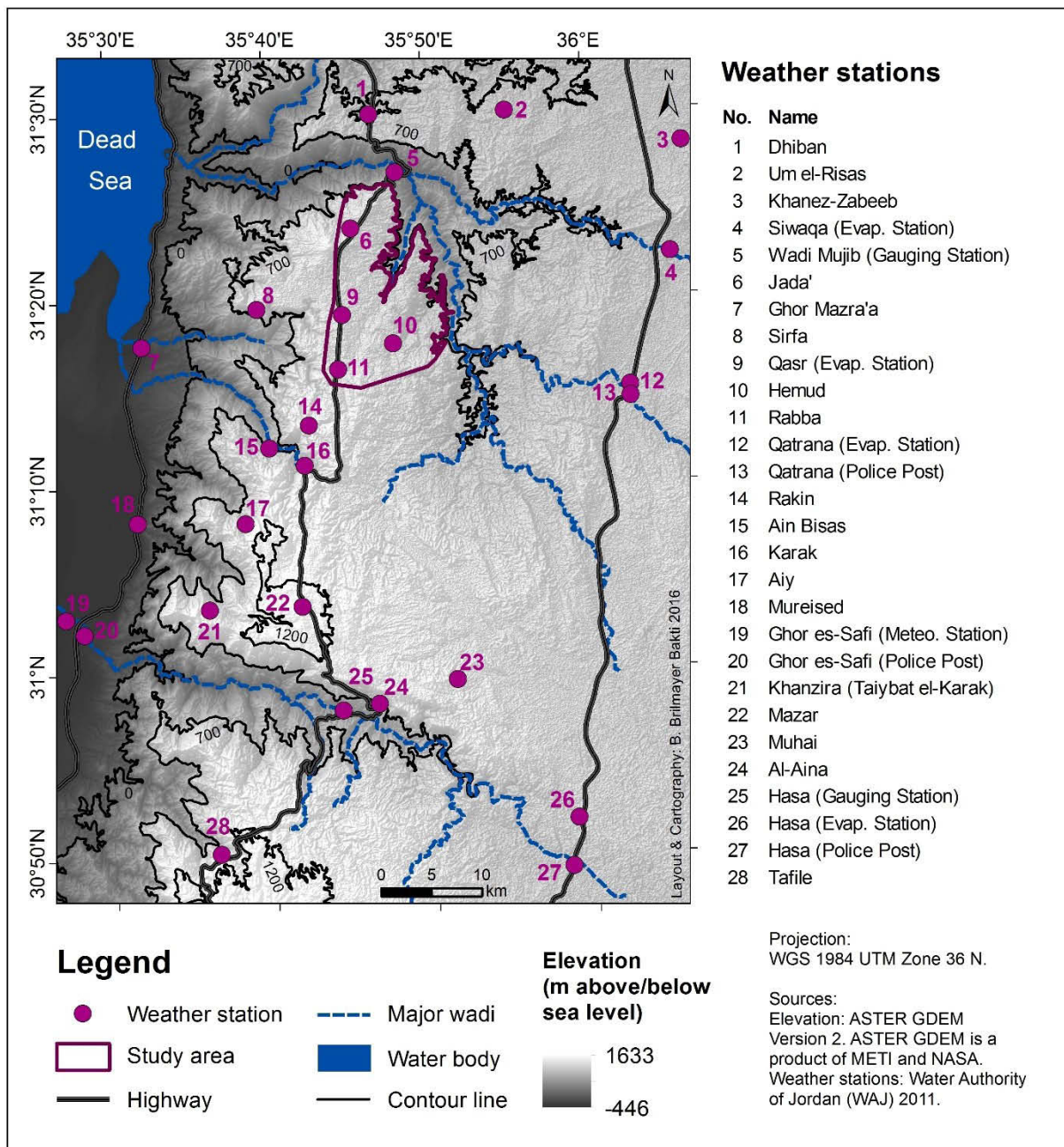
Figure 28: Locations and names of the weather stations which recorded the precipitation data used in this study. The names of the weather stations are spelled as given in the original dataset (WAJ 2011).

For the spatial interpolation of the precipitation data of the individual weather stations, a tool developed by and described in WIMMER ET AL. (2009) was employed. The approach capitalizes on a variety of different interpolation algorithms. Based on the distribution of available input data, i.e. weather stations with a precipitation record for the respective date, the program automatically selects the most suitable interpolation method. In the interpolation process, the tool also takes latitudinal and longitudinal gradients and orographic effects into account (MENZEL ET AL. 2009, TÖRNROS & MENZEL 2014). This is a particular advantage since the named factors significantly influence the spatial distribution of precipitation in the study region (see 3.3). For the adequate incorporation of these aspects, particularly the orographic effects, a DEM representing the relief must be provided for the interpolation process. Here, the

ASTER GDEM V2 was used. Its resolution was downsampled to 250 m to match the outputs of the interpolation procedure (i.e. the precipitation maps). For the latter, the spatial resolution of 250 m was found reasonable, given the total extent of the chosen region and the likely distances over which noticeable variances in precipitation could be expected. An individual precipitation raster layer was computed for each day for which at least one of the weather stations had logged a precipitation amount greater than zero. Subsequently, the daily interpolation outcomes were accumulated to obtain monthly, annual and long-term (30 years) mean precipitation (raster) data for the period 1963 - 1992.
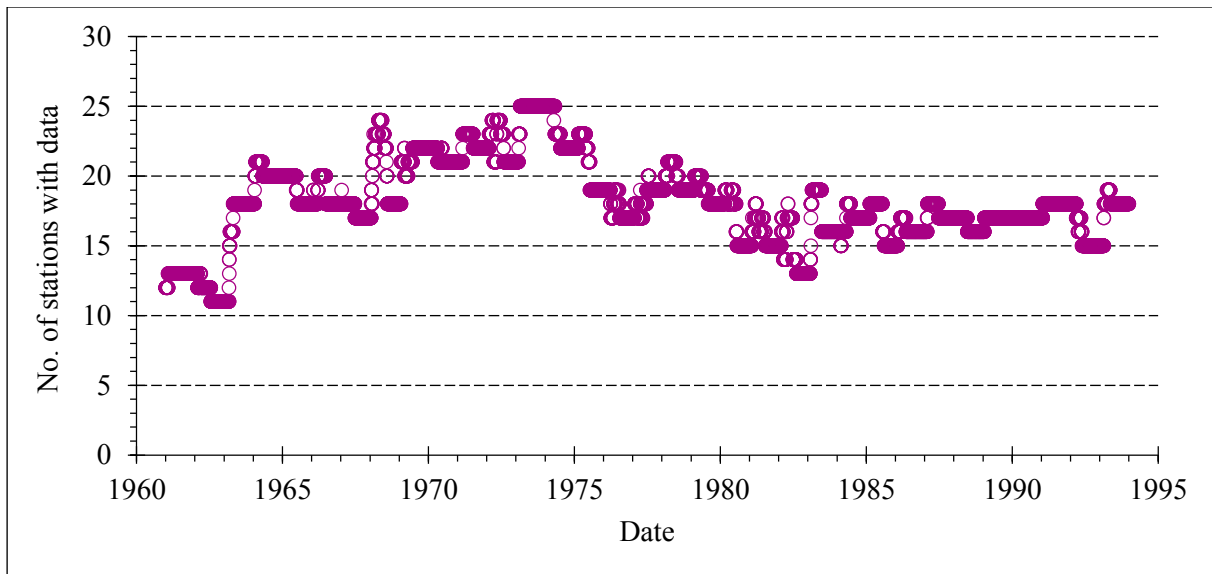
Fig. 29: Diagram of the available precipitation data for the period 1961-1994. For each day, the number of weather stations (see Fig. 28) with an available precipitation record was identified. The number of stations (y-axis) with data for a given date (x-axis) is represented as one purple circle. For an adequate representation of climatic conditions, a 30 year period with suitable data coverage had to be selected. Based on the data distribution illustrated above, the period of 1963-1992 was identified as the one with the highest data availability. Sources: precipitation records: WAJ 2011, data processing: Barbara Brilmayer Bakti & Tobias Törnros 2012.

4.2 Analysis of site characteristics and rainwater harvesting potential

In principal, the analyses outlined in this chapter served two different purposes, gaining further insights into RWH practices, past and current ones, on the one hand, and estimating the RWH potential of the area on the other. In a GIS environment, the data about the natural and the man-made environment (materials see 5.1 and 5.3-5.6, for preparation see 4.1) were analyzed in conjunction with the inventory of mapped RWH structures (see 6.1). Details on the individual (input) datasets can be found in the respective subchapters of section 5. With the use of standard GIS tools, the information contained in the different data layers were filtered, extracted, intersected and combined to identify the characteristics of RWH sites (see 4.2.1). Thus, possible relations between different factors and objects, as well as spatial

patterns could be detected. The established database of RWH facilities was also analyzed separately to examine likely relations between RWH structures of different categories. Additionally, the general RWH potential of the study area and the specific rooftop rainwater harvesting (RRWH) potential were estimated (see 4.2.2). For this purpose, the likely harvestable, annual runoff from (suitable) pervious areas and building roofs was calculated based on the LU/LC and the rooftop datasets in combination with the interpolated precipitation maps.

4.2.1 Identification of site characteristics and distances between features

In ArcMap, the information on each RWH site was gathered from the different data layers described in chapter 5. Every RWH site, defined as the location of a given RWH structure, was represented by one point, i.e. one pair of x- and y-coordinates. While cistern locations had already been recorded as points in the mapping process, bunds, ridges, check dams, dikes and similar facilities had been identified as linear structures. The center point of each object was determined and employed for the representation of the respective RWH site. Using standard tools of the ArcGIS Toolbox, for every point (RWH site), the corresponding values (attributes) were extracted from the prepared data layers. The latter existed partly as raster files, in the case of continuous, quantitative data such as e.g. elevation (DEM), and partly as vector datasets, in the case of qualitative data such as e.g. geological information. For each RWH site, the following properties were determined and stored as attributes of the respective point in the associated table: altitude above sea level, slope, type of LU/LC, mean annual precipitation, geology (formation or other unit as identified in the geological maps), and catchment information. With regard to the latter, the size, name and number of the catchment and the superordinated surface drainage (sub-) basin, within which the respective RWH site was located, were quoted. No information about individual soil types at specific sites could be retrieved from the available soil data (see 3.4, Fig. 9 and Table 4) due to its spatial resolution and the aggregated form of information provided (soil units consisting of several, heterogeneous soil types, no further spatial subdivision).

In order to examine relations between RWH objects of different classes and between RWH structures and natural or man-made features of the environment, distances between individual items of the aforementioned categories were analyzed. The approach is rooted in the "first law of geography: everything is related to everything else, but near things are more related than distant things" (TOBLER 1970, p. 236). In other words, spatial proximity suggests a relation between the concerned objects. Particularly, when a noticeable proximity between individual objects of the respective group(s) is observed in a representative number of cases, a rule or pattern can be assumed more likely. In ArcMap, the Near Analysis tool was employed to determine the Euclidean distances between individual features of one or more categories (datasets). Buffers, i.e. zones of particular radii around input objects, and spatial queries, were used

to identify and quantify features of different categories in the vicinity of RWH sites. With the aforementioned methods, for every RWH structure (input features), the nearest feature and its distance to the respective RWH site were detected in each of the following categories of target objects (near features): RWH structures (three subgroups), archaeological sites (one overall group and five subgroups according to the type of finds or remains), drainage lines, boundaries of surface water catchments, vegetation and modern settlement areas. Similarly, from the same categories, the types and numbers of near features within a specific radius around each RWH site were determined. The findings for the individual RWH sites were summarized according to the category of RWH facilities. For each of the three groups of RWH structures and each of the aforementioned categories of near features, from the outcomes of the distance analyses, the mean value, the range (minimum and maximum values) and the standard deviation were quoted. Thus, a basic, descriptive statistical summary could be given and the comparative interpretation and evaluation of the findings was facilitated.

4.2.2 Estimation of runoff and rainwater harvesting potential

In the first section of this chapter, the methodological approach is outlined which was adopted for the estimation of runoff. The relevant aspects are described that were considered in its design and contributed to the definition of the methodological particulars. Details on the computation procedure and the GIS-based processing of the involved datasets are provided in the second part. Annual runoff was computed for three different precipitation scenarios (dry year, wet year and long-term average conditions) to illustrate the likely quantitative range of runoff that could potentially be harvested in a given year.

With respect to the collection and use of runoff in different RWH schemes, two types of runoff or RWH potential were estimated. One was the annual on-site runoff which corresponds to the general RWH potential of the study area or the runoff that could theoretically be harvested from small catchments and various types of (land) surfaces. Secondly, the annual runoff from the rooftops of all buildings in the settlements of the study area was computed to assess the specific potential that could be tapped with RRWH schemes. The explanations in the following sections first refer to the calculation of on-site runoff. Subsequently, particulars concerning the estimation of runoff from rooftops are described with special regard to differences in the methodology compared to the computation of on-site runoff.

4.2.2.1 Methodological approach and background

The RWH potential of a given area depends on the amount of collectable runoff resulting from precipitation. With respect to the hydrological cycle and its quantitative expression in the water balance equation, runoff corresponds to the share of precipitation which is not consumed by evapotranspiration.

However, for shorter periods of times such as several months or years, a storage component must additionally be taken into account, since significant portions of the precipitation can be stored in soils and aquifers before they ultimately become part of the share of runoff or evapotranspiration. Several factors influence the allocation of water (precipitation) among the aforementioned competing components (surface) runoff, evaporation and storage. The factors can largely be divided into climatological influences, such as e.g. the precipitation pattern, temperature and wind conditions, and characteristics of the terrain. The latter include e.g. the vegetation cover, the type of LU/LC, the relief, the slope and the soil properties. Hence, in order to estimate the amount of (surface) runoff, not only must the amount of precipitation be known but also the intricate interplay of a multitude of influencing factors needs to be considered.

The physical processes and factors involved in the generation of runoff from precipitation are normally represented in mathematical equations or models. All formulas and models necessarily exhibit some degree of abstraction and simplification of the real world conditions. More complex equations or models include a greater number of individual parameters while in those with higher levels of simplification, several factors are aggregated and united in a single variable. Higher degrees of complexity and the incorporation of a multitude of individual variables in mathematical formulas and models are associated with a broader applicability to a variety of purposes, a higher sensitivity and adjustability to smaller changes, e.g. in single parameters, and thus, an overall enhanced accuracy of runoff prediction. The complex models and formulas are also more suitable for the estimation of runoff with higher spatial or temporal resolution. However, due to the larger number of individual parameters, the more complex equations and models also require more input data. The availability of this data and the resources (in terms of finances, labor and time) necessary for their acquisition, mostly through long-term field observations and tests, form major obstacles in detailed runoff modeling. Therefore, the selection of an appropriate model or formula for runoff estimation depends on the purpose, the temporal and the spatial scale as well as data availability.

With respect to the aforementioned considerations, the objectives of the present study and the collected data, a simple empirical formula (Eq. 1) was chosen for the estimation of runoff. Here, runoff is modeled as a function of precipitation and characteristics of the land surface. The quantitative relationship between precipitation and runoff is expressed in the runoff coefficient (RC). Different RC values are used to represent the effects of major differences in terrain and (land) surface properties, e.g. LU/LC and slope, on runoff formation. Thus, a rough estimation of runoff based on a minimum of input data is possible. For the spatial explicit estimation of runoff, only a precipitation map and a RC map are required. The latter is produced by correlating empirical data on runoff from different surfaces with spatial information about the land surface (e.g. a LU/LC map). Additional data about individual parameters which may increase or decrease runoff can be incorporated into the RC map and thus, enhance its quality. In the present study, the RC map was developed by integrating information on runoff efficiencies

given in previous studies (see Table 9) with the produced LU/LC map (see 5.1) and the slope data derived from the ALOS DEM (see 5.3). Suitable RCs for different types of land (surfaces) were determined, taking into account the particular local circumstances of the study area (see chapter 3) and their likely effects on runoff formation and amounts.

Eq. 1: $$Q = P * RC$$

In which: Q = annual runoff in mm, P = annual precipitation in mm, RC = (annual) runoff coefficient, dimensionless.

Formulas identical or akin to Eq. 1 are often found in literature on RWH, especially in technical manuals and user guidelines that are mostly published by government agencies, NGOs or NPOs and address the broader public, private individuals and landowners, as well as experts in different fields (cf. e.g. PACEY & CULLIS 1986, CRITCHLEY & SIEGERT 1991, ALI ET AL. 2009, LANCASTER 2009, WATERFALL ET AL. 2013). Within the scope of practical considerations and recommendations for the design and operation of RWH systems, formulas like Eq. 1 allow to estimate the likely amount of collectable runoff from a given area. The minimal input data requirements represent the major advantage of these simple empirical formulas and enable their widespread use. The calculation of runoff amounts with formulas like Eq. 1 is a standard procedure and an integral part of studies, guidelines and technical literature on rooftop RWH (cf. e.g. TEXAS WATER DEVELOPMENT BOARD 2005, ABDULLA & AL-SHAREEF 2006, MWENGE KAHINDA ET AL. 2010, FARRENY ET AL. 2011b). Occasionally, the same or similar formulas are also employed for the estimation of runoff in the context of other RWH practices such as micro-catchment WH and various techniques of runoff farming (cf. e.g.CRITCHLEY & SIEGERT 1991, ANSCHÜTZ ET AL. 2003). Particularly with respect to RWH practices that are based on the collection of runoff from (bare) land surfaces and larger catchment areas, more sophisticated methods of runoff estimations are often recommended to better represent the complex processes involved in runoff formation and overland flow, the intricate interplay of influencing factors and spatial heterogeneities in the two former categories.

Equation 1 and similar empirical formulas which are based on runoff coefficients, are closely linked to the rational method. At their core, these approaches employ a coefficient that depends on the terrain, surface or LU/LC characteristics to determine the share of precipitation which is converted into runoff. However, the rational formula is designed to compute the peak rate of runoff that occurs at the outlet of a given catchment during a particular rainfall event which is characterized by a specific, likely return period. In contrast, the formulas used in the context of RWH are targeted on calculating the total amount of runoff that typically results from several precipitation events during the considered time span (e.g. a month, season or year). Consequently, recommendations and empirical data published in relation to the rational formula (e.g. CHOW ET AL. 1988), particularly runoff coefficients, cannot readily be transferred and applied to formulas such as Eq. 1 which are aimed at runoff estimation for RWH purposes. However, with adequate consideration of the aforementioned specifics, empirical runoff coefficients associated

with the rational method can at least provide a basic orientation with respect to the runoff producing qualities of different types of LU/LC or surface materials.

Another method of runoff estimation that is closely related to the rational approach and the one adopted in the present study (cf. Eq. 1), is the SCS curve number (CN) method (SOIL CONSERVATION SERVICE 1985). It is probably the most widely used technique of runoff estimation in research projects on RWH (except for RRWH) (cf. e.g. VAN WESEMAEL ET AL. 1998, DE WINNAAR ET AL. 2007, KADAM ET AL. 2012, NAPOLI ET AL. 2014, KUMAR & JHARIYA 2017). Similar to the above described approaches, the SCS-CN method is also based on a comparatively simple formula that requires relatively little data input and relies on empirically determined coefficients to define the share of precipitation that corresponds to runoff. In the SCS-CN formula, runoff coefficients are expressed in curve numbers. Each curve number represents a unique combination of a specific category of LU/LC and one of the four groups of soils. The groups are defined according to differences in soils, primarily in terms of their texture as well as other properties affecting runoff and infiltration. Furthermore, the SCS-CN formula includes a variable which expresses antecedent moisture conditions. The latter have a considerable influence on initial abstraction rates and thus, the threshold of precipitation required to initiate runoff. Originally, the SCS-CN method was intended for the computation of runoff from individual precipitation events, although monthly, seasonal or annual information can be obtained through the accumulation of single (e.g. daily) runoff estimates. By including antecedent moisture conditions, the SCS-CN method is able to reflect the influence of the temporal distribution of precipitation on runoff amounts. The outlined properties and qualities characterize the SCS-CN method as more sophisticated and superior, in comparison to other, more basic empirical formulas (e.g. Eq. 1). However, the SCS-CN method also requires slightly more input information. With regard to the present study and the spatially explicit estimation of runoff at the intended resolution, the available soil data were considered inadequate for the application of the SCS curve number method.

For all hitherto described approaches, the selection of appropriate runoff coefficients is of utmost importance since this parameter ultimately defines the share of precipitation which is converted into runoff. As CRITCHLEY & SIEGERT (1991) suggested, RCs should be determined empirically by recording surface runoff from experimental catchments or fields (runoff plots) located within the study area. Longer observation periods of at least two years are recommended. Since no empirical runoff data could be collected in the present study, suitable runoff coefficients were derived from the findings and recommendations of previous studies (see Table 9). The approach was rooted in the establishment of analogies based on the described conditions. For the determination of suitable RCs, specifics of the study area (see chapter 3) such as e.g. land use practices, soil properties and local particularities of the climate, which may noticeably influence runoff efficiencies, were taken into account as general, largely spatially invariant aspects. The selected RCs were suited to the estimation of on-site runoff from small catchment areas

(e.g. micro-catchments) where distances of overland flow are marginal. With regard to collectable surface runoff from larger catchments in which distances of overland and stream flow are increased, different, typically lower runoff efficienciesmust be assumed as several empirical studies have shown (cf. e.g. SHANAN & SCHICK 1980, EVENARI ET AL. 1982, OWEIS & TAIMEH 1996, ABU-AWWAD & SHATANAWI 1997, SHANAN 2000, also see Table 9). Below, the RCs chosen for the study at hand are presented and the individual factors considered in the selection process are described.

With regard to the identification of suitable RCs for the study area, results of empirical runoff studies (see Table 9, first section) appeared most relevant. Longer periods of data collection suggested an increased reliability and representativeness of study outcomes. The transfer and application of findings seemed most justifiable for studies which were conducted in the same region or under comparable environmental conditions. Numerous other studies on RWH contained valuable information on adequate RCs to be used for the estimation of harvestable runoff (see Table 9, second section). These recommendations are typically based on comprehensive, longtime experiences of the respective authors in the field of RWH. In most cases, the suggested RCs are not tailored to specific environmental conditions in a particular area but may rather indicate the likely range of suitable RC values. Both types of information on RCs, empirical findings and recommendations, were considered together in the present study.

In terms of the identified or recommended RCs, the studies listed in Table 9 exhibit noticeable differences. These variances can most likely be attributed to individual local or regional environmental conditions, including specifics of the land surface (soils, land cover and land use practices) and weather or climate, particularly the amounts and temporal patterns of precipitation. Yet, the findings and suggestions of many of the studies overlap with respect to the range of annual RCs for bare land surfaces, with no or minor treatment, and if any, a negligible plant cover. For areas with these characteristics, under semiarid or arid climatic conditions, RCs of around 0.10 to well over 0.20 are quoted (see Table 9). Based on the meta-analysis they conducted, MAETENS ET AL. (2012) reported slightly lower RCs in general. This may be a result of the aggregation process in which findings from a large region with a broad range of environmental conditions were combined to derive mean RC values for specific categories of LU/LC.

When estimating runoff and determining appropriate RCs, slope has to be taken into account as an important factor, while the magnitude and nature of its influence can vary. Typically, steeper gradients are associated with increased runoff and reduced infiltration (cf. e.g. ABU-ZREIG ET AL. 2011), but empirical runoff studies in the Negev Desert (SHANAN & SCHICK 1980, EVENARI ET AL. 1982) revealed that negative correlations are possible too. In the Negev, decreases in runoff were observed with increasing slope, most likely due to differences in soil and land cover, particularly the amount of stones. The presence of a vegetation cover generally leads to a reduction in runoff from land surfaces although the extent of this effect may vary largely with the type of vegetation. As MAETENS ET AL. (2012) pointed out, areas

Table 9: Overview of runoff efficiencies of various kinds of pervious (unsealed) surfaces as described in selected previous studies. The first part of the table displays findings from empirical studies on runoff. Here, only data on runoff from natural precipitation was considered, whereas results from rainfall simulation were excluded. Information in the second part of the table refer to recommendations for runoff estimation. Typically, the information is based on long-term experiences of the respective authors and/or (aggregated) findings from previous studies. Therefore, no study design could be specified. If not stated otherwise, runoff coefficients are annual or equivalent seasonal means. Entries in the table were sorted according to their relevance for the present study. Priority was given to empirical studies conducted in the same region or under similar environmental conditions.

Surface	RC	Slope	Climate	Region	Study Design	Source
Part 1 – findings from empirical (research) studies and meta-analyses of empirical studies						
natural bare soil	depending on catchment size: 0.22-0.56; mean: 0.39	0-2%	arid, 150 mm mean annual precipitation	Jordan	empirical, micro-catchments	Oweis & Taimeh 1996
compacted bare soil	depending on catchment size: 0.27-0.60; mean: 0.42					
bare, smoothed soil	depending on catchment size: 0.09-0.42; mean: 0.22	1-5%	arid, 119/ 59 mm annual precipitation during study (1994-1996); 168 mm mean annual precipitation	Jordan	empirical, micro-catchments	Abu-Awwad & Shatanawi 1997
bare soil (silt clay loam), cleared, no stones	0.24	10%	arid, 206 mm annual precipitation during study (rainy season 2004/2005); 211 mm mean annual precipitation	Northern Jordan	empirical, runoff plots	Abu-Zreig et al. 2011
bare soil (silt clay loam), 5% stones	0.20	10%				
bare soil (silt clay loam), 15% stones	0.17	10%				
bare soil (clay loam), cleared, no stones	0.26	12%				
bare soil (clay loam), 5% stones	0.21	12%				
bare soil (clay loam), 15% stones	0.18	12%				
natural desert soil with stones, undisturbed	0.07-0.29; long-term mean: 0.25	10%	26-160 mm annual precipitation during study (1962-1967); 100 mm mean annual precipitation	Negev Desert, Israel	empirical, runoff plots	Evenari et al. 1982, Shanan & Schick 1980, Shanan 2000
	0.08-0.26; long-term mean: 0.22	13.5%				
	0.05-0.25; long-term mean: 0.19	17.5%				
	0.03-0.24; long-term mean: 0.16	20%				
bare desert soil with various kinds of surface treatment (removal of stones, stone mounds, surface smoothing, combination of the aforementioned)	0.05-0.35; long-term means: 0.25-0.30	10%				
	0.04-0.30; long-term means: 0.20-0.26	13.5%				
	0.03-0.58; long-term means: 0.19-0.24	17.5%				
	0.01-0.24; long-term means: 0.16-0.19	20%				
natural desert/rangeland	0.03-0-23; long-term mean: 0.13	various	93 mm mean annual precipitation		empirical, cistern watershed (1.2 ha)	
bare soil	0.20-0.42; mean: 0.30	2-5%	hyperarid, 45-158 mm annual precipitation during study (2004-2007); 111 mm mean annual precipitation	Syria	empirical, micro-catchments	Ali et al. 2010

Table 9 continued

Surface	RC	Slope	Climate	Region	Study Design	Source
natural loess slope	0.09-0.11	14%	semiarid (summer rains), 253/344 mm annual precipitation during study (1998/1999); 263 mm mean annual precipitation	China	empirical, runoff plots	Li et al. 2004
cleared loess slope	0.12-0.13					
bare soil	0.05 (weighted mean)	0-75%, mostly 8-12%	Mediterranean, annual precipitation 0-1,500 mm, mostly annual precipitation 300-1,000 mm	pan-Mediterranean (Mediterranean and adjacent regions)	meta-analysis, database of empirical results from runoff plots	Maetens et al. 2012
cropland	0.09 (weighted mean)					
fallow	0.08 (weighted mean)					
forest	0.03 (weighted mean)					
grassland	0.06 (weighted mean)					
rangeland	0.03 (weighted mean)					
shrubland	0.04 (weighted mean)					
tree crops	0.10 (weighted mean)					
Part II – suggested values for the estimation of runoff (collectable in RWH schemes) and associated conditions						
not specified, usually natural (bare) ground	0.10-0.50 to be used in conjunction with efficiency factor of 50-75%, i.e. 0.05-0.38	not specified, usually max. 5%	not specified, usually arid and semiarid climates	---	---	Critchley & Siegert 1991
typical steppe catchment with 30% bare rock cover	0.10-0.12	3-5%	100 mm annual precipitation	---	---	Ali et al. 2009
not specified, usually natural ground	0.12-0.20	not specified	---	Egypt	---	Ali et al. 2009
untreated desert soil	0.10	usually 2-7%	drylands	---	---	Fidelibus & Bainbridge 1995
prepared, bare soil	0.30-0.50	ideally 3-5%	semiarid	---	---	Fuller Renner & Frasier 1995
not specified, usually natural ground	0.17	not specified	not specified, usually arid or semiarid	---	---	Boers 1994
not specified, usually natural ground	0.10-0.25	not specified	drylands	---	---	Falkenmark et al. 2001
bare soil (all types)	0.20-0.75	flat terrain	not specified, possibly focus on arid and semiarid climates	not specified, e.g. Arizona, USA	---	Waterfall et al. 2013
bare, heavy soil (clayey soils)	0.10-0.60					
lawn on sandy soil	0.05-0.10					
lawn on heavy soil (clayey soils)	0.13-0.17					

with tree crops, vineyards and similar types of LU/LC or vegetation can exhibit considerably higher amounts of runoff in comparison to grass-, shrub- or rangeland (see Table 9).

For the estimation of runoff, several regional and local specifics of the study area need to be considered. Firstly, the high to very high clay contents of most soils on the Karak Plateau (cf. chapter 3.4) facilitate the formation of surface crusts, especially in areas with sparse or no vegetation. The phenomenon is particularly likely to occur when, within a short time, large amounts of precipitation fall onto dried out, bare soils, e.g. at the beginning of the rainy season. Due to their sealing effect, surface crusts in clayey soils typically reduce infiltration and promote runoff. Furthermore, interannual changes in the temporal distribution of precipitation can lead to a decrease or increase in (annual) runoff. In this regard, the magnitude and the frequency of intense rainfalls are decisive, as well as the number of events in which precipitation amounts exceeded the threshold for runoff initiation. Since vegetation can reduce runoff considerably, detailed spatial information about the vegetation cover are crucial for the estimation of runoff. Due to the dependence on precipitation, most of the plant growth is confined to the rainy winter half-year. This applies to the naturally occurring vegetation as well as to most of the cultivated annual plants, including agricultural crops (see chapter 3.5). Therefore, the extent of vegetated areas is expected to be significantly larger in the winter half-year than that of the mapped vegetation cover in summer. As a consequence, a reducing effect on runoff can be assumed in general. Interannual changes in the extent and location of rainfed agriculture (see 3.5.2) further affect and modify the amount and spatial distribution of runoff.

In view of the aforementioned considerations and RCs given in previous studies (see Table 9), the following RC values were chosen for the estimation of runoff in the present study:

- sealed/impervious surfaces (built-up areas, roofs, streets, asphalt, concrete, etc.)
  - all slope values   0.80
- bare ground (soil and rocks), no or minor vegetation cover and treatment
  - 0-5% slope (flat or slightly sloping terrain)   0.12
  - >5-15% slope (moderately sloping terrain)   0.15
  - >15% slope (steep sloping terrain)   0.18

- vegetated areas (in summer), mostly active, photosynthetic vegetation
  - 0-5% slope (flat or slightly sloping terrain)   0.06
  - >5-15% slope (moderately sloping terrain)   0.08
  - >15% slope (steep sloping terrain)   0.10

The category of surfaces that are largely sealed and thus, are almost or entirely impervious to water, included built-up areas, streets, roofs, parking lots and other areas covered by artificial materials like concrete or asphalt. Commonly high RCs within the range of 0.70-1.00 are assigned to this type of

LU/LC and the corresponding areas (cf. e.g. PACEY & CULLIS 1986, LANCASTER 2009, FARRENY ET AL. 2011b, WATERFALL ET AL. 2013). Here, a rather conservative but already high runoff efficiency of 80% (see above, RC 0.80) was assumed for all types of impervious areas. Potentially existing gradients in these regions were considered negligible at this point.

With regard to the remaining unsealed or pervious regions, areas of largely vegetation-free bare ground (soil and rock) were distinguished from those with significant, mostly photosynthetically active vegetation. This differentiation was essential since the vegetation typically leads to a significant decrease in runoff from corresponding pervious areas (see above and Table 9). Further subdivisions into more specific classes of LU/LC were not considered advisable with respect to the available data and the scope of the present study. Consequently, the LU/LC category of vegetation encompassed all types of plant cover. Although trees probably dominated in the detected summer vegetation, higher runoff efficiencies as described by MAETENS ET AL. (2012) for tree crops did not seem applicable here due to the mixed nature of the mapped plant cover. Additionally, as a result of the very high spatial resolution of the data, detected vegetation areas can be perceived as rather pure, i.e. excluding significant extents of other pervious areas such as e.g. bare earth between trees. Therefore, consistently lower RCs were assigned to vegetated regions in comparison to other, non-vegetated pervious areas (see above).

Besides the type of LU/LC, the gradient of the terrain was assumed to have a major influence on the formation of runoff from all unsealed surfaces. Therefore, each of the two aforementioned large categories of LU/LC was further subdivided into three classes of gradients. The necessary slope information was derived from the ALOS DEM. The occurring gradients were classified into three groups which encompassed flat or slightly sloping terrain (slope values of 0-5%), moderately sloping terrain (slope values of more than 5% to 15%) and land with steep slopes (gradients over 15%), respectively. The classes were defined with respect to the frequency of occurrence of individual gradients in the study area and slope values suggested for, or observed in, RWH schemes according to literature (see e.g. Table 9). Flat and slightly sloping land constituted approximately half (ca. 48%) of the study area. Within this category, gradients of 2-5% were most common (over 80% of the terrain in this class). In several studies (e.g. CRITCHLEY & SIEGERT 1991, FULLER RENNER & FRASIER 1995), slightly sloping land with gradients of max. 5% had been recommended as the most, or even the only suitable areas, for runoff collection, runoff farming and related RWH practices. Noticeable, but still moderate slopes of over 5% to 15% were found in ca. 44% of the land under study here. Within this group, gradients larger than 10% comprised only a minor share of ca. 25% of the corresponding area (11% of the whole study area). Most studies on runoff and RWH (see e.g. Table 9) included land with moderate gradients in the aforementioned range, thus suggesting that these regions could also constitute acceptable areas for runoff collection and various kinds of RWH schemes. Land with steeper slopes (over 15%) was normally regarded as inappropriate for RWH. Terrain with gradients of this category accounted only for ca. 8% of the study area. For all pervious areas, vegetated and non-vegetated, a positive correlation between runoff and

slope was assumed, i.e. steeper slopes were associated with higher runoff efficiencies. The effect of slope was considered to be slightly more pronounced in mostly vegetation-free pervious areas. Therefore, RCs were raised by 0.03 for the respective next higher class of slope in the category of non-vegetated pervious areas, whereas incremental steps of 0.02 were selected for RCs assigned to the different classes of slope in the category of vegetation. In general, suitable but rather conservative RC values found at the lower end of the likely range (see Table 9) were chosen in order to minimize the risk of overestimation of runoff and the RWH potential at this point.

For the estimation of runoff from rooftops and thus, the RRWH potential, a similar methodological approach was adopted. As before, the computation of runoff was based on Eq. 1. This formula has widely been used and recommended for the estimation of runoff in research and technical literature on RRWH (cf. e.g. ABDULLA & AL-SHAREEF 2009, LANCASTER 2009, FARRENY ET AL. 2011b, ASSAYED ET AL. 2013). Again, for the expedient calculation of runoff quantities with Eq. 1, the determination of suitable RCs is crucial. In this regard, besides climatological factors, the materials and characteristics of the involved rooftops must be considered. An overview of likely adequate RC values for different roof types can be found in FARRENY ET AL. (2011b). In most studies, RCs in the range of 0.70-0.90 were suggested as appropriate (cf. e.g. LI ET AL. 2010), although lower or higher values have occasionally been stated too. In the area under study here, the vast majority of buildings features flat roofs made of cement. Therefore, a RC of 0.80 was chosen and assigned as a standard value to all rooftops. Based on the available, remotely sensed data and without further ground truth, a reliable and appropriate classification into further subcategories of rooftops with different runoff efficiencies could not be attained. The selected RC of 0.80 was considered most appropriate, as lower or much higher values are normally associated with other roof materials like gravel (lower RCs) and other roof types such as e.g. pitched roofs with shingles (higher RCs). The same RC value (0.80) has also been employed in other studies on RRWH in Jordan, e.g. by PREUL (1994), ABDULLA & AL-SHAREEF (2009), and ABU-ZREIG & HAZAYMEH (2012). Additionally, the selected value is within the range of RCs identified by LANGE ET AL. (2012) who investigated runoff from rooftops in Ramallah, Palestine. However, different, typically higher RC values of e.g. 0.85 and 0.90 have also been stated in other studies on RRWH in Jordan and other countries, e.g. Spain and Kenya (e.g. DOMÈNECH & SAURÍ 2011, ASSAYED ET AL. 2013, NTHUNI ET AL. 2014, SAIDAN ET AL. 2015). In light of this, the selected value appears as a rather conservative estimate of the runoff efficiency of the involved rooftops.

4.2.2.2 Computation procedure and data processing

In ArcMap, Eq. 1 was implemented on a raster cell basis to produce a map of estimated annual on-site runoff for the study area. The required input raster datasets encompassed a precipitation map (see 5.6) for each of the three precipitation scenarios (dry, wet and long-term mean) and a RC map. The RC map was created by assigning the determined RC values (see previous section, 4.2.2.1) to the corresponding

categories of the refined LU/LC map. In the latter, the LU/LC information (see 5.1) had been integrated with the slope data derived from the ALOS DEM (see 5.3).

Before further processing, all involved datasets (i.e. the precipitation, the slope and the LU/LC data) were harmonized in terms of their spatial resolution. For this purpose, the raster files with lower resolutions, i.e. the precipitation map with a cell size of 250×250 m and the slope map with a cell size of 5×5 m, were resampled to the cell size of the data with the highest spatial resolution, i.e. the LU/LC data. As a result, all raster layers had a spatial resolution of 0.5×0.5 m per pixel. In this way, the highest level of detail, present in the LU/LC map, could be preserved while attaining a homogeneous spatial resolution in all datasets to facilitate further data processing. In the resampling process, the nearest neighbor technique was used to avoid the alteration of cell values in the output raster files as far as possible. Below, the subsequent processing steps are described that were applied to compute annual on-site runoff in the study area.

As a first step in the production of the RC map, the LU/LC and the slope data were integrated into a single raster file. In ArcMap, the Plus tool of the Spatial Analyst Toolbox was used to add up the values of the two aforementioned raster datasets on a per cell basis. Prior to this, the qualitative categories of LU/LC were each assigned a distinct numerical value (a multiple of 1,000) that did not overlap with the range of values in the slope map (0-70). Thus, in the output raster of the summation operation, cell values conveyed both information: the thousands digit indicated the category of LU/LC and the last two digits specified the gradient in percent. Subsequently, based on the encoded LU/LC and slope information, the raster cells of the created dataset were classified into eight categories of runoff efficiencies (see chapter 4.2.2.1). According to its class, each cell was then assigned the corresponding RC value (see 4.2.2.1). Clouded areas that could not be classified in terms of their LU/LC, received the value 0. Thus, a complete RC map could be produced for the study area (see Fig. 30). In accordance with Eq. 1 (see 4.2.2.1), the RC map was then multiplied with the precipitation data. To show the likely range of interannual variations in precipitation and runoff amounts, three different raster datasets were selected to represent the annual precipitation in an extremely dry year (example of 1963), an exceptionally wet year (example of 1965) and under normal, average conditions (mean values of the period 1963-1992). Using the Times tool of the Spatial Analyst extension, each of the aforementioned precipitation maps was then multiplied, one at a time, with the RC map on a per cell basis. Consequently, for every precipitation scenario, a new output raster was created in which the cell values indicated the annual on-site runoff, in mm, at the respective location.

For the estimation of runoff from rooftops, no RC map needed to be prepared since a single RC value had been identified for all rooftops (see 4.2.2.1). Hence, Eq. 1 could be applied directly by multiplying the rooftop data with the precipitation data. However, for this processing, all input datasets had to be of same type, i.e. either in the form of vector or raster data. While the precipitation information was present as raster files, the rooftop data was available as vector files. Therefore, the type of one of the two datasets

had to be adjusted. To minimize the risk of alterations resulting from the transformation process, here, the vector format of the rooftop data was selected as the standard and the precipitation raster data (original resolution of 250 × 250 m cell size) was converted into vector data. Thus, each raster cell was now represented as a polygon and its value was stored as an attribute of the respective polygon. Through the intersection of the precipitation and the rooftop data layers, annual precipitation amounts could be identified for each rooftop or its different parts, in case the rooftop was covered by two or more polygons with different values. The precipitation information derived from the three datasets corresponding to different precipitation scenarios (see previous paragraph), was written as attributes to the features (rooftops and parts of rooftop) in the output of the intersection process. By multiplying the extracted precipitation values with the selected RC of 0.80 (see 4.2.2.1) and the extent (area in m^2) of the respective feature, the annual runoff under different precipitation conditions could be calculated for each rooftop.
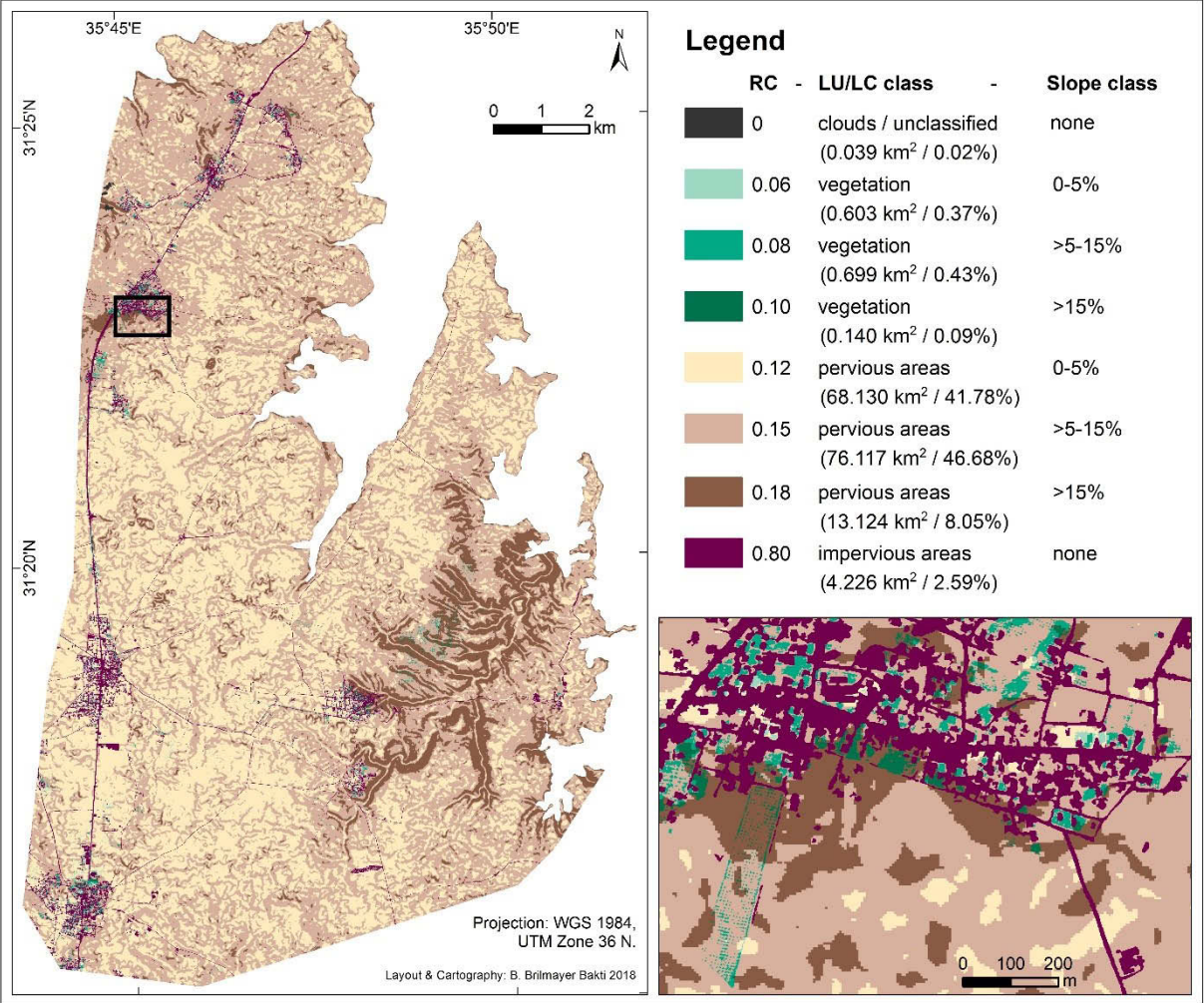
Fig. 30: Runoff coefficient (RC) map. Each RC corresponds to a specific combination of one category of LU/LC and one class of slope (see 4.2.2.1). In the legend, the area assigned to each category of RCs and its corresponding share in the study area (extent of the LU/LC map) are stated in parentheses below the class descriptions. The black rectangle in the main map indicates the location and extent of the detail map (lower right corner). For further details and sources of the individual data components, see 4.2.2.1 (RC values), 4.1.2.4 and 5.1 (LU/LC data), as well as 4.1.3 and 5.3 (slope data).

5 Materials: intermediate output and prepared datasets

In this chapter, all of the data layers are described that are employed in the spatial analyses (see section 4.2.1) as well as the estimation of the RWH potential (section 4.2.2). The database of RWH structures forms a separate category since it also forms a significant part of the outcomes with regard to the research questions raised in chapter 1. Therefore, the RWH inventory will be presented in chapter 6.1. The datasets included in the present chapter represent the outputs of the procedures outlined in section 4.1 and the input of the analyses and calculations explained in section 4.2 (also see chapter 4, Fig. 14, box 3). Some of the datasets (e.g. the DEMs and their derivative data) were also employed as input data in some of the procedures described in chapter 4.1 (e.g. preprocessing of the satellite imagery, hydrological analysis). Details on the methods and techniques used in the preparation of the individual data layers can also be found in chapter 4.1. The complexity and involved levels of processing varied strongly, ranging from almost no modification of readily available data (geological and archaeological datasets) to the production of completely new information layers (e.g. LU/LC and rooftop data) through complex analyses. For each data layer, a short description of its content and its quality including the estimated accuracy (where applicable, see e.g. 5.1 and 5.2) are given below. The characteristics of the datasets can have a significant influence on the final results presented in chapter 6 (also see discussion in 7.2).

5.1 Land use/land cover data

The LU/LC data resulting from the classification of the GeoEye-1 satellite image (see chapter 4.1.2.4) are displayed in Fig. 31. Three LU/LC classes were defined while cloud covered areas were exempt from classification results and assigned to a separate category. In general, the extent of clouded regions was rather negligible with 0.039 km^2 or 0.02% of the study area. The remaining part which could be classified amounted to 163.040 km^2. Sealed surfaces that are largely impervious to water and associated with built-up areas and related infrastructure elements, such as e.g. streets, parking lots and buildings, only accounted for a very small share of less than 3% of the study area (see Fig. 31, a and b). The gross, i.e. more than 96% of the study area, was allotted to different types of unsealed land surfaces which are pervious to water, such as e.g. agricultural fields, rangeland and various kinds of undeveloped areas or open land. Pervious surfaces with a noticeable plant cover were assigned to a separate category which constituted only a small share of less than 1% of the study area (see Fig. 31). The small extent of the vegetation class resulted from the fact that, here, only the plant cover of the dry summer month could
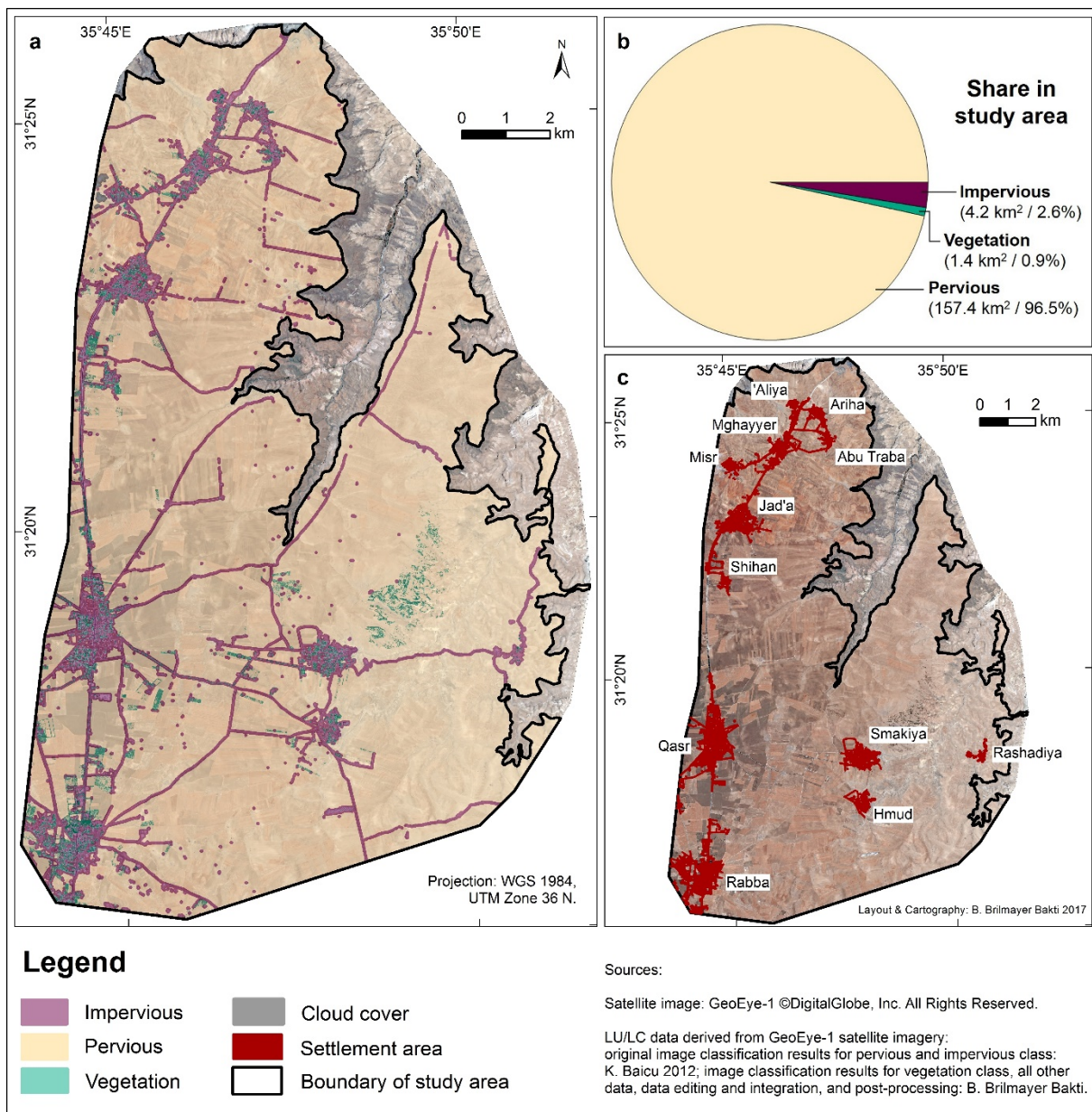
Fig. 31: Thematic map of the LU/LC (a), diagram of the shares of individual LU/LC classes in the study area (b), and thematic map of impervious surfaces which constitute different settlements (c). Each settlement is labeled with its name. For details concerning the acquisition and processing of the shown LU/LC data, see chapter 4.1.2.4.

be mapped due to the recording date(s) of the satellite imagery (see 4.1.2.1). In the semi-automatic image analysis process, primarily active, photosynthetic vegetation was detected (see 4.1.2.4 for details) which mostly consisted of various kinds of trees, and to a lesser degree, of plants grown in horticulture. While the latter is practiced in very limited areas, a considerable share of the detected vegetation is formed by plantations of permanent crops, predominantly olive and occasionally other fruit trees. Since horticulture, as well as permanent crops, often require (supplemental) irrigation during the summer (see chapter 3.5.2), the mapped vegetation is especially relevant to questions of water demand and supply.

From the regions identified as impervious, settlement areas have been delineated manually (cf. 4.1.2.4 and Fig. 31, c). These corresponded to relatively compact regions formed by continuous or adjacent

individual areas classified as impervious. The total extent of the land identified as settlement areas amounted to 3.197 km^2 which is equivalent to 76% of the area classified as impervious and 2% of the whole analyzed region. In accordance with the official, administrative data on towns and villages in the study area (see chapter 3.6, Table 6), 12 settlements were distinguished (see Fig. 31, c). These were sorted from large to small, according to the extent of the respective associated impervious area (stated below). The settlements were:

1st	Qasr	0.844 km^2	7th	Shihan (incl. Mansura)	0.123 km^2
2nd	Rabba	0.739 km^2	8th	Hmud	0.105 km^2
3rd	Jad'a	0.417 km^2	9th	Ariha	0.102 km^2
4th	Smakiya	0.262 km^2	10th	Abu Traba	0.076 km^2
5th	Mghayyer	0.262 km^2	11th	Rashadiya	0.069 km^2
6th	'Aliya	0.130 km^2	12th	Misr	0.064 km^2

The quality of the described LU/LC data can be construed from the results of the accuracy assessment. Outcomes from the evaluation of the vegetation data are presented in Table 11 and described below. Concerning the other two mapped types of LU/LC, i.e. the pervious and the impervious class, an accuracy assessment of the corresponding image classification results, prior to manual editing and integration with the vegetation data, was conducted by BAICU (2012). The accuracies described by BAICU (2012), for the two named classes, can be expected to have been enhanced through the manual editing of the classification outcomes in the present study (see section 4.1.2.4). The process of data integration, in which the edited data of the impervious and the pervious class were combined with the image classification results of the vegetation category to obtain the final LU/LC dataset (see 4.1.2.4), is not considered to have had any influence on the accuracy properties of the individual LU/LC classes.

The results of the accuracy assessment of the vegetation data (see 4.1.2.6) are displayed in the error matrix (see Table 10). From both categories, i.e. the vegetation and the background or non-vegetation class, 100 samples consisting of nine pixels each were collected and evaluated. The assessment was based on the individual pixels within each sampling unit. Therefore, when a sample unit could not be labeled as correctly or incorrectly classified in its entirety, the respective number of pixels assigned to the right or the wrong category was expressed as a fraction of one. Moreover, some of the sample units covered more than one category, i.e. the vegetation and the background region, in parts respectively. As a result, slightly fewer assessment units (pixels) fell into the vegetation category compared to the background category. In Table 10, the sum of all sample units and fractions thereof, which were assigned to the corresponding category, is given as the row total for the classification results and the column total for the reference data. The four fields at the core of the error matrix indicate the number of samples that were labeled as correctly classified (upper left and lower right field), false positives (upper right field) and false negatives (lower left field) in the evaluation process. The standard accuracy indices which are calculated based on the error matrix and its content, are stated below the table. They comprise the pro-

ducer's accuracy or error of omission, the user's accuracy or error of commission and the overall accuracy. The latter expresses the sum of correctly classified samples (all categories) as a percentage of the total number of samples. In contrast, the user's and the producer's accuracy are determined for each class separately. They represent the ratio of correctly classified samples to the row total (user's accuracy) and the column total (producer's accuracy), respectively. Since the main focus was the evaluation of the extracted vegetation data, here, only the user's and the producer's accuracy for this category are given. Further details on the use of error matrices and the computation and interpretation of the aforementioned accuracy indices can be found in several studies on the assessment of image classification outputs, e.g. CONGALTON (1991), FOODY (2002), CONGALTON & GREEN (2009) and LILLESAND ET AL. (2015).

Below, together with the traditional statistical measures of accuracy, the Kappa value is also provided. Cohen's Kappa coefficient expresses the agreement between two datasets, in this case, the classification outcomes and the reference data, which cannot be attributed to chance only. Kappa can take any value between 0 and 1. While the maximum value of 1 corresponds to a complete accordance between both datasets, the minimum value of 0 signifies no agreement other than by chance. Further information on the calculation and the interpretation of the Kappa coefficient can be found in literature (e.g. LANDIS & KOCH 1977, STEHMAN 1996, CONGALTON & GREEN 2009).The Kappa coefficient and its widespread use have received much criticism, mainly with regard to its general purpose, its value in the accuracy assessment of image classification outcomes, its arbitrariness and related interpretation problems (e.g. FOODY 2008, PONTIUS JR & MILLONES 2011). However, in most studies in the field of remote sensing and automatic image analysis, Kappa still represents an integral part of the accuracy assessment. Therefore, it is also stated here.

Table 10: Error matrix showing the results of the accuracy assessment of the vegetation data. The rows correspond to the outcomes of the semi-automatic image analysis with Feature Analyst (see 4.1.2.4). The classification output was compared to reference data (columns) which was acquired through visual-manual interpretation of the satellite imagery. A detailed description of the evaluation procedure can be found in chapter 4.1.2.6. Below the error matrix, the common, associated accuracy indices are stated. Kappa refers to the observed, unweighted coefficient according to Cohen. In the present case, due to the properties of the error matrix, Kappa could not reach its normal potential maximum of 1. Therefore, the value of Kappa in proportion to the maximum Kappa possible for the particular dataset is given too (see [a]).

		Reference data		Total	User's accuracy
		Vegetation	Background		
FA Classification results	Vegetation	78.5	7	85.5	94.58
	Background	4.5	110	114.5	
Total		83	117	200	
Producer's accuracy		91.81			
			Overall accuracy	94.25	
			Kappa [a]	0.88 / 0.91	

[a] *observed Kappa / observed Kappa as proportion of the maximum possible Kappa for the present data.*

5.2 Rooftop data

Outcomes of the semi-automatic detection of rooftops are visualized in Fig. 32-34. Each of the 24 maps in the three named figures corresponds to one image subset and shows one settlement and the rooftops identified by one of the three developed AFE models. Figure 32 displays the results from the individual application of all three models to the image subsets covering the settlements of Qasr (a-c), Rabba (d-f) and Jad'a (g-i). These image tiles were used in the development of the different AFE models. Each model was fitted to deliver the best possible object extraction results for a specific image. Consequently, Figure 32 includes original image classification outcomes as well as batch processing results obtained by applying an AFE model, which was adjusted to classify a specific image, to another image. The maps a, e, and i in Fig. 32 illustrate the original classification outputs of Model 1 (a), Model 2 (e) and Model 3 (i), resulting from the last step of model development. The other parts of Fig. 32 visualize batch processing outcomes. Figure 33 shows the rooftops detected by each AFE model in the images of Smakiya (a-c), Mghayyer (d-f) and Shihan (g-i). The named image subsets were employed for the evaluation of the developed AFE models, i.e. to test their transferability and applicability for the classification of other, similar images. Since none of the three image tiles had been used in the development stage, potential associated biases were avoided. Hence, the batch processing outcomes displayed in Fig. 33 are readily comparable and also allow estimating the broader suitability of each model.

To facilitate direct comparison, in Fig. 32 and 33, the individual classification outputs of the three AFE models were arranged side by side, in rows, according to the image subsets. Hence, in the two named figures, each column of maps displays the results from one specific AFE model, while the maps in one row show the results from the three different AFE models for the same image tile and settlement. In the maps in Fig. 32 and 33, the classification results are illustrated in combination with the reference data, to enable an independent visual assessment of the suitability of each dataset of (semi-) automatically detected rooftops. For an easier visual evaluation and comparison, the two layers, i.e. the classification and the reference data are intersected. All rooftop data are visualized on top of the analyzed satellite image subset which is shown with a true color setting (band combination 3-2-1). The reference data, i.e. the manually digitized rooftops, are displayed in orange, while the object extraction results are depicted in blue. Intersection areas in which both datasets overlap are visualized in pink. Consequently, pink areas reflect the amount and spatial distribution of correctly detected rooftops, whereas blue and orange regions indicate false positives or areas of overclassification (blue) and false negatives or areas of underclassification (orange). Hence, each map also illustrates the extent, the type and the locations of image classification errors, and thus provides further clues concerning the accuracy and the suitability of the respective outcomes and the corresponding AFE model.
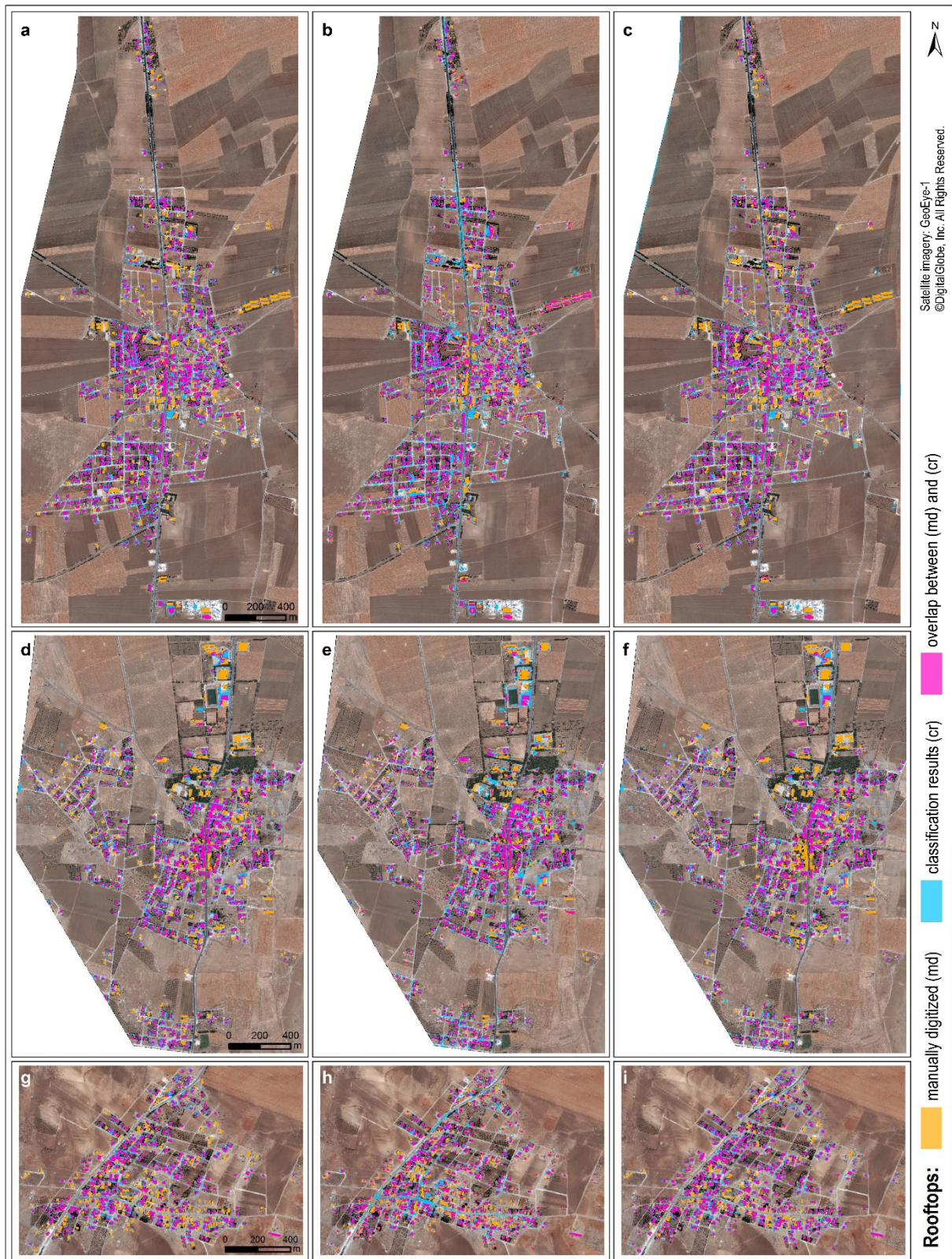
Fig. 32: Results of the semi-automatic detection of rooftops for the three image subsets used in the development of the AFE models. In each row, the outputs of the three AFE models for the same image tile are illustrated. The images in the three rows cover the settlements Qasr (a-c), Rabba (d-f) and Jad'a (g-i). The classification results of each AFE model are arranged in columns. The outputs of Model 1 are presented in the left column (a, d, g), those of Model 2 in the central column (b, e, h) and those of Model 3 in the right column (c, f, i). All maps show the image analysis results in combination with the reference data (manually digitized rooftops). An intersection of the two layers allowed the visualization of the overlap (pink) and the remaining areas in both datasets (orange and blue areas). Maps a, e and i illustrate the outputs of the AFE model specifically developed for the classification of the respective image. The classification outcomes in the other maps were obtained through batch processing.

Rooftops:

overlap between (md) and (cr)

classification results (cr)

manually digitized (md)

Fig. 33: Results of the (semi-) automatic detection of rooftops for the three image subsets used for the evaluation of the AFE models. All image classification outcomes shown here were obtained through batch processing. Except for the specified differences, the setup, design and layout of the present figure are identical to those of Fig. 32. The image tiles in the three rows depict the villages Smakiya (a-c), Mghayyer (d-f) and Shihan (g-i). The image analysis outputs of AFE Model 1 are presented in the left column (maps a, d, g), those of Model 2 in the central column (maps b, e, h) and those of Model 3 in the right column (maps c, f, i). For further details and explanations concerning the visualization of individual classification results, see Fig. 32.

Visual examination of the maps in Fig. 32 and 33 reveals a consistently high share of pink, and hence, correctly classified areas. However, all maps also contain noticeable amounts of blue and orange regions which indicate mismatches between classification outputs and reference data. In most cases, the different

colors occur in a scattered, interspersed way, which makes it difficult to visually assess the total extent of the areas covered by each color. This also affects and complicates the accurate estimation of the quality of individual classification outcomes based only on a visual evaluation. Therefore, when comparing the classification outputs of different AFE models, the datasets frequently appear to be very similar in terms of their suitability (see e.g. Fig. 32 a-c, Fig. 33 d-f) as subtle differences can go unnoticed or may not be rated appropriately in the visual examination. Batch processing results often seem just as adequate and of identical quality as the original classification outputs of the AFE model that had been developed specifically for the analysis of the respective image (see e.g. Fig. 32 a and c). In other cases, batch processing and original classification results differ visibly in regard to their suitability. For example, the original classification output of Model 3 (see Fig. 32 i) for Jad'a appears more appropriate than the batch processing outcomes obtained with Model 1 and 2. The latter apparently contain more false negatives, i.e. rooftops missed in the classification (orange areas in Fig. 32 g, Model 1) and more false positives (blue areas in Fig. 32 h, Model 2).

In the visual assessment of classification results, larger patches or clusters of erroneous areas, either false negatives or positives, are more obvious and therefore tend to be perceived as more significant. The number and the sizes of the orange regions in Fig. 32 f and g, for example, suggest a general tendency of underclassification in these results. On the contrary, a tendency of overclassification can be construed from the amount of blue patches in Fig. 32 b and h. Here, larger parts of roads, wrongly identified as rooftops, represent obvious classification errors. In several other cases, e.g. in Fig. 33 g and i, classification outcomes apparently exhibit considerable shares of false negatives, as well as false positives (orange and blue areas). While this points to an overall lower accuracy and appropriateness of the respective classification results, a specific bias (over- or underestimation) can hardly be determined visually. When the batch processing outcomes in Fig. 33 are compared, variations in suitability can be observed according to image tile. The results for Shihan (Fig. 33, g-i), for example, appear to be less accurate and fitting than those of the other image subsets shown in Fig. 33 (a-f) and Fig. 32. This lower suitability was found in the outputs of all three AFE models and hence must be linked to the individual properties of the specific image. Obviously, in some cases, discrepancies in the characteristics of the target objects and their environment can lead to less satisfactory outcomes from batch processing.

In view of the limitations pointed out above, visual evaluation alone seems insufficient for an accurate and reliable estimation and comparison of the quality of individual image analysis results. Therefore, a comprehensive accuracy assessment as outlined in chapter 4.1.2.6 was conducted. The outcomes of the assessment procedure are presented in Table 11 and 12. The collected data enabled a systematic quantitative and precise evaluation of the rooftop data gathered through (semi-) automatic image analysis. The statistical indices calculated from the gathered data allowed to express the suitability of individual datasets quantitatively. Thus, more detailed and accurate information could be gained about the quality of the image classification outcomes. This also facilitated the comparison of individual output datasets

and the performance of the different AFE models. Hence, the accuracy assessment results displayed in Table 11 and 12, and described in the following, complement the preliminary findings from the visual evaluation of the rooftop detection results (see previous paragraphs and Fig. 32 and 33). Corresponding to the content of Fig. 32, Table 11 presents the outcomes from the evaluation of the classification results for the three images used in the development of the AFE models. Table 12 parallels Fig. 33 insofar as it illustrates the findings of the three images employed in the evaluation of the developed AFE models.

In Table 11 and 12, each bloc of rows shows the assessment results for the outputs of one particular AFE model. The respective model is specified in the upper left field of each bloc. Every column in the named tables displays the outcomes for the classification results of one particular settlement or image subset. In total, 18 datasets were analyzed which resulted from the application of the three AFE models to six image tiles. For each dataset, the error matrix (first three rows in every bloc), the traditional accuracy indices (user's, producer's and overall accuracy) and the customized, unconventional object-based measures of accuracy (last four rows in each bloc) are given. Details concerning the latter are provided in chapter 4.1.2.6. Moreover, for every dataset, the quantitative, spatially unspecific congruence between the classification results and the reference data in terms of the total area of rooftops, is specified. Each set of accuracy information also includes the Kappa coefficient which has already been introduced in the previous section (5.1). Further information on Cohen's Kappa and its employment in the evaluation of image classification outcomes can be found in literature (e.g. FOODY 2002, CONGALTON & GREEN 2009). The comparison of the accuracy assessment results according to image (column) or AFE model (bloc of rows) provided deeper insights into the properties and the typical quality of classification results from a particular AFE model or image subset.

When the data presented in Table 11 are compared, original classification results regularly seem to be associated with higher degrees of accuracy than the batch processing outcomes for the same image. Normally, original classification outputs better match the reference data in terms of the total area of rooftops. Moreover, they show slightly higher overall accuracies and Kappa values. The accuracy data of original classification results are displayed in the first column (light orange) in the first bloc of rows for AFE Model 1; in the second column (medium orange) in the second bloc of rows for Model 2; and the third column (dark orange) in the third bloc of rows for Model 3 (see Table 11).

Apart from the aforementioned exceptions, the results in terms of most statistical measures, such as the user's and the producer's accuracy, and the feature scores, appear to depend primarily on the employed AFE model. With respect to some indices, e.g. the user's and the producer's accuracy, the outcomes of Model 1 and 3 are relatively similar, except for the case of "Jad'a". Here, the output of Model 3 shows better accuracies than that of Model 1. This confirms the observations pointed out in the previous paragraph, since AFE Model 3 had been adjusted specifically to detect the rooftops in the particular image

Table 11: Outcomes of the accuracy assessment of the rooftop detection results for the three image tiles used in the development of the AFE models. For each image, classification outputs from three models were evaluated.

		Image tile / settlement									
		Qasr			**Rabba**			**Jad'a**			
AFE Model 1 - Qasr		**Reference data (m²)**		Total	**Reference data (m²)**		Total	**Reference data (m²)**		Total	
		Rooftops	Background		Rooftops	Background		Rooftops	Background		
FA results (m²)	Rooftops	114529	67800	**182329**	91120	58468	**149588**	49134	25664	**74798**	
	Background	67661	6623356	6691017	74247	4215671	4289918	36535	1906841	1943376	
Total		**182191**	6691155	6873346	**165367**	4274139	4439506	**85669**	1932505	2018174	
User's Accuracy (Rooftops)		62.81%			60.91%			65.69%			
Producer's Accuracy (Rooftops)		62.86%			55.10%			57.35%			
Overall Accuracy		98.03%			97.01%			96.92%			
Kappa		0.62			0.56 / 0.59[a]			0.60 / 0.64[a]			
Area match (FA/ Reference data)		100.08% (overclassification 0.08%)			90.46% (underclassification 9.54%)			87.31% (underclassification 12.69%)			
Feature Overlap	FA results	512 of 537			469 of 489			297 of 308			
	Reference data	678 of 856			591 of 850			388 of 568			
Feature Score User's Accuracy[b]		95.34%			95.91%			96.43%			
Feature Score Producer's Accuracy[c]		79.21%			69.53%			68.31%			
AFE Model 2 - Rabba		**Reference data (m²)**		Total	**Reference data (m²)**		Total	**Reference data (m²)**		Total	
		Rooftops	Background		Rooftops	Background		Rooftops	Background		
FA results (m²)	Rooftops	112859	78405	**191264**	93398	67200	**160597**	43964	24941	**68906**	
	Background	69332	6612750	6682082	71969	4206939	4278909	41705	1907564	1949269	
Total		**182191**	6691155	6873346	**165367**	4274139	4439506	**85669**	1932505	2018174	
User's Accuracy (Rooftops)		59.01%			58.16%			63.80%			
Producer's Accuracy (Rooftops)		61.95%			56.48%			51.32%			
Overall Accuracy		97.85%			96.87%			96.70%			
Kappa		0.59 / 0.61[a]			0.56 / 0.57[a]			0.55 / 0.62[a]			
Area match (FA/ Reference data)		104.98% (overclassification 4.98%)			97.12% (underclassification 2.88%)			80.43% (underclassification 19.57%)			
Feature Overlap	FA results	710 of 972			638 of 821			453 of 557			
	Reference data	780 of 856			704 of 850			465 of 568			
Feature Score User's Accuracy[b]		73.05%			77.71%			81.33%			
Feature Score Producer's Accuracy[c]		91.12%			82.82%			81.87%			
AFE Model 3 – Jad'a		**Reference data (m²)**		Total	**Reference data (m²)**		Total	**Reference data (m²)**		Total	
		Rooftops	Background		Rooftops	Background		Rooftops	Background		
FA results (m²)	Rooftops	114995	68724	**183718**	90520	58410	**148930**	56517	29226	**85743**	
	Background	67196	6622432	6689628	74847	4215729	4290576	29152	1903279	1932432	
Total		**182191**	6691155	6873346	**165367**	4274139	4439506	**85669**	1932505	2018174	
User's Accuracy (Rooftops)		62.59%			60.78%			65.91%			
Producer's Accuracy (Rooftops)		63.12%			54.74%			65.97%			
Overall Accuracy		98.02%			97.00%			97.11%			
Kappa		0.62			0.56 / 0.59[a]			0.64			
Area match (FA/ Reference data)		100.89% (overclassification 0.89%)			90.06% (underclassification 9.94%)			100.09% (overclassification 0.09%)			
Feature Overlap	FA results	552 of 707			545 of 635			400 of 449			
	Reference data	690 of 856			637 of 850			476 of 568			
Feature Score User's Accuracy[b]		78.08%			85.83%			89.09%			
Feature Score Producer's Accuracy[c]		80.61%			74.94%			83.80%			

[a] *observed Kappa as proportion of maximum possible Kappa for the respective dataset, only stated where different from the observed Kappa.*
[b] *percentage of features in classification results which (partly) overlap with those in reference data (see Feature Overlap: FA results).*
[c] *percentage of features in reference data which (partly) overlap with those in classification results (see Feature Overlap: Reference data).*

subset. Despite some similarities, the classification outcomes of Model 1 and 3 also exhibit clear differences. The rooftop data obtained with Model 1 all show, by far, the highest Feature Score User's Accuracy (see Table 11). In each of the analyzed images, over 95% of the objects classified as rooftops at least partly overlap with the rooftops in the reference data. At the same time, only around 70% of the rooftops in the reference data are (partly) covered by the (semi-) automatically detected objects. Despite this considerable incompleteness, no severe underclassification is evident with regard to the total area of extracted rooftops. Together, these findings give insight into the type and nature of classification errors. AFE Model 1 apparently tends to overestimate the area of individual rooftops and underestimate the number of buildings. Apart from this clear bias towards omission, the detected rooftops exhibit a high level of validity with respect to actual building locations. Consequently, Model 1 identifies rooftops reliably and with a high location accuracy, but it does not detect all buildings. Moreover, the AFE model shows difficulties in capturing the exact shape and area of individual rooftops. The outputs of Model 3 are characterized by relatively similar errors of omission and commission, especially on an object-based level (see Table 11). Hence, AFE Model 3 typically recognizes more of the buildings or rooftops in the reference data (see Feature Score Producer's Accuracy). However, it also less reliably predicts actual building locations and its outputs contain a higher number of false positives (see Feature Score User's Accuracy). The classification results obtained with AFE Model 2 differ from the hitherto discussed ones with regard to several indicators. Firstly, they regularly exhibit, at least, a partial overlap with over 80-90% of the rooftops in the reference data and thus have the highest Feature Score Producer's Accuracies (see Table 11). At the same time, the outputs of Model 2 consistently show the lowest user accuracies, on an area and an object basis (Feature Score). The total areas of rooftops suggest a tendency towards under- rather than overestimation, although the classification outcomes consist of substantially more features than those of the other models (see Table 11). Hence, AFE Model 2 apparently produces classification results with high numbers of smaller individual objects. The model is able to detect, at least partly, most of the existing buildings. However, the extents of individual rooftops are commonly underestimated. Moreover, the outputs contain a considerable number of small features that are false positives. Thus, in comparison to the other two AFE models, Model 2 seems less able to identify building locations reliably and to appropriately distinguish between rooftops and other, similar surfaces.

Besides the outlined differences in accuracies that are linked to the use of different AFE models, discrepancies can also be observed in relation to the respective image analyzed. For Qasr, the rooftop detection outcomes of all three AFE models are very similar in terms of most accuracy indices (see Table 11). Regarding the total area of rooftops, the outputs of all classification models differ only slightly. They also consistently show the highest overall accuracies compared to the results of the other images included in Table 11. In contrast, the image subset of Rabba and its building inventory apparently pose a challenge for an accurate, reliable and comprehensive (semi-) automatic detection of rooftops. For this settlement, all AFE models underestimated the total area of rooftops to a certain degree. The classification outcomes for Rabba are also characterized by the lowest Kappa values in comparison to the results

of the other images (see Table 11). For Jad'a, high Kappa and user's accuracy values were found in the outputs of all classification models. This suggests that in general, the particular image subset could be analyzed fairly well with the models developed for the specific classification task. However, the results of Model 1 and 2, which were obtained through batch processing, exhibit a strong tendency towards underclassification. The original classification outputs of Model 3 are associated with a more fitting total area of rooftops and higher accuracies according to most indices (see Table 11). This indicates that here, the best possible classification results could only be achieved with an AFE model that was specifically adjusted to the particular image tile.

The accuracy assessment results presented in Table 12 provide further information about the performances of individual AFE models when they are used to classify other images (batch processing). Several of the hitherto described findings concerning the qualities of classification outcomes and differences in these, according to AFE model, are corroborated. The outputs of Model 1, for example, are regularly characterized by the highest feature score user's accuracies. On the contrary, the previously noted differences between Model 2 and 3 (see next to last paragraph) become blurred, in view of the findings displayed in Table 12. However, a clear contrast exists between Model 2 and 3 in regard to the figures for the total area of rooftops. The outcomes of Model 2 consistently exhibit a pronounced tendency towards underclassification, amounting to almost 20% in the case of Shihan, for example. In contrast, all outputs of Model 3 show a more or less strong degree of overclassification that can reach values of around 35% in the case of Mghayyer (see Table 12). These biases towards under- or overestimation can also affect the values of other accuracy indices, such as the (feature score) producer's accuracy. The latter indicates the share of the reference data that is matched by the classification results. For more comprehensive outputs, chances are higher that they also overlap with a larger portion of the reference data. Consequently, the outcomes of Model 3 show comparatively high producer's accuracies (on an object and an area basis) or low errors of omission (see Table 12). The outputs of Model 2, in contrast, exhibit larger errors of omission (lower producer's accuracies) and thus seem less complete due to the general underlying underclassification bias. Model 1 apparently produces more balanced results with no clear tendency towards systematic under- or overestimation of the total area of rooftops.

Overall, the accuracy findings presented in Table 12 are largely comparable to those displayed in Table 11. Only the results for the image subset of "Shihan" represent a rather exceptional case. For the named image tile and settlement, the outputs of all AFE models exhibit unusually low values for several accuracy indices. This finding is in good accordance with the insights gained from the visual examination of the rooftop detection results (see Fig. 33). The contrast with the outcomes from the other image tiles is most evident in the significantly lower Kappa coefficients for Shihan (see Table 12). Among the outputs of the different AFE models for the particular image subset, those of Model 2 seem most suitable. Despite the marked underclassification bias, they show the best user's, producer's and overall accuracies and the highest Kappa value for Shihan (see Table 12).

Table 12: Outcomes of the accuracy assessment of the rooftop detection results for the three image tiles used for the evaluation of the three developed AFE models. All assessed classification outcomes were obtained through batch processing.

		Image tile / settlement								
		Smakiya			**Mghayyer**			**Shihan**		
AFE Model 1 - Qasr		Reference data (m²)		Total	Reference data (m²)		Total	Reference data (m²)		Total
		Rooftops	Background		Rooftops	Background		Rooftops	Background	
FA results (m²)	Rooftops	36498	24661	**61159**	23536	19096	**42632**	7535	10492	**18027**
	Background	20073	1236064	1256137	12021	2106248	2118269	12159	1474414	1486573
Total		**56572**	1260724	1317296	**35557**	2125344	2160901	**19694**	1484906	1504600
User's Accuracy (Rooftops)		59.68%			55.21%			41.80%		
Producer's Accuracy (Rooftops)		64.52%			66.19%			38.26%		
Overall Accuracy		96.60%			98.56%			98.49%		
Kappa		0.60 / 0.63[a]			0.59 / 0.66[a]			0.39 / 0.41[a]		
Area match (FA/ Reference data)		108.11% (overclassification 8.11%)			119.90% (overclassification 19.90%)			91.54% (underclassification 8.46%)		
Feature Overlap	FA results	209 of 212			163 of 177			49 of 53		
	Reference data	261 of 342			193 of 246			58 of 137		
Feature Score User's Accuracy[b]		98.58%			92.09%			92.45%		
Feature Score Producer's Accuracy[c]		76.32%			78.46%			42.34%		
AFE Model 2 - Rabba		Reference data (m²)		Total	Reference data (m²)		Total	Reference data (m²)		Total
		Rooftops	Background		Rooftops	Background		Rooftops	Background	
FA results (m²)	Rooftops	28460	18116	**46576**	21023	13094	**34117**	9342	6769	**16111**
	Background	28112	1242608	1270720	14534	2112250	2126784	10352	1478137	1488489
Total		**56572**	1260724	1317296	**35557**	2125344	2160901	**19694**	1484906	1504600
User's Accuracy (Rooftops)		61.10%			61.62%			57.98%		
Producer's Accuracy (Rooftops)		50.31%			59.13%			47.44%		
Overall Accuracy		96.49%			98.72%			98.86%		
Kappa		0.53 / 0.59[a]			0.60 / 0.61[a]			0.52 / 0.57[a]		
Area match (FA/ Reference data)		82.33% (underclassification 17.67%)			95.95% (underclassification 4.05%)			81.81% (underclassification 18.19%)		
Feature Overlap	FA results	282 of 335			203 of 253			93 of 114		
	Reference data	276 of 342			211 of 246			94 of 137		
Feature Score User's Accuracy[b]		84.18%			80.24%			81.58%		
Feature Score Producer's Accuracy[c]		80.70%			85.77%			68.61%		
AFE Model 3 – Jad'a		Reference data (m²)		Total	Reference data (m²)		Total	Reference data (m²)		Total
		Rooftops	Background		Rooftops	Background		Rooftops	Background	
FA results (m²)	Rooftops	37822	25727	**63549**	25707	22351	**48058**	8979	11591	**20570**
	Background	18750	1234997	1253747	9849	2102994	2112843	10714	1473316	1484030
Total		**56572**	1260724	1317296	**35557**	2125344	2160901	**19694**	1484906	1504600
User's Accuracy (Rooftops)		59.52%			53.49%			43.65%		
Producer's Accuracy (Rooftops)		66.86%			72.30%			45.59%		
Overall Accuracy		96.62%			98.51%			98.52%		
Kappa		0.61 / 0.65[a]			0.61 / 0.72[a]			0.44 / 0.45[a]		
Area match (FA/ Reference data)		112.33% (overclassification 12.33%)			135.16% (overclassification 35.16%)			104.45% (overclassification 4.45%)		
Feature Overlap	FA results	232 of 261			187 of 262			77 of 102		
	Reference data	276 of 342			215 of 246			83 of 137		
Feature Score User's Accuracy[b]		88.89%			71.37%			75.49%		
Feature Score Producer's Accuracy[c]		80.70%			87.40%			60.58%		

[a] observed Kappa as proportion of maximum possible Kappa for the respective dataset, only stated where different from the observed Kappa.
[b] percentage of features in classification results which (partly) overlap with those in reference data (see Feature Overlap: FA results).
[c] percentage of features in reference data which (partly) overlap with those in classification results (see Feature Overlap: Reference data).

In order to determine the typical accuracies and characteristics of classification outcomes of each AFE model, the hitherto described assessment results were aggregated. In Table 13, for every AFE model, the observed range of values and the mean value are stated for each of the previously introduced accuracy indices. Here, only the accuracy findings of batch processing outcomes were considered since these seemed most relevant with regard to the estimation of the general quality and transferability of a given AFE model. As a result, for each AFE model, the aggregated accuracy findings shown in Table 13 were based on the assessment results from five image subsets. In all cases, the results from Smakiya, Mghayyer and Shihan (see Table 12) were included. Additionally, the outcomes from two further images (see Table 11) were taken into account. Depending on the AFE model, the data from different images were considered here, to only include findings from batch processing outputs. The figures presented in Table 13, especially the mean values, served as indicators for the typical classification performance of each AFE model and the usual quality of the outputs. Therefore, these findings formed the basis for the selection of the most suitable AFE model for the analysis of the remaining image subsets that covered the other six settlements in the study area. By extrapolating or transferring the collected data about the performance of a given AFE model and the quality of its outputs, the likely accuracies of further classification results, obtained by applying this model to other images, can be estimated. In this regard, the 95% confidence interval (CI) is particularly important, which was computed for the total area of detected rooftops. The CI defines a range for the classification results into which the actual total area of rooftops (e.g. according to the reference data) falls; with a 95% probability. In other words, the interval describes the typical magnitude of likely under- or overestimation that is observed and can be expected with regard to the total area of (semi-) automatically detected rooftops.

Comparison of the figures in Table 13 reveals large similarities in the accuracy results for the three AFE models, especially with regard to the overall accuracy and the Kappa coefficient. However, the classification models also exhibit considerable differences in the values of several indices. The specific combination of lower or higher values for individual accuracy indices is what characterizes each model and distinguishes it from the others. In this regard, the findings presented in Table 13 corroborate the previously described tendencies and differences. AFE Model 1 shows only a negligible discrepancy, on average, between classification outputs and reference data in terms of the total area of rooftops. On the whole, under- and overestimation of rooftop areas for individual images tend to even out. The 95% CI for the total area of rooftops in the classification results is defined by equal, moderate percentages of 15-16% of over- and underestimation (see Table 13). As pointed out earlier, the outputs of AFE Model 1 are characterized by exceptionally high feature score user's accuracies, which indicate a very high location accuracy and reliability of the identified rooftops. The shortcomings of the classification performance of Model 1 have also been outlined before and are reflected in the values of some of the other accuracy indices (see Table 13). Typically, a certain percentage of the rooftops in the reference data are missed by the classification model and the exact extents and shapes of individual rooftops are not captured accurately. However, some limitations and minor flaws are normally observed in all approaches

and outcomes of (semi-) automatic detection of rooftops in satellite images. For the intended use of the collected rooftop data in the present study, i.e. for the estimation of the RRWH potential, Model 1 was considered the most suitable of the developed AFE models, due to the hitherto described assessment findings. Therefore, this model was selected for the detection of rooftops in the other six image subsets.

Table 13: Mean values and ranges of values for individual accuracy indices according to AFE model. Figures were derived from the accuracy assessment results presented in Table 11 and 12. Here, only accuracy findings from classification outcomes obtained with batch processing (five datasets for each AFE model) were taken into account. This was done to compare and evaluate the classification performance of each model and the quality of its outputs specifically for batch processing conditions, i.e. when the model is used to analyze a new image.

	Model 1 (Qasr)		Model 2 (Rabba)		Model 3 (Jad'a)	
	min. - max.	mean	min. - max.	mean	min. - max.	mean
Area difference (FA/Reference data) (%)	-12.69 +19.90	-0.54	-19.57 - +4.98	-10.90	-9.94 - +35.16	+8.58
95% Confidence Interval[a]	*-16.09 - +15.01*		*-22.98 - +1.18*		*-10.17 - +27.33*	
Feature Score User's Accuracy[b] (%)	92.09 - 98.58	95.09	73.05 -84.18	80.08	71.37 - 88.89	79.93
Feature Score Producer's Accuracy[c] (%)	42.34 - 78.46	66.99	68.61 - 91.12	81.61	60.58 - 87.40	76.85
User's Accuracy (Rooftops) (%)	41.80 - 65.69	56.66	57.98 - 63.80	60.70	43.65 - 62.59	56.01
Producer's Accuracy (Rooftops) (%)	38.26 - 66.19	56.28	47.44 - 61.95	54.03	45.59 - 72.30	60.52
Overall Accuracy (%)	96.60 - 98.56	97.52	96.49 - 98.86	97.72	96.62 - 98.52	97.73
Kappa[d]	0.41 - 0.66	0.59	0.57 - 0.62	0.60	0.45 - 0.72	0.61

[a] range of likely over- and underestimation in classification results in comparison to reference data.
[b, c] see corresponding explanations in Table 11 and 12.
[d] here observed Kappa as proportion of maximum possible Kappa value for individual datasets in order to compensate biases from cases in which maximum possible Kappa is not 1.

Results of the automatic extraction of rooftops for the images of the remaining six villages in the study area, namely Ariha, Mis'r, al-'Aliya, Hmud, Abu Traba and Rashadiya, are displayed in Fig. 34. The depicted rooftop data was obtained through batch processing in which Model 1 was used to analyze the aforementioned image subsets. Visual examination of the classification outcomes suggests a good accordance between discernible buildings and automatically extracted rooftops (see Fig. 34). This supports the assumption that the rooftop detection results for the named image tiles should be similar to the previously evaluated classification outcomes, in terms of their accuracies and related properties. Therefore, the generalized findings derived from the accuracy assessment, and identified as qualities of the outputs of Model 1 (see Table 13), such as e.g. the determined 95% CI for the total area of rooftops, were transferred to the classification/batch processing outcomes shown in Fig. 34.

Figure 35 illustrates the total area of rooftops for each of the 12 settlements in the study area. Figures are based on the classification outputs of AFE Model 1. For each image subset and settlement, the total area of (semi-) automatically detected rooftops is displayed by one blue column. The height of every column reflects the size of the area. Black error bars visualize the 95% CI or the likely range into which

Fig. 34: Automatic rooftop detection results for the image subsets showing the six settlements Ariha (a), Hmud (b), Abu Traba (c), Rashadiya (d), al-'Aliya (e) and Misr (f). Classification outcomes where produced by applying AFE Model 1 to each image tile via batch processing. The total area of rooftops detected in each image is given in Fig. 35.
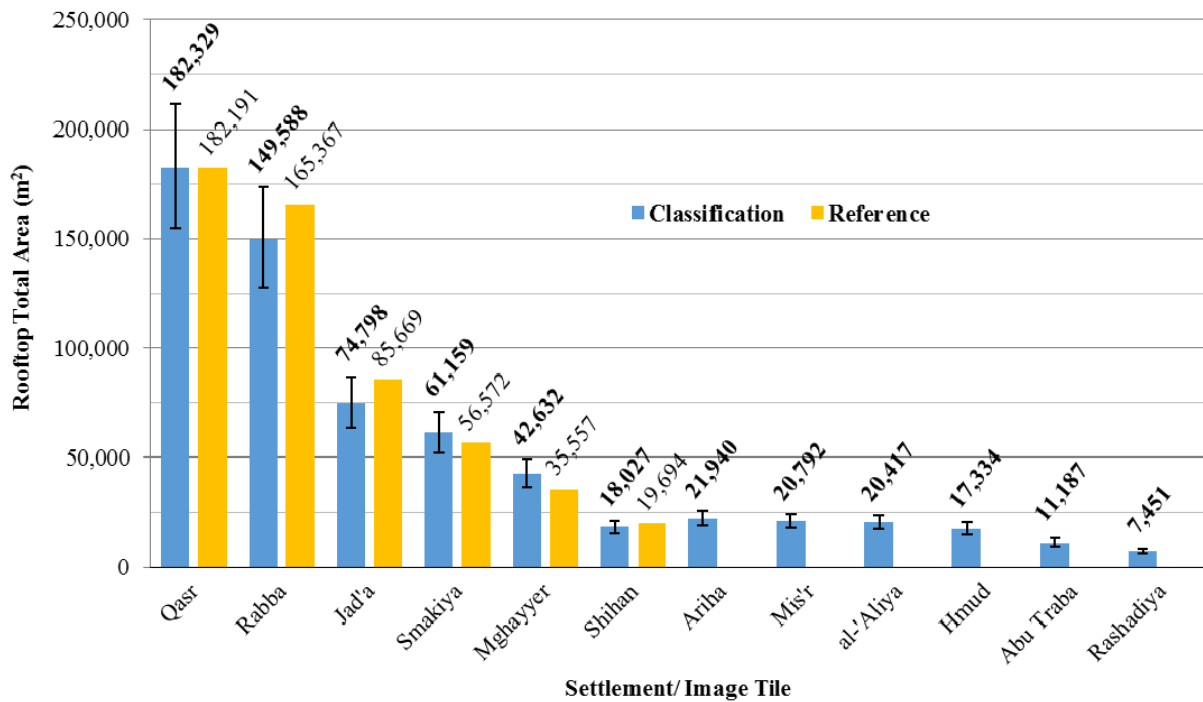
Fig. 35: Bar chart of the total areas of rooftops in individual settlements according to the image classification outcomes obtained with AFE Model 1. For the image subsets used in the development or the evaluation of the AFE models, the total rooftop areas according to the reference data (manually digitized rooftops, orange columns) are also given. Findings from (semi-) automatic object detection (blue columns) are shown in conjunction with error bars (black bars) that visualize a tolerance interval of -15% to +16%. This range of likely under- or overestimation corresponds to the 95% CI which was determined for the outputs of AFE model 1, based on the accuracy assessment results (see Table 13).

the actual total area of rooftops should fall, given the computed probable amounts of under- or overestimation in the classification outcomes. For the six images and settlements for which reference data had been acquired and classification results have been assessed, the total area of rooftops according to the reference data (orange columns) is also shown for comparison. Above each column, the total area of rooftops is stated, which was found in the respective dataset.

According to the results displayed in Fig. 35 (blue columns), the total area of rooftops detected for the 12 settlements within the study area amounts to 627,654 m^2 (0.6 km^2) altogether. With regard to the defined CI and hence, the typical range of possible over- or underestimation in classification outputs, with a possibility of 95%, the actual sum of rooftop areas should fall within the range of 533,506 - 728,079 m^2 (0.5 - 0.7 km^2). The actual rooftop area here refers to the one which would result from visual image interpretation and manual digitization of rooftops (also see reference data used in the accuracy assessment, cf. chapter 4.1.2.6). Since over- and underestimation of rooftop areas in individual settlements tend to even out overall, the above stated total area of (semi-) automatically detected rooftops can be assumed to be quite correct. Therefore, for the whole study area, the overall level of over- or underestimation of the rooftop area in the classification results is probably considerably lower than the computed range of the 95% CI suggests. For the six image subsets and settlements included in the accuracy assessment, the sum of the rooftop areas according to classification outcomes amounts to 528,533 m^2.

In the reference data, a total rooftop area of 545,050 m^2 is identified. Thus, the (semi-) automatically extracted rooftop data and the reference data differ only by 16,517 m^2 or 3%.

5.3 Digital elevation models

A closer examination of the two DEMs used in the present study, the ASTER GDEM V2 and the custom-made ALOS DEM, and their derivative products (e.g. slope maps), allows adding quantitative aspects to the description of the relief and the morphology of the area (see chapter 3.1). The ALOS DEM covers an area of 194 km^2 which comprises the northeastern part of the Karak Plateau and some of its immediate surroundings (escarpments and wadi valleys, see Fig. 36). Since the actual study area is confined to the plateau region itself, it forms a subarea of the land included in the ALOS DEM. The study area has an extent of 163 km^2 and its boundary is largely defined by the 700 m above sea level contour line (see Fig. 36). Altitudes in the study area mainly range between 700 and 1,000 m above sea level. About two-thirds of the terrain is characterized by elevations of 800 to 900 m above sea level. According to the ALOS DEM, the minimum and maximum elevations in the study area correspond to 667 m and 1010 m above sea level. Altitudes can be grouped into five classes. Elevations of the three categories of 700-799, 800-899 and 9000-1000 m above sea level are found in 13% (22 km^2), 65% (106 km^2) and 22% (35 km^2) of the study area, respectively. Areas with altitudes of less than 700 or over 1,000 m above sea level amount to less than 1 km^2. The spatial distribution of different elevations is visualized in Fig. 36.

The slope map derived from the ALOS DEM (see Fig. 36) reveals the prevalence of low to moderate inclinations in the study area. Although slopes range from a minimum of 0° to a maximum of 34°, well over 90% of the territory is characterized by gradients of less than 10°. Slopes in the categories of 0-4°, 5-9° and 10-19° are found in 72% (118 km^2), 22% (36 km^2) and 5% (8 km^2) of the study area, respectively. Less than 1% of the land (<1 km^2) exhibits steeper inclinations of 20° or more. In general, gradients of 10° and more occur mainly in the southeastern part of the study area, around Wadi Ghuwayta and its tributaries (see Fig. 36, for the location of Wadi Ghuwayta also see Fig. 38). All elevation and slope information described here and displayed in Fig. 36 were extracted or derived from the modified, enhanced version of the ALOS DEM (see chapter 4.1.3).

Elevation differences between the custom-made, revised ALOS DEM and the ASTER GDEM V2 were mostly marginal and within the range of several meters. In general, the ASTER GDEM V2 often showed slightly lower elevations compared to the ALOS DEM. For individual raster cells, differences between the two DEMs varied from 0 to 64 m (-52 m to +64 m). However, discrepancies rarely exceeded 10 m. In over 99% of the compared raster cells, i.e. those in the area covered by both DEMs, elevation differences of +/-25 m or less were observed. Still, in more than 88% of the area, discrepancies took values

of maximal +/-10 m. Hence, for the region of the present study, the two used DEMs were quite similar in terms of the elevation information they contained and the relief they displayed.

Legend

Study area on Karak plateau — Contour line

Elevation		
m above sea level	area (km^2)	share
< 300	< 1	< 1 %
300 - < 400	1	< 1 %
400 - < 500	3	1 %
500 - < 600	5	2 %
600 - < 700	9	5 %
700 - < 800	34	18 %
800 - < 900	107	55 %
900 - < 1,000	35	18 %
1,000 - 1,100	< 1	< 1 %

Slope		
gradient in degree	area (km^2)	share
0 - < 5	119	61 %
5 - < 10	38	20 %
10 - < 20	17	9 %
20 - < 30	13	6 %
30 - 50	7	4 %

Projection: WGS 1984, UTM Zone 36 N.

Sources: ALOS DEM
ALOS PRISM satellite imagery ©JAXA 2011.
DEM production: Geoserve B.V. 2011.
post-processing, data editing and production of
derivative data (slope map): B. Brilmayer Bakti.

Fig. 36: Altitudes and gradients in the study area according to the revised ALOS DEM (cf. chapter 4.1.3). For each category of elevation or slope values, the respective absolute extent (in km²) of the associated areas is given as well as the corresponding share (in percent) in the total area of the ALOS DEM.

5.4 Hydrological data layers

According to the outcomes of the hydrological analyses, almost 98% of the larger study area, which corresponds to the extent of the ALOS DEM (see Fig. 36), belongs to the surface drainage basin of Wadi al Mujib and its tributaries (see Fig. 37 and Table 14). Only small parts (ca. 2% of the study area) in the southwest were attributed to the watershed of Wadi Ibn Hammad. The latter, as well as the Wadi al Mujib, ultimately drain to the west and thus into the Dead Sea. Drainage directions within the study area vary locally depending on the (sub-) catchment. Almost 90% of the study area are part of the watersheds of Wadi Nukhayla, the southward trending branch of Wadi al Mujib, and its tributaries (see Fig. 38 and Table 14). Surface water flow in these basins is directed towards the northeast. In the area analyzed, Wadi Balua and Wadi Ghuwayta represent the main tributaries of Wadi Nukhayla. They comprise 47% and 28% of the territory, respectively (see Table 14). The remaining parts of the study area belong to the subbasins of the Lower Wadi al Mujib (8% of the area) and Wadi Ibn Hammad (ca. 2% of the area), which drain to the north and the west, respectively. With regard to the larger, regional surface water drainage situation, the study area forms only a small part (ca. 3%) of the huge basin of Wadi al Mujib (see Fig. 37 and Table 14). However, the territory makes up about two-thirds of the whole basin of Wadi Nukhayla and comprises major shares (78% and 98%, respectively) of the watersheds of Wadi Balua and Wadi Ghuwayta, two of the main western tributaries of Wadi Nukhayla (see Fig. 37 and 38 and Table 14).

For the study area, two different versions were available for each of the hydrological data layers. These represented the outcomes of the two hydrological analyses that were performed with and without data on known streams, i.e. here manually digitized drainage lines (see chapter 4.1.4). The outputs, particularly the drainage line and catchment data layers, were examined and compared to identify similarities, differences, and individual characteristics. Findings are illustrated in Fig. 38 and 39 and summarized in Table 14. The results of all hydrological analyses, including the one based on the ASTER GDEM, are in good accordance in terms of the computed main watersheds in the study area. These largely coincide, although minor differences can be observed in the details of their boundaries. For the Wadi Ibn Hammad watershed, no drainage lines could be visually identified in the satellite image. Therefore, in this case, no catchments were defined in the hydrological analysis that included the manually digitized drainage lines (see Fig. 39 and Table 14). The hydrological analysis which only relied on the DEM, without additional stream data, in contrast, yielded several drainage lines and (sub-) catchments for the watershed of Wadi Ibn Hammad (see Fig. 38 and Table 14). The catchments resulting from the hydrological analysis with the digitized streams occasionally seemed distorted, truncated or otherwise biased around the fringes of the study area and the DEM.

With regard to the overall figures for the drainage lines and catchments, the results of the two detailed hydrological analyses were very similar (see Table 14). In the process of the hydrological analysis, the

original, manually digitized streams were segmented into smaller individual parts according to junctions of tributaries. Each stream segment then corresponded to one drainage line in the output data. The resulting drainage lines were comparable to the synthetic streams, i.e. the drainage lines computed automatically based on the DEM, in terms of their number and their total length. However, the synthetic streams were slightly shorter, on average, as well as in their overall sum (see Table 14). In accordance with the drainage line results, catchment numbers in the outcomes of the two hydrological analyses were also similar. Yet, the drainage lines and catchments were distributed differently with regard to the larger watersheds (see Fig. 38 and 39 and Table 14). In most of the main watersheds, the numbers of manually digitized drainage lines and their catchments were higher than those of the synthetic streams and their catchments. This proportion was inverted for the watersheds of Wadi Ibn Hammad (see explanations above) and Wadi Balua. For the latter, outcomes from the analysis without known streams exhibited
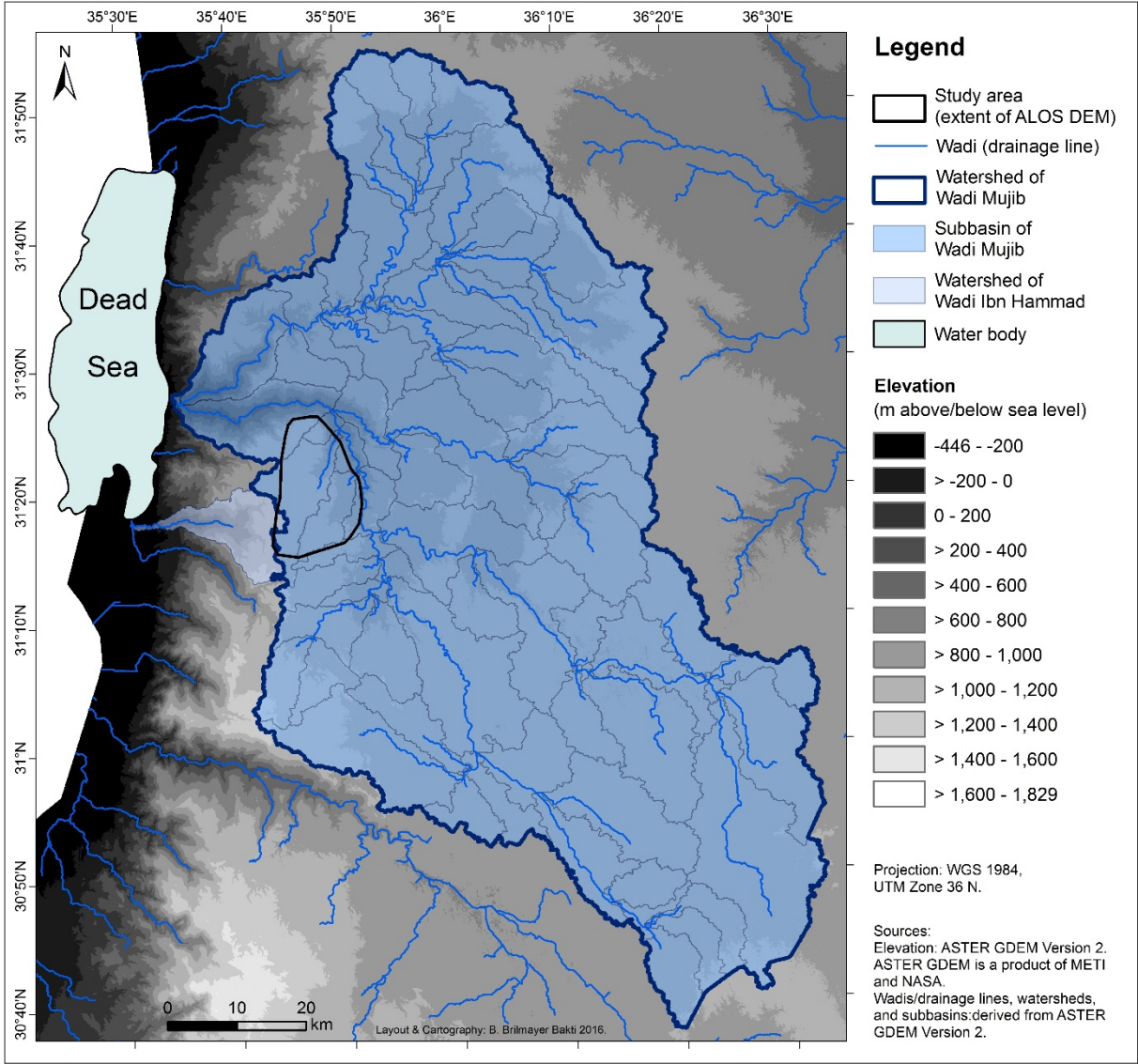
Fig. 37: Overview of the larger wadis and relevant watersheds in the wider study region. The visualized information were obtained with the broader hydrological analysis based on the ASTER GDEM V2 (see chapter 4.1.4).

Table 14: Statistical figures summarizing and describing the information contained in the hydrological data layers (drainage lines and catchments). The data correspond to the input (manually digitized streams only) and outputs (all other data) of the different hydrological analyses conducted (see chapter 4.1.4).

Parameter	Lower Mujib	Lower Nukhayla	Balua	Middle Nukhayla	Ghuwayta	Upper Nukhayla	ad-Dabba	Ibn Hammad
Major wadis and watersheds — Value: Mujib (total) → Nukhayla (total)	Lower Mujib	Lower Nukhayla	Balua	Middle Nukhayla	Ghuwayta	Upper Nukhayla	ad-Dabba	Ibn Hammad
Total area/ size (km²) — Mujib (total): 6759.63; Nukhayla (total): 263.92	165.45	15.6	116.21	25.04	55.48	51.59	36.38	126.26
Share of study area[a] in total — Mujib (total): 2.80 %; Nukhayla (total): 65.20 %	9.13 %	58.72 %	78.46 %	26.38 %	97.57 %	21.36 %	5.29 %	3.71 %
Extent in study area[a] (km²) — Mujib (total): 189.12; Nukhayla (total): 172.09	15.11	9.16	91.17	6.6	54.13	11.02	1.93	4.68
Share in study area[a] — Mujib (total): 97.59 %; Nukhayla (total): 88.80 %	7.80 %	4.73 %	47.05 %	3.41 %	27.93 %	5.68 %	0.99 %	2.41 %
Characteristics of the manually digitized drainage lines (raw data)[b]								
Number — 2090[c]; 2089; Nukhayla (total): 1804	261	151	538	162	769	184	24	0
Length per stream (km)	min. - max.: 0.02 - 21.04 ; average: 0.40							
Total length (km)	836.48							
**Characteristics of the drainage lines: synthetic streams	manually digitized streams[d]**								
Number — 4073[c]	4055[c]; 3958	4053; 3631	3523	295	489	175	285	2045	1070	120	297	1094	1528	197	343	32	41	94	0
Length per stream (km)	min. - max.: 0.00 (1 m) - 1.56	0.00 (4 m) - 3.11 ; average: 0.21	0.22							
Total length (km)	856.78	881.19							
**Characteristics of the catchments: synthetic streams	manually digitized streams[d]**								
Number of subcatchments — 4091[c]	4055[c]; 3976	4053; 3642	3523	296	489	177	285	2047	1070	127	297	1094	1528	197	343	38	41	94	0
Total area	extent (km²) — 185.00[c]	180.27[c]; 179.88	179.87; 165	165.76	12.94	13.24	9.17	9.21	86.48	86.03	6.5	6.05	52.94	54.13	9.92	10.33	1.93	0.88	4.33	0
Sizes (km²)	min. - max.: 0.00 (5 m²) - 0.40	0.00 (20 m²) - 2.83 ; average: 0.05	0.04							

[a] the study area here corresponds to the extent of the ALOS DEM
[b] original drainage line data acquired through visual interpretation of the GeoEye-1 satellite imagery and manual digitation (see 4.1.2.2)
[c] figure contains streams for which no catchment could be calculated
[d] referring to the manually digitized drainage line data (see [b]) after its preparation for the hydrological analysis. See 4.1.4, Fig. 27, b, step "create drainage line structures", in which the original digitized streams where split into individual features at intersections.
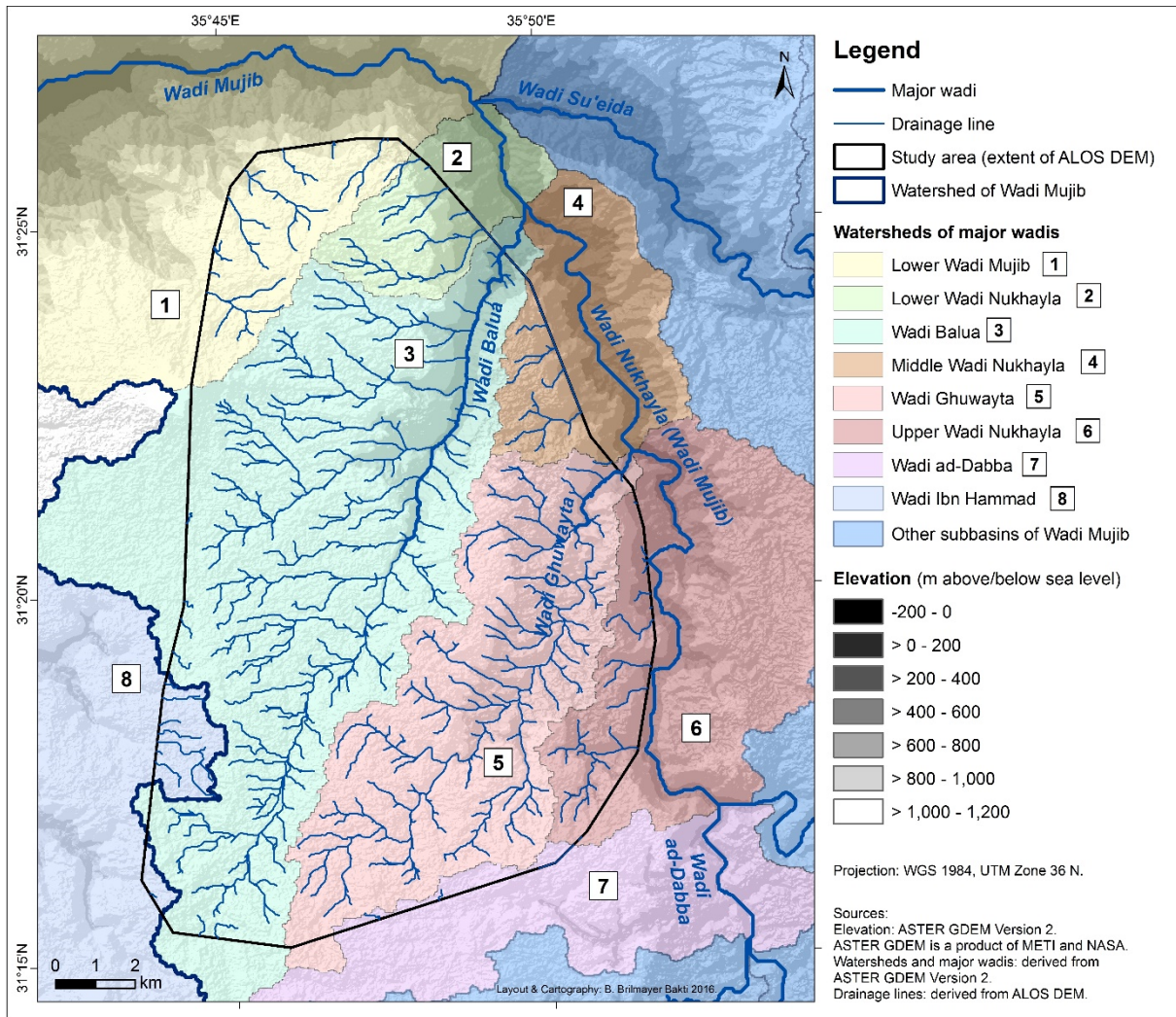
Fig. 38: Main watersheds in the study area and computed network of drainage lines (synthetic streams). The drainage line data was obtained with the hydrological analysis based on the ALOS DEM without additional information on known streams (cf. chapter 4.1.4). The displayed information on major wadis and their watersheds correspond to the outputs of the broader hydrological analysis based on the ASTER GDEM V2 (also see Fig. 37).

almost twice as many drainage lines and catchments as those of the analysis with the digitized streams (see Table 14). The watershed of Wadi Balua is the largest in the study area and covers almost half of the territory, including large portions of the flattest parts (see Fig. 36). Drainage lines and catchments derived from the DEM often show artifacts, especially in areas with marginal elevation variances. Here, parallel streams and other aberrations in the computed network of drainage lines can occur and entail an increased number of catchments, often with distorted shapes (see Fig. 39, b). On the other hand, in areas with mostly flat terrain, streams are less incised and therefore also rather difficult to visually identify in the satellite image. Often the LU/LC can further complicate their recognition. This may result in lower numbers of digitized streams and corresponding catchments. Overall, the manually digitized drainage lines and their catchments were considered more natural and plausible with respect to their shapes, sizes, and distribution, in comparison to the automatically computed drainage lines and their catchments
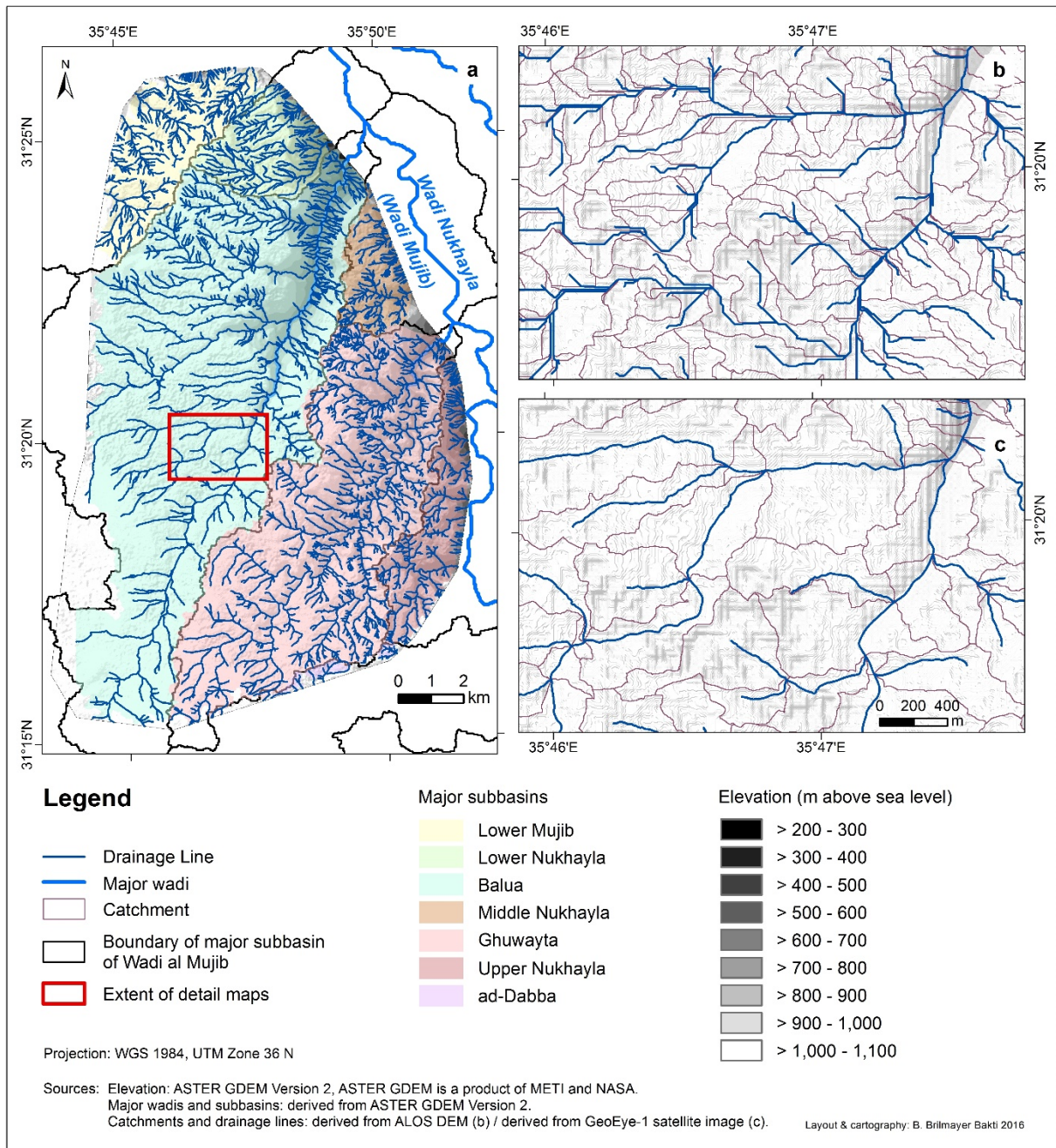
Fig. 39: Overview of the network of manually digitized streams (a) and detail maps illustrating the drainage line and catchment data which resulted from the two detailed hydrological analyses conducted for the study area (b, c) (see 4.1.4).The catchments shown in different colors according to the respective superordinated main watershed are those of the manually digitized streams. Information on major wadis and main watersheds was derived from the ASTER GDEM V2 in the broader hydrological analysis (also see Fig. 37 and 38). The location and extent of the two detail maps (b, c) are indicated with a red box in the overview map (a). Detail map b displays the drainage lines and catchments identified in the hydrological analysis based on the ALOS DEM without known streams. Map c visualizes the manually digitized drainage lines and the corresponding catchments computed in the hydrological analysis. The datasets depicted in the two detail maps (b, c) exhibit substantial similarities with regard to the overall structure of the network of drainage lines. However, larger discrepancies can be observed in the details, i.e. in the amount, location, and shape or course of smaller, tributary drainage lines and associated catchments. Source of elevation information: ALOS DEM.

(see Fig. 39, b and c). The latter, in many parts, apparently contained artifacts and distortions. Consequently, the outcomes of the hydrological analysis based on the manually digitized streams were selected as master datasets and employed in the analyses described in chapter 4.2.1. Based on the outputs of the

hydrological analysis, the catchment of any given point in the area can also be calculated. For test purposes, several cistern catchments were computed. However, the results seemed largely unsuitable. Therefore, due to suspected accuracy and reliability issues, this procedure and its results were not included in the present study.

5.5 Geological and archaeological datasets

The geological and archaeological data used in the present study were acquired from external sources and thus, the preparation of the corresponding data layers required only minimal levels of processing (cf. chapter 4.1.5). The geological and archaeological information contained in the two datasets are outlined below.

A detailed description of the geological setting in the study area can be found in chapter 3.2., which also includes a geological map. Table 15 provides a concise summary of the relevant geological units and their respective extents and shares in the study area, according to the data stored in the corresponding layer and illustrated in the geological map (see Fig. 3 in chapter 3.2).

In vast areas that amount to 124 km^2 or 76% of the study area on the Karak Plateau, more or less thick soil layers cover the sediments and other rocks. The underlying strata are primarily formed by the Al Hisa Phosphorite and its members and the various basalts of the Shihan Basaltic Group (see 3.2). The named units also predominate in the rest of the area (see Table 15). The Al Hisa Phosphorite formation

Table 15: Different geological units and their shares in the study area (plateau area). The displayed information correspond to the content of the prepared geological data layer. The areas associated with each unit and their spatial distribution are shown in the geological map (Fig. 3) in chapter 3.2.

Unit	Area (in km^2)	Share in study area
Landslide	< 1	< 1 %
Soil / soil over bedrock	124	76 %
Calcrete	5	3 %
Fluviatile and lacustrine gravels (cemented)	1	< 1 %
Basalt (not further specified)	< 1	< 1 %
Judaiyida Basalt	2	1 %
Sanina Basalt	5	3 %
Balua Basalt	< 1	< 1 %
Fraywan Basalt	3	2 %
Muwaqqar Chalk Marl	4	2 %
Al Hisa Phosphorite (not further specified)	11	7 %
Qatrana Phosphorite	7	4 %
Bahiya Coquina	< 1	< 1 %
Sultani Posphorite	1	< 1 %
Amman Silicified Limestone	< 1	< 1%

and its different members, of which the Qatrana Phosphorite is the most common in the area, occur in ca. 12% (20 km^2) of the study area, mainly in its southeastern part (see Table 15 and 3.2, Fig. 3). Basalts, among which the Sanina Basalt dominates, extend over 9 km^2 or 6% of the study area. The calcrete and the Muwaqqar Chalk Marl units cover smaller areas of 5 km^2 and 4 km^2 or 3% and 2% of the study area, respectively (see Table 15). While calcretes are mainly found in the flat areas of the northern and central parts of the plateau, the Muwaqqar Chalk Marl primarily occurs in the southeastern part of the territory, together with (cemented) fluviatile and lacustrine gravels (see 3.2, Fig. 3). The latter, as well as some other units listed in Table 15, comprise only a few smaller areas of the studied terrain.

The archaeological history of the study region has been outlined in chapter 3.6. There, a map of the archaeological sites within, and in, the surroundings of the study area can also be found (see Fig. 12 in 3.6). The visualized data, as well as additional information on each site, such as the associated periods of use and the site type according to the archaeological finds and remains discovered at the respective location, constitute the content of the archaeological data layer.

A total of 83 archaeological sites were identified in the study area, resulting in a density of ca. 1 site per 2 km^2. Additionally, more than 200 sites, which are located within a zone of a maximum distance of 6 km to the study area, were included in the prepared dataset. About half of the sites in this zone are situated on the Karak Plateau (119 sites), while the other half is found in areas of lower altitudes (114 sites).With regard to the study area itself, Figure 13 in chapter 3.6 displays, for each archaeological period, the number of sites that were associated with it, based on the estimated approximate ages of the finds and remains. For every period, the respective number of new sites, i.e. places that apparently were not occupied before, is also specified. According to the known archaeological traces, the sites in the study area were used during 1 to 13 periods, with an average of 4.4 periods. Only a few places were associated with finds or ruins from almost all eras, while the majority (over 80-90%) exhibit traces from maximal 6-7 periods. These findings similarly apply to the other archaeological sites on the Karak Plateau that were considered in the present study. The places at lower elevations, in contrast, are commonly characterized by a shorter occupation history. There, sites were obviously used during 3.2 periods, on average, with a minimum of 1 and a maximum of 11 periods. Around 80% of these sites at lower elevations apparently were occupied during 4 periods or less.

The 316 sites in the prepared archaeological data layer were grouped into four larger categories according to their types (see Fig. 12 in section 3.6). The latter were defined based on the kinds of finds and remains discovered at the respective place. With regard to the proportions of the four groups, the archaeological sites in the study area and those located in the surroundings on the Karak Plateau show a similar pattern. Places associated with military and security purposes, e.g. forts and watchtowers, or agricultural objectives in a broader sense, such as camps, hamlets, caravansaries, agricultural terraces and the like, make up shares of around 10%, respectively and thus, represent the two smallest groups. Around one quarter of the sites are characterized by ruins of more or less permanent structures, such as

buildings, and similar remains, and classified as villages, (fortified) settlements, temples, palaces, villas or tells (i.e. hills formed by the debris of several occupation phases). The shares of the aforementioned three categories are different in archaeological sites that are located in the vicinity of the study area but at lower elevations. There, sites of the last of the above described categories form the smallest group. Only about 15% of the sites exhibit settlement-related structures, ruins of buildings or similar remains. In contrast, site types linked to agricultural or military and security purposes are considerably more common. About 17% and over 20% of the archaeological sites in lower altitudes fall into these two categories, respectively. Approximately half of all archaeological sites, within and around the study area, situated either on the tableland or at lower altitudes, were assigned to the fourth category which encompasses all other, remaining site types that were not mentioned before (also see 3.6, Fig. 12). This group, which is also the biggest, comprises numerous places where sherds and similar finds have been discovered, as well as sites for which no type has been specified in the MEGA-Jordan database. The category also includes sites where (only) remains of water infrastructure elements have been found.

For each archaeological site, the presence or absence of structures and traces related to water supply and management was recorded as a separate trait in the attribute table of the prepared data layer. According to the data retrieved from the MEGA-Jordan database, the water infrastructure elements identified at the archaeological sites in the considered region were predominantly cisterns. Only a few places exhibited structures that were classified as (remains of) dams, barrages, and reservoirs. Again, major differences could be observed between archaeological sites on the tableland and their counterparts at lower elevations. About 39% of the sites on the Karak Plateau, either within or in the surroundings of the study area, featured water-related structures, which were almost exclusively cisterns (35% of the sites). At places in lower altitudes, cisterns also represented the most common type of remains linked to water management and supply. At some sites, cisterns were complemented by other water-related structures, including aqueducts. Compared to the highlands, traces of water management were identified at a significantly smaller number of sites in lower altitudes (18 out of 114, corresponding to 16%). This could be due to the differences in environmental conditions, particularly in regard to water availability, between the lower lying areas and the Karak Plateau.

5.6 Interpolated precipitation data

The outcomes of the spatial interpolation of the precipitation data recorded by the 28 weather stations in and around the study area (see 4.1.6, Fig. 28), are presented in Fig. 40-42. Figure 40 shows the locations of the different weather stations (also see 4.1.6, Fig. 28) as well as the mean annual precipitation amounts and their distribution over the study region. Spatial variations in precipitation amounts are

closely linked to the relief. Therefore, isohyets and contour lines exhibit large similarities (see Fig. 40). Mean annual precipitation in the analyzed region ranges between 107-351 mm. Values of over 200-300 mm are found only on the Karak Plateau, particularly in its central part. From there, annual precipitation amounts decline, along more or less steep gradients, towards the lower lying areas of the valleys of the major wadis (Wadi al Mujib, Wadi al Hasa) and the Dead Sea. There, the lowest precipitation amounts are observed. A clear longitudinal gradient also exists between the plateau, especially in its central part around the King's Highway, and the Eastern Desert, whose beginning or western limit is approximately marked by the Desert Highway (see Fig. 40-42, for a clear identification of the named highways, also see Fig. 2 in chapter 3.1). From west to east, over a short distance of ca. 30 km, mean annual precipitation amounts decrease from over 300 mm on the tableland to 150 mm and less in the steppe zone and finally the desert. This longitudinal gradient can also be observed in the spatial distribution of annual precipitation in the study area itself (see Fig. 40-42). However, here, the relative difference in mean annual precipitation amounts, from west to east, is slightly smaller, amounting to less than 100 mm. Absolute values range from 321 mm in the west to 224 mm in the east. In general, interpolation results are in good accordance with the general description of the regional climate given in chapter 3.3.

Although being important for the identification of general tendencies in climate, mean values from the 30 year period encompass and mask large interannual variances and extremes. The possible range of conditions is visualized in Fig. 41. Exemplified by the years 1963 and 1965, annual precipitation amounts and their spatial distribution during exceptionally dry and wet years are shown. The selected years represent the two extremes, the driest and the wettest year, of the period 1963-1992. During the dry year of 1963, the region received precipitation amounts of only 27 - 159 mm. Precipitation values in the upper half of the spectrum, between 97 and 159 mm, were observed in the study area itself. During dry years, in the moister highland areas, precipitation still reaches about half of its long term average, whereas it decreases to one third or even one quarter of the long term average in the drier areas of the steppe zone, the Eastern Desert, and around the Dead Sea (see Fig. 41). Hence, the strongest relative decreases, compared to the mean values, are found in the driest parts of the region. In 1965, the wettest year of the considered period, precipitation varied between 149 and 847 mm in the region and 395 - 677 mm in the study area on the Karak Plateau. The values identified in the study area thus roughly correspond to twice the amount of the long term average. However, the deviation from the long-term average varies considerably over the analyzed region. In its driest parts, the relative increase in precipitation, compared to the long-term mean, amounted to a surplus of 40%, whereas it was as large as 140% in the wettest parts of the highlands (see Fig. 41). Thus, in wet years, not only does the range of precipitation values expand, but local differences are also apparently intensified, with the moister parts of the region becoming even more humid. Finally, the pattern of the spatial distribution of annual precipitation changes slightly from year to year. However, the orographic influences and the previously described

longitudinal gradient always determine the underlying general pattern. Therefore, independent from interannual fluctuations, major differences in precipitation amounts can be observed between the plateau and the lower lying areas, as well as the Eastern Desert (see Fig. 40-42).
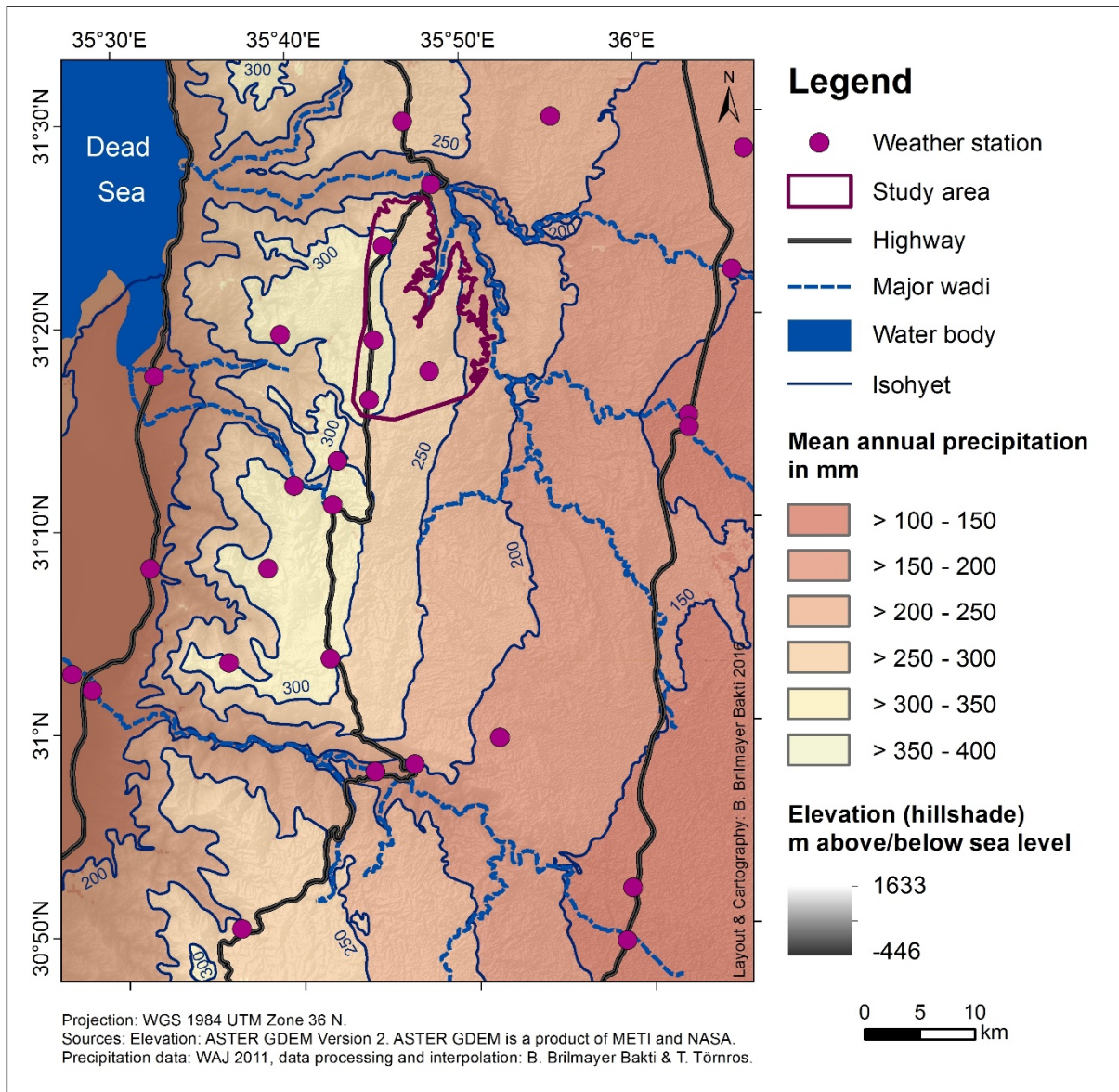
Fig. 40: Map showing the locations of the involved weather stations and the mean annual precipitation in the period 1963-1992 according to the interpolation outcomes. The names of the weather stations indicated by the points here are given in chapter 4.1.6, Fig. 28. The color scale applied to the different classes of annual precipitation amounts was selected to be consistent with the ones used for the visualization of the other precipitation interpolation results in Fig. 41 and 42. Sources: location of weather stations and raw precipitation data: WATER AUTHORITY OF JORDAN (WAJ) 2011, data processing and interpolation: B. Brilmayer Bakti & T. Törnros 2012 (also see chapter 4.1.6).
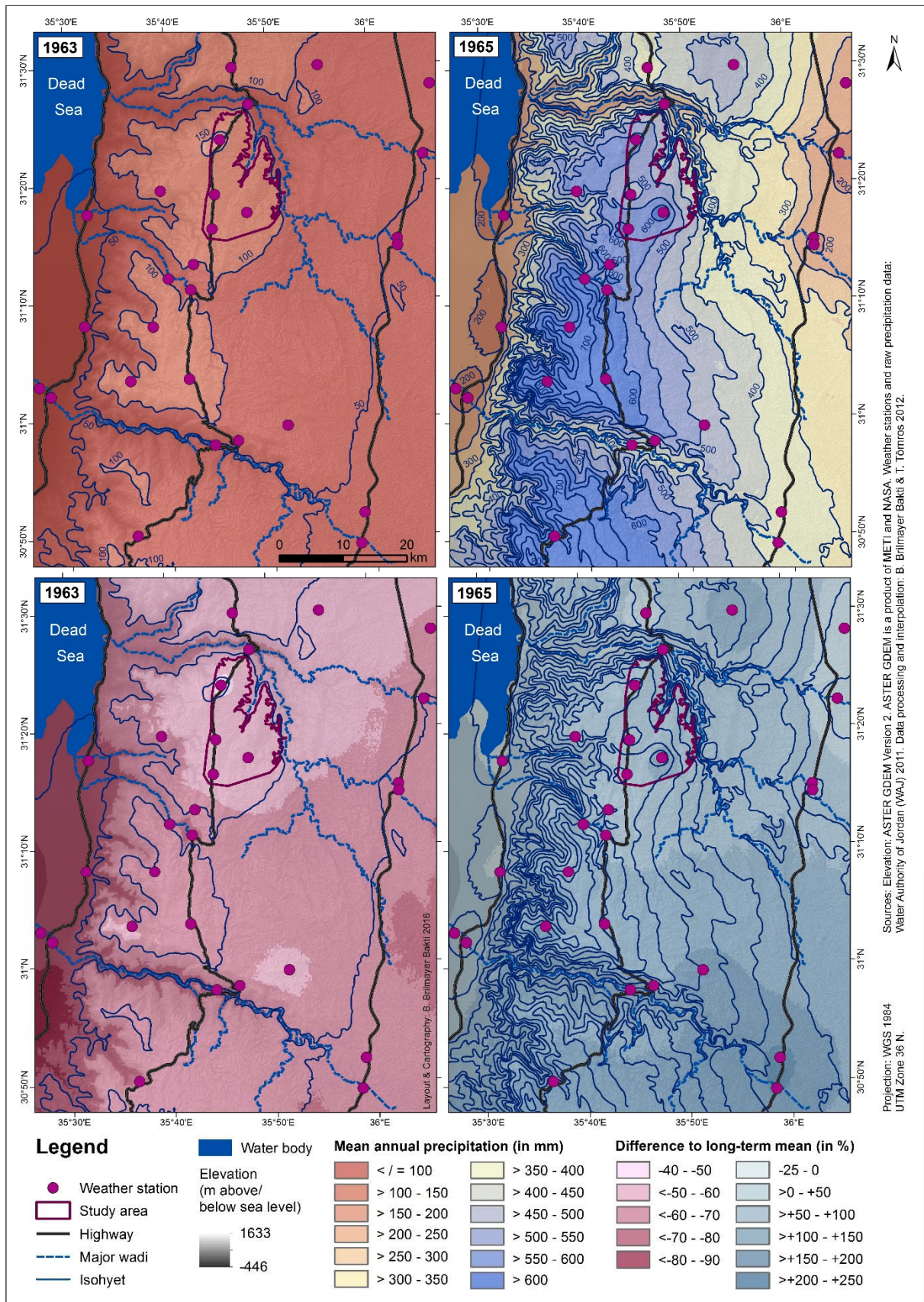
Fig. 41: Maps of the annual precipitation in the region in a dry and a wet year (top row maps) and the differences to the long-term mean (bottom row maps). A map of the mean annual precipitation in the region is presented in Fig. 40. Dry year conditions are exemplified by the precipitation data and interpolation results for 1963, wet year conditions by those for1965.

The monthly precipitation in the study region is displayed in Fig. 42. The shown results are the monthly means, which were derived from the interpolation outcomes with daily resolution for the defined 30-year period. Findings for the months of June to September were not included in Fig. 42, since precipitation in the named part of the year is close to zero, on the long-term average. The rainy season usually starts in late autumn and ends in spring (cf. section 3.3). Hence, annual precipitation is distributed over the months of October to April or May, with a strong emphasis on the winter months (see Fig. 42). On average, most precipitation occurs in January, with a secondary maximum in December. The interpolation outcomes are in line with the general description of the regional climate characteristics given in chapter 3.3. However, monthly amounts and the temporal distribution of precipitation vary interannually. In any given year, these can differ, more or less strongly, from the outcomes presented in Fig. 42. The above described overall pattern in the spatial distribution of precipitation that results from orographic and longitudinal effects, can mostly also be observed in the maps of the monthly precipitation.
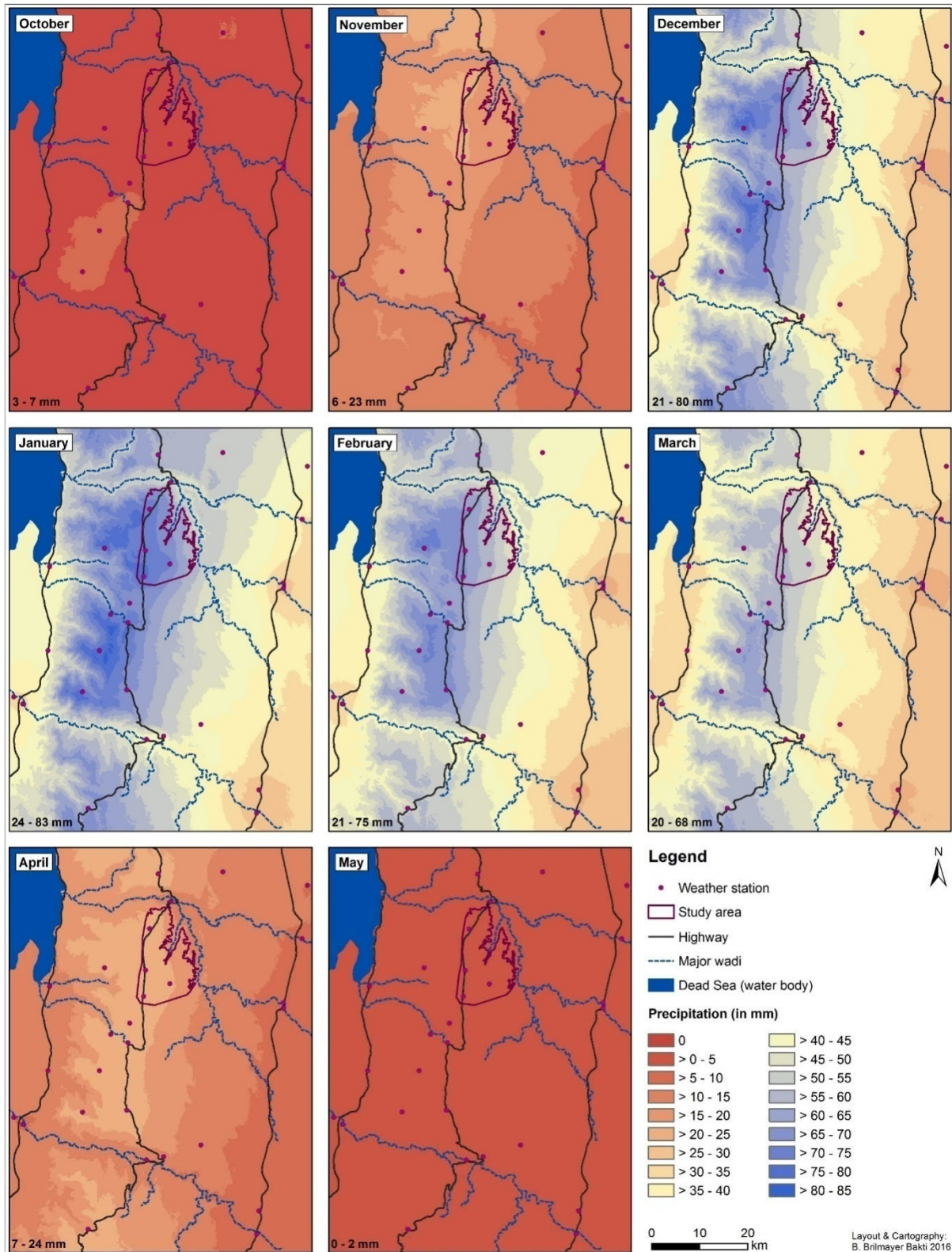
Fig. 42: Maps of the mean monthly precipitation in the study region according to the interpolation results for the period 1963-1992. For each month, the range of precipitation amounts occurring in the region is indicated in the lower left corner of the corresponding map. Negligible precipitation amounts (<0.5 mm) were identified for the summer months June to September. Therefore, no maps were included for these months. Sources: precipitation data: WAJ 2011, data processing and interpolation: B. Brilmayer Bakti & T. Törnros 2012.

6 Results

In this chapter, the analyses results and findings are presented, which are directly related to the RWH research questions that guided this study and were stated in the introduction (see chapter 1, Table 1). The first section (6.1) contains a description of the RWH inventory, i.e. the database of the mapped RWH structures in the area. Further information that could be gathered about the structures, specifically concerning e.g. their age, condition, and size, are provided as well. Outcomes of the subsequent analyses based on the RWH inventory and the additional collected datasets (see chapter 5) can be found in section 6.2. The results of the analyses of site characteristics and distances (see 4.2.1) are also presented at this point, along with statistical data that facilitate the identification of possible spatial patterns in the distribution of RWH structures (see chapter 7.3). The last section (6.3) of this chapter contains the estimates of runoff and RWH potentials. Outcomes include the computed on-site runoff and the associated general RWH potential, as well as the separately determined runoff from rooftops; thus, the RRWH potential. Runoff estimation results are described in relation and comparison to the capacities and the spatial distribution of existing RWH facilities, especially cisterns, which can serve as storage facilities for harvested rainwater and runoff.

6.1 Inventory, state and characteristics of existing rainwater harvesting structures, with particular reference to cisterns

The inventory of RWH structures mapped in the present study comprises a total of 1,477 (1,629) items which were grouped into two larger categories: cisterns and (contour) bunds, ridges, dikes, check dams, and similar structures. The latter is the largest group with 1,088 objects and encompasses all types of linear structures, mostly furrows, dikes, and shallow walls made of earth or stones which are intended to redirect, divert, spread, and retain runoff (see Fig. 43). The category of cisterns contains 389 (541) items and has been divided into three subgroups (see sections 4.1.1 and 4.1.2.2). One group is formed by the allegedly old cisterns, or "Roman Wells", as they are called by the local population, and contains 96 objects which all have been registered with GPS in field surveys (see 4.1.1). Another 293 cisterns were assigned to the subgroup of presumably modern cisterns. The objects were primarily visually identified in the satellite imagery (see 4.1.2.2). Ground truth confirmed the existence and location of a sample set of cisterns in this category; thus, corroborating the reliability of the methodological approach (also see 4.1.1 and 4.1.2.2). The third subgroup comprises 152 items which correspond to further possible cisterns. Conspicuous features discovered during the thorough visual examination of the satellite

Fig. 43: Shallow stonewalls (bunds or ridges) on the hillslopes of a branch of Wadi al-Balu, as visible in the satellite image (a) and in the landscape (b). The structures are used to direct, spread, and retain runoff and to hinder erosion. The photograph (b) was taken from a point east of the area shown in image a, with a view to the southwest. The location of the depicted structures is indicated in Fig. 45. Sources: satellite image (a): GeoEye-1 © DigitalGlobe Inc. All Rights Reserved; photograph (b): B. Brilmayer Bakti 2010.

image suggest the existence of cisterns, probably old or abandoned ones. Since in their appearance, these objects lacked the unmistakable characteristics of the other cisterns, they would each need a ground check to clarify their nature. Excluding the aforementioned questionable structures, the established RWH database thus contained 389 cisterns and 1,477 objects in total. Should all 152 suspected further possible cisterns be confirmed as such, these figures would rise to 541 cisterns and 1,629 RWH facilities in total (see numbers given in parentheses above).

Besides the hitherto described types of RWH facilities that occur numerously in many parts of the study area, a singular open reservoir, apparently designed for water storage, was found in ar-Rabba (see Fig. 44). The structure is also listed in the MEGA-Jordan database of archaeological sites and remains, and
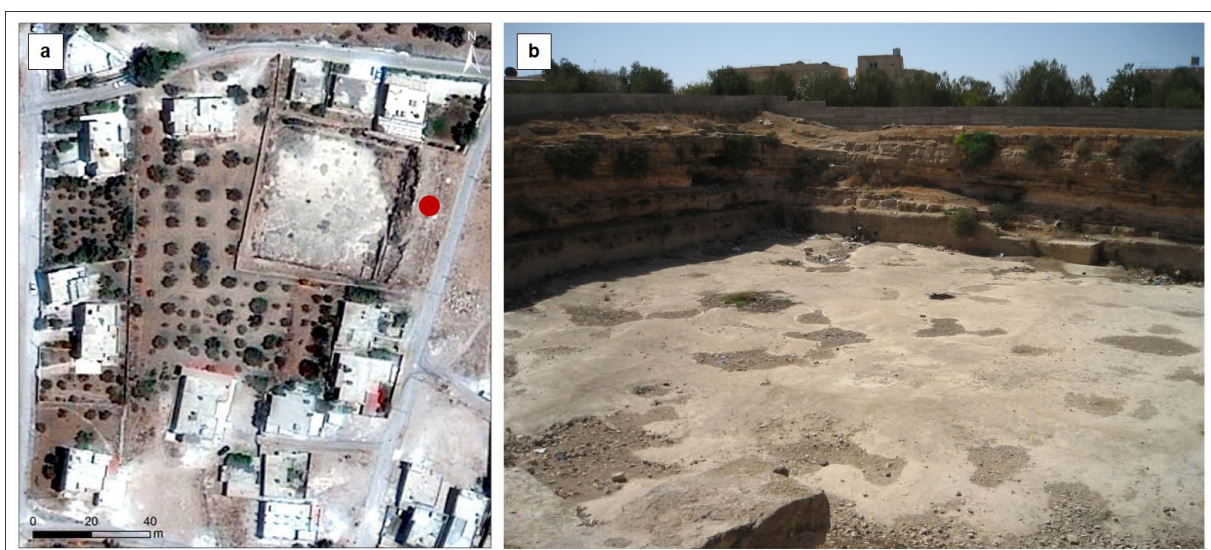
Fig. 44: The open reservoir of probably Roman age in ar-Rabba. Part a shows the reservoir as it appears in the satellite image (large rectangular object), while part b illustrates its condition and dimensions as observed during field surveys. The red dot in part a indicates the approximate point from which the photograph (b) was taken. The direction of view is towards the southwest. The location of the facility is illustrated in Fig. 45. Sources: satellite image (a): GeoEye-1 ©DigitalGlobe Inc. All Rights Reserved; photograph (b): B. Brilmayer Bakti 2010.

a Roman origin is suggested for it (THE GCI ET AL. 2010). According to the database, there should be two more, probably ancient open reservoirs, one more in ar-Rabba and one near Abu Traba (THE GCI ET AL. 2010). However, only the existence of one reservoir, located in ar-Rabba, could be confirmed through the visual examination of the satellite image and field surveys. The identified reservoir has an approximately square shape with lengths of ca. 35-40 m at each side and a depth of around 4 m and more (see Fig. 44). Hence, its capacity can roughly be estimated at 5,600 m^3 or more.

The locations of the mapped RWH facilities and their spatial distribution are illustrated in Fig. 45. Different symbols are used to signify the type and category (see above) of each RWH structure. The number of objects in each category are stated in parentheses. Cisterns that were inspected in more detail, including their interior, were assigned to a separate category and symbolized with blue points in the map.

In field surveys, information about the current conditions, functionalities, storage capacities, and construction details of cisterns, as well as evidence for their suggested ages, could also be collected. Investigations primarily concentrated on the old cisterns of the area. These were found to be in very heterogeneous conditions with some damaged or abandoned, whereas many others were still in use and often partly refurbished. Damage varied from complete or partial fillings with stones, rubbish, and other materials, purposefully or as a result of uncovered manholes (see Fig. 46 g), to impaired water holding capacities, due to insufficient sealings of cistern walls with plaster lining or roots of nearby trees growing into the cistern bodies. The latter problem particularly affected cisterns in backyards or gardens of residential houses, where olive or fruit trees had been planted in their immediate vicinity (see Fig. 46 f). Several cisterns did not show any evidence of modern use, such as repairs or alterations. In these cases, it remains unclear if the cisterns are still in use or abandoned, either permanently or temporarily. Most cisterns, however, exhibited clear signs of recent usage among which the fortification of the entry area through cementation and the attachment of a metal closing lid to cover the manhole were most common (see Fig. 46 a). In many cases old, pre-existing or new troughs for the watering of animals (sheep, goats) were incorporated in the cement work (see Fig. 46 a-b and h). This indicates the main application of cistern water nowadays, although local residents frequently stated that they were using the water for all purposes, including domestic chores, and as a source of drinking water. For a more convenient withdrawal of water, gasoline-driven water pumps were installed on some of the cisterns (Fig. 46 b-c), although this still was not very common. In some cases, the vague remains of feeding channels were discernable (Fig. 46 d-e). These shallow rills in the ground gather and lead water from a catchment area to small inlets at the manhole of a cistern. Several cisterns had small half circle ridges consisting of earth and/or stones behind them in the direction of water flow (Fig. 46 a). These structures are often used to locally slow down or impede runoff and are found in association with old and modern cisterns.

In late summer (September/October), many of the examined cisterns still contained water. This suggests that they still function as designed and store runoff collected from the surroundings. However, the possibility of active, direct filling with tap water also must be considered, as it is common practice in many

cases. Since the public water supply system provides freshwater only intermittently, normally once a week, residents usually cover their weekly demand by storing tap water, typically in plastic tanks on rooftops. Cisterns, particularly those close to residential houses, are often used as additional storage tanks to increase the weekly available amount of water. It can be assumed that this only applies to cisterns situated on private property and in the immediate vicinity of residential houses, which are connected to the public water supply system. Only a few of the mapped cisterns fulfill this requirement.
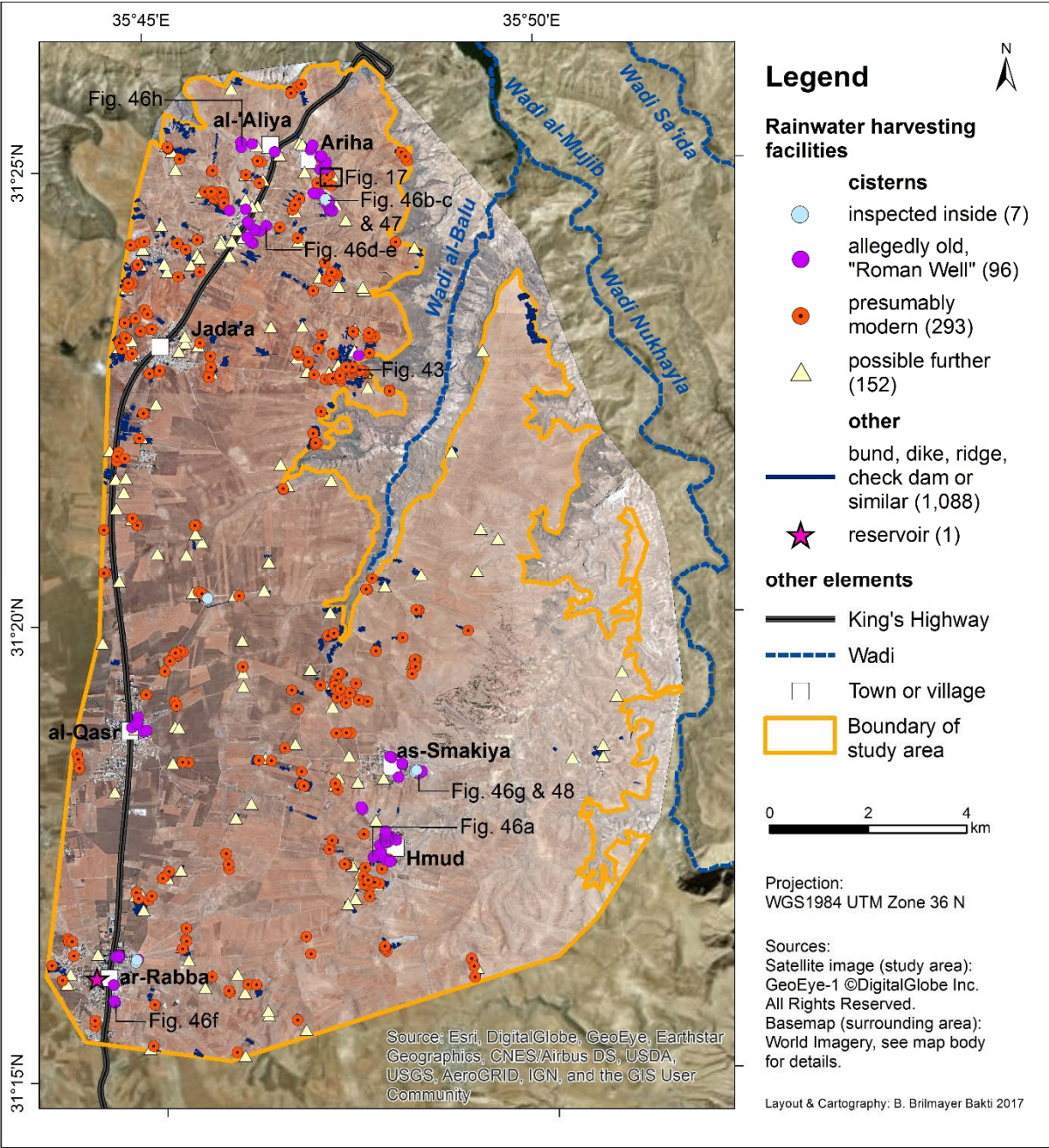
Fig. 45: Map of the existing RWH facilities in the study area. Symbols of individual features may overlap due to the map scale and the abundance of structures. In the legend, numbers given in parentheses indicate the total number of objects in the respective category. Cisterns inspected inside represent a subset of the two other groups of cisterns (old and modern ones). The locations of structures shown in other figures are indicated with the number of the respective figure in the map.

Fig. 46: Presumably old cisterns on the Karak Plateau. For locations of depicted objects see Fig. 45. a: Typical modern modification of the manhole area (cement works, metal closing lid) and half circle ridge behind a cistern. In the background, another cistern is discernible (white arrow). b: Proximity of new building and pre-existing, older cistern. While the cistern exhibits signs of current usage (e.g. water pump), it obviously has no adequate catchment area, in terms of size and type (e.g. streets). Similar circumstances were found in several towns and villages on the Karak Plateau. c: Gasoline-driven water pump installed on a cistern. d: Cemented manhole area and inlet through which water can enter the cistern. e: Weakly incised feeding channel leading water to the cistern. The white arrows in d and e indicate the course of the water along the feeding channel and towards the inlet at the manhole area of the cistern. f: Large white rock covering the opening of a cistern in an olive grove. g: Neglected, open cistern. h: Stone trough next to the manhole of a cistern. The trough is used for the watering of animals (livestock). Photographs: B. Brilmayer Bakti 2010.

Outside of modern settlement areas, where no access to the public water supply system usually exists, cisterns could directly be filled with freshwater delivered through tank wagons. Since this would be

quite expensive, the active, direct filling of cisterns with tap water is highly unlikely to be employed in rural areas and for agricultural purposes. Therefore, it can be deduced that many of the mapped cisterns still fill naturally with runoff resulting from winter rains. Apparently these cisterns are able to store the gathered runoff from the surrounding area for longer periods of time, e.g. until the end of the summer dry season or even for several years.

Examinations of the interior of seven selected cisterns revealed a variety of shapes and sizes in the underground storage rooms. All cisterns were of the rock-cut type and had one bell-shaped main room to which in some cases one to three smaller side rooms were added (see Fig. 47). Based on the different dimensions of the main room and, where applicable, the side rooms, storage capacities of 54-229 m³ were computed for each of the inspected cisterns (see Table 16). Apart from the smallest and the two largest objects with capacities of 54 m³ and around 200 m³ respectively, cisterns typically had storage volumes of around 100 m³. However, actual capacities could differ slightly since they do not only depend on the dimension of the construction, but also on the level to which the respective cistern is filled with sediments and other material. For this reason, cisterns generally have to be cleaned out regularly to ensure their full storage potential and optimal functionality. At the bottom of all main and side rooms of the inspected objects, a more or less thick layer of fine to very fine material, mostly clay, which is abundant in regional soils (see chapter 3.4), was found (see Fig. 48 b). Immediately below the manhole, usually in the middle of the main room, cisterns commonly had a pile of bigger stones and other objects. While these larger items must have fallen or have been thrown into the cisterns, sediment material usually enters the cisterns with the water inflow. Therefore, the annual influx and amount of these finer
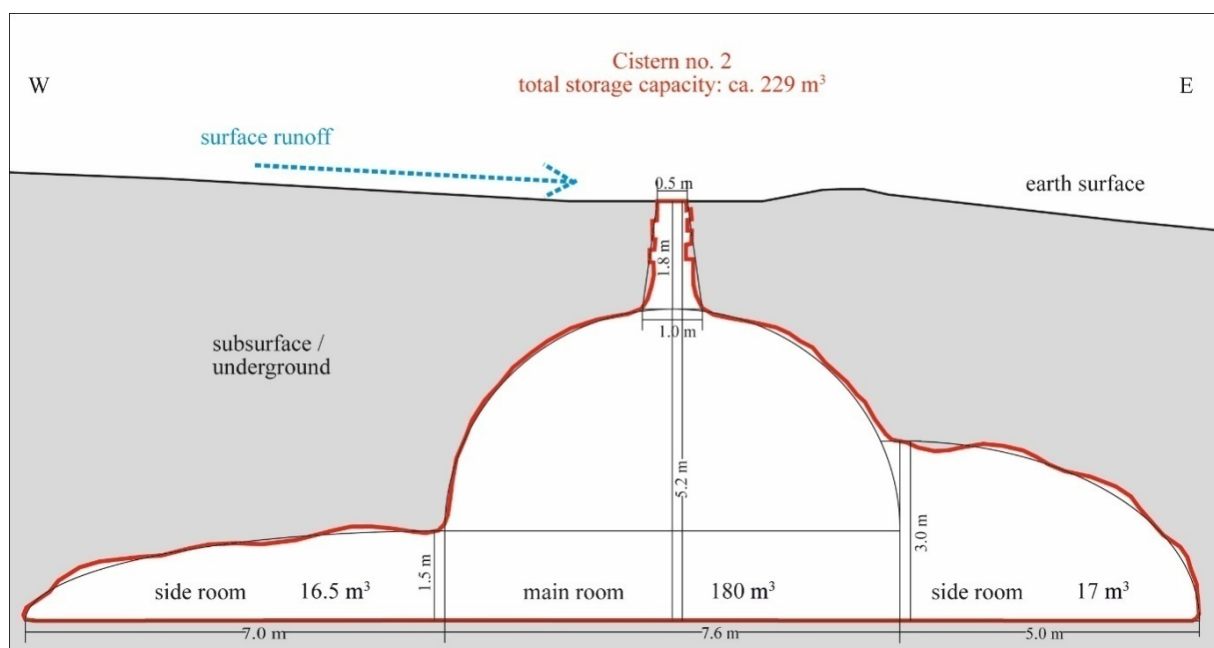
Fig. 47: Schematic cross-section of an old cistern in Abu Traba (location see Fig. 45). The cistern has one large main room and three side rooms (one not illustrated here). The red outline indicates the approximate real shape of the cistern. The fine black lines show the geometrical shapes that were used as approximations in the calculation of the storage capacity. Slope and underground conditions can vary largely between individual cistern sites.

Table 16: Storage volumes of cisterns in the study area. Depending on the category, different capacities are assumed. For the presumably modern cisterns, the typical size reported by A. Hamaideh (personal communication, May 21, 2014), ALI ET AL. (2009), and ASSAYED ET AL. (2013) was assumed as average storage capacity. The age of cistern no. 241 remains unclear. This item has tentatively been assigned to the category of modern cisterns, since its inspection did not yield sufficient evidence for a much older construction age, but rather revealed some differences to the other inspected, apparently older cisterns. However, in terms of capacity, cistern no. 241 matches the other examined cisterns, which were classified as old.

	Category		
	"Roman Wells" (old cisterns)	Modern cisterns [a]	Possible further cisterns
No. of items	96	293[a]	152
Approximate storage capacity	No. 55: 106 m^3 No. 54: 88 m^3 No. 2: 229 m^3 No. 8: 112 m^3 No. 15: 54 m^3 No. 16: 189 m^3	(No. 241[a]: 106 m^3)	?
	Mean: 130 m^3	assumed standard: 30 m^3	

[a] *These objects usually exhibited apparently modern cement works around manholes, suggesting a relatively recent construction. Nine cisterns (among them no. 241) did not show these characteristics and thus could be older than the other objects in this category.*

materials, which are deposited on the cistern grounds, strongly depend on the properties of the catchment area and the collected runoff. Upstream settling tanks reduce the sediment load of the water before it enters the cistern. These systems were not observed in any of the allegedly old cisterns, but they were integrated in the cement works around the manholes of some modern cisterns. The various amounts of sediments accumulated in the inspected cisterns indicate that they have not been cleaned out for some time, probably years, which suggests no or limited maintenance. Besides the deposited layers of (fine) sediments, larger objects (stones, rubbish, etc.) falling or being thrown into the cisterns are particularly problematic, since they can considerably decrease the capacity available for water storage.

By upscaling the findings from the inside inspections and combining them with the total number of cisterns detected, the overall storage capacity installed in the study area could be estimated. Assuming an average volume of ca. 130 m^3 for all 389 cisterns that were conclusively identified, the total capacity would amount to 50,570 m^3. It could even rise up to 70,330 m^3, if the 152 suspected additional cisterns were confirmed and had a similar capacity. More conservative estimations, assuming volumes of 130 m^3 only for the 96 "Roman Wells", and about 30 m^3 for the other 293 presumably modern cisterns, would yield a total capacity of only 21,270 m^3. The significantly smaller storage volume of 30 m^3 in modern cisterns was suggested by A. Hamaideh (personal communication, May 21, 2014) based on her involvement in cistern building projects with the MoA in Jordan. The same size was also reported by ALI ET AL. (2009) and ASSAYED ET AL. (2013). In the present study, unfortunately only a limited number of cisterns could be inspected in detail from the inside. Due to the large variety of dimensions found in the examined objects, a relatively high level of uncertainty must be accepted in the estimates of the overall capacity. The likely range is defined by the minimum and maximum figures stated above.

Six of the seven inspected cisterns exhibited signs suggesting an ancient age. Another cistern (no. 241), located northeast of al-Qasr (see Fig. 45), showed no noticeable evidence of a construction during ancient times. On the contrary, the cistern site differs from those of the other old cisterns, since it is situated on a small local basalt hill (see 6.2.1). This points to a probably younger age of the object, since the construction of cisterns in harder rock, such as some basalts, has become more feasible only relatively recently, with the availability of modern excavation machinery. Inside the other examined, probably ancient cisterns, several layers of plaster lining were often observed on the walls (see Fig. 48 a-c). This indicates repeated phases of repair, which are typically associated with a continuous or intermittent use of the cisterns over a longer time. An intact plaster lining is usually required to seal the cistern walls and prevent losses of the stored harvested water. Hence, it is crucial for the optimal functioning of the cistern. The colors of the different observed plaster linings ranged from white, to all hues of grey, beige, brown, and reddish. The plaster layers often exhibited patterns, especially dot and fishbone (see Fig. 48 c), which previously had also been documented in the cisterns of ancient Gadara (Umm Qais) in northern Jordan (see KEILHOLZ 2007). Some of the cisterns examined in detail, as well as several other presumably old ones, featured typical collar stones around the manholes. In most cases, the collar stones consisted of either one or two, apparently hand-hewn pieces of limestone or basalt with a round hole in the middle or a half circle shape on the inner side, respectively (see Fig. 48 d). Similar collar stones were
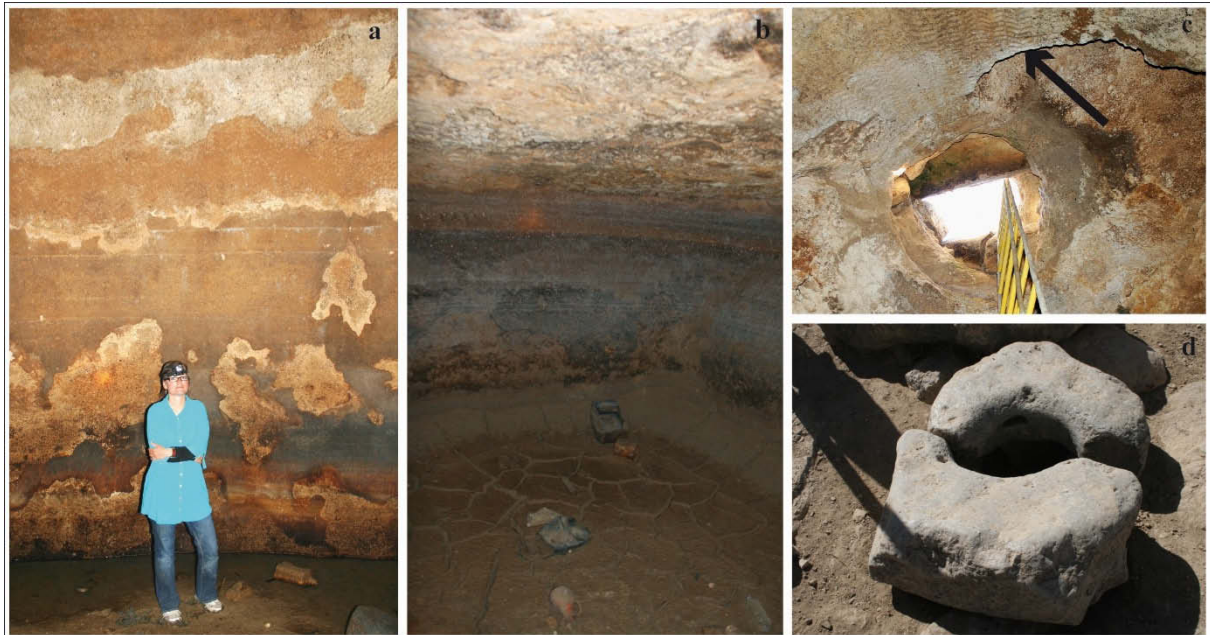
Fig. 48: Construction details of two allegedly ancient cisterns in Smakiya (see Fig. 45 for location). The illustrated details and conditions were found in several of the cisterns that were referred to as "Roman Wells" by local residents. Therefore, they can be perceived as characteristic of the old, probably ancient cisterns in the area. a: Large main room of cistern no. 16 with different layers of plaster lining on the wall (person for scale). b: Narrow side room of cistern no. 15 with cracked, dry, thick layer of fine material, probably mainly clay, on the ground. c: Manhole of cistern no. 16 and ceiling of the main room, both as seen from the inside. The plaster lining – where preserved – exhibits a distinctive fishbone pattern (see part indicated by the black arrow). d: Characteristic collar stone consisting of two half circle parts (found at the site of cistern no. 16). Collar stones typically fortify a cistern's entry area (manhole) on the earth's surface. All photographs B. Brilmayer Bakti & A. Vögele 2011.

discovered at Roman cisterns in northern Jordan (see KEILHOLZ 2014). Where the manhole areas of cisterns in the study area were modified through cementation or otherwise in modern times, the old collar stones typically were removed. Still, they could often be found in the immediate vicinity of the cistern. Altogether, the different pieces of evidence seem to corroborate the suggested ancient age of many of the "Roman Wells". However, with regard to all mapped cisterns, the prevalence of the individual characteristic traits, which were described exemplarily above, could not reliably be determined in view of the limited number of cisterns that were inspected in detail.

6.2 Rainwater harvesting sites: characteristics, spatial distribution, and distances to other elements of the natural and cultural landscape

In this chapter, the environmental conditions identified for the sites of the mapped RWH facilities are initially outlined. The information was retrieved from the datasets described in chapter 5. Subsequently, outcomes from the distance analyses are presented. This includes the determined proximities between individual RWH sites, as well as the distances between RWH structures and other elements of the natural and cultural landscape, such as vegetation areas, drainage lines or wadis, settlements, and archaeological sites. All outcomes are summarized by category of RWH sites and described and compared accordingly. Quantitative attributes are presented with essential statistical measures; such as the minimum and maximum (i.e. the range), the arithmetic mean and the standard deviation. Where necessary, particularities of the frequency distribution are additionally pointed out. From the findings outlined in this chapter, possible spatial relationships and patterns are deduced and discussed in chapter 7.3.

6.2.1 Site characteristics

Table 17 displays the environmental characteristics of the RWH sites in the study area. The collected data include information on the relief (height above sea level, slope), the geological underground, the typical annual precipitation (long-term mean), and the main surface watersheds, as well as the individual smaller catchments (see results of the hydrological analyses on different scales, chapter 4.1.4) within which the RWH structures are located. Findings for individual sites are summarized by categories of RWH facilities. The distribution of RWH sites in relation to the environmental parameters listed in Table 17 is illustrated in the maps in Fig. 49-53.

Table 17: Characteristics of RWH sites. The collected data of individual locations were accumulated according to the three defined categories of RWH structures. Quantitative attributes (marked with a yellow square) are presented with essential descriptive statistical measures to facilitate the evaluation and comparison of findings.

	Category of RWH structures		
	Allegedly old cisterns, "Roman Wells" (96)	Presumably modern cisterns (293)	Bunds, dikes, ridges, check dams, etc. (1,088) [a]
■ **Height above sea level**			
min. -max.	822 - 958 m	800 - 975 m	765 - 1,008 m
mean	884 m	876 m	871 m
standard deviation	36 m	38 m	44 m
■ **Slope**			
min.-max.	2 - 30%	1 - 18%	0 - 25%
mean	10%	7%	8%
standard deviation	5%	4%	4%
■ **Geological unit (share in study area** [b]**)**			
Soil (76%)	73 (76%)	190 (65%)	763 (70%)
Calcrete (3%)	4 (4%)	33 (11%)	110 (10%)
Basalt (all) (6%)	0	41 (14%)	132 (12%)
Judaiyida (1%)	0	21 (7%)	77 (7%)
Sanina (3%)	0	11 (4%)	41 (4%)
Balu'a (<1%)	0	9 (3%)	14 (1%)
Al-Hisa Phosphorite (7%)	19 (20%)	29 (10%)	75 (7%)
Qatrana Phosphorite (4%)	0	0	8 (1%)
■ **Mean annual precipitation (in mm)**			
min.-max.	273 - 321 mm	260 - 318 mm	234 - 320 mm
mean	294 mm	292 mm	291 mm
standard deviation	13 mm	14 mm	16 mm
■ **Major surface drainage basin (share in study area** [b]**)**			
Mujib basin (total) (97%)	96 (100%)	288 (98%)	1074 (99%)
Lower Wadi Mujib (9%)	9 (9%)	61 (21%)	382 (35%)
Wadi Nukhayla (total) (88%)	87(91%)	227 (77%)	692 (64%)
Lower Wadi Nukhayla (4%)	24 (25%)	14 (5%)	58 (6%)
Wadi Balu (48%)	28 (29%)	171 (58%)	468 (43%)
Middle Wadi Nukhayla (2%)	0	0	24 (2%)
Wadi Ghuwayta (30%)	35 (37%)	39 (13%)	121 (11%)
Upper Wadi Nukhayla (3%)	0	0	7 (1%)
Wadi ad-Dabba (1%)	0	3 (1%)	14 (1%)
Dead Sea basin (total) (3%)	0	5 (2%)	14 (1%)
Wadi Ibn Hammad (3%)	0	5 (2%)	14 (1%)
■ **Catchment information** [c]			
Total no. of catchments affected	38	135	357 (288) [d]
Total area of catchments affected	8.138 km^2	36.840 km^2	51.994 km^2 (37.260 km^2) [d]
Sizes of catchments affected			
min. - max.	0.012 - 2.828 km^2	0.009 - 7.942 km^2	0.002 - 2.828 km^2
mean	0.214 km^2	0.198 km^2	0.116 km^2 (0.129 km^2) [d]
standard deviation	0.469 km^2	0.303 km^2	0.221 km^2 (0.239 km^2) [d]
Features per catchment			
min. - max.	1 - 12	1 - 14	1 - 27 (1 - 23) [d]
mean	2.5	2.0	3.6 (3.3) [d]
standard deviation	2.2	1.9	3.3 (2.9) [d]

[a] information in this column refers to center points of linear features, except for catchment information (also see [d]).

[b] study area here refers to the actual study area on the plateau (see 3.1, Fig. 2).

[c] only catchments of drainage lines within the study area and features located in these catchments were considered. This led to a reduced number of objects in the categories of presumable modern cisterns (264 items) and bunds, dikes, ridges, check dams, and the like (969 items). Only catchments without signs of truncation (by the boundary of the study area) were included.

[d] figures in parentheses refer to center points of each feature and are given when differing from those of linear features. Differences can arise e.g. from double counts of linear features that extend over more than one catchment.

■ quantitative attributes: value(s) comprised by features in the respective category of RWH structures (column).

■ qualitative attributes: absolute number and corresponding percentage (in parentheses) of features in the respective category (column).

With regard to altitudes, the group of allegedly old cisterns exhibits the smallest range and the highest mean value (see Table 17). The presumably modern cisterns are distributed over a broader range of altitudes, while the mean elevation is slightly lower for this category. This tendency towards amplification of the elevation range is most pronounced for the group of bunds, dikes, ridges, and similar structures. At the same time, the average altitude in this category is the lowest of the three groups of RWH sites (see Table 17). As the map in Fig. 49 illustrates, the described differences in altitudes are linked with the spatial distribution of the sites of the different categories. Modern cisterns and bunds, dikes, ridges, and the like, are not only more abundant than the old cisterns, but they also tend to be more scattered over the study area. In contrast to the old cisterns, they are also found in areas of higher altitudes around mount Shihan (see 3.1, Fig. 2 for location), at the fringes of the tableland, and further east in the study area (see Fig. 49). The allegedly old cisterns, in turn, are located in steeper sloping terrain, on average, and exploit a broader range of slope conditions, in comparison to the other two categories of RWH sites (see Table 17). Bunds, dikes, ridges, and similar structures, as well as modern cisterns in particular, appear to be restricted, on average, to land in a narrower range of gradients and to relatively flat or very gently sloping terrain, (see Table 17 and Fig. 49). This finding seems rather surprising in view of the abundance of sites in the two named categories and their widespread distribution over the study area.

The link between RWH sites and specific geological underground conditions is to some degree influenced by the coverage of the different geological units in the study area (see Table 17 and Fig. 50). The distribution of bunds, dikes, ridges, and the like, to the units identified in the geological map, approximately matches the share of each unit in the total area of the examined land (see Table 17). Hence, the proportional distribution of sites roughly reflects the relative extents of the geological units. Bunds, dikes, ridges, and similar structures are largely independent from geological conditions, since they are built on the earth's surface and do not interact with the underground situation. However, geological circumstances can influence the availability of suitable building materials, e.g. stones, and thus, to a minor degree, affect the selection of sites. In contrast, cisterns fundamentally depend on the presence of adequate underground conditions. Sediment strata and other rocks with a good natural water holding capability and a relative softness to facilitate the excavation of the cistern body, are typically considered optimal. The majority of both, old and newer, modern cisterns, are situated in areas labeled as "soil (over bedrock)" in the geological map (see Table 17 and Fig. 50). The land assigned to this category is usually covered by a significant, thick soil cover and constitutes more than 70% of the study area. Depending on the local conditions and the depths of individual objects, cisterns can extend into deeper, subjacent units. Beneath the soil cover, calcrete, various types of basalts, and sediments of the Al Hisa Phosphorite unit can be expected (see chapter 3.2.). According to the findings, none of the "Roman Wells" are located directly in basalt areas, as opposed to the modern cisterns. For the latter, basalts represent the second most common type of underground (see Table 17). The other two geological units that were identified at cistern sites are calcrete (or caliche) and the Al Hisa Phosporite formation. While only 4%

of the old cisterns were built in calcrete areas, every fifth site in this group is situated in areas covered by the Al Hisa Phosphorite formation. The latter normally occurred at the sites of old cisterns in the southeastern part of the study area (see Fig. 50). The modern cisterns showed a nearly equal distribution to regions of the Al Hisa Phosphorite and the calcrete unit, although slightly more cisterns were located in calcrete areas (11% of the objects, compared to 10% in areas of the Al Hisa Phosphorite, see Table 17).
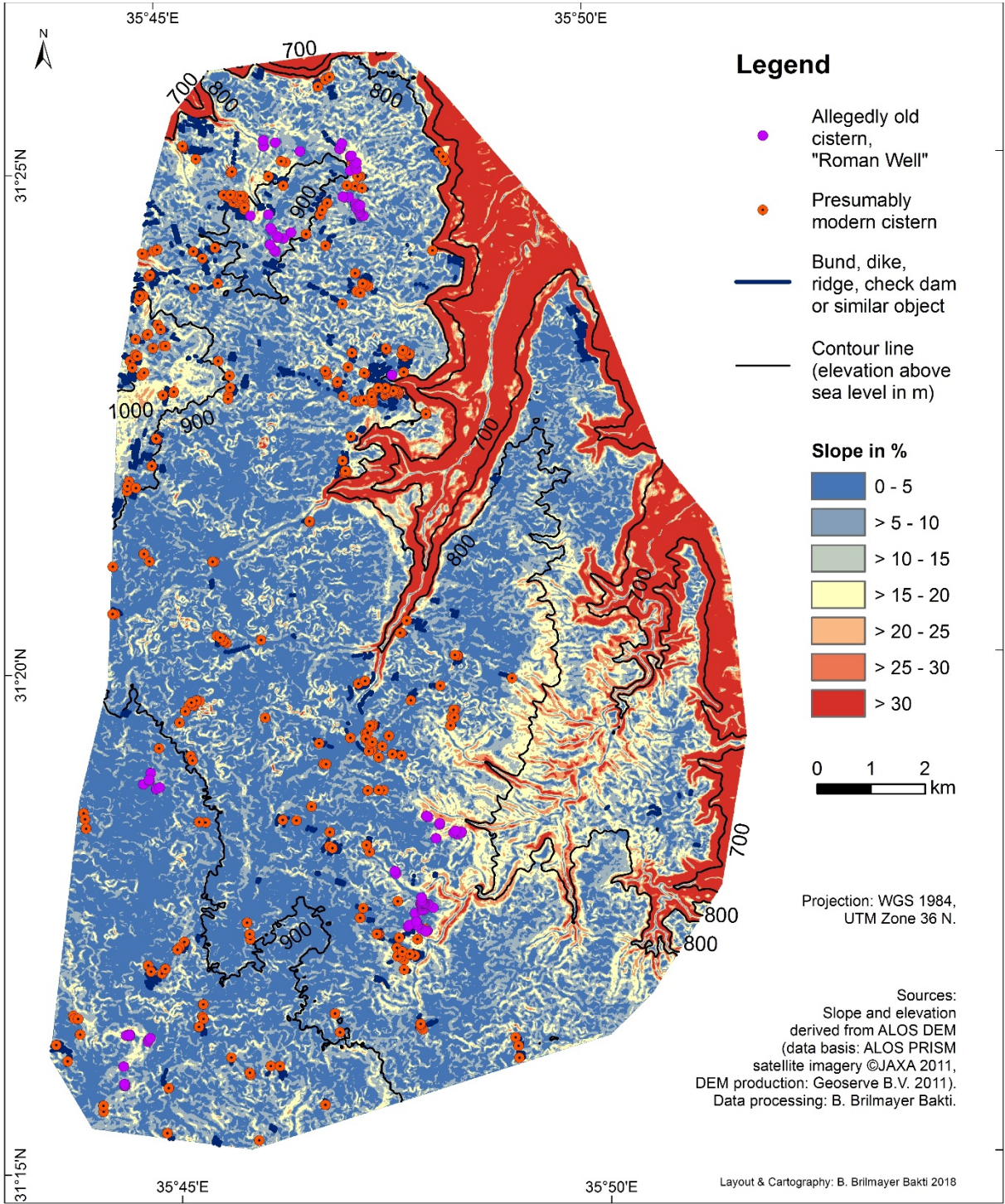
Fig. 49: RWH sites of different categories and their distribution in relation to altitudes and gradients (slope) in the study area.
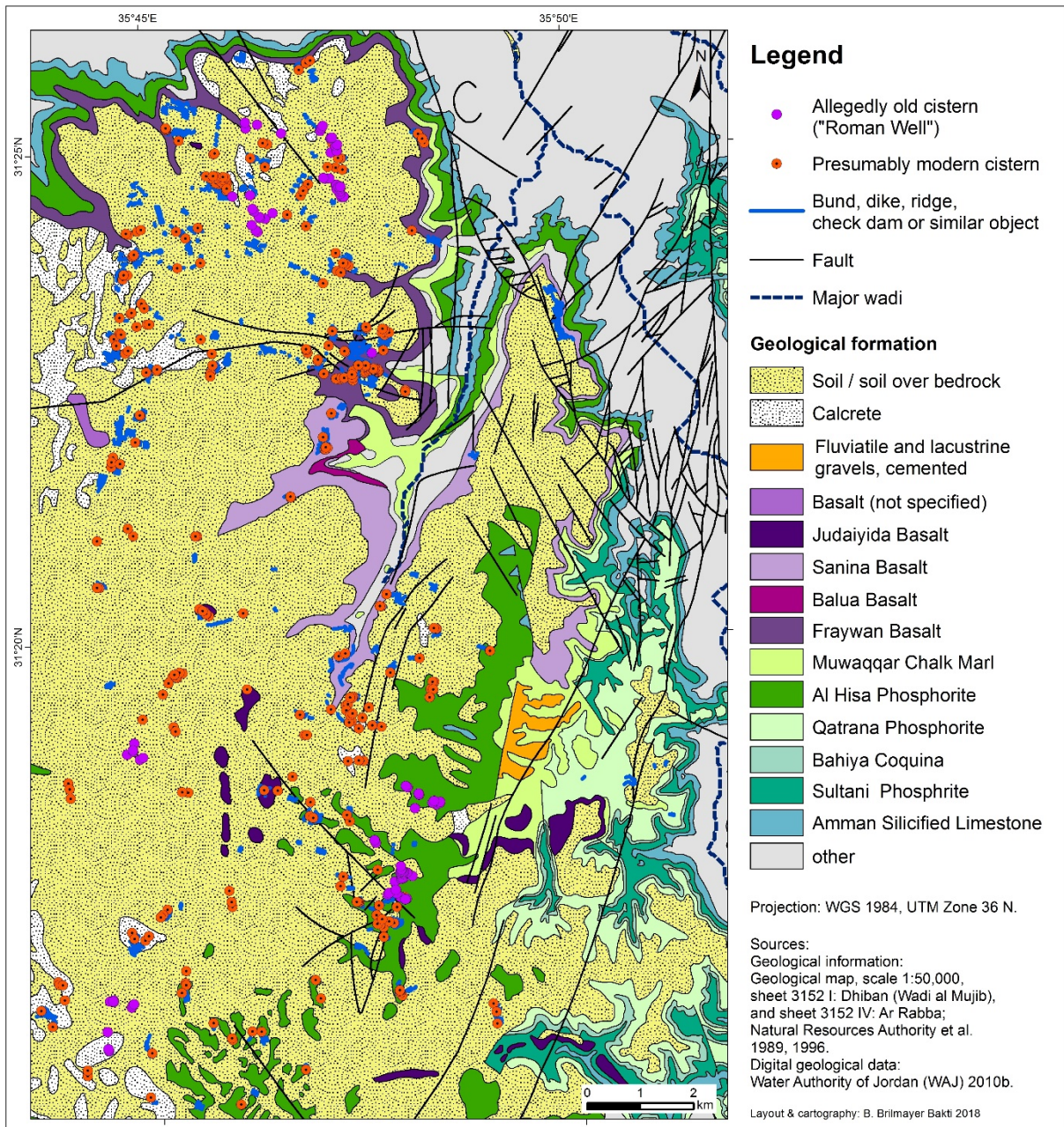
Fig. 50: RWH sites of different types and their distribution in relation to the geological situation. The units were defined according to the available geological data (see sections 4.1.5 and 5.5). Here, only the relevant geological information, i.e. the units occurring in the study area on the plateau and their respective areal extents, are shown. A more comprehensive geological map and further information in this regard can be found in chapter 3.2.

The distribution of RWH sites in relation to annual precipitation is visualized in Fig. 51. As the figures in Table 17 indicate, the three groups of RWH structures exhibit slight differences in terms of annual precipitation at their sites. In comparison to the old cisterns, modern cisterns, and in particular bunds, ridges, check dams, and similar structures, are distributed over areas within a broader range of mean annual precipitation amounts. This especially includes drier areas. Therefore, the mean values of annual precipitation were lower in these two categories than that of the old cisterns (see Table 17). These findings largely parallel the observations concerning altitudes, which were outlined earlier in this section.

As before, the broad variety of annual precipitation amounts can be related to the abundance and extensive distribution of modern cisterns and bunds, dikes, ridges, and the like (see Fig. 51). Sites in the eastern half are primarily associated with lower annual precipitation figures. In contrast, the old cisterns are limited to a few areas which are characterized by slightly higher annual precipitation amounts (see Table 17 and Fig. 51).

The widespread, scattered distribution of modern cisterns and bunds, ridges, dikes, and the like, also affects the number of corresponding sites identified in each of the main watersheds in the area (see Table 17 and Fig. 52). While the old cisterns are all located in only four out of the eight defined main watersheds, modern cisterns are found in six, and bunds, check dams, ridges, and similar structures in all of the watersheds. This includes the watersheds of Wadi Ibn Hammad and Wadi ad-Dabba which comprise smaller parts of the studied terrain in the southwest and the southeast. These watersheds only feature modern cisterns and bunds, ridges, check dams, and similar structures, but none of the old cisterns. In the watersheds of the middle and the upper part of Wadi Nukhayla, bunds, ridges, and the like represent the only RWH structures. The old cisterns, on the one hand, and the modern cisterns and bunds, check dams, and similar structures, on the other, exhibit complementary tendencies with regard to the proportional distribution of sites to individual watersheds. For example, less than 10% of the old cisterns are located in the watershed of the Lower Wadi Mujib and 25% in that of the Lower Wadi Nukhayla (see Table 17 and Fig. 52). In contrast, only 5% of the modern cisterns and 6% of the bunds, ridges, and similar structures are situated in the watershed of the Lower Wadi Nukhayla, whereas over 20% and 35% of the sites in the named two categories were found in the watershed of the Lower Wadi Mujib. Similar site distribution patterns were observed in regard to the two largest watersheds in the study area, that of Wadi Ghuwayta and Wadi Balu'a. Considerably more old cisterns are located in the watershed of Wadi Ghuwayta than in that of Wadi Balu'a (37% versus 29%). On the contrary, notably more modern cisterns and bunds, ridges, check dams, and the like were sited in the watershed of Wadi Balu'a (58% and 43% of the objects, respectively), while only around 10% of the objects of two named categories were situated in the watershed of Wadi Ghuwayta (see Table 17 and Fig. 52).

The three classes of RWH structures also show considerable differences in regard to the distribution of their sites to individual catchments (see Fig. 53), as computed in the detailed hydrological analysis based on the manually digitized drainage network (see chapters 4.1.4 and 5.4). The old cisterns are sited in a limited number of catchments and thus, the corresponding total area of all catchments affected is relatively small (see Table 17). In contrast, RWH sites of the other two categories are distributed over a larger variety of different catchments. This can partly be explained by the widespread occurrence and high number of objects in these classes. Compared to the results for the group of modern cisterns, for the category of bunds, dikes, ridges and the like, the number of catchments and their total area seem rather small in proportion to the quantity of sites. This tendency is especially noticeable in the results
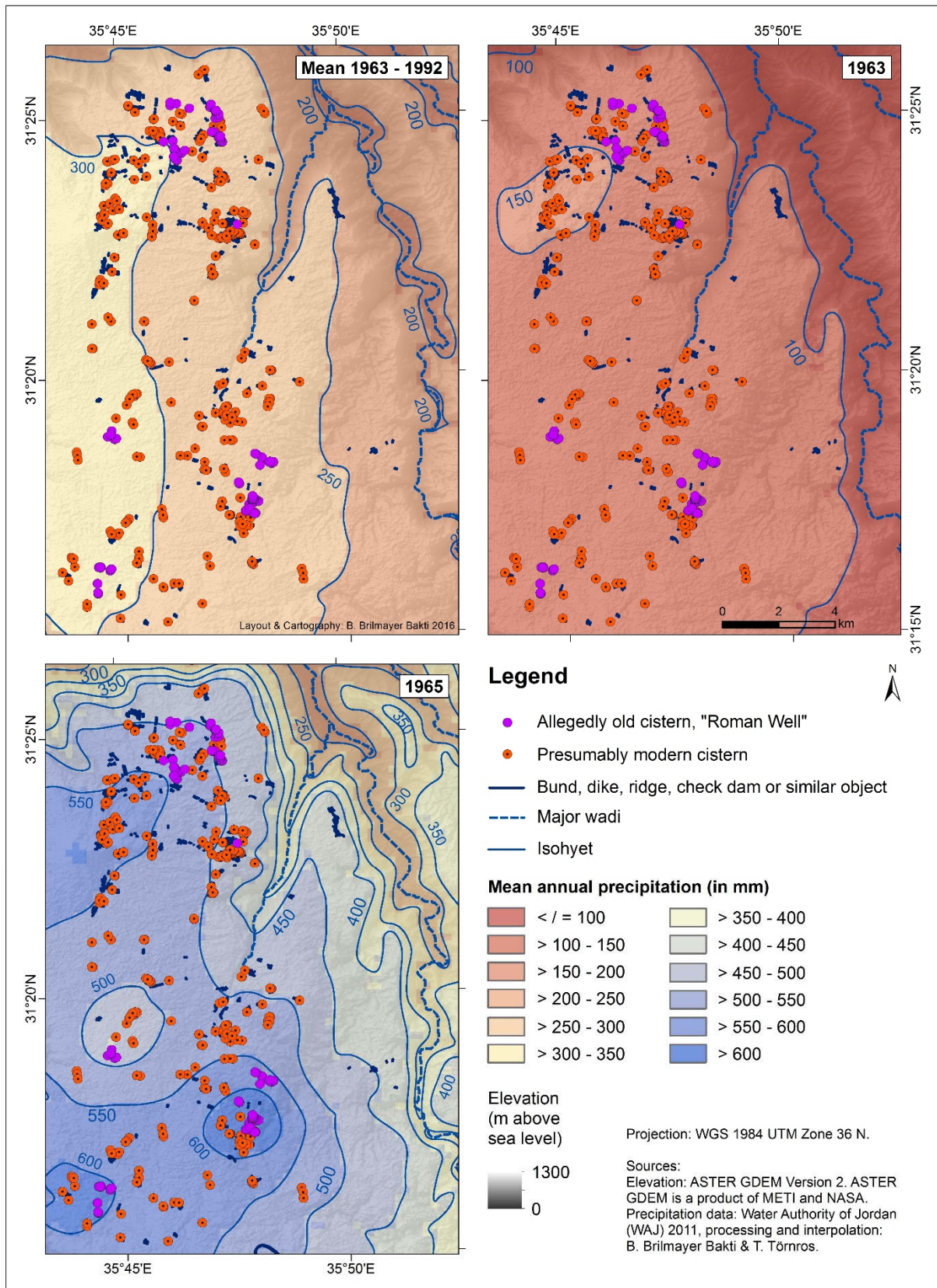
Fig. 51: RWH sites of different categories and their distribution in relation to annual precipitation. The maps illustrate the distribution and amounts of annual precipitation under three different conditions: long-term mean (1963-1992, upper left), dry year (1963, upper right), and wet year (1965, lower left).
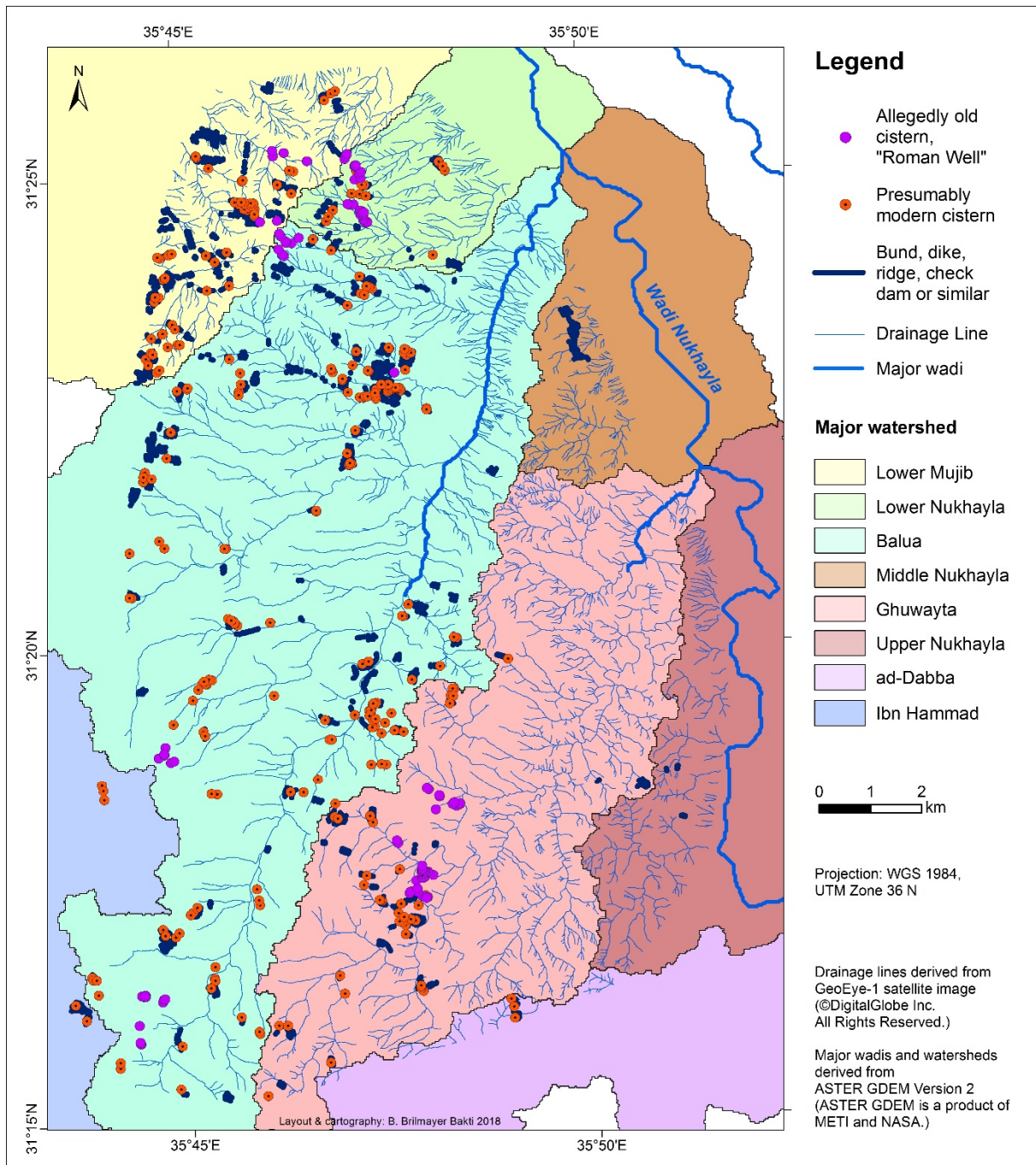
Fig. 52: RWH sites of different categories and their distribution in relation to drainage lines and watersheds of major wadis. The drainage lines (thin blue lines) were digitized manually based on the visual interpretation of the satellite image (see chapters 4.1.2.2, 4.1.4 and 5.4). The major wadis and their watersheds were computed in the broader, regional hydrological analysis (see 4.1.4 and 5.4). The number of RWH sites in each of the depicted watersheds is given in Table 17.

excluding double counts (see figures in parentheses in Table 17). The latter resulted from bunds, ridges, check dams, and other linear RWH structures extending over two catchments. To avoid this effect, objects were assigned to exactly one catchment based on their center point. The reduced number and total area of catchments in proportion to the quantitative size of the group of bunds, ridges, dikes, and the like suggests a higher number of objects per catchment, on average, and probably smaller catchment sizes. Both assumptions are confirmed by the collected statistical information about catchment sizes and

sites per catchment (see Table 17). In general, the identified ranges of catchment sizes are very broad and similar for all types of RWH facilities (see respective minimum and maximum values in Table 17). For all three categories, most of the catchments which accommodate RWH sites are relatively small, while large catchments with extents at the upper end of the identified ranges rather represent exceptions. Hence, frequency distributions of catchment sizes are skewed to the right and about 75-79% of the concerned catchments are smaller than the calculated average (see mean values in Table 17). Although the described tendency is similar for all three groups, the average catchment size varies with the category of RWH structures. While the difference between the two groups of cisterns, the old and the modern ones, is rather small in this regard, the computed mean catchment size is significantly lower for the class of bunds, ridges, check dams, and the like.

The two groups of cisterns also show substantial similarities in the findings concerning the number of objects per catchment (see Table 17). In contrast, the outcomes for the category of bunds, dikes, ridges, and the like differ noticeably, as they are characterized by a wider range, which results from a higher maximum, and an increased average number of objects per catchment. Naturally, these figures are slightly smaller when double counts of structures extending over two catchments (see explanation in previous paragraph) are eliminated (see figures in parentheses in Table 17). Nevertheless, the higher mean value suggests that several bunds, ridges, check dams, and the like are typically sited together in the same catchment. As the maximum value indicates, the number of structures in some catchments is very high. In contrast, 45% of the catchments in which an old cistern is found contain only a single object of this category. Another 39% of the catchments feature 2-4 old cisterns. In the category of modern cisterns, this tendency towards lower quantities of objects per catchment is even more pronounced. In 61% of the catchments concerned, only one modern cistern was detected and 32% of the catchments accommodated 2-4 modern cisterns. On the contrary, in the category of bunds, dikes, ridges, and the like, about 30% of the catchments feature only a single structure of this type and in ca. 45% of the catchments, 2-4 objects of this category are found. In combination with the findings regarding catchment sizes, the described results indicate a local concentration of bunds, dikes, ridges and similar structures in various areas. Being sited together in mostly rather small catchments, several objects of this type likely form groups of different sizes. The suggested clustering tendency is examined further in section 6.2.2, where the results of the distance analyses are presented.

The spatial distribution of RWH structures to catchments is visualized in Fig. 53. The corresponding drainage network, which formed the basis for the computation of the catchments, is illustrated in Fig. 52. The density of drainage lines obviously varies across the study area. Therefore, some of the hitherto described differences between the three classes of RWH structures could be a direct result of the different spatial distribution of sites in each category. For example, the lower mean catchment size identified for the category of bunds, ridges, dikes, and the like could be related to the fact that many of the sites in
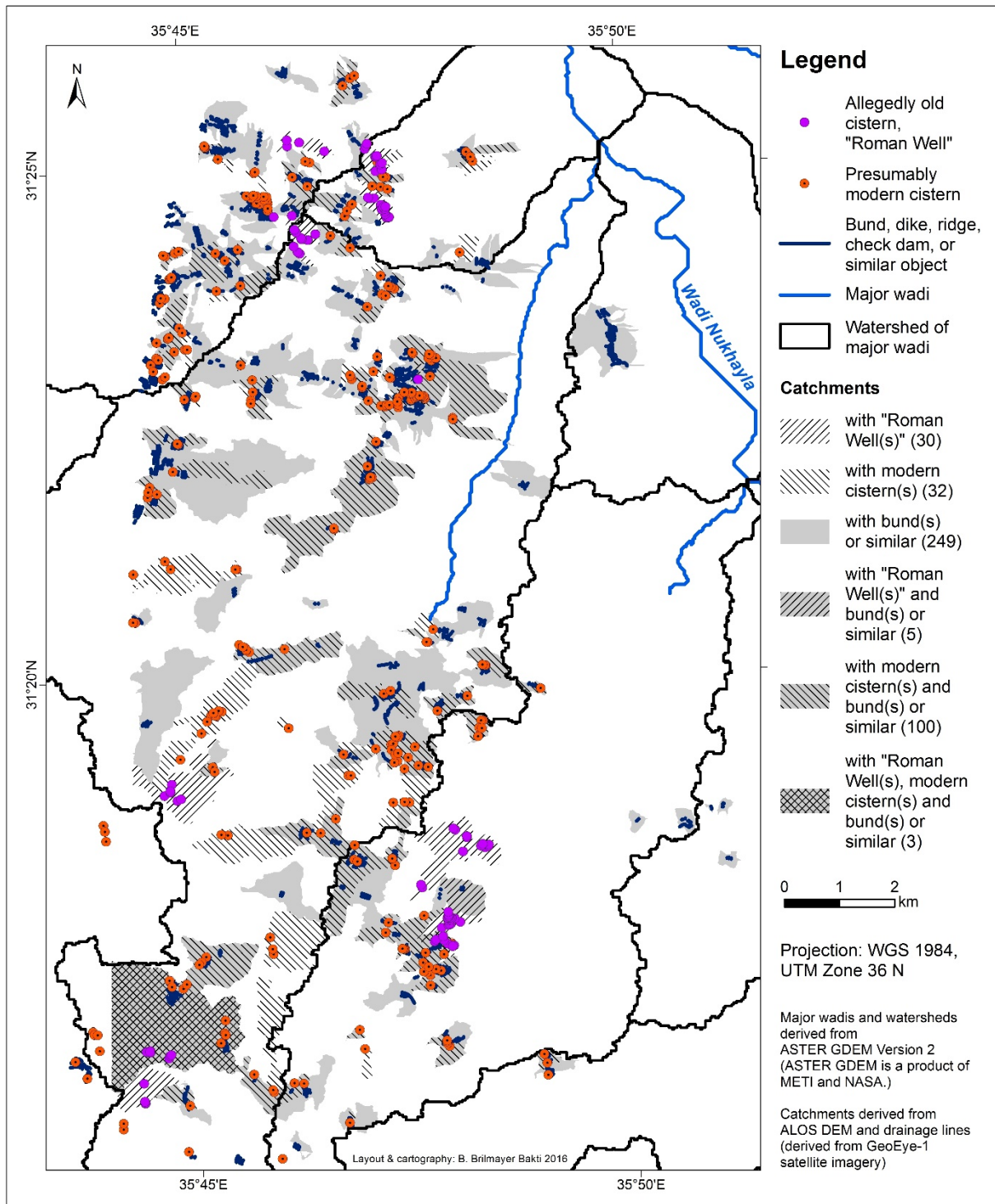
Fig. 53: RWH sites of different categories and their distribution to individual catchments. The catchments were computed based on the manually digitized drainage network, which is depicted in Fig. 52. According to the type(s) and – where applicable – combinations of RWH structures they contain, catchments were classified into different categories. The number of catchments in each category is stated in parentheses after the class description in the legend. In no catchment, objects of both cistern groups, old ("Roman Wells") and modern ones, were found. Where bunds, dikes, ridges and the like extended over two catchments, both catchments were considered as containing a structure of the named category. The catchment data resulted from the detailed hydrological analysis based on the ALOS DEM and the manually digitized drainage lines (details see chapters 4.1.4 and 5.4).

this category are found in the more dissected northern and eastern parts of the study area and around the fringes of the plateau (see Fig. 52 and 53). In these areas, the network of drainage lines is denser and

catchments are typically smaller. Figure 53 illustrates the overlap between the different categories of RWH facilities in regard to the affected catchments. Most of the catchments (311 out of 419) accommodate only one type of RWH structures. In particular, more than 70% of the catchments which contain either an old cistern or a bund, dike, ridge or similar object, do not feature a RWH structure of any other category. In contrast, only in 24% of the catchments with one or more modern cistern no other RWH structure of a different category is found. Most of the catchments (74%) that contain a modern cistern also accommodate one or more bunds, dikes, ridges, or similar structures (see Fig. 53). Other combinations of different types of RWH facilities are found only in a few catchments.

The hitherto described findings revealed several differences between the three categories of RWH facilities in regard to site characteristics. These differences were observed in the collected data on altitudes, mean annual precipitation amounts, geology, major watersheds, and catchments. In contrast to the fewer locations with old cisterns, a broader variety of local environmental conditions were usually associated with the numerous sites of modern cisterns and linear RWH structures, such as bunds, dikes, ridges, check dams, and the like. Only the results concerning slope values showed a contrary tendency indicating that modern cisterns and bunds, dikes, ridges, and similar structures tend to be restricted to areas of flatter terrain. With regard to catchments containing RWH structures, differences between the two groups of cisterns, old and modern ones, were rather small, compared to the larger ones that existed between cisterns and bunds, dikes, ridges, and the like. Overall, in regard to the findings for the three categories of RWH structures, many of the observed differences in site characteristics seem to be linked to discrepancies in the quantity of objects, and the spatial distribution pattern.

6.2.2 Distances and spatial relationships

In this chapter, the outcomes of the proximity analyses (see 4.2.1) are presented. Firstly, findings concerning the distances between individual RWH structures are described. The second section then focuses on the distances and potential spatial relations between RWH sites and other, natural or man-made elements of the landscape, such as vegetation, drainage lines, settlements, and archaeological sites. The spatial distribution of RWH structures, archaeological sites, vegetation, and settlements is illustrated in Fig. 54. The synoptical visualization of the named data in the map provides a first impression of possible spatial patterns and correlations. The statistical figures and information given in Table 18-20 complement the map and enable a more detailed, quantitative assessment of typical proximities between features of different categories.

Findings concerning the Euclidean distances between individual RWH structures of the three different types are summarized in Table 18. The first bloc shows the results from the analysis regarding the closest other RWH structure for each site. Typically, the nearest object is one of the same category, except for

the modern cisterns. In this category, only roughly one third of the sites have another modern cistern as the closest RWH structure, while for all other sites, a bund, dike, ridge or similar structure represents the nearest object. In the category of bunds, dikes, ridges, and the like, only slightly more than 10% of the sites have a (modern) cistern as the closest RWH structure, whereas for the overwhelming majority (87%) another object of the same type is the nearest one (see Table 18). This strong tendency of intra-group spatial relation or clustering is even more pronounced in the category of old cisterns. For more than 90% of the objects in this class, another old cistern represents the next closest RWH structure. Almost all other old cisterns have a bund, ridge, check dam or similar structure as the nearest RWH object. In contrast, in only one case, an old cistern forms the closest RWH facility of a bund, dike, ridge, or similar structure. A close proximity between old and modern cisterns is likewise uncommon (see Table 18). Apart from some rather exceptional cases, most of the nearest RWH structures are found at similar distances. On average, the next closest RWH structure is located less than 100 m or even less than 50 m away (see mean values in Table 18). Although distances to the nearest feature can vary considerably (see minimum and maximum values in Table 18), close proximities prevail, while greater distances, particularly those at the upper end of the identified range, beyond 250-300 m, are rather atypical. Hence, the frequency distributions of the outcomes are strongly right skewed. The map in Fig. 45 illustrates the described findings concerning the typical groupings of RWH structures and the associated observed distances.

The previously outlined clustering tendencies and typical spatial associations of different RWH structures are also evident in the outcomes from the analysis of distances between each RWH site and the nearest RWH structure in each of the three categories (see Table 18). The types of RWH facilities that are often sited together exhibit significantly lower average distances to the nearest object in the respective category (see mean values in the second bloc of Table 18). All three groups of RWH structures show the lowest average distances to the nearest objects of the same category, respectively. Moreover, the low mean distance between modern cisterns and the nearest bund, dike, ridge, or similar object indicates a frequent close proximity of these structures. On average, the distances between bunds, ridges, check dams, and the like and the closest modern cistern are higher. Although several of the linear RWH structures are found in close proximity to modern cisterns, a high number of objects in this category are located in greater distances and thus, are apparently unrelated to cisterns. In the discussed proximity analysis, combinations of input and near features with a likely spatial relation, indicated by a frequent close proximity, were not distinguished from those which are characterized by greater distances and thus, are less likely to be related. Therefore, the absolute values are less significant here, while the data can provide valuable relative information when compared. Furthermore, the outcomes should be considered in conjunction with the other results given in Table 18.

Legend

- 🟨 Archaeological site
- 🟣 Allegedly old cistern, "Roman Well"
- 🔴 Presumably modern cistern
- ▬ Bund, dike, ridge, check dam or similar object
- — Contour line of 700 m above sea level (altitude)
- 🟩 Vegetation
- ⬜ Settlement area
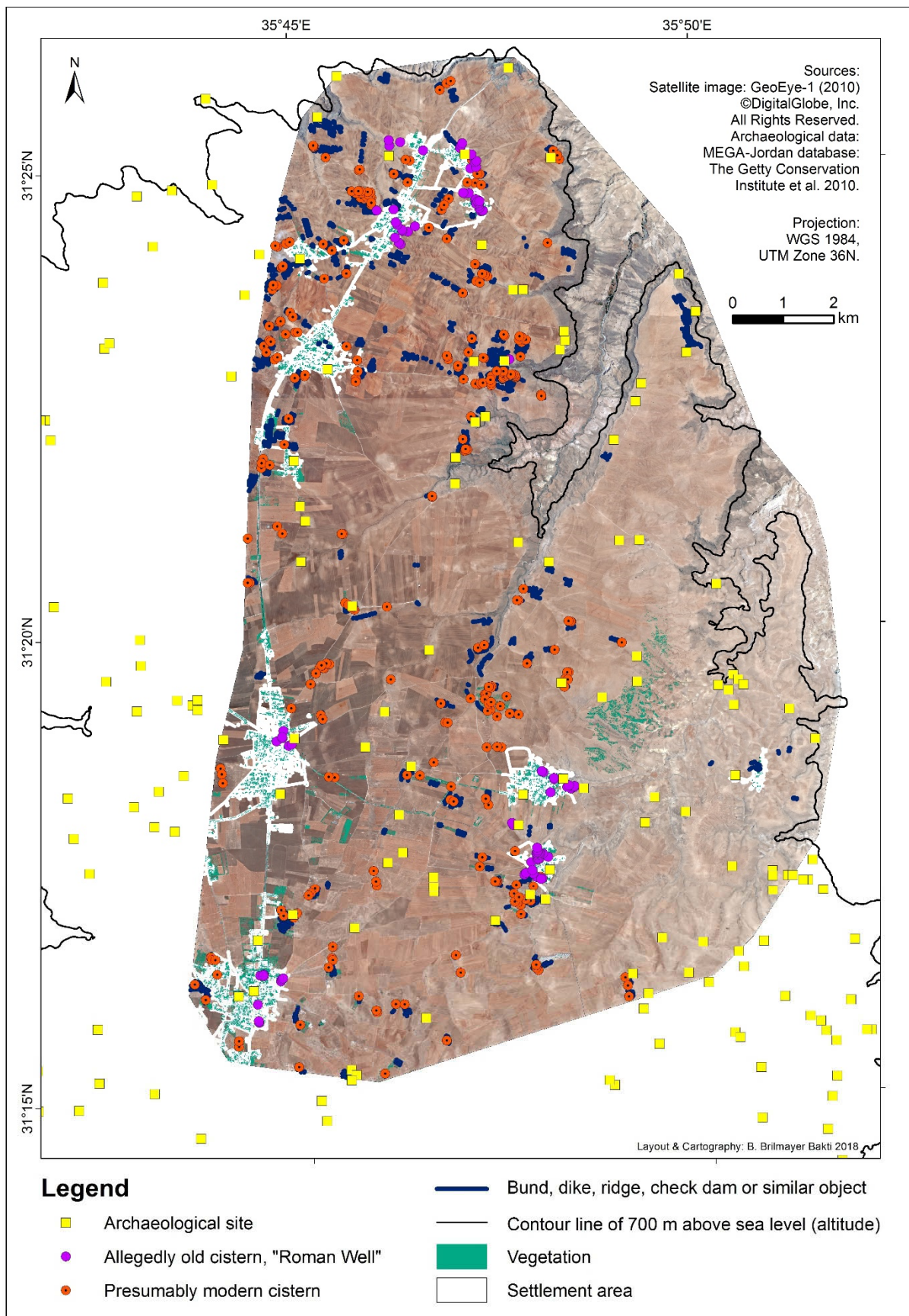
Fig. 54: RWH sites of different categories and their distribution in relation to the locations of archaeological sites, vegetation areas, and modern settlements. The data on vegetation and settlement areas is limited to the study area (see chapter 5.1).The archaeological data includes all sites which are located either within the study area or on the Karak Plateau and in a zone of a maximum distance of 6 km around the study area (see chapter 5.5). Statistical data concerning the distances between the illustrated features can be found in the Tables 18-20.

The determination of the number and type(s) of RWH structures in a given radius around each RWH site provided further insights into clustering tendencies and common spatial associations of different types of RWH facilities (see third bloc in Table 18). Here, a radius of 250 m was chosen since this seemed a reasonable maximum distance with regard to potential (intentional) relationships between objects. While being not too broad, the selected radius was also large enough to yield the most comprehensive and indicative results. The outcomes, i.e. the quantity of sites in each category that have one or more RWH structures of a specific class (same or different) in their vicinity, largely reflect the previously described patterns. These include the strong intra-group clustering tendency, which is observed in all categories, and the frequent close proximity between modern cisterns and bunds, ridges, dikes, and the like. Since not only the nearest, but rather all RWH structures in the vicinity of a given site, were detected in the analysis, common spatial associations became more evident. This especially applies to the frequent grouping of modern cisterns and the combined arrangement of modern cisterns with linear RWH structures. More than 80% of the modern cisterns and 60% of the bunds, dikes, ridges, and similar structures have a modern cistern in their immediate surroundings (see Table 18). Information about the number of further RWH structures that are found in the 250 m radius around each RWH facility is given, according to category, in the last section of Table 18. These figures provide an insight into the sizes of clusters of RWH structures. Since the results do not include any information about the commonness of these clusters, they must be considered in conjunction with the previously described findings. The significance and informative value are highest for the outcomes concerning those combinations of types of RWH structures, for which a frequent close proximity had been observed. Those types of RWH structures that are rarely sited together, e.g. old cisterns and modern cisterns or bunds, dikes, ridges, and the like, usually also have a small number of sites of the respective categories in the analyzed radius (see mean, minimum, and maximum values in the last bloc of Table 18). In contrast, the types of RWH facilities that are frequently situated in proximity to each other, on average, are also characterized by a higher number of five, and more, objects of the respective categories within the radius of 250 m. For these common combinations and the involved categories, the number of structures detected in the vicinity of a given site also vary over a broader range (see corresponding minima and maxima in Table 18). Whereas the largest figures at the upper end of the identified range represent rather exceptional cases, mean values usually quite adequately reflect typical amounts of near features (i.e. observed quantities are approximately normally distributed). The comparison of the results revealed slight differences between the individual categories of RWH facilities which are often found in close proximity to each other. Maximum and mean values of the number of near objects indicate that bunds, dikes, ridges, and the like typically form parts of larger local clusters. These consist of a higher number of individual objects, either only of the named category or of the named type and the class of modern cisterns. In contrast, clusters of cisterns, either old or modern, without linear RWH structures, comprise only about half the amount of objects (see number of near features for the respective categories in Table 18).

Table 18: Outcomes of the analysis of distances between individual RWH structures according to their category. The spatial distribution of the different types of RWH structures is illustrated in Fig. 45.

| | Input Features – RWH category | | |
Near Features – RWH category	Allegedly old cisterns, "Roman Wells"	Presumably modern cisterns	Bunds, dikes, ridges, check dams and similar
Nearest feature according to category and corresponding distances [a]			
Allegedly old cisterns, "Roman Wells"	88 (92 %)	3 (1 %)	1 (<1 %)
min. - max.	9 - 325 m	33 - 479 m	4 m
mean	54 m	194 m	-
standard deviation	53 m	202 m	-
Presumably modern cisterns	1 (1 %)	92 (31 %)	141 (13 %)
min. - max.	33 m	4 - 290 m	5 - 145 m
mean	-	61 m	22 m
standard deviation	-	59 m	35 m
Bunds, dikes, ridges, check dams and similar	7 (7 %)	198 (68 %)	946 (87 %)
min. - max.	4 - 304 m	5 - 993 m	0 - 757 m
mean	96 m	38 m	27 m
standard deviation	89 m	84 m	35 m
Distance to the nearest feature of the respective type			
Allegedly old cisterns, "Roman Wells"			
min. - max.	9 - 2,987 m	33 - 5,221 m	4 - 5,117 m
mean	94 m	1,534 m	1,644 m
standard deviation	306 m	1,104 m	1,195
Presumably modern cisterns			
min. - max.	33 - 1,640 m	4 - 1,363 m	5 - 4,636 m
mean	531 m	138 m	332 m
standard deviation	364 m	194 m	631 m
Bunds, dikes, ridges, check dams and similar			
min. - max.	4 - 1,019 m	5 - 2,199 m	0 - 984 m
mean	432 m	132 m	31 m
standard deviation	282 m	299 m	56 m
Near features according to type in a max. distance of 250 m [b]			
Allegedly old cisterns, "Roman Wells"	90 (94 %)	11 (4 %)	59 (5 %)
Presumably modern cisterns	18 (19 %)	252 (86 %)	722 (66 %)
Bunds, dikes, ridges, check dams and similar	28 (29 %)	257 (88 %)	1,082 (99 %)
Number of near features according to type in the 250 m zone [c]			
Allegedly old cisterns, "Roman Wells"			
min. – max.	1 - 15	1 - 7	1 - 7
mean	5.5	2.7	2.1
standard deviation	3.9	2.0	1.5
Presumably modern cisterns			
min. – max.	1 - 3	1 - 20	1 - 24
mean	1.5	5.4	4.7
standard deviation	0.7	4.6	4.4
Bunds, dikes, ridges, check dams and similar			
min. - max.	1 - 19	1 - 47	1 - 49
mean	4.2	10.5	11.6
standard deviation	4.1	9.2	10.0

[a] *Number (percentage) of input features whose nearest RWH structure belongs to this category, and corresponding distances.*
[b] *Number (percentage) of input features which have a RWH structure of the respective type within a max. distance of 250 m.*
[c] *Number of near features of the respective category which are located at a max. distance of 250 m to individual input features.*

In conclusion, the outcomes of the analysis of distances between RWH structures indicate clear grouping tendencies. All three categories of RWH structures exhibit a considerable intra-group clustering tendency, which is strongest in the classes of old cisterns and linear RWH structures. It is slightly less pronounced in the category of modern cisterns, which includes a few more isolated objects that are located further away from the other cisterns. Nonetheless, the vast majority of modern cisterns are situated in close proximity to other objects of the same type. Intergroup relations and spatial associations appear to be strongest for the combination of modern cisterns and bunds, ridges, dikes, and the like. RWH structures of the two named categories are frequently sited in proximity to each other. Nevertheless, about one third of the linear RWH structures are located at greater distances to modern cisterns and thus, can be considered largely unrelated to them. In contrast, almost 90% of the modern cisterns have a bund, dike, ridge or similar structure in their immediate vicinity. With respect to the sizes of the described common groups, clusters of old or modern cisterns usually consist of considerably fewer objects than those of bunds, ridges, dikes and the like. The latter types of RWH structures form (part of) the largest clusters with significantly higher numbers of objects, in either case, whether they are sited independently or together with modern cisterns.

The outcomes of the analysis of distances between RWH structures and other natural or man-made features of the environment are summarized in Table 19 and 20. To obtain valuable clues to possible spatial patterns, correlations, and interdependencies between the analyzed elements, the results need to be considered and evaluated comparatively, with regard to their relative information content rather than their absolute values. Therefore, in the following, similarities and differences in the findings for the three categories of RWH structures are highlighted.

The distances between RWH structures and their nearest archaeological sites can indicate the likelihood of features of the two named groups being related in some way. In the proximity analyses, only archaeological sites on the Karak Plateau, i.e. those at altitudes of at least 700 m above sea level, were taken into account (see 4.1.5 and 5.5 for details on the data). Possible links to the mapped RWH facilities seemed more likely for these sites, which are situated at similar altitudes as the RWH structures. For all three class of RWH facilities, distances to the nearest archaeological site vary over a comparable range (see minima and maxima in Table 19). On average, however, the distance is noticeably lower for the old cisterns than for the other two types of RWH facilities (see Table 19). These results suggest that, compared to the other groups of RWH structures, a larger percentage of the old cisterns are located in the vicinity of archaeological sites. To facilitate the assessment and comparison of the distance information, particularly in regard to frequency distributions, the data was analyzed based on selected thresholds. For each category of RWH facilities, the number of objects were determined, whose nearest archaeological site was found at a distance of up to a specific limit. In Table 19, the results for the maximum distances of 250 m and 500 m are presented. The relative findings underpin the aforementioned contrast between the category of old cisterns and the other two classes of RWH structures. Over 20% of

the old cisterns are situated at distances of up to 250 m to archaeological sites. In contrast, only slightly more than 10% of the modern cisterns and the bunds, ridges, dikes, and similar structures exhibit a similar proximity to archaeological sites. The described pattern is also observed in the results for the maximum distance of 500 m. Whereas more than 60% of the old cisterns have an archaeological site in the named radius, the same applies to only about one third of the structures in the other two categories.

Table 19: Different types of RWH structures and nearest archaeological sites on the Karak Plateau. The spatial distribution of RWH structures and archeological sites and the resulting proximities between both are visualized in Fig. 54.

Near Features	Input Features – RWH category		
	Allegedly old cisterns, "Roman Wells"	Presumably modern cisterns	Bunds, dikes, ridges, check dams and similar
Archaeological sites (202) [a]			
■ *Distance to nearest on plateau*			
min. - max.	103 - 1,640 m	25 - 1,559 m	5 - 1,785 m
mean	535 m	692 m	659 m
standard deviation	391 m	364 m	360 m
■ *Nearest in up to 250 m* [b]	23 (24%)	35 (12%)	159 (15%)
■ *Nearest in up to 500 m* [b]	60 (63%)	99 (34%)	404 (37%)
■ *Number of different nearest sites* [c]	11	49	56
■*Nearest site type* [d]			
Settlement (fortified), tell, temple, palace, village, villa or similar (51) [e]	8	19	18
Fortress, tower or similar (19) [e]	1	3	6
Camp, caravansary, hamlet, agricultural terrace or similar (25) [f]	0	5	6
Cistern, reservoir or similar (28) [e]	1	8	7
Other or not specified (79) [f]	1	14	19
■ *Number of periods at nearest sites* [g]			
min. - max.	4 - 10	1 - 13	1 - 11
mean	6	5	5
standard deviation	2	3	3

[a] archaeological sites fulfilling three criteria: dated to periods before 1918 AD or not dated yet (water structures only), located within or in a zone of up to 6 km distance around the study area, and situated on the Karak Plateau, i.e. at altitudes of at least 700 m above sea level. For sources and details see 4.1.5 and 5.5.
[b] number (percentage) of input features (RWH structures) whose nearest archaeological site is found at a distance of less than or equal to 250m/500 m.
[c] number of different archaeological sites that appear as nearest to the RWH structures of the respective category.
[d] site types (broad categories) of the archaeological sites which appear as nearest features.
[e] sites of these types were considered rather complex and permanent. In parentheses: number of sites in the respective category that were included in the analysis.
[f] sites of these types were regarded as less complex and rather ephemeral. In parentheses: number of sites in each category which were included in the analysis.
[g] number of different periods per site; number of periods associated with each of the archaeological sites that appear as nearest features.
■ quantitative attribute: value(s) comprised by the features in the respective category of RWH structures.
■ qualitative attribute: absolute number and percentage (in parentheses) of RWH structures in the respective category which possess this attribute.
■ number of nearest archaeological sites that fall into the respective categories. For total number of different nearest sites see row above.

Additional information about the archaeological sites that are found, more or less, close to the RWH structures can offer further clues to the possible relationships between the sites of the two named categories. The number of different archaeological sites which appear as nearest features reveal if the RWH structures are located near a small subgroup of specific sites or in the vicinity of many different, probably random, places with archaeological finds or remains. For the old cisterns, only 11 of the 202 archaeological sites were identified as nearest features. This number is markedly higher (49 and 56) for the other two groups of RWH facilities: the modern cisterns and the bunds, dikes, ridges, and similar structures

(see Table 19). These results are in line with the quantities and spatial distribution patterns of the different types of RWH facilities. Whereas the old cisterns are fewer in number and mostly found in limited areas, the numerous RWH structures of the other two categories are widely dispersed over the study area (see Fig. 45). Furthermore, the site type of each of the nearest archaeological places was recorded (see Table 19). The different site types can broadly be divided into more complex, rather permanent ones, and less complex, rather ephemeral ones. Sites with (remains of) buildings or building-like structures, such as e.g. houses, watch towers, temples, and the like, or water facilities (cisterns, large reservoirs, etc.), were considered quite complex and rather permanent. The named structures have often been preserved, at least in part, over long periods of time and are typically stable in terms of their location. All sites of the other two broad categories, such as e.g. campsites, agricultural fields or terraces, or sites for which no type has been specified, and places of (surface) finds like sherds and similar items, were regarded as less complex and rather ephemeral. The structures and objects found at these types of sites are typically more temporal in nature and are abandoned, destroyed, or relocated more easily. In terms of the types of their nearest archaeological sites, the three classes of RWH facilities show noticeable differences. The old cisterns are located almost exclusively in the vicinity of archaeological sites of rather complex and permanent types, primarily (fortified) settlements and villages (73% of the nearest sites, see Table 19). With regard to absolute numbers, archaeological sites of these types also form many of the nearest features in the other two groups of RWH facilities. However, when seen in relation to the higher number of different archaeological sites that appear as nearest features, sites with remains of rather complex and permanent structures are less common, since they only account for about 60% of all nearest sites (see Table 19). About 15% of the archaeological sites which are closest to modern cisterns or bunds, dikes, ridges, and the like, are places which were primarily linked to remains of water infrastructure elements, such as e.g. cisterns or reservoirs (and did not comprise any remains of other rather complex and permanent structures). Archaeological sites that were considered less complex and rather ephemeral, based on their site type, constitute about 40% of the nearest features for the two aforementioned two groups of RWH structures.

The number of periods that were associated with each of the nearest archaeological sites can be seen as an indicator for the diachronic use and thus, likely significance of a given place. The corresponding findings concerning the nearest archaeological sites for each group of RWH structures are summarized in Table 19. Apparently, the old cisterns are situated in the vicinity of sites which exhibited finds or remains from 4-10 archaeological periods, respectively. On average, these nearest sites were linked to six periods. This finding matches the previously described results, which pointed to a predominant proximity between old cisterns and archaeological sites of more complex, rather permanent types. All of the sites that appear as nearest features for the old cisterns were used over a longer time, either continuously or intermittently during several time intervals. For the archaeological sites nearest to modern cisterns or bunds, ridges, check dams, and the like, the number of associated periods varies over a broader range, including sites with traces from only one period. The average number of periods linked to these sites is

slightly lower than that of the sites closest to the old cisterns (see Table 19). This is in line with the aforementioned higher shares of archaeological sites of less complex and rather ephemeral types in the nearest features of modern cisterns and bunds, dikes, ridges, and the like.

For each of the archaeological sites that appear as nearest features, its type and the number of RWH structures for which it is the nearest site were determined. The corresponding outcomes largely reflected the shares of the different categories of site types in the nearest features and therefore, were not included in Table 19. For example, for most of the old cisterns, their nearest archaeological site is one of the more complex and permanent types, whereas this tendency is less pronounced for the modern cisterns and the linear RWH structures. Thus, the distribution of RWH facilities to individual nearest features and categories of archaeological sites largely reinforces the patterns described earlier. In the map in Fig. 54, the spatial distribution of RWH structures and archaeological sites is visualized.

Furthermore, distances between RWH facilities and modern settlements were analyzed. Outcomes are summarized in Table 20. The spatial distribution of RWH structures in relation to settlement areas is also illustrated in Fig. 54. The employed data on current settlements and their areas is presented in chapter 5.1., while the data acquisition and all related processing steps are described in section 4.1.2.4. When the distance results of the different classes of RWH structures are compared, a stark contrast becomes evident between the old cisterns, on the one hand, and the modern cisterns and bunds, dikes, ridges, and the like on the other. The vast majority of the old cisterns is situated in close proximity to modern settlements. On average, the distance between an old cistern and the nearest settlement is only 59 m. The range of distances between the old cisterns and the nearest settlement appears to be relatively broad, however, it is smaller than that observed for the modern cisterns and the linear RWH structures. For the latter two types of RWH facilities, the maximum distance to the nearest settlement is considerably higher than that of the old cisterns (see Table 20). On average, modern cisterns and bunds, dikes, ridges, and the like are located more than one kilometer away from settlement areas. Additionally, for each group of RWH structures, the number of objects which are found at distances of up to 250 m from settlement areas, were determined. The results underpin the previously described differences between the old cisterns and the other two groups of RWH facilities. While 95% of the old cisterns are situated at distances of no more than 250 m from settlement areas, the same applies to only about one third, or less, of the modern cisterns and the bunds, dikes, ridges, and similar structures (see Table 20). Overall, in terms of distances to settlements, modern cisterns and linear RWH structures show large similarities.

In regard to the distances to vegetation, the different types of RWH structures exhibit patterns which are very similar to those observed in relation to settlements. The vegetation here primarily corresponds to the photosynthetically active plant cover of the summer half year, which mainly consists of permanent plants, such as trees, and some other (seasonal) plants grown in small-scale horticulture (for further details on the vegetation data see chapter 5.1). The distances between individual old cisterns and the

Table 20: Distances between RWH structures of different types and settlements, vegetation areas, drainage lines, and catchment boundaries. The spatial distribution of the features of the named categories and the resulting proximities are visualized in Fig. 52-54.

Near Features	Input Features – RWH category		
	Allegedly old cisterns, "Roman Wells"	Presumably modern cisterns	Bunds, dikes, ridges, check dams and similar
Settlement areas (3.19 km²) [a]			
▪ *Distance to nearest*			
min. - max.	0 - 2,661 m	0 - 3,318 m	1 - 4,917 m
mean	59 m	1,119 m	1,073 m
standard deviation	275 m	937 m	1,077 m
▪ *Nearest in up to 250 m [b]*	91 (95%)	79 (27%)	357 (33%)
Vegetation areas (1.44 km²) [c]			
▪ *Distance to nearest*			
min. - max.	0 - 390 m	2 - 1,482 m	0 - 1,524 m
mean	44 m	259 m	293 m
standard deviation	68 m	331 m	391 m
▪ *Nearest in up to 250 m [b]*	93 (97%)	198 (68%)	706 (65%)
Drainage lines (total length 629 km) [d]		*	*
▪ *Distance to nearest*			
min. - max.	2 - 520 m	1 - 425 m	0 - 384 m
mean	120 m	99 m	59 m / 75 m [e]
standard deviation	116 m	77 m	68 m / 68 m [e]
Catchment boundaries (3,561 catchments) [f]		*	*
▪ *Distance to nearest*			
min. - max.	1 - 194 m	0 - 271 m	0 - 347 m
mean	49 m	42 m	34 m / 49 m [e]
standard deviation	41 m	45 m	49 m / 52 m [e]
▪ **Quotient distance to drainage line / to catchment boundary [g]**		*	*
min. - max.	0 - 109	0 - 1,240	0 - 1,077
mean	6	15	7 / 12 [e]
standard deviation	13	79	52 / 70 [e]

[a] impervious surfaces and areas assigned to individual settlements, see Fig. 54, for description of dataset see 5.1.

[b] number (percentage) of input features (RWH structures) whose nearest settlement/vegetation area is found at a distance of less than or equal to 250m/500 m.

[c] primarily photosynthetically active vegetation of the summer half year, for details on the vegetation data and its acquisition see 5.1 and 4.1.2.4.

[d] manually digitized drainage lines, see 5.4, 4.1.4 and 4.1.2.2.

[e] figures when including/excluding structures like check dams, which intersect drainage lines (202 objects). Number of other structures (bunds, ridges, etc.) considered: 759. For further restrictions leading to a reduced number of features here, also see *

[f] output of the detailed hydrological analysis based on the ALOS DEM and the manually digitized drainage lines, see 5.4 and 4.1.4.

[g] quotient calculated for each RWH structure individually by dividing its distance to the nearest drainage line by its distance to the closest catchment boundary.

* for the figures in this section, only RWH structures located within the catchments of drainage lines originating in the study area (see 5.4 and Fig. 52-53) were considered. This included all of the 96 old cisterns, 259 of the 293 modern cisterns, and 961 of the 1,088 bunds, dikes, check dams and similar structures.

▪ quantitative attribute: value(s) comprised by features in the respective category of RWH structures.

▪ qualitative attribute: absolute number and percentage (in parentheses) of input features (RWH structures) to which the statement applies.

nearest vegetation area vary over a significantly smaller range than those identified for the other two categories of RWH structures (see respective minimum and maximum values in Table 20). The smaller range of distances in the group of old cisterns results from a substantially lower maximum. On average, the distance of an old cistern to the nearest vegetation patch is less than 50 m. In comparison to this, the modern cisterns, as well as the bunds, dikes, check dams, and similar structures, show a broader range of distances, and on average, their distance to the nearest vegetation area is more than 250 m. In all three categories of RWH facilities, a high percentage of features is found at distances of less than or equal to 250 m to vegetation. For 97% of the old cisterns, the nearest vegetation area is located no more than 250

m away. In the categories of the modern cisterns and the bunds, ridges, check dams, and similar structures, about two thirds of the features exhibit a similar proximity to vegetation areas (see Table 20). The spatial distribution of RWH structures in relation to vegetation areas is illustrated in Fig. 54.

With respect to the distances to drainage lines and catchment boundaries, the differences between the three classes of RWH objects are rather subtle. The old cisterns show the broadest range of distances and largest mean distance to the nearest drainage line. In contrast, bunds, dikes, ridges, and similar structures exhibit the closest proximities to drainage lines. This is evident from the lower mean and the reduced maximum distance, as well as the smaller range of distances to the nearest drainage line (see Table 20). The findings for the modern cisterns range between those of the two aforementioned groups of RWH facilities. In the category of linear RWH structures, approximately 21% of the features intersect with drainage lines and hence, are characterized by a distance value of zero. Most, if not all, of these structures very likely qualify as check dams. In regard to the distances to catchment boundaries, the three groups of RWH facilities are very similar. On average, the different types of RWH structures are located at distances of around 40-50 m to catchment boundaries. In the category of linear RWH structures, the mean distance differs, depending on whether or not check dams and similar features crossing drainage lines are taken into account. When these types of structures are included, the mean distance decreases significantly (34 m instead of 49 m, see Table 20). The range of distances to catchment boundaries varies for each group of RWH facilities, according to the respective identified maximum distance. The smallest range and the lowest maximum were observed for the old cisterns, whereas modern cisterns and particularly bunds, dikes, ridges, and the like were associated with higher maximum distances and thus, also a broader range (see Table 20).

For each RWH structure, a quotient was computed, which describes the proportion of the distance to the nearest drainage line to the distance to the nearest catchment boundary. In Table 20, the results are summarized according to category of RWH structures. The quotient can serve as an indicator of the relative size of the potential (upstream) catchment area, which could probably be linked to a given RWH structure. It does not reflect the actual extent of the potentially available catchment area, since other influencing factors like directions of overland flow, individual catchment shapes, and the number of adjacent RWH structures, are not taken into consideration here. The quotient and the corresponding findings can rather reveal differences between RWH sites in regard to the possible relative extent of the upstream part of the surrounding natural catchment (also see 6.2.1, Table 17, Fig. 53). In general, smaller values are normally associated with RWH locations close to drainage lines and rather far away from catchment boundaries. Thus, a low quotient suggests that a relatively large area or part of the respective catchment lies upstream from the analyzed point. Relatively low quotients were observed for the old cisterns. In the named category, the lowest mean and maximum values, as well as the smallest range were found. In contrast, the range of quotient values identified for the modern cisterns and bunds, dikes, ridges, and similar structures, was significantly broader, due to much higher maxima (see Table 20).

The findings for the two aforementioned groups of RWH facilities are quite similar, at least when check dams and similar structures crossing drainage lines are not taken into account. When the latter subtypes of linear RWH structures are included, the mean value decreases to a level similar to that of the old cisterns. Overall, the findings suggest larger upstream, potential catchment areas for the old cisterns and those linear RWH structures which intersect with drainage lines. For all other linear RWH structures, as well as the modern cisterns, the parts of the computed catchments that are found upstream of their sites, often seem to be considerably smaller.

6.3 Runoff and rainwater harvesting potential

This chapter presents the outcomes of the runoff estimation. The calculated amounts of runoff are equated with the theoretical maximum RWH potential of the study area based on the simple assumption that all annually accruing runoff can be collected and used directly or stored. Limiting aspects, which can lead to a lower, actual, practical and feasibly realizable RWH potential, are outlined in chapter 7.4.2. In the following sections, firstly, the total annual (on-site) runoff or general RWH potential in the study area is described. Then, the estimated runoff from rooftops and thus, the equivalent, more specific RRWH potential are presented.

6.3.1 Estimated surface runoff and overall rainwater harvesting potential

Below, outcomes concerning the annual on-site runoff, i.e. the yearly sum of local surface runoff arising from individual precipitation events, are described. The calculated annual figures presuppose that the local surface runoff from each precipitation event is collected and either utilized directly or stored in a way that prevents losses, e.g. through evaporation, before use at a later date. The term local or on-site runoff refers to the surface runoff that can be collected from a small catchment area, such as a micro-catchment. Catchments of these sizes are employed in many RWH schemes, particularly those belonging to the group of micro-catchment WH or runoff farming practices. Due to the small extents of the catchments, losses like those resulting from longer distances of overland flow and transmission losses in wadi channels, which occur in larger catchments and reduce the amount of collectable runoff at the outlet, are negligible here. Therefore, when compared on a per square meter basis, the amounts of on-site runoff are typically significantly higher than the runoff amounts measured at the outlets of larger watersheds (cf. e.g. SHANAN & SCHICK 1980).

The outcomes of the runoff estimations for the three annual precipitation scenarios are visualized in the maps in Fig. 55. The distribution patterns of on-site runoff primarily reflect spatial differences in annual precipitation (see chapter 5.6, Fig. 40 and 41), LU/LC, and slope (cf. 4.2.2.2, Fig. 30). The strongest contrast in regard to runoff exists between areas and surfaces classified as impervious (to water) and those identified as pervious in the LU/LC map (see Fig. 55 and Table 21). The highest amounts of annual on-site runoff, in absolute terms, as well as in relation to the precipitation at a given site, are always found in impervious areas, such as that of settlements and connecting roads. In contrast, the lowest amounts of local runoff result from vegetated areas in relatively flat terrain (slopes of max. 5%). In general, annual quantities of on-site runoff decrease towards the east, where annual precipitation amounts are also lower compared to the central parts of the Karak Plateau (cf. 3.3 and 5.6). The sites where the absolute minimum and maximum amounts of runoff are observed can vary from year to year, as a function of interannual variances in the quantity and spatial distribution of precipitation. The results showed the lowest amount of annual on-site runoff can be expected near Rashadiya in the southeastern corner of the study area in normal (long-term average) and dry years, and near Ariha in the northernmost part of the plateau during wet years. Despite these interannual variances, the aforementioned stark contrast between vegetated areas in flat terrain, which produce the least runoff, and impervious areas from which the highest runoff amounts result, always remains the dominant trait of the spatial distribution patterns of local runoff (see Fig. 55).

The total amount of on-site runoff or the annual general RWH potential of the study area corresponds to approximately 16% of the annual precipitation, independent of the respective precipitation scenario (see Table 21). This proportion is primarily determined by the LU/LC pattern, i.e. the extents and distribution of the areas covered by the individual types of LU/LC, which are associated with different runoff efficiencies. With regard to absolute quantities of on-site runoff in the study area, large interannual differences can be observed, resulting from considerable variances in precipitation. In exceptionally dry years, such as 1963, the total amount of on-site runoff was reduced by more than 50% compared to the long-term mean. Deviations from mean can even be larger in extremely wet years. Results for the wet year of 1965 showed a surplus of more than 80% and thus, a total amount of on-site runoff that equaled about 180% of the calculated long-term average. In absolute terms, most of the study area's annual surface runoff stems from pervious areas (see Table 21). Although runoff efficiencies of sealed surfaces are considerably higher, only around 14% of the area's annual on-site runoff originates from impervious areas. This is a result of the strong imbalance between the two categories of LU/LC in regard to their extents. While pervious land constitutes about 97% the study area, impervious surfaces only cover ca. 3% of the terrain.
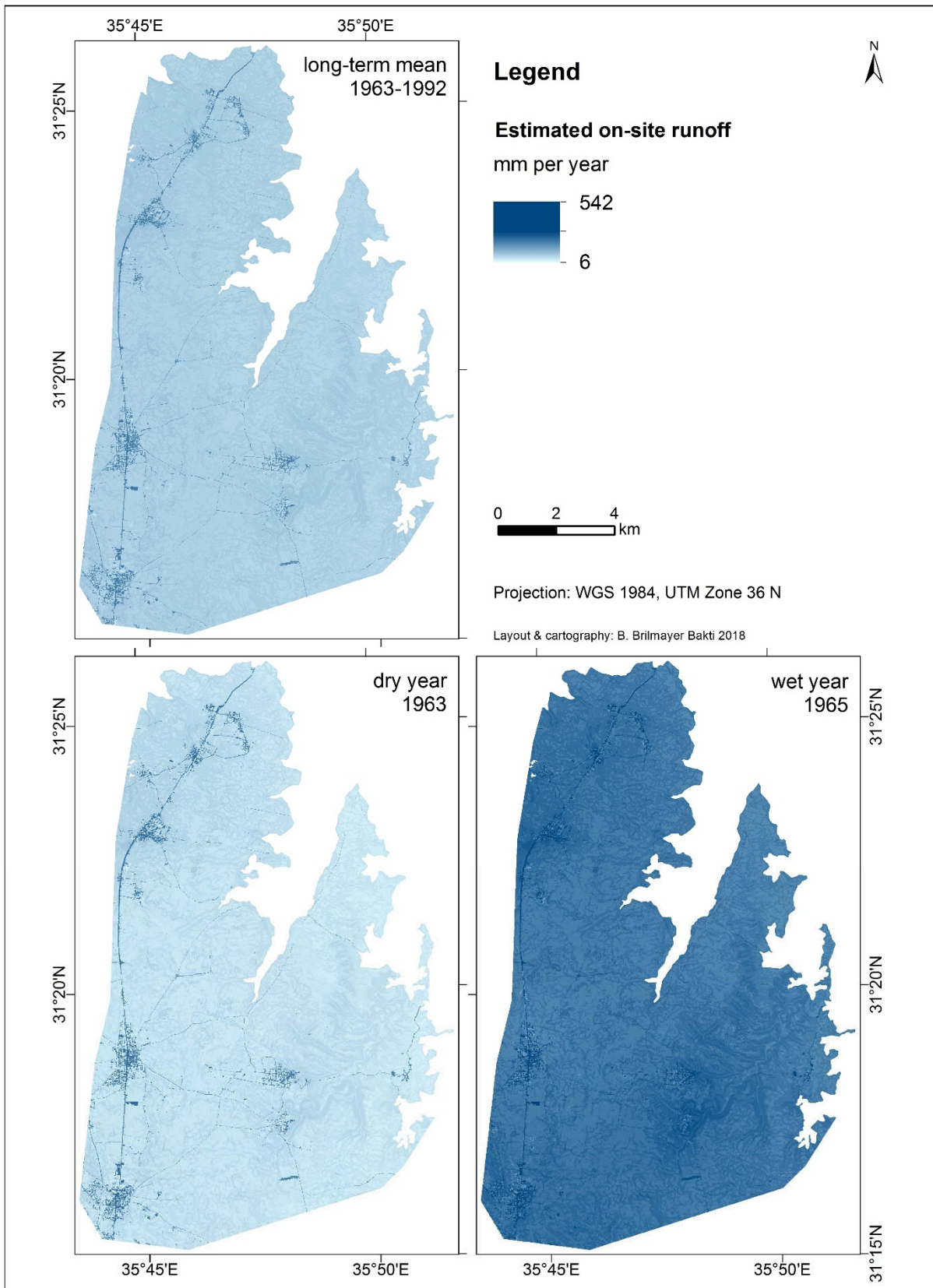
Fig. 55: Maps visualizing the spatial distribution of estimated amounts of annual on-site runoff (in mm per m²) under three different precipitation scenarios. Together, the maps illustrate the likely interannual variances in local runoff or the expectable range of annual runoff amounts. The spatial variances in runoff result from differences in precipitation amounts, LU/LC, and slope. A singular graded color scale was used to visualize the estimated annual amounts of local runoff from all precipitation scenarios. Hence, the values at the lower and the upper end of the range correspond to the absolute minimum and maximum occurring in at least one of the maps. For minimum and maximum runoff under specific precipitation conditions and further statistical key data, see Table 21.

Table 21: Estimated annual on-site runoff: statistical key data and summary for the study area. For each of the three different precipitation scenarios, the annual precipitation and the computed amounts of annual local runoff from pervious and impervious areas, as well as the study area as a whole, are given in million cubic meter (MCM, 10^6 m³) in the "total" column. Additionally, the associated minima, maxima, mean, and standard deviation (SD) of the annual precipitation and on-site runoff are stated in mm per m².

	Long-term mean conditions (1963-1992)		Dry year conditions (1963)		Wet year conditions (1965)	
		total		total		total
Precipitation						
min.	224 mm	46.184 MCM	97 mm	21.203 MCM	395 mm	84.885 MCM
max.	321 mm		159 mm		677 mm	
mean	273 mm		128 mm		523 mm	
SD	28 mm		18 mm		72 mm	
Runoff						
pervious areas		6.219 MCM		2.856 MCM		11.443 MCM
min.	14 mm		6 mm		26 mm	
max.	58 mm		29 mm		121 mm	
impervious areas		1.019 MCM		0.469 MCM		1.853 MCM
min.	186 mm		82 mm		334 mm	
max.	257 mm		127 mm		542 mm	
overall		7.238 MCM		3.325 MCM		13.296 MCM
mean	62 mm		29 mm		123 mm	
SD	70 mm		33 mm		138 mm	

Based on the figures presented in Table 21, the size of the catchment area can be determined which would be required to collect an adequate amount of runoff to fill a cistern (see Table 22) (for cistern capacities see 6.1, Table 16). Since local runoff amounts per square meter vary considerably throughout the study area, according to differences in precipitation and characteristics of the land surface, necessary catchment sizes also differ depending on local circumstances. The range of required catchment sizes could be derived from the identified minimum and maximum amounts of runoff per m². The highest discrepancy in the required extent was observed between impervious and pervious catchment areas, as these were associated with strong differences in runoff per m² (see Fig. 55 and Table 21). Here, a distinction was drawn only between impervious and pervious areas, and the latter category included all types of unsealed surfaces, i.e. land with and without vegetation. For each of the three precipitation scenarios, the respective areas needed to collect sufficient quantities of runoff to fill a cistern are stated in Table 22. Irrespective of the specific local circumstances and the LU/LC, in comparison to the results

Table 22: Estimated catchment areas needed to harvest sufficient runoff to fill one cistern once per year.

Type of catchment area	Required catchment area (min. - max.) under the respective conditions		
	long-term mean annual precipitation (1963-92)	dry year (1963)	wet year (1965)
Pervious areas			
for an old cistern (130 m³)	2,241-9,286 m²	4,483-21,667 m²	1,074-5,000 m²
for a modern cistern (30 m³)	517-2,143 m²	1,034-5,000 m²	248-1,154 m²
Impervious areas			
for an old cistern (130 m³)	506-699 m²	1,024-1,585 m²	240-389 m²
for a modern cistern (30 m³)	117-161 m²	236-366 m²	55-90 m²

for normal, average years, the catchment area would at least have to be doubled to harvest enough runoff during dry years. In contrast, during wet years, slightly more than half of the catchment area required under long-term average conditions would already yield sufficient runoff to fill a given cistern.

For a variety of reasons, such as differences in runoff efficiency and water purity levels, not all areas and surfaces are equally suited for the collection of runoff. Impervious surfaces are generally associated with high runoff rates, but most of these areas are normally excluded from RWH mainly due to water quality concerns. Rooftops represent an exception in this regard, as they are usually considered excellent or even the only appropriate catchment areas for RWH purposes. Details on rooftop RWH can be found in section 6.3.2. Vegetated areas are typically characterized by low to very low runoff efficiencies, and are therefore normally regarded as inadequate catchments for RWH. Of the remaining pervious areas, only those with slopes of no more than 15% were considered as potentially suitable for the collection of runoff. Steeper sloping catchments are usually associated with increased erosion and thus, higher sediment loads in runoff. Additionally, runoff from steeper sloping terrain is more difficult to control and hence, its collection would at least require larger investments and more elaborate, complex RWH schemes that are specifically adjusted to these conditions. Finally, individual pervious areas meeting the aforementioned criteria had to be of sufficient size to be suitable for RWH and serve e.g. as catchment areas for cisterns. The minimum extent was defined by the catchment area required to collect enough runoff to fill a modern cistern to its capacity once per year, under normal precipitation conditions. On average, the calculated on-site runoff from pervious land without vegetation and with gradients of no more than 15% was 0.039 m^3 per m^2 in years with normal, i.e. long-term mean, precipitation. Hence, a catchment area of 769 m^2 would be necessary to harvest sufficient runoff to fill a modern cistern with an assumed typical capacity of 30 m^3 (see 6.1). The pervious areas that fulfilled the aforementioned qualifications, including that of a minimum size of 769 m^2 at a given location, amounted to a total of 143.890 km^2 altogether. This corresponds to 88% of the whole study area or more than 90% of the land

Table 23: Estimated amounts of annual local runoff and catchment areas required to collect enough runoff to fill a cistern once per year, when considering only pervious areas without vegetation, with slopes of up to 15%, and a minimum extent of 769 m^2 per patch. Since these areas are regarded as potentially suitable for RWH, the runoff figures below illustrate the (theoretical) RWH potential of the study area, excluding the RRWH potential which is described in section 6.3.2.

	Results under the respective precipitation conditions		
	long-term mean (1963-1992)	dry year (1963)	wet year (1965)
Estimated annual on-site runoff / RWH potential in the study area			
total amount	5.547 MCM	2.549 MCM	10.188 MCM
min. - max. per m^2	27-48 mm	12-24 mm	47-102 mm
mean per m^2	37 mm	17 mm	71 mm
standard deviation	6 mm	3 mm	13 mm
Required catchment area			
for an old cistern (130 m^3)	2,708-4,815 m^2	5,417-10,833 m^2	1,275-2,766 m^2
for a modern cistern (30 m^3)	625-1,111 m^2	1,250-2,500 m^2	294-638 m^2

classified as pervious in the LU/LC map (all gradients, excluding vegetation). Table 23 displays the annual amount of on-site runoff and the sizes of required catchment areas for cisterns when considering only the pervious areas which meet the described criteria of slope and minimum extent.

In the estimation of the RWH potential (see Table 23), other, competing forms of use of the pervious areas, e.g. for agricultural purposes, and possible further restrictions, such as boundaries of individually owned parcels of land, were not taken into account. These circumstances may reduce the extent of the areas actually available for RWH and thus, the harvestable amount of runoff. To assess the combinability of the existing RWH facilities and the likely suitable catchment areas, both datasets need to be compared with regard to the spatial distribution of individual features (objects or patches). Almost all modern cisterns (290 of 293) and bunds, dikes, ridges, and similar structures (1,070 of 1,088), as well as 84 of the 96 old cisterns, were found either within, or at distances of no more than 10 m to, pervious areas determined as potentially suitable for RWH.

6.3.2 Runoff from rooftops and associated rainwater harvesting potential

In Table 24 and 25, the estimated annual amounts of runoff from rooftops are given for each settlement in the study area. The calculated amounts of runoff are tantamount to the annual RRWH potential of each town or village. Findings for the six settlements that were identified as the largest, according to resident and/or household numbers (cf. 3.6, Table 6), are displayed in Table 24. The outcomes for these settlements include the figures which resulted from the semi-automatic object extraction outcomes, as well as those which were based on the reference data (manually digitized rooftops). Results for the six smaller settlements are shown in Table 25. The findings exclusively rely on automatically detected roof-top information, as for these villages, no reference data was collected (see 4.1.2.6 and 5.2). Since runoff was computed as a direct function of rooftop area and precipitation, the total area of the rooftops (see 5.2) and the annual amount of precipitation (see 5.6) are also stated for each settlement in Table 24 and 25. All runoff estimates that were based on semi-automatically detected rooftop data, are given in conjunction with the likely range of uncertainty (see "tolerance" in Table 24 and 25). The minimum and maximum amounts of runoff were computed based on the likely degrees of over- or underestimation in the image classification results (see chapter 5.2). The tolerance range corresponds to a subtraction of 15% and an addition of 16% to the respective annual amount of runoff. To facilitate the comparison of the individual RRWH potentials of the different towns and villages, independent of their size (i.e. the respective total area of rooftops), the mean annual runoff per square meter is also stated in Table 24 and 25. Figures of runoff per m^2 directly reflect spatial differences in precipitation. Besides runoff estimates for long-term average precipitation conditions, those for exceptionally dry and wet years, exemplified by the years 1963 and 1965, are included in Table 24 and 25 as well. Together, these findings illustrate

typical yearly runoff quantities, as well as the expected range of variances in annual runoff, which result from interannual differences in precipitation. In addition to the figures presented in Table 24 and 25, the RRWH potentials of the individual settlements under different precipitation conditions are also visualized in Fig. 56 to facilitate the comparative assessment of the results.

Table 24: RRWH potentials of the six larger settlements in the study area. For each settlement, the total area of rooftops, the annual precipitation in the settlement area, and the resulting estimated annual runoff from rooftops are given. Findings for three different precipitation scenarios are included, namely normal or long-term mean conditions (based on the period 1963-1992), dry years (exemplified by 1963), and wet years (exemplified by 1965).

	Town or village					
	Qasr	**Rabba**	**Jad'a**	**Smakiya**	**Mghayyer**	**Shihan**
Rooftop area [a]						
classification	182,329 m^2	149,588 m^2	74,798 m^2	61,159 m^2	42,632 m^2	18,027 m^2
reference	182,191 m^2	165,367 m^2	85,669 m^2	56,572 m^2	35,557 m^2	19,694 m^2
Long-term average conditions (1963-1992)						
Annual precipitation [b]						
min. - max.	304 - 319 mm	299 - 321 mm	299 - 318 mm	273 - 291 mm	290 - 303 mm	302 - 315 mm
mean	314 mm	313 mm	307 mm	284 mm	298 mm	307 mm
standard deviation	3 mm	5 mm	4 mm	5 mm	3 mm	3 mm
Annual runoff [c]						
classification	46,187 m^3	37,821 m^3	18,495 m^3	13,931 m^3	10,211 m^3	4,427 m^3
tolerance	39,254 - 53,619 m^3	32,144 - 43,907 m^3	15,719 - 21,471 m^3	11,840 - 16,172 m^3	8,679 - 11,854 m^3	3,762 - 5,139 m^3
reference	46,133 m^3	41,798 m^3	21,185 m^3	12,880 m^3	8,515 m^3	4,837 m^3
per m^2	0.253 m^3	0.253 m^3	0.247 m^3	0.228 m^3	0.240 m^3 (0.239 m^3) [d]	0.246 m^3
Dry year conditions (1963)						
Annual precipitation [b]						
min. - max.	133 - 139 mm	128 - 150 mm	146 - 156 mm	126 - 135 mm	140 - 154 mm	139 - 149 mm
mean	136 mm	140 mm	152 mm	132 mm	147 mm	143 mm
standard deviation	1 mm	5 mm	3 mm	2 mm	3 mm	2 mm
Annual runoff [c]						
classification	20,031 m^3	17,212 m^3	9,146 m^3	6,482 m^3	5,053 m^3	2,035 m^3
tolerance	17,024 - 23,254 m^3	14,629 - 19,982 m^3	7,773 - 10,617 m^3	5,509 - 7,525 m^3	4,295 - 5,866 m^3	1,730 - 2,363 m^3
reference	20,007 m^3	19,045 m^3	10,466 m^3	5,992 m^3	4,213 m^3	2,240 m^3
per m^2	0.110 m^3	0.115 m^3	0.122 m^3	0.106 m^3	0.119 m^3 (0.118 m^3) [d]	0.113 m^3 (0.114 m^3) [d]
Wet year conditions (1965)						
Annual precipitation [b]						
min. - max.	447 - 552 mm	584 - 616 mm	542 - 588 mm	543 - 607 mm	519 - 560 mm	531 - 572 mm
mean	503 mm	604 mm	565 mm	578 mm	539 mm	546 mm
standard deviation	26 mm	7 mm	11 mm	17 mm	9 mm	9 mm
Annual runoff [c]						
classification	72,843 m^3	72,945 m^3	34,125 m^3	28,393 m^3	18,547 m^3	7,834 m^3
tolerance	61,909 - 84,563 m^3	61,996 - 84,682 m^3	29,003 - 39,615 m^3	24,131 - 32,961 m^3	15,763 - 21,531 m^3	6,658 - 9,095 m^3
reference	72,477 m^3	80,521 m^3	39,074 m^3	26,238 m^3	15,462 m^3	8,597 m^3
per m^2	0.400 m^3 (0.398 m^3) [d]	0.488 m^3 (0.487 m^3) [d]	0.456 m^3	0.464 m^3	0.435 m^3	0.435 m^3 (0.437 m^3) [d]

[a] *total area of rooftops in the respective settlement, according to the semi-automatic image analysis outcomes (row "classification") and the reference data (manually digitized rooftops; row "reference"). For details on the rooftop data and its acquisitions see 4.1.2.5 and 5.2.*
[b] *figures here refer to the area covered by the respective satellite image subset used in the rooftop mapping process (see 4.1.2.5 and 5.2).*
[c] *annual runoff from rooftops or RRWH potential as calculated based on the total area of rooftops in the semi-automatic image analysis results (row "classification") and the reference data (row "reference"). Also see rooftop area above. For the figures based on the (semi-) automatically detected rooftop data, a tolerance range is given. The error margin is derived from the 95% confidence interval of the classification results (see 5.2) and reflects the likely under- or overestimation of the RRWH potential by 16% and 15%, respectively.*
[d] *numbers in parentheses indicate the average annual runoff per square meter of rooftop as computed based on the reference data. Figures are only given where they differ from those relying on the classification results with regard to the displayed precision (number of decimals).*

Table 25: RRWH potentials of the six smaller settlements within the study area. Also see description of Table 24, which is similarly structured and designed.

	Town or village					
	Ariha	**Mis'r**	**al-'Aliya**	**Hmud**	**Abu Traba**	**Rashadiya**
Rooftop area [a]						
classification	21,940 m²	20,792 m²	20,417 m²	17,334 m²	11,187 m²	7,451 m²
Long-term average conditions (1963-1992)						
Annual precipitation [b]						
min. - max.	278 - 292 mm	301 - 306 mm	287 - 295 mm	286 - 299 mm	278 - 286 mm	239 - 243 mm
mean	286 mm	303 mm	291 mm	294 mm	283 mm	241 mm
standard deviation	3 mm	1 mm	2 mm	4 mm	3 mm	1 mm
Annual runoff [c]						
classification	5,034 m³	5,040 m³	4,737 m³	4,092 m³	2,525 m³	1,437 m³
tolerance	4,278 - 5,843 m³	4,283 - 5,851 m³	4,026 - 5,500 m³	3,478 - 4,750 m³	2,146 - 2,931 m³	1,222 - 1,669 m³
per m²	0.229 m³	0.242 m³	0.232 m³	0.236 m³	0.226 m³	0.193 m³
Dry year conditions (1963)						
Annual precipitation [b]						
min. - max.	129 - 140 mm	150 - 159 mm	135 - 143 mm	132 - 137 mm	131 - 137 mm	106 - 109 mm
mean	135 mm	154 mm	139 mm	135 mm	135 mm	107 mm
standard deviation	2 mm	2 mm	2 mm	2 mm	2 mm	1 mm
Annual runoff [c]						
classification	2,380 m³	2,544 m³	2,252 m³	1,884 m³	1,198 m³	642 m³
tolerance	2,023 - 2,763 m³	2,162 - 2,953 m³	1,914 - 2,615 m³	1,601 - 2,187 m³	1,018 - 1,390 m³	546 - 746 m³
per m²	0.108 m³	0.122 m³	0.110 m³	0.109 m³	0.107 m³	0.086 m³
Wet year conditions (1965)						
Annual precipitation [b]						
min. - max.	479 - 519 mm	544 - 569 mm	499 - 528 mm	627 - 677 mm	485 - 506 mm	445 - 459 mm
mean	501 mm	556 mm	511 mm	653 mm	498 mm	451 mm
standard deviation	9 mm	5 mm	10 mm	15 mm	5 mm	4 mm
Annual runoff [c]						
classification	8,840 m³	9,195 m³	8,298 m³	9,173 m³	4,428 m³	2,708 m³
tolerance	7,513 - 10,263 m³	7,815 - 10,675 m³	7,053 - 9,633 m³	7,796 - 10,649 m³	3,763 - 5,140 m³	2,301 - 3,143 m³
per m²	0.403 m³	0.442 m³	0.406 m³	0.529 m³	0.396 m³	0.363 m³

[a] *total area of rooftops in the respective settlement, according to the semi-automatic image analysis outcomes (classification; see 5.2).*
[b] *figures here refer to the area covered by the respective satellite image subset used in the rooftop mapping process (see 4.1.2.5 and 5.2).*
[c] *annual runoff from rooftops or RRWH potential as calculated based on the total area of automatically detected rooftops (classification). Also see rooftop area above. Additionally, a tolerance range is given, which is derived from the 95% confidence interval of the classification results (see 5.2). The error margin reflects the likely under- or overestimation of the RRWH potential by 16% and 15%, respectively.*

The RRWH potential of each town or village is primarily determined by its size, or more precisely, the total area of rooftops from which water potentially could be collected. Consequently, differences in RRWH potential largely correspond to those in the total area of rooftops. Hence, the settlements with the largest total areas of detected rooftops, namely Qasr, Rabba, and Jad'a, also show the highest amounts of collectable runoff from precipitation. The lowest RRWH potentials are found in the smallest villages of the study area: Abu Traba in the north and Rashadiya in the very east. For five other settlements, moderate RRWH potentials of 4,000-5,000 m³ runoff per year under normal, i.e. long-term average precipitation conditions, were computed. These settlements, namely Ariha, Mis'r, al-'Aliya, Shihan, and Hmud, were characterized by very similar total areas of rooftops (see Table 24 and 25). Therefore, the identified differences in the RRWH potentials of these villages must be chiefly attributed

to spatial disparities in annual precipitation. In some cases, settlements with a smaller total area of rooftops can even exhibit a higher RRWH potential than those with a slightly larger rooftop area. This finding may apply to all, or only to, specific precipitation scenarios. The village of Mis'r, although being smaller in terms of the total area of rooftops, features a higher RRWH potential under all precipitation conditions than the slightly larger village of Ariha (see Table 25 and Fig. 56). In the small village of Hmud, the total amount of annual runoff from rooftops only exceeds that of the larger settlements Ariha, al-'Aliya, and Shihan in years with exceptionally high precipitation, as the results indicate (see Table 24 and 25). Similarly, the highest RRWH potential in wet years is found in Rabba, while Qasr, the town with the largest total area of rooftops, only ranks second under these conditions (see Table 24 and Fig. 56). Apparently, shifts in the spatial distribution of precipitation in unusually dry or wet years (see section 5.6, Fig. 41) can noticeably influence the RRWH potentials of individual settlements.

The figures for the average runoff per m^2 of rooftop allow the comparison of the respective RRWH potentials of each settlement under specific precipitation conditions, independent from the settlement size. Under all precipitation scenarios, Rashadiya exhibits the least RRWH potential per m^2, due to its location in the easternmost part of the study area, where precipitation amounts are lowest (see Table 25). The largest RRWH potentials per m^2 are found in different settlements, depending on the precipitation scenario. Under normal, i.e. long-term average conditions, Qasr and Rabba feature the highest amounts of mean annual runoff per m^2 of rooftop area. In contrast, during dry years, the largest RRWH potentials per m^2 are found in Jad'a and Mis's, as the results show (see Table 24 and 25). In wet years, Hmud exhibits the highest amounts of runoff per m^2 of rooftop area. These variances in mean annual runoff per m^2 in combination with the differences in the total area of rooftops, lead to the individual RRWH potentials of each settlement (see Fig. 56).

In total, the RRWH potential of all settlements in the study area amounts to 153,937 m^3 per year under long-term mean precipitation conditions. However, findings indicate that the sum of annual runoff from all rooftops can be as low as 70,859 m^3 during dry years and as high as 277,329 m^3 in wet years. Irrespective of the particular precipitation conditions, the overall RRWH potential of the six larger towns and villages is almost six times as high as that of the six smaller villages together (see Table 24 and 25). When runoff estimations are based on reference data, where available, instead of (semi-) automatically detected rooftops, the computed total amounts of annual runoff from rooftops are slightly higher, with 158,213 m^3, 72,863 m^3, and 285,011 m^3 in years with average, extremely low, and very high precipitation, respectively. Yet, the differences in computed runoff quantities, which result from the use of reference data or (semi-) automatic image classification outcomes, are small to moderate, and usually within the specified tolerance range (see Table 24). Only for the village of Mghayyer, the difference in runoff amounts is slightly higher due to the lower appropriateness of the total area of automatically detected rooftops in this specific case (see chapter 5.2, Table 12).
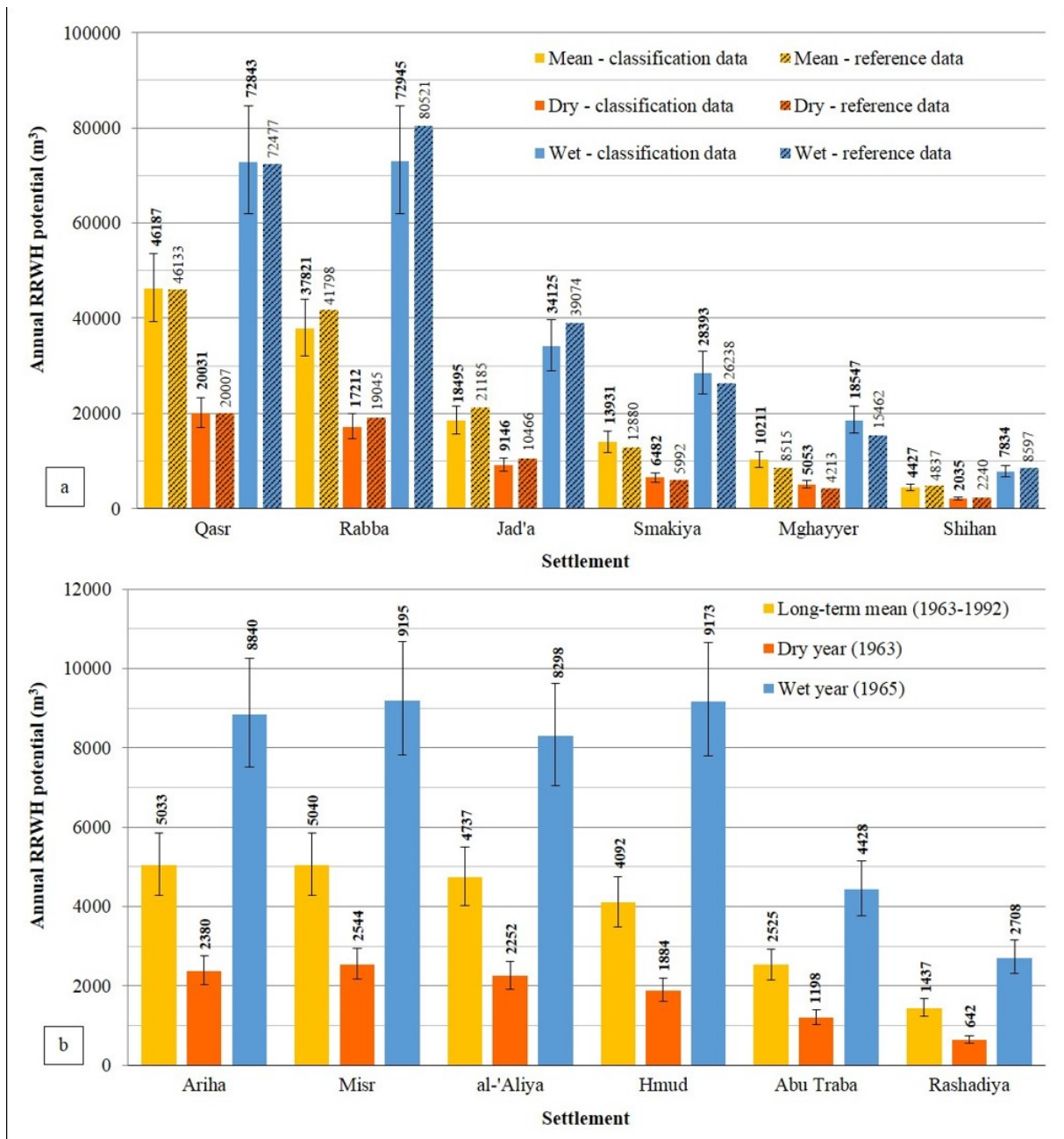
Fig. 56: Individual RRWH potentials of the settlements in the study area. For each town or village, the annual RRWH potential, i.e. the estimated runoff from all rooftops, under three different precipitation scenarios is illustrated: normal or long-term mean conditions, as derived from the data for the period of 1963-1992 (orange yellow bars), dry year conditions exemplified by the year 1963 (red bars), and wet year conditions represented by the year 1965 (blue bars). Part a shows the results for the six larger settlements (see Table 24) and part b displays the outcomes for the six smaller villages in the study area (see Table 25). The hatched bars in part a illustrate the RRWH potential calculated based on the reference data (manual digitized rooftops). The plain bars in both diagrams visualize the runoff quantities which were computed using the semi-automatically detected rooftop data (classification outputs). Error bars show the tolerance range which was derived from the likely over- or underestimation (95% confidence interval) of the total area of rooftops in the image classification outcomes (see chapter 5.2). The color of each bar indicates the respective precipitation scenario. Above every bar, the corresponding estimated RRWH potential (annual amount of runoff from all rooftops, see Table 24 and 25) is stated.

As pointed out before, runoff quantities can vary substantially from year to year, due to the larger inter-annual variances in precipitation. The identification of likely minimum and maximum quantities and thus, the expectable range of annual runoff amounts, is important for a detailed assessment of the RRWH

potential and associated planning purposes, such as the design of RWH systems and the dimensioning of cisterns or other storage components. Absolute amounts of annual runoff from rooftops under different precipitation scenarios have been presented in Table 24 and 25 and Fig. 56. In Fig. 57, for each settlement, the relative reduction or surplus of annual runoff in exceptionally dry or wet years, compared to the long-term mean, is visualized. In dry years, the RRWH potential decreases by around 50% in relation to the long-term mean. The degree of reduction, i.e. the percentage change, is very similar in all settlements (see Fig. 57). In contrast, the relative increase in wet years varies largely from one village or town to another. The surplus in annual runoff from rooftops can be as little as 58% (Qasr), but may also reach well over 100%. The highest relative increases, compared to long-term mean values, are found in some of the eastern most villages: Hmud and Smakiya. In general, the percentage changes in runoff are significantly larger in wet years than in dry years. In some settlements, primarily those in the eastern part of the study area, these tendencies are apparently especially pronounced.
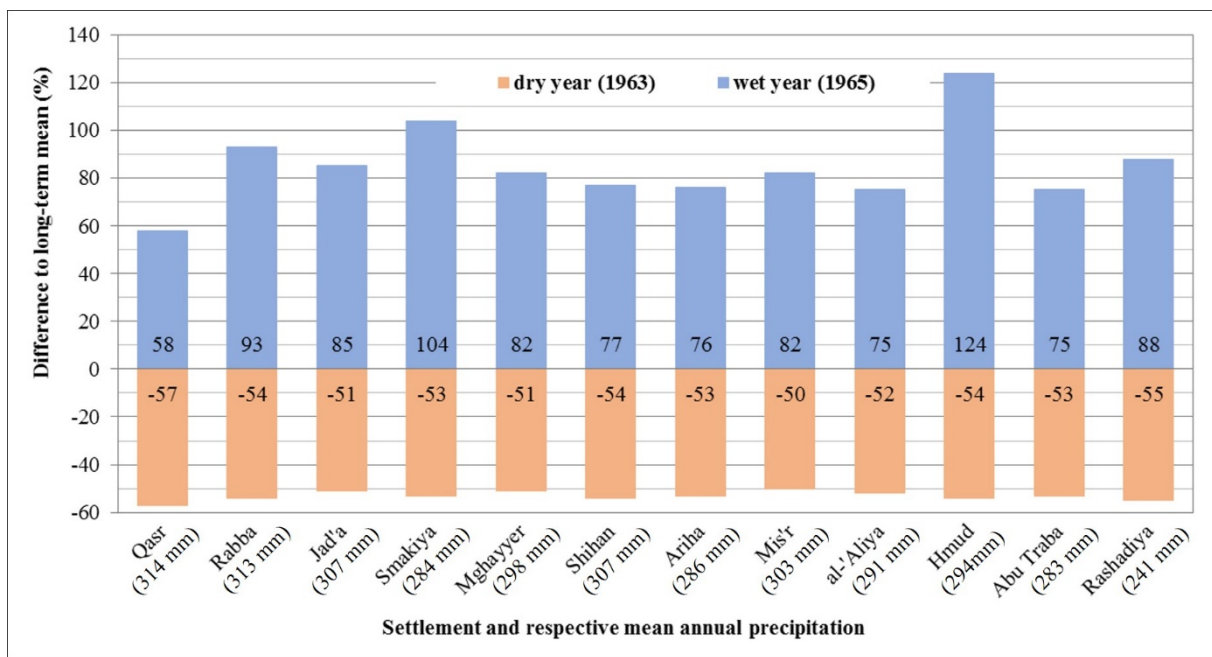
Fig. 57: Differences in annual RRWH potentials (runoff from rooftops) in years with exceptionally low or high precipitation, compared to long-term mean values. The bars indicate the individual deficit (red parts) and surplus (blue parts) in annual runoff from rooftops in each settlement in the study area. All values express the percentage change compared to the annual runoff under normal, long-term mean precipitation conditions (see Table 24 and 25 and Fig. 56). Dry and wet year conditions are exemplified by the data for the years 1963 and 1965, respectively. To illustrate spatial differences in mean annual precipitation amounts, the corresponding values are stated below the name of each settlement, in parentheses.

Finally, the estimated annual RRWH potential of each settlement was compared to the total storage capacity of the cisterns located in the vicinity of the buildings. The results are summarized in Table 26. Based on these findings, mismatches between the storage capacities of existing cisterns and the annual quantities of potentially harvestable runoff from rooftops can be identified. Deficits in available storage capacities and location discrepancies between existing cisterns and buildings can impede the full and efficient exploitation of RRWH potentials. On the other hand, many of the old cisterns lack adequate

catchment areas for the collection of runoff (see 6.1), which restricts their functionality. Therefore, a critical assessment that identifies possible deficits and constraints is the necessary first step to an optimal exploitation of the RRWH potential and to an improved use of the existing RWH infrastructure.

Key data on runoff from rooftops and existing cisterns in the proximity of buildings are provided in Table 26. Besides the findings for each settlement individually, summarized information for the entirety of the villages and towns in the study area are also given. The smallest and easternmost settlement, Rashadiya, was not included in Table 26, since there, and in the immediate surroundings, no cisterns were discovered. For each settlement, firstly, the respective rooftop area is stated which is needed to collect a suitable quantity of runoff to fill an allegedly old or a presumably modern cistern to its capacity once per year. While the old cisterns each require rooftop catchment areas of 500-600 m^2, for a modern cistern, around 120-130 m^2 are sufficient to harvest an adequate amount of runoff. This discrepancy results from the fundamental difference in storage volumes assumed for the two groups of cisterns (see 6.1, Table 16). The differences between individual settlements in regard to the exact extent of the necessary rooftop catchment area are comparatively small and result from spatial variances in precipitation and annual runoff per m^2 of rooftop (see Table 24 and 25). All figures in Table 26 refer to the estimated annual amounts of runoff under normal, long-term mean precipitation conditions.

Secondly, the number of cisterns is given which were identified as suitable for the integration into RRWH schemes. Only cisterns close to buildings, at distances of no more than 250 m, were regarded as eligible for RRWH. The named threshold was assumed as the maximum distance over which an existing cistern as storage component could probably be connected to a building rooftop serving as runoff collection area, while at the same time, limiting the required piping system and related construction and maintenance costs to a reasonable extent. As the overall findings for the study area show, the majority of the cisterns which possibly qualify for integration into RRWH schemes, were old ones (see Table 26). With regard to individual settlements, the number of potentially eligible old or modern cisterns differs largely. In each of the analyzed towns or villages, between 2 and 23 old cisterns and 2 to 13 modern cisterns were identified in the vicinity of buildings (250 m radius; see Table 26). In some places, such as Shihan, Jad'a, and Mis'r, no old cistern potentially suitable for RRWH was detected at all. Similarly, no eligible modern cistern was found in the area of Abu Traba and in that of Smakiya.

For each of the qualifying cisterns, i.e. those with a building within the radius of 250 m, the distance to the nearest rooftop was also determined. For the eligible old cisterns, distances of less than 1 m to almost 200 m were identified, with an average of 47 m (see Table 26). The suitable modern cisterns were often characterized by higher distances of around 30 m to more than 200 m to the nearest building, although occasionally, distances of less than 1 m were observed too. The average distance between an eligible modern cistern and the closest rooftop is 126 m. However, in individual settlements, the distances between cisterns and the next closest buildings can vary significantly.

Table 26: Comparison of RRWH and available storage potentials in individual settlements. All figures concerning necessary rooftop areas or runoff from rooftops refer to normal, i.e. long-term average precipitation conditions. The required roof area corresponds to the rooftop catchment area necessary to collect an adequate amount of runoff to fill an old or modern cistern (storage capacities see 6.1, Table 16) once per year. Cisterns eligible for RRWH are those situated at distances of no more than 250 m from the closest rooftop. Similarly, eligible rooftops must be located, at least partly, with a radius of 250 m around a cistern. Cisterns with sufficient roof area are those which have rooftops with a total extent at least as big as the respective specified threshold (see roof area required) in their vicinity (250 m radius). All results, except those stated in parentheses, were computed based on semi-automatically detected rooftops. Figures in parentheses were obtained using the reference data (i.e. manually digitized rooftop data) instead of the image classification outcomes in the analyses. Reference data was only available for six settlements (see 5.2) and the corresponding results are only stated where they differ from the outcomes based on the (semi-) automatically acquired rooftop data.

Settlement	Allegedly old cisterns, "Roman Wells"	Presumably modern cisterns
Qasr		
Roof area required, per cistern	514 m^2	119 m^2
Potentially eligible cisterns	6	2 (3)
Distance to nearest rooftop		
min. - max.	6-40 m (11-31 m)	128 m / 225 m (127-205 m)
mean	17 m (16 m)	- (173 m)
standard deviation	12 m (7 m)	- (33 m)
Total area of eligible rooftops	56,238 m^2 (52,274 m^2)	3,312 m^2 (4,912 m^2)
Annual runoff from eligible roofs	14,228 m^3 (13,225 m^3)	838 m^3 (1,243 m^3)
Estimated total capacity of eligible cisterns	780 m^3	60 m^3 (90 m^3)
Eligible cisterns with sufficient roof area	6	1 (3)
Rabba		
Roof area required, per cistern	514 m^2	119 m^2
Potentially eligible cisterns	12	8
Distance to nearest rooftop		
min. - max.	7-74 m (11-76 m)	0-211 m (30-146 m)
mean	39 m (31 m)	95 m (77 m)
standard deviation	23 m (19 m)	70 m (41 m)
Total area of eligible rooftops	61,696 m^2 (73,627 m^2)	21,918 m^2 (22,362 m^2)
Annual runoff from eligible roofs	15,609 m^3 (18,628 m^3)	5,545 m^3 (5,658 m^3)
Estimated total capacity of eligible cisterns	1,560 m^3	240 m^3
Eligible cisterns with sufficient roof area	12	8
Jad'a		
Roof area required, per cistern	526 m^2	121 m^2
Potentially eligible cisterns	-	12 (13)
Distance to nearest rooftop		
min. - max.	-	63-166 m (24-187 m)
mean	-	124 m (93 m)
standard deviation	-	25 m (44 m)
Total area of eligible rooftops	-	19,114 m^2 (21,497 m^2)
Annual runoff from eligible roofs	-	4,721 m^3 (5,310 m^3)
Estimated total capacity of eligible cisterns	-	360 m^3 (390 m^3)
Eligible cisterns with sufficient roof area	-	12
Smakiya		
Roof area required, per cistern	570 m^2	132 m^2
Potentially eligible cisterns	10	-
Distance to nearest rooftop		
min. - max.	0-154 m (2-78 m)	-
mean	58 m (35 m)	-
standard deviation	53 m (26 m)	-
Total area of eligible rooftops	41,987 m^2 (39,084 m^2)	-
Annual runoff from eligible roofs	9,573 m^3 (8,911 m^3)	-
Estimated total capacity of eligible cisterns	1,300 m^3	-
Eligible cisterns with sufficient roof area	7	-

Table 26 continued

Settlement	Allegedly old cisterns, "Roman Wells"	Presumably modern cisterns
Mghayyer		
Roof area required, per cistern	542 m^2	125 m^2
Potentially eligible cisterns	11	12 (13)
Distance to nearest rooftop		
min. - max.	2-117 m (3-117 m)	29-243 m (31-246 m)
mean	50 m (49 m)	164 m (171 m)
standard deviation	40 m	66 m (66 m)
Total area of eligible rooftops	26,366 m^2 (23,369 m^2)	1,001 m^2 (775 m^2)
Annual runoff from eligible roofs	6,328 m^3 (5,585 m^3)	240 m^3 (185 m^3)
Estimated total capacity of eligible cisterns	1,430 m^3	360 m^3 (390 m^3)
Eligible cisterns with sufficient roof area	11 (9)	1
Shihan		
Roof area required, per cistern	528 m^2	122 m^2
Potentially eligible cisterns	-	7
Distance to nearest rooftop		
min. - max.	-	40-205 m (30-215 m)
mean	-	115 m (139 m)
standard deviation	-	73 m (69 m)
Total area of eligible rooftops	-	7,003 m^2 (2,739 m^2)
Annual runoff from eligible roofs	-	1,723 m^3 (674 m^3)
Estimated total capacity of eligible cisterns	-	210 m^3
Eligible cisterns with sufficient roof area	-	5
Ariha		
Roof area required, per cistern	568 m^2	131 m^2
Potentially eligible cisterns	10	6
Distance to nearest rooftop		
min. - max.	14-177 m	0-137 m
mean	96 m	67 m
standard deviation	42 m	49 m
Total area of eligible rooftops	13,093 m^2	5,123 m^2
Annual runoff from eligible roofs	2,998 m^3	1,173 m^3
Estimated total capacity of eligible cisterns	1,300 m^3	180 m^3
Eligible cisterns with sufficient roof area	8	6
Mis'r		
Roof area required, per cistern	537 m^2	124 m^2
Potentially eligible cisterns	-	10
Distance to nearest rooftop		
min. - max.	-	29-240 m
mean	-	137 m
standard deviation	-	72 m
Total area of eligible rooftops	-	9,966 m^2
Annual runoff from eligible roofs	-	2,412 m^3
Estimated total capacity of eligible cisterns	-	300 m^3
Eligible cisterns with sufficient roof area	-	6
al-'Aliya		
Roof area required, per cistern	560 m^2	129 m^2
Potentially eligible cisterns	2	3
Distance to nearest rooftop		
min. - max.	47 m / 199 m	60-167 m
mean	-	111 m
standard deviation	-	44 m
Total area of eligible rooftops	9,917 m^2	8,970 m^2
Annual runoff from eligible roofs	2,301 m^3	2,081 m^3
Estimated total capacity of eligible cisterns	260 m^3	90 m^3
Eligible cisterns with sufficient roof area	2	3

Table 26 continued

Settlement	Allegedly old cisterns, "Roman Wells"	Presumably modern cisterns
Hmud		
Roof area required, per cistern	551 m²	127 m²
Potentially eligible cisterns	23	4
Distance to nearest rooftop		
min. - max.	0-86 m	16-218 m
mean	35 m	145 m
standard deviation	26 m	81 m
Total area of eligible rooftops	16,087 m²	1,247 m²
Annual runoff from eligible roofs	3,797 m³	294 m³
Estimated total capacity of eligible cisterns	2,990 m³	120 m³
Eligible cisterns with sufficient roof area	13	2
Abu Traba		
Roof area required, per cistern	575 m²	133 m²
Potentially eligible cisterns	17	-
Distance to nearest rooftop		
min. - max.	2-60 m	-
mean	32 m	-
standard deviation	19 m	-
Total area of eligible rooftops	11,221 m²	-
Annual runoff from eligible roofs	2,536 m³	-
Estimated total capacity of eligible cisterns	2,210 m³	-
Eligible cisterns with sufficient roof area	15	-
Total, all settlements		
Roof area required, per cistern	544 m²	126 m²
Potentially eligible cisterns	91	64 (67)
Distance to nearest rooftop		
min. - max.	0-199 m	0-243 m
mean	47 m	126 m
standard deviation	41 m	68 m
Total area of eligible rooftops	236,605 m² (238,673 m²)	77,655 m² (77,592 m²)
Annual runoff from eligible roofs	57,370 m³ (57,981 m³)	19,027 m³ (19,030 m³)
Estimated total capacity of eligible cisterns	11,830 m³	1,920 m³ (2,010 m³)
Eligible cisterns with sufficient roof area	74 (72)	44 (46)

Together, the extents of all rooftops within the radius of 250 m around cisterns constitute the total area of eligible rooftops. For each settlement, as well as the whole study area, the corresponding figures were computed separately for the two categories of cisterns, old and modern ones. The individual results depended on the total number of eligible cisterns, the locations of the cisterns, and the number and extents of rooftops in their surroundings. In line with the previously described findings, for the study area as a whole, the total area of qualifying rooftops is about two times bigger for the old cisterns than that for the modern ones (see Table 26). However, for individual settlements, figures and proportions can vary significantly. The amount of potentially harvestable runoff was computed based on the identified total area of eligible rooftops and the mean annual runoff per m² of rooftop in the respective settlement(s). Here, differences in annual precipitation, according to the locations of individual rooftops, appeared to have rather negligible effects on calculated runoff quantities. Obviously, the latter primarily depend on the total area of eligible rooftops. Therefore, when considering the whole study area, the difference between old and modern cisterns, in regard to the estimated annual amount of runoff from

nearby rooftops, is largely proportional to the respective total area of these rooftops (see last section in Table 26). The calculated quantities of annual runoff from rooftops, identified in the vicinity of cisterns, are considered the readily exploitable RRWH potential, which could probably be tapped with the existing RWH infrastructure and minor amendments.

The amount of runoff from rooftops close to cisterns was then compared to the overall storage capacity of the cisterns labeled as suitable for RRWH (see Table 26). This allowed determining to which degree the runoff quantities and storage potentials computed for each settlement, and for the study area as a whole, matched each other. Thus, possible deficits in catchment areas or storage capacities could be identified. Overall, the findings show a significant surplus in annual runoff from rooftops close to cisterns, compared to the storage potential of the existing eligible cisterns. The total storage capacity of all old and all modern cisterns that were regarded as possibly suitable for RRWH, respectively corresponds to about 20% (old cisterns) and 10% (modern cisterns) of the annual runoff from rooftops in their vicinity (see Table 26, last section). However, with regard to individual towns or villages, the proportions between runoff quantity and storage potential can differ strongly. Depending on the settlement, between less than 10% (e.g. in Qasr) to nearly 90% (e.g. in Abu Traba) of the annual runoff from eligible rooftops could probably be stored in nearby old cisterns (see Table 26). The percentage of runoff that the modern cisterns in the vicinity of buildings could likely contain varies considerably from settlement to settlement. Normally, annual quantities of runoff from eligible rooftops by far exceed the storage capacity of nearby modern cisterns. The exception is the case of Mghayyer, where the storage potential of the eligible modern cisterns is substantially higher than the estimated runoff from rooftops in their vicinity (see Table 26).

The comparison of the described runoff and storage figures provided a first overview of their proportions and further insights into the RRWH potential and possible options for improvement in this regard. Yet, the summarized findings for individual settlements, or the whole study area, may obscure spatial disparities and discrepancies on a smaller scale. Therefore, assumed storage volumes and estimated amounts of annual runoff from nearby rooftops were compared at the level of individual cisterns. Several rooftops had more than one cistern within the analyzed radius of 250 m. The areas of these rooftops and the associated runoff were partly ascribed, with equal shares, to each of the nearby cisterns. Overall, among the cisterns classified as potentially suitable for RRWH, about 80% of the allegedly old and around 70% of the presumably modern ones have sufficiently large rooftop areas in their vicinity (250 m radius) to harvest adequate amounts of runoff to fill them once a year (see Table 26). Again however, these average figures do not necessarily reflect the circumstances in individual settlements, as those can vary considerably. In almost all of the towns or villages, the majority of old cisterns are surrounded by sufficiently large rooftop areas. Hmud represents an exception in this regard, since here, only slightly more than half of the eligible old cisterns have rooftop areas of adequate extents in their proximity. This village also exhibits the highest number of old cisterns close to buildings, i.e. potentially suitable for RRWH (see

Table 26). The highest number of modern cisterns in the proximity of buildings were found in Jad'a and Mghayyer. In Jad'a, all of these cisterns were surrounded by sufficiently large rooftop areas. In Mghayyer, in contrast, only the rooftop area in the vicinity of one out of the 12-13 eligible modern cisterns was big enough for the collection of an adequate amount of annual runoff (see Table 26).

The described findings reveal compatibilities and mismatches between the RRWH potential, i.e. the estimated annual runoff from rooftops, and storage capacities, on the local scale of individual cisterns. The collected data also allows determining the dimensions of discrepancies and the locations concerned. Thus, possibilities and obstacles for the integration of individual cisterns into RRWH schemes can be identified. In general, the old cisterns appear to be particularly suitable for RRWH, in comparison to the modern ones. This conclusion was drawn from the higher number of old cisterns found in proximity to buildings, the high percentage of objects in this group that had sufficiently large rooftop areas in their vicinity, and the typically closer proximities between old cisterns and nearby rooftops (see Table 26).

Individual findings, such as the number of cisterns and rooftops eligible for RRWH in a given settlement or the number and total area of rooftops in the vicinity of a specific cistern, can differ slightly, depending on whether (semi-) automatic image classification outcomes or reference data are used as rooftop information in the analyses (see Table 26). This is a direct consequence of the discrepancies between the two datasets (see 5.2). For individual locations, this can lead to strongly differing findings, e.g. concerning the suitability for RRWH or the RRWH potential. However, with regard to the estimated RRWH and storage potentials in many settlements, and particularly in the study area as a whole, the differences in results are rather small, with discrepancies of less than 5 % (whole study area, see Table 26).

7 Interpretation and discussion of results

In this chapter, the outcomes presented in chapter 6 are interpreted and discussed with regard to the research questions outlined in the introduction (see chapter 1, Table 1). The interpretation is based on a synoptic view of the gathered information and individual findings. The quality of the collected data and outcomes and the resultant implications for their use and interpretation are discussed. Findings are compared to those of previous studies and possibilities for enhancement, upgrading, and extension are pointed out. Moreover, the employed methods and materials (see chapters 4 and 5) are evaluated with regard to specific advantages and disadvantages, their suitability for the objectives of the present study, and possible effects on outcomes.

7.1 Quality, suitability, and limitations of the rainwater harvesting inventory

The RWH inventory can be assumed to be highly reliable in regard to the existence and locations of the listed RWH structures. This high correctness can be attributed to the multi-method approach in which remote sensing techniques and field work were employed together for the acquisition and evaluation of the data. Information gained through field work, including GPS recordings, was used in the training stages of the remote sensing-based analyses and as ground truth for the assessment of the data collected with remote sensing techniques. This sandwich approach, in which remote sensing analyses were framed by precedent and subsequent field work, ensured the best possible accuracy and reliability in outcomes, as well as a precise evaluation of the quality of the RWH database. The application of remote sensing products and techniques enabled the time-efficient analysis of a larger area, which would not have been possible with field work alone. The absence of a significant vegetation cover for the most part, and the very high resolution of the satellite imagery, facilitated the image interpretation and the mapping of the RWH structures. Additionally, structures that resembled RWH objects in some ways, but could not clearly be identified as ones, were assigned to a separate category in the remote sensing-based mapping process. Thus, the higher uncertainties associated with these structures could not decrease the overall accuracy of the whole RWH inventory. The described image interpretation and detection problems only occurred in the mapping of cisterns, which in general were more difficult to identify in the satellite image than other, e.g. linear structures, such as bunds, ridges, dikes, and check dams. Including these ambiguous objects as "possible further cisterns" in the database ensured the best possible completeness of the RWH inventory. Thus, locations for further ground checks were marked and the likely range of uncertainty concerning the number of actually existing RWH facilities could be determined.

A tendency towards overestimation or false positives, i.e. the assumption of RWH facilities where in reality there are none, could nearly be excluded in the mapping process. However, each of the employed methods was linked to individual possibilities of underestimation of the actual number of RWH structures. The GPS-based mapping of RWH facilities, primarily cisterns, in the first field survey essentially depended on the knowledge of the local guides and the accessibility of sites. Therefore, cisterns and other structures which are located in hidden, inaccessible spots or on private property or are largely unknown to the local community, could have been missed. Similarly, remote sensing-based mapping approaches that rely on the interpretation of optical satellite images do not allow for the detection of e.g. cisterns integrated into buildings, structures hidden by vegetation or clouds, or objects otherwise obscured from direct view. These structures, which are not visible in the satellite imagery, have to be mapped with other methods, such as field surveys. However, the remote sensing-based approach offers the systematic overview and "access" to all areas which is not provided in field surveys. Hence, through a combination of both mapping approaches, the shortcomings of each method can be counterbalanced and overcome. Since the employed mapping procedure included both methods, an enhanced, good degree of completeness is assumed for the established RWH inventory. When further information becomes available, the created database can readily be expanded, updated, and improved.

In regard to the defined categories of RWH facilities, some degree of uncertainty had to be accepted for the two classes of cisterns. While the discrimination between cisterns and other RWH structures, such as check dams, bunds, dikes, and the like, was straightforward and unambiguous, the further classification of cisterns into ancient or (very) old and modern ones had to be based on several details and pieces of evidence. Besides the statements of local residents and community leaders, construction details offered further valuable clues to the likely ages of the cisterns. However, only a small number of cisterns could be examined in detail, from the inside. Hence, for the majority of cisterns this detailed information was not available. Further evidence could be derived from the results of the proximity analyses. In contrast to the presumably modern cisterns, the allegedly old cisterns were frequently found in close proximity to archaeological sites. This finding was considered an additional indication for the similarly old, likely ancient ages of the cisterns that had tentatively been labeled as old. Thus, with respect to the groups of old and modern cisterns on the whole, the evidence seemed sufficient to support and justify the differentiation and classification.

The ages of individual cisterns could be determined more certainly with absolute dating methods. Plaster linings inside cisterns frequently contain small pieces of charcoal, which can be dated with the radiocarbon or 14C method (e.g. LICHTENBERGER ET AL. 2015). However, this requires that the original plaster lining has been preserved, which may not be the case for all old cisterns. Since many cisterns were used over a long period of time or are still in use today, later modifications and repairs are common. These often include the renovation of the plaster lining to ensure an optimal water holding capability. Hence, the age of the plaster lining not necessarily always corresponds to the age of the cistern itself.

Besides these restrictions, absolute dating would be feasible only for a small number of selected cisterns, due to the involved efforts and costs. Findings then could not be applied to other cisterns without accepting huge uncertainties. Cisterns were probably built during all phases of history and similar materials and construction techniques were often used over several centuries and in different cultural settings. Hence, the upscaling potential and the transferability of insights gained from the absolute dating of a few cisterns are limited. Consequently, absolute dating methods can offer further clues but most likely no definite answers concerning the age distribution of the cisterns in the study area.

Some uncertainties also exist in regard to the conditions and functionality of many of the mapped RWH structures, and the storage capacities of cisterns in particular. Estimates of the total storage capacity of all cisterns in the study area were based on several assumptions. These include the (mostly) correct classification of the cisterns into old and modern ones, the different average cistern sizes for the two named groups, and finally, the appropriateness of the determined typical storage capacities. Information on the latter was derived from external sources (other studies), in the case of modern cisterns, and a limited amount of data (measurements from cisterns inspected inside) collected during field work, in the case of the old cisterns. Additional data could probably enhance the validity, reliability, and accuracy of the findings (mean figures and total estimates). The collected data already illustrate the high variability in storage volumes of individual cisterns. Therefore, the application of average figures cannot sufficiently represent individual circumstances and available storage capacities at specific sites. For optimal planning of new RWH schemes and measures or new construction intended to rehabilitate, enlarge, or otherwise improve existing RWH facilities, the information gathered in the present study could be complemented by further data from field surveys and the examination of more cisterns.

To adequately evaluate the outcomes of the present study, the findings are compared to those of previous studies. Thus, common traits and general patterns, as well as local particularities can be identified. Additionally, the transferability and upscaling potential of the results can be gauged.

The RWH structures examined in the study at hand, particularly the cisterns, exhibit strong similarities to RWH facilities found at other sites, e.g. in Jordan at ancient Nakhl (MATTINGLY ET AL. 1998) and in Madaba (BIKAI 2004), at Shivta in Israel (TSUK 2002), in Syria and Egypt (ALI ET AL. 2009), as well as in many other parts of West Asia and North Africa (OWEIS ET AL. 2004). In regard to several construction details, such as shapes, collar stones, and patterns in plaster linings, the cisterns in the study area parallel those discovered at a number of archaeological sites in the broader region (cf. PACE 1996, BASTERT & LAMPRICHS 2004, KEILHOLZ 2007). This significant overlap in findings underpins the estimation that many of the cisterns in the study area date back to ancient, e.g. Roman, Nabataean, Hellenistic, or Byzantine times. Despite the large similarities, the RWH infrastructure of a given area typically slightly differs from that of another region, e.g. with respect to some of the construction materials or techniques used. For example, at some places, mainly or only, rock-cut or built cisterns are found, whereas at other sites, cisterns were roofed with stone slabs or developed from natural caves (OLESON

1991, AL ZEEZ SHQAIRAT ET AL. 2010). These variances are, most likely, rooted in different cultural influences and periods of construction, as well as the specific environmental circumstances at a given site. A broad variability can also be observed in the documented shapes and sizes of cisterns. Storage capacities can range from just a few cubic meters to several thousands (WÅHLIN 1997, OWEIS ET AL. 2004, KOELBEL 2009, ASSAYED ET AL. 2013, MAYS ET AL. 2013). With volumes of ca. 30-230 m^3, the cisterns of the study area rank among the small to medium ones. Differences in cistern sizes may represent adaptations to the respective environmental conditions at a given location. Geological circumstances and anticipated harvestable runoff quantities, which result from annual precipitation amounts and extents and characteristics of available catchment areas, can constitute limiting factors. Additionally, cisterns are dimensioned according to the amount of water that needs to be stored. Thus, individual storage capacities depend on the water demand and its spatial distribution. These aspects again are influenced by socio-political circumstances. Important factors in this regard are population figures and the structure of cistern ownership, i.e. whether cisterns are mostly private or community property. The storage capacities of the "Roman Wells" or old cisterns in the study area suggest a rural setting in the past, in which each cistern covered the water demands of a relatively small number of residents and their domestic animals, and was typically family owned (cf. WÅHLIN 1997). The more recently constructed, modern cisterns are usually significantly smaller. One reason for this could be changes in feasibility. Modern excavation machinery most likely facilitated the construction of cisterns in a broader variety of geological conditions and led to a relative reduction in the investments required to build a new cistern. Additionally, today, more cisterns are probably owned privately, by individuals or small groups of people. The smaller storage volumes of modern cisterns may also reflect the different role of cisterns today. Changes in the purposes of use of cistern water and the availability of alternative sources of freshwater may have led to decreases in the amount of water needed to be harvested and stored at a given location. Together, the described aspects can probably explain the smaller sizes and increased number of modern cisterns, which are distributed over many different sites – in other words, the extensification of RWH and cistern use.

The data on existing RWH structures that is available from other sources is scarce and limited to cisterns. For the northern Karak Plateau, LANCASTER & LANCASTER (1995a) created a map showing the locations of individual cisterns or groups of cisterns that were used during the period 1990-1993. However, no information about the number of objects – in total or at individual sites – was provided. In its census of 2015, for the governorate of Karak, the Jordanian DEPARTMENT OF STATISTICS (2015) lists 346 housing units as relying on rainwater and/or a well as the main source of drinking water. ASSAYED ET AL. (2013) claim to have founded 222 cisterns in the same area. In the present study, 389 cisterns were definitely identified in a subarea of the Karak governorate. The extent of this subarea corresponds to only about 4% of the governorate's total area. In light of this, the figures given by ASSAYED ET AL. (2013) and the DEPARTMENT OF STATISTICS (2015) obviously cannot nearly reflect the possible number of actually existing cisterns in the whole governorate. The described limitations of the available data underpin the

necessity for a comprehensive, current database of existing RWH structures. The latter represents the essential foundation for all spatial planning tasks in regard to RWH, since it helps to ensure that the plans and efforts match the specific regional circumstances. Moreover, such a database is particularly indispensable for larger RWH projects in which individual efforts need to be coordinated.

7.2 Evaluation of methods and materials: advantages and limitations of the applied remote sensing and GIS techniques and quality of the resulting data

This chapter discusses the advantages and limitations of the methodological approaches adopted in this study. In particular, the suitability and applicability of the employed methods and datasets for research, planning, and management purposes, in relation to RWH, are reviewed. The evaluation focuses on remote sensing products and techniques as well as GIS procedures and analyses, as these were used in the acquisition, processing, and analysis of the data. In conjunction with the procedures, the quality and suitability of the input and output data, including intermediate results, such as the LU/LC and the rooftop data, are also discussed. Methodological aspects, specifically pertaining to the RWH data base and its creation, have already been presented in the previous section and therefore are not part of this chapter.

7.2.1 Opportunities and limitations linked to the remote sensing-based approach

One major advantage of the application of optical remote sensing is its ability to provide an overview and unrestricted access to all areas of the world. In contrast to field surveys, satellite images allow the expeditious examination of larger areas, typically with reduced risks and efforts, and fewer expenses. The imagery provides a bird's eye view of the area, which facilitates the mapping of structures that are not (easily) recognizable from a pedestrian's point of view or are located in terrain that is difficult to access. However, due to this fixed perspective, some features in the images, particularly smaller ones at ground level, such as cistern manholes, can be obscured by larger, possibly overhanging, nearby objects, e.g. trees. What is similarly ambivalent is the inherent characteristic of images to "freeze" a specific point in time, i.e. to depict the situation at the moment of image recording. All data derived from the imagery also refer to the date of image recording; a circumstance which can interfere with the need for up-to-date information. This limitation can be overcome with the acquisition, interpretation, and comparison of several satellite images recorded at different points in time. Thus, for example, seasonal variations in plant cover, as well as all kinds of other temporal or permanent changes in LU/LC, can be identified. This allows the creation of enhanced derivative information products, e.g. LU/LC maps, and

provides insights into change dynamics and the development of a region. The fact that each image documents a situation at a specific time also represents an opportunity, as older satellite images, e.g. the declassified ones of the former US military satellite CORONA, can serve as windows into former times. Through analysis and interpretation of these images, long-term changes, particularly in regard to profound differences in LU/LC and the state of natural and cultural heritage sites, can be traced and assessed.

The suitability of a given satellite image for a specific purpose, e.g. a certain mapping, research, or planning task, largely depends on the image characteristics, particularly the spatial resolution. The latter crucially influences whether the target objects or structures are recognizable in the imagery and hence, the desired information can be extracted. The use of VHR satellite images, such as the one employed in the present study, enables the recognition of a broad variety of details and (small) objects, e.g. individual buildings and RWH structures. As US federal regulations, which previously restricted the resolution of commercially available satellite images to 0.50 m for civil purposes, including research, were modified in 2014, remote sensing products with even higher spatial resolutions became available. Further advances in technology, the launch of new satellite sensors, such as WorldView-3 and SuperView-1 (GaoJing-1), and the continuance of earlier launched satellite missions, together, enhance the availability of VHR remote sensing products. The broader variety of images and reduced prices for selected products, such as archived images of some satellite sensors, offer new opportunities for the use of remote sensing, e.g. for various research or spatial planning tasks and objectives. Through the ongoing integration of new VHR satellite images into applications like Google Earth, the wider public, too, gains access to this type of remote sensing products. Hence, the amount and quality of derivative information, e.g. on the locations of RWH facilities and new buildings, can also be easily increased and improved. Yet, data from field studies is still indispensable to complement remote sensing-based information.

7.2.2 Currentness and validity of the remote sensing-based data

All information derived from the GeoEye-1 satellite imagery refers to its recording date(s) in July 2010. The respective degree of validity, which can be assumed for the individual datasets in the medium to long term, depends on the involved LU/LC change dynamics. The general character of the study area continues to be a rural one and the overall pattern of LU/LC remains relatively stable, with only moderate, gradual changes over time. This can be confirmed from recent satellite images (e.g. from 2017), e.g. via Google Earth. Along with increases in local resident numbers, a general trend towards further surface sealing can be observed. This encompasses the expansion of existing settlement areas and related infrastructure. Hence, with regard to the established LU/LC map and the respective shares of the individual classes, a slowly progressing shift from pervious to impervious can be expected. Pervious areas adjacent

to impervious ones, especially settlement areas, are most likely to be converted, thus forming larger, contiguous, impervious regions. As the number of buildings increase, RRWH potentials are modified too. This applies to the total amount of runoff from rooftops as well as the spatial distribution of the potential. However, these developments are expected to occur at a moderate pace, resulting in gradual changes over time.

A relatively high medium- to long-term validity is assumed for the vegetation data collected in the present study, at least with regard to possible interannual differences in the plant cover of the specific season. Since the satellite imagery, from which the vegetation information was extracted, was recorded in July, the mapped vegetation is that of the summer half year. The (photosynthetically active) vegetation during this part of the year primarily consists of permanent plants, such as trees, and, to a lesser extent, of other, e.g. annual, plants grown in horticulture. Therefore, major interannual variances in the extent and the spatial distribution of the summer vegetation are rather unlikely. However, due to the strong seasonal differences, the collected vegetation data does not allow for the estimation of the extent of the plant cover during the winter half year. Additionally, the latter can vary strongly from year to year, due to interannual differences in precipitation.

In regard to the drainage line data and its validity in the long term, the environmental circumstances which may facilitate rapid changes in the drainage line network, need to be considered. In (semi-) arid areas with flat terrain, the runoff from a single intense rainfall event can alter the courses of shallow wadis. Moreover, small drainage lines may be modified, e.g. enlarged, and new rills and gullies, which often later develop into wadis, may form. One area that is particularly prone to some of the described changes is the central part of the Karak plateau, around ar-Rabba and Qasr, where wadis are not deeply incised and the terrain is mostly flat. The northern part of the study area, in particular, exhibits a heightened risk of (linear) erosion. This results from several factors, most notably, the LU/LC and the area's proximity and large altitudinal differences to the local erosion base. Thus, the conditions in this area facilitate the formation and enlargement of rills, gullies, and other small drainage lines.

For the RWH inventory of the area itself, minor to moderate changes over time are anticipated. Besides existing facilities and currently applied RWH practices, there are also efforts to increase the adoption of RWH measures. Consequently, the total number of RWH structures is growing. The recently built cisterns, and those under construction at the time of the field studies, attest to this trend. Shifts in environmental conditions and LU/LC patterns, as described above, may lead to the abandonment or modification of RWH practices and associated facilities. The capital, material, and labor investments necessary for the construction of new RWH structures imply that only a limited number of new schemes can usually be built within a given period of time, and thus, established, functioning facilities are mostly valued and maintained. Hence, the spatial distribution and total number of RWH objects probably change rather slowly, with minor to moderate degrees of modification.

7.2.3 Methodological evaluation of the preprocessing, analysis and interpretation of the satellite imagery

The quality of the data derived from satellite images is also influenced by the level and suitability of the preprocessing applied to the imagery. Here, the atmospheric corrections of the GeoEye-1 imagery were particularly time consuming, as they entailed a substantial amount of empirical testing of settings, parameters, and adjustments to obtain satisfying results. This was necessary since standard procedures and recommendations were mostly not available. However, the procedure was considered indispensable to ensure optimal outcomes in the subsequent image analysis and interpretation. Moreover, insights gained in the present study can be used to facilitate and accelerate similar tasks, such as the preprocessing of GeoEye-1 and comparable VHR satellite images. Thus, further secondary information, e.g. updates on the rooftop, LU/LC, and RWH data, can be obtained more quickly as well.

For the analysis and interpretation of VHR satellite images, and thus, the extraction of the desired information, several methods and techniques are available. Despite the variety of different (semi-) automatic approaches that have been developed so far, the visual image examination and manual digitization of target areas or objects by a trained user often still outperform these methods. The main reason for this is the complexity of human visual perception and decision making. In the image interpretation process, users incorporate a variety of information, such as the shapes, colors, sizes, and environment of the target objects or areas. To obtain similarly suitable or even better results through (semi-) automatic analysis and classification of images, the software Feature Analyst tries to mimic human visual perception (see chapter 4.1.2.3). Additionally, FA relies on a machine learning approach, in which an individual set of classifiers – an ensemble of established algorithms – is developed and used for each image classification task (cf. 4.1.2.3). This equips the software with a high adaptability to diverse images and different classification objectives and circumstances. However, when analyzing images, human operators also employ all background knowledge they have in relation to the specific interpretation task. This unique ability of the human user can hardly be emulated by technology, even with machine learning approaches. Most of the latter developed so far, including FA, can also be described as template matching approaches, as the software "learns" to identify certain objects or areas based on their similarity to the examples given by the user. The quality of the outcomes in these cases crucially depends on the appropriateness – in terms of both, quality and quantity – of the training data provided by the user. With adequate training data, machine learning methods can represent sophisticated and powerful tools of (semi-)automatic image analysis, particularly for VHR imagery, as the results of the present study show. Yet, for certain tasks, visual-manual image interpretation by an expert is still indispensable. This particularly applies to target objects or areas that are very small and/or exhibit a large heterogeneity in their appearance, such as e.g. the RWH structures mapped in this study. Major drawbacks of the visual-manual image interpretation are that the method is usually time-consuming, labor-intensive, and depends on the availability of suitable, trained personnel (cf. e.g. BLUNDELL & OPITZ 2006). Additionally, outcomes

produced by different users can exhibit considerable differences (cf. e.g. PAUL ET AL. 2013), which result from natural, mostly inevitable, personal variances in perception and decision making. In contrast, (semi-) automatic image analysis, when applied successfully, can be more time-efficient, can reduce labor costs, and can lead to consistent, high-quality results (cf. e.g. O'BRIEN 2003, QUACKENBUSH 2004, OPITZ & BLUNDELL 2008b). Often the combination of both approaches, e.g. by manually editing and/or completing (semi-) automatic image classification results, is suggested or applied, in order to optimally exploit the complementary advantages of both methods (e.g. TSAI ET AL. 2011, PAUL ET AL. 2013, CAGGIANO ET AL. 2016).

Aside from these general methodological considerations, the semi-automatic image analysis and interpretation approach adopted in the present study is characterized by several specific advantages and disadvantages. Most of these are directly linked to the properties and the functionality of the employed software. One major advantage of FA is the simplicity of its user interface and workflows, compared to other (true) OBIA software solutions, such as e.g. eCognition. For each 'learning' or classification pass, the user essentially needs to digitize – or select, during hierarchical learning – suitable training examples. This task largely corresponds to visual-manual image interpretation. The actual image classification or object extraction is then performed automatically by the software. The learning settings comprise a number of parameters, which can be configured as necessary for the respective task (see 4.1.2.3). However, at this point, the user can also choose a template, which then automatically sets all learning parameters to suitable values. Templates are available for a variety of common object extraction and image classification objectives. These characteristics, particularly the high degree of automation and the use of training examples, make the workflows in FA largely intuitive and easy to learn. Thus, for the successful application of FA, less training is required than for most other OBIA software solutions. The latter commonly rely on image segmentation and a subsequent rule-based classification of these segments, instead of training examples and machine learning. Therefore, users typically need to specify and configure a comparatively complex set of (abstract) parameters and rules. To obtain suitable classification results, comprehensive expert knowledge and training is usually required to understand and manage the intricate interplay of individual parameters and to master the application of the software. At the same time, the high degree of automation also constitutes a fundamental disadvantage of FA. Large parts of the software's functionality, including crucial information on how many and which algorithms are involved in a specific classification pass, are "hidden behind the scenes" and remain inaccessible to the user. While this perfectly serves to protect the proprietary nature of the software, it also renders much of the sophisticated functioning of FA intransparent. Decisive parameters cannot be identified and the classification process cannot be totally reconstructed.

Another drawback of the FA approach is the strong dependence of the (quality of the) results on the training data provided by the user. This includes the initial examples, as well as those provided during hierarchical learning. Any variations in these samples can lead to significant differences in outcomes,

even when all learning parameters remain identical and the training data evidently does not change in terms of quality or quantity. Therefore, image analysis results are difficult, to virtually impossible, to reproduce. Every training dataset differs at least slightly from another, even if both were digitized by the same person, and probably even more so if several users were involved in the digitization process. Nonetheless, through trial and error, and with some effort, it is usually possible for different users and with different training data to obtain image classification results of comparable quality. Although outcomes are typically not identical, their accuracy, completeness, and reliability can be at a very similar level at the same time.

An additional positive aspect of FA is the automatic generation of AFE models for all classification cycles. Thus, for all outputs, including intermediate ones from a multi-stage hierarchical learning procedure, a corresponding AFE model is available. Through thorough evaluation, the most suitable results can be identified and the corresponding classification model can be applied to other images to analyze and interpret them in the same fashion. Thus, the desired information can be easily and quickly extracted, and in a consistent manner from a larger set of images, which are typically needed to cover a broader area or for change detection purposes. Normally, the transferability of a given classification model is limited to images that are similar to the initial one, based on which the model was established. However, with additional training data and further learning passes, an existing AFE model can be refined to better suit a particular image and thus, improve the corresponding outcomes. In any case, even if the model needs to be adjusted, the batch processing function, i.e. the application of an existing AFE model to another image, allows the time-efficient and effortless production of first classification results. The benefits of this approach and the transferability of AFE models have been demonstrated in the present study for different image classification objectives, such as the detection of rooftops and vegetation areas.

The performance of FA was especially convincing, exceeding expectations, in the detection of rooftops. The target objects – mostly flat concrete rooftops – exhibited large similarities to a variety of other areas, in terms of spectral characteristics ("color"), sizes, shapes, and environment. Therefore, the identification and delineation of these rooftops represented a particularly challenging task for any image analysis software. This generally applies to most cases of (semi-) automatic mapping of buildings (i.e. building footprints) or rooftops in satellite or aerial images. The good performance of FA in regard to this task, i.e. the extraction of building data from VHR satellite imagery, particularly in comparison to other, similar software solutions, such as ENVI FX, has also been pointed out by TSAI ET AL. (2011). The special ability of FA to produce particularly suitable outcomes for the discussed task probably results from the machine learning approach, which incorporates genetic algorithms and ensemble learning, whereas most other software solutions rely on a singular specific classification algorithm and approach.

7.2.4 Quality and suitability of the land use/land cover and rooftop data derived from the satellite imagery

The LU/LC and the rooftop data, which were derived from the GeoEye-1 satellite image through (semi-) automatic image analysis and interpretation, both exhibited an expedient, good quality and were suitable for the purposes of the study at hand. These overall findings were based on a comprehensive evaluation of the data, which included both a thorough visual examination and a detailed accuracy assessment. The importance and value of visually assessing image classification outcomes has been emphasized by MLADINICH (2010). Additionally, a systematic accuracy assessment is indispensable, since it allows for the quantitative evaluation and expression of quality, by means of numerical data and statistical measures, such as the overall, the user's, and the producer's accuracy, and the kappa coefficient.

A minimum value of 85% in some of the traditional statistical measures of accuracy (at least the overall accuracy) has often been suggested as the desired level of accuracy for data obtained through (semi-) automatic classification of satellite images (FOODY 2008). This recommendation resulted from the need to define a threshold that would indicate a satisfactory quality of the data, based on the accuracy assessment outcomes. Although the aforementioned value can represent a feasible and reasonable goal for some classification tasks, for others, it may induce undue and disproportionate harshness in the evaluation of the outcomes (FOODY 2008). Depending on the imagery, the specific analysis and interpretation goals, the details of the accuracy assessment procedure, and similar aspects, accuracies of 85% and higher can be difficult or impossible to obtain with reasonable efforts. Moreover, for many purposes and under several circumstances, image classification results with lower accuracies may still be well acceptable. For this reason, the acceptance and use of image-derived data with accuracies below the aforementioned threshold is common practice (FOODY 2002).

The produced LU/LC data was characterized by accuracies of around 90% and better, for the overall accuracy, as well as the user's and producer's accuracies of the individual classes (see chapter 5.1 and BAICU 2012). According to BAICU (2012), the unedited, raw image classification outcomes for the impervious and pervious class were associated with a Kappa coefficient of 0.80. For the vegetation detection results, a Kappa value of 0.88 was identified (see 5.1, Table 10). Based on the commonly applied interpretation scale of LANDIS & KOCH (1977), these Kappa values indicate a substantial to almost perfect agreement between the image classification outcomes and the reference data and thus, suggest a high accuracy of the LU/LC data. With the manual editing and refinement of the initial classification results, the accuracy of the data of the pervious and the impervious class most likely further improved in the present study. Hence, the values stated by BAICU (2012) – although based on a rather minimal accuracy assessment – can be considered as the minimum accuracy of the pervious and the impervious class in the final LU/LC dataset (see chapter 5.1). The vegetation data, which was extracted separately here, was characterized by accuracies of over 90% (see 5.1, Table 10). Compared to the above stated

accuracy goal of 85%, the identified values suggest a very high accuracy for the collected LU/LC data. The quality is at a similarly high level throughout the dataset, without significant differences between the individual LU/LC classes. These findings compare well with the results of other studies with similar mapping approaches and image classification objectives (e.g. YUAN 2008, MILLER ET AL. 2009, MADSEN ET AL. 2011, SUGG ET AL. 2014, ZWEIG ET AL. 2015). The high accuracies observed in several studies, including the one at hand, must probably (at least partly) be attributed to the nature of the classification tasks. The definition of only a few, broad LU/LC classes and clear differences between these in terms of spectral signatures, typical shapes, sizes, and environments, facilitate a successful (semi-automatic) image classification, leading to quite accurate outcomes.

Most of the wrongly labeled areas in the unedited image analysis results for the pervious and the impervious class could be associated with a few specific classification difficulties. Particularly in the context of settlement areas, the software was not always able to correctly discriminate between pervious and impervious regions and to accurately capture their boundaries. This difficulty is probably related to the complex pattern of mostly small patches of different pervious and impervious surfaces, which are typically found in these areas. Pervious regions with a shallow soil cover or highly compacted, dry, bare earth can often hardly be distinguished from the dust-covered impervious surfaces of roads, paths, courts, parking sites, and the like, particularly when the different areas of the two classes border on each other. In general, pervious areas with shallow soils, bare rock, or a patchy mixture of both, were often classified as impervious, due to their similarities to some impervious surfaces, such as concrete. The named pervious and impervious (concrete) areas are typically both characterized by high reflectance values in all spectral bands of the satellite image. The described type of misclassification was particularly common in that part of the imagery which showed the southeastern section of the study area. Consequently, a significant part of the manual editing was applied to the classification results for this areas (cf. chapter 4.1.2.4, Fig. 21). SUGG ET AL. (2014) encountered very similar difficulties and flaws in their classification outcomes when mapping impervious surfaces. They suggested that these classification errors could pertain specifically to semiarid areas, in which the vegetation cover is often limited and sparse. Thus, bare, natural, pervious surfaces regularly border on impervious surfaces. At the same time, the areas of both classes are often very similar in regard to their appearance in the imagery. Hence, these circumstances can represent a particular challenge for the accurate and correct delineation of pervious and impervious areas in the semi-automatic image classification process.

The high accuracy commonly observed in semi-automatically extracted vegetation data is at least partly rooted in the distinctive spectral signature of active, i.e. photosynthetic, vegetation. Its high reflectance values in the near infrared (NIR) band of satellite images clearly distinguishes the vegetation from other areas and objects and thus, makes it easy to map. However, this characteristic is absent in inactive or non-photosynthetic vegetation, which consists e.g. of dead or dormant plants. The spectral signatures, sizes, shapes, and contexts of individual features or areas of non-photosynthetic vegetation can vary and

therefore, this subtype of vegetation cannot reliably be identified based on satellite imagery alone, even with visual-manual image interpretation by an expert. The problem could probably be addressed with additional data, e.g. comprehensive ground truth. In the semi-automatic classification of satellite images alone, existing, but photosynthetically inactive, vegetation can easily be confused with other objects and surfaces, particularly shadow areas. This can introduce considerable classification errors in the resulting mapped vegetation data.

In the present study, only the vegetation that could unambiguously be identified visually in the satellite image, was mapped. This primarily encompassed vegetation with some level of photosynthetic activity. To a lesser extent, non-photosynthetic vegetation was included as well, as far as it could clearly be visually recognized in the imagery and thus, suitable training data could be provided for the semi-automatic image classification. The visual identification of the inactive vegetation was usually based on several clues, such as the spectral signature, size, and context (e.g. association with active vegetation), which together formed converging evidence. Nonetheless, the majority of the observed classification errors occurred in areas with a scarce plant cover and/or vegetation with no or very little photosynthetic activity. The accuracy values computed for the vegetation data thus can be regarded as averages, which result from very high accuracies in the regions with photosynthetically active vegetation and lower accuracies in the other areas with a scarce and/or mostly inactive plant cover. Since, here, the active vegetation was primarily mapped, the accuracy values determined for the whole dataset are high. The actual vegetation during summer can be expected to contain a substantial amount of inactive plants, as summer dormancy represents an adaptation strategy to periodic dryness and the climate of the region is semiarid. Yet, the exact extent and spatial distribution of the inactive part of the summer vegetation could not be determined with the employed remote sensing-based methods and data.

Additional data is required for more complete information about the vegetation dynamics in the study area and the plant cover during different seasons. The necessary information could be derived from suitable satellite images recorded at different points in time. Data about the extent, the spatial distribution, and further characteristics of the vegetation in the winter half year would be particularly crucial, also in regard to runoff dynamics and the estimation of runoff. Since almost all of the precipitation occurs during the winter half year, vegetation conditions during this time can have a significant influence on runoff formation, runoff quantities, and associated processes, such as e.g. erosion. This particularly applies to rural areas, such as the one under study, in which agricultural fields, rangeland areas, and other types of open land constitute the dominant types of LU/LC. The vegetation cover and LU/LC pattern in the study area during the winter half year can vary strongly from year to year, according to changes in annual precipitation amounts. To adequately factor in these interannual variances, comprehensive vegetation data should be derived from several satellite images of different years.

In the evaluation and discussion of the rooftop data and its quality, the specific characteristics of this image interpretation task should also be taken into consideration. As mentioned earlier (cf. 7.2.3), the

semi-automatic extraction of rooftop or building (footprint) data from satellite or aerial images, without additional data, usually represents a particularly challenging image analysis and interpretation task. Consequently, outcomes are often characterized by lower accuracies, with noticeable deficits in correctness and/or completeness, compared to the results from other image classification tasks, such as e.g. the mapping of pervious and impervious areas (cf. e.g. OPITZ & BLUNDELL 2008a, PSALTIS & IOANNIDIS 2008, YUAN 2008, MILLER ET AL. 2009). For a fair assessment, the extracted rooftop data should primarily be compared to outcomes from classification operations with similar objectives or equivalent levels of complexity. However, with regard to the rooftop detection carried out here, almost no directly comparable studies exist. Most studies, in which rooftops or building footprints were mapped in satellite images (e.g. DU ET AL. 2009, DINIS ET AL. 2010, FREIRE ET AL. 2010, WIGINTON ET AL. 2010, SANTOS ET AL. 2011), exhibit substantial differences in terms of the employed classification procedure(s), the input data, and the conducted accuracy assessment. Therefore, here, the quality of the rooftop data is primarily evaluated independently, based on the accuracy assessment results.

Firstly, in the visual examination, the delineated features corresponded fairly well to the rooftops discernible in the satellite imagery (see 5.2, e.g. Fig. 34). As emphasized by MLADINICH (2010), the visually perceived quality importantly determines the overall acceptance of the classification results. Secondly, in regard to the total area of rooftops, for most of the settlements, the semi-automatically extracted data showed no severe under- or overestimation (see 5.2, Table 11 and 12). In most cases, the total area of rooftops in the classification outcomes closely matched those in the reference data. With regard to the total area of rooftops in the whole study area, over- and underestimations in individual settlements tended to even out, thus leaving only a marginal difference of 0.5% between image classification results and reference data (cf. 5.2, Table 13). Similarly, WIGINTON ET AL. (2010) reported an absolute error of 15% when comparing the rooftop area in their classification outcomes to that in the reference data. However, they also observed the tendency for over- and underestimation errors to counterbalance each other, which, in their data, led to a remaining difference of 2% between classification and reference data, in regard to the total area of rooftops.

The target accuracy of 85% or higher was met by the overall accuracies of all assessed rooftop datasets. The values of the named index varied between 96 and 99%, while for the data extracted with AFE Model 1 (Qasr), average overall accuracies of 98% were computed (see 5.2, Table 11-13). In contrast, the user's and producer's accuracies for the detected rooftops were significantly lower, mostly ranging between ca. 55 to 65%. Lower or higher values were occasionally observed. Although these figures do not align with the accuracy standard of 85%, they cannot be considered sufficient evidence for an inappropriately low quality in the extracted rooftop data, due to two reasons. Firstly, the accuracy target of 85% was originally suggested for different image classification tasks and broader LU/LC classes, and thus, probably does not represent a reasonable standard for the outcomes of the specific, narrowly defined object

extraction task discussed here. Secondly, for a fair judgment of the quality of the rooftop data, all accuracy assessment results, i.e. the values of the different indices, need to be considered synoptically. In addition to the aforementioned traditional measures of accuracy, the developed object-based indices (feature scores) are able to provide further insights into possible biases and common types of error in the image classification results. On average, 95% of the objects labeled as rooftops in the classification outcomes obtained with AFE Model 1 (Qasr) could at least be partly verified as such (see 5.2, Table 13, feature score user's accuracy, mean), based on a visual assessment of the satellite image (reference data, see 4.1.2.6). In contrast, a considerable number (ca. 33%, on average) of the rooftops in the reference data were not detected by the software and the developed classification model (see 5.2, Table 13, feature score producer's accuracy, mean). Consequently, AFE Model 1, which was selected as the overall most suitable classification model for the detection of the rooftops, can be characterized as highly specific but less sensitive, at least on the object-based level. Overall, the results of the accuracy assessment, i.e. the feature scores and the values of the traditional, area-related measures of accuracy, in combination with the findings from the visual assessment, suggest that FA was able to distinguish fairly well between rooftops and other areas (background). While a varying number of rooftops typically were not recognized by the software (underclassification, false negatives), the classification outcomes contained almost no independent false positives, i.e. discrete features in other areas labeled as rooftops (cf. 5.2). Areas of overclassification usually resulted from the imprecise delineation of correctly identified rooftops and an overestimation of their extent. Hence, in the assessment of the extracted rooftop data, substantial weaknesses in the correct, accurate delineation of the target objects, and thus, the recognition of the precise shapes, sizes, and boundaries of the rooftops, could be identified as the main classification issues. These findings coincide with the classification errors observed by CZEREPOWICZ ET AL. (2012) when detecting shelterbelts in a VHR satellite image with FA.

To correctly interpret the findings, the methodological details of the accuracy assessment procedure also need to be considered, since these can influence results considerably (cf. e.g. STEHMAN & WICKHAM 2011). In the present study, classification outcomes and reference data were compared on the level of individual rooftops. Instead of samples, the complete rooftop detection results of six individually analyzed image tiles were assessed (see 4.1.2.6). Hence, the conducted accuracy assessment was rather detailed and rigorous. This could be one reason why the identified accuracy values here were lower than those presented by DU ET AL. (2009) for the building footprint data they extracted from a KOMPSAT-2 image using eCognition. Their accuracy assessment, which comprised an error matrix, as well as the traditional measure of accuracy, was based on random point samples. Compared to other approaches, the use of single points or pixels as sample units in the assessment can introduce a certain degree of positive bias, particularly when the sample size is also relatively small. As a result, higher accuracies may be identified for the classification outcomes (cf. e.g. CZEREPOWICZ ET AL. 2012).

The evaluation and comparison of the rooftop data extracted from different image tiles revealed that the most suitable and accurate outcomes were usually obtained when an AFE model individually developed for, or adjusted to, the respective image was used in the detection process. However, this classification approach is much more time consuming and labor intensive as the fast, straightforward, and convenient batch processing procedure, which is highly automated and relies on an already established AFE model to extract the desired information. Hence, a certain tradeoff must obviously be accepted between the highest possible quality in outcomes and the fastest, most efficient, and most convenient image classification procedure. Nonetheless, the results of the present study have shown that the (re-) use of earlier established AFE models for the classification of further images can still lead to outcomes of good quality. The differences between the outputs from the two named image classification methods are usually rather marginal. Thus, the advantages of the batch processing procedure normally outweigh possible slight demerits in the accuracy or completeness of the outcomes. Consequently, the batch processing method can be recommended for the time-efficient and expedient analysis and classification of larger images, time series, and other sets of similar or related images.

A few suggestions can be derived from the insights gained in other studies on the extraction of building (footprint) or rooftop data from satellite or aerial images (e.g. OPITZ & BLUNDELL 2008a, DINIS ET AL. 2010, FREIRE ET AL. 2010, FREIRE ET AL. 2011, SANTOS ET AL. 2011) with regard to possible further improvements of the semi-automatic mapping procedure and the quality of the resulting rooftop or building (footprint) data. Probably, the most promising approach here is the integration of DSMs of very high spatial resolution into the image classification process. The combined use of a satellite or aerial image and a VHR DSM, and thus, the integrated interpretation of both, optical and elevation data, apparently leads to more accurate and reliable outcomes in (semi-automatic) building (footprint) or rooftop detection procedures (cf. e.g. OPITZ & BLUNDELL 2008a, FREIRE ET AL. 2010, SANTOS ET AL. 2011). Suitable DSMs should approximately match the employed imagery in terms of recording date and spatial resolution. Such DSMs are typically produced from airborne LiDAR data or stereoscopic VHR satellite imagery, which often is not readily available and is recorded only upon request. The usually high costs associated with this procedure prevent the wider use of these DSMs. However, where VHR DSMs are available, they also enable the true orthorectification of VHR satellite imagery. This increases the geometric and location accuracy of information derived from the imagery, such as e.g. building data.

The use of satellite images with even higher spatial resolutions (<0.5 m), which have only recently became available, can lead to more accurate and reliable image classification outcomes. Finer resolutions allow a better recognition of details and subtle differences and thus, facilitate a precise image classification and accurate delineation of individual target objects or areas. This may improve classification results, particularly in those cases where previously, the extents, shapes, and boundaries of target objects or areas were not always captured correctly nor exactly. Hence, for example, more accurate

rooftop data could probably be derived from satellite images with the highest currently available resolution. Moreover, the quality of derivative datasets that were produced through (semi-) automatic image analysis and interpretation can often be enhanced through manual editing. Thus, the advantages of both methods, the (semi-) automatic image classification and the visual-manual image interpretation by an expert, can beneficially be combined to obtain optimal results. In the present study, this well-known, straightforward, and advantageous integrated approach was adopted to improve the LU/LC data (see 4.1.2.4). Similarly, manual editing could also be applied to further enhance the quality of the semi-automatically extracted rooftop data. Errors in the extents and outlines of individual rooftops could be corrected by reshaping features, and rooftops not recognized by the software could be digitized to complete the data.

In the discussion of the quality of the data obtained through semi-automatic image classification, i.e. the LU/LC information (vegetation class) and the rooftop data, consideration also has to be given to the methodological details of the accuracy assessment. Besides the sample size and unit, the reference data, to which the classification outcomes are compared, is decisive. Here, through visual image interpretation and manual digitization, the reference data was derived from the same satellite image as the classification results (see 4.1.2.6). The acquisition of reference data in this way represents a feasible option when actual ground truth is not available. Therefore, this approach has been used in many studies, although it has also received well-founded criticism (e.g. CONGALTON & GREEN 2009). The main concern is that reference data acquired through visual-manual image interpretation does not necessarily accurately reflect real-world circumstances. The data can be biased by e.g. image interpretation uncertainties, inconsistencies in the digitization, or possible (residual) location errors and geometric distortions in the imagery. In particular, the latter must be assumed to be present, to a certain degree, in the satellite imagery employed in the study at hand, since here no true orthorectification could be performed due to the absence of suitable elevation data (VHR DSM). Hence, the manually digitized reference data itself would need to be evaluated with adequate ground truth to assess the possible degree of bias or distortion compared to actual circumstances. In the absence of suitable ground truth, with the reference data collected here, only the relative quality of the classification results can be determined which is a function of the employed image interpretation approach. To assess the absolute quality of the data extracted from the imagery, a comparison to ground truth data is required.

On the whole, the data derived from the satellite imagery was well-suited for the intended purpose and the scope of the present study. The LU/LC map, with its three broad classes, allowed the rough, but spatially explicit, estimation of local runoff. Thus, a map of the theoretical RWH potential in the area could be produced. The rooftop data enabled a first estimation of the RRWH potential in individual settlements. Based on the collected data, the approximate spatial distribution of the RRWH potential at the local scale, within a given settlement, could also be computed. Yet, the quality of the extracted rooftop data is not comparable to that typically found in the building data of cadastral land registers –

where this information is available. Thus, for detailed planning purposes, e.g. prior to the construction of RRWH systems, and similar tasks, the collected building data would have to be assessed with suitable ground truth to determine its actual quality, and edited where necessary to improve its accuracy, reliability, and completeness. Despite the described limitations, the acquired LU/LC and rooftop data is highly valuable, since up to now, no similar datasets with comparable levels of detail (resolution) and quality were available from other sources (e.g. government agencies). The selected method of data acquisition, through (semi-automatic) image interpretation, is highly flexible and customizable and thus, can be employed to gather further data, and to update or expand the existing information. A particular advantage in this regard is the possibility to reuse the developed AFE models for the fast and easy classification of further satellite images.

7.2.5 Quality of the digital elevation models and the derivative data and resulting implications

The quality and characteristics of the employed DEMs directly affected the representation of the relief and the properties, accuracy, and reliability of the derivative data, such as the slope map and the hydrological data layers (see 5.3 and 5.4). Both DEMs used in the present study, the ASTER GDEM V2 and the ALOS DEM, were derived from optical satellite images and obtained as ready-to-use products from third parties (see 4.1.3). To evaluate the DEMs in terms of their quality, their elevation values were compared on a per cell basis. Thus, the relative accuracy and reliability of the data could be assessed. Since the DEMs were derived from completely different source data, identical errors or biases were highly unlikely. For the most part, the two models were in good accordance and exhibited very similar values (cf. 5.3). This suggests a satisfactory relative accuracy and adequate quality in both DEMs and thus, a suitable representation of the relief as well .In the absence of appropriate ground truth, the absolute accuracy of the elevation information could not be determined here. Yet, information on typical error margins for the aforementioned types of DEMs are available from various sources and may serve as first estimates in this regard.

Further insights concerning the quality and suitability of the DEMs can also be gained from a close examination of the derivative data. In the visual assessment, the slope map derived from the originally obtained ALOS DEM showed noticeable artefacts (see 4.1.3, Fig. 26). Through subsequent processing of the DEM, these artefacts could be eliminated and the quality of the slope map could be improved (see 4.1.3, Fig. 26 and 5.3, Fig. 36). The quality of the hydrological information, i.e. the drainage line (stream) and catchment data derived from the DEMs in the hydrological analyses (see 4.1.4), was evaluated by comparing the different datasets. Thus, insights could be gained into the relative accuracy and validity of the data. The synthetic streams, or automatically computed drainage lines, derived from the ALOS DEM and the ASTER GDEM V2, were compared with each other and to the drainage lines

visually-manually identified in the GeoEye-1 satellite image (see 4.1.2.2, 4.1.4, and 5.4). In general, all datasets exhibited vast similarities, e.g. in regard to the positions, directions, and courses of drainage lines. This was especially true for areas with a more pronounced relief, where drainage lines were more deeply incised, and for streams of higher order; further away from headwaters. Noticeable differences between the data derived from the ALOS DEM and the manually digitized drainage lines were primarily observed in areas of relatively flat terrain and for drainage lines of lower stream order (see 5.4, Fig. 39, Table 14). This underpins the significance of the resolution and the accuracy of the DEM, as these properties have a crucial influence on the quality and characteristics of the derived hydrological information. The sensitivity to details of the DEM also depends on the characteristics of the displayed terrain and the level of detail of the hydrological data. Overall, findings suggested a good suitability of the ALOS DEM and its resolution and accuracy for the objectives of the present study, particularly in regard to the cost-benefit ratio and possible alternatives. Yet, the ALOS DEM and others of similar resolution and accuracy may not be applicable for hydrological questions and analyses at a very detailed level. For these purposes, apparently, very accurate and usually still costly VHR DEMs are required.

In addition to the data collected here, information about the individual catchments of the mapped RWH structures, particularly the cisterns, would be highly desirable, since it could provide valuable further insights into the current functioning of existing RWH schemes and improvement possibilities in this regard. In the context of the hydrological analysis, based on the provided DEM, the catchment for any given point within the analyzed area can be calculated. This option was used at the end of the detailed hydrological analysis, which relied on the ALOS DEM, to compute the catchments for some of the mapped cisterns. In general, the produced catchment data always reflects the resolution and accuracy of the input (raster) data, i.e. the DEM that was employed in the analysis. Here, most of the catchments calculated for the cisterns were very small, comprising only a few raster cells or square meters, and characterized by a narrow linear shape. These findings can be explained in two ways. Assuming the results adequately reflect actual circumstances, specifically the catchment sizes, then the findings would highlight the importance of linear RWH structures (bunds, ridges, dikes, feeding channels, etc.) to redirect runoff and thus, enlarge natural catchment areas. This would then suggest that in most cases, linear structures need to be integrated into RWH schemes in order to create sufficiently large catchments for the cisterns and thus, to collect adequate amounts of runoff. On the other hand, the shapes and sizes of the computed catchments could have resulted from an inadequate resolution and inaccuracies of the DEM employed in the analysis. In this case, the outcomes would not be able to give an appropriate account of the real world circumstances and hence, would not be suitable to assess the actual catchment areas of cisterns. In view of the limited data on the accuracy of the employed ALOS DEM and its still quite coarse resolution, compared to VHR DEMs, possible biases could not be ruled out to an adequate degree for the computed catchments of individual cisterns. Due to these accuracy and reliability concerns, the corresponding data was not included in the present study. Yet, the findings illustrate and emphasize the need for, and dependence upon, suitable, accurate and detailed input data, such as VHR

DEMs. From appropriate VHR elevation data, more accurate and reliable detailed catchment information, e.g. for cisterns, can also be derived, as demonstrated e.g. by KRAUSHAAR (2016). Consequently, data availability and the characteristics of the data employed in a study crucially influence which, and how adequately, research questions can be addressed.

7.2.6 Quality and suitability of the precipitation maps and other datasets employed in this study

Since precipitation represents one of the most decisive parameters in regard to runoff, it was given particular attention in the present study. The precipitation maps produced here were derived from daily precipitation records of 28 measuring stations within and around the study area (see 4.1.6, Fig. 28). The data of these measuring stations covered different periods of time, in most cases including either a large part or all of the selected 30-year period (1963-1992, see also 4.1.6, Fig. 29). Independent of the covered period, the precipitation data of almost all stations exhibited gaps, resulting from technological failure, maintenance problems, staff shortage, or other temporal difficulties. For these time intervals, which ranged from a few days to several months or even years, either no precipitation data or only estimates or summary values for longer time spans (i.e. weekly or monthly instead of daily data) were available. Nevertheless, for each day in the chosen 30-year period, an adequate amount of available data could be ensured, due to the high number of weather stations contributing data, and since recording errors did not occur at all measuring stations at the same time (also see 4.1.6, Fig. 29). Overall, the available precipitation data was considered suitable for the objectives of the present study and allowed the identification of representative average values, as well as the determination of the typical range of interannual variances in precipitation. The data was also able to reflect the temporal and spatial patterns of precipitation distribution due to the high temporal and spatial resolution available with the daily precipitation records from 28 measuring stations.

Besides the availability of adequate precipitation data, the selection of a suitable interpolation approach was crucial for the production of high-quality precipitation maps for the whole study area. Here, a sophisticated method and tool could be used for this purpose (see 4.1.6). One major strength of the approach was its ability to factor in multiple aspects, which can influence the spatial distribution of precipitation over a given area, such as altitudinal effects and latitudinal and longitudinal gradients. Moreover, depending on the available input data in each case (here each day), the most appropriate interpolation technique was selected automatically (cf. 4.1.6 and WIMMER ET AL. 2009). In view of these benefits, the employed interpolation approach is regarded as one of the best possible solutions for this task. Consequently, the outcomes – the precipitation maps – are also assumed to be of high quality, i.e. quite accurate and reliable, and thus, to adequately show the spatial distribution of precipitation and the amount of rainfall at any given point in the study area.

In addition to the precipitation data, further information, e.g. on other climate parameters, such as wind, temperature, and evaporation, would be desirable to enable a more detailed modeling of rainfall-runoff relationships and thus, improve the assessment of the spatial and temporal distribution of runoff. Additionally, this could probably lead to more accurate and reliable estimates of runoff quantities. In regard to the latter, the temporal distribution of precipitation and the intensity and magnitude of individual rainfall events is especially decisive. Therefore, precipitation records with even higher temporal resolution, e.g. hourly measurements, could also contribute to an enhanced estimation of runoff amounts. Finally, precipitation records covering a more recent time span would allow the assessment of potential effects of climate change on precipitation and runoff. The data and outcomes of the present study could then serve as basis of comparison.

The geological and soil information that was available for the present study represents a good foundation which could be improved and updated with additional data in the future. For all (research) questions concerning runoff and RWH, soil maps with finer resolutions and a higher level of detail would be especially useful. The currently available soil maps for the area only distinguish individual soil units, similar to groups. Each unit is characterized by a specific composition of different soil types, which comprise defined shares in the respective unit (see 3.4, Fig. 9 and Table 4). Hence, most soil map units encompass two or more, often highly heterogeneous, soil types, which exhibit different capacities for water infiltration and moisture retention, and different runoff efficiencies. Here, more detailed, spatially explicit information about the occurrence and distribution of the different soil types would be desirable. With respect to runoff and RWH, maps that distinguish between different, relatively homogeneous groups of soils, and show the corresponding areas covered by each group, would be sufficient. The soils included in a given group or soil map unit should be similar, e.g. in regard to their textures and typical depths, since variations in these properties are closely connected to differences in infiltration capacity and runoff efficiency. The analysis and interpretation of VHR satellite images and DEMs could probably facilitate the preparation of such a soil map, as the remote sensing-based approach may allow an enhanced extrapolation of (existing) soil data from field surveys. In combination with ground truth, land cover and relief information, derived from images and DEMs, could enable the identification of e.g. hill crest, summit, and steeper slope areas, which are typically covered by shallow soils (Leptosols), and areas of relatively flat terrain, where normally deeper soils (various Cambisols) are found (see chapter 3.4). Particularly in regions without a significant vegetation cover, soils and their properties have a crucial influence on surface runoff. Therefore, detailed information on the different soils and their distribution is essential for the accurate and reliable prediction of runoff in regard to RWH.

Comprehensive information on archaeological sites in the study area, and finds and remains discovered there, could be retrieved from the MEGA-Jordan database (see 4.1.5 and 5.5). In an ongoing revision process, the information stored in the database is revised, updated, and completed where necessary and possible, to ensure an optimal accuracy, reliability, and completeness. For this purpose, the (visual)

examination and interpretation of optical remote sensing data – new VHR imagery, or older, now de-classified military satellite images – could offer additional possibilities. The current condition of known archaeological sites and remains could be assessed and new, previously unknown or now destroyed structures and places with archaeological relevance could be discovered. Moreover, through the identification of sites in satellite images and/or GPS data from field studies, the location accuracy of older data can be improved. Many archaeological sites and remains were examined and documented decades ago and thus, could not be mapped as accurately and reliably as it is possible today, with modern technology. No profound changes are expected to result from the ongoing review of the source database with regard to the archaeological data employed in the present study. In several extensive field surveys, the structural remains and archaeological places in the study area have been well mapped and documented (cf. e.g. GLUECK 1934, MILLER 1979 and 1991, PARKER 1987 and 2006, MATTINGLY 1996a, MATTINGLY & PACE 2007, also see 3.6). As the data of these studies has been integrated in the MEGA-Jordan database, the retrieved information is assumed to be quite accurate, reliable, and complete.

As it has been pointed out thus far in the discussion, the quality and validity of the findings from RWH studies and runoff estimations are closely related to the accuracy, reliability, and appropriateness of the employed input data, such as precipitation records, LU/LC and soil maps, as well as archaeological and geological information. Therefore, further improvements and new insights in the named fields crucially depend on the availability of suitable, accurate, and reliable input data.

7.3 Site characteristics, interrelations, and spatial patterns: how site preferences could be linked to functions and roles of rainwater harvesting structures

The characteristics of the RWH sites, their distances to various features of the natural or man-made environment, and apparent patterns in their spatial distribution have been described in chapter 6.2. On the one hand, the outcomes are a result of the prevailing environmental circumstances in the study area, and on the other, they also reflect the functions of the different types of RWH structures. Several differences were identified between the two major categories of RWH facilities, the cisterns for water storage and the linear structures for runoff retention, deflection, and spreading, in regard to their spatial distribution and the typical characteristics of their sites. These differences can be related to the respective, particular function of the RWH structures. The two named broad types of RWH facilities serve fundamentally different purposes and have different requirements concerning suitable conditions and sites. For example, bunds, dikes, ridges, and similar surface structures obviously are not bound to specific underground conditions and thus can be installed independently of the geological setting. In contrast, the construction of underground cisterns is usually restricted to areas with suitable geological conditions,

found in e.g. near-surface sediments that can easily be excavated and offer a good natural water-holding capacity. Nevertheless, many of the identified site characteristics were very similar for all groups of RWH facilities. Where differences between the three groups of RWH structures were observed, these were often rather small (see 6.2.1, Table 17). This overlap in site attributes may partly result from the fact that different types of RWH structures are often combined and sited together to achieve optimal, synergistic effects, e.g. with ridges, bunds, or dikes (re-) directing runoff to cisterns. In these cases, which include more than half of all linear RWH structures (cf. 6.2.2, Table 18), in all likelihood, the place of the bund, ridge, or similar object is predetermined by the cistern and its site requirements.

Besides their role as auxiliary structures within larger RWH schemes, bunds, dikes, ridges, and the like also serve a variety of other purposes. They are commonly used to increase water infiltration and moisture in the soil layer(s), particularly where they are sited independently of cisterns. Due to their capacity to slow down and spread surface runoff, the linear RWH structures also help to minimize soil erosion. Given the environmental conditions in the study area (see chapter 3), erosion undoubtedly is a serious problem, which manifests itself e.g. in (incipient) gully formation. This phenomenon can especially be observed in the northern part of the study area. Hence, erosion control certainly represents an additional aim or even the main reason for which bunds, dikes, ridges, and similar structures are installed. Depending on the primary purpose of each of these linear RWH structures, probably different environmental factors are considered and emphasized during site selection. The possible resulting differences in site preferences could not be investigated here, as the mapped linear RWH structures were not further subdivided into different classes according to their respective nature or main purpose.

The findings of the present study indicate some general tendencies with regard to the whole group of bunds, dikes, ridges, check dams, and similar objects. The named linear RWH structures usually appear in groups, most likely in order to be most effective at a given site or for a certain, perhaps larger area. As the survey revealed, bunds, dikes, ridges, and similar structures are abundant in the study area, probably due to two main reasons. Firstly, the aforementioned objects can serve a variety of slightly different purposes, as described above, and are often associated with multiple advantageous effects. Secondly, the discussed RWH structures are typically inexpensive and easy to construct, and as such, require comparatively little investments in terms of money, building materials, labor, and time. These aspects mark bunds, dikes, ridges, and the like as highly beneficial structures, particularly for different runoff farming and micro-catchment RWH strategies, as well as for erosion control. Therefore, the named structures and associated techniques have most likely been employed for several millennia or even longer, similar to other water management facilities and strategies. Remains at numerous archaeological sites testify to the long history of RWH and water management structures, including bunds, ridges, channels, check dams, and similar objects (see chapter 2.1 and e.g. OLESON 1991, LABIANCA 1995, MATTINGLY ET AL. 1998, SHANAN 2000, ABDELKHALEQ &ALHAJ AHMED 2007). In regard to the possible ages of the mapped linear RWH structures, no reliable estimation can be given. While bunds, dikes, ridges, check

dams, and the like have most likely been constructed and used for millennia on the Karak plateau (cf. e.g. MATTINGLY ET AL. 1998), individual objects have probably been destroyed, rebuilt, modified or constructed newly over time, thus possibly leading to shifts in locations and distribution patterns as well.

Within the category of (definitely identified) cisterns, allegedly old cisterns or "Roman Wells" were distinguished from presumably modern ones. Therefore, in the following, the results for both (sub-) groups, i.e. their respective typical site characteristics and potential patterns in their spatial distribution, are discussed comparatively. Thus, similarities and differences between the two groups of cisterns can be highlighted. Moreover, this allows for the identification of possible changes over time in site preferences and the relevance of different aspects in the selection of suitable locations for cisterns.

First of all, the allegedly old cisterns and the presumably modern ones are distributed differently in regard to the various geological units (see 6.2.1). The old cisterns are restricted to soil or calcrete areas or regions of the Al-Hisa Phosphorite, according to the geological map, whereas a significant share (14%) of the modern cisterns are also found in basalt areas (see 6.2.1, Table 17). One explanation for the apparently new exploitation of basalt areas could be the availability of modern excavation equipment. Many of the basalts in the study area are likely characterized by a low permeability, which can be associated with a good natural water holding capacity in cisterns. However, the hardness of most of these rocks can render excavations a difficult and arduous task. Therefore, areas with basalts, at or close to the earth's surface, apparently were not considered very suitable for the construction of cisterns in the past, when all excavation work had to be done manually. Here, the advent and availability of modern excavation equipment and machinery probably opened up new possibilities, leading to basalt areas now being considered suitable for the construction of underground cisterns. Additionally, modern cisterns are usually smaller in size and thus, require less excavation work.

In contrast to their modern counterparts, the majority of the mapped old cisterns are found at relatively short distances to archaeological sites (see 6.2.2, Table 19 and Fig. 54). Additionally, the old cisterns tend to cluster around only a few archaeological sites, primarily places with remains of rather permanent structures typically linked to settlement and related activities. Moreover, the old cisterns show a strong association with modern settlement areas, as most of them are situated within or in the immediate surroundings of towns and villages. In all likelihood, both findings, the proximity to archaeological sites and the relation to settlement areas, are interconnected, since modern settlements in most cases were built upon, around, or in close proximity to earlier settled places or other ruins and remains of ancient structures (see 3.6, Fig. 12). Their close relation to built-up areas renders the old cisterns eligible for integration – as storage units– into RRWH schemes. Around 75-95% of the mapped old cisterns were regarded as especially suitable for this purpose (see 6.3.2, Table 26). At the same time, due to the locations in and around built-up areas, rooftops can often represent the only suitable surfaces that are available for the collection of runoff in the vicinity of the old cisterns. With respect to the required proximity to buildings, only a few (15-23 %) of the mapped modern cisterns were identified as potentially eligible

for RRWH. The overwhelming majority of the modern cisterns are located outside of villages and towns; relatively far away from buildings. There, they often form parts of larger RWH schemes and are typically found in groups of 2-20 objects (see 6.2.2, Table 18). As the outcomes of the proximity analyses indicate, modern cisterns are also often sited together with bunds, ridges, dikes, check dams, and similar structures, which can slow down runoff and/or (re-)direct it towards the cistern(s). While the distribution pattern of the old cisterns shows a similar tendency for intra-group clustering, the old cisterns are rarely spatially associated with modern cisterns or bunds, dikes, ridges, or similar structures (see 6.2.2, Table 18). This finding is most likely linked to the locations of the old cisterns in and around built-up areas. There, no natural ground catchment areas are available for the collection of runoff and thus, the setting does not allow for e.g. micro-catchment RWH practices, which typically include linear RWH structures.

Furthermore, compared to the locations of other RWH structures, the sites of the allegedly old cisterns were associated with higher slope values, which manifested in an increased minimum (2%), maximum (30%), and mean figure (10%) (see 6.2.1, Table 17). These results, i.e. the observed gradients, partly contradict common recommendations, according to which sites with steeper slopes are less suitable or even inappropriate for RWH, or more specifically, the collection of runoff from ground (micro-)catchments (see e.g. CRITCHLEY & SIEGERT 1991, suggesting a max. slope of 5%, and ALI ET AL. 2009, recommending slopes of 3-15%). Before further interpretation, the possibility of errors in the described results also has to be considered. Here, inaccuracies of the DEM, from which the slope values were derived, could considerably affect the findings. Based on the insights gained concerning the quality of the employed DEM (see 5.3, and 7.2.5), potential biases are expected to be rather small. The DEM and the derived slope information is assumed to be characterized by a fairly high relative accuracy, and thus, a sufficient reliability and validity too. Additionally, in view of the number of analyzed sites, possible minor inaccuracies in absolute slope values of single locations most likely do not lead to substantial differences in overall outcomes. Excluding significant data errors, two other explanations are conceivable for the observed tendency towards higher slope values in the group of old cisterns. For one, these cisterns could have been part of RWH schemes that do not rely on ground catchments for the collection of runoff. Here, particularly RRWH systems seem likely, since most of the old cisterns are situated in or around villages or towns today and also frequently exhibit a close proximity to archaeological sites, of which many were linked to settlement and related activities. An integration into RRWH schemes or other uses that do not involve ground catchments would render the cisterns, and the suitability of their sites, largely independent of the slope. The cistern sites then could have been primarily selected based on other factors, such as the vicinity to buildings or the geological underground. Alternatively, assuming a combination with ground (micro-) catchments for the old cisterns, sites could have been chosen despite being less favorable in terms of slope. In this case, other environmental or socio-economic aspects could have been given priority in the site selection process. Cisterns may have been constructed where access to fresh water was most necessary, or where they could best serve the intended purpose. For example, for larger, e.g. community owned, cisterns that should primarily provide drinking water for a number of

people, locations in the proximity of (residential) houses, in the center of a settlement, or near other central points could have appeared most suitable. In regard to other factors, such as the gradient of the terrain, then a broader variety of conditions could have been considered acceptable as long as these did not render RWH impossible.

Overall, the two groups of cisterns, old and modern, show large differences in their spatial distribution over the study area. These discrepancies in their spatial distribution pattern are connected to differences in the observed site characteristics and in the suitability for specific RWH strategies, such as RRWH or micro-catchment RWH practices. It can be hypothesized that old and modern cisterns were constructed to serve slightly different purposes, which in turn led to different site preferences.

A synoptical interpretation of all findings concerning the characteristics of the different RWH sites and the outcomes of the conducted proximity analyses allowed for the identification of one general, over-arching tendency: that of the extensification of RWH in modern times. This refers to all RWH structures for which a relatively recent construction date can be assumed, i.e. the presumably modern cisterns and all bunds, dikes, ridges, dams, and similar objects, and to the numerous ways in which the findings for these groups differed from those for the old cisterns. Compared to the outcomes for the latter group, the results for the sites of modern cisterns and linear RWH structures generally tended to cover broader ranges of values, thus suggesting an amplification in regard to the site characteristics and environmental circumstances considered acceptable for RWH sites. This diversification tendency was observed in the outcomes for the categories of elevation, annual precipitation amounts, and geological underground, as well as in the distribution of sites according to catchment (see chapter 6.2.1). Absolute minimum and mean figures indicated that modern cisterns and bunds, ridges, check dams, and the like, are often located at slightly lower elevations and in areas with lower annual precipitation amounts, compared to the old cisterns. These findings can be explained by an expansion towards the fringes of the highland and the east. Hence, a significant share of the modern RWH structures, but almost none of the older cisterns, are found in these areas. Moreover, the modern cisterns and linear RWH structures are widely distributed over different geological areas (units) and a large number of mostly comparatively small catchments (cf. section 6.2.1, especially Table 18). Overall, in regard to the spatial distribution of RWH sites, these findings support the idea of a greater (spatial) diversification and extensification in modern times. At the same time, locally, an intensification and concentration of RWH efforts can also be observed, especially where several modern cisterns and bunds, dikes, ridges, and similar structures are sited together, and in close proximity to each other, thus forming larger RWH schemes.

It can be hypothesized that, when a wide range of natural environmental circumstances are considered acceptable for RWH, these aspects become less critical and pivotal in the site selection process, and other criteria, such as socio-economic factors, may gain increasing significance. Suitable locations for new RWH schemes can then be chosen according to the primary purpose(s) of the respective RWH structures or where additional water is most needed. Collected and stored rainwater can be assumed to

have been the main or the only source of freshwater directly available on the Karak plateau during most of history. Therefore, the primary function of cisterns most likely was to provide the essential (drinking) water for the local population. To optimally serve this purpose, the old cisterns probably were constructed where the geological underground was found to be suitable and access to freshwater was most crucial and could best benefit a number of people – e.g. in the vicinity of residential houses or at the center of a settlement.

In contrast, modern RWH structures, particularly the modern cisterns, apparently fulfill a different role. Since the villages and towns on the Karak plateau have been connected to the public water supply system, this source typically represents the main source of (drinking) water for the residents of the area. The supplied water mostly corresponds to a mix of surface and groundwater from various sources and regions (of Jordan) that is then redistributed through the pipeline network to all parts of the country as needed. Additionally, at many places, modern machinery and deep drilling enabled the installation of public and private wells, which provide access to groundwater and thus, form another, year-round available source of fresh water. Hence, RWH schemes are not the only locally available, and therefore, vitally important source of water any more, but rather constitute an additional alternative. Since RWH systems normally represent low-cost and low-tech, independently applicable on-site (i.e. local) solutions, they can be especially valuable in remote areas, where no access to public water supply exists. In areas with increased water demand, e.g. for (supplemental) irrigation, RWH can provide additional water resources, which otherwise would not be available or would be too expensive. In summary, the described aspects can explain why modern cisterns, in contrast to their older counterparts, are regularly found outside of settlements and often at quite remote locations.

Overall, the findings suggest that factors like the spatial distribution of water demand and availability, and the local ratio of the former to the latter, are pivotal in the site selection process, whereas aspects concerning the natural environment (e.g. slope, geology, etc.) seem to be less decisive. Unless they render a given location completely inappropriate for RWH, a high flexibility apparently exists in regard to the natural environmental characteristics of a site. This indicates that RWH schemes can be adjusted to a variety of settings and local circumstances as dictated by the need for (additional) water resources.

In the present study, the investigation of spatial patterns and relations was based on site factors and proximity analyses as well as on a comparative evaluation and interpretation of the collected data and outcomes, including basic descriptive statistical measures. Thus, substantiated hypotheses could be formulated about suitable RWH sites, their identification and spatial distribution, as well as changes in RWH strategies over time. Additional (statistical) analyses, such as e.g. spatial regression analyses, and the resulting data could provide further valuable insights in regard to spatial patterns, the significance of specific aspects, and the degree of correlation or the nature of relations between individual features or factors. Research studies from other disciplines, such as social sciences, and outcomes obtained with

other methods, such as interviews, can contribute further information concerning the implementation of RWH and the socio-economic circumstances that encourage it.

7.4 Tapping the rainwater harvesting potential: benefits, constraints, and necessary preconditions

In this section, firstly, the computed RWH potential and the estimated total water storage capacity available with the mapped cisterns are evaluated, and compared to the water demand of the local population of the area. Subsequently, the requirements and necessary preconditions for an optimal exploitation of the estimated RWH and storage potentials are outlined and possible obstacles in this regard are described. Finally, the benefits that can be expected from an intensification of RWH efforts are pointed out, and the potential role of RWH in a modern society and an integrated water management is discussed.

7.4.1 Evaluation of the estimated rainwater harvesting and storage potentials and comparison to the water demand

In order to adequately assess current RWH efforts and the calculated RWH potential, the storage capacity available with existing cisterns, the amount of potentially collectable runoff, and the water demand of the local population are compared. Detailed descriptions of the computed storage potential, the estimated on-site runoff, and the runoff from rooftops can be found in chapters 6.1, 6.3.1, and 6.3.2, respectively. Information about the water demand is given later in this chapter. About 88% of the study area were classified as pervious areas which are potentially suitable for the collection of surface runoff from small catchments or micro-catchments. This excluded vegetated areas, terrain with gradients over 15%, and very small patches of land (see 6.3.1). On-site or local runoff from the remaining pervious area that is possibly suitable for RWH was estimated at $5.5 \cdot 10^6$ m^3, $2.5 \cdot 10^6$ m^3, and $10.2 \cdot 10^6$ m^3 per year under long-term average, dry, and wet precipitation conditions, respectively. Assuming an average volume of 30 m^3 per object, the total storage capacity of the 293 reliably identified and presumably modern cisterns amounted to 8,790 m^3. Consequently, in years with average precipitation, 0.16% of the estimated local runoff from eligible pervious areas could be stored in the mapped modern cisterns. This share changes to 0.34% for dry and 0.09% for wet year conditions. When taking into account the mapped old cisterns ("Roman Wells") as well, a significantly larger fraction of the computed on-site runoff could be stored. Based on an assumed average volume of 130 m^3 per object, the total storage capacity of the 96 identified old cisterns is estimated at 12,480 m^3. Consequently, both groups of cisterns, the allegedly old and the

presumably modern ones, together probably could store around 21,270 m^3 of water. This capacity corresponds to ca. 0.38% of the on-site runoff from potentially suitable pervious areas under normal (long-term average) precipitation conditions, and 0.83% and 0.21% of the analogous on-site runoff in extremely dry or exceptionally wet years, respectively. However, as has been pointed out before (see 7.3), not all cisterns are equally suited for an integration into RWH schemes of a given type, due to differences in characteristics of their sites. In most cases, those cisterns situated close to appropriate pervious areas, from which runoff could be collected, were labeled as modern. Hence, in regard to RWH schemes that rely on on-site runoff from potentially suitable pervious areas, the number and sizes of modern cisterns and the resulting total storage capacity are most relevant.

In contrast, the identified old cistern are mostly situated close to buildings and within, or in the vicinity of, settlement areas and thus, are regarded as especially suitable for integration into RRWH schemes. The total RRWH potential, defined as the annual runoff from detected rooftops, of the 12 settlements in the study area, is estimated at 153,936 m^3 in years with average precipitation, and 70,859 m^3 and 277,329 m^3 in exceptionally dry or wet years, respectively. The aforementioned figures are based on the rooftop data derived from the GeoEye-1 satellite image through semi-automatic image analysis (see chapter 6.3.2, Table 24 and 25, and Fig. 56, plain bars). In view of the error margin (95% confidence interval) identified for the image classification outcomes (see 5.2, Table 13), runoff estimates relying on this data also need to be stated with a corresponding tolerance range. With respect to the likely degree of over- or underestimation, the annual RRWH potential in the study area was expected to be in the range of 130,830-178,704 m^3 under average precipitation conditions, 60,223-82,260 m^3 in dry years, and 235,702-321,951 m^3 in wet years. With an estimated total storage capacity of 12,480 m^3, the mapped old cisterns together could store shares of 8.11% (6.98-9.54%), 17.61% (15.17-20.72%), and 4.50% (3.88-5.29%) of the computed annual runoff from all detected rooftops under normal, dry, and wet precipitation conditions, respectively (figures in parenthesis refer to the tolerance ranges stated above). Here, only the total storage capacity of the old cisterns was considered, since most of the modern cisterns are located quite far away from buildings and thus, were not regarded as suitable for RRWH. The total figures stated here can give an initial impression of the dimensions of the RRWH and storage potentials and the water demand, and the proportions of these three to each other. However, these quantities and proportions can vary largely in individual settlements, as the outcomes presented in chapter 6.3.2 show. Impervious areas, other than rooftops, were not considered suitable for RWH and thus, excluded from the estimates of RWH potentials, mainly due to water quality concerns in regard to the runoff from these areas.

The share of runoff, either from rooftops or potentially suitable pervious areas, which can be stored in the mapped existing cisterns, can in effect be higher or lower than the estimated one, due to several factors. Besides the design, the size, and construction details, the current condition of a cistern also has

a significant influence on its storage capacity and water holding ability. Cracks in the walls or insufficient or damaged plaster linings can cause considerable leakages, and thus severely compromise the water holding ability and functioning of a cistern. Accumulated (fine) sediments, rocks, and oftentimes rubbish inside cisterns can also decrease their storage capacities substantially. On the other hand, multiple fillings of cisterns over the course of a year are common and can significantly raise the total annual amount of water that can be stored (partly consecutively). For the Karak Plateau, Assayed et al. (2013) reported that partial multiple fillings increased the storage potential of the cisterns they studied by 30%. Based on this finding, the actual shares of runoff from rooftops and pervious areas, which can be stored in the mapped cisterns, could be 30% larger than previously estimated (see above). Another factor which could lead to an actually higher storage potential is the existence of further cisterns. Several conspicuous structures, which might indicate cisterns but would require individual ground checks to clarify their nature, were mapped and assigned to a separate category (see 4.1.2.2 and 6.1). Moreover, the existence of further cisterns that could not be mapped in the present study (see 7.1), seems likely in view of the general popularity of cisterns in the area. Based on these considerations, the total figures given above, i.e. the total capacity of all cisterns and the corresponding storable shares of runoff, can be regarded as conservative or minimum estimates. Although occasionally, the functioning and capacities of individual (old) cisterns are limited by their current condition, the possibility of multiple fillings and the likely existence of further cisterns, on the whole, point to a rather larger than smaller total storage potential. However, even a total storage capacity twice as high as estimated would equal only a relatively small share of the theoretically annually harvestable runoff or RWH potential (see figures in previous paragraphs). Not taking into account other types of RWH schemes and practices, e.g. those relying only on bunds, ridges, check dams, and the like, this suggests a relatively large remaining RWH potential, which could probably be tapped with additional RWH facilities. This applies especially to local (on-site) runoff from pervious areas. Of the estimated runoff from rooftops, a considerable share (about 8-20%) could already be stored with the existing (old) cisterns (see above and chapter 6.3.2, Table 26). Necessary preconditions and possible constraints for the exploitation of the estimated RWH potentials are described later in this chapter.

The estimated RWH and storage potentials are compared here to the water demand of the population in the study area. According to the data of the Jordanian DEPARTMENT OF POPULATION STATISTICS (DoPS 2015), in 2015, about 23,614 people resided in the towns and villages in the study area (see 3.6, Table 6). The water demand per person per day is estimated at 80 liters, at least in rural areas, as suggested by ASSAYED ET AL. (2013) and the Jordanian MINISTRY OF WATER AND IRRIGATION (MWI 2016a,b). The named amount of water is thought to cover all domestic needs in the broadest sense, including drinking, cooking, washing, and cleaning purposes, as well as the watering of livestock and plants (gardening) (MWI 2016b). Based on these figures, the total water demand of the residents in the study area then amounts to 1,889 m^3 per day and 689,529 m^3 per year. The calculated total storage capacity of all cisterns (21,270 m^3) thus corresponds to approximately 3% of the annual water demand of the local population

or the water demand of 728 residents. While the water stored in a modern cistern (30 m^3) would roughly equal the annual domestic water demand of one person, an old cistern with an estimated average volume of 130 m^3 could provide enough water for more than four people each year. This illustrates the importance of being able to use the maximum possible storage volume of every cistern. Early cleaning and maintenance, at regular intervals, is needed to eliminate all factors which can reduce the storage capacity or water holding ability of a cistern, e.g. cracks causing leakages or debris, rubbish, and sediments accumulating in the cisterns. The figures above also highlight the potential that lies in the rehabilitation and reuse of the old cisterns, especially in view of their typically relatively large storage volumes.

In effect, the proportion of the storage potential of the existing cisterns to the water demand of the local population may be slightly more favorable than the above described estimates suggest, due to several factors. Firstly, with multiple fillings per year, cisterns would be able to supply more water. Assuming an increase of 30%, owing to multiple fillings, as described by ASSAYED ET AL. (2013) (see above), the annual amount of water that could be harvested and stored in the existing cisterns would then correspond to 4% of the annual domestic water demand of the local residents or the water demand of 947 people. Additionally, the likely existence of further cisterns in the area, as discussed earlier in this chapter, could lead to a further rise in the yearly storage potential. On the other hand, the annual per capita freshwater demand for domestic purposes might actually be smaller than the suggested 80 l per day. According to the Jordanian MINISTRY OF WATER AND IRRIGATION (2016b), the daily per capita water demand for municipal purposes – of which 87% is attributed to domestic water demands – amounted to only 55 l in the Karak Governorate in 2014, as calculated from water bills. However, in the same year, the daily freshwater supply to the area was equivalent to 179 l per person (MWI 2016b). The difference between the two aforementioned figures, an incredible share of around 70% of the annual water supply, was declared as losses. To what extent this unaccounted-for or non-revenue water corresponded to actual losses, e.g. through leakages in pipelines, or somehow still contributed to the water supply of the area, e.g. through illegal tapping, cannot be determined. Excluding the latter and considering only the metered water supply, this suggests a daily per capita water demand of well below 80 liters. Additionally, the aforementioned estimate of domestic water demand includes a broad variety of purposes (see above), far beyond the very basic needs for a healthy survival. Yet, not all water uses require the same water quality. While for some purposes, drinking quality water is indispensable, for other purposes, e.g. the flushing of toilets, the use of less pure or even gray-water would be acceptable. Thus, the overall demand for freshwater could be reduced through water reuse, e.g. by utilizing residual water from cooking for the watering of plants. Water demand management comprises a variety of different strategies and tools which can effectively help reduce the demand for fresh water.

Based on the above-mentioned estimate of the annual water demand of the population in the study area (689,529 m^3), the share of runoff can be calculated which would have to be collected and stored, if RWH were to provide all the necessary water supply. According to the outcomes of the present study, at most,

only ca. 22% of the annual domestic water demand of the residents could be covered by RRWH, even if the computed runoff from all rooftops – about 153,936 m^3 under normal precipitation conditions – was collected. In other words, the estimated runoff from all detected rooftops would be sufficient to meet the annual water demand of approximately 5,272 people, assuming a per capita demand of 80 liters per day. Alternatively, in a year with average precipitation, about 13% of the computed amount of on-site runoff from potentially suitable pervious areas (see 6.3.1, Table 23) would have to be harvested (and stored) to cover the estimated domestic water demand of the population in the study area.

In the above evaluation and discussion, only the water demand for municipal or domestic purposes has been considered. However, these uses typically account for less than 40% of the whole water demand occurring in Jordan annually. Most of the remaining share of supplied fresh water (around 60%) is devoted to agricultural purposes, while the amount of water used by the country's industry is comparably small (ca. 3%) (MWI 2016a,b). Depending on regional particularities, throughout Jordan, some differences can be observed in the described distribution of water demand according to sector. In the Karak Governorate, which receives only ca. 8% of the country's total water supply, a higher percentage (13%) of the provided fresh water is applied to industrial purposes and a somewhat lower share (22%) to municipal (mainly domestic) purposes (MWI 2016b). Within the governorate, most of the water demand for agricultural purposes emanates from the Jordan Valley. In the highlands, to which the study area belongs, agriculture normally relies on precipitation. There, irrigation is usually restricted to smaller areas and typically applied only as supplemental irrigation, e.g. for trees (see 3.5.2). To some extent, particularly in the highlands, the water demand of the agricultural sector can probably be covered by RWH schemes consisting of bunds, dikes, ridges, check dams, and the like. These structures can increase soil moisture and thus enhance plant growth and agricultural production. Hence, the water demand, e.g. for irrigation, may decrease. The pressure on the country's water resources can be reduced in this way. For the study area, the aforementioned linear RWH structures are especially beneficial, since they also represent effective erosion mitigation measures. The exact actual effects of these structures are difficult to quantify. A reliable assessment typically requires the acquisition and comparative evaluation of empirical, preferably long-term, data on soil moisture and/or plant growths in areas with and without these RWH structures (cf. e.g. AL-SEEKH & MOHAMMAD 2009, ALI ET AL. 2010, ABU-ZREIG & TAMIMI 2011, GAMMOH 2013).

7.4.2 Possible obstacles and necessary preconditions for the realization of the rainwater harvesting potential

Several possible constraints and necessary preconditions have to be considered with respect to the realizability of the hitherto described RWH potentials. In regard to the quantity of harvestable water, the

actual extent of suitable and available catchment areas is decisive. The realizable RRWH potential, first and foremost, depends on the actually existing rooftop area. Since the rooftop data in the present study was derived from satellite imagery, ground truth is indispensable in determining the degree of congruency with real-world conditions (see 7.2.4). In the absence of suitable ground truth, only a limited accuracy assessment of the rooftop data was possible (see 4.1.2.6 and 7.2.4). Hence, the existing RRWH potential in reality could be somewhat larger or smaller than the findings suggest.

Competing uses can limit the extent of the areas which are actually available for the collection of runoff and thus, integration into RWH schemes. This applies to the rooftop, as well as, the pervious areas, which were identified as potentially suitable for RWH in this study. The rooftops of most buildings in the study area are partly occupied by water tanks and often used as storage areas too. The characteristics of the rooftops, e.g. their inclination, surface materials, and similar details, can further limit the usability of these areas for RRWH purposes. In regard to the study area, these concerns probably play a minor role and most rooftops can be considered suitable for the collection of runoff. Parts of the mapped pervious areas that were identified as potentially adequate catchment areas for RWH schemes are very likely used for agricultural purposes, which normally render the simultaneous collection of runoff from these areas impossible or inefficient. This applies especially to areas with relatively flat terrain and deep soils, since this is where most of the agricultural fields are found.

In addition to the surface properties of potential runoff catchment areas, other factors can also significantly influence the suitability of a given location for RWH purposes. Here, particularly the land cover and land uses in the immediate surroundings of a site can play a crucial role. In the study area, roads, agricultural fields, and industrial, waste, and quarry sites, as well as intensive chicken factory farms are the main land uses and areas that are often associated with runoff of low, or even problematic, quality. The inadequate water quality results from possible contaminations with fuel and oil spilled on roads, insecticides and fertilizers washed out from soils, and various other chemicals or problematic substances. When runoff from these areas, and with the described characteristics, enters RWH systems, the quality of all collected water can be severely degraded, to the degree where it becomes unusable. To minimize pollution risks and to ensure the best possible quality in the collected water, RWH sites should be selected carefully, taking into account the environment of the intended location. This can further reduce the extent of available, suitable pervious areas for RWH purposes, as some sites may be ruled out due to their proximity to areas with the aforementioned land uses and the associated water contamination risks. The described considerations apply to all RWH schemes that rely on ground catchment areas, whereas they are usually less relevant in regard to RRWH systems, particularly when rooftops serving as runoff collection areas are cleaned regularly or the runoff from the first rain after the dry season is discarded (first flush elimination).

The applicability of RWH schemes based on bunds, dikes, ridges, and similar structures, which aim at the deceleration and retention of runoff and the increase of infiltration, is limited to pervious areas with

adequate soils. Since the runoff 'harvested' by these structures is normally intended to be stored locally in the soil profile, the soil has to be able to absorb and retain the additional water. At the same time, the infiltrated water has to be stored at depths and forms that allow plants to access it, i.e. above the wilting point, in order to benefit plant growth, which is typically one of the main goals of these RWH structures. Therefore, besides the depths of soil layers, the soil properties, such as the grain size distribution, are also important, as they crucially influence the ability of a given soil to store moisture in plant available forms and to support plant growth. The availability and extent of areas with suitable soils can represent a limiting factor in the site selection process, and in regard to the upscaling potential of the implementation of the above-named types of RWH structures and practices.

Besides the selection of appropriate sites or areas, several organizational, economic, and other planning questions have to be addressed for the successful implementation of RWH schemes. Major aspects that need to be considered concern the initial establishment and maintenance (e.g. repairs and regular cleaning of cisterns) of RWH systems, as well as the distribution and use of the harvested water, where applicable. Thorough planning, with respect to the aforementioned aspects, includes the determination of necessary steps, tasks, and adequate schedules, as well as the assignment of duties, responsibilities, and rights to individuals and/or parties involved with the respective RWH scheme. All stakeholders need to agree upon the distribution of any benefits, and their respective contributions to the initial, as well as, ongoing investments. This is especially crucial for large RWH schemes, which are severally owned and/or shared by multiple beneficiaries. Addressing these questions as early as possible, e.g. at the initial planning stage, not only helps to avoid later conflicts over access and rights to collected water resources., but it also minimizes the risks of poor or under-functioning of the respective RWH system, due to deficient maintenance, and its deterioration over time. The best possible long-term benefits from initial investments associated with the construction or restoration of RWH facilities can be ensured when these stipulations are followed.

Similar considerations must form an essential part of the planning of RWH projects on a larger, e.g. regional or national, scale. Thorough and comprehensive planning is one of the most decisive factors for the advancement of RWH and the successful realization of related projects. First and foremost, the financial and spatial scale of an envisioned RWH project has to be determined, and all possible stakeholders, such as donors, managing institutions or organizations, and beneficiaries, need to be identified. All (groups of) stakeholders, especially those intended to benefit from the new RWH schemes, should be involved in the planning process right from the start, in order to avoid a suboptimal top-down approach. Typical stakeholders in larger RWH projects are government agencies, development aid organizations and other NGOs or NPOs, usually functioning as donors or investors, as well as, local residents, farmers, organizations, or small businesses. The latter named groups are normally the receivers or beneficiaries of the investments into RWH structures. In the planning process, local and regional stakeholders, e.g. residents and farmers, and their interests must be given particular attention, since they can be

directly affected by the RWH strategies. Generally, the implementation of RWH schemes can entail changes in runoff, which through downstream effects, can affect broad areas, far beyond the actual RWH site. Ensuring the broad acceptance of all stakeholders and people, who likely will be affected by the planned structures, is a crucial prerequisite for the successful realization of RWH projects and long-term benefits from the associated investments. The thorough planning of RWH projects should also address organizational and administrative questions concerning the time beyond the initial implementation phase. Here, schedules and responsibilities, e.g. with regard to the maintenance of RWH systems, need to be determined. Finally, all RWH projects should ideally include some kind of quality control or assessment of the outcomes as well. A critical evaluation of completed RWH projects, especially in regard to long-term effects of outcomes, can be particularly beneficial to define lessons learned, and thus to improve the planning and application of any new RWH strategies. The described aspects illustrate the complexity of RWH projects and the numerous steps, considerations, and potential pitfalls involved. Research findings, such as those from the present study, can make an important contribution to the improvement and advancement of RWH strategies. Yet, the successful practical application of the findings in new RWH projects depends on a variety of factors, particularly thorough and appropriate planning which adequately acknowledges local particularities. Additional data and insights from other disciplines, such as cultural or social sciences, may further enhance the understanding and implementation of RWH. An integrative, multidisciplinary approach in research and planning, as well as, the acquisition of adequate data are crucial prerequisites for the overall success of RWH efforts, the long-term effectiveness of investments, and an optimal cost-benefit ratio in RWH strategies.

7.4.3 Suitability and benefits of rainwater harvesting for the study area and beyond

Additional water that becomes available through RWH can principally be used for different purposes, at least when runoff is collected and stored in ways which allow for its convenient accessibility, e.g. in cisterns. Runoff from RWH schemes that are designed to retain runoff and increase infiltration, is stored in soils and thus, can usually only be used for plant growth. The usability of water from other RWH systems that rely on e.g. open reservoirs or cisterns, mostly depends on the quality of the collected and stored water and the intended purpose of use. The quality of water from RWH systems is largely determined by two decisive factors: the catchment area and the storage conditions. Firstly, the selection of appropriate catchment areas is crucial to ensure a good initial quality in the collected runoff. Suitable areas should be pollutant-free, as clean and smooth as possible, and feature adequate, nonhazardous (nontoxic) surfaces. Thus, the risk of contamination and the amount of sediments, stones, leaves, and other materials, which can enter the storage units of RWH system with the runoff, can be minimized. Rooftops commonly represent excellent catchment areas, as they are usually characterized by appropriate surface materials and are impervious to water. Their elevated position protects them from most of

the pollution risks (a detailed discussion of RRWH systems, the quality of the harvested water, and influencing factors can be found in e.g. MEERA & MANSOORAHAMMED 2006, FARRENY ET AL. 2011b). Despite these positive aspects, most of the rooftops in the study area are currently not used for RWH purposes. At the same time, many, mostly old, cisterns located in the vicinity of these buildings, lack adequate catchment areas and are also not integrated into RWH systems. Therefore, rooftops representing excellent runoff collection areas and (old) cisterns providing necessary water storage capacities, should be connected to form efficient RRWH systems. In many cases, this would probably require only minor investments and adaptations, such as the installation of gutters, downspouts, and similar connecting pipework, and the restoration of cisterns where necessary.

In order to preserve the initial quality of the harvested water, appropriate conditions must be ensured during storage. Protection from possible pollution and low temperatures are crucial. Cool temperatures impede bacterial growth which otherwise can lead to a serious decline in water quality over time. Longer storage times are usually associated with higher risks of contamination and the deterioration of water quality. In semi-arid areas, rainwater harvested during the winter half year and stored, is typically used, gradually, over the dry season, and thus, part of it needs to be stored over several months, until the end of summer. Consequently, the best possible conditions for water storage are essential and storage units of RWH systems must be designed accordingly. As closed underground cavities, cisterns are usually able to provide optimal storage conditions. The water is largely protected against external influences, including high summer temperatures. Several studies suggested that in most cases, the water from RWH systems and cisterns is characterized by an acceptable. to good, quality, at least when the corresponding RWH systems are designed properly, when reasonable precautions are taken, and when basic water treatment is applied where necessary (e.g. GOULD 1999, SALAMEH 2004, MEERA & MANSOU-RAHAMMED 2006, SAZAKLI ET AL. 2007, HELMREICH & HORN 2009, RADAIDEH ET AL. 2009, AL-SALAYMEH ET AL. 2011, DE KWAADSTENIT ET AL. 2013). The quality of cistern water fundamentally depends on the initial quality of the collected runoff and thus, on the location, design, functionality, and maintenance of the whole RWH system and on the catchment area in particular. Besides the described aspects concerning catchment areas and storage conditions, suitable measures of water treatment, such as filtering, UV treatment, and boiling, can further enhance the quality of water from RWH systems and cisterns. Adequate water treatment is normally recommended before use to ensure a safe drinking water quality that meets international standards, at least for human consumption, e.g. drinking or cooking purposes.

According to local residents and farmers, the collected and stored water of RWH systems, and particularly, cisterns in the study area, is of good quality. In personal communications during fieldwork, locals consistently expressed their satisfaction with the water quality and that they consider the cistern water suitable for all purposes, including drinking. Nevertheless, one of the primary uses of the harvested rainwater is the watering of livestock. This can be concluded from the information provided by local

residents in personal communications and the widespread occurrence of troughs at or around the manholes of cisterns.

The storage of water in cisterns entails another major advantage: the protection from evaporation. In semiarid or arid areas, which are characterized by high rates of (potential) evaporation, at least during several months of the year, safeguarding water resources from evaporation is crucial. According to estimates, (effective) evaporation in Jordan takes up over 80-90% of the country's annual precipitation (e.g. ALLISON ET AL. 2000, SALAMEH & HADDADIN 2006, HADADIN ET AL. 2010). By collecting and storing parts of the rainwater in cisterns, additional water resources, which otherwise would be lost to evaporation, become available for use.

Another important advantage of RWH in general is the decentralized way in which it is normally applied. The area of runoff collection, and that of its application or the place of water consumption, are usually adjacent or found at short distances to each other. Thus, an extensive network of pipelines for the distribution of water over longer distances is not required. This is not only advantageous economically, in view of the investments necessary for the construction and maintenance of an extensive pipeline network and the required energy expenses for water pumping, but it also minimizes the risk of losses during water distribution, which is a major problem in Jordan (see e.g. BARHAM 2004). Each year, government agencies responsible for the management and distribution of the country's water resources, observe a significant difference between the amount of supplied fresh water and water consumption according to bills. The share of supplied water that is not metered and paid for is declared as losses during water distribution. The percentage of these losses, also termed non-revenue or unaccounted-for unaccounted for water, varies in the different parts of Jordan. In 2014, it amounted to ca. 52% on a nationwide average, and almost 70% in the Karak governorate (MWI 2016b). It is difficult to estimate to what extent these losses arise from technical problems, such as leakages, pipe bursts, and similar issues, or they must be attributed to fraudulent tapping and illegal connections to water supply lines. Yet, these figures illustrate the risks and potential inefficiencies connected to large pipeline networks and a centralized approach in the management of water resources. The various RWH measures, which generally focus on the local development of (additional) water resources, can represent advantageous, complementary, alternative solutions for water supply and management.

Apart from the advantages pointed out above, various other beneficial aspects of RWH in general have been described in numerous studies (e.g. ABUJABER 1995, LABIANCA 1995, PRINZ 1996, JABER & MOHSEN 2001, SALAMEH 2004, ABDULLA & AL-SHAREEF 2009, HELMREICH & HORN 2009, STURM ET AL. 2009, ABU-ZREIG & HAZAYMEH 2012, OWEIS ET AL. 2012, YOUSIF & BUBENZER 2013) (also see chapter 2.4). Among others, these benefits include the alleviation of water stress, which will probably be aggravated in the wake of global and climate change (e.g. PANDEY ET AL. 2003), the improvement of agriculture in dry areas (e.g. OWEIS 2005), and (socio-)economic, as well as, ecological advantages, especially in regard to sustainable development (e.g. GUTTMANN-BOND 2010). Therefore, ancient as

well as new RWH techniques have recently been attracting increasing interest, particularly with regard to those parts of the world where access to adequate freshwater resources is limited. In Jordan, ranked among the ten driest countries of the world in terms of available per capita freshwater resources, the recent, renewed interest in RWH manifests itself in the construction of numerous new cisterns and other RWH structures, such as check dams, bunds, ridges, and the like, and in the rehabilitation of old cisterns. Great interest in the application and improvement of RWH strategies has frequently been expressed by local residents in personal communications as well. The establishment, application, and dissemination of different types of RWH schemes and practices, especially those based on cistern use, have also been the main focus of several projects. The wider scope of these projects was the improvement of living conditions, of opportunities for economic activities (mostly farming and animal husbandry), and of the general development in rural areas, such as the Karak Plateau (cf. e.g. MOP & JICA 1990, JENSSEN 2006, HUMPAL ET AL. 2012, ASSAYED ET AL. 2013). Pilot projects like the aforementioned are usually led by international development aid organizations, NPOs or NGOs, typically in cooperation with local Jordanian organizations or government agencies. Besides promoting traditional and modern strategies of RWH and water management, these projects and the involved organizations also provide the necessary funds or loans for the construction of new RWH facilities, particularly cisterns, which otherwise often could not be realized due to financial constraints. Necessary initial investments for some RWH schemes and structures, such as cisterns, can be quite high, at times even unaffordable for many people, e.g. smallholder farmers or nomads. Therefore, the existing cisterns are extremely valuable, independent of their current condition, as the rehabilitation of old cisterns is normally time- and cost-efficient compared to the construction costs of any new ones. Other RWH structures, such as bunds, ridges, check dams, and the like, which are made of earth and/or stones, are comparably inexpensive and usually require less investments in terms of labor, material and time. Yet, they can be very beneficial and effective for RWH and the reduction of soil erosion. They can form important elements of larger RWH schemes, e.g. in combination with cisterns, in which they serve to (re-)direct, channel and control runoff. Apart from that, bunds, ridges, and similar structures are often employed to improve crop production. Typically installed in groups of several elements, they are used to increase infiltration and soil moisture. In this way, crop production can be enhanced and/or the risk of crop failure can be reduced, particularly in dry areas where water availability is a limiting factor for plant growth. Although occasionally, the efficiency and adequacy of these RWH structures, especially in regard to the cost-benefit ratio of their application, have been questioned (e.g. FLESKENS ET AL. 2005), most studies highlighted the above described benefits of these structures (e.g. SHATANAWI 1994, OWEIS & HACHUM 2006, QADIR ET AL.2007). For optimal results, the suitability of a given RWH approach should be determined individually for each region and site, and RWH schemes need to be adjusted to local circumstances and requirements.

7.4.4 Possible contribution of rainwater harvesting to modern integrated water management

Finally, the relevance of RWH and its possible role in contemporary and future water management and modern societies must be discussed. With respect to the country of Jordan and its ever increasing water shortage, most studies include the adoption of RWH approaches in their recommendations for securing access to adequate water resources (e.g. JABER & MOHSEN 2001, SALAMEH 2004, MOE & UNDP 2009, HADADIN ET AL. 2010, HUMPAL ET AL. 2012, MWI 2016a). However, RWH and the various strategies that are subsumed under this term represent only one option among several for the mitigation of water shortages. The different approaches can largely be divided into two groups: those focusing on the enhancement of water supply and the development of (new) water resources, and those which are related to water demand and aim at an improved management of existing water resources. The main targets of practices of the latter category are typically a reduction of the water demand and a more efficient water use. In regard to the first group of strategies, to which RWH practices can also be assigned, it is debatable if the total amount of annually available water resources can still be increased. Even if this is not the case, approaches of the named category are still valuable and important as to secure access to adequate water resources in the long term. By offering alternatives, the various approaches aimed at the improvement of water availability can lead to a diversification of water resources and thus, an enhanced resilience to droughts and water shortages. Moreover, with further alternatives available, the pressure on nonrenewable and/or non-sustainable sources of freshwater, such as e.g. fossil groundwater reserves and overused aquifers, can be relieved and a greater sustainability may be achieved in the water sector.

Currently a variety of approaches are proposed for the development of additional or alternative water resources. Besides the application of RWH practices, the suggested methods primarily include the desalination of seawater or brackish groundwater, water treatment and recycling, and (grey) water reuse. Mega projects like the planned connection between the Red Sea and the Dead Sea for water transfer and desalination (cf. e.g. AL-KURDI 2008, RABADI 2016) are intended to drastically increase available water resources and with lasting effects through the implementation of a single project. However, projects of these dimensions require huge investments and are still difficult to realize due to the extent and complexity of the necessary construction works and related installations. Moreover, the consequences and effects of such complex mega projects like the Red Sea-Dead Sea connection are often difficult to anticipate and to estimate correctly and reliably, especially with regard to environmental impacts. In comparison to these mega projects, the possible contribution of RWH approaches to the region's water resources and water supply appears rather small. The reliance on RWH as the main or even only source of freshwater seems rather challenging, particularly in view of today's standards in water supply, in terms of quantity and quality. Yet, RWH can represent a valuable additional alternative source of fresh water, and can thus complement the ensemble of available water sources. As such, RWH can help to reduce the pressure on heavily used or overused groundwater aquifers or to replace water supplies currently drawn from nonrenewable sources; mainly fossil groundwater reserves. The amount of freshwater

gained through RWH, and thus the relevance of these practices, also depend on the scale of their implementation. In order to make a significant contribution to the region's water resources, RWH has to be applied extensively, i.e. on a large scale. Numerous individual RWH structures and complex RWH schemes need to be established and large areas have to be reserved for the collection of runoff. Since RWH is a decentralized strategy that is implemented locally, a broad variety and high number of different stakeholders are often involved in coordinated, large scale RWH efforts. The successful implementation and effectiveness of RWH schemes crucially depends on the efforts of the individuals, groups, and organizations responsible for the establishment, supervision, and regular maintenance of the RWH systems. In contrast to the above mentioned large projects and most other water resources, which are extracted in a concentrated manner, i.e. by government agencies and at a limited number of sites, RWH schemes are difficult to manage, monitor, and control by central (government) organizations, particularly with regard to the amount of collected water. On the positive side, RWH typically is a low-tech approach and the necessary facilities for its implementation usually require only small investments, in contrast to many other, major projects in the water sector, e.g. the construction of larger dams. Most RWH techniques and structures have a long history and therefore, are time-tested and well-known and -established. They are sustainable and suitable for a variety of (environmental) settings. The design of RWH schemes can be adapted individually to fit particular local environmental conditions and requirements. RWH alone is probably not able to cover today's water demand. However, it can represent a valuable, complementary approach, especially for the enhancement of water availability in rural and remote areas that are outside of the focus of other, major water projects.

8 Conclusion

Findings of the present study are summarized and put into a broader context in the following chapters. At the same time, the research questions posed in the introduction are answered. For a more convenient correlation between the information provided here and the questions raised in the introduction, the present chapter is subdivided into five sections corresponding to the five subtopics and parts of Table 1 (see chapter 1). The research questions themselves can be found in chapter 1 and are not reproduced here to facilitate a concise, synoptic summary and conclusion.

8.1 Existing rainwater harvesting infrastructure

RWH has long been practiced on the Karak Plateau, probably ever since the area was first settled, and therefore can be seen as an essential part of traditional water management. The reason for this long tradition in RWH most likely lies in the semi-arid climate and the natural environment of the tableland. Other easily accessible sources of fresh water, such as streams and springs, are found only at the fringes and the escarpments of the plateau and in the valleys and lower lands surrounding it. Hence, before the advent of groundwater wells and a public water supply system in modern times, residents, travelers, and farmers on the Karak Plateau had to rely on precipitation as the main source of freshwater for their survival. Since precipitation is largely limited to the winter half year, rainwater and associated runoff had to be collected and stored to ensure sufficient water availability during the dry summer half year. Today a variety of sources of fresh water, including groundwater, are available and the water demand of the local population is primarily covered by the public water supply (tap water). Nevertheless, RWH techniques are still applied and represent an important part of local water resources and water management strategies. Facilities installed for RWH purposes are diverse and mainly comprise open reservoirs and underground cisterns for water storage, more or less complex (modern) RRWH systems, and various linear RWH structures, such as dikes, ridges, bunds, check dams, and similar objects. These shallow channels or walls made of earth or stones are often used to (re-) direct runoff to nearby storage facilities like cisterns, thereby e.g. enlarging the catchment area or redistributing runoff from a large catchment to several cisterns. In most other cases, where they are sited independently from storage facilities, the aforementioned RWH structures are applied to decelerate, spread, retain and ultimately decrease runoff and foster infiltration. Thereby, the amount of water stored in the soil profile should increase in order to benefit enhanced plant growth. The named structures are also able to reduce soil erosion and associated phenomena such as gully formation due to their influence on runoff.

The inventory of RWH structures in the study area provides plenty of evidence for the long history of use, as well as the current application and modern adaptation of (traditional) RWH practices. In many RWH structures, their design and the materials used strongly suggest a recent construction or modification of older structures, thus testifying to the continuing use of the corresponding RWH strategies. Several other RWH facilities, in particular many cisterns, exhibit details that are usually related to a construction during ancient or former times, e.g. the Nabatean, Roman, or Byzantine era. The continued use or current reuse of several of the presumably old cisterns is often indicated by apparently recent modifications such as the attachment of metal closing lids and locks, the installation of modern gas powered or electric water pumps, and/or the reinforcement of old manhole openings of cisterns with modern cement. In contrast to the other RWH practices and facilities, the use of open reservoirs for the storage of (harvested rain-) water obviously has been abandoned. The few existing large, open basins (pools) are commonly considered to be old, probably built during antiquity, and linked to archaeological sites and ruins in the vicinity. In conversations with local residents and at the basins themselves, no evidence could be found for their current use. New, recently constructed open reservoirs have not been detected in the area in the framework of this study. Several disadvantages inherent in this way of water storage may have led to the abandonment of this method and corresponding facilities, particularly when more suitable alternatives for water storage and supply (storage tanks, tap water, etc.) became available. Water contained in open reservoirs is exposed to high risks of contamination and potentially high rates of evaporation. Rising temperatures during warm summer months also facilitate bacterial growth, thus leading to a deterioration of water quality. These risks and drawbacks usually increase with the duration of water storage. They also apply to water contained in pools formed behind small dams across minor wadis. Therefore, runoff collected or stored in this way can only be used for a limited number of purposes, of which groundwater recharge forms the major and most common objective. In the study area, dams and reservoirs are rare and exist only in the southeastern part where the terrain is more rugged and the landscape is that of a dry steppe or semi-desert, with almost no settlement or agricultural areas.

RWH efforts in the study area manifest themselves in large numbers of structures, facilities, and complex schemes of different types at many individual sites all over the tableland. Hence, their comprehensive documentation can pose a challenge, particularly in terms of quantity and spatial extent. GPS based recordings of individual facilities and their locations in fieldwork probably delivers the most reliable and accurate results. However, this approach is usually labor intensive, time-consuming, and restricted to (easily) accessible areas (e.g. public land with moderate relief and little vegetation). Remote sensing techniques, in this case the interpretation of VHR (optical) satellite images, allow for the time-efficient mapping of numerous objects and the examination of a larger area. They also provide a better overview and enable the convenient analysis of even remote or inaccessible terrains. However, not all RWH structures are equally easily discernible in satellite images. Therefore, appropriate mapping procedures must be chosen according to the characteristics of the specific group or type of target objects that should be mapped, and their respective environment. As has been shown in the present study, under appropriate

conditions and with suitable input data, even RWH structures such as cisterns with only small above ground components (in this case manholes) can be detected in satellite images. In order to be reliably identifiable on satellite images, target objects such as RWH facilities should appear as characteristic, distinct features; ideally, they should be located in a contrasting environment (e.g. bare ground area), and they must not be obscured, e.g. by vegetation or buildings. At least in semiarid areas in summer, linear RWH structures typically fulfill the aforementioned requirements and therefore their identification in VHR satellite images is quite straightforward. Nevertheless, all RWH facilities included in the present study are usually so small and diverse in their appearance that they cannot be detected (semi-) automatically with sufficient accuracy. Rather, they should be mapped with visual image interpretation and on-screen digitization by a trained expert. For the best possible results in terms of completeness, accuracy, and reliability, the remote sensing based mapping process should be complemented and enhanced with independent training data and ground truth, both acquired in fieldwork, such as e.g. GPS data. Both mapping approaches, fieldwork and on-screen digitization based on the interpretation of satellite imagery, should be integrated and combined to optimally exploit advantages and overcome inherent limitations of both methods.

RWH structures documented and surveyed during fieldwork were found to be in very heterogeneous conditions, varying from obviously fully functioning, recently constructed or rehabilitated objects to neglected, deteriorated or completely destroyed ones, e.g. due to collapsing or being filled with debris, in the case of cisterns. Particular attention was given to allegedly old cisterns. Several of these could be inspected from the inside and further evidence for their current condition, functionality, age, and history could be collected. In some cisterns, different layers of plaster lining could be observed which suggest discrete phases of repair and a long history of use. Typical stone collars around cistern mouths and characteristic patterns in some of the plaster linings inside cisterns provided further valuable clues to the possible time of construction of these cisterns. Findings largely parallel those from other studies, which investigated archaeological sites and their corresponding RWH and water management structures elsewhere in Jordan. Since these studies strongly suggest a construction during Nabataean, Hellenistic, or Roman times for many of the examined water infrastructure elements, and in view of the resemblances, similar periods of construction can be assumed at least for some of the cisterns in the study area. Absolute dating of cisterns and their materials (mortar or plaster lining inside cisterns) could not be applied in the framework of the present study. In contrast to cisterns, RWH structures such as bunds, dikes, ridges, check dams, and similar objects are typically more temporary in nature and can be relatively easily destroyed and rebuilt, particularly given the design, building materials (earth, loose natural stones), and the small size of these structures in the study area. Therefore, a rather recent time of construction can be assumed for most RWH schemes of this category. Although such currently existing structures most likely did not persist in their current form and location over centuries or even millennia, underlying RWH techniques and largely identical or similar structures have probably been used during,

and since, ancient times. This is suggested by remains identified as possible RWH structures that were associated with other archaeological discoveries or sites on the Karak Plateau.

8.2 Spatial patterns

A broad variety of aspects of the natural and human environment can influence the selection of suitable sites for RWH schemes. Natural environmental circumstances such as the geological underground, soil types and depths, slope, and relief, obviously determine if a location, in general, fits the requirements to accommodate RWH facilities of a given type. Aspects concerning the man-made environment and social, cultural, and economic conditions seem to primarily control which of the generally suitable, potential areas are actually selected as RWH sites. In this regard, factors such as competing land uses (e.g. agriculture), locations of and distances to industrial or mining sites (as potential sources of pollution), settlement areas and related infrastructure (e.g. roads), and the availability of alternative sources of freshwater, play a major role. The latter is partly determined by natural environmental circumstances such as the existence of (perennial) streams and natural springs. It is also influenced by the conditions of the man-made environment, essentially, the access to groundwater through corresponding wells, or to tap water through a connection to the distribution network of the public water supply. The availability or absence of other water resources, together with the spatial distribution of different types of land use, such as e.g. settlement areas, grazing land, or agricultural fields with permanent plants (e.g. fruit trees), usually control where the demand for (additional) water is highest, and thus, where RWH schemes will more likely be sited.

Depending on the type of RWH technique and structures, different locations can be considered appropriate or inappropriate as RWH sites. Cisterns are usually excavated in rock with low permeability and a good natural water holding ability. Suitable sediments or other types of rock should also be available in shallow depth, i.e. near the earth surface, and ideally be characterized by little hardness. Consequently, cistern sites are limited to areas with appropriate geological underground conditions. In comparison to many other RWH structures (e.g. bunds, ridges, and similar), the construction of cisterns is also quite costly in terms of time, labor, and the financial investments required. Therefore, RWH schemes based on cisterns are commonly employed where water of comparatively high quality and multi-purpose usability is required, and/or the collected water needs to be stored for longer periods of time during which evaporation and the deterioration of the water quality must be prevented. In these cases, other, simpler and less expensive RWH techniques and structures most likely do not meet the requirements, and thus may not be applicable. In contrast, the selection of sites for the construction of bunds, dikes, ridges, check dams, and similar structures is probably based on different criteria and takes

into account a different set of factors. For example, these types of RWH facilities may be installed especially in steeper sloping terrain and where a reduction of soil erosion should additionally be achieved. In general, such structures are applied to areas where both runoff should be reduced and retained, and infiltration should increase. Ultimately, besides erosion mitigation, in most cases, the intended purpose of these RWH structures is to increase soil moisture, and thus to sustain and enhance plant growth, e.g. of agricultural crops. Therefore, suitable sites for these types of RWH schemes must feature adequate soil types and depths that allow for the (quick) infiltration and retention of harvested runoff. The water must be plant available, i.e. stored in the soil profile above the wilting point. Soils also need to be suitable for the cultivation of the respective plant species. In other cases, where bunds, dikes, ridges and similar structures are employed for the deceleration, deflection, and/or (re-) direction of runoff to storage units such as cisterns, the selection of appropriate sites is probably largely governed by the conditions required for those, i.e. cisterns, reservoirs, and similar structures.

Noticeable patterns seem to emerge when examining the spatial distribution of RWH sites in conjunction with other data on the natural and human environment. These can be assumed to result from various factors that can influence site selection (see above) and from the weighting of individual aspects. The detection of possible diachronic changes in these patterns and associated site preferences, was primarily based on cistern data as these facilities are quite abundant in the study area and typically are rather permanent in nature. Once constructed, cisterns usually persist over long periods of time. Many of the presumably old cisterns of the Karak Plateau are located in the vicinity of ancient ruins and other archaeological sites that have typically been associated with multiple historical periods. In these places, (fortified) settlements, temples, villas, watchtowers, and similar infrastructure once existed, and at least traces of these are still preserved until today (e.g. a Nabataean temple in Qasr and Roman and Byzantine buildings in ar-Rabba). The proximity between many of the mapped cisterns probably dating to the same periods (see 8.1), and the aforementioned archeological sites, suggests a possible relation. From this it can be inferred that cisterns were built to cover the water demand of the local population at that time. In view of the required investments, cisterns were probably preferably constructed at suitable and central locations, where people could best benefit and where the water supply was most crucial, e.g. for human survival (drinking and other basic needs). Therefore, cisterns were most likely an essential and integral part of the (residential) infrastructure. As capacities of several cisterns suggest, they were probably intended to be shared by larger groups of people. Already existing water supply infrastructures in the form of cisterns could also have been a reason for the continuous use or re-use after the abandonment of a specific place, e.g. as a settlement area, during several periods of time. Since modern settlements mostly were established around, near, or even exactly in the places of ancient buildings and other archaeological remains, most of the presumably old cisterns are nowadays situated close to, or within, modern villages and towns.

In contrast to the described spatial pattern in the distribution of old cisterns, modern RWH facilities, especially modern cisterns, seem to exhibit a different, apparently opposite tendency in their spatial dissemination. In most cases they are located outside of settlement areas and can frequently be found in rather remote places, e.g. at the fringes of the plateau. Since in these areas, and in general outside of modern towns and villages, no access to the network of public water supply (tap water) usually exists. Cisterns are then probably preferably constructed in these specific areas to provide necessary water resources e.g. for the watering of livestock grazing in the area, nomad campsites, or supplemental irrigation of (olive) trees. Environmental aspects seem to play a rather minor role in the site selection process, although locations surely must fulfill some basic requirements for the installation of RWH schemes. However, the range of acceptable natural environmental conditions appears to be rather broad, and hence vast areas of the Karak Plateau can be considered suitable for the application of RWH. This probably increased flexibility, regarding environmental characteristics, manifests itself e.g. in the range of annual precipitation amounts at RWH sites (including drier areas) and the variety of geological settings at cistern locations. The latter is perhaps linked to the use of modern machinery and drilling equipment which render the excavation of underground cisterns more feasible even in areas with harder rock, such as basalt. However, sites of modern RWH structures seem to be generally confined to a narrower range of slope gradients and relatively flat terrain. Nevertheless, apparently modern RWH facilities are distributed over vast areas of the Karak Plateau. Although individual RWH structures (of the same type or different categories) often form clusters or larger RWH schemes, the number of different sites associated with modern RWH is quite high. This dispersed occurrence is also reflected in the relatively large number of small (sub-) catchments within which modern RWH structure are located. At the same time, capacities of modern cisterns are commonly significantly smaller than those of old cisterns. The overall pattern identified in the spatial distribution of modern RWH facilities is best described as a tendency towards extensification (higher number of sites throughout the study area) and local intensification, e.g. in the form of larger, complex RWH schemes at certain sites.

The findings and spatial patterns outlined above should be refined, revised, and corroborated (where applicable) with further data and (statistical, spatial) analyses, such as e.g. a spatial regression analysis. Thus, the understanding of correlations and possible causal relationships between individual aspects of the natural and human environment could be deepened, and further insights could be gained into the site selection process and the formation of patterns in the distribution of RWH sites.

Described patterns in the spatial distribution of RWH structures and diachronic changes in those seem to reflect the respective role and function of RWH nowadays, and in the past. From being the essential, main or probably only source of freshwater on the Karak Plateau, the role of RWH and RWH with cisterns, in particular, has shifted to an alternative, additional source of freshwater which can complement tap water supplies from the public distribution network and water supplies from other sources, such as e.g. groundwater. Along with this, the scope and objectives of RWH approaches have changed.

In the past, the water harvested and stored in cisterns was most likely used for all purposes; primarily, to sustain the survival of the local population. Today the cistern water is mainly used for the watering of livestock and in agriculture (e.g. supplemental irrigation of fruit trees). Sometimes it is also applied to other, domestic purposes such as drinking, cleaning, or the watering of plants in horticulture. With the advent of modern technology and machinery, access to further water resources and new ways of water supply and management became possible and feasible, e.g. with deep drilling to access ground-water resources and the construction and operation of a public water supply system that relies on the centralized management of nationwide water resources, and an extensive pipeline network for water distribution. Hence, the dependence on RWH for water supply decreased and, consequently, many fa-cilities and techniques were given up. In many regions, recent developments such as climate change and population growth have led to a higher variability, or decline in the availability of water resources, and simultaneously an increased water demand. Especially in dry areas, water scarcity is exacerbated and new challenges have arisen with regard to water management and adequate water supply. Against this background, traditional, as well as, new RWH techniques have received new attention and renewed interest as alternative, complementary strategies for the sustainable management of water resources. At the same time, modern machinery and technology, e.g. in the form of excavation machinery and remote sensing and geoinformation technology, have significantly altered the conditions for RWH, in terms of context, possibilities and methodologies. All this has resulted in changes in the feasibility and applica-bility of RWH schemes and different, new, approaches in the planning, site selection process, and man-agement of RWH projects and facilities.

8.3 Rainwater harvesting potential and strategies

The estimated, theoretical annual RWH potential in the study area is as high as $5.70 \cdot 10^6$ m^3 in years with average precipitation conditions (see chapter 6.3). This figure corresponds to all theoretically har-vestable on-site runoff from potentially suitable pervious (i.e. unsealed ground) areas and runoff from the total area of all rooftops of the settlements in the study area. Most of the computed RWH potential (97% or $5.55 \cdot 10^6$ m^3) is made up by on-site runoff from pervious areas, whereas runoff from rooftops constitutes a comparatively small part (3% or $0.15 \cdot 10^6$ m^3). In the calculation of the annual RWH potential, all rooftop areas were considered and those pervious areas that were vegetation-free (at least in summer and according to the acquired LU/LC data), exhibited slope gradients of up to 15%, and had an extent of at least 769 m^2. Accordingly, 88% of the study area, or 90% of the land classified as pervious (to water) in the LU/LC map, were regarded as potentially suitable for the collection of on-site runoff, e.g. with RWH systems based on small plots of bare ground (microcatchments). However, in effect, not all of the theoretically applicable areas can probably be employed for RWH due to several other limiting

factors, such as competing forms of land use (e.g. agricultural production in the rainy winter half year) or required investments for the construction, operation, and maintenance of suitable RWH systems. Thus, with respect to these factors and the feasibility and profitability of RWH schemes compared to other possible sources of water supply, the actual RWH potential in the study area might be significantly lower, depending on the prevailing variable socio-economic conditions. Apart from these considerations, the (theoretical) RWH potential and the appropriateness of its estimation largely depend on the input data (on climate, LU/LC, building footprints, etc.) and its quality. The data used for the calculation of the RWH potential in the present study is assumed to be of high accuracy, although an optimal quality assessment would require further, comprehensive ground truth data. Particularly, inaccuracies in the detected rooftop dataset can affect the estimated RRWH potential significantly. Due to the high amounts of runoff per m^2 and a relatively small total area, here rather small biases in the input data can lead to considerable differences in outcomes, i.e. estimated RRWH potentials. Finally, the annual RWH potential is subject to interannual variations as a direct result of the high variability in annual precipitation. According to data and findings of the study at hand, RWH systems on the Karak Plateau typically collect approximately 50% less runoff in dry years, and up to around 100% more water in exceptionally wet years, compared to long-term average precipitation conditions and the corresponding RWH potential.

Based on statistical data, in 2015, there were assumed to be 23,614 residents in the study area (see 3.6, Table 6) with a water demand of ca. 80 l per person per day for all domestic purposes in the wider sense, including the watering of domestic animals (small-scale animal husbandry) and plants (gardening). Consequently, the essential (domestic) water demand that has to be met amounts to 1,889 m^3 per day and 689,529 m^3 per year in total. Comparing these figures to the calculated theoretical annual RWH potential reveals that the on-site runoff from ca. 13% of the pervious areas classified as potentially suitable for RWH harvesting would have to be collected and stored for subsequent use. In contrast, if all of the estimated annual runoff from rooftops could be harvested, the amount of water would still only meet the annual demand of approx. 5,272 persons, or in other words, correspond to ca. 22% of the required water supply for domestic purposes. These figures do not include the fresh water needed for other uses, e.g. for industrial or agricultural productions. For the study area itself, water demand of these sectors is difficult to quantify. However, especially with regard to agriculture, a variety of RWH systems, including those featuring cisterns, as well as those consisting mainly of bunds, ridges, and similar structures, could probably make a significant contribution to the required water supply. Nevertheless, although probably theoretically possible, as figures suggest, RWH is very likely not suitable as the only strategy of water supply to cover all current demands. Due to required investments and several other obstacles and constraints for the widespread application of RWH, the real annual RWH potential, and hence the amount of water that can practically be collected and supplied, may in effect be considerably smaller.

Besides the quantity of water, the quality of the harvested water is also decisive as it crucially determines its suitability and applicability. In general, with appropriate measures, water from RWH systems can be

used for all, or at least, a broad variety of purposes. The water quality essentially depends on the employed RWH technique and characteristics of the RWH system, e.g. its condition (maintenance), mode of operation, and design, especially regarding the way of water storage and the area from which the runoff is collected. According to the water quality and intended purposes, different types and degrees of water treatment (e.g. filtering, boiling, or disinfection with chemicals or UV light) may be required before water usage. Typically, a more complex, multi-stage, thorough treatment must be applied whenever a safe drinking water quality has to be ensured, whereas for some domestic purposes, such as the flushing of toilets, gardening in some cases, and similar usages, the water from RWH systems, especially RRWH systems, can usually be employed with no, or basic treatment (e.g. particle filtering). Thus, water from RWH schemes can partly replace water from the public supply system (tap water). Thereby the dependence on centralized water resources and their management, as well as the public water supply, can be decreased. This may also reduce associated problems such as the high amounts of losses (ca. 70% of the supplies in the Karak Governorate) during distribution through the extensive pipeline network. RWH typically represents an alternative, complementary source of freshwater used for selected purposes. However, in places with no access to the public water supply network, it can also form the only source of water. Moreover, RWH can also deliver water for agricultural purposes, e.g. for increased moisture availability in soils for plant growth, small-scale supplemental irrigation of permanent plants like trees, livestock husbandry, and horticulture. Thus, other sources such as groundwater reserves may be spared and agricultural production can be improved.

In order to tap the potential of the study area, a variety of RWH techniques can be employed. Apparently, the most suitable and relevant RWH strategies typically have a long tradition and are also applied nowadays. The use of cisterns is especially long-established, very common, and of particular value and relevance. Underground cisterns can provide excellent storage conditions for water, even over longer periods of time. For the best possible water quality and fully functional RWH systems, cisterns need to be combined with suitable areas for the collection of runoff. Rooftops usually represent comparably smooth and clean catchment areas. Hence, RRWH systems, including cisterns or similar storage elements, are particularly valuable. Small plots of bare ground and similar earth surfaces can also be used as catchments of cisterns or other RWH facilities. However, collected runoff from these areas is typically characterized by a higher risk of contamination. Therefore, the harvested water needs intense treatment before use or it can be applied for different purposes, which do not require drinking water quality, e.g. agricultural uses instead of domestic ones. The advantage of RWH systems relying on ground catchments is its upscaling potential. Vast areas on the Karak Plateau can also benefit from the application of bunds, dikes, ridges, check dams, and similar RWH structures that reduce runoff and facilitate infiltration. With respect to relief and soils, large parts of the study area are highly suitable for agriculture, while water availability often represents a limiting factor. The aforementioned RWH structures are able to enhance soil moisture and improve water availability for plant growth. Their application seems particularly advantageous since they can also reduce erosion.

The use of open reservoirs as storage elements in RWH schemes is connected to a number of drawbacks, and therefore should be avoided and replaced by other solutions wherever possible. Consequently, existing ancient open pools are not employed in RWH today (see 8.1). Conditions in the study area also seem unsuitable for flood water harvesting and similar RWH schemes that operate on a larger scale, i.e. involving large catchment areas per individual structure, or collecting runoff from (ephemeral) streams instead of overland flow. This includes dams across wadis to retain and store runoff in reservoirs within the wadi. Occasionally, new RWH approaches and systems or modifications of existing, traditional ones are developed. Their applicability and suitability for a specific area have to be examined individually, particularly regarding the involved cost-benefit ratio, before any recommendations are given.

In order to improve RWH efforts in the study area, the rehabilitation of existing facilities, especially cisterns, and their integration into fully functioning RWH systems, is of utmost importance. Since the excavation of cisterns is usually quite costly, existing, but neglected and deteriorated objects, represent valuable elements of the RWH inventory of the area. They can be reused with comparably small investments for repair, rehabilitation, and modification where necessary. Existing RWH elements often also need to be combined and complemented with additional structures to create fully functional RWH systems. Specifically, the mapped old cisterns, which are mostly located within modern settlement areas, could relatively easily be connected to rooftops in their vicinity to form RRWH systems. However, to be able to exploit a considerable share of the estimated RWH potential, further, new RWH systems and particularly additional facilities for water storage, such as cisterns, have to be constructed as well. The total storage capacity of the 96 presumably old cisterns that were detected in this study was calculated to amount to 12,480 m^3, based on an average capacity of 130 m^3 per object (see chapter 6.1). Accordingly, theoretically, 8% of the estimated annual runoff from rooftops in the study area could be stored. For the 293 mapped, probably modern, cisterns that are usually located outside of settlements and combined with ground catchment areas, an average volume of 30 m^3 per object, and thus a total capacity of 8,790 m^3, was assumed. This overall storage capacity is equivalent to ca. 0.16% of the long-term average annual on-site runoff from all pervious areas that are potentially suitable for RWH. With multiple fillings, the amount of water that could annually be stored in existing cisterns, may rise by 30%. Nonetheless, the storage capacity of all 389 identified cisterns would then still correspond to only ca. 4% of the estimated annual (domestic) water demand of the local population, or the annual water demand of around 947 residents. These results, which do not include other limiting factors, illustrate the necessity of further RWH facilities. The outcomes from the present study and the collected (geo-) data can serve as a first basis for the planning of RWH strategies. For this purpose, the established database can also easily be updated and expanded with further information, as needed.

8.4 Methodological evaluation

For approximately two decades now, research studies and applied projects in the field of RWH have increasingly made use of geoinformation technology. For example, spatial decision support systems have been set up and employed to detect suitable locations for various RWH schemes. In the present study, this approach has virtually been inverted, in that information on RWH sites and their surroundings were gathered and analyzed to identify spatial patterns and possible factors that led to the selection of these sites. At least in the framework of RWH related research, the involved geodata and procedures have perhaps been used for the first time in this way in the present study. The unique aspect should be seen in the specific combination of different GIS and remote sensing (related) techniques, as well as in how these were applied. With respect to mapping procedures and data acquisition, the interpretation of optical VHR satellite images enables the time- and cost-efficient, precise and comprehensive analysis of a larger area and documentation of higher numbers of objects. Thus, access to quantitative aspects and associated research questions is improved and overview and mapping are facilitated, particularly in less accessible, remote areas or difficult terrain. GIS techniques have proved especially beneficial for the processing of (geo-) data and all types of investigations concerning spatial questions, including the detection of spatial patterns and possible correlations between individual features or characteristics. In general, the various methods from the field of geoinformatics can support RWH projects and studies in many ways and at all stages. In the planning phase, they can facilitate the identification of suitable areas, e.g. by integrating all data and processes in a (spatial) decision support system. In the final phase of a project, remote sensing and GIS analyses can be used to control and monitor outcomes and changes. Furthermore, geodata, GIS, and remote sensing can be employed in the management of existing RWH schemes.

The application of different geoinformation methods is connected to individual advantages and drawbacks, and hence each approach exhibits a different suitability for specific purposes and associated limitations. Remote sensing products, techniques, and related procedures have greatly facilitated the acquisition of geodata and information on (objects on) the earth's surface, particularly with regard to larger datasets. Analysis and interpretation of optical (VHR) satellite images allow for the relatively quick, convenient, and inexpensive collection of comprehensive, detailed, and accurate information, e.g. in mapping processes. However, all data derived from satellite images, the imagery itself, and all other products and procedures relying on remote sensing, typically require at least a minimum amount of data from fieldwork, as ground truth, in order to calibrate and evaluate remotely sensed information, and thus ensure an adequate accuracy and reliability in the resulting collected data. With the appropriate processing and auxiliary data (ground truth), VHR satellite images can be employed for the mapping of even very small objects and details. This could be demonstrated in the present study in the context of the detection of RWH structures; particularly cisterns. Regarding the method of image analysis, the

mapping objectives and properties of the target objects or areas determine whether a (semi-) automatic procedure can be applied or a manual approach needs to be adopted. Here, the RWH structures were represented by relatively small details with a very heterogenic appearance, and they were embedded in a variety of different environments. Therefore, their detection had to be based on visual examination of the imagery and manual digitization of objects by a trained expert. In contrast, (semi-) automatic image classification could be employed for the production of the LU/LC map. Thus, satisfactory results could be achieved when the image classification process was largely performed by the software automatically and only minimal input (training templates, classification parameters, etc.) was required from the user. In contrast to the visual-manual image interpretation by an expert, which usually leads to the best, i.e. the most accurate and complete outcomes, the main advantage of (semi-) automatic image analysis is the fast acquisition of consistent results. However, both methods can also be combined to optimally exploit the benefits and overcome the drawbacks of each approach. Outputs of (semi-) automatic image classification can be edited manually, according to visual image interpretation, to complement, edit, revise, control, and thus improve results, as has been shown for parts of the LU/LC map in the present study. The possibility of serial, highly automated analysis of several similar satellite images has additionally been demonstrated. By using Overwatch's Feature Analyst, an automatic feature extraction model could be established and employed in the detection of rooftops that could potentially be suitable for RRWH. Thus, the necessary rooftop data could be acquired with a high degree of automation. The procedure and the developed AFE model can also possibly be used for the rapid detection of rooftops in other (comparable) imagery. With FA, all image interpretation procedures could also be conducted in a GIS environment, in this case ESRI's ArcGIS Desktop, in which most of the other data processing steps and analyses were performed as well. Only the preprocessing of the satellite imagery, which mainly consisted of orthorectification and atmospheric corrections, had to be done with specialized software for the processing of remote sensing data. For all other tasks, ESRI's ArcGIS Desktop, and the various extensions and add-ons available to broaden its functionality, proved to be a versatile and comprehensive integrated solution for the handling and processing of geodata, including visual image interpretation and on-screen digitization, data editing, data management, and visualization with maps. Moreover, within ArcGIS Desktop, spatial analyses could be performed for the determination of RWH site characteristics and the detection of possible spatial relations and patterns in the distribution of features and/or sites. Yet, field work is still indispensable for the acquisition of additional, complementary data. With regard to the study at hand, besides ground truth, this particularly applies to data on the condition of cisterns, typical capacities, and similar information.

Progress in RWH research, and improvement in the planning and application of RWH projects, crucially depend on the quality of available input data. Besides a comprehensive, up-to-date database on existing RWH structures, current, accurate, and detailed LU/LC data is essential. In addition to the LU/LC data acquired in the present study, further relevant information in this regard could comprise (geo-) data on

land parcels and ownership (i.e. data normally contained in a cadastral land register), implemented agricultural practices, vegetation during the winter half year (rainy season during which most of the agriculture is carried out), and more detailed soil maps than the currently available ones. Another type of important, necessary data is ground truth. Concerning the study at hand, further field data or ground truth would be needed to clarify the nature of objects identified as possible additional cisterns based on the interpretation of the satellite imagery. Moreover, helpful additional data, which can only be collected in field work, could comprise (further) exemplary information on the real extents of rooftops and the respective area that could effectively be used for RRWH, as well as the actual conditions of cisterns and their respective storage capacities. The availability of a DEM (DSM) with very high resolution (1 m^2 per pixel or finer) would provide new possibilities for analysis, and thus deeper insights regarding RWH. For example, VHR DEMs would enable the computation of catchments of individual RWH structures and the detection of changes in hydrological features, e.g. catchments, when existing RWH facilities are removed or modified or new RWH structures are installed. VHR DSMs can also be employed for the extraction of building footprints (potential rooftop area), either independently or in combination with (optical) satellite imagery. The accuracy of data acquired in this way is typically higher than that of building data derived from satellite imagery alone. Finally, for the estimation of runoff and RWH potentials, more comprehensive climate data and precipitation records of recent years would be desirable to allow for an assessment of the impact of climate change and the effects of the temporal distribution of precipitation and variations in other parameters (temperature, wind, etc.).

8.5 Synopsis and transferability of outcomes

The study at hand can equally be used as a basis for further research and for practical applications, e.g. improved planning, extension, and operation of RWH schemes. The comprehensive RWH inventory that was established is probably the first of its kind. While the mapping and documentation approach can be transferred to many other areas, the created database itself can serve as a (planning) basis for the enhancement and expansion of RWH efforts and related research in the study area. The benefits of the employment of remote sensing products and techniques could be demonstrated in the context of mapping RWH facilities as well as in connection with the acquisition of other, supplemental data, e.g. on LU/LC, hydrological features (e.g. wadis), and buildings or rooftops. The interpretation of VHR satellite images, either visually-manually or (semi-) automatically, facilitates the time-efficient collection of data and surveys of a broader area. Thereby, questions can also be addressed which require larger datasets and/or concern quantitative aspects. With regard to the building data necessary for the estimation of the RRWH potential, a reusable, transferable classification or AFE model could be developed. The AFE model can be employed for the rapid, automatic detection of rooftops in other satellite images, provided

that the image, the (environmental) setting, and the target objects (i.e. building rooftops) exhibit sufficient similarities to those of the original image analysis task. The application of established AFE models represents the highest degree of automation in image analysis and classification.

The collected data and the analyses performed in a GIS environment allowed deeper insights into the spatial distribution of RWH structures and potential factors that govern site preferences. In environmental settings such as that of the Karak Plateau, where most of the area is considered roughly suitable for RWH (in terms of precipitation, slope, relief, geology, etc.), the precise natural circumstances at a given location seem to be of rather subordinate importance in the site selection process. Apparently, site preferences are largely determined by aspects of the human environment and directly reflect the role and purposes of RWH schemes, for example, when RWH structures are sited together with olive plantations to provide additional water for the supplemental irrigation of these trees.

Additionally, the theoretical annual RWH harvesting potential of the study area was determined and compared to the (domestic) water demand of the local population. Besides this general RWH potential, the annual amount of runoff that could possibly be collected from rooftops was computed. For the estimation of the RRWH potential, a highly automated, straightforward, and yet very accurate methodological approach and workflow could be shown. The employment of actual, recent and comprehensive building data derived from VHR optical satellite imagery was new, compared to previous studies on RRWH potentials in Jordan. Moreover, specific measures and approaches for the enhancement of RWH strategies in the study area could be suggested based on the collected data and outcomes of the present study. Research and data deficits and possibilities for the improvement of involved methods and procedures were pointed out.

Based on the collected data, analyses, and outcomes of the present study, assumptions could also be formulated regarding the role of RWH strategies for human survival and prosperity in a semiarid environment, such as the Karak Plateau. Findings suggest that the role of RWH changed fundamentally over the centuries and millennia. From the beginning of the settlement of the area until the advent of deep groundwater wells and a public water supply system, RWH schemes were most likely the only, and essential, source of freshwater on the Karak Plateau and in other areas without perennial streams or springs. Today, in view of the access to alternative sources, this dependence and reliance on RWH has decreased significantly and RWH schemes rather represent an additional, complementary source of water. Nevertheless, there is a trend for renewed interest in RWH, valuing it as an alternative, time-tested and sustainable source of water which requires relatively little investments and technology and can be applied individually and independently from centralized, public water management schemes. Thus, the use of RWH strategies can reduce the dependence and pressure on other sources, such as e.g. (fossil) groundwater reserves and transfers from other regions (public water supply), particularly at times when these are in short supply or temporarily not available. Although RWH can cover a broad variety of purposes, its main objectives today are typically the supply of additional water for enhanced plant

growth and optimized crop production. RWH structures, primarily cisterns, also appear to be the main source of water for animal husbandry, livestock breeding, and pasture farming, particularly in the case of (semi-) nomadic herders and their animals (mostly sheep and goats). Additionally, RWH schemes, usually based on cisterns, can be the only essential source of water supply for people living, or staying temporarily, in dry, remote locations where no access to a public water supply system or other reliable water resources is given. Furthermore, bunds, ridges, check dams, and similar structures can be applied to reduce erosion and thus, to preserve the vital, irreplaceable soil cover in erosion prone areas.

Owing to the multiple benefits associated with its various techniques and structures, RWH can be worthwhile and offer many benefits for almost any region of the world. Traditionally, especially semiarid, and to some extent arid, areas are perceived as predestined for RWH strategies, due to their natural water shortage. Therefore, these regions regularly feature (relics of) numerous old RWH structures that testify to the long tradition of, and dependence on, RWH that often began with the first settlement of the respective area. Additionally, the existence of modern RWH schemes frequently underpin the contemporary relevance of these techniques. Based on the Jordanian Karak Plateau, exemplarily roles, purposes, (advantageous) effects, history, and potential of RWH in a semiarid area were investigated and pointed out in the present study. Beyond regions with comparable climatic and environmental conditions, slightly drier areas, and regions with higher amounts of annual precipitation, can also benefit from RWH. Besides (low) overall annual precipitation amounts which may entail natural water shortages, the characteristic that most strongly suggests the application of RWH in a given area is the occurrence of strong seasonal differences in precipitation, and hence typically, a temporary, seasonal surplus, alternating with a deficit in water availability. In regions with seasonally high amounts of precipitation and/or frequent intense rainfalls, RWH measures that reduce, retain, spread, decelerate or otherwise modify runoff amounts, dynamics, and properties, can help reduce detrimental effects of episodic or seasonal intense precipitation events, such as e.g. (flash) floods and other problems related to short-term occurrences of high amounts of runoff. In areas that are also characterized by episodic or seasonal deficits in water availability (dry season, frequent droughts, and similar circumstances), RWH schemes that collect and store rainwater and associated runoff can serve as an important source of water during dry periods with water shortages. Through improved water availability, RWH structures designed to retain runoff and increase infiltration and moisture stored in soil profiles are able to enhance agricultural crop production and plant growth in general, particularly in semiarid areas. In the latter, and other regions where erosion is a major problem, primarily due to climatic factors and relief, RWH structures such as bunds, dikes, ridges, and similar objects can significantly reduce the loss of (fertile) soil covers. Independent from climatic circumstances, RWH schemes, especially RRWH systems including cisterns and similar storage elements, can constitute a local and relatively reliable and safe source of freshwater for all purposes, including drinking (with appropriate water treatment). This makes RWH especially interesting and suitable for remote, and other, areas where no access to a public water supply system exists, or the water supply from other sources is associated with increased risks or otherwise is problematic, e.g. due to

frequent contamination, intermittent, unreliable, or inadequate supply, salinization, or decline or depletion of (fossil) groundwater resources. For all areas that fall into one or more of the aforementioned categories, RWH can represent an expedient, valuable, alternative solution to secure access to a sufficient water supply. Depending on individual local circumstances, findings from the study at hand are potentially transferable to other, particularly semiarid, areas. Thus, the present study can provide useful basic information and guidance regarding e.g. methodological approaches, the planning or optimization of RWH schemes, and the (regional) history of RWH and related archaeological topics, well beyond the Karak Plateau and Jordan.

The possible role of RWH, especially with respect to the alleviation of (future) water stress, is strongly connected to the inherent benefits and limitations of the various low-tech, decentralized strategies subsumed under the term RWH. To some degree, the specific suitability, advantages, and constraints also depend on, and vary with, the respective RWH techniques and structures employed. Overall, RWH can represent a valuable, time-tested, and well-established strategy of securing and managing water resources and supply, above all, in a sustainable way. The latter ensures long-term applicability of the involved methods and facilities. In contrast to most other commonly used water resources, RWH is typically applied locally, close to the place of water demand and consumption. Hence, on a larger scale (e.g. nationwide), RWH efforts are accomplished through a large number of independent RWH schemes and systems at many different sites. This decentralized, local, extensive character of the RWH approach also entails the involvement of a large number, and variety, of different parties and stakeholders concerned with the planning, implementation, management, and maintenance of individual RWH schemes. Therefore, on a larger, e.g. national, scale, RWH efforts are rather difficult to organize, monitor, control (e.g. in terms of quantity of actually harvested water), and integrate into the public system of water supply and management. The application of RWH practices and systems shifts responsibilities for an adequate water supply back, at least to some extent, onto local water consumers, i.e. residents, farmers, businesses, communities, local (government) agencies, and other groups and organizations with a similar spatial range. As findings of the present study, particularly estimations of RWH potentials, suggest, RWH should probably best be considered as an alternative, additional source of water that can complement any water supply from other sources, such as surface water reservoirs (dams on major rivers or wadis), groundwater, desalination, and water treatment and recycling. Nevertheless, RWH can form an important, integral part of the diversification of water resources. Diversification, i.e. development of and access to a variety of different sources of water, is probably the best strategy for an enhanced resilience to water stress and water shortages, and any other underlying problems, like dry spells and droughts, overused, depleted or otherwise declining (fossil) groundwater resources, contamination of surface waters, or deficits in the public water supply due to other reasons. Increasing the resilience to water related problems is particularly important in view of an ever-increasing water demand as a result of population growth and heightened risks of water shortages and droughts, due to a decline, and higher variability in

precipitation as a (regional) effect of climate change. However, in order to be really effective, all strategies aimed at securing water supplies, including RWH, must be combined with policies and techniques that improve the management of available water resources. This primarily encompasses various strategies targeting the enhancement of efficiency, such as e.g. water reuse and the elimination of water losses through leakages in pipelines, and thus the reduction of (overall or per capita) water demand. Without an improved management of water demand, efficiency, and resources, all approaches and techniques for the development of, and access to, water resources and an enhanced water supply will fall short of ameliorating the situation in many regions of the world. In many areas, especially arid and semiarid lands with natural water scarcity, water will always be a limited, essential, and hence, precious resource that cannot be wasted or used thoughtlessly, particularly when it should cover the demand of a large population. Consequently, all efforts need to be combined to prevent and reduce water scarcity, droughts, water stress, and related crises and to develop an increased resilience to the aforementioned difficulties. Since the best possible solution is most likely a multipart or multimodal one, all individual approaches and strategies, including RWH, can only represent one part of the puzzle.

References

ABDELKHALEQ, R.A. / ALHAJ AHMED, I. (2007): Rainwater harvesting in ancient civilizations in Jordan. In: Water Science & Technology: Water Supply 7 (1), 85-93.

ABDULLA, F.A. / AL-SHAREEF, A.W. (2006): Assessment of rainwater roof harvesting systems for household water supply in Jordan. In: P. HLAVINEK, T. KUKHARCHYK, J. MARSALEK, I. MAHRIKOVA (Eds.): Integrated urban water resources management. Dordrecht: Springer, 291-300. (NATO Security through Science Series C).

ABDULLA, F.A. / AL-SHAREEF, A.W. (2009): Roof rainwater harvesting systems for household water supply in Jordan. In: Desalination 243, 195-207.

ABU-AWWAD, A.M. / SHATANAWI, M.R. (1997): Water harvesting and infiltration in arid areas affected by surface crust: examples from Jordan. In: Journal of Arid Environments 37, 443-452.

ABUDANH, F. (2007): The water supply systems in the region of Udhruh. In: Studies in the History and Archaeology of Jordan 9, 482-496.

ABUJABER, R.S. (1995): Water collection in a dry farming society. In: Studies in the History and Archaeology of Jordan 5, 737-744.

ABUJABER, R. (2007): The Jordanian countryside as a corridor for population movements and trade. In: Studies in the History and Archaeology of Jordan 9, 89-95.

ABU-SHARAR, T.M. (2006): The challenges of land and water resources degradation in Jordan: diagnosis and solutions. In: W.G. KEPNER, J.L. RUBIO, D.A. MOUAT, F. PEDRAZZINI (Eds.): Desertification in the Mediterranean Region: a security issue. Dordrecht: Springer, 201-226. (NATO Security through Science Series C, 3).

ABU SHMAIS, A.I. (2007): Notes on the old water system and the integrated of Jordan future. In: Studies in the history and archaeology of Jordan 9, 97-102.

ABU-ZREIG, M. / HAZAYMEH, A. (2012): Urban rainfall harvesting to alleviate water shortages and combat desertification in the arid land of Jordan. In: Journal of Arid Land Studies 22 (1), 87-90.

ABU-ZREIG, M. / TAMIMI, A. (2011): Field evaluation of sand-ditch water harvesting technique in Jordan. In: Agricultural Water Management 98, 1291-1296.

ABU-ZREIG, M., ATTOM, M., HAMASHA, N. (2000): Rainfall harvesting using sand ditches in Jordan. In: Agricultural Water Management 46, 183-192.

ABU-ZREIG, M.M., TAMIMI, A., ALAZBA, A.A. (2011): Soil erosion control and moisture conservation of arid lands with stone cover. In: Arid Land Research and Management 25 (3), 294-307.

AGARWAL, A. / NARAIN, S. (Eds.) (1997): Dying wisdom: rise, fall and potential of India's traditional water harvesting systems. New Delhi: Centre for Science and Environment. (State of India's environment: a citizens' report, 4).

AGNEW, C.T., ANDERSON, E., LANCASTER, W., LANCASTER, F. (1995): Mahafir: a water harvesting system in the Eastern Jordan (Badia) Desert. In: GeoJournal 37 (1), 69-80.

AKASHEH, T.S. (2004): Nabataean and modern watershed management around the Siq and Wadi Musa in Petra. In: H.-D. BIENERT/ J. HÄSER (Eds.): Men of dikes and canals: the archaeology of water in the Middle East: international symposium held at Petra, Wadi Musa (H. K. of Jordan), June 15-20, 1999. Rahden: Marie Leidorf, 109-121. (Orient-Archäologie, 13).

AKPINAR FERRAND, E. / CECUNJANIN, F. (2014): Potential of rainwater harvesting in a thirsty world: a survey of ancient and traditional rainwater harvesting applications. In: Geography Compass 8 (6), 395-413.

AL-ADAMAT, R. (2008): GIS as a decision support system for siting water harvesting ponds in the basalt aquifer/ NE Jordan. In: Journal of Environmental Assessment Policy and Management 10(2), 189-206.

AL-ADAMAT, R., DIABAT, A., SHATNAWI, G. (2010): Combining GIS with multicriteria decision making for siting water harvesting ponds in Northern Jordan. In: Journal of Arid Environments 74, 1471-1477.

AL-ADAMAT, R., ALAYYASH, S., AL-AMOUSH, H., AL-MESHAN, O., RAWAJFIH, Z., SHDEIFAT, A., AL-HARAHSHEH, A., AL-FARAJAT, M. (2012): The combination of indigenous knowledge and geo-informatics for water harvesting siting in the Jordanian Badia. In: Journal of Geographic Information System 4, 366-376.

ALAYYASH, S., AL-ADAMAT, R., AL-AMOUSH, H., AL-MESHAN, O., RAWJEFIH, Z., SHDEIFAT, A., AL-HARAHSHEH, A., AL-FARAJAT, M. (2012): Runoff estimation for suggested water harvesting sites in the Northern Jordanian Badia. In: Journal of Water Resources and Protection 4, 127-132.

AL ALI, M. (2012): Soil water conservation and water balance model for micro-catchment water harvesting system. Dissertation, Loughborough Univ., Dept. of Civil and Building Engineering. Loughborough.

AL-ANSARI, N., AL-HANBALY, M., KNUTSSON, S. (2013): Hydrology of the most ancient water harvesting schemes. In: Journal of Earth Sciences and Geotechnical Engineering 3 (1), 15-25.

AL-AZEEZ SHQIARAT, M.A. (2008): The archaeology of water control in the Nabataean and Roman-Byzantine periods in Jordan: overview and case studies from key sites. In: C. OHLIG (Ed.): Cura Aquarum in Jordanien: Proceedings of the 13th international conference on the history of water management and hydraulic engineering in the Mediterranean Region, Petra/ Amman, March 31-April 09, 2007. Siegburg: Deutsche Wasserhistorische Gesellschaft (DWhG), 21-45.

AL-AZEEZ SHQIARAT, M.A., ABUDANH, F.Q., TWAISSI, S.A. (2010): Water management and rock-cut cisterns with special reference to the region of Udhruh in Southern Jordan. In: Jordan Journal for History and Archaeology 4 (2), 205-227.

AL-BAKRI, J.T., AJLOUNI, M., ABU-ZANAT, M. (2008): Incorporating land use mapping and participation in Jordan: an approach to sustainable management of two mountainous areas. In: Mountain Research and Development 28 (1), 49-57.

AL-BAKRI, J., SULEIMAN, A., ABDULLA, F., AYAD, J. (2011): Potential impact of climate change on rainfed agriculture of a semi-arid basin in Jordan. In: Physics and Chemistry of the Earth, Parts A/B/C 36 (5), 125-134.

AL-BASHAIREH, K. / HODGINS, G.W.L (2011): AMS 14C dating of organic inclusions of plaster and mortar from different structures at Petra – Jordan. In: Journal of Archaeological Science 38, 485-491.

ALBERT, R., PETUTSCHNIG, B., WATZKA, M. (2004): Zur Vegetation und Flora Jordaniens. In: W. WAITZBAUER, R. ALBERT, B. PETUTSCHNIG, G. AUBRECHT (Eds.): Reise durch die Natur Jordaniens. Linz: Biologiezentrum der Oberösterreichischen Landesmuseen, 133-220. (Denisia, 14).

AL-EISAWI, D.M. (1985): Vegetation in Jordan. In: Studies in the History and Archaeology of Jordan 2, 45-58.

AL-EISAWI, D. (1996): Vegetation of Jordan. Cairo: UNESCO Regional Office for Science and Technology for the Arab States.

AL FARAJAT, M. (2001): Hydrogeo-Eco-Systems in Aqaba, Jordan – coasts and region: natural settings, impacts of land use, spatial vulnerability to pollution and sustainable management. Dissertation, Univ. of Wuerzburg, Dept. of Geosciences, Institute of Geology. Wuerzburg.

AL-HOMOUD, A.S., ALLISON, R.J., SUNNA, B.F., WHITE, K. (1995): Geology, geomorphology, hydrology, groundwater and physical resources of the desertified Badia environment in Jordan. In: GeoJournal 37 (1), 51-67.

ALI, A., OWEIS, T., SALKINI, A.B., EL-NAGGAR, S. (2009): Rainwater cisterns: traditional technologies for dry areas. Aleppo: ICARDA.

ALI, A., YAZAR, A., AAL, A.A., OWEIS, T., HAYEK, P. (2010): Micro-catchment water harvesting potential of an arid environment. In: Agricultural Water Management 98, 96-104.

ALKHADDAR, R. (2003): Water harvesting in Jordan using earth ponds. In: Waterlines 22 (2), 19-21.

ALKHADDAR, R., PAPADOPOULOS, G., AL-ANSARI, N. (2003): Water harvesting schemes in Jordan. In: Proceedings of the 2nd international conference on efficient use and management of urban water supply, Tenerife (Canary Islands, Spain), April 2-4, 2003. Paper 10087.

ALKHATEEB, O.H. (2007): Evaluation of water harvesting techniques under semi arid environment north of Jordan. Unpublished master thesis, Jordan Univ. of Science and Technology (JUST), Faculty of Graduate Studies. Irbid.

AL-KURDI, O. (2008): The water situation in Jordan. In: C. OHLIG (Ed.): Cura aquarum in Jordanien: proceedings of the 13th international conference on the history of water management and hydraulic engineering in the Mediterranean region, Petra/ Amman, March 31-April 09, 2007. Siegburg: Deutsche Wasserhistorische Gesellschaft (DWhG), 11-20.

AL-LABADI, A.M. (1994): Water harvesting in Jordan: existing and potential systems. In: FAO: Water harvesting for improved agricultural production. Rome: FAO, 211-230. (Water Reports, 3).

ALLISON, R.J., GROVE, J.R., HIGGITT, D.L., KIRK, A.J., ROSSER, N.J., WARBURTON, J. (2000): Geomorphology of the eastern Badia basalt plateau, Jordan. In: Geographical Journal 166 (4), 352-370.

AL QUDAH, B. (2001): Soils of Jordan. In: P. ZDRULI, P. STEDUTO, C. LACIRIGNOLA, L. MONTANARELLA (Eds.): Soil resources of southern and eastern Mediterranean countries. Bari: CIHEAM, 127-141. (Options Méditerranéennes: Série B, 34).

AL-SALAYMEH, A., AL-KHATIB, I.A., ARAFAT, H.A. (2011): Towards sustainable water quality: management of rainwater harvesting cisterns in southern Palestine. In: Water Resources Management 25 (6), 1721-1736.

AL-SEEKH, S.H. / MOHAMMAD, A.G. (2009): The effect of water harvesting techniques on runoff, sedimentation, and soil properties. In: Environmental Management 44, 37-45.

ANDERSSON, J.C.M., ZEHNDER, A.J.B., JEWITT, G.P.W., YANG, H. (2009): Water availability, demand and reliability of in situ water harvesting in smallholder rain-fed agriculture in the Thukela River Basin, South Africa. In: Hydrology and Earth System Sciences 13, 2329-2347.

ANSCHÜTZ, J., KOME, A., NEDERLOF, M., DE NEEF, R., VAN DE VEN, T. (2003): Water harvesting and soil moisture retention. 2nd ed. Wageningen: Agromisa Foundation. (Agrodok, 13).

ANTONIOU, G., KATHIJOTES, N., SPYRIDAKIS, D.S., ANGELAKIS, A.N. (2014): Historical development of technologies for water resources management and rainwater harvesting in the Hellenic civilizations. In: International Journal of Water Resources Development 30 (4), 680-693.

APLIN, P. / SMITH, G.M. (2008): Advances in object-based image classification. In: The International Archives of the Photogrammetry, Remote Sensing and Spatial Information Sciences 37 (Part B7), 725-728.

ARCE, I. (2004): The Umayyad hydraulic system at Amman citadel – collection, storage, distribution, use and sewage. In: H.-D. BIENERT/ J. HÄSER (Eds.): Men of dikes and canals: the archaeology of water in the Middle East: international symposium held at Petra, Wadi Musa (H. K. of Jordan), June 15-20, 1999. Rahden: Marie Leidorf, 243-260. (Orient-Archäologie, 13).

ASHRAF, S., BRABYN, L., HICKS, B.J. (2012): Image data fusion for the remote sensing of freshwater environments. In: Applied Geography 32, 619-628.

ASSAYED, A., HATOKAY, Z., AL-ZOUBI, R., AZZAM, S., QBAILAT, M., AL-ULAYYAN, A., ABU SALEEM, M., BUSHNAQ, S., MARONI, R. (2013): On-site rainwater harvesting to achieve household water security among rural and per-urban communities in Jordan. In: Resources, Conservation and Recycling 73, 72-77.

ASTER GDEM VALIDATION TEAM (2011): ASTER Global Digital Elevation Model Version 2: summary of validation results. http://www.jspacesystems.or.jp/ersdac/GDEM/ver2Validation/Summary_GDEM2_validation_report_final.pdf (access August 3, 2016).

BAICU, K. (2012): Landschaftsklassifikation des jordanischen Karak-Plateaus mithilfe von Feature Analyst. Unpublished master thesis, Insitute of Geography, Heidelberg University. Heidelberg.

BALDERAMA, O.F. (2014): Technical and institutional options of water harvesting systems for climate change adaptation in agriculture. In: W. LEAL FILHO (Ed.): Handbook of climate change adaptation. Berlin/ Heidelberg: Springer, 1-19.

BALKE, K.-D. (2009): Annex 1: case study: rainwater harvesting: final report: STOA Project "Agricultural Technologies for Developing Countries". European Technology Assessment Group (ETAG).

BANDEL, K. / SALAMEH, E.M. (2013): Geologic development of Jordan: evolution of its rock and life. Amman: Elias Mechael Salameh. (National library of the Hashemite Kingdom of Jordan, deposit no. 2013).

BANDEL, K. / SHINAQ, R. (2003): The sea in the Jordan Rift (Northern Jordan) during Oligocene/ Miocene transition with implications to the reconstruction of the geological history of the region. In: Freiberger Forschungshefte C 499: Paläontologie, Stratigraphie, Fazies 11, 97-115.

BARHAM, N. (2004): Human impact on the water problem. In: H.-D. BIENERT/ J. HÄSER (Eds.): Men of dikes and canals: the archaeology of water in the Middle East: international symposium held at Petra, Wadi Musa (H. K. of Jordan), June 15-20, 1999. Rahden: Marie Leidorf, 273-285. (Orient-Archäologie, 13).

BARRON, J. (Ed.) (2009): Rainwater harvesting: a lifeline for human well-being. United Nations Environment Programme (UNEP)/ Stockholm Environment Institute (SEI).

BASTERT, K. / LAMPRICHS, R. (2004): The Wadi Qattar catchment area: ancient techniqes of water usage and storage: an archaeological perspective. In: H.-D. BIENERT/ J. HÄSER (Eds.): Men of dikes and canals: the archaeology of water in the Middle East: international symposium held at Petra, Wadi Musa (H. K. of Jordan), June 15-20, 1999. Rahden: Marie Leidorf, 57-64. (Orient-Archäologie, 13).

BECKERS, B. (2012): Ancient food and water supply in drylands: geoarchaeological perspectives on the water harvesting systems of the two ancient cities Resafa, Syria and Petra, Jordan. Berlin: FU Berlin.

BECKERS, B., SCHÜTT, B., TSUKAMOTO, S., FRECHEN, M. (2013): Age determination of Petra's engineered landscape - optically stimulated luminescence (OSL) and radiocarbon ages of runoff terrace systems in the Eastern Highlands of Jordan. In: Journal of Archaeological Science 40, 333-348.

BELLWALD, U. (2008): The hydraulic infrastructure of Petra - a model for water strategies in arid land. In: C. OHLIG (Ed.): Cura Aquarum in Jordanien: proceedings of the 13th international conference on the history of water management and hydraulic engineering in the Mediterranean region, Petra/ Amman, March 31-April 09, 2007. Siegburg: Deutsche Wasserhistorische Gesellschaft (DWhG), 47-94.

BENDER, F. (1968): Geologie von Jordanien. Berlin: Gebrüder Borntraeger. (Beiträge zur regionalen Geologie der Erde, 7).

BENDER, F. (1975): Geology of the Arabian Peninsula: Jordan. Washington: U.S. Dept. of the Interior, Geological Survey. (Geological Survey Professional Paper, 560-I).

BETTS, A.V.G. / HELMS, S.W. (1989): A water harvesting and storage system at Ibn El-Ghazzi in Eastern Jordan: a preliminary report. Levant 21, 3-11.

BIENERT, H.-D. (2000): Water shortage in Jordan since prehistoric times – lessons from history. In: ICID Journal 49 (4), 17-37.

BIENERT, H.-D. / HÄSER, J. (Eds.) (2004): Men of dikes and canals: the archaeology of water in the Middle East: international symposium held at Petra, Wadi Musa (H. K. of Jordan), June 15-20, 1999. Rahden: Marie Leidorf. (Orient-Archäologie, 13).

BIKAI, P.M. (2004): Madaba's water systems. In: H.-D. BIENERT/ J. HÄSER (Eds.): Men of dikes and canals: the archaeology of water in the Middle East: international symposium held at Petra, Wadi Musa (H. K. of Jordan), June 15-20, 1999. Rahden: Marie Leidorf, 231-235. (Orient-Archäologie, 13).

BLASCHKE, T. (2010): Object based image analysis for remote sensing. In: ISPRS Journal of Photogrammetry & Remote Sensing 65 (1), 2-16.

BLASCHKE, T., LANG, S., HAY, G.J. (Eds.) (2008): Object-based image analysis: spatial concepts for knowlege-driven remote sensing applications. Berlin, Heidelberg: Springer. (Lecture notes in geoinformation and cartography).

BLUME, H.P., BRÜMMER, G.W., HORN, R., KANDELER, E., KÖGEL-KNABNER, I., KRETZSCHMAR, R., STAHR, K., WILKE, B.M. (2010): Scheffer/ Schachtschabel: Lehrbuch der Bodenkunde. 16th edition. Heidelberg: Spektrum.

BLUNDELL, J.S. / OPITZ, D.W. (2006): Object recognition and feature extraction from imagery: the Feature Analyst® approach. In: International Archives of Photogrammetry, Remote Sensing and Spatial Information Sciences 36 (4), C42.

BOCANEGRA-MARTÍNEZ, A., PONCE-ORTEGA, J.M., NÁPOLES-RIVERA, F., SERNA-GONZÁLEZ, M., CASTRO-MONTOYA, A.J., EL-HALWAGI, M.M. (2014): Optimal design of rainwater collecting systems for domestic use into a residential development. In: Resources, Conservation and Recycling 84, 44-56.

BOERS, T.M. (1994): Rainwater harvesting in arid and semi-arid zones. Wageningen: International Institute for Land Reclamation and Improvement (ILRI). (Publication 55).

BOERS, T.M. / BEN-ASHER, J. (1982): A review of rainwater harvesting. In: Agricultural Water Management 5, 145-158.

BRUINS, H.J., EVENARI, M., NESSLER, U. (1986): Rainwater-harvesting agriculture for food production in arid zones: the challenge of the African famine. In: Applied Geography 6, 13-32.

BULCOCK, L.M. / JEWITT, G.P.W. (2013): Key physical characteristics used to assess water harvesting suitability. In: Physics and Chemistry of the Earth 66, 89-100.

BURDON, D.J. (1959): Handbook of the geology of Jordan. Colchester: Benham.

CAGGIANO, M.D., TINKHAM, W.T., HOFFMAN, C., CHENG, A.S., HAWBAKER, T.J. (2016): High resolution mapping of development in the wildland-urban interface using object based image extraction. In: Heliyon 2 (10), e00174.

CALZINI GYSENS, J. (2008): Interim report on the Rabbathmoab and Qaṣr Rabbah Project. In: East and West 58 (1-4), 53-86.

CHESWORTH, W. (Ed.) (2008): Encyclopedia of soil science. Dordrecht, Berlin, Heidelberg, New York: Springer.

CHIBI, M.C. / VAN DUUREN, F.A. (2010): Rainwater harvesting: a technical guide. Pretoria: CSIR, Division of Water Technology.

CHOW, V.T., MAIDMENT, D.R., MAYS, L.W. (1988): Applied hydrology. International Edition. Singapore: McGraw-Hill.

CHU, S.C. (Ed.) (1991): Rainwater catchment for future generations: proceedings of the 5th international conference on rain water cistern systems, Keelung, August 4-10, 1991. Keelung: National Taiwan Ocean University.

COHEN, K.M., FINNEY, S.C., GIBBARD, P.L., FAN, J.-X. (2013, updated): The ICS International Chronostratigraphic Chart. In: Episodes 36, 199-204. http://www.stratigraphy.org/ICSchart/ChronostratChart2018-08.pdf (access April 15, 2019).

CONGALTON, R.G. (1991): A review of assessing the accuracy of classifications of remotely sensed data. In: Remote Sensing Environment 37, 35-46.

CONGALTON, R.G. / GREEN, K. (2009): Assessing the accuracy of remotely sensed data: principles and practices. 2nd edition. Boca Raton: CRC Press.

CORDOVA, C.E. (2007): Millennial landscape change in Jordan: geoarchaeology and cultural ecology. Tucson: The University of Arizona Press.

CORDOVA, C.E., FOLEY, C., NOWELL, A., BISSON, M. (2005): Landforms, sediments, soil development, and prehistoric site settings on the Madaba-Dhiban Plateau, Jordan. In: Geoarchaeology 20 (1), 29-56.

CRITCHLEY, W. / SIEGERT, K. (1991): Water harvesting: a manual for the design and construction of water harvesting schemes for plant production. Rome: FAO.

CROOK, D. (2009): Hydrology of the combination irrigation system in the Wadi Faynan, Jordan. Journal of Archaeological Science 36, 2427-2436.

CZEREPOWICZ, L., CASE, B.S., DOSCHER, C. (2012): Using satellite image data to estimate aboveground shelterbelt carbon stocks across an agricultural landscape. In: Agriculture, ecosystems & environment 156, 142-150.

DANIN, A. (2003-2016a): Flora of Israel online: analytical flora. [Online database]. http://flora.org.il/en/plants/ (access May 10, 2016).

DANIN, A. (2003-2016b): Vegetation of Israel and neighboring countries. http://flora.org.il/en/books/ vegetation-of-israel-and-neighboring-countries/ (access May 10, 2016).

DAVIAU, P.M.M. / FOLEY, C.M. (2007): Nabataean water management systems in the Wadi ath-Thamad. In: Studies in the history and archaeology of Jordan 9, 357-365.

DAVIES, C.P. / FALL, P.L. (2001): Modern pollen precipitation from an elevational transect in central Jordan and its relationship to vegetation. In: Journal of Biogeography 28 (10), 1195-1210.

DEARMAN, J.A. (Ed.) (1989): Studies in the Mesha inscription and Moab. Atlanta: Scholars Press. (Archaeology and biblical studies, 2).

DEBUSK, K. / HUNT, W.F. (2014): Rainwater harvesting: a comprehensive review of literature. Raleigh (North Caroline): Water Resources Research Institute, Univ. of North Carolina. (Report, 425).

DE JAEGER, C. / DE DAPPER, M. (2002): Tectonic control in the geomorphologic development of the Wadi el-Mujib canyon (Jordan). In: EGU Stephan Mueller Special Publication Series 2, 83-94.

DE KWAADSTENIET, M., DOBROWSKY, P.H., VAN DEVENTER, A., KHAN, W., CLOETE, T.E. (2013): Domestic rainwater harvesting: microbial and chemical water quality and point-of-use treatment systems. In: Water, Air, & Soil Pollution 224, 1629.

DEPARTMENT OF ANTIQUITIES (DoA), MINISTRY OF TOURISM AND ANTIQUITIES (n.d.): Jordan cultural heritage: the history of a land. http://doa.gov.jo/en/inside.php?src=sublinks&SlID=5024&MlID=8 (access May 30, 2016).

DEPARTMENT OF POPULATION STATISTICS (DoPS), POPULATION AND SOCIAL STATISTICS DIRECTORATE (2015): The population of the kingdom by administrative divisions, according to the general census of population and housing results 2015. Amman: Department of Statistics.

DEPARTMENT OF STATISTICS (DoS), THE HASHEMITE KINGDOM OF JORDAN (1994): Population (by sex), number of households, housing units and buildings in Karak governorate by administrative division, as of 10/12/1994. http://www.dos.gov.jo/sdb_pop/karak_e.htm (access May 30, 2016).

DEPARTMENT OF STATISTICS (DoS), THE HASHEMITE KINGDOM OF JORDAN (2013): Jordan statistical yearbook 2013. Amman: Department of Statistics.

DEPARTMENT OF STATISTICS (DoS), THE HASHEMITE KINGDOM OF JORDAN (2015): Population and housing census 2015: Table 2.5: Distribution of occupied housing units by private or collective households by main source of drinking water, type of housing unit, urban/rural and governorate. http://www.dos.gov.jo/dos_home_a/main/population/census2015/HousingUnits/Housing_2.5.pdf (access October 5, 2019).

DE VRIES, B. (1987): The el-Lejjun water system. In: S.T. PARKER (Ed): The Roman frontier in Central Jordan: interim report on the Limes Arabicus Project, 1980-1985, Oxford: B.A.R., 399-428.

DE WINNAAR, G., JEWITT, G.P.W., HORAN M. (2007): A GIS-based approach for identifying potential runoff harvesting sites in the Thukela River basin, South Africa. In: Physics and Chemistry of the Earth 32: 1058-1067.

DILE, Y. T., KARLBERG, L., TEMESGEN, M., ROCKSTRÖM, J. (2013): The role of water harvesting to achieve sustainable agricultural intensification and resilience against water related shocks in sub-Saharan Africa. In: Agriculture, ecosystems & environment 181, 69-79.

DINIS, J., NAVARRO, A., SOARES, F., SANTOS, T., FREIRE, S., FONSECA, A., AFONSO, N. TENEDÓRIO, J. (2010): Hierarchical object-based classification of dense urban areas by integrating high spatial resolution satellite images and LiDAR elevation data. In: E.A. ADDINK & F.M.B. VAN COILLIE (Eds.): GEOBIA 2010: geographic object-based image analysis, Ghent, June 29 - July 2, 2010. International Society for Photogrammetry and Remote Sensing (ISPRS), 280-286. (The International Archives of the Photogrammetry, Remote Sensing and Spatial Information Sciences, XXXVIII-4/C7).

DÖRING, M. (2008): Qanat Firaun – über 100 km langer unterirdischer Aquädukt im nordjordanischen Bergland. In: C. OHLIG (Ed.): Cura Aquarum in Jordanien: Proceedings of the 13th international conference on the history of water management and hydraulic engineering in the Mediterranean Region, Petra/ Amman, March 31-April 09, 2007. Siegburg: Deutsche Wasserhistorische Gesellschaft (DWhG), 189-204.

DOMÈNECH, L. / SAURÍ, D. (2011): A comparative appraisal of the use of rainwater harvesting in single and multi-family buildings of the metropolitan area of Barcelona (Spain): social experience, drinking water savings and economic costs. In: Journal of Cleaner Production 19, 598-608.

DOMÈNECH, L., HEIJNEN, H., SAURÍ, D. (2012): Rainwater harvesting for human consumption and livelihood improvement in rural Nepal: benefits and risks. In: Water and Environment Journal 26 (4), 465-472.

DU, Y., BIJKER, W., WANG, C. (2009): Verification of post-tsunami housing reconstruction projects by object-oriented building extraction from high resolution satellite imagery. In: ACRS 2009: proceedings of the 30th Asian conference on remote sensing: geo-referenced images of capitals in Asia, Beijing, October 18-23, 2009. Wuhan: Wuhan University Press, 5 p.

EADIE, J.W. / OLESON, J.P. (1986): The water-supply systems of Nabatean and Roman Humayma. Bulletin of the American Schools of Oriental Research 262, 49-76.

EITEL, B. (2001): Bodengeographie. Braunschweig: Westermann.

EL-NAQA, A. (1993): Hydrological and hydrogeological characteristics of Wadi el Mujib catchment area, Jordan. In: Environmental Geology 22, 257-271.

EL-NAQA, A. (1994): Estimation of transmissivity from specific capacity data in fractured carbonate rock aquifer, central Jordan. In: Environmental Geology 23, 73-80.

ENVIRONMENTAL SYSTEMS RESEARCH INSTITUTE (ESRI) (2010-2018): ArcGIS Desktop Advanced. Versions 10.0-10.6. [Computer program]. Redlands (CA, USA): ESRI, Inc.

ENVIRONMENTAL SYSTEMS RESEARCH INSTITUTE (ESRI) (2014-2017): Arc Hydro for ArcGIS. Versions 2.0.1.156-10.5.0.50. [Computer program]. Redlands (CA, USA): ESRI, Inc.

ENVIRONMENTAL SYSTEMS RESEARCH INSTITUTE (ESRI) (2016): How Topo to Raster works. http://pro.arcgis.com/en/pro-app/tool-reference/spatial-analyst/how-topo-to-raster-works.htm (access August 5, 2016).

ERDAS (2009-2011): ERDAS IMAGINE Professional. Versions 2010 and 2011. [Computer program]. Norcross (GA, USA): ERDAS, Inc.

ERDAS (2010): ERDAS IMAGINE 2010 help document. Norcross (GA, USA): ERDAS, Inc.

ESRI, DELORME PUBLISHING COMPANY, INC. (2015): World Countries. [Feature service]. ESRI. https://services.arcgis.com/P3ePLMYs2RVChkJx/arcgis/rest/services/World_Countries_analysis_trim/FeatureServer (last access December 15, 2015).

ESRI, DIGITALGLOBE, GEOEYE, EARTHSTAR GEOGRAPHICS, CNES/AIRBUS DS, USDA, USGS, AEROGRID, IGN, THE GIS USER COMMUNITY (2015-2019): World Imagery. [Map service]. ESRI. https://services.arcgisonline.com/ArcGIS/rest/services/World_Imagery/MapServer (last access November 3, 2019).

EVENARI, M., SHANAN, L., TADMOR, N. (1982): The Negev: challenge of a desert. 2nd ed. Cambridge: Harvard Univ. Press.

FALKENMARK, M., FOX, P., PERSSON, G., ROCKSTRÖM, J. (2001): Water harvesting for upgrading of rainfed agriculture: problem analysis and research needs. Stockholm: Stockholm International Water Institute (SIWI). (SIWI Report 11).

FAO (1994): Water harvesting for improved agricultural production. Rome: FAO. (Water Reports, 3).

FAO (2006): Guidelines for soil description. 4th edition. Rome: Food and Agriculture Organization of the United Nations (FAO).

FARAHBAKHSH, K., DESPINS, C., LEIDL, C. (2009): Developing capacity for large-scale rainwater harvesting in Canada. In: Water Quality Research Journal of Canada 44 (1), 92-102.

FARDOUS, A.A.-N., TAIMEH, A., JITAN, M. (2004): Indigenous water-harvesting systems in Jordan. In: T. OWEIS, A. HACHUM, A. BRUGGEMAN (Eds.): Indigenous water harvesting systems in West Asia and North Africa. Aleppo (Syria): ICARDA, 42-60.

FARRENY, R., GABARRELL, X., RIERADEVALL, J. (2011a): Cost-efficiency of rainwater harvesting strategies in dense Mediterranean neighbourhoods. In: Resources, Conservation and Recycling 55, 686-694.

FARRENY, R., MORALES-PINZÓN, T., GUISASOLA, A., TAYA, C., RIERADEVALL, J., GABARRELL, X. (2011b): Roof selection for rainwater harvesting: quantity and quality assessments in Spain. In: Water research 45, 3245-3254.

FEINBRUN, N. / ZOHARY, M. (1955): A geobotanical survey of Transjordan. In: Bulletin of the Research Council of Israel 5D, 5-35.

FEWKES, A. (2006): The technology, design and utility of rainwater catchment systems. In: D. BUTLER/ F.A. MEMON (Eds.): Water demand management. London: IWA Publishing, 27-61.

FIDELIBUS, M.W. / BAINBRIDGE, D.A. (1995): Microcatchment water harvesting for desert revegetation. In: Soil Ecology and Restoration Group (SERG) Restoration Bulletin 5, 1-12.

FLESKENS, L., STROOSNIJDER, L., OUESSAR, M., DE GRAAFF, J. (2005): Evaluation of the on-site impact of water harvesting in southern Tunisia. In: Journal of Arid Environments 62, 613-630.

FOODY, G.M. (2002): Status of land cover classification accuracy assessment. In: Remote sensing of environment 80 (1), 185-201.

FOODY, G.M. (2008): Harshness in image classification accuracy assessment. In: International Journal of Remote Sensing 29 (11), 3137-3158.

FRASIER, G.W. (1987): Water harvesting for collecting and conserving water supplies. In: ICRISAT (INTERNATIONAL CROPS RESEARCH INSTITUTE FOR THE SEMI-ARID TROPICS): Alfisols in the semi-arid tropics: proceedings of the consultants' workshop on the state of the art and management alternatives for optimizing the productivity of SAT Alfisols and related soils, INCRISAT Center (Patancheru, India), December 1-3, 1983. Pantacheru (India): ICRISAT, 67-78.

FRASIER, G.W. (1994): Water harvesting/ runoff farming systems for agricultural production. In: FAO: Water harvesting for improved agricultural production. Rome: FAO, 57-71. (Water Reports, 3).

FRASIER, G.W. (1998): Water harvesting for rangeland water supplies: a historic perspective. In: Proceedings of a symposium on environmental, economic, and legal issues related to rangeland water development, Tempe, Arizona, Nov. 13-15, 1997. Tempe (Arizona): The Center for the Study of Law, Science, and Technology, Arizona State Univ., 17-24.

FRASIER, G.W. / MYERS, L.E. (1983): Handbook of water harvesting. Berkeley (California): U.S. Department of Agriculture. (Agriculture Handbook No. 600).

FREIRE, S., SANTOS, T., GOMES, N., FONSECA, A., TENEDÓRIO, J.A. (2010): Extraction of buildings from QuickBird imagery for municipal planning purposes: quality assessment considering existing mapping standards. In: The International Archives of the Photogrammetry, Remote Sensing and Spatial Information Sciences 38 (4): C7.

FREIRE, S., SANTOS, T., GOMES, N., FONSECA, A., TENEDÓRIO, J.A. (2011): Extraction of buildings from QuickBird imagery: what is the relevance of urban context and heterogeneity? In: Geospatial data and geovisualization: environment, security, and society. Special joint symposium of ISPRS Commission IV and AutoCarto 2010 in conjunction with ASPRS / CaGIS 2010 Special Conference, Orlando (Florida), November 15-19, 2010. International Society for Photogrammetry and Remote Sensing (ISPRS). (ISPRS Archives, XXXVIII Part 4).

FREIWAN, M. / KADIOGLU, M. (2008): Spatial and temporal analysis of climatological data in Jordan. In: International Journal of Climatology 28, 521-535.

FROT, E., VAN WESEMAEL, B., BENET, A.S., HOUSE, M.A. (2008): Water harvesting potential in function of hillslope characteristics: a case study from the Sierra de Gador (Almeria province, south-east Spain). In: Journal of Arid Environments 72, 1213-1231.

FRY, L.M., COWDEN, J.R., WATKINS JR, D.W., CLASEN, T., MIHELCIC, J.R. (2010): Quantifying health improvements from water quantity enhancement: an engineering perspective applied to rainwater harvesting in West Africa. In: Environmental Science & Technology 44 (24), 9535-9541.

FUJII, S. (2007): Wadi Abu Tulayha and Wadi Ruweishid ash-Sharqi: an investigation of PPNB barrage systems in the Jafr Basin. In: Neo-Lithics 2/07, 6-16.

FUJII, S. (2010): Domestication of runoff water: current evidence and new perspectives from the Jafr Pastoral Neolithic. In: Neo-Lithics 2/10, 14-32.

FULLER RENNER, H. / FRASIER, G. (1995): Microcatchment water harvesting for agricultural production. In: Rangelands 17 (3), 72-82.

GAMMOH, I.A. (2013): An improved wide furrow micro-catchment for large-scale implementation of water-harvesting systems in arid areas. In: Journal of Arid Environments 88, 50-56.

GARFUNKEL, Z. / BEN-AVRAHAM, Z. (1996): The structure of the Dead Sea basin. In: Tectonophysics 266, 155-176.

GEBEL, H.G.K. (2004): The domestication of water: evidence from early Neolithic Ba'ja? In: H.-D. BIENERT/ J. HÄSER (Eds.): Men of dikes and canals: the archaeology of water in the Middle East: international symposium held at Petra, Wadi Musa (H. K. of Jordan), June 15-20, 1999. Rahden: Marie Leidorf, 25-36. (Orient-Archäologie, 13).

GEOEYE (2009): GeoEye product guide. Version 1.0.1. Dulles (Virginia): GeoEye.

GEOEYE (2010): Product order metadata. Thornton (Colorado): GeoEye.

GEOSYSTEMS (2011): ATCOR for ERDAS IMAGINE 2011: haze reduction, atmospheric and topographic reduction: user manual ATCOR2 and ATCOR3. Manual version 04/01/2011. Germering: GEOSYSTEMS.

GEOSYSTEMS (2012): ATCOR: Answers to the FAQs. http://www.geosystems.de/atcor/faqs/index.html (access October 15, 2012).

GHRAYYIB, R. / RONZA, M.E. (2007): Archaeological evidence of water distribution and quarrying activity at Qasr al-Hallabat. In: Studies in the history and archaeology of Jordan 9, 423-429.

GLUECK, N. (1934): Explorations in Eastern Palestine, I. In: The Annual of the American Schools of Oriental Research 14, 1-113.

GLUECK, N. (1939): The Nabataean temple of Qasr Rabbah. In: American Journal of Archaeology 43 (3), 381-387.

GOULD, J. (1999): Is rainwater safe to drink? A review of recent findings. In: Proceedings of the 9th international rainwater catchment systems conference. Petrolina (Brazil), July 1999. http://www.eng.warwick.ac.uk/ircsa/9th.html (access November 3, 2015).

GOULD, J. / NISSEN-PETERSEN, E. (1999): Rainwater catchment systems for domestic supply: design, construction and implementation. London: Intermediate Technology Publications.

GREEN, M.D. (2004a): An analysis of the possible influence of climate in settlement shifts across the Karak Plateau and surrounding region, Jordan: chalcolithic through Umayyad periods. In: The Arab World Geographer 7 (3), 193-205.

GREEN, M.D. (2004b): Roman and Umayyad settlements on the Karak Plateau: using technology to determine site location factors on a regional scale. In: Near Eastern Archaeology 67 (4), 220-225.

GREENBAUM, N., BEN-ZVI, A., HAVIV, I., ENZEL, Y. (2006): The hydrology and paleohydrology of the Dead Sea tributaries. In: Y. Enzel, A. Agnon, and M. Stein (Eds.): New frontiers in Dead Sea paleoenvironmental research. Boulder (Colorado, USA): The Geological Society of America, 63-93. (Special Paper, 401).

GÜNERALP, İ., FILIPPI, A.M., HALES, B. (2014): Influence of river channel morphology and bank characteristics on water surface boundary delineation using high-resolution passive remote sensing and template matching. In: Earth Surface Processes and Landforms 39 (7), 977-986.

GUNNELL, Y. / KRISHNAMURTHY, A. (2003): Past and present status of runoff harvesting systems in dryland peninsular India: a critical review. In: AMBIO: A Journal of the Human Environment 32 (4), 320-324.

GURUNG, T.R. / SHARMA, A. (2014): Communal rainwater tank systems design and economies of scale. In: Journal of Cleaner Production 67, 26-36.

GUTTMANN-BOND, E. (2010): Sustainability out of the past: how archaeology can save the planet. In: World Archaeology 42 (3), 355-366.

HADADIN, N., QAQISH, M., AKAWWI, E., BDOUR, A. (2010): Water shortage in Jordan – sustainable solutions. In: Desalination 250, 197-202.

HADADIN, N., SHAWASH, S., TARAWNEH, Z., BANIHANI, Q., HAMDI, M.R. (2012): Spatial hydrological analysis for water harvesting potential using ArcGIS model: the case of the north-eastern desert, Jordan. In: Water Policy 14, 524-538.

HARLAN, J.R. (1985): The Early Bronze Age environment of the Southern Ghor and the Moab Plateau. In: Studies in the History and Archaeology of Jordan 2, 125-130.

HARRISON, T.P. (1997): Shifting patterns of settlement in the highlands of Central Jordan during the Early Bronze Age. In: Bulletin of the American Schools of Oriental Research 306, 1-37.

HAYEK, B.O. (2009): Water resources in the Arab World: a case study on Jordan. In: H.G. BRAUCH, Ú. OSWALD SPRING, J. GRIN, C. MESJASZ, P. KAMERI-MBOTE, N.C. BEHERA, B. CHOUROU, H. KRUMMENACHER (Eds.): Facing global environmental change: environmental, human, energy, food, health and water security Concepts. Berlin, Heidelberg: Springer, 615-621. (Hexagon series on human and environmental security and peace, 4).

HEEMEIER, B., RAUEN, A., WALDHÖR, M., GROTTKER, M. (2008): Tall Hujayrat al-Ghuzlan – das wasserwirtschaftliche System einer prähistorischen Siedlung in Südjordanien. In: C. OHLIG (Ed.): Cura Aquarum in Jordanien: Proceedings of the 13th international conference on the history of water management and hydraulic engineering in the Mediterranean Region, Petra/ Amman, March 31-April 09, 2007. Siegburg: Deutsche Wasserhistorische Gesellschaft (DWhG), 119-153.

HELMREICH, B. / HORN, H. (2009): Opportunities in rainwater harvesting. In: Desalination 248, 118-124.

HELMS, S.W. (1981): Jawa: lost city of the Black Desert. London: Methuen.

HIRT, C. (2014): Digital terrain models. In: E. GRAFAREND (Ed.): Encyclopedia of geodesy. Living reference work, continuously updated edition. Basel, Cham: Springer International.

HOMÈS-FREDERICQ, D. / FRANKEN, H.J. (1986): Pottery and potters – past and present: 7000 years of ceramic art in Jordan. Tuebingen: Attempto. (Ausstellungskataloge der Universitaet Tuebingen, 20).

HUMPAL, D., EL-NASER, H., IRANI, K., SITTON, J., RENSHAW, K., & GLEITSMANN, B. (2012). A review of water policies in Jordan and recommendations for strategic priorities. USAID.

HUSSAIN, I., ABU-RIZAIZA, O.S., HABIB, M.A.A., ASHFAQ, M. (2008): Revitalizing a traditional dryland water supply system: the karezes in Afghanistan, Iran, Pakistan and the Kingdom of Saudi Arabia. In: Water International 33 (3), 333-349.

HUTCHINSON, M.F. (1989): A new procedure for gridding elevation and stream line data with automatic removal of spurious pits. In: Journal of Hydrology 106, 211-232.

HUTCHINSON, M.F. (1996): A locally adaptive approach to the interpolation of digital elevation models. In: Proceedings of the third international conference/ workshop on integrating GIS and environmental modeling, Santa Fe (New Mexico, USA), January 21-25, 1996. Santa Barbara (California, USA): National Center for Geographic Information and Analysis (NCGIA), 390-396. http://escholarship.org/uc/item/43x094z3 (access August 11, 2016).

HUTCHINSON, M.F. / GALLANT, J.C. (2000): Digital elevation models and representation of terrain shape. In: J.P. WILSON, J.C. GALLANT (Eds.): Terrain analysis: principles and applications. New York: Wiley, 29-50.

HUTCHINSON, M.F., XU, T., STEIN, J.A. (2011): Recent progress in the ANUDEM elevation gridding procedure. In: T. HENGEL, I.S. EVANS, J.P. WILSON, M. GOULD (Eds.): Proceedings of the Geomorphometry 2011 conference and workshop, Redlands (California), September 7-9, 2011. International Society for Geomorphometry, 19–22.

HUTCHINSON, M.F., STEIN, J.A., STEIN, J.L., XU, T. (2009): Locally adaptive gridding of noisy high resolution topographic data. In: R.S. ANDERSSEN, R.D. BRADDOCK, L.T.H. NEWHAM (Eds.): Proceedings of the 18th world IMACS congress and MODSIM09 international congress on modelling and simulation, Cairns (Australia), July 13-17, 2009. Modelling and Simulation Society of Australia and New Zealand and International Association for Mathematics and Computers in Simulation, 2493–2499.

IBRAHIM, K.M., MOH'D, B.K., MASRI, A.I., AL-TAJ, M.M., MUSLEH, S.M., ALZUGHOUL, K.A. (2014): Volcanotectonic evolution of central Jordan: evidence from the Shihan Volcano. In: Journal of African Earth Sciences 100, 541-553.

INTWATER (n.d.): Welcome to INTwater: the International Network on Traditional Water Use is a global network promoting historical documentation and rehabilitation perspectives of traditional water use objects. http://www.intwater.uni-freiburg.de (access September 14, 2015).

IRCSA (n.d.a): International Rainwater Catchment Systems Association: conference abstracts. http://www.eng.warwick.ac.uk/ircsa/conference_abstracts.html (access October 27, 2015).

IRCSA (n.d.b): International Rainwater Catchment Systems Association: international conference proceedings. http://ircsa.ir/files/site1/english/conference/index.html (access April 11, 2019).

ISLAM, M.M., CHOU, F.N.-F., KABIR, M.R., LIAW, C.-H. (2010): Rainwater: a potential alternative source for scarce safe drinking and arsenic contaminated water in Bangladesh. In: Water resources management 24 (14), 3987-4008.

IUSS WORKING GROUP WRB (2007): World Reference Base for Soil Resources 2006. Rome: FAO. (World Soil Resources Reports, 103).

JABER, J.O. / MOHSEN, M.S. (2001): Evaluation of non-conventional water resources supply in Jordan. In: Desalination 136, 83-92.

JAPAN AEROSPACE EXPLORATION AGENCY (JAXA) / EARTH OBSERVATION RESEARCH CENTER (EORC) (n.d.): About ALOS-PRISM. http://www.eorc.jaxa.jp/ALOS/en/about/prism.htm (access August 3, 2016).

JENSSEN, S.M. (2006): Traditional rainwater harvesting in Jordan: a qualitative study of Project Rainkeep (1994-1995). Master thesis. Bergen: The University of Bergen.

JET PROPULSION LABORATORY (JPL), CALIFORNIA INSTITUTE OF TECHNOLOGY (CALTECH), NASA (2012): ASTER Global Digital Elevation map announcement. https://asterweb.jpl.nasa.gov/gdem.asp (access August 3, 2016).

JIMÉNEZ, C., TEJEDOR, M., DÍAZ, F. (2004): The impact of water harvesting on soil properties in the island of Fuerteventura, Spain. In: Soil Use and Management 20 (1), 89–91.

JOHNS, J. (1992): Islamic settlement in Ard Al-Karak. In: Studies in the History and Archaeology of Jordan 4, 363-369.

JOUKOWSKY, M.S. / CLOKE, C.F. (2007): The Petra Great Temple's water strategy. In: Studies in the history and archaeology of Jordan 9, 431-437.

KADAM, A.K., KALE, S.S., PANDE, N.N., PAWAR, N.J., SANKHUA, R.N. (2012): Identifying potential rainwater harvesting sites of a semi-arid, basaltic region of Western India, using SCS-CN method. In: Water Resources Management 26 (9), 2537-2554.

KANA'AN, R. / MCQUITTY, A. (1994): The architecture of Al-Qasr on the Kerak Plateau: an essay in the chronology of Vernacular architecture. In: Palestine Exploration Quarterly 126, 127-154.

KEILHOLZ, P. (2007): Die Zisternen der antiken Stadt Gadara (Umm Qais, Jordanien). In: C. OHLIG (Ed.): Antike Zisternen. Siegburg: Deutsche Wasserhistorische Gesellschaft (DWhG), 195-228.

KEILHOLZ, P. (2014): The ancient cisterns of Hellenistic Gadara/ Umm Qais (Jordan). In: T. SCHÄFER, F. SCHÖN, A. GERDES, J. HEINRICHS (Eds.): Antike und Moderne Wasserspeicherung: Internationaler Workshop vom 11. - 14.05.2011 in Pantelleria (Italien). Rahden: Marie Leidorf, 27-36. (Tübinger Archäologische Forschungen, 12).

KEMPE, S., AL-MALABEH, A., AL-SHREIDEH, A., HENSCHEL, H.-V. (2006): Al-Daher Cave (Bergish), Jordan, the first extensive Jordanian limestone cave: a convective Carlsbad-type cave? In: Journal of Cave and Karst Studies 68 (3), 107-114.

KHRESAT, S.A. (2001): Calcic horizon distribution and soil classification in selected soils of north-western Jordan. In: Journal of Arid Environments 47, 145-152.

KHRESAT, S.A. / TAIMEH, A.Y. (1998): Properties and characterization of vertisols developed on limestone in a semi-arid environment. In: Journal of Arid Environments 40, 235-244.

KHRESAT, S.A., AL-BAKRI, J., AL-TAHHAN, R. (2008): Impacts of land use/ cover change on soil properties in the Mediterranean region of northwestern Jordan. In: Land Degradation & Development 19 (4), 397-407.

KIRK, A. (1998): A synthesis of climatic data with specific interest in the precipitation record. In: R.W. DUTTON, J.I. CLARKE, A. BATTIKHI (Eds.): Arid land resources and their management: Jordan's desert margin. London: Kegan Paul International, 47-66.

KLEMM, O., SCHEMENAUER, R. S., LUMMERICH, A., CERECEDA, P., MARZOL, V., CORELL, D., VAN HEERDEN, J., REINHARD, D., GHEREZGHIHER, T., OLIVIER, J., OSSES, P., SARSOUR, J., FROST, E., ESTRELA, M.J., VALIENTE, J.A., FESSEHAYE, G.M. (2012): Fog as a fresh-water resource: overview and perspectives. In: Ambio 41 (3), 221-234.

KOELBEL, J. (2009): Survey and assessment of ancient cisterns in the West Bank. Bethlehem: Applied Research Institute of Jerusalem (ARIJ).

KOUCKY, F.L. (1987a): Survey of the Limes zone. In: S.T. PARKER (Ed.): The Roman frontier in Central Jordan: interim report on the Limes Arabicus Project, 1980-1985. Vol. 1. Oxford: B.A.R.. (BAR International Series, 340), 41-105.

KOUCKY, F.L. (1987b): The regional environment. In: S.T. PARKER (Ed.): The Roman frontier in Central Jordan: interim report on the Limes Arabicus Project, 1980-1985. Vol. 1. Oxford: B.A.R.. (BAR International Series, 340), 11-40.

KRAUSHAAR, S. (2016): Soil erosion and sediment flux in northern Jordan: analysis, quantification and the respective qualitative impacts on a reservoir using a multiple response approach. Switzerland: Springer International. (Springer Theses).

KRAUSHAAR, S., OLLESCH, G., SIEBERT, C., VOGEL, H. J., FUCHS, M. (2015): Long-term sediment export estimates from northern Jordan using Roman cisterns as sediment traps. In: Geoarchaeology 30 (4), 369-378.

KUMAR, T. / JHARIYA, D.C. (2016): Identification of rainwater harvesting sites using SCS-CN methodology, remote sensing and Geographical Information System techniques. In: Geocarto International 32 (12), 1367-1388.

KUNAPO, J., SIM, P.T., CHANDRA, S. (2005): Towards automation of impervious surface mapping using high resolution orthophoto. In: Applied GIS 1 (1), 3.1-3.19.

LABIANCA, O.S. (1995): On-site water retention strategies: solutions from the past for dealing with Jordan's present water crisis. In: Studies in the History and Archaeology of Jordan 5, 771-777.

LABIANCA, O.S. / YOUNKER, R.W. (1998): The kingdoms of Ammon, Moab and Edom: the archaeology of society in Late Bronze/ Iron Age Transjordan (ca. 1400-500 BCE). In: T.E. LEVY (Ed.): The archaeology of society in the Holy Land. London: Leicester University Press, 399-415.

LANCASTER, B. (2009): Rainwater harvesting for drylands and beyond. Vol. 1: Guiding principles to welcome rain into your life and landscape. Tucson (Arizona): Rainsource Press.

LANCASTER, W. / LANCASTER, F. (1995a). Land use and population in the area north of Karak. In: Levant, 27 (1), 103-124.

LANCASTER, W. / LANCASTER, F. (1995b): Traditional systems of water conservation in the Eastern Badiya of Jordan. In: Studies in the History and Archaeology of Jordan 5, 767-776.

LANCASTER, W. / LANCASTER, F. (1999): People, land and water in the Arab Middle East: environments and landscapes in the Bilâd ash-Shâm. Amsterdam: Harwood. (Studies in environmental anthropology, 2).

LANDIS, J.R. / KOCH, G.G. (1977): The measurement of observer agreement for categorical data. In: Biometrics 33 (1), 159-174.

LANGE, J., HUSARY, S., GUNKEL, A., BASTIAN, D., GRODEK, T. (2012): Potentials and limits of urban rainwater harvesting in the Middle East. In: Hydrology and Earth System Sciences 16 (3), 715-724.

LAUREANO, P. (2004): Traditional techniques of water management: a new model for a sustainable town and landscape: from the first water harvesting surfaces to Paleolithic hydraulic labyrinths. In: Perspectivas Urbanas 4, 1-7.

LAVEE, H., POESEN, J., YAIR, A. (1997): Evidence of high efficiency water-harvesting by ancient farmers in the Negev Desert, Israel. In: Journal of Arid Environments 35, 341-348.

LAVENTO, M., HUOTARI, M., JANSSON, H., SILVONEN, S., FIEMA, Z.T. (2004): Ancient water management systems in the area of Jabal Haroun, Petra. In: H.-D. BIENERT/ J. HÄSER (Eds.): Men of dikes and canals: the archaeology of water in the Middle East: international symposium held at Petra, Wadi Musa (H. K. of Jordan), June 15-20, 1999. Rahden: Marie Leidorf, 163-172. (Orient-Archäologie, 13).

LAVIGNE, D.A., HONG, G., ZHANG, Y. (2006): Performance assessment of automated feature extraction tools on high resolution imagery. In: MAPPS/ ASPRS 2006 Fall Conference, San Antonio (Texas), November 6-10, 2006. http://www.asprs.org/a/publications/proceedings/fall2006/0026.pdf (access December 15, 2016).

LEIN, H. (2004): Managing the water of Kilimanjaro: irrigation, peasants, and hydropower development. In: GeoJournal 61 (2), 155-162.

LEROY, S.A.G. (2010): Pollen analysis of core DS7-1SC (Dead Sea) showing intertwined effects of climatic change and human activities in the Late Holocene. In: Journal of Archaeological Science 37 (2), 306-316.

LI, W. / GUO, Q. (2013): A new accuracy assessment method for one-class remote sensing classification. In: IEEE Transactions on Geoscience and Remote Sensing 52 (8), 4621-4632.

LI, X.-Y., XIE, Z.-K., YAN, X.-K. (2004): Runoff characteristics of artificial catchment materials for rainwater harvesting in the semiarid regions of China. In: Agricultural Water Management 65, 211-224.

LI, X., ZHANG, R., GONG, J., XIE, Z. (2002): Effects of rainwater harvesting on the regional development and environmental conservation in the semiarid loess region of Northwest China. In: Proceedings of the 12th ISCO Conference, Beijing (China), May 26-31, 2002. Tsinghua University Press, 482-486.

LI, Z., BOYLE, F., REYNOLDS, A. (2010). Rainwater harvesting and greywater treatment systems for domestic application in Ireland. In: Desalination 260, 1-8.

LICHTENBERGER, A., LINDROOS, A., RAJA, R., HEINEMEIER, J. (2015): Radiocarbon analysis of mortar from Roman and Byzantine water management installations in the Northwest Quarter of Jerash, Jordan. In: Journal of Archaeological Science: Reports 2, 114-127.

LIGHTFOOT, D.R. (1997): Qanats in the Levant: hydraulic technology at the periphery of early empires. In: Technology and Culture 38 (2), 432-451.

LIGHTFOOT, D.R. (2000): The origin and diffusion of qanats in Arabia: new evidence from the northern and southern peninsula. In: The Geographical Journal 166 (3), 215-226.

LILLESAND, T.M., KIEFER, R.W., CHIPMAN, J.W. (2015): Remote sensing and image interpretation. 7th ed. Hoboken (New Jersey): Wiley.

LINDNER, M. (2005): Water supply and water management at ancient Sabra (Jordan). In: Palestine Exploration Quarterly 137 (1), 33-52.

LUCKE, B. (2007): Demise of the Decapolis: past and present desertification in the context of soil development, land use and climate. Dissertation, Brandenburg Univ. of Technology (BTU) Cottbus, Faculty of Environmental Sciences and Process Engineering. Cottbus.

LUCKE, B., ZIADAT, F., TAIMEH, A. (2013): The soils of Jordan. In: M. ABABSA (Ed.): Atlas of Jordan: history, territories and society. Beirut: Presses de l'Ifpo, Institut français du Proche-Orient, 72-76. (Contemporain publications (CP), 32).

LUCKE, B., KEMNITZ, H., BÄUMLER, R., SCHMIDT, M. (2014): Red Mediterranean soils in Jordan: new insights in their origin, genesis, and role as environmental archives. In: Catena 112, 4-24.

LUEBKER, T. / SCHAAB, G. (2008): Identifying benefits of pre-processing large area QuickBird imagery for object-based image analysis. In: T. BLASCHKE, S. LANG, G.J. HAY (Eds.): Object-based image analysis: spatial concepts for knowledge-driven remote sensing applications. Berlin, Heidelberg: Springer, 203-220. (Lecture notes in geoinformation and cartography).

MACDONALD, B. (2001): Climatic changes in Jordan through time. In: B. MACDONALD, R. ADAMS, P. BIENKOWSKI (Eds.): The archaeology of Jordan. Sheffield (UK): Sheffield Academic Press, 595-601.

MADSEN, M.D., ZVIRZDIN, D.L., DAVIS, B.D., PETERSEN, S.L., ROUNDY, B.A. (2011): Feature extraction techniques for measuring pinon and juniper tree cover and density, and comparison with field-based management surveys. In: Environmental Management 47 (5), 766-776.

MAETENS, W., VANMAERCKE, M., POESEN, J., JANKAUSKAS, B., JANKAUSKIENE, G., IONITA, I. (2012): Effects of land use on annual runoff and soil loss in Europe and the Mediterranean: a meta-analysis of plot data. In: Progress in Physical Geography 36 (5), 599-653.

MAGELLAN NAVIGATION, INC. (2008): MobileMapper™ 6: getting started guide. Santa Clara (USA): Magellan Navigation, Inc.

MAHMOUD, S.H., MOHAMMAD, F.S., ALAZBA, A.A. (2015): Delineation of potential sites for rainwater harvesting structures using a geographic information system-based decision support system. In: Hydrology Research 46 (4), 591-606.

MALIVA, R. / MISSIMER, T. (2012): Arid lands water evaluation and management. Heidelberg: Springer. (Environmental Science and Engineering: Environmental Science).

MARGANE, A., HOBLER, M., ALMOMANI, M, SUBAH, A. (2002): Contributions to the hydrogeology of Northern and Central Jordan. In: Geologisches Jahrbuch C 68, 3-52.

MATOS, C., SANTOS, C., PEREIRA, S., BENTES, I., IMTEAZ, M. (2013): Rainwater storage tank sizing: case study of a commercial building. In: International Journal of Sustainable Built Environment 2, 109-118.

MATOS SILVA, C., SOUSA, V., VAZ CARVALHO, N. (2015): Evaluation of rainwater harvesting in Portugal: application to single-family residences. In: Resources, Conservation and Recycling 94, 21-34.

MATTINGLY, G.L. (1996a): Al-Karak Resources Project 1995: a preliminary report on the pilot season. In: Annual of the Department of Antiquities of Jordan 40, 349-368.

MATTINGLY, G.L. (1996b): The King's Highway, the Desert Highway, and Central Jordan's Kerak Plateau. In: ARAM 8, 89-99.

MATTINGLY, G.L. / PACE, J.H. (2007): Crossing Jordan: by way of the Karak plateau. In: T.E. LEVY, P.M.M. DAVIAU, R.W. YOUNKER, M. SHAER (Eds.): Crossing Jordan: North American contributions to the archaeology of Jordan. London, Oakville: Equinox, 153-159.

MATTINGLY, G.L., PACE, J.H., STEPHENSON, R.A., WAGNON, E.P. (1998): The water catchment system of Nakhl, Jordan. In: Annual of the Department of Antiquities of Jordan 42, 331-341.

MAYS, L.W. (Ed.) (2010): Ancient water technologies. Dordrecht, Heidelberg: Springer.

MAYS, L.W. / GOROKHOVICH, Y. (2010): Water technology in the ancient American societies. In: L.W. MAYS (Ed.): Ancient water technologies. Dordrecht, Heidelberg: Springer, 171-200.

MAYS, L.W., KOUTSOYIANNIS, D., ANGELAKIS, A.N. (2007): A brief history of urban water supply in the antiquity. In: Water Science & Technology: Water Supply 7 (1), 1-12.

MBILINYI, B.P., TUMBO, S.D., MAHOO, H., MKIRAMWINYI, F.O. (2007): GIS-based decision support system for identifying potential sites for rainwater harvesting. In: Physics and Chemistry of the Earth 32, 1074-1081.

MCCARTHY, J.J., CANZIANI, O.F., LEARY, N.A., DOKKEN, D.J., WHITE, K.S. (Eds.) (2001): Climate change 2001: impacts, adaptation, and vulnerability: contribution of Working Group II to the third assessment report of the Intergovernmental Panel on Climate Change. Cambridge (UK): Cambridge University Press, IPCC.

MEERA, V. / MANSOOR AHAMMED, M. (2006): Water quality of rooftop rainwater harvesting systems: a review. In: Journal of Water Supply: Research and Technology – AQUA 55 (4), 257-268.

MENZEL, L., KOCH, J., ONIGKEIT, J., SCHALDACH, R. (2009): Modelling the effects of land-use and land-cover change on water availability in the Jordan River region. In: Advances in Geosciences 21, 73-80.

MILLER, J.E., NELSON, S.A., HESS, G.R. (2009): An object extraction approach for impervious surface classification with very-high-resolution imagery. In: The Professional Geographer 61 (2), 250-264.

MILLER, J.M. (1979): Archaeological survey of Central Moab: 1978. In: Bulletin of the American Schools of Oriental Research 234, 43-52.

MILLER, J.M. (Ed.) (1991): Archaeological survey of the Kerak Plateau: conducted during 1978 - 1982 under the direction of J. Maxwell Miller and Jack M. Pinkerton. Atlanta: Scholars Press. (ASOR Archaeological Reports, 1).

MILLER, R. (1980): Water use in Syria and Palestine from the Neolithic to the Bronze Age. In: World Archaeology 11 (3), Water Management, 331-341.

MILWRIGHT, M. (2008): The fortress of the raven: Karak in the Middle Islamic period (1100-1650). Leiden, Boston: Brill. (Islamic History and Civilization, 72).

MINISTRY OF AGRICULTURE (MoA), DIRECTORATE OF RANGELANDS AND BADIA DEVELOPMENT (2013/ 2014): Updated rangeland strategy for Jordan. Amman: Ministry of Agriculture, The Hashemite Kingdom of Jordan.

MINISTRY OF AGRICULTURE (MoA), THE HASHEMITE KINGDOM OF JORDAN (2011): Soil map data level 2: central highlands (Karak). [Data files]. Amman: Ministry of Agriculture, The Hashemite Kingdom of Jordan.

MINISTRY OF ENVIRONMENT (MoE), THE HASHEMITE KINGDOM OF JORDAN (2006): National strategy and action plan to combat desertification. Amman: Ministry of Environment, The Hashemite Kingdom of Jordan/ United Nations Development Programme (UNDP).

MINISTRY OF ENVIRONMENT (MoE), THE HASHEMITE KINGDOM OF JORDAN (2015): Integrated investment framework for sustainable land management in Jordan. Amman: Ministry of Environment, The Hashemite Kingdom of Jordan/ United Nations Development Programme (UNDP).

MINISTRY OF ENVIRONMENT (MoE), THE HASHEMITE KINGDOM OF JORDAN / UNITED NATIONS DEVELOPMENT PROGRAMME (UNDP) (2009): Jordan's second national communication to the United Nations Framework Convention on Climate Change (UNFCCC). Amman: Ministry of Environment, The Hashemite Kingdom of Jordan.

MINISTRY OF PLANNING (MoP), THE HASHEMITE KINGDOM OF JORDAN / JICA (1990): Feasibility study on agricultural development for the Karak-Tafila Development Region. Unpublished report. Tokyo: Japan International Cooperation Agency (JICA).

MINISTRY OF WATER AND IRRIGATION (MWI), THE HASHEMITE KINGDOM OF JORDAN (2016a): National water strategy 2016-2025. Amman: Ministry of Water and Irrigation (MWI), The Hashemite Kingdom of Jordan.

MINISTRY OF WATER AND IRRIGATION (MWI), THE HASHEMITE KINGDOM OF JORDAN (2016b): Water reallocation policy. Amman: Ministry of Water and Irrigation, The Hashemite Kingdom of Jordan.

MITHEN, S. (2010): The domestication of water: water management in the ancient world and its prehistoric origins in the Jordan Valley. In: Philosophical Transactions of the Royal Society A 368, 5249-5274.

MLADINICH, C.S. (2010): An evaluation of object-oriented image analysis techniques to identify motorized vehicle effects in semi-arid to arid ecosystems of the American west. In: GIScience & Remote Sensing 47 (1), 53-77.

MOORMANN, F.R. (1959): The soils of East Jordan: report to the government of Jordan. Rome: FAO. (Expanded Technical Assistance Program, 1132).

MULDER, V.L., DE BRUIN, S., SCHAEPMAN, M.E., MAYR, T.R. (2011): The use of remote sensing in soil and terrain mapping – a review. In: Gederma 162, 1-19.

MWENGE KAHINDA, J., TAIGBENU, A.E., BOROTO, R.J. (2010): Domestic rainwater harvesting as an adaption measure to climate change in South Africa. In: Physics and Chemistry of the Earth 35, 742-751.

MWENGE KAHINDA, J., LILLIE, E.S.B., TAIGBENU, A.E., TAUTE, M., BOROTO, R.J. (2008): Developing suitability maps for rainwater harvesting in South Africa. In: Physics and Chemistry of the Earth 33, 788-799.

MWENGE KAHINDA, J., TAIGBENU, A.E., SEJAMOHOLO, B.B.P., LILLIE, E.S.B., BOROTO, R.J. (2009): A GIS-based decision support system for rainwater harvesting (RHADESS). In: Physics and Chemistry of the Earth 34, 767-775.

MYERS, D. / DALGITY, A. (2012): The Middle Eastern Geodatabase for Antiquities (MEGA): an open source GIS-based heritage site inventory and management system. In: Change Over Time 2 (1), 32-57.

MYERS, L.E. (1975): Water harvesting – 2000 B.C. to 1974 A.D. In: G.W. FRASIER (Ed.): Proceedings of the water harvesting symposium, Phoenix, Arizona, 26-28 March, 1974. Berkeley (California, USA): U.S. Department of Agriculture, Agricultural Research Service, 1-7.

NAPOLI, M., CECCHI, S., ORLANDINI, S., ZANCHI, C.A. (2014): Determining potential rainwater harvesting sites using a continuous runoff potential accounting procedure and GIS techniques in central Italy. In: Agricultural Water Management 141, 55-65.

NASA, METI, AIST, JAPAN SPACESYSTEMS, U.S./JAPAN ASTER SCIENCE TEAM (2009): ASTER Global Digital Elevation Model. [Data set]. NASA EOSDIS Land Processes DAAC. https://doi.org/10.5067/ASTER/ASTGTM.002 (access October 18, 2019).

NATIONAL SOIL MAP AND LAND USE PROJECT, MINISTRY OF AGRICULTURE, THE HASHEMITE KINGDOM OF JORDAN, HUNTING TECHNICAL SERVICES LTD. UK, SOIL SURVEY AND LAND RESEARCH CENTRE UK (1993a): The soils of Jordan: level 1: reconnaissance soil survey. Vol. 2: Main report. Amman: Ministry of Agriculture, The Hashemite Kingdom of Jordan.

NATIONAL SOIL MAP AND LAND USE PROJECT, MINISTRY OF AGRICULTURE, THE HASHEMITE KINGDOM OF JORDAN, HUNTING TECHNICAL SERVICES LTD. UK, SOIL SURVEY AND LAND RESEARCH CENTRE UK (1993b): The soils of Jordan: level 1: reconnaissance soil survey. Vol. 3: Representative profiles and soil analyses. Amman: Ministry of Agriculture, The Hashemite Kingdom of Jordan.

NATIONAL SOIL MAP AND LAND USE PROJECT, MINISTRY OF AGRICULTURE, THE HASHEMITE KINGDOM OF JORDAN, HUNTING TECHNICAL SERVICES LTD. UK, SOIL SURVEY AND LAND RESEARCH CENTRE UK (1994a): The soils of Jordan: level 2: semi-detailed studies. Vol. 2: Main report. Amman: Ministry of Agriculture, The Hashemite Kingdom of Jordan.

NATIONAL SOIL MAP AND LAND USE PROJECT, MINISTRY OF AGRICULTURE, THE HASHEMITE KINGDOM OF JORDAN, HUNTING TECHNICAL SERVICES LTD. UK, SOIL SURVEY AND LAND RESEARCH CENTRE UK (1994b): The soils of Jordan: level 2: semi-detailed studies. Vol. 3: Appendices. Amman: Ministry of Agriculture, The Hashemite Kingdom of Jordan.

NATIONAL SOIL MAP AND LAND USE PROJECT, MINISTRY OF AGRICULTURE, THE HASHEMITE KINGDOM OF JORDAN, COMMISSION OF THE EUROPEAN COMMUNITIES, SOIL SURVEY AND LAND CLASSIFICATION SECTION, DEPARTMENT OF AFFORESTATION AND FORESTS, HUNTING TECHNICAL SERVICES LTD. UK, SOIL SURVEY AND LAND RESEARCH CENTRE UK (1994c): Semi detailed soil map, scale 1:50,000. Sheet 16: Al Karak. Amman: The Royal Jordanian Geographic Centre.

NATURAL RESOURCES AUTHORITY, GEOLOGY DIRECTORATE, MINISTRY OF ENERGY AND MINERAL RESOURCES, HASHEMITE KINGDOM OF JORDAN, GEOLOGICAL MAPPING DIVISION, NATIONAL MAPPING PROJECT, MASRI, A. (1996): Geological map, scale 1:50,000. Sheet 3152 I: Dhiban (Wadi al Mujib). Amman: The Royal Jordanian Geographic Centre.

NATURAL RESOURCES AUTHORITY, GEOLOGY DIRECTORATE, MINISTRY OF ENERGY AND MINERAL RESOURCES, THE HASHEMITE KINGDOM OF JORDAN, GEOLOGICAL MAPPING DIVISION, NATIONAL MAPPING PROJECT, MOH'D, B.K. (1989): Geological map, scale 1:50,000. Sheet 3152 IV: Ar Rabba. Amman: The Royal Jordanian Geographic Centre.

NEUBERT, M. / MEINEL, G. (2005): Atmospheric and terrain correction of IKONOS imagery using ATCOR3. In: C. HEIPKE, K. JACOBSEN, M. GERKE (Eds.): Proceedings of the ISPRS Hannover Workshop 2005: high-resolution earth imaging for geospatial information, Hannover, May 17-20, 2005. International Society for Photogrammetry and Remote Sensing (ISPRS).

NGIGI, S.N. (2003): What is the limit of up-scaling rainwater harvesting in a river basin? In: Physics and Chemistry of the Earth 28, 943-956.

NTHUNI, S.M., LÜBKER, T., SCHAAB, G. (2014): Modelling the potential of rainwater harvesting in western Kenya using remote sensing and GIS techniques. In: South African Journal of Geomatics 3 (3), 285-301.

O'BRIEN, M.A. (2003): Feature extraction with the VLS Feature Analyst system. In: Proceedings of the ASPRS Annual Conference, Anchorage (Alaska), May 5-9, 2003. Bethesda (Maryland, USA): American Society for Photogrammetry and Remote Sensing (ASPRS).

OLESON, J.P. (1991): Aqueducts, cisterns, and the strategy of water supply at Nabataean and Roman Auara (Jordan). In: T.A. HODGE (Ed.): Future currents in aqueduct studies. Leeds: Cairns, 45-62.

OLESON, J.P. (1995): The origins and design of Nabataean water-supply systems. In: Studies in the History and Archaeology of Jordan 5, 707-719.

OLESON, J.P. (2001): Water supply in Jordan through the ages. In: B. MACDONALD, R. ADAMS, P. BIENKOWSKI (Eds.): The archaeology of Jordan. Sheffield (UK): Sheffield Academic Press, 603-614.

OLESON, J.P. (2007): Nabataean water supply systems: appropriateness, design, and evolution. In: Studies in the History and Archaeology of Jordan 9 (Cultural interactions through the ages), 167-174.

OPITZ, D. / BLUNDELL, S. (2008a): Feature extraction with the VLS Feature Analyst system. In: Proceedings of the ASPRS Annual Conference "Bridging the horizons – new frontiers in geospatial collaboration", Portland (Oregon, USA), April 28 - Mai 2, 2008. Bethesda (Maryland, USA): American Society for Photogrammetry and Remote Sensing (ASPRS).

OPITZ, D. / BLUNDELL, S. (2008b): Object recognition and image segmentation: the Feature Analyst® approach. In: T. BLASCHKE, S. LANG, G.J. HAY (Eds.): Object-based image analysis: spatial concepts for knowlege-driven remote sensing applications. Berlin, Heidelberg: Springer, 153-167. (Lecture notes in geoinformation and cartography).

ORTLOFF, C.R. (2005): The water supply and distribution system of the Nabataean city of Petra (Jordan), 300 BC - AD 300. In: Cambridge Archaeological Journal 15 (1), 93-109.

OTT, M. (1998): Landwirtschaft in Jordanien: Agrarstrukturmerkmale am Beispiel der Provinz Al-Karak. In: Mitteilungen der Fränkischen Geographischen Gesellschaft 45, 337-376.

OUESSAR, M., ABDELLI, F., YAHYAOUI, H., MAATI, M. (2004): Assessment of water harvesting techniques: impacts on soil water and erosion in an arid catchment. In: C. CANTERO-MARTÍNEZ, D. GABIÑA (Eds.): Mediterranean rainfed agriculture: strategies for sustainability: proceedings of the final seminar of the Regional Action Programme on Rainfed Agriculture (RAP-RAG) of the EC (Europe Aid) CIHEAM Cooperation Project 19982003, Zaragoza (Spain), June 2-3, 2003. Zaragoza: CIHEAM/ EC Europe Aid, 55-61. (Options Méditerranéennes: Série A, 60).

OUESSAR, M., BRUGGEMAN, A., ABDELLI, F., MOHTAR, R.H., GABRIËLS, D., CORNELIS, W.M. (2009): Modelling water-harvesting systems in the arid south of Tunisia using SWAT. In: Hydrology and Earth System Sciences 13, 2003-2021.

OVERWATCH (2010): Feature Analyst® 5.0 for ArcGIS®: reference manual. Missoula (Montana): Overwatch.

OVERWATCH / TEXTRON SYSTEMS (2012-2017): Feature Analyst for ArcGIS, professional. Versions 5.0.0.119-5.2.0.4. [Computer program]. Sterling (VA, USA): Overwatch Systems, Ltd. / Textron Systems Geospatial Solutions.

OWEIS, T.Y. (2005): The role of water harvesting and supplemental irrigation in coping with water scarcity and drought in the dry areas. In: D.A. WILHITE (Ed.): Drought and water crises: science, technology, and management issues. Boca Raton: CRC Press, 191-213.

OWEIS, T. / HACHUM, A. (2006): Water harvesting and supplemental irrigation for improved water productivity of dry farming systems in West Asia and North Africa. In: Agricultural Water Management 80, 57-73.

OWEIS, T.Y. / TAIMEH, A.Y. (1996): Evaluation of a small basin water-harvesting system in the arid region of Jordan. In: Water Resources Management 10, 21-34.

OWEIS, T., HACHUM, A., BRUGGEMAN, A. (Eds.) (2004): Indigenous water harvesting systems in West Asia and North Africa. Aleppo (Syria): ICARDA.

OWEIS, T., HACHUM, A., KIJNE, J. (1999): Water harvesting and supplementary irrigation for improved water use efficiency in dry areas. Colombo (Sri Lanka): International Water Management Institute (IWMI). (SWIM Paper, 7).

OWEIS, T., PRINZ, D., HACHUM, A. (2001): Water harvesting: indigenous knowledge for the future of the drier environments. Aleppo (Syria): ICARDA.

OWEIS, T.Y., PRINZ, D., HACHUM, A.Y. (2012): Water harvesting for agriculture in the dry areas. Leiden (The Netherlands): CRC Press/ Balkema.

PACE, J.H. (1996): The cisterns of the al-Karak Plateau. In: Annual of the Department of Antiquities of Jordan 40, 369-374.

PACEY, A. / CULLIS, A. (1986): Rainwater harvesting: the collection of rainfall and run-off in rural areas. London: Intermediate Technology Publications.

PANDEY, D.N., GUPTA, A.K., ANDERSON, D.M. (2003): Rainwater harvesting as an adaption to climate change. In: Current Science 85 (1), 46-59.

PARKER, S.T. (Ed.) (1987): The Roman frontier in central Jordan: interim report on the Limes Arabicus Project, 1980 - 1985. Oxford: BAR. (BAR International Series, 340).

PARKER, S.T. (1992): The Limes and settlement patterns in Central Jordan in the Roman and Byzantine periods. In: Studies in the History and Archaeology of Jordan 4, 321-327.

PARKER, S.T. (Ed.) (2006): The Roman frontier in central Jordan: final report on the Limes Arabicus Project, 1980 - 1989. Washington, D.C.: Dumbarton Oaks Research Library and Collection. (Dumbarton Oaks studies, 40).

PARKER, S.T. (2007): Projecting power on the periphery: Rome's Arabian frontier east of the Dead Sea. In: T.E. LEVY, P.M.M. DAVIAU, R.W. YOUNKER, M. SHAER (Eds.): Crossing Jordan: North American contributions to the archaeology of Jordan. London, Oakville: Equinox, 349-357.

PAUL, F., BARRAND, N.E., BAUMANN, S., BERTHIER, E., BOLCH, T., CASEY, K., FREY, H., JOSHI, S.P., KONOVALOV, V., LE BRIS, R., MÖLG, N., NOSENKO, G., NUTH, C., POPE, A., RACOVITEANU, A., RASTNER, P., RAUP, B., SCHARRER, K., STEFFEN, S., WINSVOLD, S. (2013): On the accuracy of glacier outlines derived from remote-sensing data. In: Annals of Glaciology 54 (63), 171-182.

PERSELLO, C. / BRUZZONE, L. (2010): A novel protocol for accuracy assessment in classification of very high resolution images. In: IEEE Transactions on Geoscience and Remote Sensing 48 (3), 1232-1244.

PONTIUS JR, R.G. / MILLONES, M. (2011): Death to Kappa: birth of quantity disagreement and allocation disagreement for accuracy assessment. In: International Journal of Remote Sensing 32 (15), 4407-4429.

PORTER, D.O., PERSYN, R.A., SILVY, V.A. (2008): Rainwater harvesting. College Station (Texas): AgriLife Extension Service, Texas A&M System.

PORTER, B.W., ROUTLEDGE, B.E., SIMMONS, E.M., LEV-TOV, J.S.E. (2014): Extensification in a Mediterranean semi-arid marginal zone: an archaeological case study from Early Iron Age Jordan's Eastern Karak Plateau. In: Journal of Arid Environments 104, 132-148.

POWELL, J.H. (1989): Stratigraphy and sedimentation of the Phanerozoic rocks in central and south Jordan: Part B: Kurnub, Ajlun and Belqa Groups. Amman: Geology Directorate, Natural Resources Authority, Ministry of Energy and Mineral Resources, The Hashemite Kingdom of Jordan. (1:50,000 Geological Mapping Series, Geological Bulletin, 11).

POWELL, J.H. / MOH'D, B.K. (2011): Evolution of Cretaceous to Eocene alluvial and carbonate platform sequences in central and south Jordan. In: GeoArabia 16 (4), 29-82.

PRAG, K. (2007): Water strategies in the Iktanu Region of Jordan. . In: Studies in the history and archaeology of Jordan 9, 405-412.

PREUL, H.C. (1994): Rainfall-runoff water harvesting prospects for Greater Amman and Jordan. In: Water International 19 (2), 82-85.

PRINZ, D. (1996): Rainwater harvesting: past and future. In: L.S. PEREIRA, R.A. FEDDES, J.R. GILEY, B. LESAFFRE (Eds): Sustainability of irrigated agriculture: proceedings of the NATO Advanced Research Workshop on sustainability of irrigated agriculture, Vimeiro, Portugal, March 21-26, 1994. Dordrecht: Kluwer Academic Publishers, 137–168. (NATO ASI series E, 312).

PRINZ, D. (2002): The role of water harvesting in alleviating water scarcity in arid areas. In: Proceedings of the international conference on water resources management in arid regions, Kuwait, March 23-27, 2002. Kuwait: Kuwait Institute for scientific research, 107-122.

PRINZ, D., TAUER, W., VÖGTLE, T. (1994): Application of remote sensing and geographic information systems for determining potential sites for water harvesting. In: FAO: Water harvesting for improved agricultural production. Rome: FAO, 136-144. (Water Reports, 3).

PSALTIS, C. / IOANNIDIS, C. (2008): Simple method for cost-effective informal building monitoring. In: Surveying and Land Information Science 68 (2), 65-79.

QADIR, M., SHARMA, B.R., BRUGGEMAN, A., CHOUKR-ALLAH, R., KARAJEH, F. (2007): Non-conventional water resources and opportunities for water augmentation to achieve food security in water scarce countries. In: Agricultural Water Management 87, 2-22.

QUACKENBUSH, L.J. (2004): A review of techniques for extracting linear features from imagery. In: Photogrammetric Engineering & Remote Sensing 70 (12), 1383-1392.

QUENNELL, A.M. (1951): The geology and mineral resources of (former) Transjordan. In: Colonial Geology and Mineral Resources 2 (2), 85-115.

RABADI, A. (2016): The Red Sea-Dead Sea desalination project at Aqaba. In: Desalination and Water Treatment 57 (48-49), 22713-22717.

RADAIDEH, J., AL-ZBOON, K., AL-HARAHSHEH, A., AL-ADAMAT, R. (2009): Quality assessment of harvested rainwater for domestic uses. In: Jordan Journal of Earth and Environmental Sciences 2 (1), 26-31.

RAHMAN, A., KEANE, J., IMTEAZ, M.A. (2012): Rainwater harvesting in Greater Sydney: water savings, reliability and economic benefits. In: Resources, Conservation and Recycling 61, 16-21.

RAPPOLD, G.D. (2005): Precipitation analysis and agricultural water availability in the Southern Highlands of Yemen. In: Hydrological Processes 19, 2437-2449.

REGNER, H.J. (2002): Historical and modern use of rainwater harvesting systems in Egypt. In: C. OHLIG, Y. PELEG, T. TSUK (Eds.): Cura Aquarum in Israel: Proceedings of the 11th international conference on the history of water management and hydraulic engineering in the Mediterranean Region, Israel, May 7-12, 2001. Siegburg: Deutsche Wasserhistorische Gesellschaft (DWhG), 267-278.

REMINI, B., KECHAD, R., ACHOUR, B. (2014): The collecting of groundwater by the qanats: a millennium technique decaying. In: LARHYSS Journal 20, 259-277.

RICHTER, R. / SCHLAEPFER, D. (2011): Atmospheric/ topographic correction for satellite imagery: ATCOR-2/3 user guide. Version 8.0.2. Wil (Switzerland): ReSe Applications Schlaepfer.

RICHTER, R., DEUTSCHES ZENTRUM FÜR LUFT- UND RAUMFAHRT (DLR), GEOSYSTEMS, ERDAS (2010-2011): ATCOR for ERDAS IMAGINE. Version(s) 2010-2011. [Computer program].Germering: GEOSYSTEMS GmbH.

ROEBUCK, R.M., OLTEAN-DUMBRAVA, C., TAIT, S. (2011): Whole life cost performance of domestic rainwater harvesting systems in the United Kingdom. In: Water and Environment Journal 25 (3), 355-365.

ROUTLEDGE, B. (2004): Moab in the Iron Age: hegemony, polity, archaeology. Philadelphia: University of Pennsylvania Press.

SAIDAN, M.N., AL-WESHAH, R.A., OBADA, I. (2015): Potential rainwater harvesting: an adaptation measure for urban areas in Jordan. In: Journal AWWA (American Water Works Association) 107 (11), E594-E602.

SALAMEH, E. (2004): Ancient water supply systems and their relevance for today's society in Jordan. In: H.-D. BIENERT/ J. HÄSER (Eds.): Men of dikes and canals: the archaeology of water in the Middle East: international symposium held at Petra, Wadi Musa (H. K. of Jordan), June 15-20, 1999. Rahden: Marie Leidorf, 285-291. (Orient-Archäologie, 13).

SALAMEH, E. / HADDADIN, M.J. (2006): The population-water resources equation. In: M.J. HADDADIN (Ed.): Water resources in Jordan: evolving policies for development, the environment, and conflict resolution. Washington, DC: Resources for the Future/ RFF Press, 7-27.

SALAMEH, H.R. (1997): Geomorphology of the eastern coast of the Dead Sea, Jordan. In: GeoJournal 41 (3), 255-266.

SANTOS, T., FREIRE, S., FONSECA, A., TENEDÓRIO, J.A. (2011): Producing a building change map for urban management. In: EARSel eProceedings 10 (1), 56-65.

SAVAGE, S.H. (2007): Controlling space at the regional level: geographic information systems (GIS) and JADIS in Jordan. In: T.E. LEVY, P.M.M. DAVIAU, R.W. YOUNKER, M. SHAER (Eds.): Crossing Jordan: North American contributions to the archaeology of Jordan. London, Oakville: Equinox, 37-46.

SAZAKLI, E., ALEXOPOULOS, A., LEOTSINIDIS, M. (2007): Rainwater harvesting, quality assessment and utilization in Kefalonia Island, Greece. In: Water Research 41, 2039-2047.

SCHÄFER, T., SCHÖN, F., GERDES, A., HEINRICHS, J. (Eds.) (2014): Antike und moderne Wasserspeicherung: internationaler Workshop vom 11.-14.05.2011 in Pantelleria (Italien). Rahden: Marie Leidorf. (Tübinger Archäologische Forschungen, 12).

SCHIETTECATTE, W., OUESSAR, M., GABRIELS, D., TANGHE, S., HEIRMAN, S., ABDELLI, F. (2005): Impact of water harvesting techniques on soil and water conservation: a case study on a micro catchment in southeastern Tunisia. In: Journal of Arid Environments 61, 297-313.

SCHMID, S.G. (2008): Die Wasserversorgung des Wadi Farasa Ost in Petra. In: C. OHLIG (Ed.): Cura Aquarum in Jordanien: Proceedings of the 13th international conference on the history of water management and hydraulic engineering in the Mediterranean Region, Petra/ Amman, March 31-April 09, 2007. Siegburg: Deutsche Wasserhistorische Gesellschaft (DWhG), 95-117.

SCHMIDT, M., LUCKE, B., BÄUMLER, R., AL-SAAD, Z., AL-QUDAH, B., HUTCHEON, A. (2006): The Decapolis region (Northern Jordan) as historical example of desertification? Evidence from soil development and distribution. In: Quaternary International 151 (1), 74-86.

SEKAR, I. / RANDHIR, T.O. (2007): Spatial assessment of conjunctive water harvesting potential in watershed systems. In: Journal of Hydrology 334, 39-52.

SEYLER, F., MULLER, F., COCHONNEAU, G., GUIMARAES, L., GUYOT, J.L. (2009): Watershed delineation for the Amazon sub-basin system using GTOPO30 DEM and a drainage network extracted from JERS SAR images. In: Hydrological Processes 23 (22), 3173-3185.

SHADEED, S. / LANGE, J. (2010): Rainwater harvesting to alleviate water scarcity in dry conditions: a case study in Faria Catchment, Palestine. In: Water Science and Engineering 3 (2), 132-143.

SHANAN, L. (2000): Runoff, erosion, and the sustainability of ancient irrigation systems in the Central Negev desert. In: M.A. HASSAN, O. SLAYMAKER, S.M. BERKOWICZ (Eds.): The hydrology-geomorphology interface: rainfall, floods, sedimentation, land use (Proceedings of the Jerusalem Conference, May 1999). Wallingford: IAHS Publ., 75-106. (IAHS Publication 261).

SHANAN, L. / SCHICK, A.P. (1980): A hydrological model for the Negev Desert Highlands: effects of infiltration, runoff and ancient agriculture. In: Hydrological Sciences Journal 25 (3), 269-282.

SHARMA, S.K. (2009): Potential of roof-top rainwater harvesting techniques in urban areas: a case study from India. In: J. FEYEN, K. SHANNON, M. NEVILLE (Eds.): Water and urban development paradigms: towards an integration of engineering, design and management approaches. London: Taylor & Francis, 491-495.

SHATANAWI, M.R. (1994): Water harvesting in Jordan and the region: present situation and future needs. In: FAO: Water harvesting for improved agricultural production. Rome: FAO, 391-399. (Water Reports, 3).

SHEHADEH, N. (1985): The climate of Jordan in the past and present. In: Studies in the History and Archaeology of Jordan 2, 25-38.

SHINAQ, R., SHEREIDEH, S., SAIFULDIN, N. (2006): Microfacies and depositional environment of Upper Cretaceous phosphorites in northern Jordan. In: Paläontologie, Stratigraphie, Fazies 14, Freiberger Forschungshefte C 511, 45-58.

SHOWLEH, T. (2007): Water management in the Bronze Age: Greece and Anatolia. In: Water Science & Technology: Water Supply 7 (1), 77-85.

SOIL CONSERVATION SERVICE (SCS), US DEPARTMENT OF AGRICULTURE (USDA) (1985): National engineering handbook. Section 4, Hydrology. Washington, DC: USDA.

SOIL SURVEY STAFF (1990): Keys to Soil Taxonomy. 4th edition. Blacksburg, Virginia: Virginia Polytechnic Institute and State University. (SMSS technical monograph, 6).

STAHN, H. / TOMINI, A. (2009): A drop of rainwater against a drop of groundwater: does rainwater harvesting really allow us to spare groundwater? Marseille: GREQAM (Groupement de Recherche en Economie Quantitative d'Aix-Marseille – UMR-CNRS 6579, Ecole des Hautes Etudes en Sciences Sociales, Universités d'Aix-Marseille II et III). (Document de Travail, 2009-43).

STEFFEN, J., JENSEN, M., POMEROY, C.A., BURIAN, S.J. (2013): Water supply and stormwater management benefits of residential rainwater harvesting in U.S. cities. In: Journal of the American Water Resources Association (JAWRA) 49 (4), 810-824.

STEHMAN, S.V. (1996): Estimating the Kappa Coefficient and its variance under stratified random sampling. In: Photogrammetric Engineering & Remote Sensing 62 (4), 401-407.

STEHMAN, S.V. / WICKHAM, J.D. (2011): Pixels, blocks of pixels, and polygons: choosing a spatial unit for thematic accuracy assessment. In: Remote Sensing of Environment 115, 3044-3055.

STURM, M., ZIMMERMANN, M., SCHÜTZ, K., URBAN, W., HARTUNG, H. (2009): Rainwater harvesting as an alternative water resource in rural sites in central northern Namibia. In: Physics and Chemistry of the Earth 34, 776-785.

SU, M.D., LIN, C.H., CHANG, L.F., KANG, J.L., LIN, M.C. (2009): A probabilistic approach to rainwater harvesting systems design and evaluation. In: Resources, Conservation and Recycling 53, 393-399.

SUGG, Z.P., FINKE, T., GOODRICH, D.C., MORAN, M.S., YOOL, S.R. (2014): Mapping impervious surfaces using object-oriented classification in a semiarid urban region. In: Photogrammetric Engineering & Remote Sensing 80 (4), 343-352.

TAHERI TIZRO, A., AKBARI, K., VOUDOURIS, K. (2009): Assessment of groundwater artificial recharge from water storage structures in a rural region of west Iran. In: J. FEYEN, K. SHANNON, M. NEVILLE (Eds.): Water and urban development paradigms: towards an integration of engineering, design and management approaches. London: Taylor & Francis, 447-453.

TAIMEH, A.Y. / KHRESAT, S.A. (1988): Vertisols in Jordan: properties and distribution. Amman: Univ. of Jordan.

TAQIEDDIN, S.A., AL-HOMOUD, A.S., AWAD, A., AYYASH, S. (1995): Geological and hydrological investigation of a water collection system in arid Jordanian lands. In: Environmental Geology 26, 252-261.

TARAWNEH, S. (2004): Fog water harvesting five sites of Mazar-Karak (1992-1994) Jordan. Alexandria Engineering Journal 43 (1), 55-65.

TARAWNEH, Q. / KADIOGLU, M. (2003): An analysis of precipitation climatology in Jordan. In: Theoretical and Applied Climatology 74 (1), 123-136.

TEXAS WATER DEVELOPMENT BOARD (2005): The Texas manual on rainwater harvesting. 3rd ed. Austin (Texas): Texas Water Development Board.

THE AGRICULTURAL COMMITTEE (2002): National strategy for agricultural development 2002-2010. Amman. http://faolex.fao.org/docs/pdf/jor145312.pdf (access May 24, 2016).

THE GETTY CONSERVATION INSTITUTE (GCI), WORLD MONUMENTS FUND (WMF), DEPARTMENT OF ANTIQUITIES (DOA), THE HASHEMITE KINGDOM OF JORDAN (2010): MEGA-Jordan: the national heritage documentation and management system. [Online database]. http:// megajordan.org (access November 5, 2015).

THE HASHEMITE KINGDOM OF JORDAN (2001): Agricultural resources management project: mid-term evaluation report. International Fund for Agricultural Development, Report No. 1159.

THE WORLD BANK GROUP (2015): Data: Jordan. http://data.worldbank.org/country/jordan (access October 31, 2015).

THOMAS, R.B., KIRISITS, M.J., LYE, D.J., KINNEY, K.A. (2014): Rainwater harvesting in the United States: a survey of common system practices. In: Journal of Cleaner Production 75, 166-173.

TOBLER, W.R. (1970): A computer movie simulating urban growth in the Detroit region. In: Economic Geography 46 (Supplement: Proceedings. International Geographical Union. Commission on Quantitative Methods), 234-240.

TÖRNROS, T., MENZEL, L. (2014): Leaf area index as a function of precipitation within a hydrological model. In: Hydrology Research 45 (4-5), 660-672.

TRIMBLE NAVIGATION LIMITED (2013): MobileMapper® 20: getting started guide. Westminster (USA): Spectra Precision Division, Trimble Navigation Limited.

TSAI, Y.H., STOW, D., WEEKS, J. (2011): Comparison of object-based image analysis approaches to mapping new buildings in Accra, Ghana using multi-temporal QuickBird satellite imagery. In: Remote Sensing 3 (12), 2707-2726.

UNESCO / ACSAD (1986): The major regional project on rational utilization and conservation of water resources in the rural areas of the Arab States with emphasis on the traditional water systems. Paris: UNESCO/ ACSAD.

VAN DER STERREN, M., RAHMAN, A., DENNIS, G.R. (2012): Rainwater harvesting systems in Australia. In: K. VOUDOURIS (Ed.): Ecological water quality: water treatment and reuse. InTech, 471-496.

VAN DIJK, J. / REIJ, C. (1994): Indigenous water harvesting techniques in sub-Saharan Africa: examples from Sudan and the West African Sahel. In: FAO: Water harvesting for improved agricultural production. Rome: FAO, 101-112. (Water Reports, 3).

VAN WESEMAEL, B., POESEN, J., SOLÉ BENET, A., CARA BARRIONUEVO, L., PUIGDEFÁBREGAS, J. (1998): Collection and storage of runoff from hillslopes in a semi-arid environment: geomorphic and hydrologic aspects of the aljibe system in Almeria Province, Spain. In: Journal of Arid Environments 40, 1-14.

VÖGELE, A. (2012): Bodengeographische Untersuchungen auf der Karak-Hochebene (Jordanien): Mächtigkeiten, Verbreitung, Eigenschaften. Unpublished Master Thesis, Insitute of Geography, Heidelberg University. Heidelberg.

VOHLAND, K. / BARRY, B. (2009): A review of in situ rainwater harvesting (RWH) practices modifying landscape functions in African drylands. In: Agriculture, Ecosystems and Environment 131, 119-127.

WÅHLIN, L. (1997): The family cistern: 3,000 years of household water collection in Jordan. In: M. SABOUR/ K.S. VIKØR (Eds.): Ethnic encounter and culture change: papers from the third Nordic Conference on Middle Eastern Studies, Joensuu, 1995. Bergen: Nordic Society for Middle Eastern Studies, 233-249. (Nordic Research on the Middle East, 3).

WAITZBAUER, W. / PETUTSCHNIG, B. (2004a): Zum Klima Jordaniens. In: W. WAITZBAUER, R. ALBERT, B. PETUTSCHNIG, G. AUBRECHT (Eds.): Reise durch die Natur Jordaniens. Linz: Biologiezentrum der Oberösterreichischen Landesmuseen, 77-87. (Denisia, 14).

WAITZBAUER, W. / PETUTSCHNIG, B. (2004b): Zur Geologie Jordaniens. In: W. WAITZBAUER, R. ALBERT, B. PETUTSCHNIG, G. AUBRECHT (Eds.): Reise durch die Natur Jordaniens. Linz: Biologiezentrum der Oberösterreichischen Landesmuseen, 89-112. (Denisia, 14).

WAITZBAUER, W. / PETUTSCHNIG, B. (2004c): Zur Hydrogeologie Jordaniens. In: W. WAITZBAUER, R. ALBERT, B. PETUTSCHNIG, G. AUBRECHT (Eds.): Reise durch die Natur Jordaniens. Linz: Biologiezentrum der Oberösterreichischen Landesmuseen, 55-76. (Denisia, 14).

WARD, S., MEMON, F.A., BUTLER, D. (2010): Rainwater harvesting: model-based design evaluation. In: Water Science & Technology 61 (1), 85-96.

WARD, S., MEMON, F.A., BUTLER, D. (2012): Performance of a large building rainwater harvesting system. Water Research 46, 5127-5134.

WATER AUTHORITY OF JORDAN (WAJ) (2010a): Boundaries: international boundary of Jordan and boundaries of administrative units (governorates) in Jordan. [Data files]. Amman: Water Authority of Jordan.

WATER AUTHORITY OF JORDAN (WAJ) (2010b): Geology 50000: digital data of the geological maps of the scale 1:50,000 for Jordan. [Data files]. Amman: Water Authority of Jordan.

WATER AUTHORITY OF JORDAN (WAJ) (2010c): Surface water basins of Jordan. [Data files]. Amman: Water Authority of Jordan.

WATER AUTHORITY OF JORDAN (WAJ) (2011): Daily precipitation records of 28 weather stations for varying periods of time. [Data files]. Amman: Water Authority of Jordan.

WATERFALL, P.H., BICKELMANN, C., RANSOM, D. (2013): Harvesting rainwater: guide to water-efficient landscaping. Tucson (AZ, USA): City of Tucson Water.

WERZ, H. (2006): The use of remote sensing imagery for groundwater risk intensity mapping in the Wadi Shueib, Jordan. Dissertation, Univ. of Karlsruhe, Dept. of Civil Engineering, Geo- and Environmental Sciences. Karlsruhe.

WIGINTON, L.K., NGUYEN, H.T., PEARCE, J.M. (2010): Quantifying rooftop solar photovoltaic potential for regional renewable energy policy. In: Computers, Environment and Urban Systems 34, 345-357.

WIMMER, F., SCHLAFFER, S., MENZEL, L. (2009): Distributed modelling of climate change impacts on snow sublimation in Northern Mongolia. In: Advances in Geosciences 21, 117-124.

WISSER, D., FROLKING, S., DOUGLAS, E.M., FEKETE, B.M., SCHUMANN, A.H., VÖRÖSMARTY, C.J. (2010): The significance of local water resources captured in small reservoirs for crop production – a global-scale analysis. In: Journal of Hydrology 384, 264-275.

WITHARANA, C., CIVCO, D.L., MEYER, T.H. (2013): Evaluation of pansharpening algorithms in support of earth observation based rapid-mapping workflows. In: Applied Geography 37, 63-87.

WOLF, L., WERZ, H., HOETZL, H., & GHANEM, M. (2007): Exploring the potential of managed aquifer recharge to mitigate water scarcity in the Lower Jordan River Basin within an IWRM approach. In: P. FOX (Ed.): Management of aquifer recharge for sustainability: Proceedings of the 6th international symposium on managed artificial recharge of groundwater, ISMAR6, Phoenix, Arizona USA, October 28-November 2, 2007. Phoenix (Arizona): Acacia, 30-46.

WORSCHECH, U. (1992): Ancient settlement patterns in the northwest Ard Al-Karak. In: Studies in the History and Archaeology of Jordan 4, 83-89.

YANG, B., KIM, M., MADDEN, M. (2012): Assessing optimal image fusion methods for very high spatial resolution satellite images to support coastal monitoring. In: GIScience & Remote Sensing 49 (5), 687-710.

YOUN, S.G., CHUNG, E.S., KANG, W.G., SUNG, J.H. (2012): Probabilistic estimation of the storage capacity of a rainwater harvesting system considering climate change. In: Resources, Conservation and Recycling 65, 136-144.

YOUSIF, M. / BUBENZER, O. (2013): Integrated remote sensing and GIS for surface water development: case study: Ras El Hekma area, northwestern coast of Egypt. In: Arabian Journal of Geosciences 6 (4), 1295-1306.

YOUSIF, M. / BUBENZER, O. (2015): Geoinformatics application for assessing the potential of rainwater harvesting in arid regions: case study: El Daba'a area, northwestern coast of Egypt. In: Arabian Journal of Geosciences 8 (11), 9169-9191.

YOUSSEF, K. (1998): Evaluation of different water harvesting techniques at two different sites of Jordan. Master thesis, Univ. of Jordan, Faculty of Graduate Studies. Amman. Unpublished.

YUAN, F. (2008): Land-cover change and environmental impact analysis in the Greater Mankato area of Minnesota using remote sensing and GIS modelling. In: International Journal of Remote Sensing 29 (4), 1169-1184.

ZAYADINE, F. (1985): Caravan routes between Egypt and Nabataea and the voyage of Sultan Baibars to Petra in 1276. In: Studies in the History and Archaeology of Jordan 2, 159-175.

ZAYADINE, F. (2007): The Gaza-Damascus road in the medieval periods. In: Studies in the History and Archaeology of Jordan 9, 367-378.

ZENG, C., WANG, J., LEHRBASS, B. (2013): An evaluation system for building footprint extraction from remotely sensed data. In: IEEE Journal of Selected Topics in Applied Earth Observations and Remote Sensing 6 (3), 1640-1652.

ZIADAT, F.M., MAZAHREH, S.S., OWEIS, T.Y., BRUGGEMAN, A. (2006): A GIS-based approach for assessing water harvesting suitability in a Badia benchmark watershed in Jordan. In: Proceedings of the 14th international soil conservation organization conference, Marrakech (Morocco), May 14-19, 2006. Marrakech (Morocco): International Soil Conservation Organization (ISCO), 1-5.

ZIADAT, F., BRUGGEMAN, A., OWEIS, T., HADDAD, N., MAZAHREH, S., SARTAWI, W., SYUOF, M. (2012): A participatory GIS approach for assessing land suitability for rainwater harvesting in an arid rangeland environment. In: Arid Land Research and Management 26 (4), 297-311.

ZOHARY, M. (1962): Plant life of Palestine: Israel and Jordan. New York: Ronald Press. (Chronica Botanica: New Series of Plant Science Books, 33).

ZOHARY, M. (1973): Geobotanical foundations of the Middle East. Stuttgart: Gustav Fischer/Amsterdam: Swets & Zeitlinger. (Geobotanica selecta, 3).

ZWEIG, C.L., BURGESS, M.A., PERCIVAL, H.F., KITCHENS, W.M. (2015): Use of unmanned aircraft systems to delineate fine-scale wetland vegetation communities. In: Wetlands 35 (2), 303-309.

Acknowledgements

NATURWISSENSCHAFTLICH-MATHEMATISCHE
GESAMTFAKULTÄT

COMBINED FACULTY OF NATURAL SCIENCES AND
MATHEMATICS

RUPRECHT-KARLS-
UNIVERSITÄT
HEIDELBERG

Eidesstattliche Versicherung gemäß § 8 der Promotionsordnung für die Naturwissenschaftlich-Mathematische Gesamtfakultät der Universität Heidelberg / Sworn Affidavit according to § 8 of the doctoral degree regulations of the Combined Faculty of Natural Sciences and Mathematics

1. Bei der eingereichten Dissertation zu dem Thema / The thesis I have submitted entitled

   ………………………………………………………………………………………………………

   ……………………………………………………………………………………………………….

   handelt es sich um meine eigenständig erbrachte Leistung / is my own work.

2. Ich habe nur die angegebenen Quellen und Hilfsmittel benutzt und mich keiner unzulässigen Hilfe Dritter bedient. Insbesondere habe ich wörtlich oder sinngemäß aus anderen Werken übernommene Inhalte als solche kenntlich gemacht. / I have only used the sources indicated and have not made unauthorised use of services of a third party. Where the work of others has been quoted or reproduced, the source is always given.

3. Die Arbeit oder Teile davon habe ich wie folgt/bislang nicht[1] an einer Hochschule des In- oder Auslands als Bestandteil einer Prüfungs- oder Qualifikationsleistung vorgelegt. / I have not yet/have already[1] presented this thesis or parts thereof to a university as part of an examination or degree.

   Titel der Arbeit / Title of the thesis: ……………………………………………………………

   Hochschule und Jahr / University and year: ……………….……………………………………….......

   Art der Prüfungs- oder Qualifikationsleistung / Type of examination or degree: …………………………

4. Die Richtigkeit der vorstehenden Erklärungen bestätige ich. / I confirm that the declarations made above are correct.

5. Die Bedeutung der eidesstattlichen Versicherung und die strafrechtlichen Folgen einer unrichtigen oder unvollständigen eidesstattlichen Versicherung sind mir bekannt. / I am aware of the importance of a sworn affidavit and the criminal prosecution in case of a false or incomplete affidavit.

Ich versichere an Eides statt, dass ich nach bestem Wissen die reine Wahrheit erklärt und nichts verschwiegen habe. / I affirm that the above is the absolute truth to the best of my knowledge and that I have not concealed anything.

…………………………………….. ……………………………….………………………..
Ort und Datum / Place and date   Unterschrift / Signature

[1] Nicht Zutreffendes streichen. Bei Bejahung sind anzugeben: der Titel der andernorts vorgelegten Arbeit, die Hochschule, das Jahr der Vorlage und die Art der Prüfungs- oder Qualifikationsleistung. / Please cross out what is not applicable. If applicable, please provide: the title of the thesis that was presented elsewhere, the name of the university, the year of presentation and the type of examination or degree.

The German text is legally binding.